

LOW HEADROOM TRANSFER CHUTE FOR UNDERGROUND BELT CONVEYORS:

Analysis of Coal Flow through
Ninety Degree Transfer Point & Preliminary Design

FINAL TECHNICAL REPORT

as of
MAY, 1978

NOTICE
This report was prepared as an account of work sponsored by the United States Government. Neither the United States nor the United States Department of Energy, nor any of their employees, nor any of their contractors, subcontractors, or their employees, makes any warranty, express or implied, or assumes any legal liability or responsibility for the accuracy, completeness or usefulness of any information, apparatus, product or process disclosed, or represents that its use would not infringe privately owned rights.

This report represents completion by the Interior Department's Bureau Of Mines of a part of a program that was transferred to the Department Of Energy on October 1, 1977.

Terrell L. Holliday

Fairchild Space & Electronics Company
Germantown, Maryland 20767

Date Published
MAY, 1978

U.S. DEPARTMENT OF ENERGY
Assistant Secretary for Energy Technology
Solid Fuels Mining and Preparation

EB

DISCLAIMER

This report was prepared as an account of work sponsored by an agency of the United States Government. Neither the United States Government nor any agency thereof, nor any of their employees, makes any warranty, express or implied, or assumes any legal liability or responsibility for the accuracy, completeness, or usefulness of any information, apparatus, product, or process disclosed, or represents that its use would not infringe privately owned rights. Reference herein to any specific commercial product, process, or service by trade name, trademark, manufacturer, or otherwise does not necessarily constitute or imply its endorsement, recommendation, or favoring by the United States Government or any agency thereof. The views and opinions of authors expressed herein do not necessarily state or reflect those of the United States Government or any agency thereof.

DISCLAIMER

Portions of this document may be illegible in electronic image products. Images are produced from the best available original document.

REPORT DOCUMENTATION PAGE		1. REPORT NO. FE/2415-1	2.	3. Recipient's Accession No.
4. Title and Subtitle Low Headroom Transfer Chute for Underground Belt Conveyors: Analysis of Coal Flow Through Ninety Degree Transfer Point and Preliminary Design			5. Report Date May, 1978	
			6.	
7. Author(s) Terrell L. Holliday			8. Performing Organization Rept. No. 908-DR-3000	
9. Performing Organization Name and Address Fairchild Space & Electronics Company 20301 Century Boulevard Germantown, Maryland 20767			10. Project/Task/Work Unit No.	
			11. Contract(C) or Grant(G) No. (C) HO 166113 (G)	
12. Sponsoring Organization Name and Address U. S. Department of Energy Fossil Energy, Solid Fuels Mining and Preparation Pittsburg, Pennsylvania 15213			13. Type of Report & Period Covered Final July 1976 to April, 1977	
			14.	
15. Supplementary Notes				
16. Abstract (Limit: 200 words) A study program combining computer math modelling and scale model tests has evolved a preliminary design for a 90-degree transfer chute for belt conveyors in underground coal mines. The principal design objective was to achieve chute flow characteristics that minimize coal spillage, dust generation, and belt wear. This preliminary design will serve as a conceptual baseline for detailed design, fabrication, and testing---both above ground and in a coal mine---of a full size, 90-degree transfer chute between a 36-inch wide, input belt conveyor and a 42-inch wide, receiving belt conveyor. The study concludes that a double curvature-type surface will most nearly achieve the performance objectives for the 90 degree belt conveyor transfer chute. The surface recommended for full scale, above-ground testing resembles a portion of a 90 degree smoke pipe elbow, corresponding to a jointed approximation of a basic torus geometry. For the 36 inch wide belt, 450 fpm, feed conveyor case, the torus has a 36-inch major radius and an 18 inch minor radius. Work performed under this study includes 1) technology surveys of transfer point design, bulk flow theory, and underground coal mine operations; 2) math modeling and associated computer programming of free fall, impact, and frictional flow dynamics; 3) evolution and evaluation of several candidate chute geometries; 4) construction and laboratory testing of one-sixth scale models; and 5) preliminary design of the recommended chute.				
17. Document Analysis a. Descriptors Belt Conveyors Coal Mining Bulk Handling Coal Mines Chutes Mine Haulage Coal Dust b. Identifiers/Open-Ended Terms Transfer Point Design Pseudo Plastic Flow Torus Smoke Pipe Torus c. COSATI Field/Group Earth Sciences and Oceanography/Mining Engineering				
18. Availability Statement Release Unlimited		19. Security Class (This Report) Unclassified		21. No. of Pages 414
		20. Security Class (This Page) Unclassified		22. Price

TABLE OF CONTENTS

<u>Section</u>	<u>Title</u>	<u>Page</u>
1.0	REPORT DOCUMENTATION PAGE	
2.0	EXECUTIVE SUMMARY	9
3.0	PRELIMINARY DESIGN	15
3.1	Structural Description	15
3.1.1	General	15
3.1.2	Design Details	24
3.1.2.1	Surface Plate Segment	24
3.1.2.2	Plate Segment Support Structure	29
3.1.2.3	Base Support Structure	30
3.2	Chute Positional Adjustment Procedures	32
3.2.1	Rotational Adjustment	32
3.2.1.1	Roll Adjustment	33
3.2.1.2	Pitch Adjustment	34
3.2.1.3	Yaw Adjustment	34
3.2.2	Translational Adjustment	34
3.2.2.1	X-Adjustment	35
3.2.2.2	Y-Adjustment	35
3.2.2.3	Z-Adjustment	35
3.3	Nominal Pitch and Yaw Adjust	35
3.4	Transfer Point Installation Clearances	36
4.0	DATA SOURCES	39
4.1	Consultant Support	39
4.2	State of the Art Surveys	40
4.2.1	Mine Site Survey	40
4.2.1.1	Mines Visited	40
4.2.1.2	General Techniques of Right Angle Transfer	40
4.2.1.3	Chute Configurations Observed	41
4.2.1.4	Performance Characterization	41
4.2.1.5	Flow Materials Characterization	43
4.2.1.6	Chute Frictional Slope Analysis	44
4.2.1.7	Construction Details	44
4.2.1.8	Mine Interfaces	45
4.2.1.9	Conveyor Data	46
4.2.1.10	Transfer Part Operations	46
4.2.1.11	Ancillary Equipment	46
4.2.1.12	Other Data from Mine Site Surveys	47
4.2.2	Other Surveys	47
4.2.2.1	Program Bibliography	47
4.2.2.2	Materials Properties	48
4.3	Chute Development Guidelines	48

TABLE OF CONTENTS (Cont'd)

<u>Section</u>	<u>Title</u>	<u>Page</u>
5.0	DYNAMIC THEORY AND MATH MODELING	59
5.1	Phase 1. Free Fall Trajectory and Impact	59
5.1.1	General Definition	59
5.1.2	Math Model of Free Fall Phase	60
5.1.3	Computer Program for Free Fall Phase	62
5.2	Frictional Flow Phase	65
5.2.1	General	65
5.2.2	Math Model	65
5.2.3	Frictional Flow Computer Program	67
5.2.3.1	Phase 1 Interface	67
5.2.3.2	Program Sequence	68
6.0	CHUTE DESIGN CONCEPTS AND MATH MODELS	73
6.1	Conceptual Design and Evaluation	73
6.2	Chute Math Model	81
7.0	DYNAMIC ANALYSIS RESULTS	85
7.1	Free Fall/Impact Phase	85
7.2	Frictional Flow Phase	88
8.0	LABORATORY CHUTE SCALE MODELS AND TEST EQUIPMENT	89
8.1	Scale Model Considerations	89
8.1.1	Dimensional Analysis	89
8.1.2	Laboratory Test Scale Size	92
8.2	Laboratory Test Equipment	92
8.2.1	Test Conveyors	92
8.2.2	Flow Feed Provisions	94
8.3	Chute Scale Models	94
8.3.1	Conceptual Scale Model Phase	94
8.3.1.1	Conical Models	97
8.3.1.2	Cylindrical Models	97
8.3.1.3	Toroidal Models	97
8.3.2	Additional Torus Configuration Scale Models	105
9.0	LABORATORY TESTING	113
9.1	Flow Materials Utilized	113
9.2	Initial Lab Testing of Development Concepts	115
9.2.1	Cone Model Tests	115
9.2.2	Cylinder Model Tests	121
9.2.3	Initial Torus Configuration	121
9.3	Revised Torus Model Tests	136

TABLE OF CONTENTS (Cont'd)

Volume II	Appendices	
A	Bibliography Accessed in Technology Survey for Low Headroom Transfer Chute Program	A-1
B	Math Model for Phase I Dynamics - Free Fall and Impact Dynamics Phase	B-1
C	Phase I Dynamics Computer Program - Free Fall and Impact Dynamics Phase	C-1
D	Math Model for Phase II Dynamics - Frictional Flow Phase	D-1
E	Phase 2 Dynamics Computer Program - Frictional Flow Dynamics Phase	E-1
F	Trajectory Study of Candidate Transfer Chute Concepts	F-1
G	Torus Chute Math Model	G-1
H	Computer Analytical Results	H-1

LIST OF FIGURES

<u>Figure</u>	<u>Title</u>	<u>Page</u>
3-1a	Chute Installation Layout Front View	16
3-1b	Chute Installation Layout - Side View	17
3-1c	Chute Installation Layout - Top View	18
3-2a	Chute Assembly	19
3-2b	Chute Assembly Continued	20
3-3a	Ring Support Structure Weldment - Forward Portion	21
3-3b	Ring Support Structure Weldment - Forward Portion (contd)	22
3-3c	Ring Support Structure Weldment - Aft Extension	23
3-4	Plate Segment - Typical	25
3-5	Flat Pattern Layout for Chute Segments	26
4-1a	Flow Properties of Raw Coal, Site J, 12 Percent Moisture Content	50
4-1b	Wall Yield Loci of Raw Coal, Site J, 12 Percent Moisture Content	51
4-2	Typical Average Size Distribution of Raw Bituminous Coal	52
5-1	Coordinate Axes, Translational and Rotational Sign Convention	63
5-2	Basic Flow Diagram, Phase I (Free Fall/Impact) Computer Program	64
6-1	Cone, Opening Half Angle Concept	74
6-2	Cone Concept With Flat Impact Plate	75
6-3	Zero Half Angle Cone Concept	76
6-4	Cylinder Concept, Single Surface	77
6-5	Cylinder Concept, Compound Surface	78
6-6	True Torus Concept	79
6-7	Smoke Pipe Torus Concept	80
6-8	Computer Plate and Rotation Definition	83
8-1	Free Fall Trajectory Parameters	90
8-2	Six Inch and Eight Inch Test Conveyors	93
8-3	Transfer Point Test Setup	95
8-3a	Hopper Lift	96
8-4	15° Cone Scale Model	96
8-5	Cone Baseplate	98
8-6	Lower Quadrant, Cone Model	99
8-7	Upper Quadrant, Cone Model	100
8-8	Cone Model with Flat Impact Plate	101
8-9	Zero Opening Angle Cone	102
8-10	Quarter Cylinder Model, Single Surface	103
8-11	Compound Quarter Cylinder Model	104
8-12	Torus Model I, 6" Dia	106
8-13	Torus II Model	107
8-14	Smoke Pipe Torus Models	108-10
8-15a	Torus III Model	111
8-15b	Torus III Model	112
8-15c	Torus III Installation	112
8-16	Torus I Installation	112

LIST OF FIGURES (Cont'd)

<u>Figure</u>	<u>Title</u>	<u>Page</u>	<u>Figure</u>	<u>Title</u>	<u>Page</u>
9-1	Run of Mine Coal Samples	114	9-47	Run 125	134
9-2	Correlation between Theoretical and Test Trajectory Shapes	116	9-48	Run 126	134
9-3	Run 201	118	9-49	Run 131	134
9-4	Run 201A	118	9-50	Run 131	134
9-5	Run 202	118	9-51	Run 51	138
9-6	Run 204	118	9-52	Run 52	138
9-7	Run 205	119	9-53	Run 62	138
9-8	Run 205		9-54	Run 62	138
9-9	Run 206		9-55	Run 63	139
9-10	Run 151	119	9-56	Run 65	139
9-11	Run 152	120	9-57	Run 65	139
9-12	Run 1	120	9-58	Run 68	139
9-13	Run 3	120	9-59	Run 67	140
9-14	Run 4	120	9-60	Run 71	140
9-15	Run 5	126	9-61	Run 72	140
9-16	Run 6	126	9-62	Run 81	140
9-17	Run 7	126	9-63	Run 82	141
9-18	Run 8	126	9-64	Run 83	141
9-19	Run 9	127	9-65	Run 461	141
9-20	Run 10	127	9-66	Run 462	141
9-21	Run 11	127	9-67	Run 481	144
9-22	Run 12	127	9-68	Run 483	144
9-23	Run 13	128	9-69	Run 484	144
9-24	Run 22	128			
9-25	Run 25	128			
9-26	Run 26	128			
9-27	Run 100	129			
9-28	Run 102	129			
9-29	Run 103	129			
9-30	Run 104	129			
9-31	Run 105	130			
9-32	Run 106	130			
9-33	Run 107	130			
9-34	Run 111	130			
9-35	Run 112	131			
9-36	Run 114	131			
9-37	Run 115	131			
9-38	Run 116	131			
9-39	Run 117	132			
9-40	Run 119	132			
9-41	Run 120	132			
9-42	Run 121	132			
9-43	Run 121	133			
9-44	Run 122	133			
9-45	Run 123	133			
9-46	Run 124	133			

LIST OF TABLES

<u>Table</u>	<u>Title</u>	<u>Page</u>
3-1	Chute Locational Parameters	36
3-2	Transfer Point Installation Clearances	37
4-1	Applicable Coal Properties from Test Data	49
4-2	Low Headroom Chute Development Guidelines	53
8-1	Belt Speed Variation Provision in Scale Model Conveyors	94
9-1	Sand Mixtures Used in Scale Model Testing	113
9-2	Scale Model Test Results for Cone Chute Configurations	117
9-3	Scale Model Test Results for Cylindrical Chute Con- figurations	122-123
9-4	Scale Model Test Results for Initial Torus Chute Con- figurations	124-125
9-5	Scale Model Test Results for Second Group of Torus Chute Configurations	137
9-6	Scale Model Test Results for Torus III Chute Configura- tions	143



2.0 EXECUTIVE SUMMARY

2.1 INTRODUCTION

This report summarizes the results of a study program to evolve a preliminary design for a 90-degree transfer chute for belt conveyors in underground coal mines. This preliminary design is intended to provide a conceptual baseline for detailed design, fabrication, and testing---both above ground and in a coal mine---of a full size, 90-degree transfer chute between a 36-inch wide, input belt conveyor and a 42-inch wide, receiving belt conveyor.

2.2 PROJECT SUMMARY

Consistent with the above objective of this program, this study has addressed candidate chute configurations from the standpoint of flow characteristics that will minimize coal spillage, dust generation, and belt wear. In order to achieve this, the work performed in this study has included the following:

- 1) Technology surveys of transfer point design, bulk flow theory, and underground coal mine operations, the last including visits to several mines.
- 2) Math modeling and associated computer programming of dynamics covering both free fall and impact, as well as frictional flow.
- 3) Evaluation of several candidate chute geometries, including mathematical formulation of the most promising ones for analysis.
- 4) Construction and laboratory testing of one-sixth scale models of preliminary chute concepts.
- 5) Preliminary design of the recommended chute configuration, including installation interfaces.

FSEC's work in evolution, analysis, and testing of chute surfaces was initiated by an extensive bibliography study into pertinent subject areas related to underground belt conveyor transfer points and was further augmented by specific consultant support in transfer point technology, bulk flow theory, and mine operations. In this last-mentioned area, FSEC inspected transfer points in a total of eight underground mines. This overall survey phase of the study program is covered in Section 4.0.

Math modelling effort during the program involved mathematical definition and associated computer programming in two basic areas: 1) dynamic flow; and 2) mathematical definition of specific chute geometry to support the flow study.

Two distinct dynamic phases were modelled, namely, those of free fall and frictional flow. Provision was made in these models for introduction of three principal groups of parameters: 1) conveyor interface characteristics; 2) material characteristics; and 3) the chute itself. Definition of the dynamic phases of the modelling is covered in section 5.0 while the chute configuration model is developed in section 6.0, following evolution and screening of candidate chute surface concepts.

The free fall portion of the dynamic model was uniformly successful in providing locations and angles of impact of the initial trajectory. The frictional flow portion of the model, however, involved a considerable period of shakedown and debugging that was not entirely resolved in this program. The problems were ultimately related to mathematical convergence problems in the incrementally defined velocities and shapes of the several stream flow elements, into which the mass cross section was divided to establish the effects of deformation. As a result of this, modifications of the math model were dictated until the end of the program, and the results in the area of frictional flow are limited to a few dynamic parameters.

In the math model of the torus, a broad flexibility is provided for parametric variation both of details of the surface configuration and of rotational and translational definition relative to the feed conveyor pulley.

The results of the flow analysis utilizing the above math models, covered in Section 7.0, includes development of design definition data utilized in Section 3.0. derived from dynamic trajectories generated during the free fall and functional phases.

The basic toroidal surface configuration was selected from a number of candidate surface geometries evaluated during preliminary analysis and testing. The details of this conceptual development phase, other configurations evaluated, and the tradeoffs involved are discussed in Section 6.0. The torus geometry was not the simplest type of those considered, and extensive consideration was given to the question of producibility, as ultimately reflected in Section 3.0. It was, however, evident from the tradeoffs involved that the potential performance of the torus offered the best opportunity for advancing the state of the art in transfer point design, particularly from the standpoint of minimized turbulence, scatter, and --- thereby --- dust evolution.

Construction of one-sixth (1/6) size scale models for laboratory testing involved about seven preliminary candidate designs, which were included in the conceptual evolution and tradeoff analysis discussed above. These configurations, which included basic conical and cylindrical geometries, as well as several iterations of the torus shape, are described and shown in Section 8.0.

Laboratory testing of the scale models provided ultimate insight into several critical phases of flow characteristics. The most important of these were 1) the behavior of flow at impact, 2) the tendency toward convergence/divergence during the frictional phase; and 3) the output direction of the flow trajectory relative to the receiving conveyor. In the first-mentioned area, several trial positions and attitudes for many chute model configurations were dictated to achieve impact flow that did not 1) fork or divide, as a result of variable angle of impact at different areas in the impact zone; and 2) interfere with the subsequent frictional flow. Extensive photographic coverage was provided of this work, which is summarized in Section 9.0.

Analysis and testing conducted in this study program indicates that a double curvature-type surface will most nearly achieve the performance objectives for the 90 degree belt conveyor transfer chute. The surface specifically recommended for full-scale, above-ground testing approximates the outer portion of a 90 degree smoke pipe elbow. This elbow is itself a jointed approximation of a basic torus geometry, which for the 36 inch wide belt, feed conveyor case, has a 36-inch major radius and an 18 inch minor radius. The chute configuration specified herein for a nominal feed conveyor input velocity of 450 fpm is shown in Figures 3-2a and 2b, while the overall transfer point layout is shown in Figures 3-1a, -1b, and 1-c.

The basic conceptual approach taken in this preliminary design is fourfold:

1. Establish the location of initial contact of the free fall trajectory with the chute as close as possible to the feed conveyor to initiate the 90 degree turn of the material early and minimize the headroom utilized for the turn. This location can be varied at installation along three axes of translational adjustment.
2. Orient the initial contact surface approximately tangential to the free fall trajectory vector to minimize turbulence and scatter originating at impact. This is achieved both by the surface shape as well as provisions for three degrees of rotational adjustment for the chute at installation.
3. Provide a vertical curve frictional trajectory in the direction of the receiving conveyor to achieve the most efficient geometry from a headroom standpoint, to maintain and/or accelerate flow. This vertical curve is parallel to the major radius of the torus geometry.
4. Provide converging curvature crosswise to the above vertical curve in order to contain random movement and spillage as well as to direct and center the flow mass relative to the receiving conveyor. This convergence curvature corresponds to the minor radius of the torus.

The smoke pipe approximation of the torus geometry was chosen in order to achieve both producibility, as well as maintainability of worn portions of the chute surface. The surface is built up of single-radius-of-curvature, or cylindrical, segments. These segments can be either cut from a flat pattern and formed individually or else cut from a common piece of rolled stock. The design provides for assembly and replacement of the segments as individual pieces by means of bolted attachment. Details of fabrication and assembly are provided in Section 3.0.

The base support structure defined for the chute provides for floor mounting and is primarily related to requirements of above ground testing. While this configuration is applicable to a below-ground installation, the particular requirements of mines vary, involving in some cases either or both vertical or lateral support from the feed conveyor boom structure or else from the floor roof, via roof bolts. In this context the chute base support structure will require review during planning for below-ground testing, as well as during production design.



3.0 PRELIMINARY DESIGN

This section describes the preliminary design of a transfer point chute which has evolved from the studies performed in this program. It addresses alternate configurations for different feed conveyor input velocities. The basic chute surface approximates a portion of a torus. It is constructed of a series of jointed cylindrical surfaces and resembles therefore a cutout from a "smokepipe" 90 degree elbow.

3.1 STRUCTURAL DESCRIPTION

3.1.1 General

The overall transfer point configuration is shown in Figures 3-1a, -1b, and -1c, which include side, end, and top views, relative to the two interfacing conveyors. The basic dimensional parameters cited are the following:

- Input Belt Width - 36"
- Receiving Belt Width - 42"
- Input Belt Velocity - 450 FPM (For the particular chute position shown)

The two principal structural elements in the design are the following:

1. The Chute Assembly (Figures 3-2a and 3-2b)
2. The Base Support Structure (Figures 3-1a, -1b, and 1c)

The Chute Assembly consists of a series of cylindrically curved plate segments mounted in a multiple-ring, plate segment support structure weldment. (Figures 3-3a and 3-3b.) The inside radius of curvature of each plate segment is 18 inches, while the orthogonal, or major, radius approximated by the series of plates is 54 inches.

This ring support structure weldment, which in part resembles a boat hull skeleton, (Figure 3-3b), includes a wheelbarrow handle-like extension (Figure 3-3c, that pivotally attaches the aft end of the entire Chute Assembly to the Base Support Structure. The opposite end is also supported by the Base Support Structure, suspended by a wire rope-type loop. This permits the Chute Assembly to move up around the aft-located pivot, relative to the receiving conveyor direction, when large run of mine coal lumps arrive from an upstream feed point.

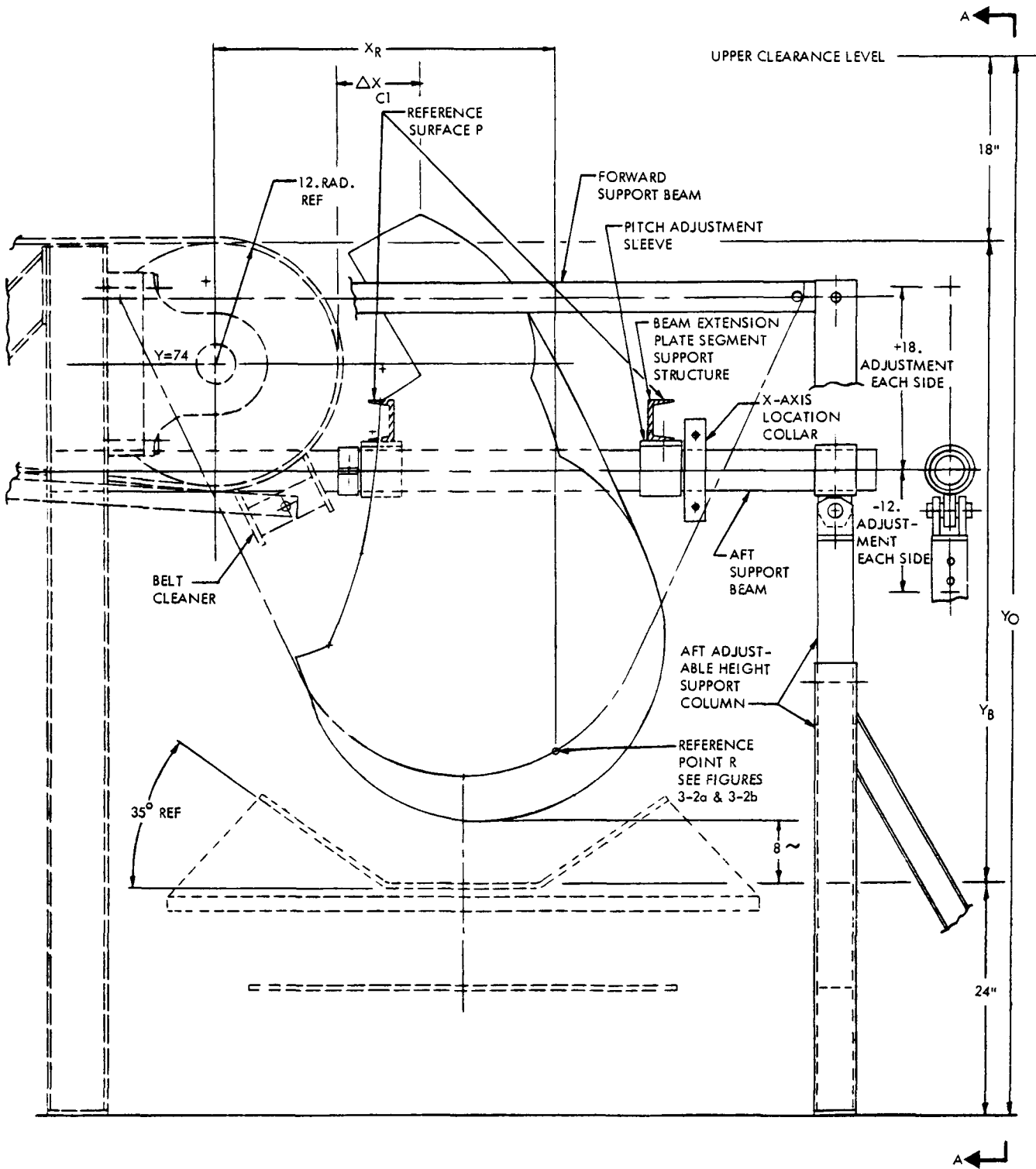
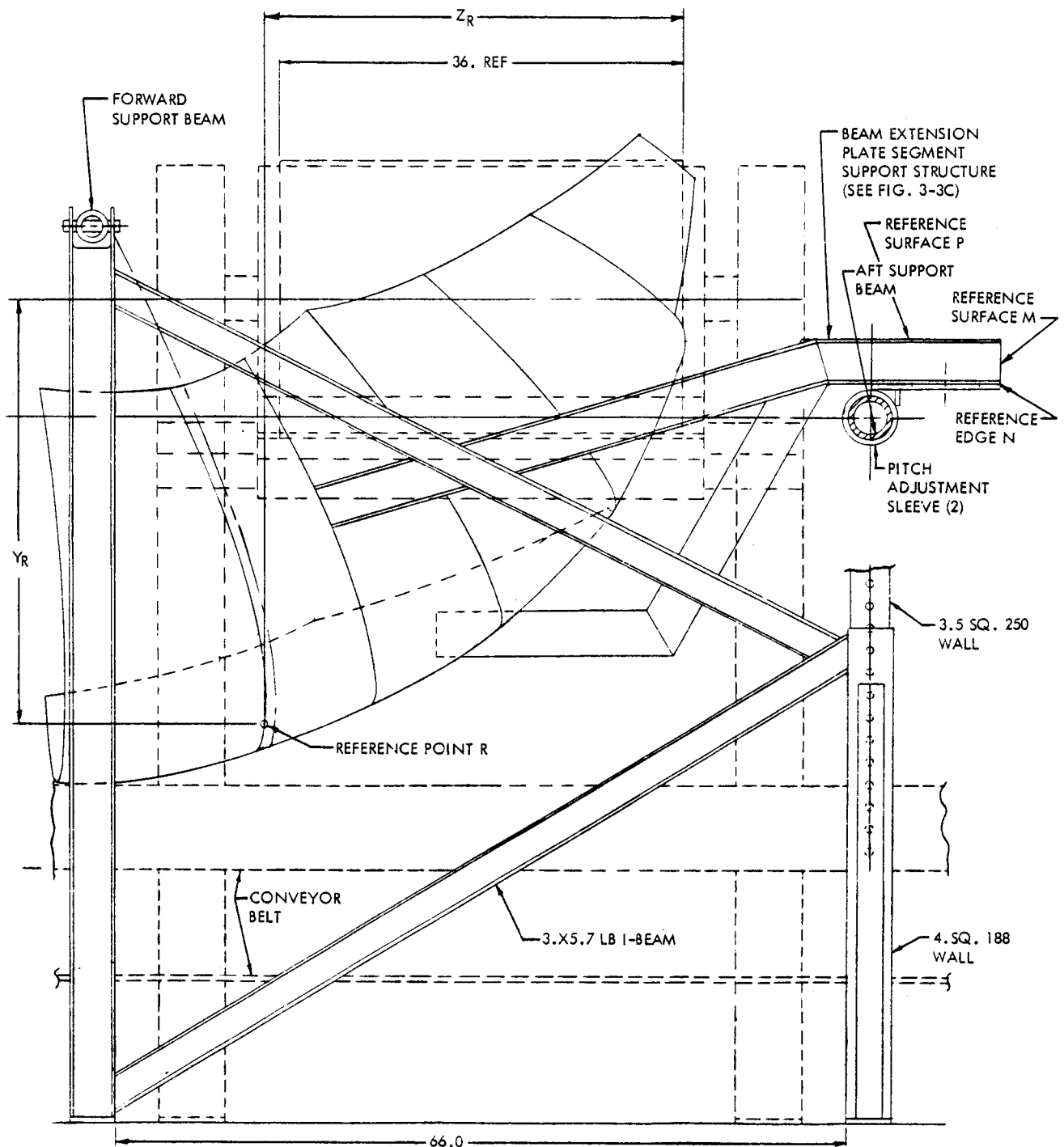


Figure 3-1.a. Chute Installation Layout-Front View
 (Looking Parallel to Down Stream Conveyor)



VIEW SHOWING CHUTE INSTALLED IN
 NORMAL DESIGN POSITION WITH
 ROLL = 30°, PITCH = 15°, AND YAW = 5°

Figure 3-1b. Chute Installation Layout - Side View,
 Looking Parallel to Upstream Conveyor
 (View A-A in Figure 3-1a)

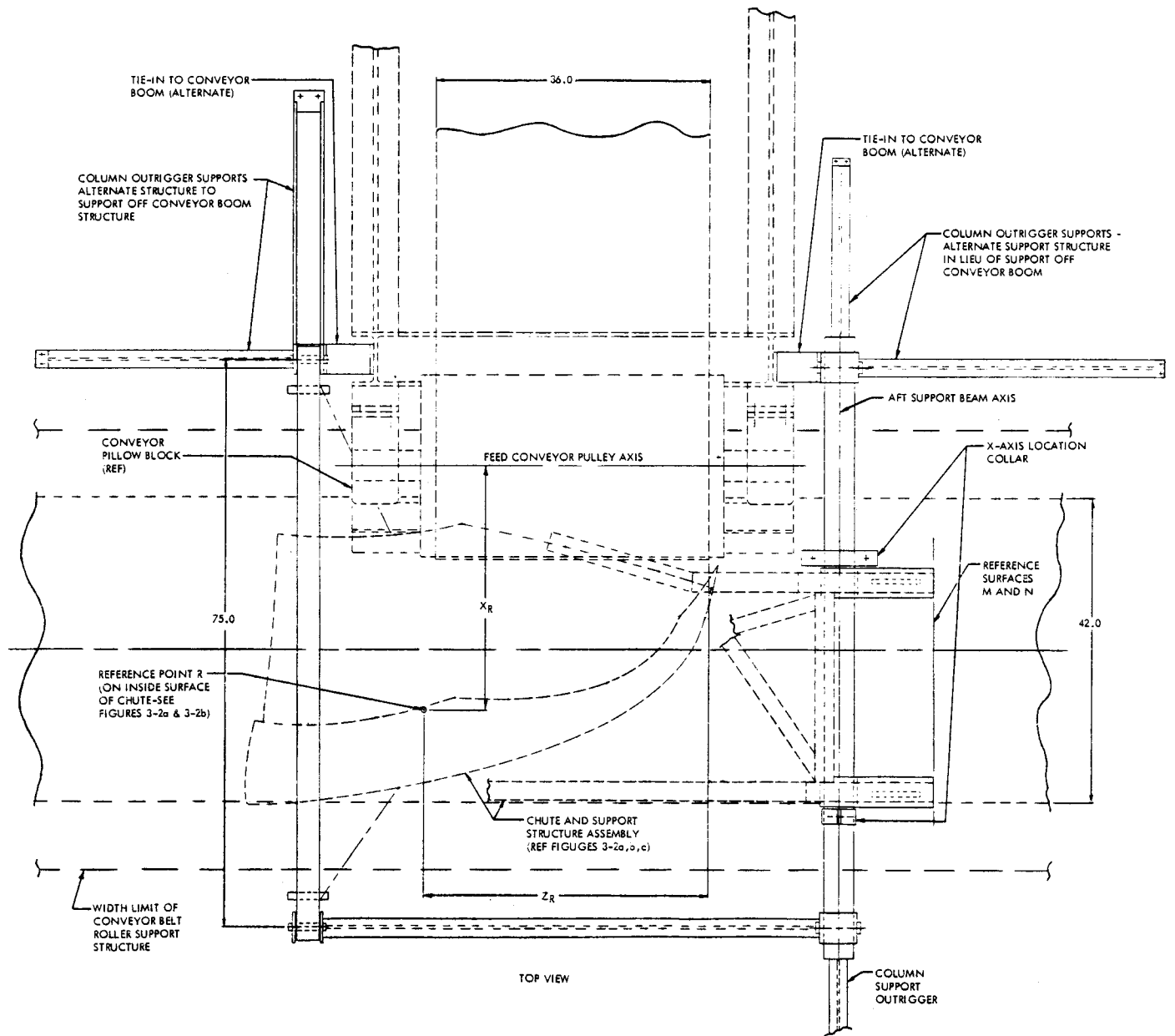
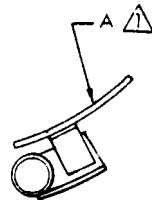


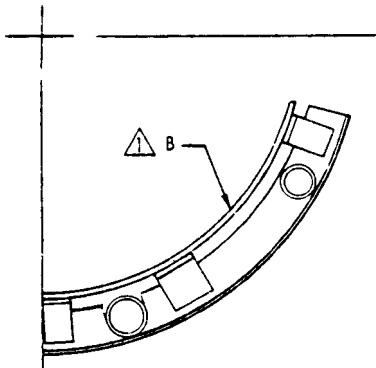
Figure 3-1c. Chute Installation Layout - - Top View

NOTES:

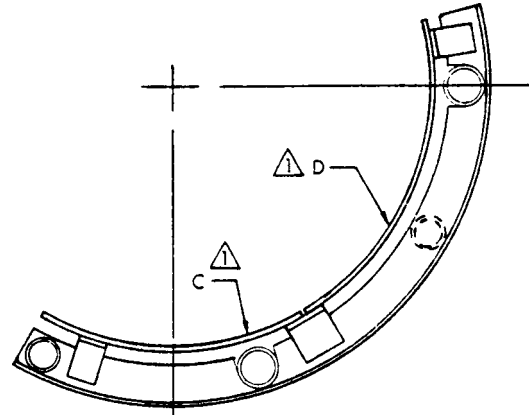
- ⚠ SEE FIGURE 3-5 FOR PLATE LETTER DESIGNATIONS.
- ⚠ SEE FIGURE 3-2a FOR SECTIONS A, B, & C.



SECT F-F (ROTATED 73-30° INTO PLANE)



SECT E-E (ROTATED 60° INTO PLANE)



SECT D-D (ROTATED 45° INTO PLANE)

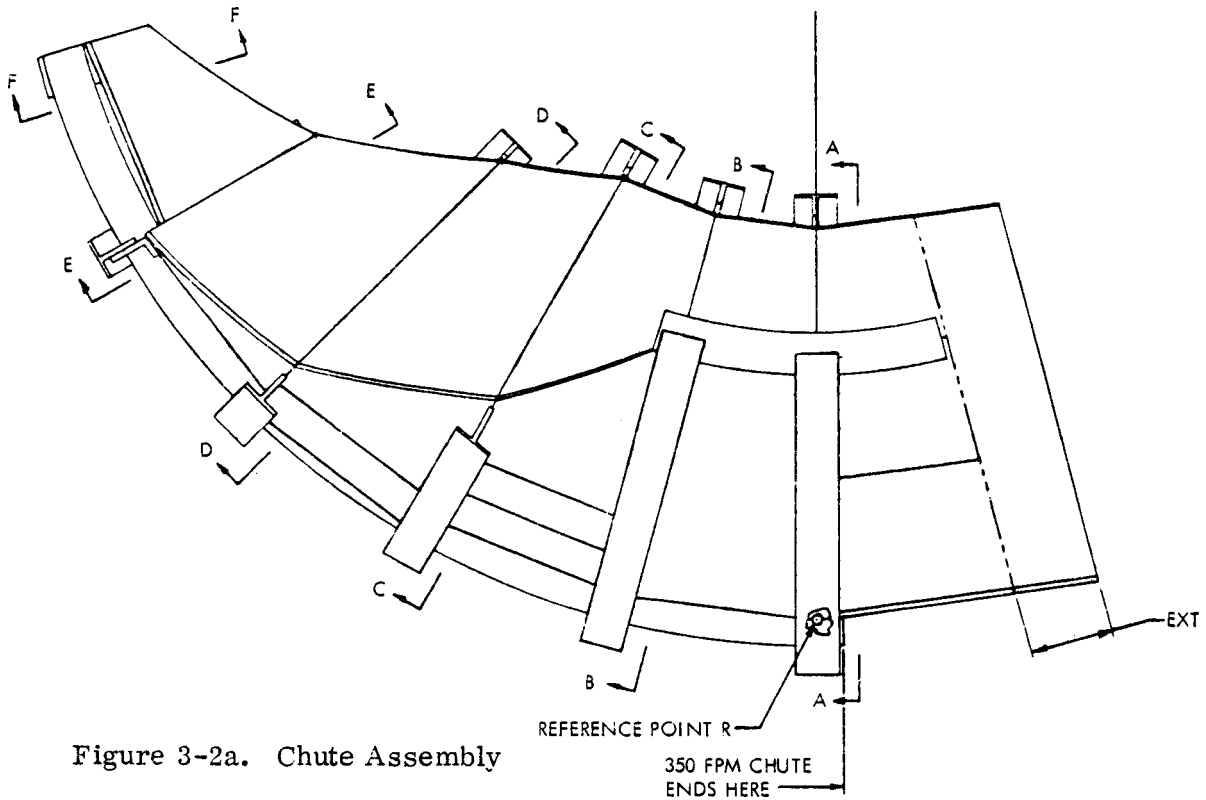


Figure 3-2a. Chute Assembly

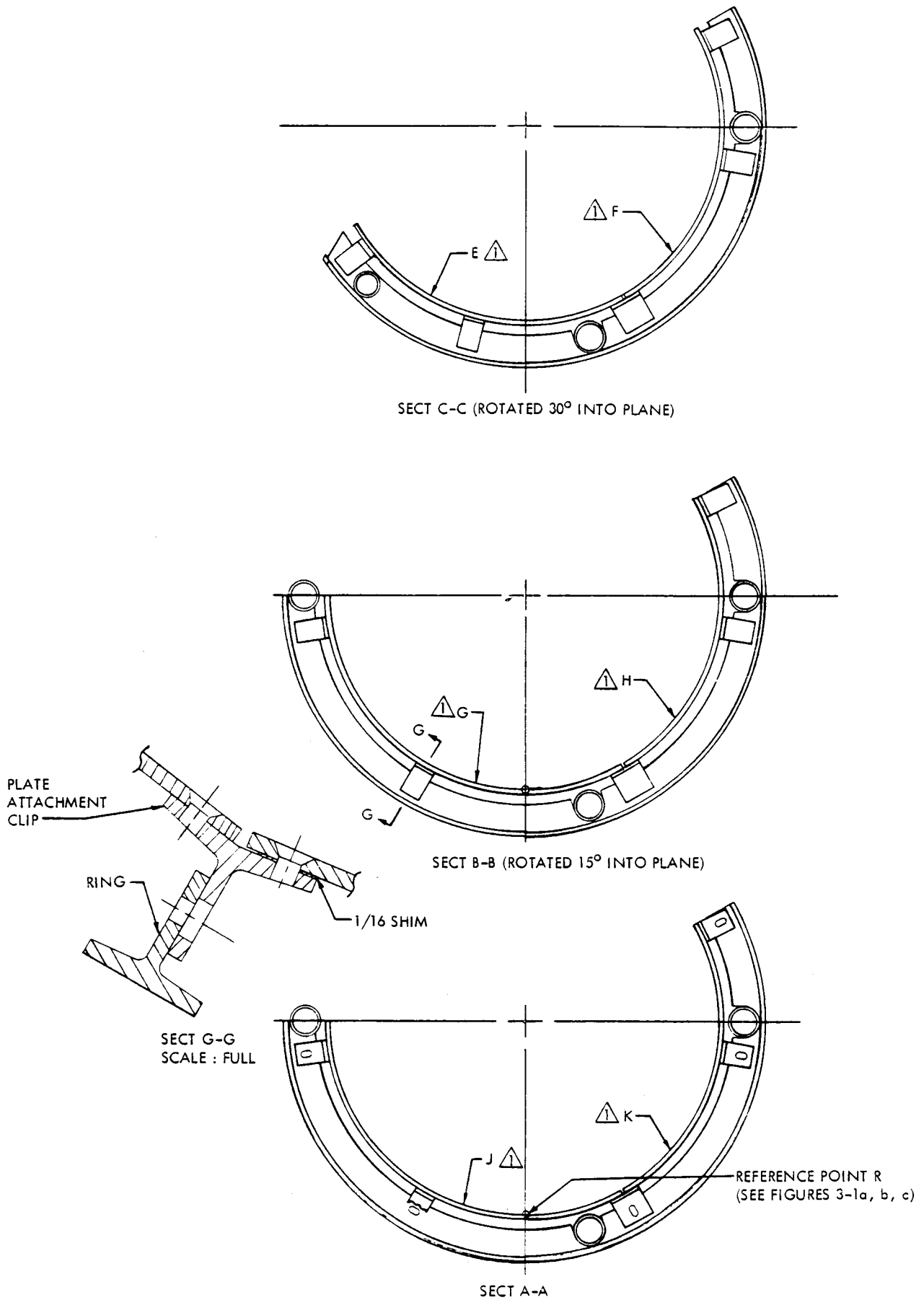


Figure 3-2b. Chute Assembly - Continued (Additional Sections)

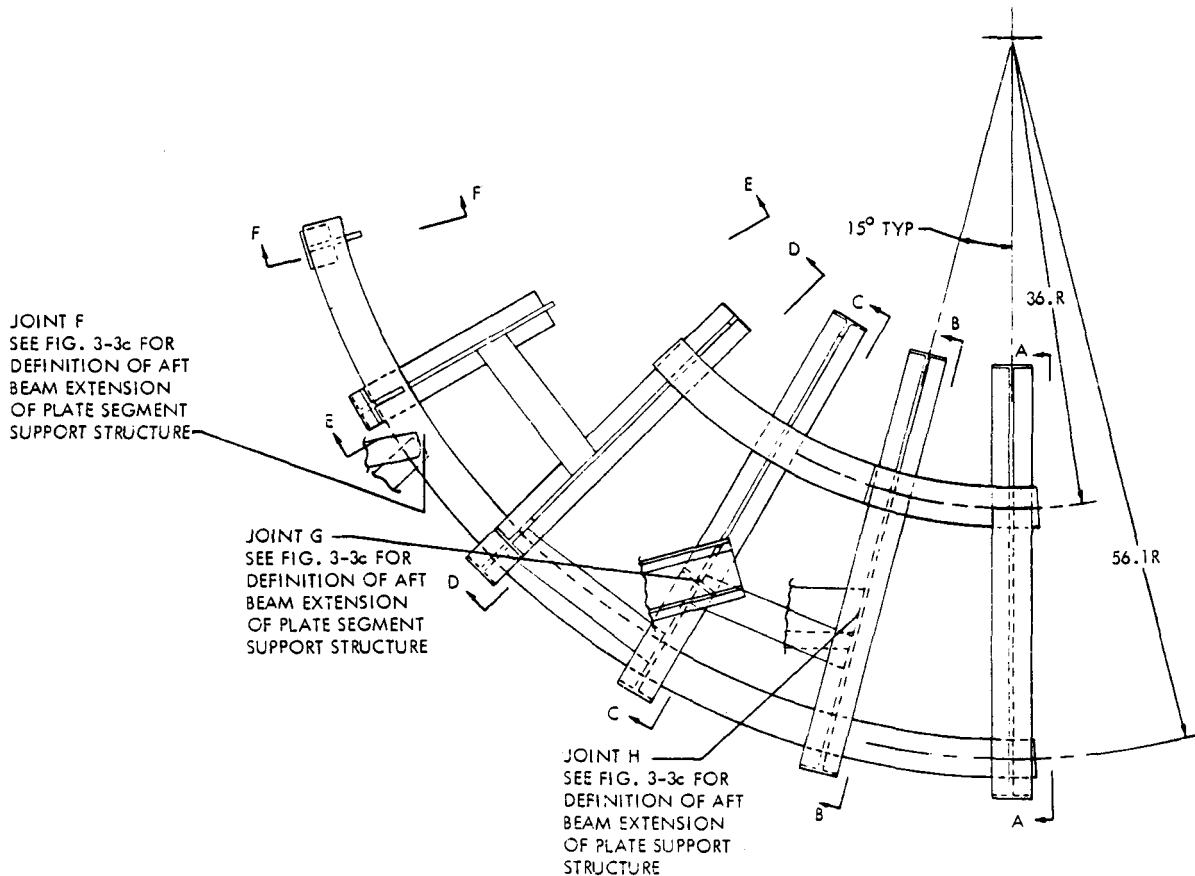
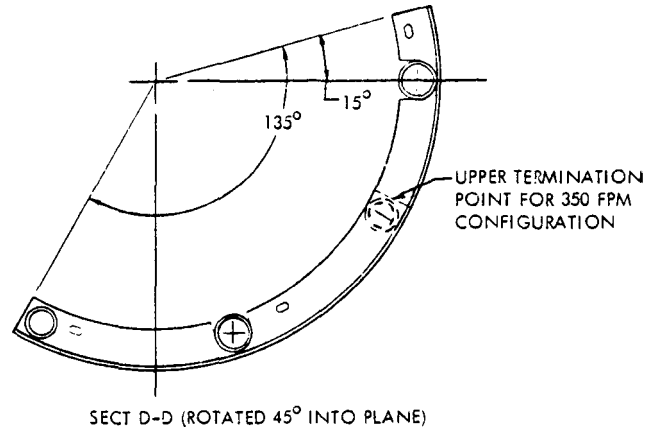
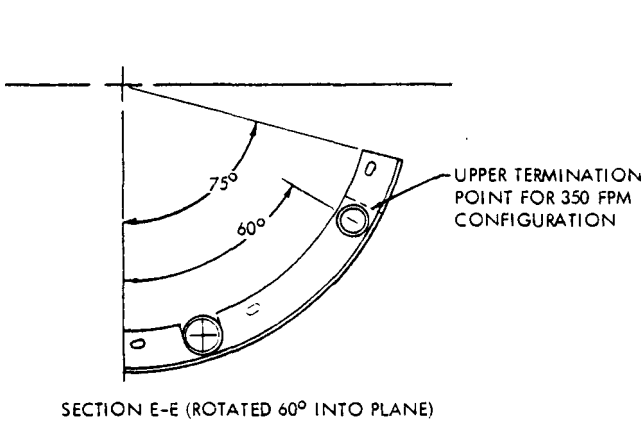
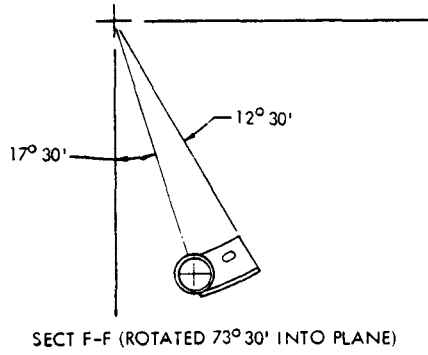
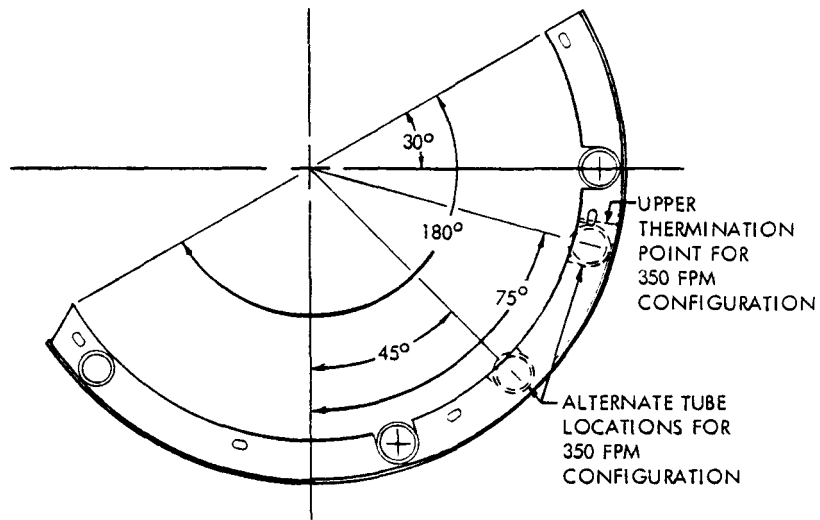
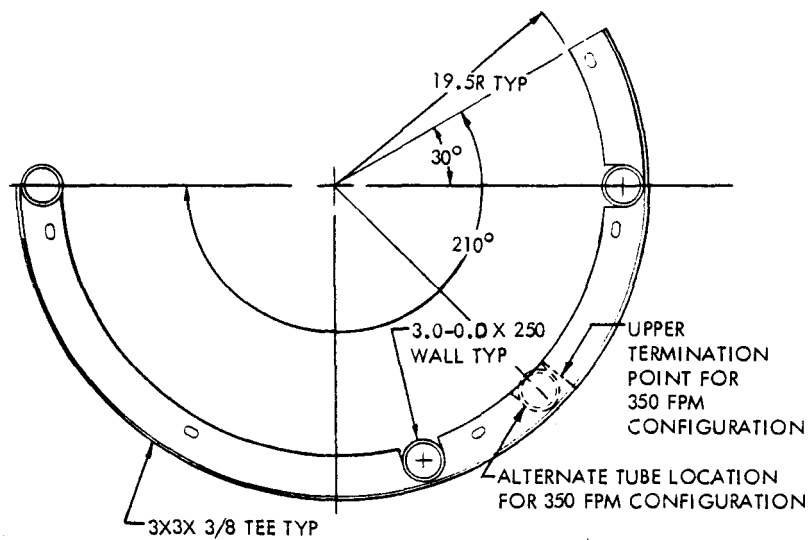


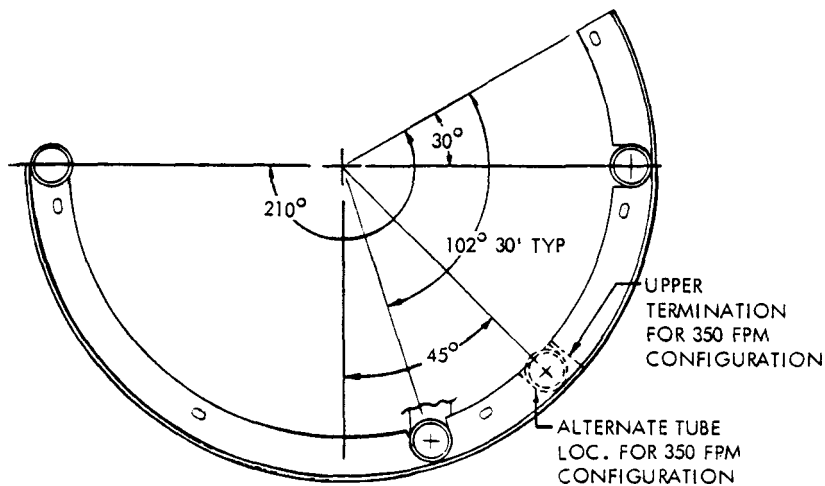
Figure 3-3a. Ring Support Structure Weldment - Forward Portion



SECT C-C (ROTATED 30° INTO PLANE)

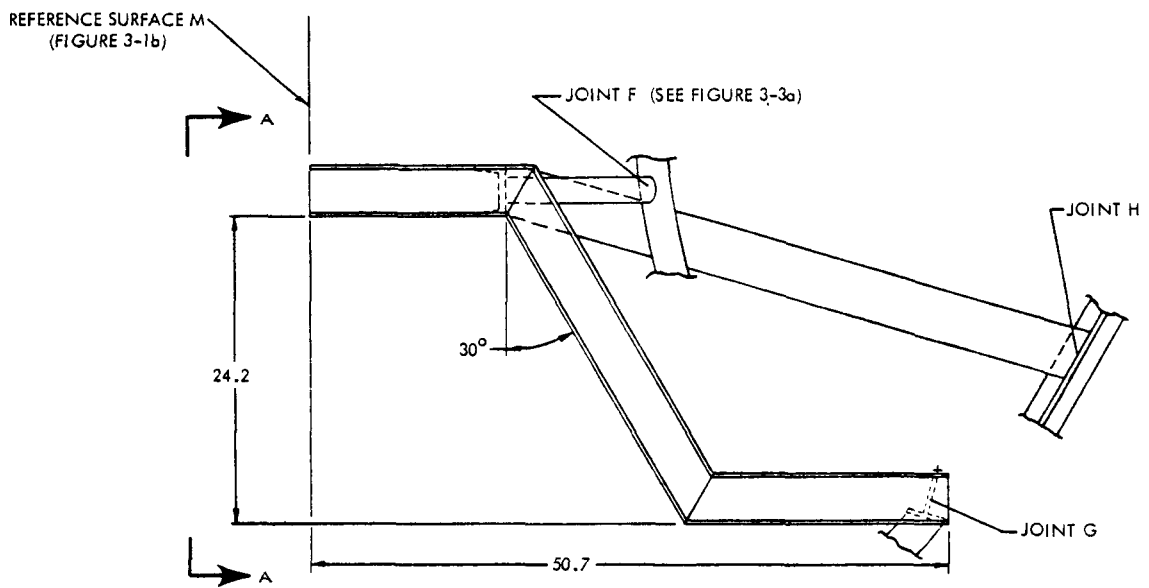
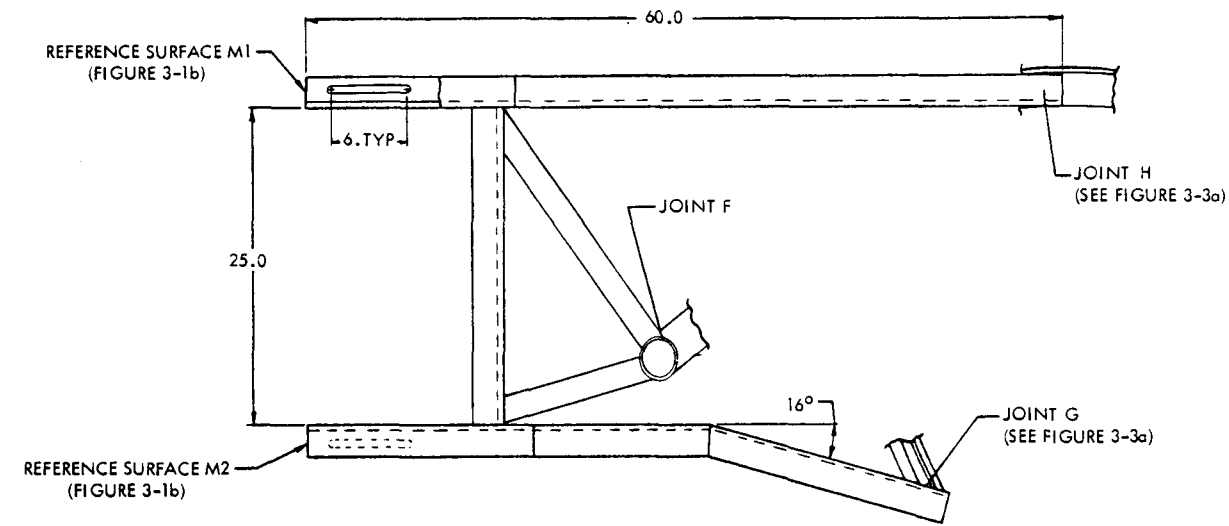


SECT B-B (ROTATED 15° INTO PLANE)



VIEW A-A (PARTIAL)

Figure 3-3b. Ring Support Structure Weldment, Forward Portion
(Additional Sections Taken in Figure 3-3a)



NOTE:
 AFT BEAM EXTENSION PORTION OF
 PLATE SEGMENT SUPPORT STRUCTURE
 SHOWN WITH CHUTE ATTITUDE OF
 30° ROLL, 15° PITCH, AND 5° YAW

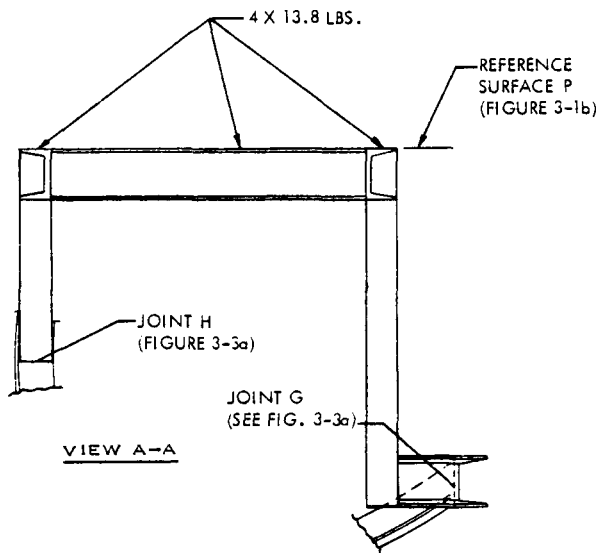


Figure 3-3c. Ring Support Structure - AFT Extension Structure

3.1.2 Design Details

3.1.2.1 Surface Plate Segment

3.1.2.1.1 Basic Configuration

Figure 3-4 shows a typical curved plate element of which the frictional flow surface of the Chute Assembly is constructed. Defined here as a basic flat pattern as well as a curved section, the surface segments are machine-torch cut from 3/8 inch steel plate. Tolerances of $\pm 1/16$ inch, which are achievable by this cutting method, will be adequate for matching of the plates at assembly into a continuous flow surface.

Definition of an entire chute surface, in terms of the initial flat patterns for all plate segments required, is provided in Figure 3-5. The solid, phantom, and dashed outlines correspond to the dynamic conditions involved for input conveyor velocities of 450, 600, and 350 feet per minute, respectively. The patterns shown are for the plate neutral planes, but can be readily extrapolated in the direction of curvature to outside surface dimensions. This alternative is mentioned in connection with a proposed spares philosophy wherein basic stock is obtained with the 18 inch curvature for local mine inventory, and then cut to specific flat pattern shapes when worn pieces are to be replaced. The plate width dimensions are 1/4 inch less than the nominal corresponding to a edge-to-edge-fit.

In the flat patterns defined, the upper edge of the plates on the outboard side have a minimum " ΔXC " clearance with the extreme end of the conveyor pulley, corresponding to the specific numbered points in the respective flat pattern (Figure 3-6). The important feature of these clearances is that they increase along the directions of the 90 degree turn and that of the receiving conveyor. These clearances are specified in Section 3.4.

The chute segments, when rolled up, correspond approximately to 15° sections in a 90 degree smoke pipe elbow. In the case of the 450 and 600 FPM configurations the lower most sections (from flat patterns J and K) include a tangential extension beyond the 15 degree central angle, required to center the flow prior to discharge. The tangential extension distance EXT, will involve some final sizing during above ground tests as a function of the coefficient of friction, but six inches is judged to be a good nominal starting value.

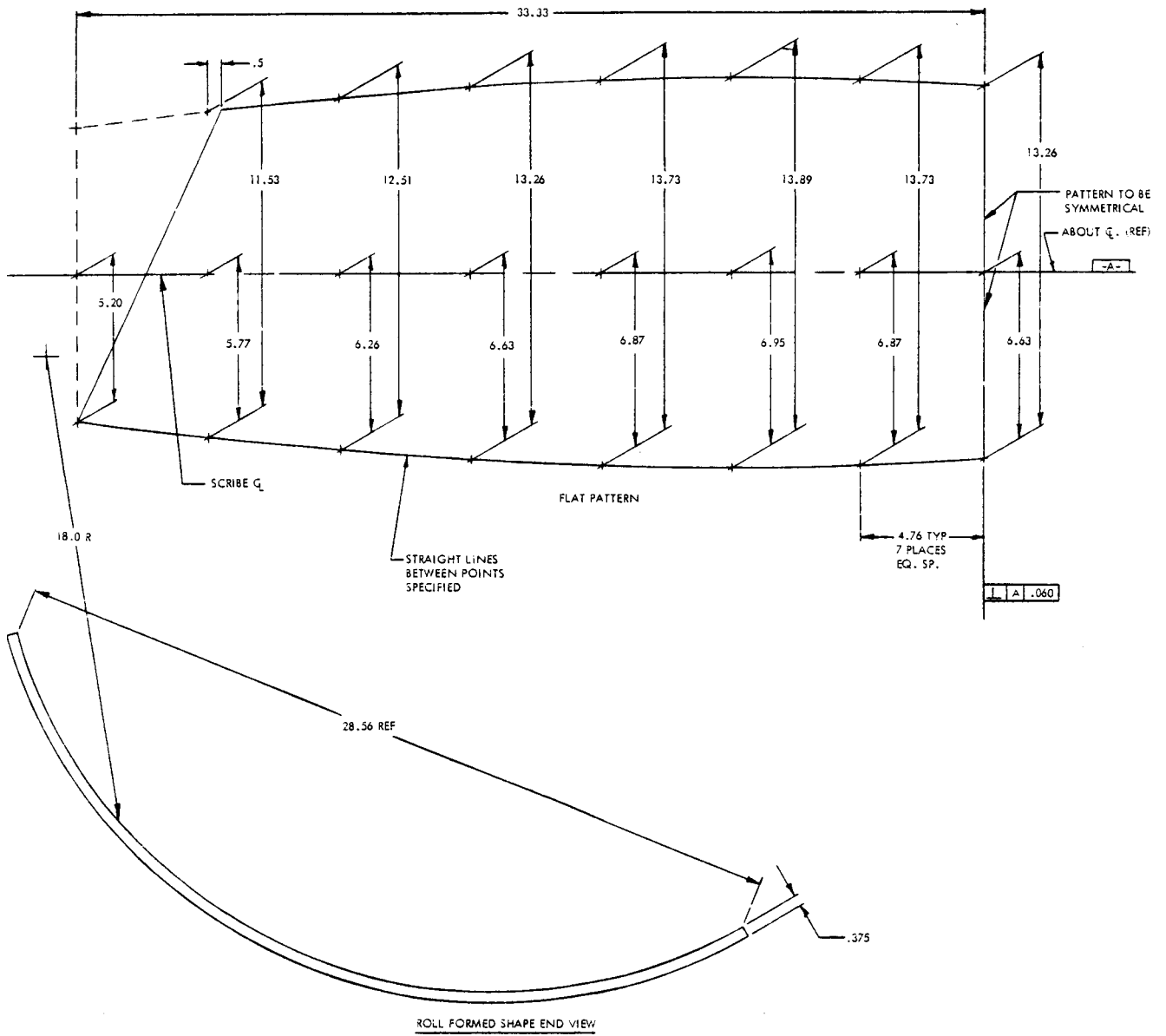


Figure 3-4. Plate Segment, Typical

NOTES:

- ▲ SOLID PLATE OUTLINE DEFINES FLAT PATTERN FOR 450 FPM CONFIGURATION.
- ▲ PHANTOM LINE ----- DEFINES DEPARTURES FROM 450 FPM CONFIGURATION FOR 600 FPM CONFIGURATION.
- ▲ DASHED LINE ----- OUTLINE DEFINES DEPARTURES FROM 450 FPM CONFIGURATION FOR 350 FPM CONFIGURATION. PLATES J AND K ARE NOT USED IN 350 FPM CONFIGURATION.
- ▲ FOR THE 600 FPM CONFIGURATION EXT = 12 INCHES AND FOR THE 450 FPM CONFIGURATION, EXT = 6 IN.
- ▲ NOMINAL CLEARANCE BETWEEN PLATES = 1/4 INCH.
- ▲ CIRCLED NUMBERS CORRESPOND TO REFERENCED CLEARANCE POINTS ALONG OUTBOARD EDGE OF CHUTE, OPPOSITE TO INPUT CONVEYOR PULLEY.

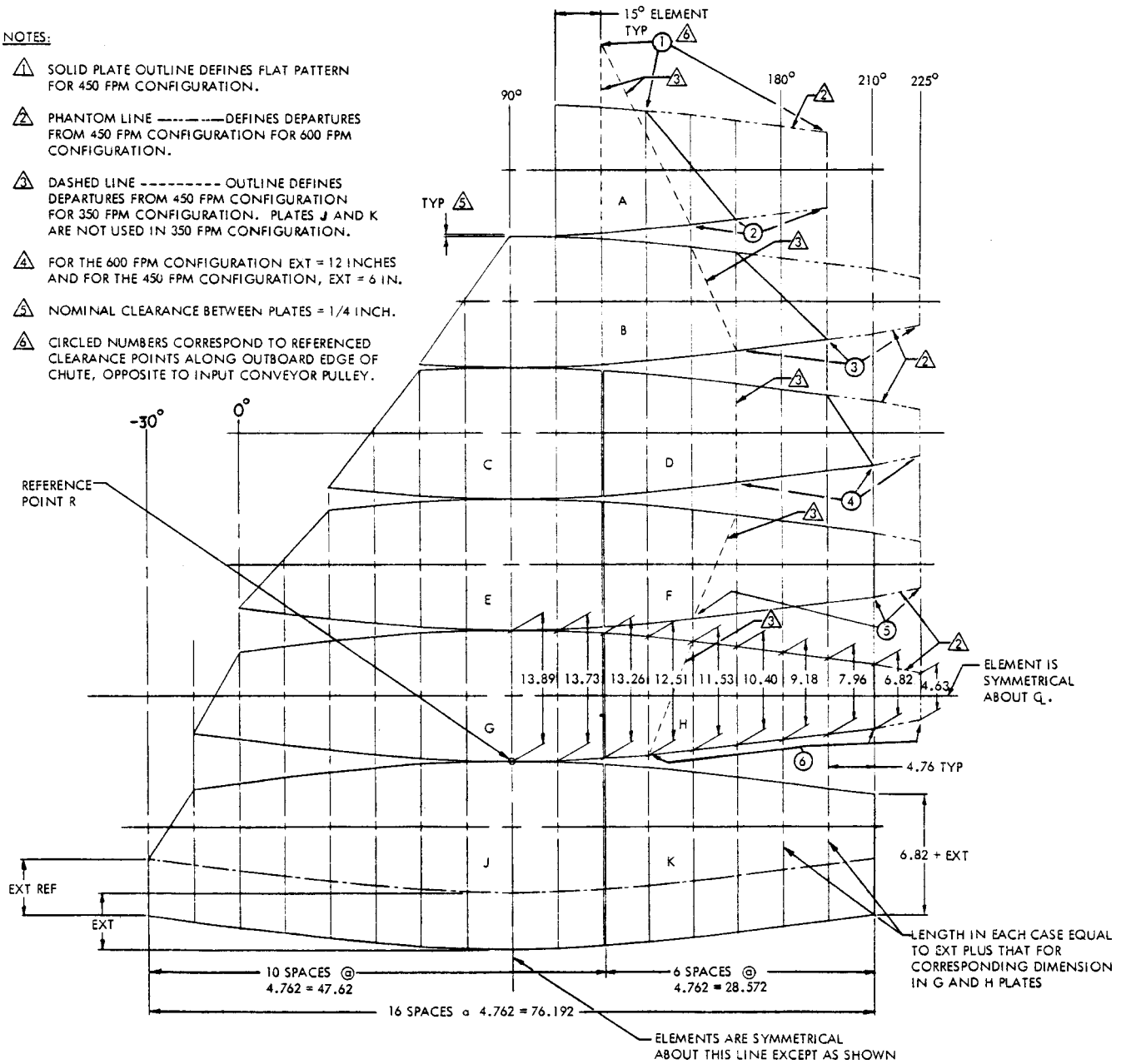


Figure 3-5. Flat Pattern Layout for Chute Segments

3.1.2.1.2 Materials

Some very pertinent design tradeoffs are involved in defining the specific surface material. Five basic alternatives, relative to the surface wear environment, are identified here:

- An austenitic stainless steel
- A high abrasion resisting steel, such as US Steel T-1 (various brinell hardnesses) or Jones and Laughlin Jallo
- A nonmetal, such as ceramic or UHMW
- A standard carbon steel, which will wear out most quickly.
- A standard carbon steel surface treated with a plasma spray-on material such as tungsten carbide

The choice must be made in the context of initial cost and replacement considerations as well as of performance.

Apart from its cost, stainless steel is evidently not presently favored by the mining industry as an option for a chute liner material because of the relative difficulties involved in cutting and welding in under field conditions. However, stainless is attractive because of its relatively low coefficient of friction with run of mine coal (Table 4-1), and may necessarily be considered in the case of very sticky flow cases.

UHMW and ceramic have often been suggested for use in high abrasion environments, such as for a coal chute surface. Potential questions concerning UHMW in the areas of flammability and associated toxic gas by products have been partially addressed by means of additives to the basic mix. These additives, however, are known to degrade the abrasion resistant properties of the material. Consideration of UHMW was, in this regard, put in limbo during the survey on this subject, when it was determined from MESA that new criteria on permissibility of materials in underground mines were in the process of being prepared. In that these criteria were expected, in the area of flammability, to involve performance against specific tests, it was evident that no early resolution concerning UHMW was likely, and it was dropped from further consideration.

Use of ceramic bricks for aboveground coal hopper and chute liners has been introduced, according to industrial literature. However, it is indicated that the brick or "tile" thickness must be quite large to avoid impact-type fractures. Moreover, introduction of tile mosaic configurations into underground mine environments, while literally feasible, raises questions concerning maintenance and inspection that are beyond the scope of this program to resolve. The key factor that seems to militate against enthusiasm over this option for the present design under consideration is that the provision for ready quick replacement of plate segments makes it possible to use materials with less wear life with minimum penalty.

The high abrasion resisting steels are an obvious candidate for the chute plate surface, having already experienced wide use in coal mines for this application. The cylindrical forming requirement for the plates in this present design involves a potential problem here, however. A major fabricator contacted concerning use of these steels indicates that some initial sample rolling fabrication should be performed to insure that the plate's "springiness", inherent in the heat treated condition, does not cause the radius of the formed segments ultimately to relax due to shipping or handling shock. It is recommended that such tests be performed on a full size sample plate segment in Phase II of the program. Assuming that the results are favorable in the area of dimensional stability, a high abrasion resisting steel is the recommended plate segment material for this chute design, except where friction dictates stainless.

A fall-back choice of materials is a standard, low carbon steel. While replacement of worn pieces will be dictated more frequently, this requirement is inherently well-addressed for in the proposed design, which provides for bolted attachment of the individual plates to the Plate Segment Support Assembly.

A fifth plate design alternative considered was a low carbon steel with a plasma-sprayed coating of a high abrasion-resisting quality, such as tungsten carbide. A process commercially identified as Metco flame spraying was studied in this connection. This option is inherently attractive from the standpoints of 1) the potential economics relative

to initial cost and mine maintenance and 2) the geographically widespread availability of the flame spraying process, as well as the number of very hard coating materials available. However, its typical application has characteristically not involved the broad plate areas under consideration here; and it is also indicated that the surface roughness of a plasma coating such as tungsten carbide will typically exceed 200 RMS, resembling a sand paper configuration. Altogether, it is clear that some developmental work in this area would be required to confirm its feasibility here.

3.1.2.2 Plate Segment Support Structure

The plate segment support structure consists of 6 radially - formed, three inch deep, T sections of various lengths (as shown in Figures 3-3a and 3-3b) welded to orthogonally curved, 3 inch O.D. tubular sections. Viewed prior to any chute rotation*, this support structure has a main tubular section securing all six T-section ring segments at an outboard radial location about 60 degrees down from the horizontal at each ring cross section. A second outboard tubular section, located on the horizontal of each cross section, secures the lowest four ring segments, while a second tubular segment at 60° ties the fourth and fifth rings. A series of shorter tubular sections join pairs of adjacent rings together along the inboard side. As indicated in Figures 3-3a and 3-3b, the Plate Segment Support will be configured slightly differently for the 350 fpm configuration.

The plates are secured to the ring sections by means of T-shaped clips. When plates meet going around the principal radius of the torus, the upstream plate edge is shimmed as required so that its surface is flush or slightly above the downstream plate edge (Detail G-G in 3-2b). The T-clips, which are all identical, have slotted holes for their attachment to the ring sections, in order to provide assembly flexibility. The corresponding ring section holes are also slotted at 90° to the above slots for additional adjustment flexibility.

*See 3.2

The aft beam extension of the Plate Segment Support Structure is configured so that the nominal rotational attitude of the chute, prior to utilizing the adjustment features, are the following:

- Roll - 30°
- Pitch - 15°
- Yaw - 5°

The adjustment provisions are discussed in the next section and the required chute attitude requirements are introduced in Section 3.3.

Standard structural steel materials are proposed for all elements of the Plate Segment Support Structure. A number of alternatives exist for fabricating the basic cross section defined for the T clip. Immediate options involve welding a 3/8 plate stem to a cap which has been dihedrally break-formed to the 15 degree angle required. Another involves bending the cap ends on a standard structural Tee section, each by $7\ 1/2$ degrees, in opposite directions.

3.1.2.3 Base Support Structure

3.1.2.3.1 Structural Interface

The Base Support Structure (Figures 3-1a, -1b, and -1c) has been defined primarily in the context of preliminary, above ground testing requirements and without final specification of a feed conveyor to dictate an interface requirement. The support approach is, accordingly, entirely floor-mounted. It is clear, however, that other alternatives in the underground coal mine industry include 1) provision of either or both vertical and lateral support from the ceiling or 2) support on the chute inboard side (relative to the feed conveyor pulley) directly from the pulley boom. These alternatives must be addressed for individual mine installation requirements.

It will be seen that the principal support interface to the chute assembly (Figures 3-2a and 3-2b) involves forward and aft support tubular beams, supported on individual columns. The columns on the outboard side are braced together for lateral support, parallel to the receiving belt conveyor; and the aft column is supported with an outboard stanchion or outrigger. The two inboard columns have outrigger supports also, although it is envisioned that alternate, lateral support to the conveyor head pulley structure may be feasible.

3.1.2.3.2 Adjustment Features

Adjustment procedures and requirements relative to chute position and alignment are discussed in 3.3 and 3.4, respectively. The structural features involved in these adjustments are identified here.

The aft pair of support columns consist each of a pair of square tubes, sized so that the upper tube sections, which are pivotally attached to the aft beam, slide inside the lower tube sections and can be fixed at various heights by means of a pin-through connection. By this means the chute can be either 1) raised or lowered, or 2) rotated when seen in Figure 3-1a, (pitch rotation).

The forward end of the chute assembly can be raised or lowered by means of shortening or lengthening the loop length of a wire-rope provision attachment to the forward beam. The details of the rope and the attachments are not defined in the preliminary design. The movement inherent here is either vertical adjustment, in conjunction with the previous adjustment, or else rotation of the chute, when seen in Figure 3-1b.

The structural interface between 1) the aft extension structure, or "wheelbarrow handle" portion of the chute assembly, and 2) the aft tubular beam consists of two "pitch adjustment sleeves", as identified in Figure 3-1b. This feature permits the following relative movements:

- 1) Rotation of the chute around the aft beam axis.
- 2) Sliding of the chute along the aft beam axis, as constrained by the X-axis adjustment collars. (The wire rope loop must be correspondingly capable of being slid along the forward beam).

In addition, the "pitch" adjustment sleeve is slotted at the attachment point with the aft extension structure of the chute assembly. This permits two further adjustments:

- 3) Movement of the chute assembly relative to the aft tubular beam, parallel to the axis of the feed pulley.
- 4) Rotation of the chute assembly when viewed in Figure 3-1c.

It should be noted that the nature of the adjustment features inherently involves some cross coupling of rotations and translational adjustments, since they are not independent of each other. Relatively small angular and translational adjustment ranges are involved, however, as noted in the following paragraphs. Furthermore, because of the inherent interim nature of these provisions relative to full scale testing, more sophisticated adjustment features are not warranted.

3.2 CHUTE POSITIONAL ADJUSTMENT PROCEDURES

In order to provide for the range of dimensional and dynamic parameters associated with the transfer point configuration, as well as design uncertainties at this stage of the program, provision in the support design has been described for six-degree of freedom adjustment of the chute assembly. Figure 5-1 defines the ultimate coordinate system for these adjustments. The procedure recommended for achieving the required adjustments involves first setting the required rotational attitude of the chute about the midpoint of the aft support beam, and then achieving the required translational position in terms of coordinates X_R , Y_R , Z_R .

3.2.1 Rotational Adjustment

As defined in Figures 3-1a, -1b, and -1c, the position of the chute shown corresponds to the following geometry.

<u>Physical Condition</u>	<u>Corresponding Angular Attitude</u>
1. Surface P (See also Figure 3-3c) is horizontal in X direction, or as viewed in Front View of Figure 3-1a.	Roll Angle = 30°

3.2.1 (contd)

<u>Physical Condition</u>	<u>Corresponding Angular Attitude</u>
2. a. Aft support beam axis is perpendicular to pulley axis (vertical as viewed in Fig. 3-1c). b. Reference surface M (M1 and M2 in Figure 3-3c) is flush or parallel to Reference Surface N in Fig. 3-1b.	} Yaw Angle = 5°
3. Surface P is horizontal in Z direction, or as seen in side view of Fig.	Pitch Angle = 15°

As previously discussed, adjustments can be made relative to the designated surfaces. A bubble type inclinometer is required for measuring roll and pitch adjustments, while a scale is needed for yaw adjustments.

Prior to making any of the rotational adjustments, the required vertical clearance distance between the lowest point of the chute assembly and the receiving conveyor should be approximately set, using the forward end wire rope support. It is suggested that 8 inches be used here.

3.2.1.1 Roll Adjustment

The roll adjustment is performed by raising and lowering the upper ends of the aft support columns, in opposite directions, as required, by equal amounts. For the 75 inch separation between columns shown, the simultaneous raising/lowering increment is 0.65 inches per degree of roll, or a total vertical movement of ± 6.5 inches on each side for achieving a range of 15 ± 10 degrees of roll. The angle can be monitored by a bubble inclinometer on surface P.

3.2.1.2 Pitch Adjustment

This adjustment is achieved by raising or lowering the aft columns in the same direction, by equal amounts. Based on the approximate 60 inch diagonal separation between the aft pivot axis and the forward support point on the chute assembly, and an initial angle of this diagonal with the horizontal of 30° , the additional height adjustment required in the aft columns for achieving a range of $15 \pm \frac{5}{10}$ degrees of pitch is approximately $\pm \frac{5}{10}$ inches or 15 inches, total.

Since the wire rope attachment should be secured at the forward-most support ring, raising of the aft pivot axis to increase pitch will have the net effect of raising the forward end slightly, while lowering the aft pivot axis (decreasing pitch) will have the effect of lowering the forward end slightly. This is because the horizontal distance between the lower attachment point and the aft support axis will be changing, causing the angle of the wire rope to the lower support point also to change. This vertical movement will be a second order effect, however.

Once again, an inclinometer will be used on surface P to measure the desired pitch angle

3.2.1.3 Yaw Adjustment

Yaw adjustment is achieved by turning the chute crosswise in the top view (Figure 3-1c) so that the distances between edge surfaces M and N on back side change by equal amounts in opposite directions. At the 25 inch baseline between surfaces M1 and M2 (Figure 3-3c), this corresponds to 0.21 inches per degree of yaw change, or about ± 1 inch for a $5 \pm 5^{\circ}$ yaw range.

3.2.2 Translation Adjustment

A point along the axis of the pulley, even with the belt edge on the upstream side is chosen as the translation (X, Y, Z) origin. (Figure 5-1).

The initial 90° point R on the chute surface between plates G and H (Figures 3-2 and 3-5) is chosen as the common chute reference point for any input velocity chute configuration. The X, Y, and Z distances, then become those indicated in Figures 3-1a, -1b, and -1c, as X_R , Y_R , and Z_R .

3.2.2.1 X-Adjustment

X adjustment is achieved by relocating the X-adjustment collars and sliding the chute along the aft beam shaft until X_R is achieved. (The wire rope loop will simultaneously slide in the X-direction.)

3.2.2.2 Y-Adjustment

Y adjustment is achieved by simultaneously adjusting the heights at the forward and aft support locations, the former by changing the wire rope loop length and the latter by adjusting the aft tubular support columns. The remaining adjustment length available in the aft columns, starting with a total available range of $\pm 12^{18}$ inches and subtracting ± 6.5 inches and $\pm 10^5$ inch for the previously defined roll and pitch adjustments, respectively, is $\pm 1.5^{6.5}$ inches.

It is not anticipated that the chute will be lowered toward the receiving belt appreciably once the initial 8 inch clearance is set.

3.2.2.3 Z-Adjustment

Z adjustment is accomplished by means of the same adjustment provision as for the yaw angle. The attachments between the chute assembly aft beam structure and the pitch adjustment sleeves are loosened and reference surface M is moved relative to reference surface N, in the required Z direction.

3.3 NOMINAL CHUTE POSITION AND ATTITUDE

For the three designated input conveyor velocities, Table 3-1 gives the nominal rotational and translational requirements for the chute position, in terms of the six reference parameters, roll, pitch, yaw, and X_R , Y_R , and Z_R .

Table 3-1
Chute Locational Parameters

Parameter		Input Conveyor Velocity, FPM		
Name	Units	450	600	350
Roll	Degrees	30	30	25
Pitch	Degrees	15	20	0
Yaw	Degrees	5	10	0
X _R	Inches	33.6	39.3	23.12
Y _R	Inches	-38.0	-37.3	-37.8
Z _R	Inches	37.9	30.7	52.8

3.4 TRANSFER POINT INSTALLATION CLEARANCES

Two other primary dimensional parameters for the chute involve 1) the clearance ΔX_C between points along the outboard edge of the chute and the end of the feed conveyor head pulley and 2) the net head room clearances ΔY_B and ΔY_O , dictated at the transfer point. Table 3-2 summarizes these parameters for the chute configurations proposed for the 350, 450, and 600 fpm input belt velocities.

The chute outboard points referenced in the table are defined in Figure 3-5, being seen to occur at the joints between the plate segments.

Their ΔX_C clearance with the pulley, which assume a 12 inch pulley radius, increase to a minimum of 20 inches in the direction of the turn, and are considered adequate for the large lumps of coal and (or rock encountered in underground mining operations (See 4.2.1.5).

The overall clearance, Y_O , assumes a minimum 18 inch clearance above the input feed conveyor surface.

The headroom clearances, ΔY_B and ΔY_O , are defined in Figure 3-1a and -1b. The overall clearance Y_O assumes a minimum 18 inch clearance above the input feed conveyor surface and a 24 inch distance from the lower belt surface down to the floor.

Table 3-2
Transfer Point Installation Clearances

Clearance		Feed Belt Velocity Case			
		350 fpm	450 fpm	600 fpm	
1.	" ΔX " Clearance Between End of Feed Conveyor Pulley and Chute Out Board Edge at Following Chute Points:				
	<u>Point*</u>	<u>At Plate Joint</u>			
	0	A (350 Case)	3.0	-	-
	1	A (450/600 Case)	-	7.8	2.5
	2	A/B	12.7	16.7	18.4
	3	B/D	16.0	18.8	20.1
	4	D/F	19.	18.6	23.2
	5	F/H	20.8	20.5	25.6
6	H/K	20.4	21.5	27.3	
2.	Headroom				
	Belt/Belt Y_B	59.4	62.9	64.1	
	Overall Y_O	101.4	104.9	106.1	

*See Figure 3-5.



4.0 DATA SOURCES

Data sources for this program were of two types: 1) consultant support and 2) state-of-the-art surveys, involving literature searches and visits to underground coal mines. The details of the information gained from these sources are summarized in this section.

4.1 CONSULTANT SUPPORT

FSEC retained the following consultant support in Phase I:

	<u>Consultant</u>	<u>Field</u>
1.	Jenike and Johanson North Bellerica, Massachusetts	Bulk Material Flow
2.	Hendrik Colijn Monroeville, Pennsylvania	Transfer Point Design
3.	Reese E. Mallette Assoc. Birmingham, Alabama	Mining Operations
4.	John T. Boyd Co. Pittsburg, Pennsylvania	Mining Operations

Dr. Jerry Johanson of Jenike and Johanson defined the basic model of mathematical equations that describes the dynamic effects of both internal and external boundary friction of a deforming mass as it moves across a surface under gravity. The details of this work and its application in a general math model of overall transfer point dynamics is discussed in Section 5.

Mr. Hendrik Colijn provided support in 1) technology and design practice associated with belt conveyor transfer points and 2) in laboratory test characterization of run of mine coal properties, related to parameters pertinent to flow dynamics (See 4.2.2).

Reese E. Mallette Associates and John T. Boyd Company assisted FSEC in gaining specific insight into operational details and constraints at belt conveyor transfer points in underground coal mines. This involved the primary activity of identifying, and conducting survey trips to, a series of underground mines where a range of transfer point configurations and constraints could be observed. John T. Boyd Company was retained for the last four mine trips when Reese Mallette was not able to support an additional series of mine visits by FSEC. The data obtained from the mine site survey are discussed in 4.2.1.

4.2 STATE-OF-THE-ART SURVEYS

4.2.1 Mine Site Survey

4.2.1.1 Mines Visited

FSEC studied belt conveyor transfer point configurations in a total of eight underground mines, located in eastern and midwestern states. These sites, for which trip reports were included in monthly contract progress reports, were located in the following geographic areas:

1. Alabama, Birmingham vicinity
2. Illinois, western
3. Kentucky, western
4. West Virginia, Charleston vicinity
5. Pennsylvania, western

4.2.1.2 General Techniques of Right Angle Transfer

Provisions for turning the flow through 90 degrees at the transfer points observed by FSEC can be classified in three types, in order of hardware sophistication:

1. No Chute: Flow trajectory impacts belt directly

2. Deflector Plate: Flow trajectory impacts vertical backboard plate, which is parallel to second belt motion, and either suspended above the center of this belt or located alongside this belt and opposite the feed conveyor head pulley.
3. Chute: Flow channeled by plate structure down a slide incline, after its initial direction has been deflected by an impact surface (see next section).

It is worth noting that the third type of provision was made for transfers from 36 inch to 42 inch belt transfer points in only five of the eight mines visited. In one of the mines with the most sophisticated conveyor haulage systems, chutes were used only for 42 inch belt feed cases, while the 36 inch to 42 inch transfer points were served by the deflector plate technique.

4.2.1.3 Chute Configurations Observed

As implied above, chute configurations observed generally had a channel-type cross section to converge flow to the area above the receiving belt. Most of these channel sections had a flat inclined bottom, with vertical or sloped flat side walls, ranging from elementary, two-plate shapes to multiple flat plate configurations. In two instances, the side wall was curved, following the 90° turn.

The other general design class was characterized by curved bottoms cross wise to flow. In some cases the curved surface, a cylinder, was bounded by flat side walls, while in another mine visited the chutes were virtually 180° cylindrical sections.

4.2.1.4 Performance Characterization

Of principal interest to FSEC during the site visits were the following performance characteristics at the transfer chutes:

- Spillage
- Dust
- Belt Wear

4.2.1.4.1 Spillage

In general, loss of material at the transfer points with chutes was successfully controlled, any accumulation on the mine floor being very gradual and due primarily to bouncing around the periphery of the mass flow cross sections as it made initial contact with the chute. There were cases where the flow in the chute tended to back up and spill over the back or sides, owing principally to an insufficient slope angle of the slide base. In this case the material generally still landed on the belt.

Major spillage was observed only at one site, where transfer was attempted onto the tail end of the receiving conveyor, without even a backboard provision. A three sided frame-type structure, slightly raised above the belt surface, was the only converging device. It was evident in all transfer points not using a chute that tolerable operation depended on generally low flow conditions, and that occurrence of peak flow for more than a few seconds would have resulted in sometimes significant spillage.

4.2.1.4.2 Dust

With few exceptions, measurable levels of dust were generated at the transfer points, even with water spray suppression devices in use. The exceptions were in cases where the flow itself had a high moisture content. At the opposite extreme, an unusually heavy dust condition at one particular transfer point was attributed by mine personnel in part to the dryness of the air, corresponding to climatic conditions for that time of year.

It appeared that the exposure of the mass cross section periphery during the airborne or free fall, phase of the transfer is a factor in dust generation approaching that of the impact and frictional flow phases. In the heavy dust condition case identified above, mine personnel indicated that the reason for not using grizzly bars (see 4.2.1.11) was to preclude segregation of the fine material from the coarse. Segregations renders this fine material vulnerable to scattering by air currents during the period of gravity descent to the receiving belt.

One mine employed a dust suppression device known commercially as Roto-Clone at its mainline transfer points. This involves covering the transfer point under a hood and vacuuming the dust as it is generated. The dust is then mixed with water and expelled on the receiving belt.

4.2.1.4.3 Belt Wear

Observations in the area of belt wear provided no quantitative means for relating this parameter to chute evaluation. Even on a qualitative basis a measurable reference in this area was not available, in that worn surfaces were not clearly discernable at any of the mines visited. Evidence of sensitivity of mine personnel to this type of wear mechanism was correspondingly absent. At one of the most up-to-date mines visited, technologically speaking, means of turning flow at the 36 inch to 42 inch transfer points involved only a deflector plate, identified in an earlier paragraph. This required the flow to drop vertically to the second belt, there to be accelerated from zero to full belt speed while sliding on the belt.

There appears to be some question among experienced people in this area concerning the criticality of the belt wear mechanism. That impact with the receiving belt at a direction other than approximately tangential and at a speed other than that of the belt surface involves some wear function is clear. Certainly a chute configuration that most nearly produces a flow output velocity matching that of the receiving belt constitutes a design objective, all other considerations being equal. On the other hand, an issue that has been raised by at least one consultant to FSEC in this area is that belt failure and/or replacement due to belt wear of this type is comparatively insignificant to those of 1) catastrophic events and 2) belt edge wear.

4.2.1.5 Flow Materials Characterization

Principal flow constituency parameters of interest include maximum size; size distribution; moisture content; internal and external coefficients of friction; hardness; and basic definition from a materials constituency standpoint. Detailed data in several of these area was developed during the literature survey, and is covered in 4.3.

Of note here are observations defining anomalies in run of mine coal from the standpoint of maximum size and makeup. While not specifically observed by FSEC during the field visits, the maximum lump dimensions was, according to interviews of mine personnel, judged to run up to 18 to 20 inches. This usually involved roof rock, sandstone, etc., rather than coal. The most unusual article observed was a roof bolt.

Refuse, or non-coal constituents in the flow, ran typically 30 to 40 percent.

4.2.1.6 Chute Frictional Slope Angles

Slope angles, relating to the inclination of the chute bottom when viewing the receiving belt from the side, ranged from 32 degrees to 49 degrees, or slightly higher, with the horizontal. The steeper cases yielded, of course, positive dynamics from a self cleaning standpoint, but the shallowest angles noted appeared to work reasonably well during the period of observation, even when the flow material characterized a mud slide. Some potentially marginal conditions existed, however.

4.2.1.7 Construction Details

Quarter to 3/8 inch-thick steel plate was in normal use for chute configurations observed. High-abrasion resisting alloys, including U. S. Steel T-1 and Jones and Laughlin Jalloxy were frequently used.

Welded construction for joints between principal chute sections was the typical means of fabrication. Replacement of worn sections was ordinarily accomplished piecewise by torch cutting and welding in a filler piece or else simply welding over patch pieces. In one mine visited significant use was made of bolted-in sections of predetermined size for replacement. The original plates were attached by means of flat socket head cap screws, making quick replacement possible.

One of the reasons cited for the absence of stainless steel construction for the chutes at any of the transfer points visited was the comparatively greater difficulty, over other steels, in torch-cutting and welding stainless on site.

4.2.1.8 Mine Interfaces

Mine interface details are grouped in four areas here: chute structural support; elevation distance between conveyors at the transfer point; chute clearance above the belt; and roof clearances at these points.

Methods of chute structural support, in the typical case of chutes located at intermediate points along the receiving belt, included as a general rule a pivotable mounting at the aft, or upstream end of the chute and cable or chain suspensions, sometimes with shock springs, at the forward, or downstream end. The pivoted end is hinged on a shaft in varying configurations, the shaft itself having simple beam supports on opposite sides of the receiving conveyor. On the feed conveyor side, attachment is typically to the head conveyor structure itself, while on the opposite, or outboard end, support is provided by a column. Similar two point support is provided for a cross beam above the downstream end of the chute, from whence hang the cable supports identified above.

Less common means of support for the aft pivot shaft and forward cross beams involved attachment to roof bolts or attachment to cantilevered beams extending across from the head pulley structure.

The distance between conveyor surfaces at transfer points utilizing chutes ranged from 79 inches down to about 45 inches, with a mean estimated at about 60 to 66 inches. For deflector plate type transfer points, this elevation difference was as little as 30 to 36 inches.

Clearances between the bottom of the chute and the receiving conveyor belt ranged from 6 to 18 inches, with 12 inches being common.

In connection with the chute to receiving conveyor interface, mine operation practice observed uniformly stressed the need for aligning in plain view the flow discharge vector parallel to the receiving belt motion, in order to prevent belt mis-tracking.

No attempt was evident at the vast majority of transfer points witnessed to minimize roof height or headroom. This height was rarely less than seven feet at 36 inch to 42 inch belt transfer points and frequently was up to 9 to 10 feet, giving a more than adequate distance above the feed conveyor.

4.2.1.9 Conveyor Data

The maximum pulley radius observed for the 36 inch feed conveyor was 12 inches, corroborating catalogue data.

Input conveyor speeds, where known, ranged between 450 to 500 feet per minute, with catalogue data defining a probable maximum range of 350 to 600 fpm. Receiving belt speeds, often not known at specific sites, were most commonly estimated at 550 to 600 fpm.

At all transfer points visited, the elevation angle of the feed conveyor belt was essentially zero, i. e. , horizontal, although it was evident from the head pulley structure configuration that this angle was variable up to 10 to 15 degrees above the horizontal.

All feed conveyors utilized belt cleaning devices of various configurations of a factory or local design. The effluent from this cleaner is normally caught on an inclined surface and fed onto the receiving conveyor. This surface is sometimes steel but is more commonly old conveyor belting or an elastomer material.

4.2.1.10 Transfer Point Operations

Transfer points for 36 to 42 inch belt cases are moved, according to personnel interviewed, at frequencies as little as every 4 months up to 2 years or more. A typical period required for movement of both the conveyor head section and the transfer chute is one week.

4.2.1.11 Ancillary Equipment

Some of the most common types of ancillary equipment at transfer points included skirt boards, dust suppression spray systems and grizzly bars. The function of these items are well understood in the industry. In particular, the purpose of grizzly bars --- which are in reality a part of the transfer chute --- is to lay a protective bed of fine material on the belt, by virtue of falling between the bars, prior to impact of the

larger, heavier lumps which cannot drop to the belt prior to reaching the end of the grizzly bars. It was noted earlier, however, that the view on the value of this provision, at least among some mining personnel, is divided, owing to the increased vulnerability of the now isolated fines to be scattered by air currents.

4.2.1.12 Other Data From Mine Site Surveys

FSEC performed photographic coverage of all but two of the mines visited. In conjunction with this work, FSEC's mining consultant assisted in gathering and identifying geologically samples from about five coal mine operations.

4.2.2 Other Surveys

In addition to mine site inspections, extensive data gathering in the areas of mining technology, transfer chute design, bulk flow theory, and run of mine coal properties was undertaken through the routes of literature surveys and consultant contacts. This section summarizes 1) bibliography accession from the literature survey and 2) run of mine coal properties applicable to bulk flow, gained from both literature and consultant sources.

4.2.2.1 Program Bibliography

In Appendix A are identified reports, books, magazine articles, and correspondence from consultants, which were obtained and reviewed during this program. They are organized by subject matter in the following areas:

1. Chute design, general
2. Chute materials
3. Coal mining at face
4. Underground haulage
5. Dust
6. Specific coal mines
7. Safety
8. Bulk flow, general
9. Bulk flow, theory
10. Coal properties
11. Sampling
12. Scale modelling

4.2.2.2 Materials Properties

Table 4-1 summarizes several test-derived properties for various types of coal samples from a total of 11 mine sites. While "cleaned" coal samples as well as raw coal are included, the properties cited are not found to vary significantly, and this is confirmed by the consultant source for this data. While the actual test data for samples given by site letter code cannot be identified, one (J) has given such permission, and the test report data from which the tabulated friction and moisture figures for Site J are taken is included herein as Figure 4-1.

Partly based on the above data and partly based on consultant experience, the following mean property values are given:

1.	Moisture, percent	6-7
2.	Sliding Friction Angle, degrees	
	Stainless Steel	20
	Rusted Carbon Steel	35
	UHMW	20
3.	Effective Angle of Internal Friction, Deg.	55
4.	Angle of Internal Friction, Deg.	38

The profile distribution of lump sizes in run-of-mine coal depends initially on whether it has been mined with conventional or continuous mining equipment. Figure 4-2 shows a logarithmically plotted size distribution for typical distributions using each method. Mean average sizes are seen to be less than a half inch for continuously mined coal and close to 3/4 inch for conventionally mined coal, with mean peak sizes of 4 1/2 and 8 inches, respectively. The maximum sizes here are superseded by the 18 to 20 inch sizes observed during the mine visits, however.

4.3 CHUTE DEVELOPMENT GUIDELINES

Table 4-2 summarizes guidelines, derived from the various data surveys reported in this section, to serve as a baseline in this program for the development of chute configurations and associated mine interfaces.

Table 4-1

Applicable Coal Properties From Test Data

Site Code	Type of Coal	Effective Angle of Friction δ , Deg.	Angle of Internal Friction ϕ Deg.	Moisture Content %	Angle of External (Wall) Friction		
					UHMP* Deg.	Rusted Steel Deg.	Stainless 304-2B Deg.
A	Clean	50	36	3.5		35	21
		60	40	13.0		39	23
B	Clean	50	39	23	19	33	20
		50	40	31	19	35	20
C	Raw	50	38	6	18	23	20
D	Clean	50	39	8			24
		52	39	11			29
		55	40	15			30
		60	41	18			26
E	Clean	50	40	5		32	22
		53	40	9		33	22
F	Clean	49	39	12	16	33	16
		50	40	15	18	33	18
G	Clean	54	40	10	17	30	15
		56	40	13	18	34	20
H	Clean	56	38	8	23	40	21
I	Clean	58	39	18	20	35	19
		53	39	15	21	35	21
J	Raw	50	39	12	16	34	16
K	Raw	60	45	7 1/2	20	36	17
		51	37	7	18	36	20
		55	40	9	20	37	23
		60	40	15	22	44	28
L	Clean	56	38	10	19	36	18
		58	40	7	21	35	20

*Ultra High Molecular Weight Polyethylene

Figure 4-1a
 FLOW PROPERTIES OF RAW COAL SITE J
 12.0% MOISTURE CONTENT

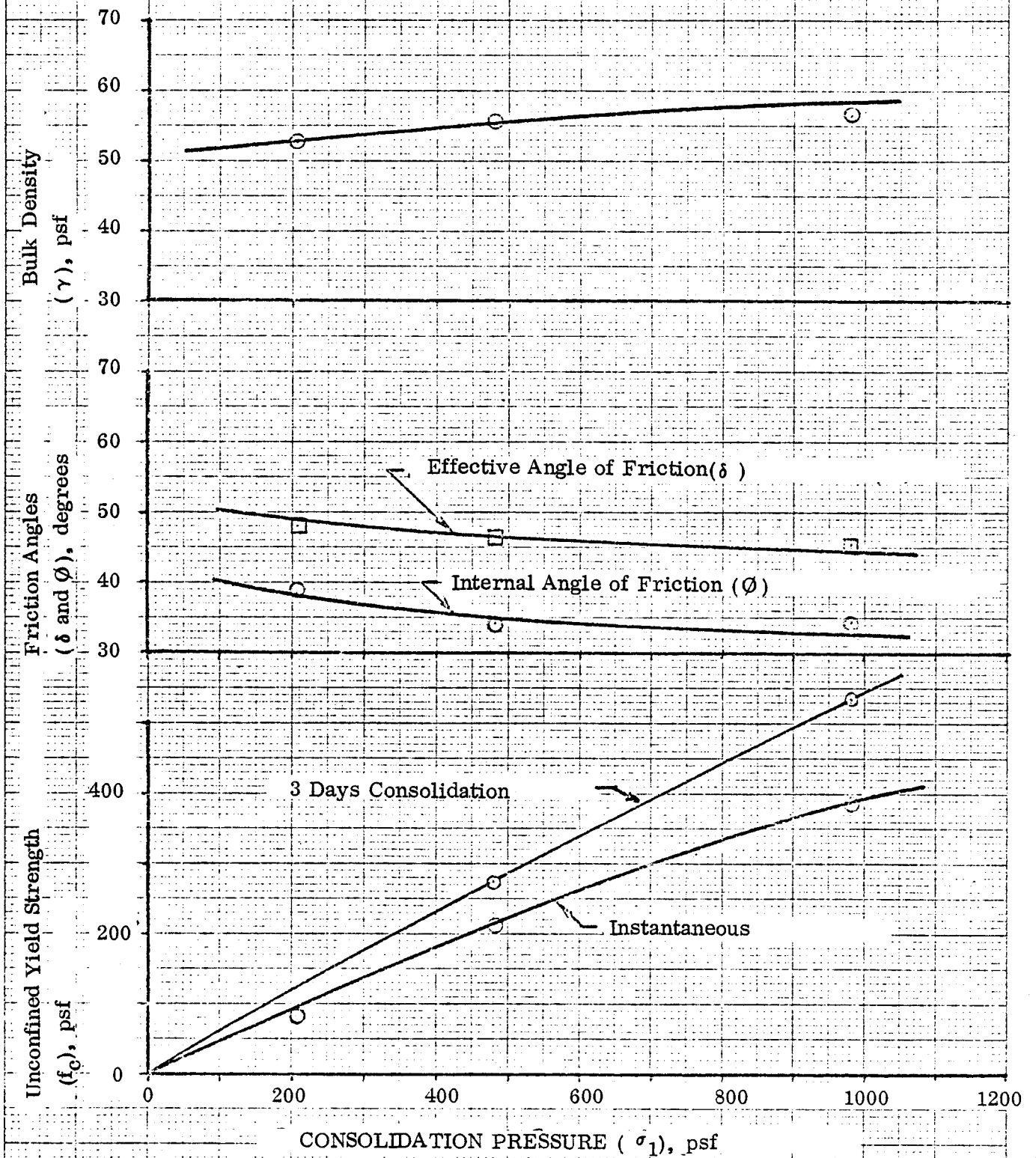
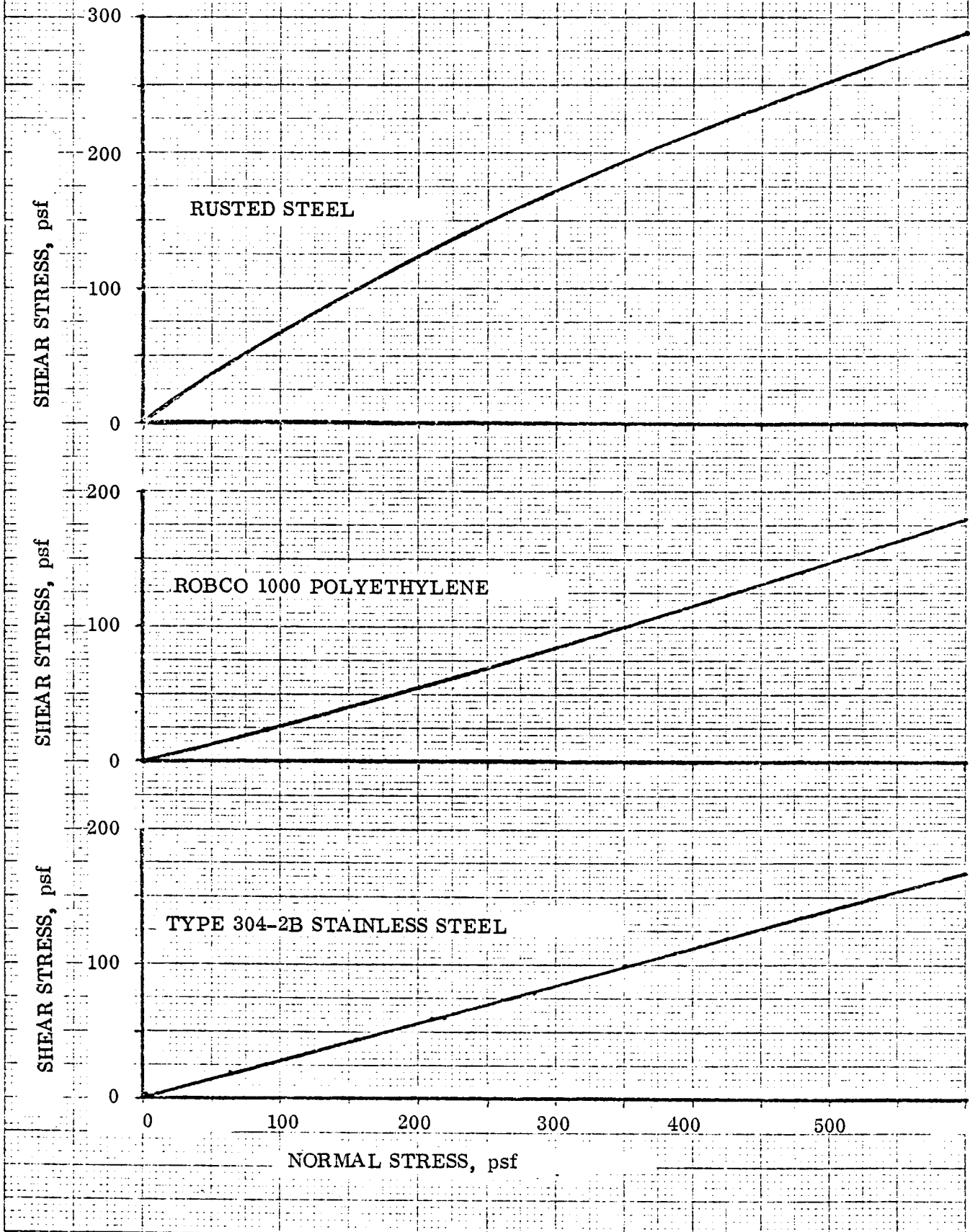
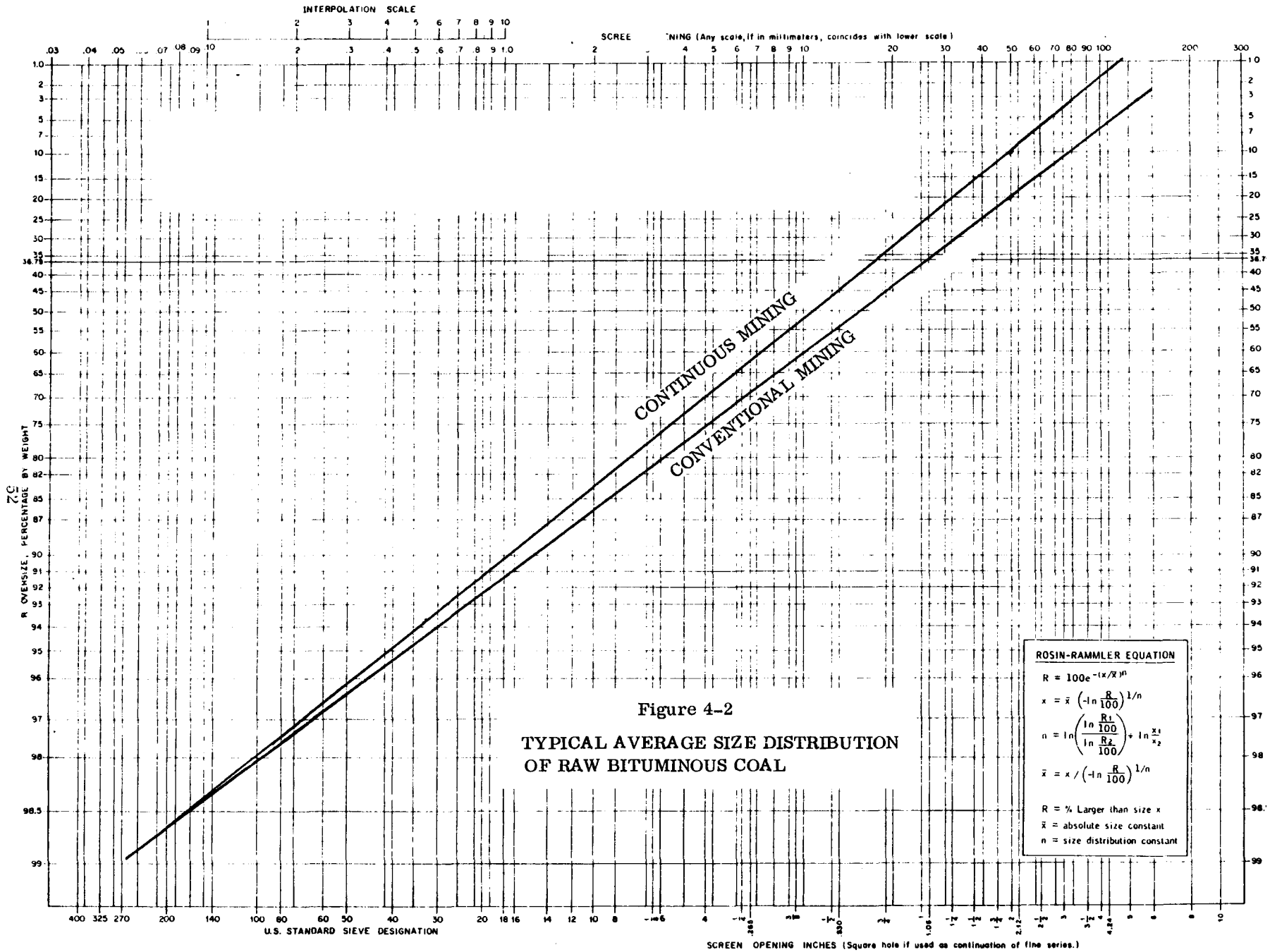


Figure 4-1b
WALL YIELD LOCI OF RAW COAL
12.0% MOISTURE CONTENT

SITE J





GRAPHICAL FORM FOR REPRESENTING DISTRIBUTION OF SIZE OF BROKEN COAL

Table 4-2

Low Headroom Chute Development Guidelines

GUIDELINE			REFERENCE SOURCE REQUIREMENT					
GENERAL	PARAMETER SPECIFIC	REQUIREMENT	FUNCTIONAL PERFORMANCE	MAINTENANCE			SAFETY	
				SPILLAGE	WEAR	OTHER	DUST	OTHER
1. Bulk Material Characteristics	a. <u>Moisture Range</u> Raw Coal, Percent	Peak Average	X	X		X (Corrosion)		
	b. <u>Sliding Friction Φ</u> Degrees (for 6% moisture)							
	1)Mild Steel, Rusted	29 ^o -40 ^o	X	X	X			
	2)Stainless, 304 2 B	15 ^o -29 ^o	X		X			
	c. <u>Effective Angle of Friction δ</u>							
	• Average	50 ^o -60 ^o	X					
	• Maximum	40 ^o -65 ^o	X					
	d. <u>Angle of Internal Friction Φ</u>		X					
	• Average	35 ^o -40 ^o						
	• Maximum	12 ^o -43 ^o						
e. <u>Coefficient of Restitution, Chute Wall with Coal</u>	Function: 1)Angle of Incidence 2)Run of Mine Particle Size and Material; 3)Chute Wall Thickness		X	X	X			
2. Dynamic Constraints	a. <u>Pulley Diameter</u>		(Influence on Trajectory)					
	• Maximum	24"	X					
	• Minimum	16"	X					

Table 4-2, cont'd

Low Headroom Chute Development Guidelines

GUIDELINE			REFERENCE SOURCE REQUIREMENT						
GENERAL	PARAMETER SPECIFIC	REQUIREMENT	FUNCTIONAL PERFORMANCE	MAINTENANCE			SAFETY		
				SPILLAGE	WEAR	OTHER	DUST	OTHER	
2. Dynamic Constraints (Cont'd.)	b. <u>Belt Speeds (FPM)</u> 1) Feed Conv. (36") • Minimum • Average • Peak 2) Recv. Conv. (42") • Minimum • Average • Peak	350	X						
		450-500	X						
		600	X						
		500	X						
		550-600	X						
		800	X						
	c. <u>Feed Trajectory Angle</u> (above horizontal, climbing)	0°-15°	X		X				
	d. <u>Impact Location on Receiving Belt</u> • Crosswise to Recv. Belt (Convergency)	Center 1/3 of Belt Width, Approx.			X		X (Tracking)	X	
		• Lengthwise to Recv. Belt	Centered Between Idlers Approx. (Max. Idler Pitch of 18" to 30")		X	Belt			
	e. <u>Elevation Drop</u> (From Top of Feed Conveyor to Top of Receiving Conveyor)	Goal	42"	X					
		Current Mean Range	60"-66"						
f. <u>Stream Cross Section</u> • Cohesion	Avoid: 1) Stream Splitting 2) Peripheral Scatter 3) Impact Bounce 4) Chute Flow Buildup 5) Impact Interference with Sliding Stream		X		X		X		

Table 4-2, cont'd

Low Headroom Chute Development Guidelines

GUIDELINE			REFERENCE SOURCE REQUIREMENT					
GENERAL	PARAMETER SPECIFIC	REQUIREMENT	FUNCTIONAL PERFORMANCE	MAINTENANCE			SAFETY	
				SPILLAGE	WEAR	OTHER	DUST	OTHER
2. Dynamic Constraints, Cont.	g. <u>Final Flow Vector at Impact</u> <ul style="list-style-type: none"> ● Direction of Horizontal Component ● Magnitude 	Parallel to Receiving Conveyor		X	X	X (Tracking)	X	
		Near-Match to Receiving Conveyor Velocity (See also 4. a.)		X	X		X	
3. Construction Details	a. <u>Materials</u> 1) Surface 2) Plastics (UHMW, etc.) 3) Weldability	High Abrasion Resistance in Wear Areas (See also 3. b.) Ruled Out			X (Chute)			oFlame spread oToxic by-products when burnt
		Peremptorily for Present Design Consideration because of Uncertainty Pending MESA Action on Materials Permissibility Standards for Underground Mines						
		1) Weldability Underground Desirable 2) Torch Cuttable 3) Low Skill Req'd.					X (Minimum Downtime Underground)	X
	b. <u>Fastening</u>	Bolted Replacement of High Wear Surfaces Desirable			X	X (Minimum Downtime Underground)		
4. Ancillary Constraints	a. Impact Control on Receiving Belt	Provide Grizzly bars, to provide initial bed of fine material for cushioning of impact by large pieces				X		

CC

Table 4-2, cont'd

Low Headroom Chute Development Guidelines

GUIDELINE			REFERENCE SOURCE REQUIREMENT						
GENERAL	PARAMETER SPECIFIC	REQUIREMENT	FUNCTIONAL PERFORMANCE	MAINTENANCE			SAFETY		
				SPILLAGE	WEAR	OTHER	DUST	OTHER	
4. Ancillary Constraints (Cont'd)	b. <u>Skirtboard</u> (If Required) 1) Belt Interface	Minimum Gap		X			X		
		●Support Skirtboard on Idlers							
		●Minimize Idler Pitch Along Skirtboard Length (18")							
	2) Material	Elastomer Wearstrip			X				
	3) Length	Sufficient to Contain Material During Deposition on Belt							
	c. <u>Belt Cleaner</u> (Accommodation, clearances for)	1) Location Around Pulley	135° from Top, Approx.		X				
		2) Feeds	Receiving Belt		X				
	d. <u>Troughing Angle</u> (Both Conveyors)	27°; 35°		X					
	e. <u>Overflow</u>	Consider Cutoff Switch for Feed Conveyor Based on Overflow Sensor		X	X			X	
	f. <u>Dust Control</u>	1) Water Spray	Use at Impact Area						
2) Active System (At 42" and 48" feeder transfer points only)		Consider hood & exhaust which mixes dust with water and dumps on receiving conveyor							
g. <u>Min. Clearance Between Bottom of Chute and Conveyor Belt</u>	8" to 18" (Also, chute to be Pivoted for Large Pieces)		X	X					



5.0 DYNAMIC THEORY AND MATH MODELLING

Two distinct dynamic phases are involved in analytically modelling the mass flow of material at a right angle conveyor belt transfer point:

1. The free fall phase, from the instant of leaving the input conveyor until contact with the chute.
2. The frictional phase, from initial contact with the chute until departure from the lower end.

Section 5 is concerned with 1) the identification of the applicable dynamic theory in these areas; 2) the structuring of a mathematical model adequate to represent the physical conditions; and finally 3) the creation of a computer program covering these phases, suitable for parametric analysis of the candidate chute model or models. In order to define entirely these areas, the method for representing mathematically a generalized chute surface will also be introduced. However, parametric analysis of specific geometric configurations will be addressed in section 7, following the presentation of candidate chute concepts and mathematical representation of a specific concept in section 6.

5.1 PHASE 1. FREE FALL TRAJECTORY AND IMPACT

5.1.1 General Definition

In Phase 1, the principal objectives involve tracking of the periphery of the mass cross section in terms not only of location but of the direction of the velocity vector. It is necessary to know the trajectory location in order to insure that the chute is positioned to intercept the flow; while it is equally important to know the trajectory direction, in order to monitor the angle of impact with the chute surface. Subject to verification by testing in both laboratory scale models and full-size configurations, one goal for the analytical task is to maintain this impact angle with the chute surface as small as possible, in order to minimize the tendency for bouncing and ricocheting. It is also necessary to know the angle and magnitude of the velocity vector at impact in order to calculate the initial velocity of the flow in the friction phase.

5.1.2 Math Model of Free Fall Phase

Appendix B summarizes the equations involved in the free fall trajectory phase. The main steps involved are the following:

1. Division of the total flow cross section into piece-wise segments across the head pulley, for purposes both of defining a chute impact trace and for tracking the later frictional movement.
2. Determination of the position and direction of the trajectory when it leaves the head pulley.
3. Mathematical representation of the subsequent trajectory path at the top, center of gravity, and bottom of the flow segments.
4. Solution for the impact point by means of simultaneous solution of mathematical equations for the trajectory, found above; and for the chute surface.
5. Computation of the following additional impact data:
 - Impact angle between velocity vector and normal to plate, and the complement of this angle.
 - Stream velocity immediately before and after impact

Some general points concerning the math model theory are addressed here.

Definition of the direction of the stream segments and their position on the head pulley at the instant of departure is taken from the chapter on discharge trajectories from the CEMA Bulk Materials Handbook. The theory here, briefly, assumes the trajectory of all elements of the flow mass follows that of a point mass located at the center of gravity of the flow cross section. This theory assumes a relatively smooth, tangential departure from the pulley radius, and does not address a phenomenon sometimes referred to as "humping", wherein the material does not reach the pulley perimeter tangentially, but rather

experiences an impact component with the pulley. A review of this subject was undertaken with one of FSEC's consultants, whose joint conclusion, with two other sources especially contacted on this matter, is that the effect referred to is not significant for conveyor speeds less than 800 to 900 feet per minute. This range is considerably above the peak speed of 600 fpm defined for this study.

As shown in Parts 1 and 2 of Appendix A, determination of the initial velocity and location of the piece-wise-defined segments, or streams, of the flow cross section entails introduction of the following parameters:

1. Belt speed, V
2. Conveyor belt inclinator with the horizontal θ
3. Idler configuration angle
4. Surcharge angle
5. Pulley radius (belt thickness is disregarded) R
6. Number of stream subdivisions assumed, n
7. Belt width, b
8. Edge distance, from belt to flow mass, e

Tracking the free fall trajectory of the flow cross section thus becomes a straightforward mathematical exercise. In the matter of defining the chute impact location and velocity for each stream, however, the model becomes closely dependent on the means of representation, as opposed to the specific shape, of the chute. As will be discussed later, this involves initial approximation of the chute surface by a mosaic of finite, rectangular, flat plate segments.

This representation is independent of whether the chute configuration actually consists of a smooth curved surface or is segmented in flat plates. As shown in part 4 of Appendix B, this convention leads to the solution of two simultaneous equations: 1) that of the second degree trajectory path for a given stream and 2) the line defining the intersection

between the plane of this stream trajectory, and the plane of the plate segment of the chute. In order to utilize a means convenient for computer solution for the specific plate impacted and the coordinates of the impact point, each rectangular plate is divided into a pair of discretely identified triangular sections. This permits the actual determination of the impact point to be broken into two phases, involving a test of each predetermined, triangular segment in the chute to determine whether it satisfies two conditions:

1. Where, if at all, does the trajectory intersect the plane in which the triangular segment lies?
2. Does the computed hit point lie within the triangle?

In both the free fall trajectory phase of the analysis and the subsequent frictional phase, the coordinate convention for locating stream positions and chute plate locations is that defined in Figure 5-1. In particular, the convention involves an XYZ axes system wherein the origin is on the pulley axis, even with the edge of the belt on the upstream side, relative to the motion of the receiving conveyor.

5.1.3 Computer Program for Free Fall Phase

The math model developed in Appendix B was written in FORTRAN language as a computer program, which is presented in Appendix C. As an aid to following the detailed steps in the program compilation, it will be seen that extensive use therein is made of annotations in the form of comment statements. Figure 5-2 is a flow chart of the basic logic in the Phase 1 computer program.

As an aid both to design and analysis of various chute configurations, the FSEC computer has a routine available called NASTRAN which prepares in each of three orthogonal views, and also a perspective view, a plot of the X, Y, Z coordinates of all corners of the flat plate mosaic representation of the chute. In addition to these points, the NASTRAN routine will also store the coordinates of the hit points on the chute, as well as other useful data, such as the relative location of the feed conveyor head pulley. (Figure 5-1).

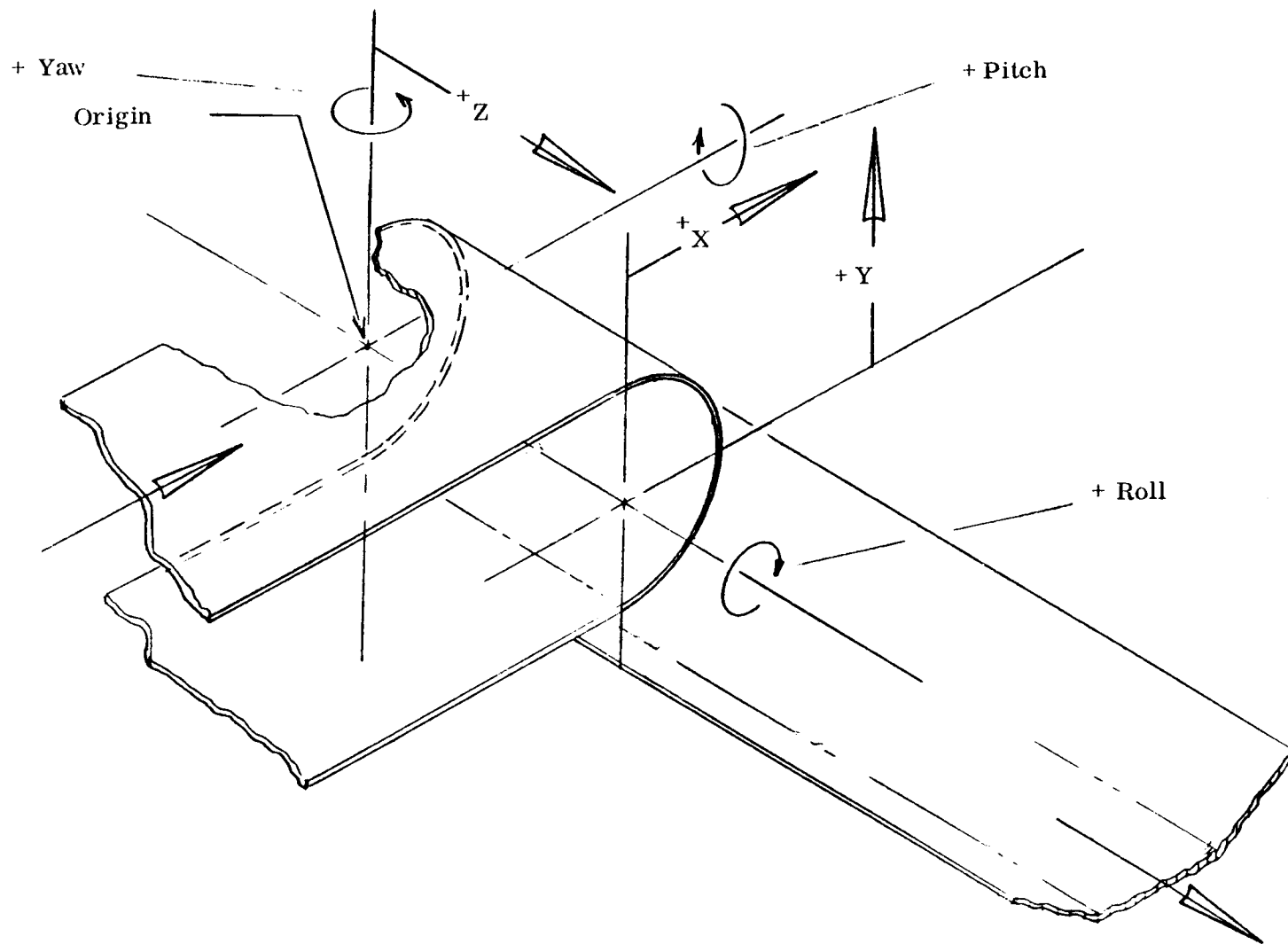
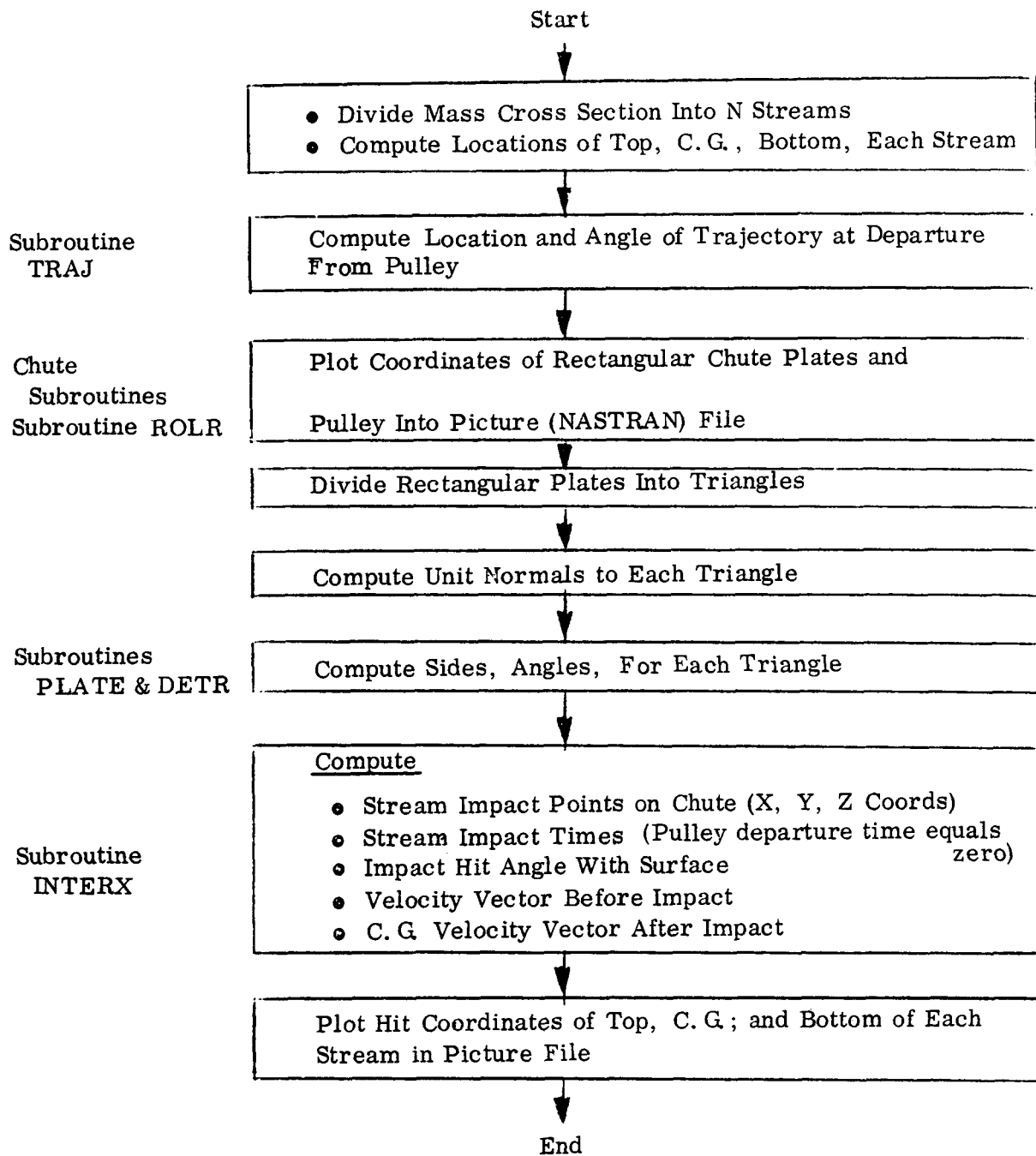


Figure 5-1 , Coordinate Axes
Translation and Rotational Sign Convention



** See Section 6.2

Basic Flow Diagram
Phase 1 (Free Fall/Impact) Computer Program

Figure 5-2

5.2 FRictionAL FLOW PHASE

5.2.1 General

The frictional flow math model covers the phase of the transfer beginning immediately after impact with the chute and extending down to exit of the flow from the chute. The basic theory accounts for the dynamic effects upon flow both at the periphery and within the interior of the flow mass cross section, the latter case arising because of deformation of the mass cross section.

5.2.2 Math Model

Briefly outlined, the theory treats the flow cross section in a series of piece-wise segments, whose mass in each case is concentrated at its center of gravity. After chute impact, these point masses are treated initially as independent dynamic entities. The velocity after impact for each stream is in a plane which is defined by the impact vector and the unit normal vector to the chute plate surface at the point of impact.

Because the moving c.g.'s represent streams of finite width and height, however, they must interact. Their relative locations and motions are traced in the model as they are combined into a stream net during initial movement down the chute. Before and after the net formation phase, the dynamic interaction at hypothetical interface planes or "dividing planes" between the streams is analyzed in terms of normal and shear forces. Together with 1) normal and friction forces at the chute wall; 2) gravity; and 3) centrifugal forces associated with chute curvature, these internal, interactive forces are applied iteratively to a stream "cell" of unit length during a series of stepwise movements down the chute surface. At the end of each step, which has a predetermined length, the velocity, shape, and boundary conditions for each stream are recomputed. The cells along a given cell wavefront of the streams are "locked" together, in that each is advanced some variable distance during each step, as a function of its velocity, width, and height, relative to those of adjacent streams.

The details of this model, including explanatory theory, are covered in Appendix D.

The flow theory utilized in this math model is sometimes referred to as the "pseudo-plastic" theory in bulk dynamics study. In a broad sense it assumes that the flow is governed primarily by dynamic mechanisms involving the fine particles in the mass cross section. Flow criticality, that is, is a function of what the fines "do", and, generally speaking, analysis of this type will give a conservative cast applied to cases where large lumps predominate, without a significant presence of fines.

The major premise of this conclusion relates to the fact that the independent parameter of record utilized in pseudo plastic analyses, the effective coefficient of friction δ , is a test-derived data point, obtained in tests where the maximum particle size is about a number 8 mesh size, or about one tenth of an inch. The reason for this is that shear tests involving maximum particle size significantly larger than the number 8 mesh size have historically exhibited considerable scatter in the results. FSEC is advised by its consultant in the bulk dynamics theory area, however, that obtaining test data for using uniformly graded material of about 1/8 inch should be achievable with some laboratory equipment now in use. Because the effect of the fines would have therefore been isolated from the material tested, the data obtained would be immediately extrapolable to uniformly graded sizes much larger than the 1/8 inch material, since the inter angular mechanisms involved in the shear measurements would not be dependent on a specific particle size.

The use of the mathematical model defined herein is not, then, ultimately limited to fine particle-governed dynamics. On the other hand it is judged, from observations of the flow material at the transfer points visited by FSEC, that the prevalence of fines is sufficiently common that this conservative approach is entirely justified, and in fact is the only approach justified, in order to ensure that flow is maintained. It is recognized, in this connection, that observations by experienced people in the field show that some segregation of the fines and coarse particles occur in transit to the transfer points, and that as a result the coarse pieces at the top of the flow cross section leaving the feed conveyor

head pulley may reach slide portions of the chute where flow is not pseudo-plastic, owing to the absence of the fines. This is still considered to be a nonconservative approach, however; the mechanism of the fines elsewhere on the slide will still be the pacing case from the standpoint of maintaining flow. The path of the coarse pieces must, of course, also be confined.

5.2.3 Frictional Flow Computer Program

Appendix E contains a compilation of the computer program for the Phase 2 frictional phase of the 90 degree transfer analysis. The program is extensively annotated and can be followed by one familiar with FORTRAN IV after he familiarizes himself with the friction flow math model (Appendix D) and the following discussion.

5.2.3.1 Phase 1 Interface

The Phase 2 computer program is run in sequence with the Phase 1 program, which provides it, in the form of a punched computer deck or else in disk or tape memory, the following data for a given set of chute configuration, mass properties, and feed conveyor characteristics:

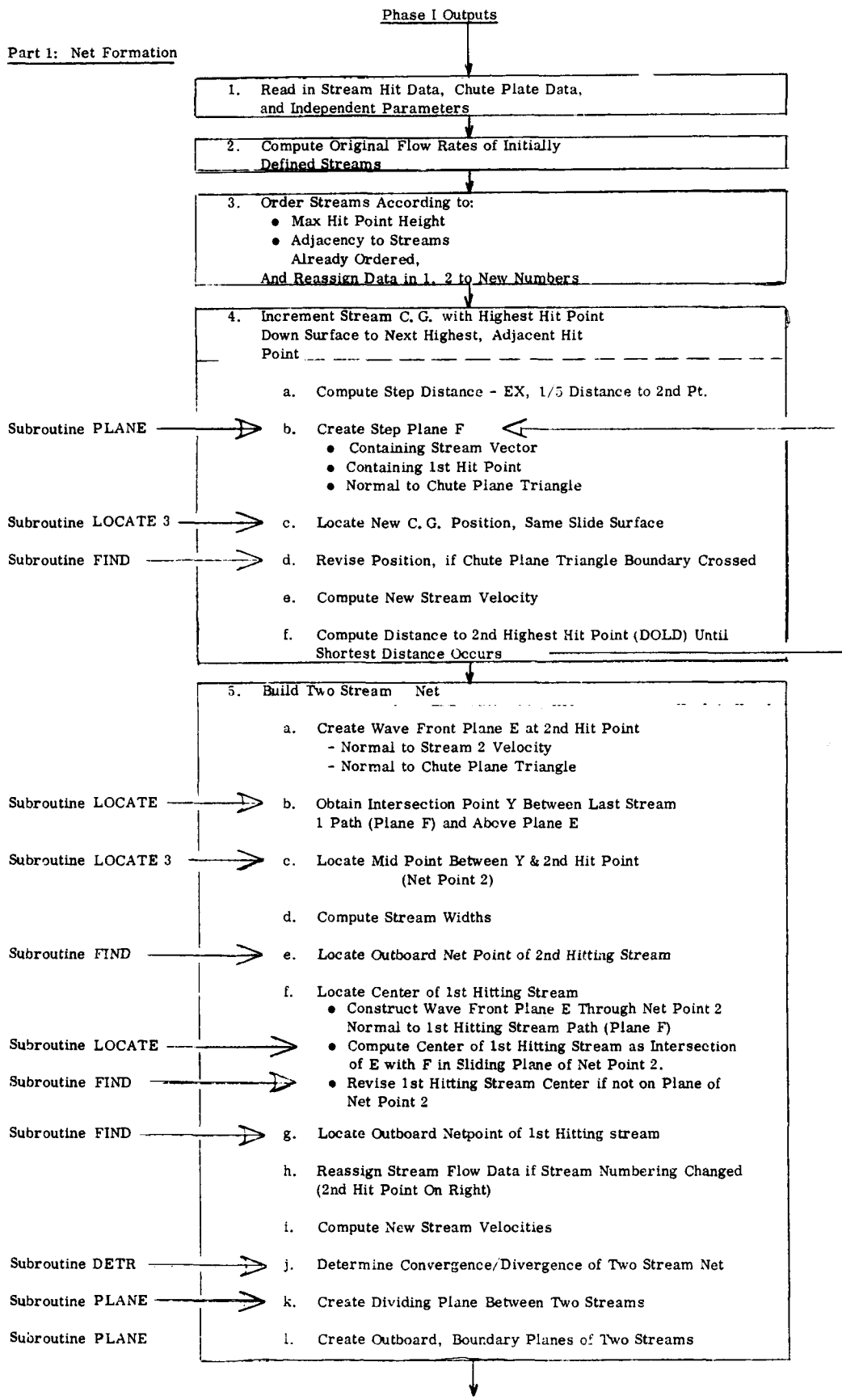
1. The X, Y and Z coordinates of the corners of the rectangular plates of the chute (See section 6.2).
2. The X, Y, and Z coordinates of the corners of the triangular subdivisions of each plate.
3. The X, Y, and Z directional cosines of the unit normal to each plate surface.
4. The lengths of the sides and the vertex angles of each triangle.
5. The coordinates of each stream impact point and the identification of the plate/triangle hit.
6. All eight parameters defined in paragraph 5.1.2.
7. Run-of-mine coal properties, including angle of dynamic wall friction and effective angle of internal friction.

5.2.3.2 Program Sequence

Figure 5-4 is a flow chart summary of the basic steps involved in the Phase 2 computer program shown in Appendix E, identifying also major subroutines and their functions.

It will be seen that the Phase 2 frictional program is itself divided into two parts: the first tracks the flow as the individual streams are sequentially incorporated into a common net; the second part then tracks the flow down to the point where the end of the chute is reached. In the second part, the fact that the identities of the original independent streams have been maintained discretely, for the previously discussed purpose of measuring internal normal and shear forces, is utilized to track the incremental departure of the flow from the chute, as various portions across its width reach the chute edge in that area.

Figure 5-4
Phase 2 Math Model Computer Program Flow Chart



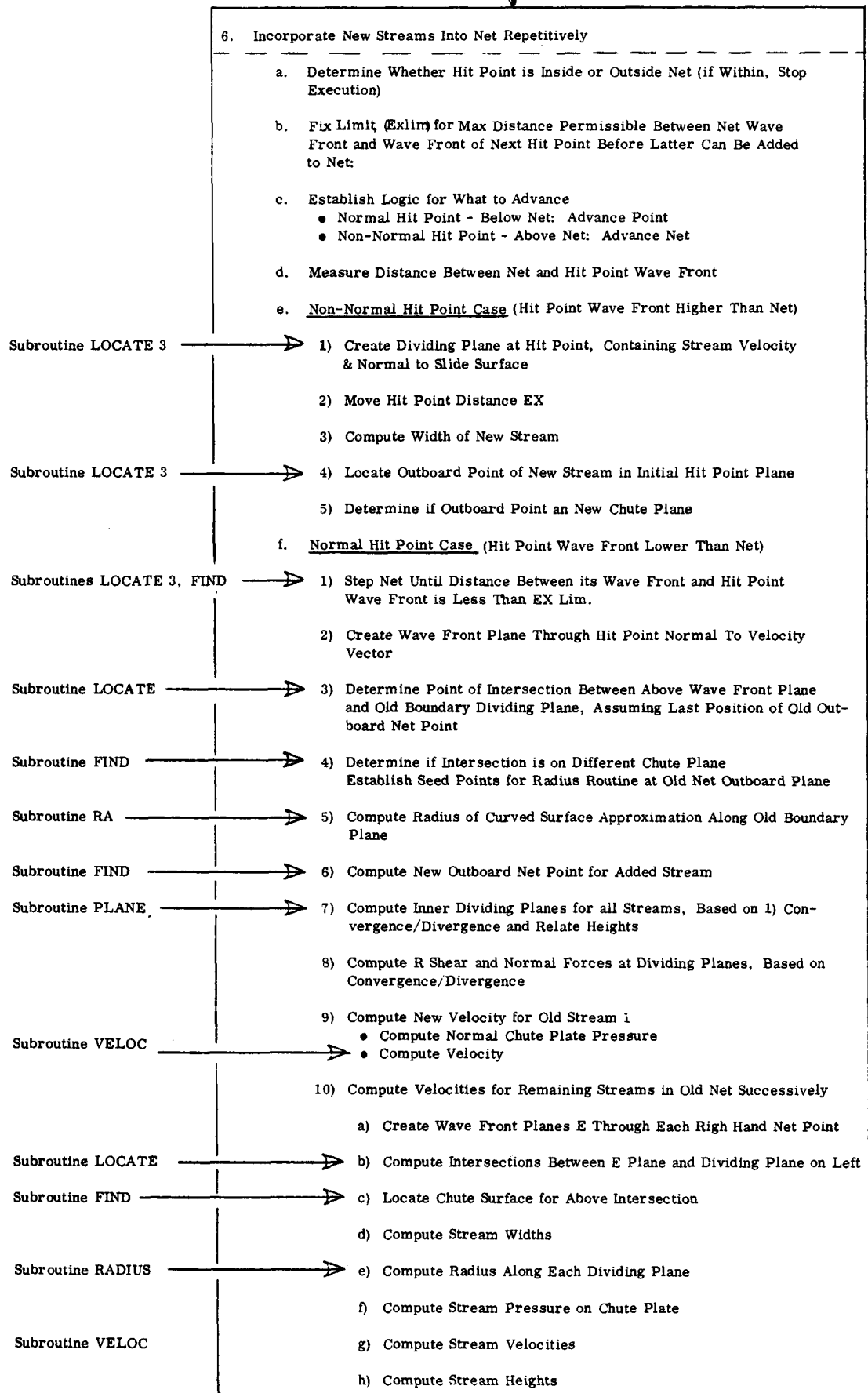


Figure 5-4 (cont'd)

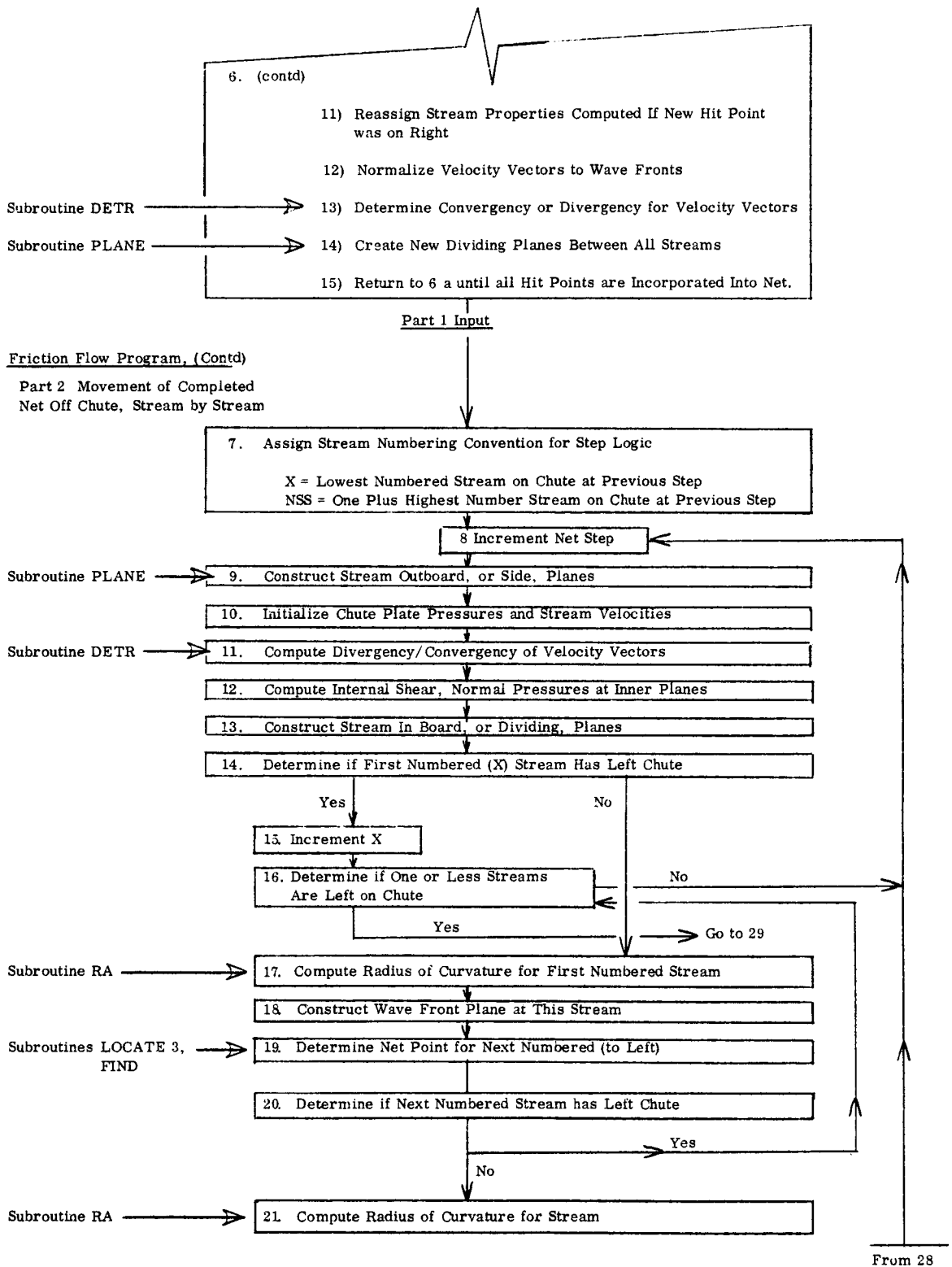


Figure 5-4 (cont'd)

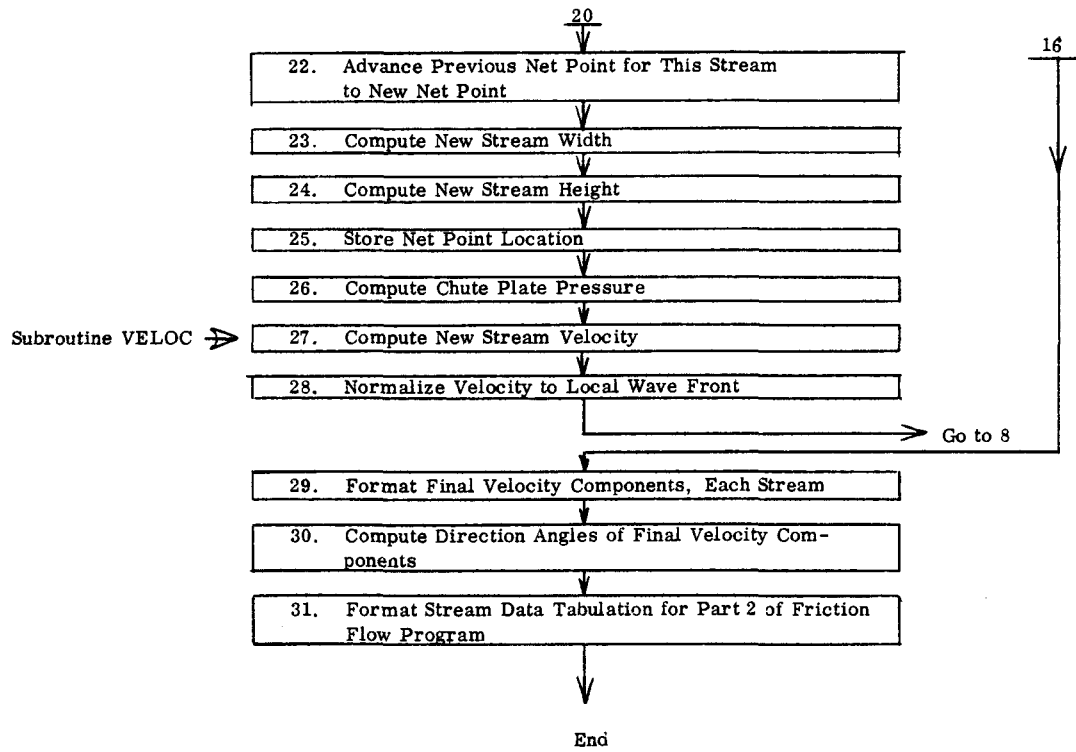


Figure 5-4 (cont'd)

6.0 CHUTE DESIGN CONCEPTS AND MATH MODELS

Prior to mathematically analyzing flow on specific chute surfaces, a series of concepts were evolved and evaluated as candidate configurations for the ninety degree transfer chute. The most promising concepts were screened by early lab testing (see Section 8 and 9); and in two cases chute math models were developed, namely, for toroidal and conical geometries. The torus geometry was selected for detailed analysis.

6.1 CONCEPTUAL DESIGN AND EVALUATION

Of numerous concepts considered, above seven distinct shapes were evaluated in detail. The seven configurations are derived from three basic geometries, namely, a cone, a cylinder, and a torus:

<u>Item</u>	<u>Basic Geometry</u>	<u>Concept Designation</u>	<u>Reference Figure</u>
1	Cone	Opening Half Angle	6-1
2	Cone	Flat Impact Plate	6-2
3	Cone	Zero Half Angle	6-3
4	Cylinder	Single Surface	6-4
5	Cylinder	Compound Surface	6-5
6	Torus	True (Smooth)	6-6
7	Torus	Smoke Pipe (Jointed)	6-7

These candidate concepts were screened in a tradeoff analysis against the following ten criteria, covering the three general areas of performance, compatibility with mine operations, and economics.

1. Stream (Mass Cross Section) Cohesion
2. Belt Impact Vector
3. Freedom of Flow
4. Convergence
5. Jam Clearance
6. Minimum Headroom
7. Installation Complexity
8. Maintainability
9. Producibility

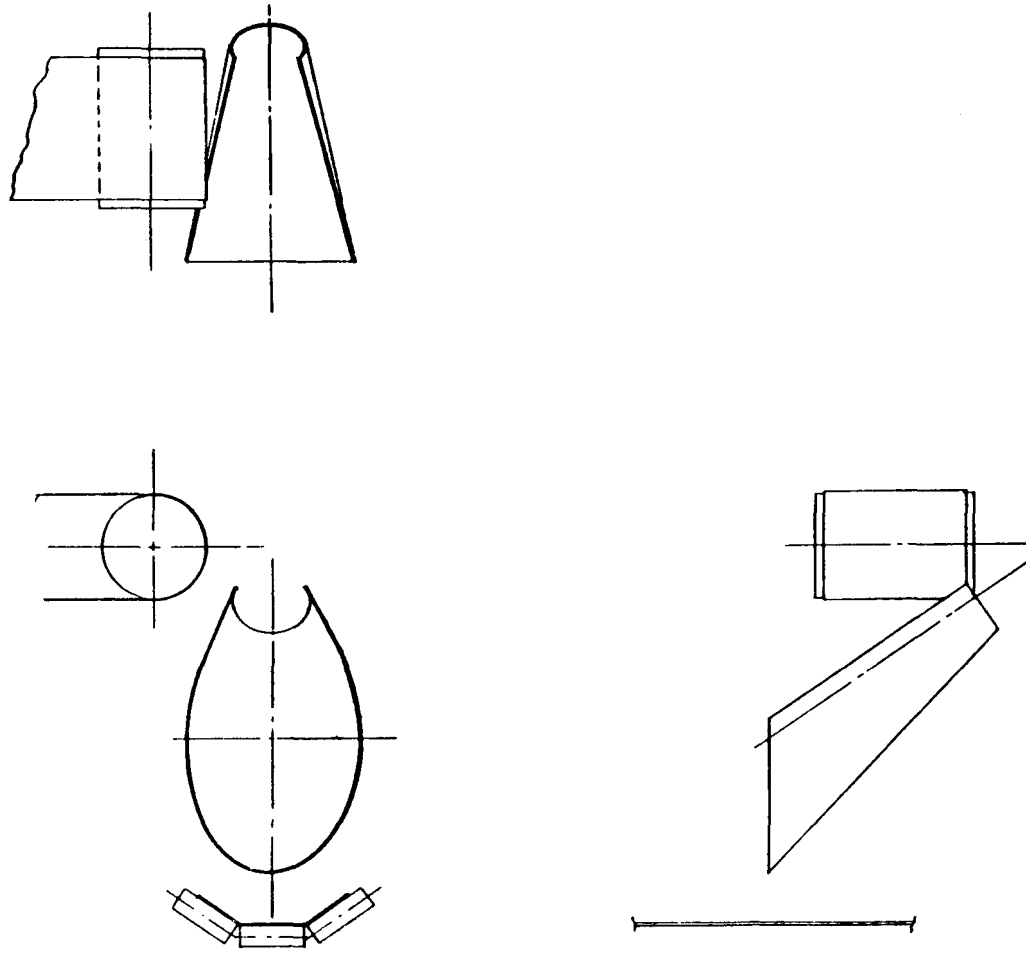


Figure 6-1 Cone, Opening Half Angle Concept

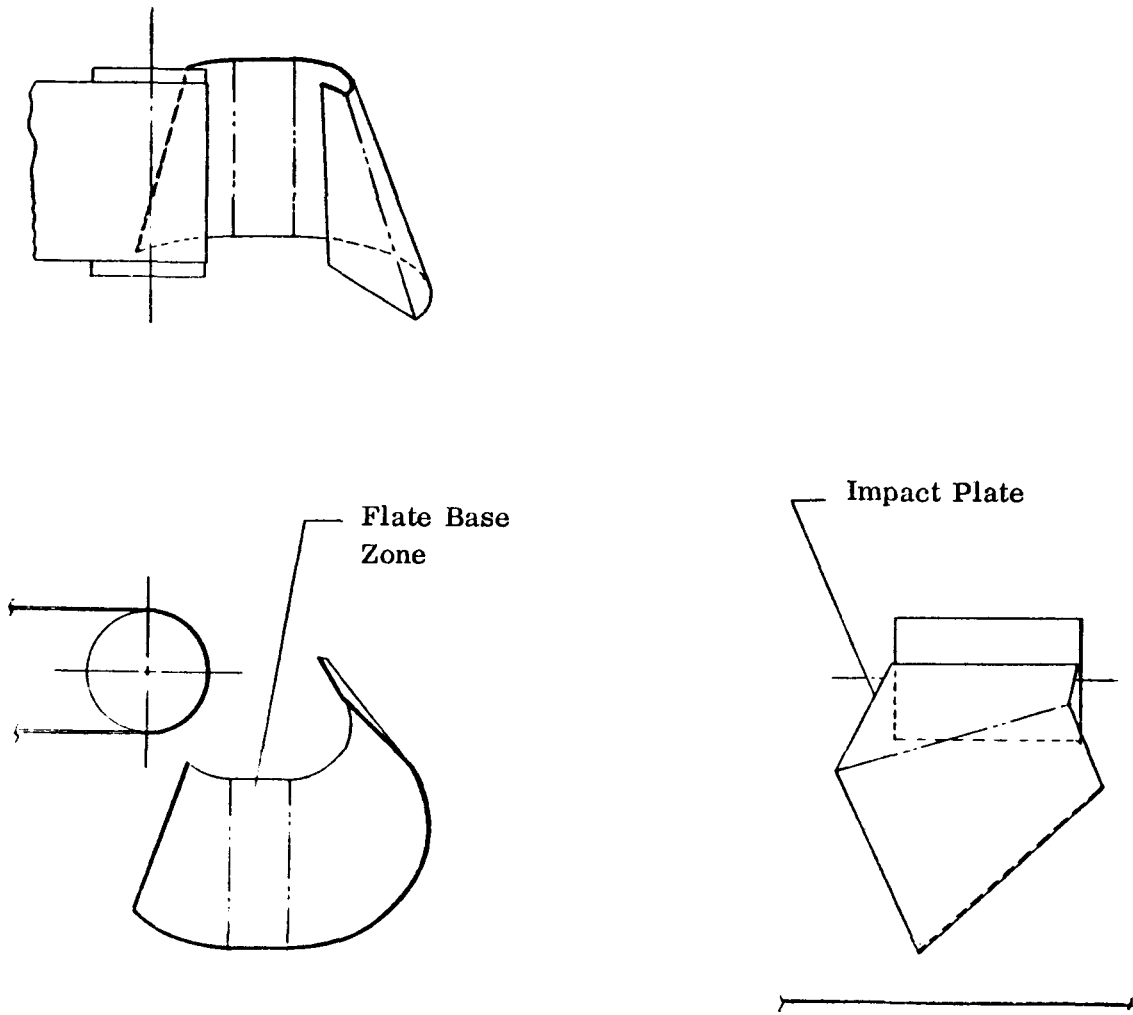


Figure 6-2, Cone Concept With Flat Impact Plate

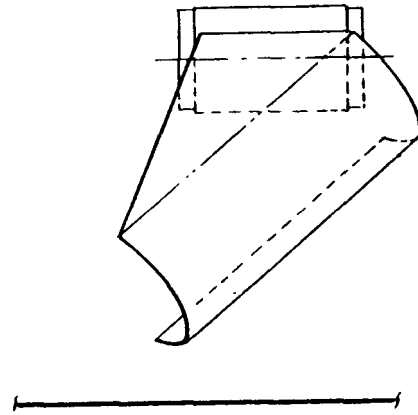
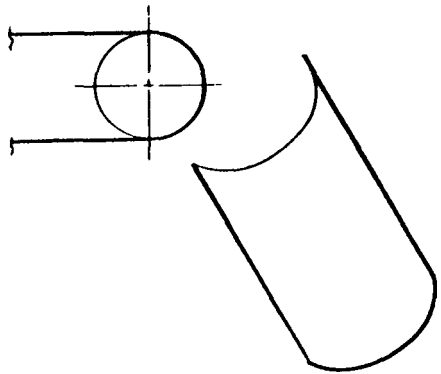
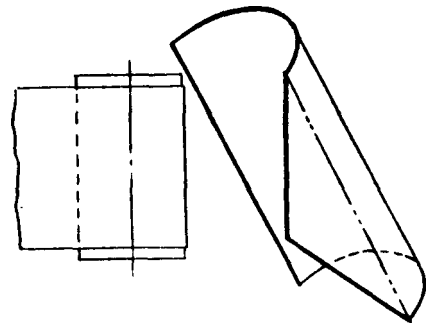


Figure 6-3, Zero Half Angle Cone Concept

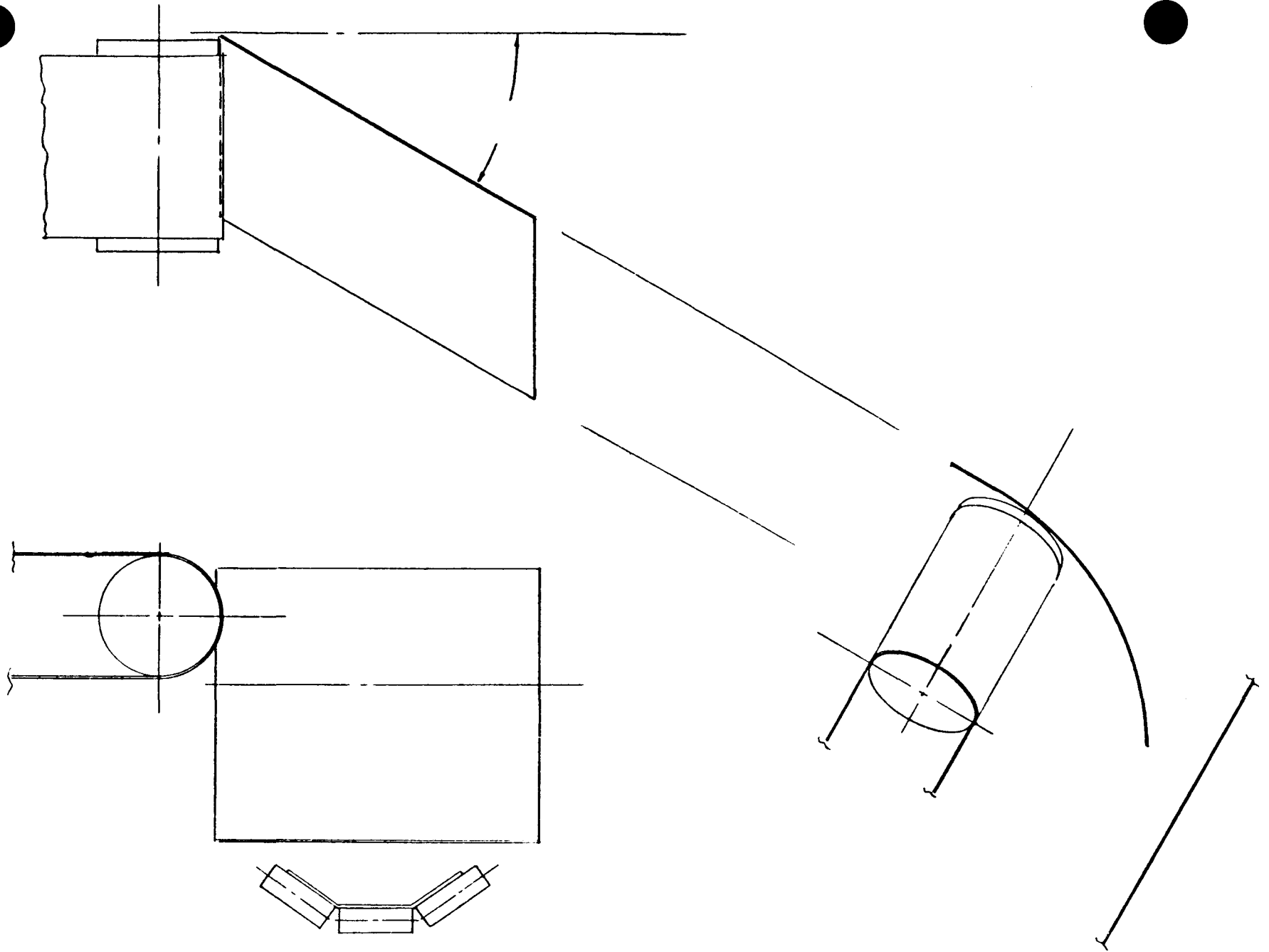


Figure 6-4, Cylinder Concept, Single Surface

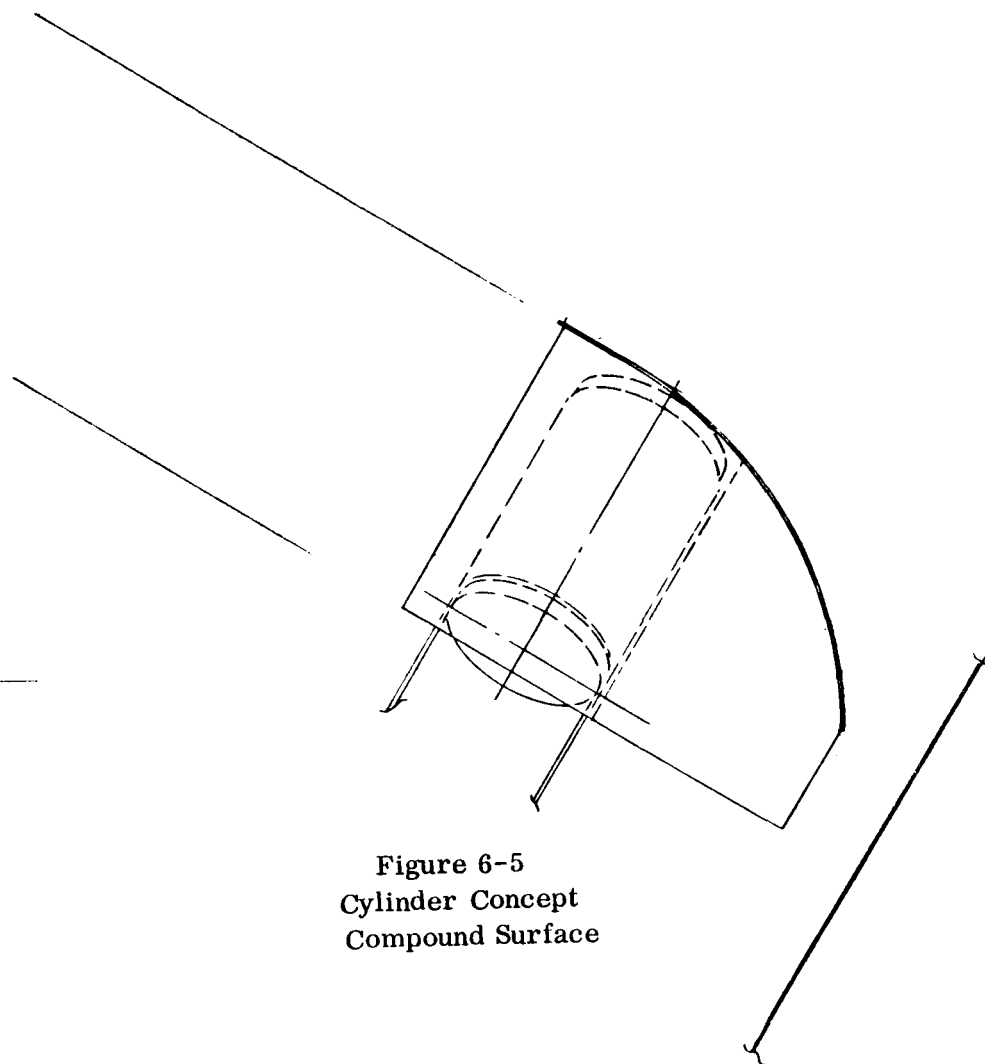
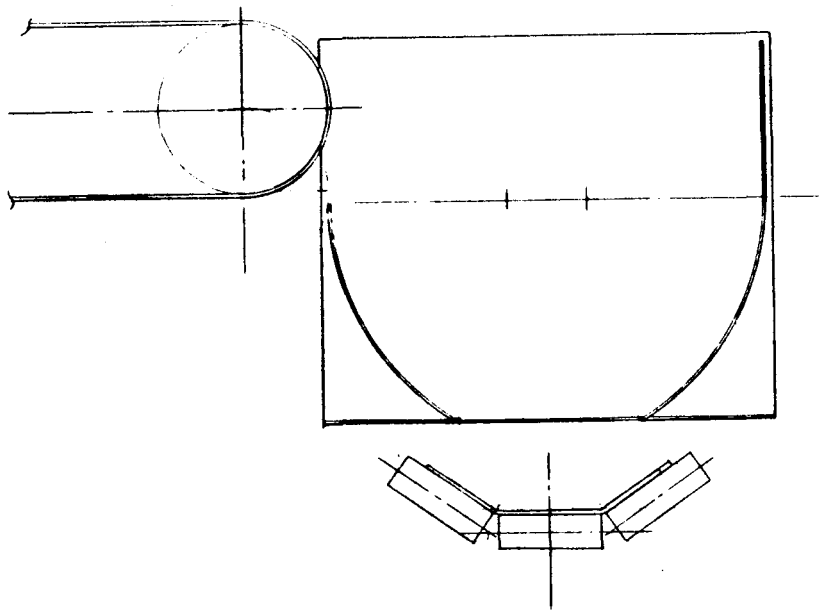
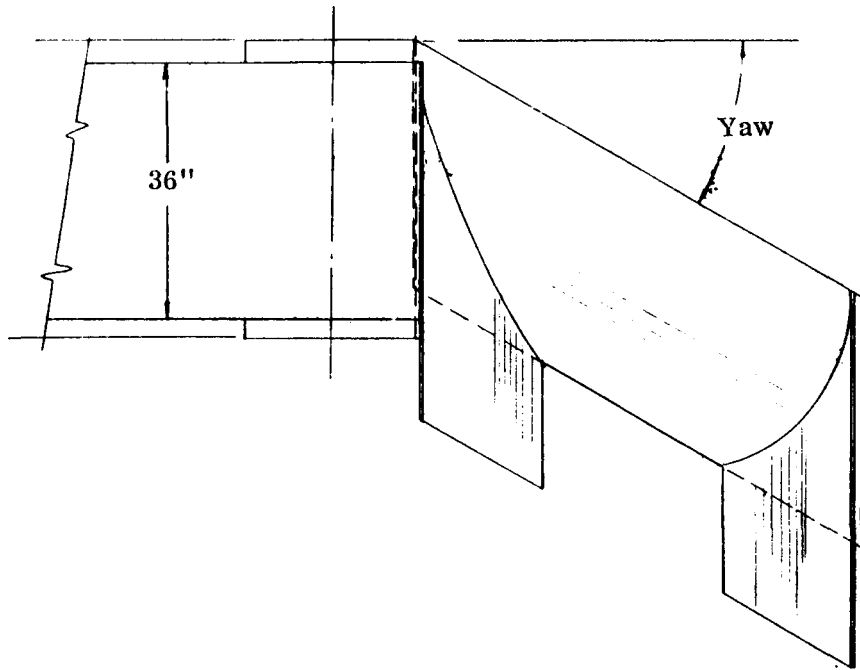
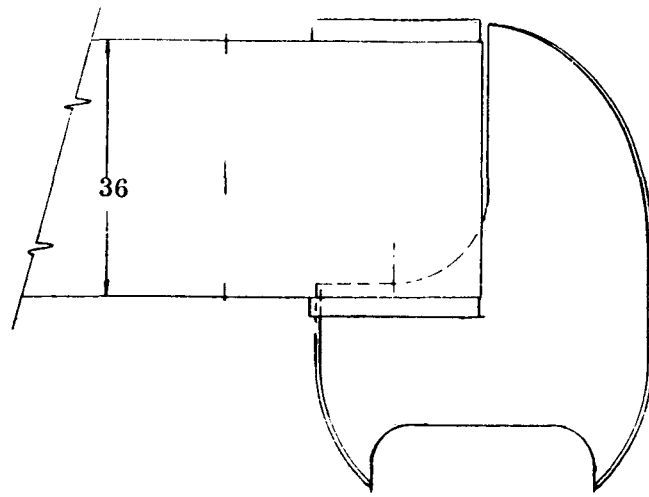
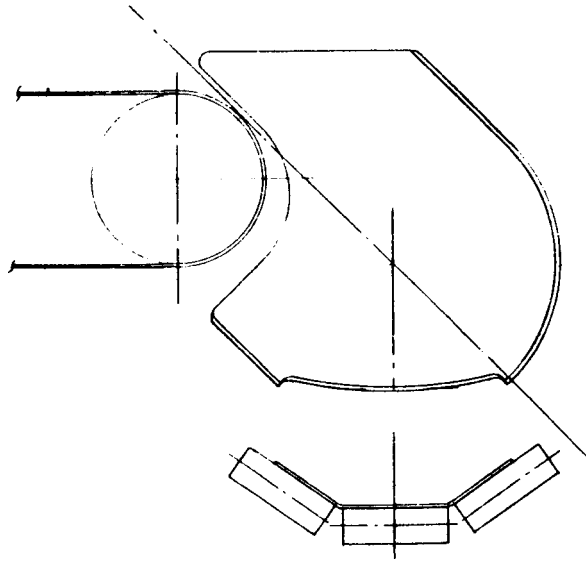


Figure 6-5
Cylinder Concept
Compound Surface



79



Alternate Roll Position

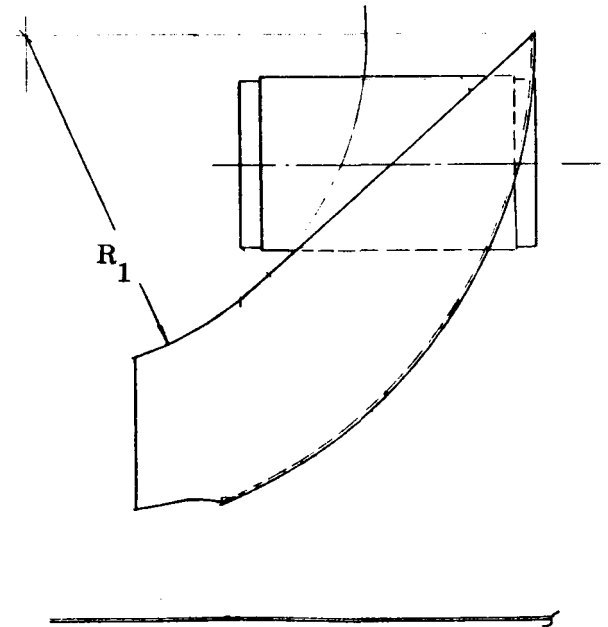
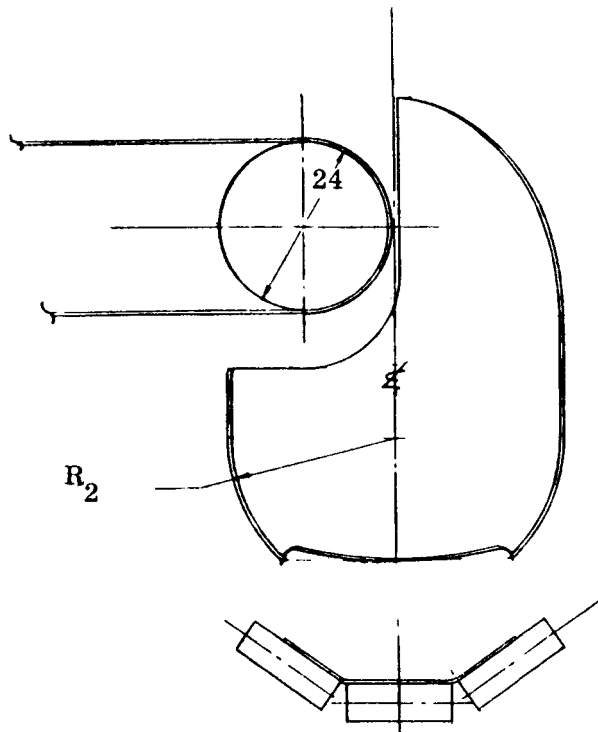


Figure 6-6 True Torus Concept

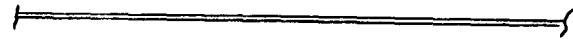
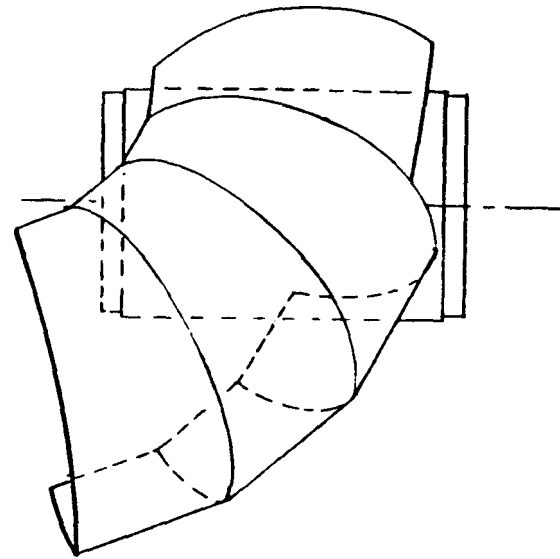
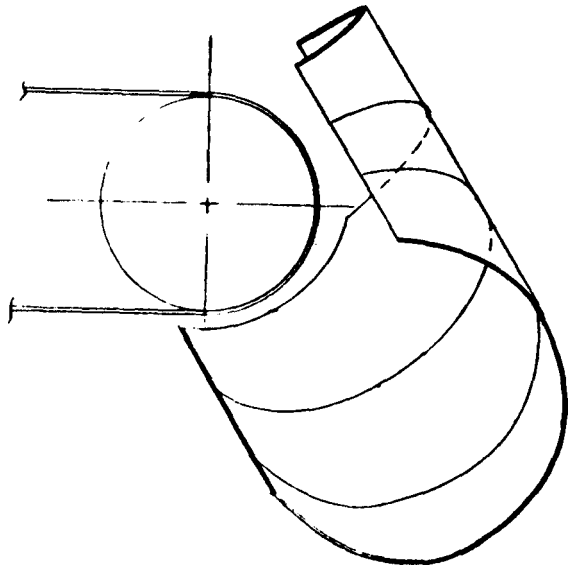
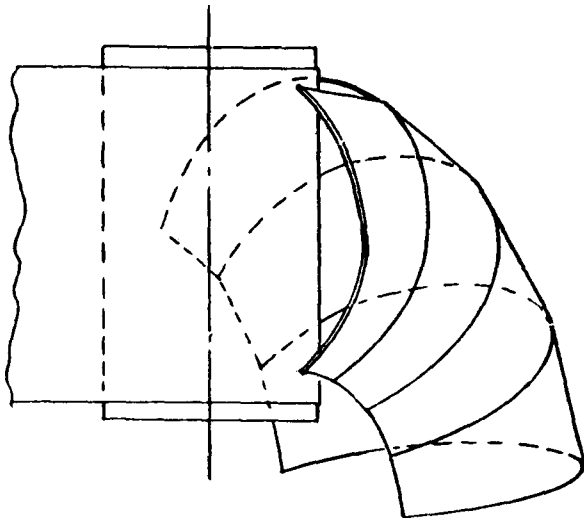


Figure 6-7, Smoke Pipe Torus Concept

Appendix F is a report of the tradeoff analysis performed. In addition to a discussion of both the candidate concepts and above criteria, it provides a rationale for application of a numerical weighting to these criteria in terms of relative importance.

The conclusion of this tradeoff analysis is that the smokepipe torus achieves the best overall rating in performance, mine compatibility, and economics. Moreover, because of one or more prohibitive drawbacks found to characterize each of the other concept configurations, the smokepipe torus is the only one judged to be suitable for detailed analysis and preliminary design.

6.2 CHUTE MATH MODEL

As discussed in Section 5, the general math model for flow analysis introduces the chute configuration effectively as an independent group parameter, along with sets of parameters relating to 1) the feed conveyor and pulley; 2) flow material parameters. This introduction is achieved by means of a specific chute subroutine to Phase I of the flow analysis computer program, given in Appendix C.

The chute subroutines provided are TORUS and CONE. They are capable, with prespecified modification, of generating in mathematical space three dimensional representations of any of the correspondingly designated chute surfaces listed in previous section 6.1. These surface representations are defined by flat plate-subdivided approximations of the nominal geometrical curved surface, where the degree of approximation can be achieved to any degree of precision simply by specifying a finer subdivision.

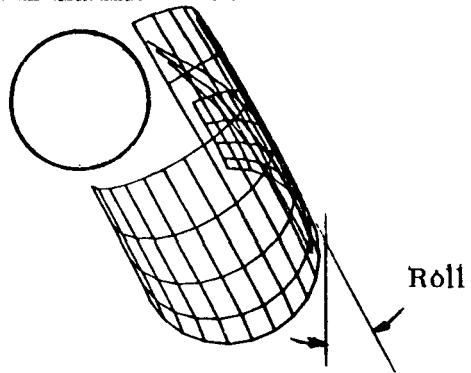
One purpose of the chute subroutine, then, is to supply to the two main routines of the flow analysis program the locating X, Y, Z, coordinates of the four corners of each rectangular subdivision. These plate definitions are immediately subdivided into triangles by the program for the purposes both of locating initial free fall trajectory hit points and of tracing the subsequent frictional flow path.

A second, prior function of the chute subroutine is to compute the space location of these plate coordinates, given basic independent parameters relating 1) to the particular geometrical shape and 2) to the location and attitude of the chute relative to the feed conveyor pulley. Thus in the case of the torus, the following base parameters would be specified for a given run:

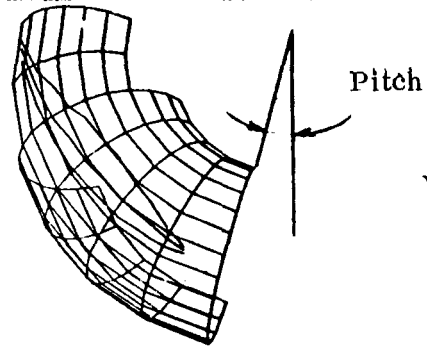
1. Major Radius RT 1
2. Minor Radius RT 2
3. Number of Flat Plate Subdivisions Along Major Radius of Curvature
NT1
4. Number of Flat Plate Subdivisions Along Minor Radius of Curvature
NT2
5. Coordinates of top, aft edge of torus section from pulley origin : X_T ,
 Y_T , Z_T (See Figures G-1 and G-2 of Appendix G)
6. Attitude of chute, relative to pitch, yaw, and roll angles, about the
principal axes through origin (Figure 6-8).

The torus math model whereby the computer programs subroutine develop the corner coordinates of the subdivided rectangular plates is provided in Appendix G. A similar math model is available for the cone computer program subroutine (Appendix C), but is omitted here in the interests of brevity, since this subroutine is not utilized in the proposed configuration. (Some of the cone chute models generated by this subroutine are shown in Figures 1B, 2B, and 3B of Appendix F).

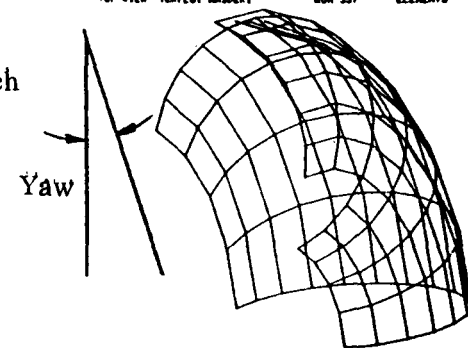
FRONT VIEW TEMPLAT HASDEK1 RUN 327 ELEMENTS 1.99999



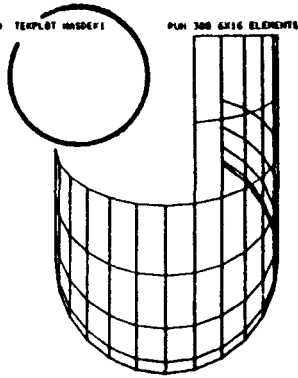
SIDE VIEW TEMPLAT HASDEK1 RUN 327 ELEMENTS 1.99999



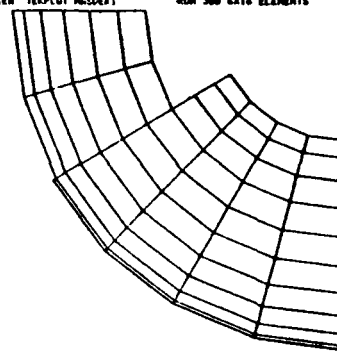
TOP VIEW TEMPLAT HASDEK1 RUN 327 ELEMENTS 1.99999



FRONT VIEW TEMPLAT HASDEK1 RUN 300 6X16 ELEMENTS 1.99999



SIDE VIEW TEMPLAT HASDEK1 RUN 300 6X16 ELEMENTS 1.99999



TOP VIEW TEMPLAT HASDEK1 RUN 300 6X16 ELEMENTS 1.99999

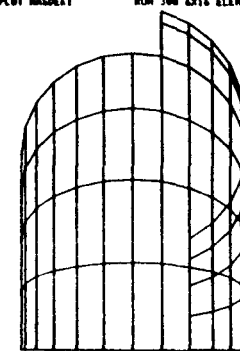


Figure 6-8. Computer Plate and Rotation Definition

Some other considerations in the actual chute geometry involve the fact that the surface is toroidal down to the last section, but at this point the plates in the final section developed in the model are each extensions of the adjacent plates in the previous section. This tangential departure from the "donut" shape is provided with a computer-designated length factor "EXT", to center the flow in the chute for some flow cases.

Another provision in the computer subroutine torus is the capability of specifying removal for clarity and appearance of particular flat plates from the basic mosaic pattern computed (Figure 6-8).

As shown in Figure G-4 of Appendix G, nominal plate numbering is along each cross section segment of the torus in sequence, beginning with the top section and going to the lowest. The numbering along each cross section begins on the side nearest the pulley and goes to the outboard side. When plates are removed, the numbering simply skips those plates. In the final configuration the entire top row of plates and the left side of the second row are so eliminated, since no streams impact in that upper area of the torus math model.

A "sub" subroutine called DIST is used to compute basic plate dimensions, depending on the number of subdivisions and the total angular lengths chosen for (NT1) X(NT2)plates. This is a design aid and the subroutine is not called for every parametric run.

7.0 DYNAMIC ANALYSIS RESULTS

For convenience of presentation, the results of the computer studies are included as Appendix H, in Volume II. Sections H-1 and H-2 of this Appendix cover the free fall/impact and the frictional flow studies, respectively. Discussions in this section, which addresses the 350, 450 and 600 fpm input belt velocity cases, will be in reference to Appendix H. The free fall/impact studies include chute configuration data which is used extensively as a design aid.

7.1 FREE FALL/IMPACT PHASE

1. 350 FPM Trajectory Case

The results of the free fall/impact analysis for a given trajectory vs chute orientation case are presented in Appendix H in the following formats, making illustrative reference here to Run 626, which corresponds to the nominal chute orientation: for the 350 fpm trajectory.

- Input Data (Page H-4), covering parameters on the feed conveyor, the torus chute, run of mine coal, and run convention constants
- Output Data, (Page H5 to H10), covering 1) basic geometry outputs; 2) the X, Y, Z coordinates of the four corners of each of the plates into which the chute is subdivided; and 3) the hit data, which includes for each stream into which the flow mass is subdivided: the time of impact, its angle of impact with the chute surface, and the X, Y, Z coordinates of the hit point. Because of bulk, the output information for all run cases except the nominal ones will be limited to the hit data.
- Design Plots, (Pages H11-H14) covering four (4) computer-plotted views of the conveyor pulley, the chute, and the hit pattern on the chute surface.

Run 626 corresponds to the nominal design orientations presented for the 350 fpm trajectory in section 3.3. The "Y min" value, which is the Y coordinate of the lowest point on the chute, is used to determine the belt-to-belt clearance Y_B in Table 3-2 of section 3 by adding the 12 inch radius above the pulley centerline, plus 8 additional

inches of clearance below the chute. Similarly, the roll, pitch, and yaw rotations specified in Table 3-1 are taken directly from the input data sheet of the computer run (H-4). This same procedure is used for establishing locational and rotational parameters for the nominal chute positions in the 450 and 600 fpm cases.

The X_R , Y_R , and Z_R coordinate locations for the 350 fpm trajectory case are taken from the fourth corner of the 33rd plate, which corresponds to the bottom edge of the chute prior to any rotation. .

The chute position here defines approximately that in run number 72 in section 9.0, where the X, Y, Z locating coordinates of -0.2, -2.0 and -0.5 in Table 9-5, correspond within a quarter of an inch to the first corner of plate 1 (page H-4), if the 0.305, 11.176 and -1.427 are divided by 6 to correspond to the 1/6 scale of the lab chute.

It will be seen with few exceptions that the hit angles at the c. g. , top, and bottom of each stream are less than 30 degrees.

The chute outboard edge, shown by dashed lines in the side view plot of page H-16 was located to clear the upper impact trace by approximately 6 inches, in the event that final translational or rotational adjustment causes this impact line to rise. The corresponding side view in Run 627 shows, for example, the change in the location of the top of the impact zone if the R point on the chute is lowered about a half inch and brought in toward the pulley about 1 inch. The allowance for material above the final hit zone must be minimized to obtain maximum clearance with the pulley.

It will be seen from the front view plot (H-12) that material corresponding to approximately two plates, must be removed in the chute design. In that each plate corresponds to a 30 degree segment, and that the left edge of the cutout shown in H-12 is at the centerline, the final left edge should be at 30 degrees to the right of this centerline. Referring to the flat pattern for the 350 fpm plate segment flat pattern in Figure 3-5, it will be seen that this is where the left edge lies, including a additional triangular area about the upper segment, which corresponds to the second row of plates in the H-12 figure.

2. 450 FPM Trajectory Case

Run 746 corresponds to the nominal design chute position for the 450 fpm trajectory. Reference point R in Table 3-1 corresponds to the fourth corner of plate 29, which is numbered differently from that in the 350 fpm case because the latter contains an additional row of four plates at the upper end. Run 746 also ties in approximately with test runs 481 and 482, whose locational coordinates in Table 9-6 correspond to those at the fourth corner of plate 32, the latter being at full scale.

The outboard edge of the chute wall, as shown in the side view plot of Run 746, is well above the hit zone, and will accommodate shifts of this zone due to rotational ranges introduced during the testing phase, such as that shown in Figure 706. The peculiar hump at the lower end of the hit zone in the Figure 706 side view is an anomaly due to the coarseness of the plate subdivision chosen. When the subdivision is 15° plate segments instead of 30° , as shown on the page immediately following for a shorter chute at the same location and orientation, the hit zone is seen to smooth out.

3. 600 FPM Trajectory Case

Run 846 corresponds to the nominal design chute position for the 600 fpm trajectory. Reference point R in Table 3-1 corresponds to the fourth corner of plate 29, as in the 450 fpm case. This run also corresponds to Test run 462, for which the locating coordinates given in Table 9-6, tie to the fourth corner of plate 32, at full scale.

The location of the outboard edge above the hit zone is shown in the side view plot, where again the top of the former shows perturbations due to the coarseness of the plate subdivision.

A problem of wave front stability still existed in final computer runs of the model for frictional flow down the surfaces of the nominal chute configurations defined in the previous section. A number of steps were taken regarding the modification of the initial math model (Appendix D) to correct the problem, including changing the logic as to the direction of the hypothetical dividing planes between stream subdivisions of different height. Various step increment sizes were tried for the moving of the net down to the surface. It was found also that additional work was required on the surface radius computation, upon which the centrifugally derived friction effect depends.

Page H-66 and H-67 show one of the typical computer log formats for maintaining the dynamic parameters of each stream during its stepwise movement. In addition, the right hand four (4) columns present the successive locations of the stream wavefront, given, respectively, in terms of X, Y, Z coordinates, and plate number location (referring to H-4 to H-8, for example).

The balance of Appendix H-2 presents computer plots taken from preliminary friction flow runs at 0 and 20 degrees, for various trajectories. It will be seen that, for the most part, the general flow directions are evident, despite the random perturbations associated with point location, which correspond to computer overflow conditions due to the remaining math model instabilities. Some of the random data in the runs has been removed from the plots for clarity.

Prior to attempting higher wall friction coefficients ($\tan(\phi')$), it would be necessary to model a smoother inter-relationship between adjacent streams, as well as improve the radius subroutine.

It will be noted that the plot data shown, as well as the tabular data identified above, relates to the movement of the stream net, once all streams have been incorporated into this common net, after initial impact. The net formation phase, which is documented in a cumbersome computer printout format not presented here, is a very smooth process, ranging up to 40 steps in itself, prior to the step sequence in the table on H-66, 67. The computer plots shown record wavefronts at every tenth step after the full net is formed.

8.0

LABORATORY CHUTE SCALE MODELS AND TEST EQUIPMENT

FSEC constructed a number of one-sixth size scale models of chutes during this study program. The modeling efforts related to two different activities:

1) the development and evaluation of various concepts, which were screened in the tradeoff analysis discussed in Section 6; and 2) to testing of that chute geometry identified for detailed study, the torus. This section describes the various scale models fabricated and tested, together with basic test equipment utilized, and the scaling considerations involved.

8.1 SCALE MODEL CONSIDERATIONS

8.1.1 Dimensional Analysis

Two groups of parameters are involved in addressing options and constraints relative to scale model testing: 1) material flow characteristics applicable to free, open channel flow; and 2) chute geometry and associated material trajectories.

Because free, open channel flow characterizes the functional flow mechanism of interest in transfer point chutes, all of the materials flow characteristics applicable to the analysis are effectively dimensionless. In particular, because steady velocity profiles in a mass-flow configuration characterize chute flow, only two material parameters are involved:¹

1. Effective angle of internal friction δ
2. Kinetic angle of wall sliding friction ϕ'

In an actual laboratory size scale test, one additional constraint applied to materials parameters is that the largest lump size should not be greater than about 1/4 to 1/3 of the belt width, relating to the idler trough.

In the pre-friction flow phase of the transfer point analysis, it is necessary to duplicate the shape of the free fall trajectory relative to the chute scale size selected, as well as the pulley diameter applicable. Referring to Figure 8-1, the relationship required between the scale size selected (s) and the full size configuration (f) is

$$\xi_s = \xi_f$$

¹ Modelling Flow of Bulk Solids, J. R. Johnson, Powder Technology, May 14, 1971

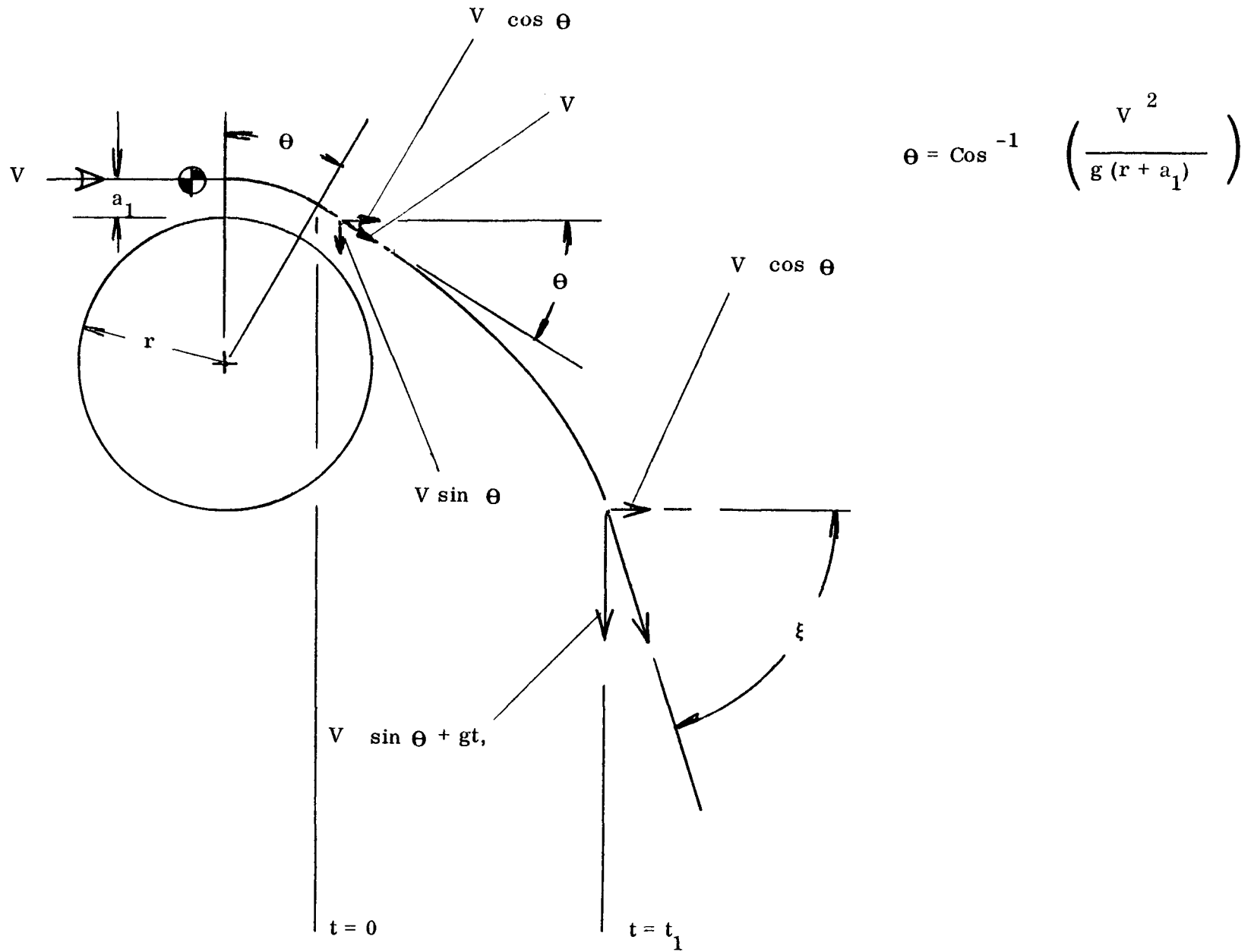


Figure 8-1 Free Fall Trajectory Parameters

That is,

$$\frac{V_s \sin \theta_s + gt_s}{V_s \cos \theta_s} = \frac{V_f \sin \theta_f + gt_f}{V_f \cos \theta_f} \quad (2)$$

or

$$\tan \theta_s + \frac{gt_s}{V_s \cos \theta_s} = \tan \theta_f + \frac{gt_f}{V_f \cos \theta_f} \quad (3)$$

By definition of equivalency of trajectory shape,

$$\theta_s = \theta_f \quad (4)$$

Also, in the horizontal direction, for either case,

$$t = \frac{X}{V \cos \theta} \quad (5)$$

Hence, substituting equations (4) and (5) in equation (3) and clearing common terms

$$\frac{X_s}{V_s^2} = \frac{X_f}{V_f^2} \quad (6)$$

This can be expressed in the form,

$$\frac{V_s}{V_f} = \sqrt{\frac{X_s}{X_f}}, \quad (7)$$

indicating that for any scale factor X_s/X_f chosen, the ratio of the velocities must be the square root of this ratio.

It will be seen from section 2 of Appendix B, that because the following relationship holds

$$\theta = \cos^{-1} \left[\frac{V^2}{g(r + a_1)} \right]$$

the above dimensional relationship between the velocity and the pulley size holds identically to that for the velocity and the chute size.

8. 1. 2 Laboratory Test Scale Size

Because relatively minor dynamic constraints govern selection of the scale size for laboratory testing, it is possible to choose one where the cost and inconvenience of handling and storing large amounts of bulk materials can be minimized and also where the most readily available conveyor test equipment can be chosen. In the case of the 1/6 scale model chosen, it will be seen that the normal peak flow rate, at full scale, of about 18 tons per minute on a 600 fpm, 36 inch belt conveyor reduces to

$$\begin{aligned} Q_s &= (18 \times 2000 \text{ lbs}) \times \left(\frac{\text{Cross Sectional}}{\text{Area Scale Factor}} \right) \left(\frac{\text{Velocity}}{\text{Scale Factor}} \right) \\ &= 36,000 \times (1/6) \times \left(\sqrt{1/6} \right) \\ &= 408 \text{ lbs/min} \end{aligned}$$

For a test run of one minute, this figure corresponds to the following volumetric requirements;

<u>Material</u>	<u>Density</u>	<u>1-minute Flow Volume</u>
Coal	55 lb/ft ³	7.4 ft ³
Sand	100 lb/ft ³	4.1 ft ³

8. 2 LABORATORY TEST EQUIPMENT

8. 2. 1 Test Conveyors

The most practical means of producing flow volumes with the required trajectory shapes and uniformly reproducible flow rates was judged to be a 1/6 scale size conveyor, i. e. , with a 6 inch wide belt. One further critical feature required, in order to obtain the trajectory shape, is that the radius to the belt surface also be 1/6 that of the full size case in order to duplicate the full scale radial angle of departure θ of the flow mass from the pulley. For 24 inches the largest size pulley diameter available for a 36-inch wide belt conveyor, the exterior scale size radius must then be 2 inches for the feed conveyor.

Figure 8-2 shows the scale model conveyors utilized in testing, together with a typical scale mode chute (see 8. 3. 5). The feed conveyor has a 6 inch wide, slider bed-type, troughed conveyor and is 10 feet in length. Its 3 1/2 inch pulley diameter and

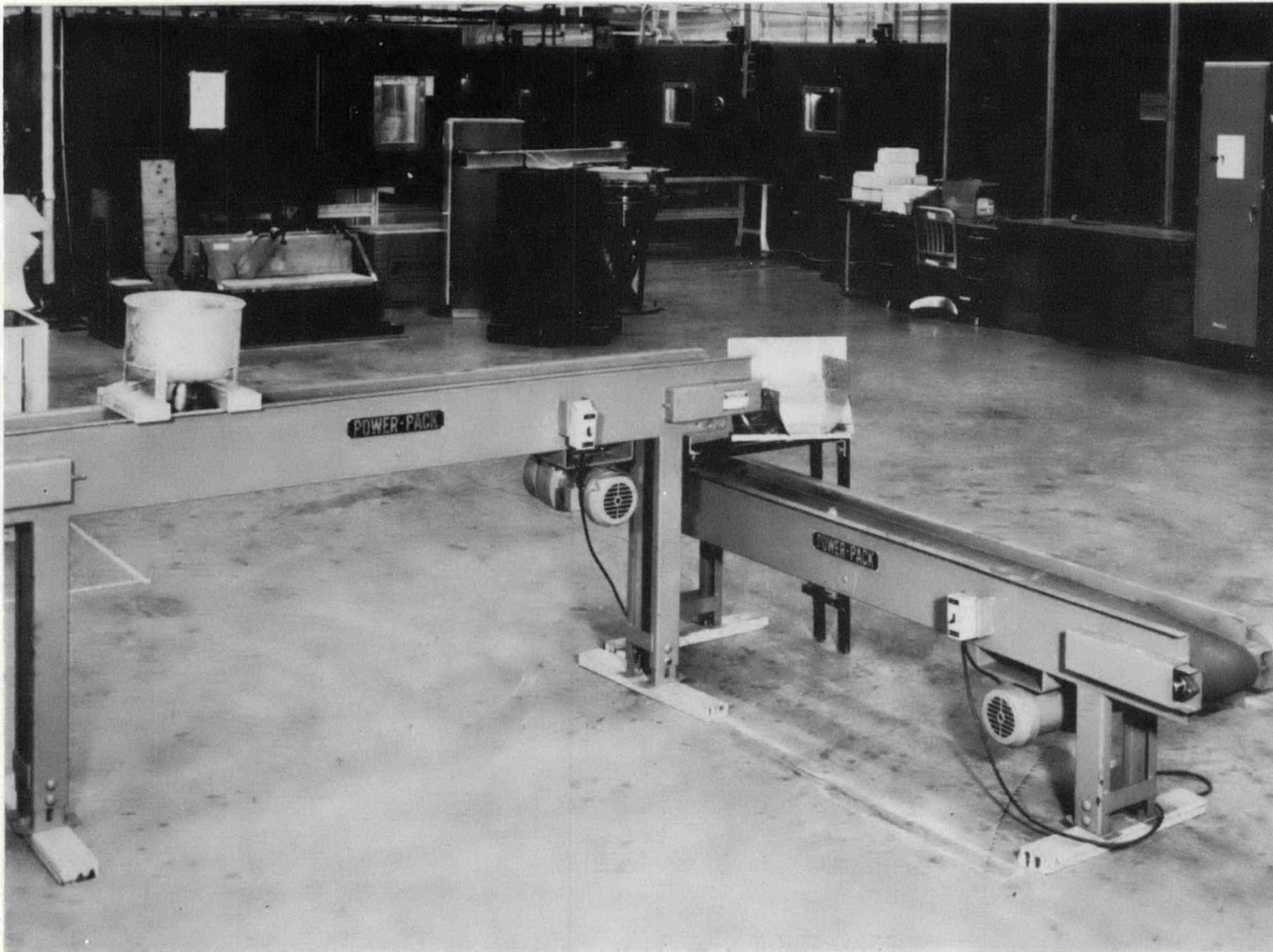


Figure 8-2. 6-Inch & 8-Inch Test Conveyors

1/4 inch thick belt yields the required exterior 2 inch radius.

The receiving conveyor, also 10 feet long, has an 8-inch belt width. For the 1/6 scalefactor, this corresponds to a full size conveyor of 48 inches.

Each conveyor is driven by a 1/3 hp motor, utilizing a chain sprocket drive reduction to the pulley shift to obtain the required belt speed. Provision was made in the chain drive assembly to adjust the belt speeds to values which are average value and limiting values for the applicable range at full scale. Table 8-1 summarizes the details of this provision:

Table 8-1
Belt Speed Variation Provision in Scale Model Conveyors

Scale Model Conveyr	Speed Range Value	Sprocket Provision			Belt Velocity, Fpm	
		No. Teeth DrivrSpkt	No. Teeth Drvr Spkt	R ratio	Scale Model	Full Size Equiv. (X 6)
6" (Input)	low	14	26	1.84	143	350
	average	14	20	1.43	184	451
	high	14	15	1.07	246	602
8" (Output)	low	16	21	1.29	204	500
	average	16	17	1.07	245	600
	high	16	14	.88	301	737

8.2.2 Flow Feed Provision

A conical hopper with about a 4.5 cubic foot capacity was constructed to provide about a minute's flow at peak capacity for test sand, Figure 8-3 shows the hopper in place above the feed conveyor. After filling, the hopper is raised to the position shown on a hydraulic fork lift. (Figure 8-3a).

8.3 CHUTE SCALE MODELS

8.3.1 Conceptual Scale Model Phase

The following models were developed during the conceptual development phase. Conceptual rationale for the various iterations is also discussed in 9.2 and 9.3.

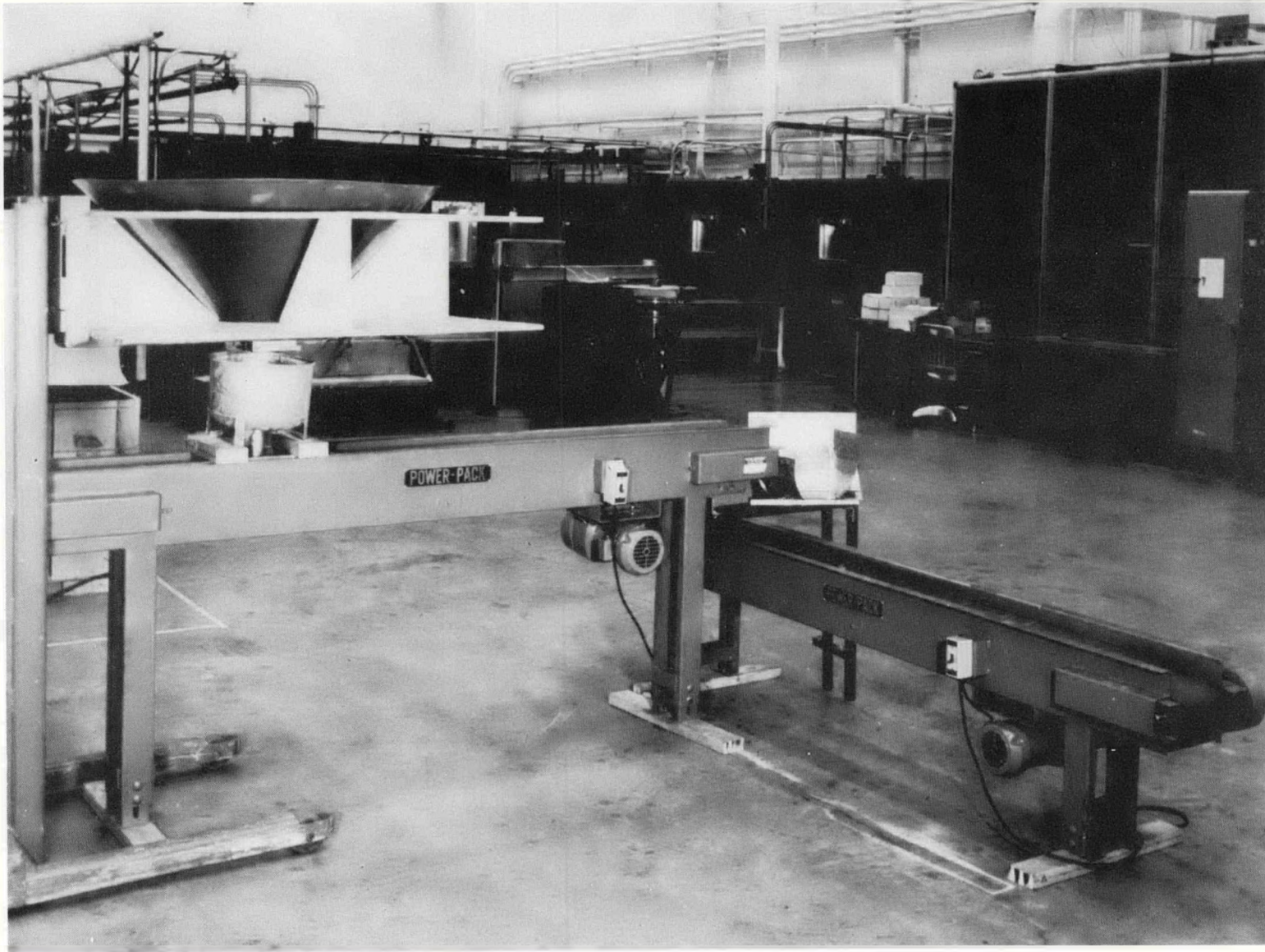


Figure 8-3. Transfer Point Test Setup

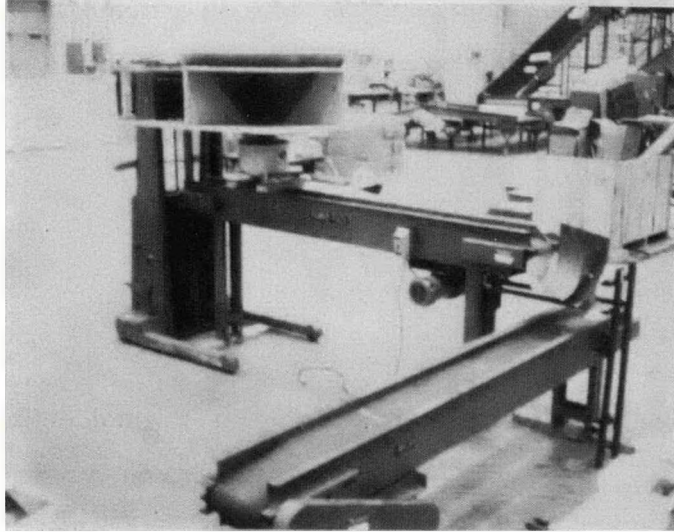


Figure 8-3a. Hopper Lift

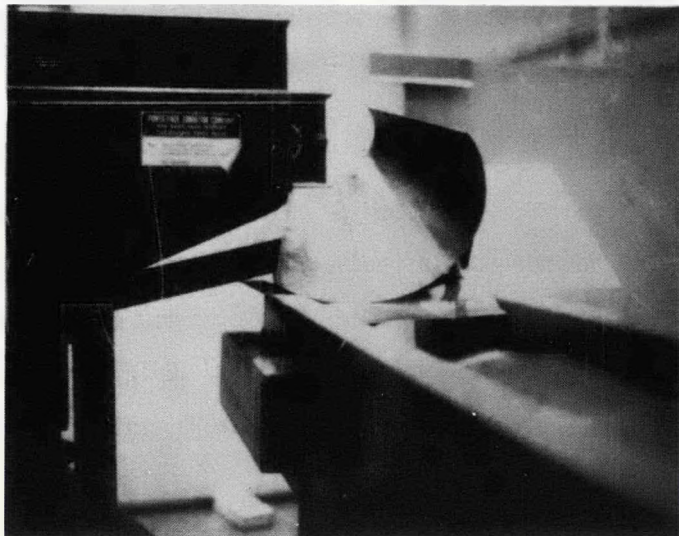


Figure 8-4. 15° Cone Scale Model

8.3.1.1 Conical Models

Two different types of cone scale models were designed and constructed. The first was an multi-section assembly, with a fifteen degree opening angle (Figure 8-4). It consists of the following elements:

- Piece 1 (Figure 8-5)
A base section, containing the curved portion of the cone on the inboard (to the pulley) cone side and a flat section located along the lowest quadrant, which is capable of being varied in width by sliding Piece 2 on it.
- Piece 2 (Figure 8-6)
The lower outboard quadrant of the cone.
- Piece 3 (Figure 8-7)
The upper, outboard section of the cone, which defines a variable cone arc above piece 2 by varying its degree of overlap therewith.
- Piece 4 Figure 8-8)
A flat, initial impact plate, which is an optional attachment to Piece 3.

A second type of cone section is depicted in Figure 8-9. Nominally called a cone because of its similarity to the previous configuration in the manner of its alignment orientation, the opening angle of this cone is zero degrees.

8.3.1.2 Cylindrical Models

Two basic cylindrical geometries were defined and constructed. The first is an approximately 90 degree cylindrical quadrant, terminating at the upper end with a flat vertical wall (Figure 8-10). The second configuration is a compound version of the first, consisting of a pair of additional cylindrical quadrants, which are provided as side constraints on the flow as it slides down the main cylindrical section. (Figure 8-11)

8.3.1.3 Toroidal Models

Two groups of torus chute scale models were designed and fabricated

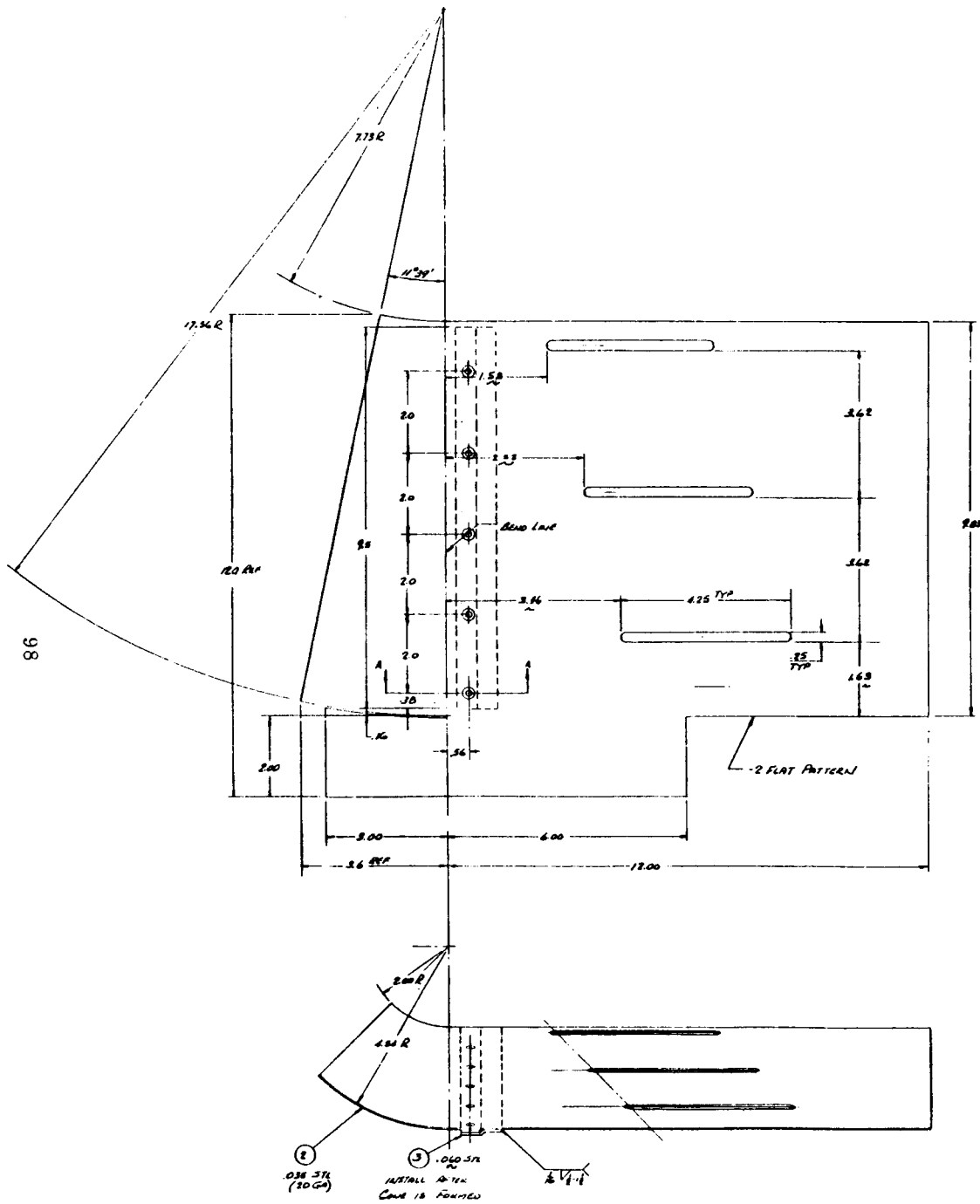
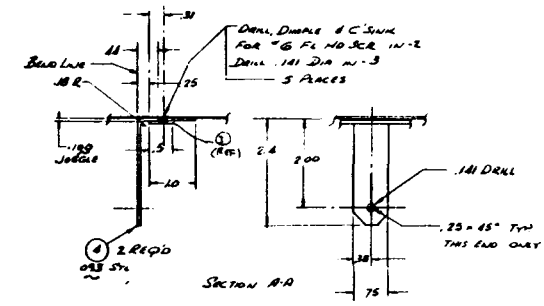


Figure 8-5, Cone Baseplate



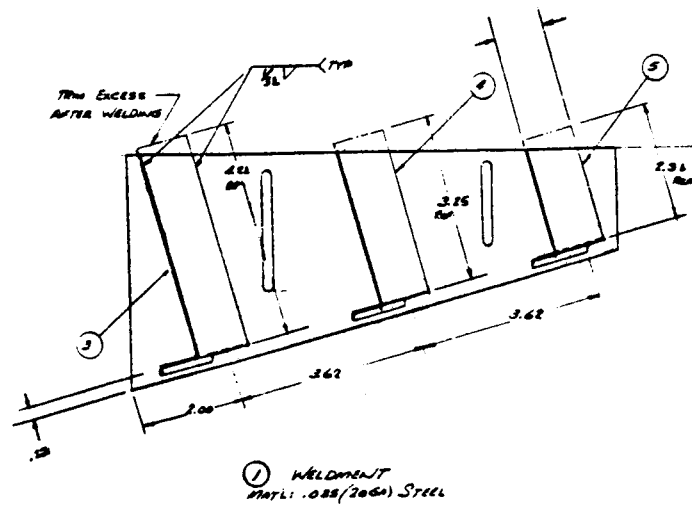
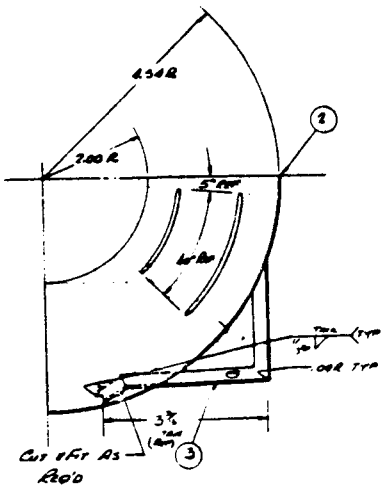
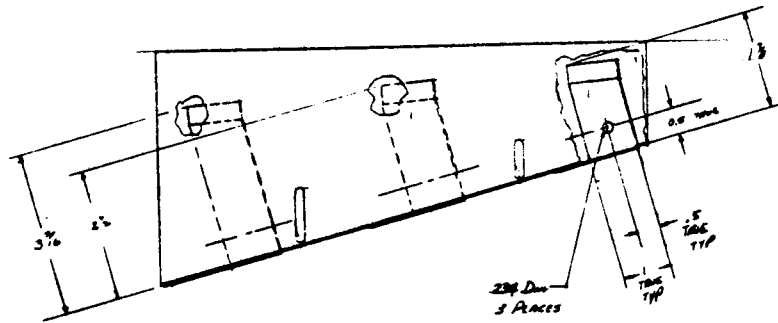
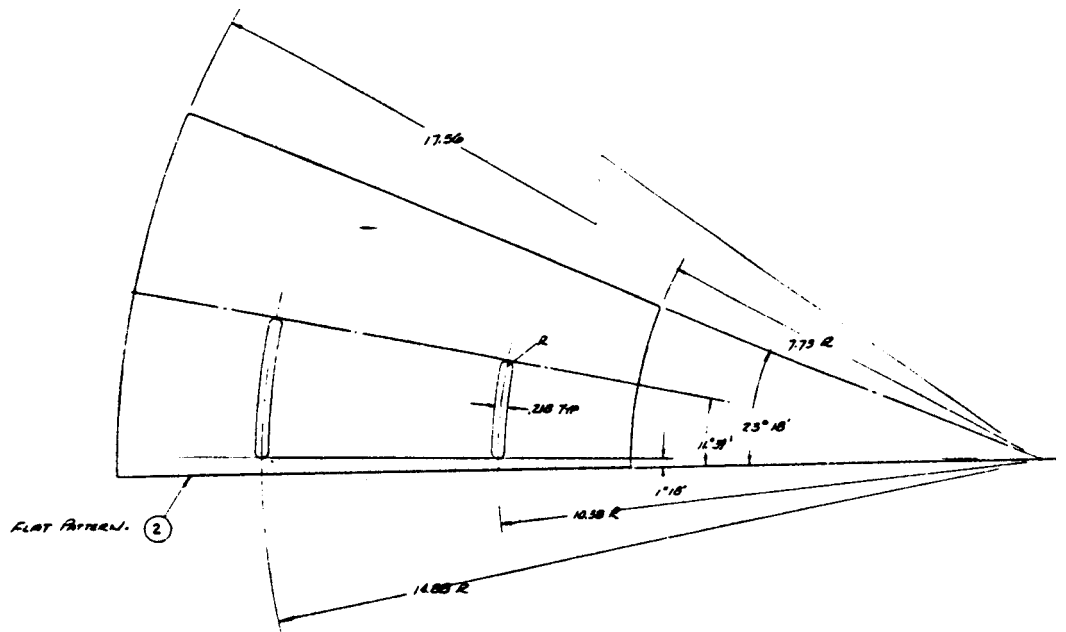


Figure 8-6. Lower Quadrant, Cone Model

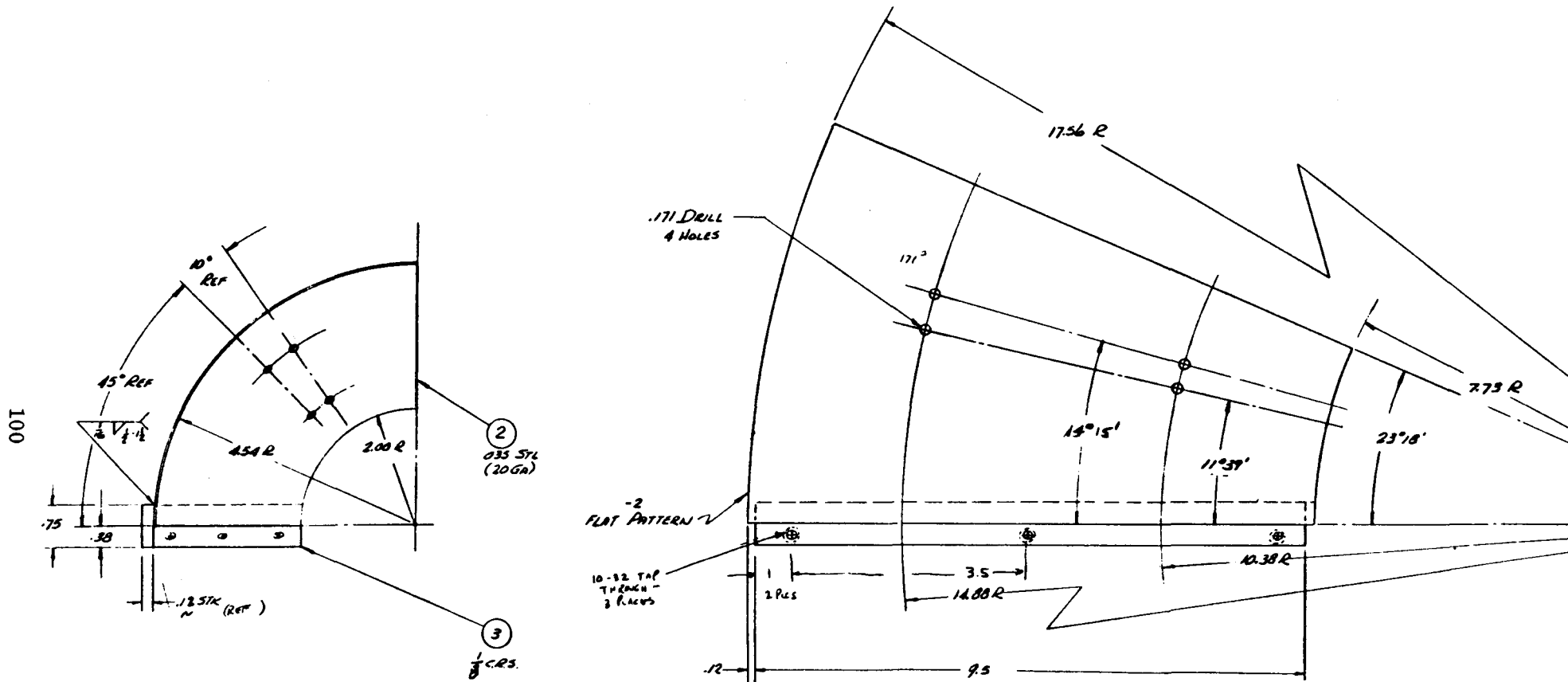
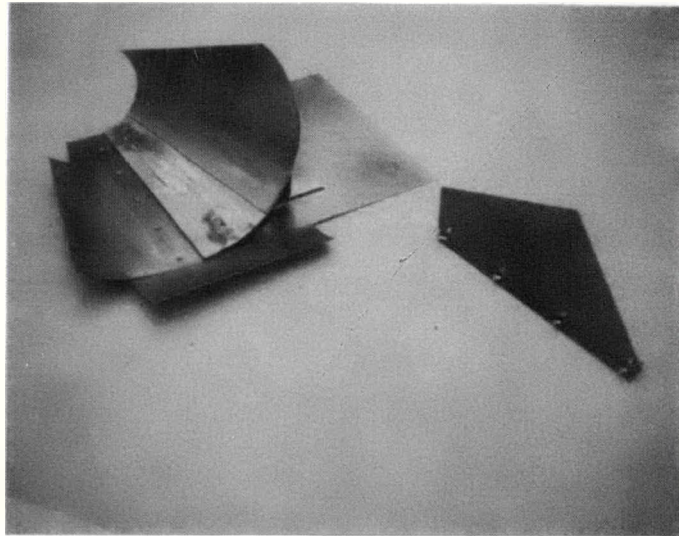
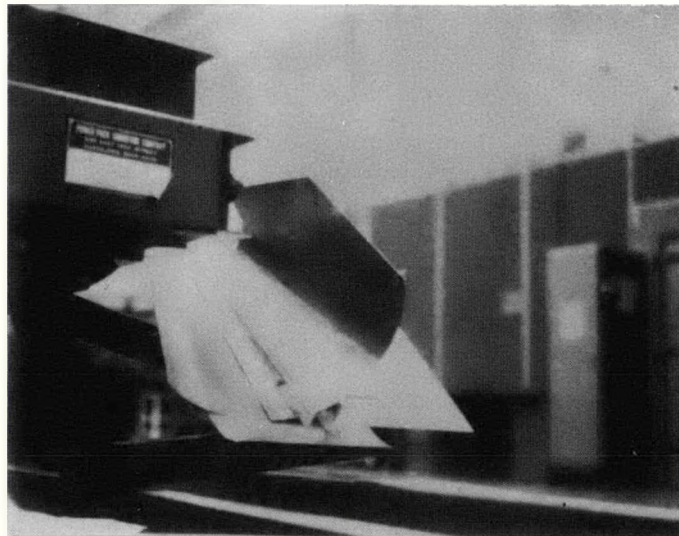


Figure 8-7. Upper Quadrant, Cone Model

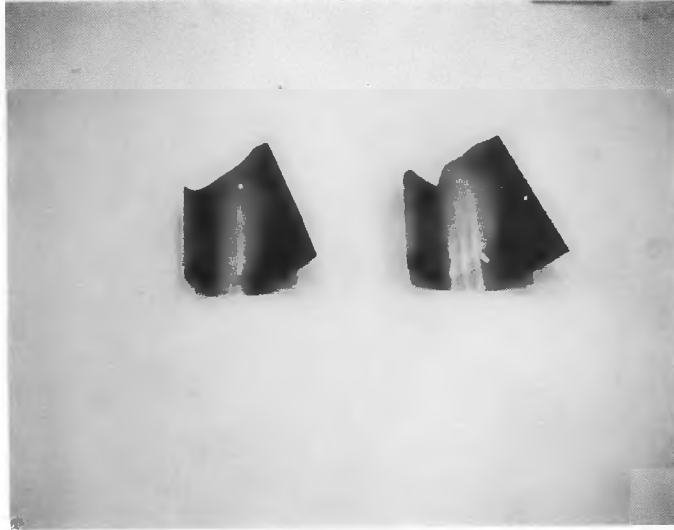


Impact Plate Separate

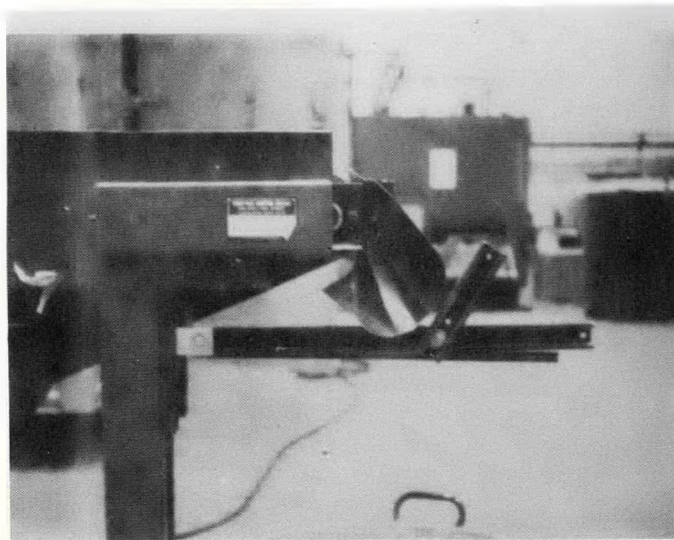


Installation

Figure 8-8. Cone Model with Flat Impact Plate

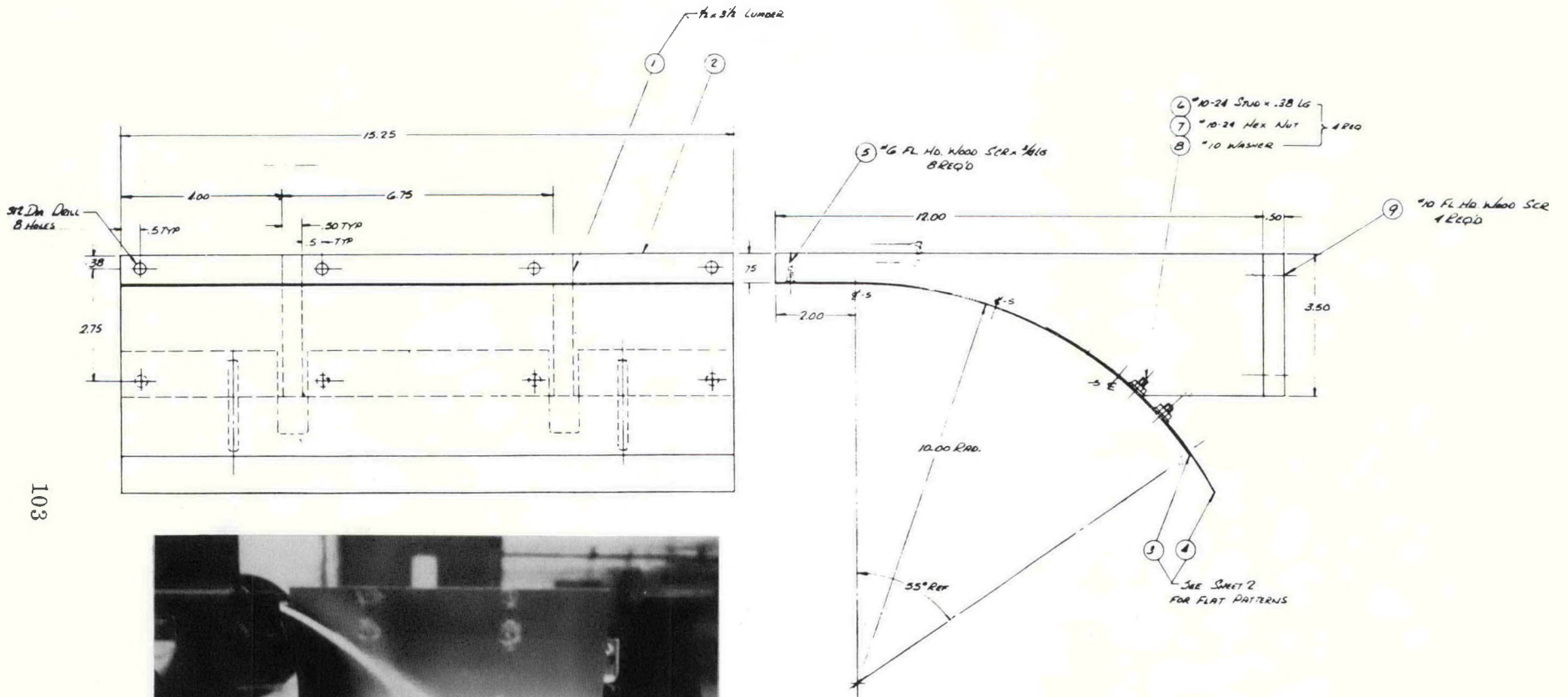


6" Dia. 8" Dia.



Installation, 6" Dia.

Figure 8-9. Zero Opening Angle Cone



103

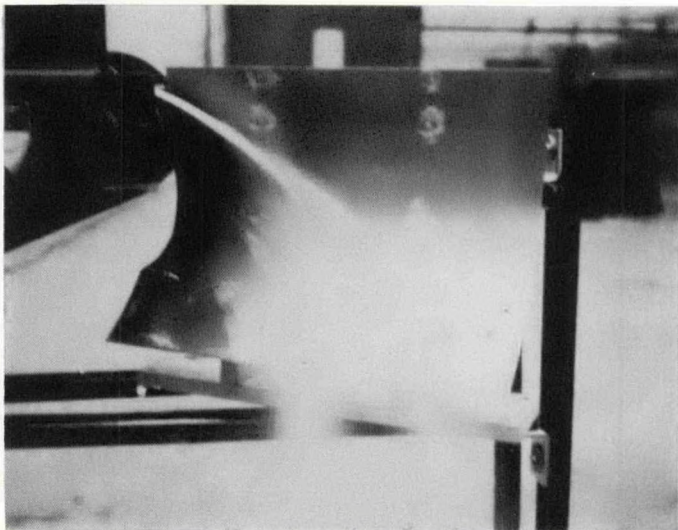


Figure 8-10. Quarter Cylinder Model, Single Surface

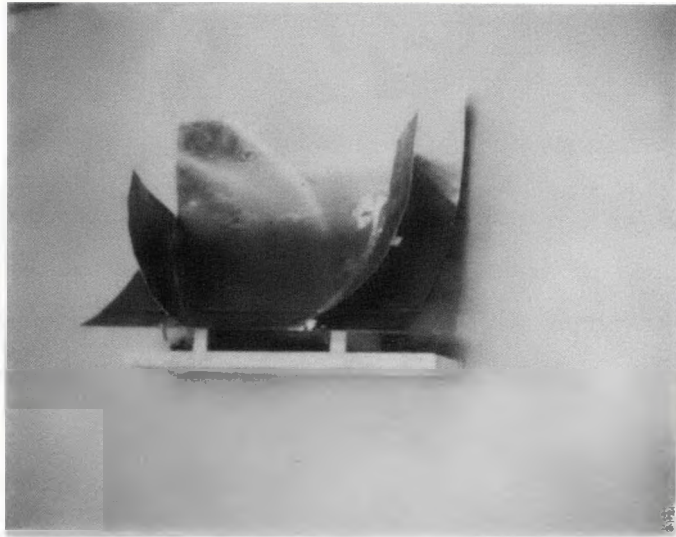
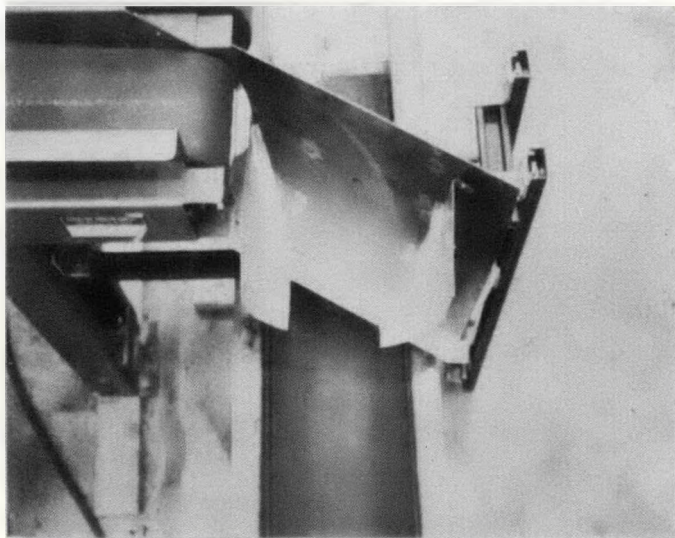


Figure 8-11. Compound Quarter Cylinder Model



iteratively during the initial conceptual stage. The first group involved a series of smooth toroidal surfaces, corresponding to sections cut from 90-degree welding elbows. The second group were similar in basic geometry, except that they were cut from 90-degree, "smoke pipe " elbows, or hot air ducts. The fabrication of the second group involved very informal methods, the purpose of these models being to determine whether significant departures in flow pattern occurred when a smooth toroidal surface is broken into series of intersecting cylinders.

8.3.1.3.1 Smooth Torus Configuration

Smooth torus configurations were constructed in 6 inch and 8 inch minor scale size diameters. The first set designed are shown in Figure 8-12. Their outboard wall, relative to the pulley side was found during testing to be cut too low. The length of the vertical curve along the major radius was similarly made too short.

A second torus configuration was built to redeem the shortcomings of the first. Shown in Figure 8-13, it consisted of a much higher outboard wall; and its vertical curve length was extended by virtue of a two piece construction. The lower section was provided to guide the final flow vector leaving the end of the torus. The lower section is a rotatable attachment to the upper one, provided to realign the slot opening with the bottom of the first section as its roll position varies.

8.3.1.3.2 Smoke Pipe Torus Configurations

The smoke pipe torus configurations modelled involved various modifications of basic 90 degree, 4-section, hot air duct elbows. Although a number were investigated, the most typical ones are shown in Figure 8-14. They include modifications of both 6-inch and 8-inch minor diameters, where once again the variations involved pertain to the amount of outboard sidewall retained as well as to the length of the vertical curve.

8.3.2 Additional Torus Configuration Scale Models

Subsequent to selection of the torus shape as the preferred chute geometry, an additional design iteration was performed to define configurations suitable for 350 fpm

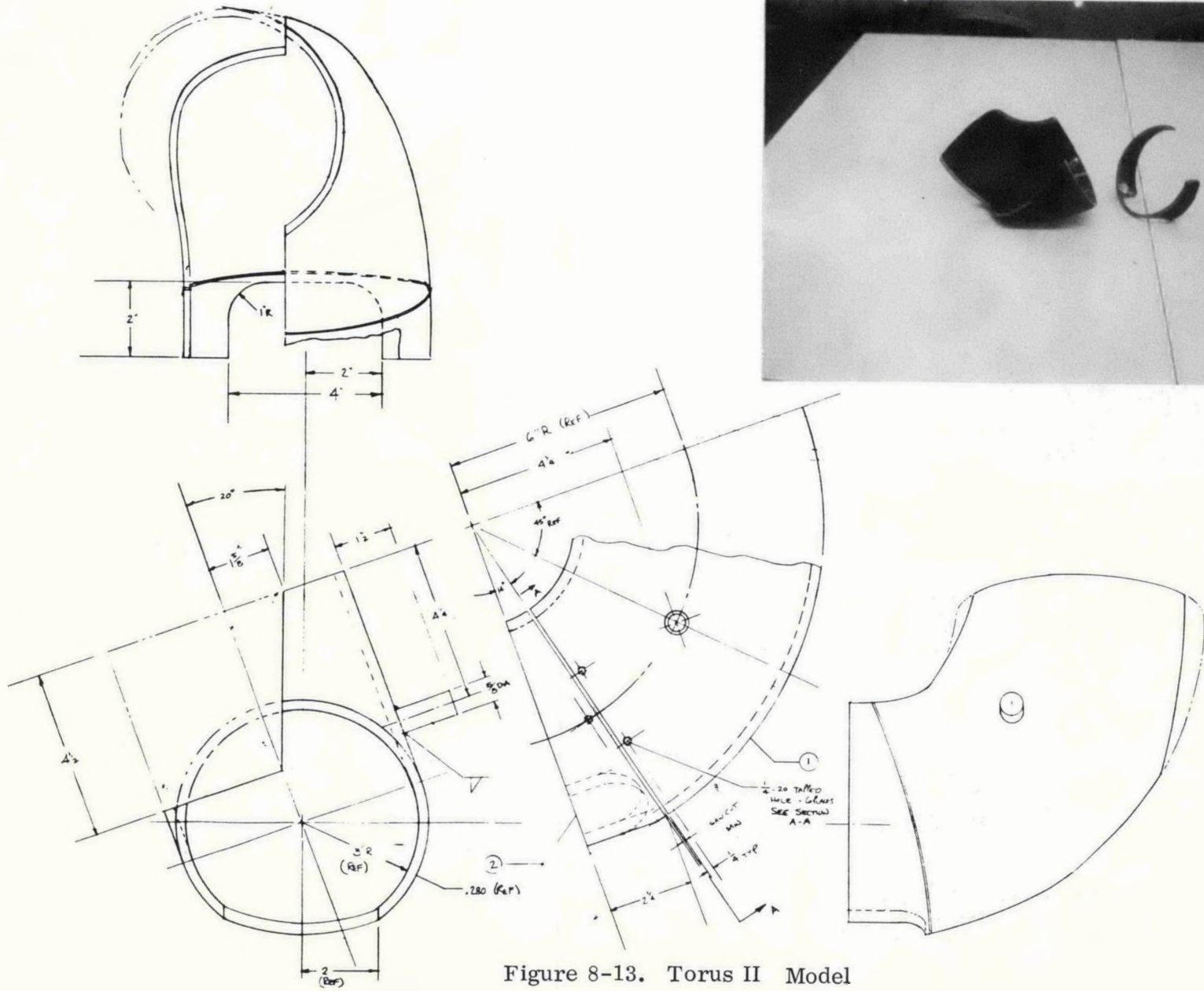
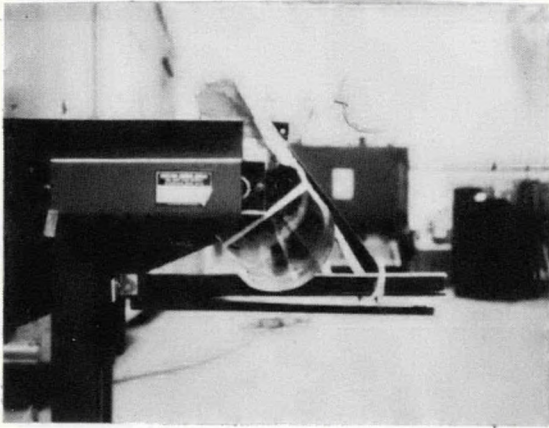
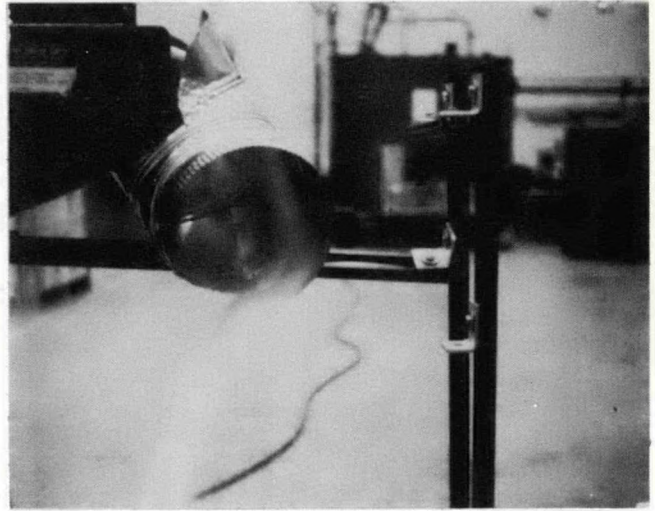


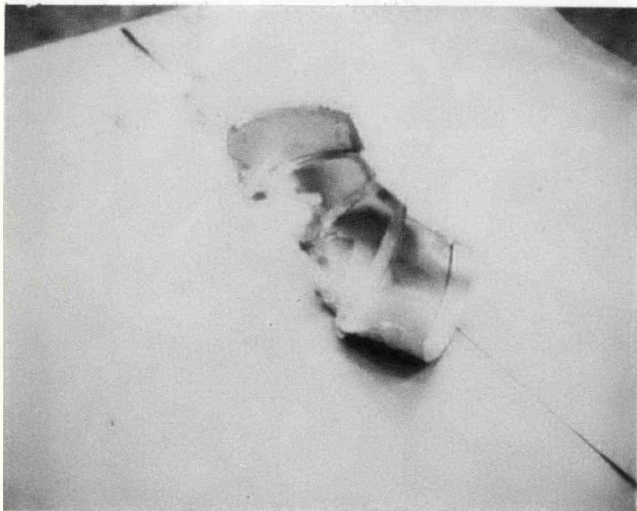
Figure 8-13. Torus II Model



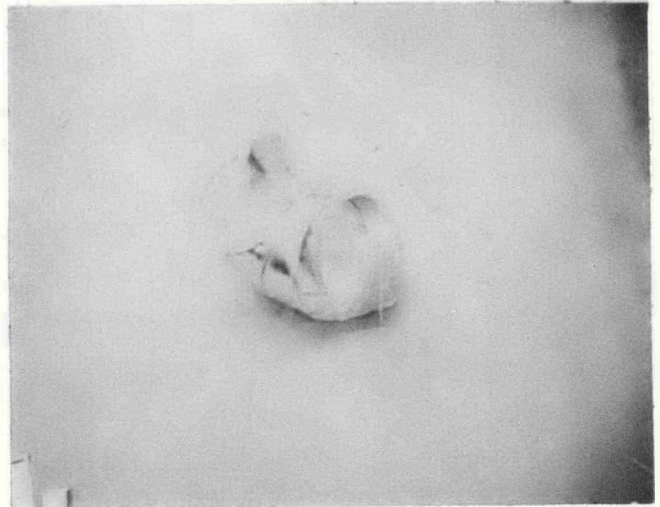
Installation: Run 126



Installation: Run 111

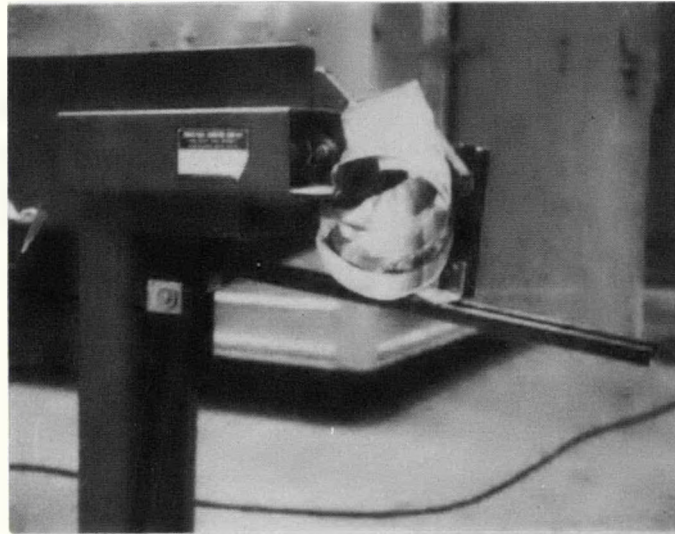


8" Minor Dia. High Configuration

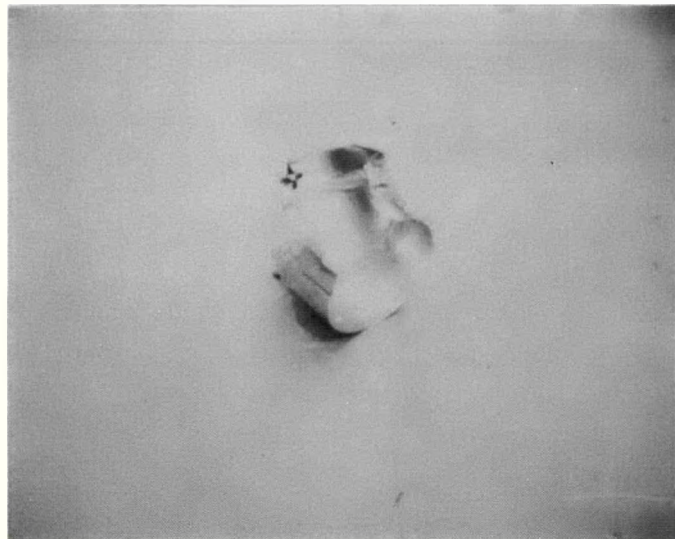


8" Minor Dia. Low Configuration

Figure 8-14a Smoke Pipe Torus Models - 8"



Installation: Run 131



6" Minor Dia.

Figure 8-14b Smoke Pipe Torus Model - 6"

and 450 fpm input flow velocities, as well as the 600 fpm figure used in the conceptual screening phase of the work. This resulted in the configuration shown in Figure 8-15, covering the specific 450 and 600 fpm cases and generally an approximate range between 400 to 600 fpm, for which the angle θ of trajectory departure from the pulley surface is 0 degrees. In addition, the configuration for the 350 fpm case, covering up to about 400 fpm is shown in Figure 8-16. This last scale model is the one defined in the drawing depicted in Figure 8-13.

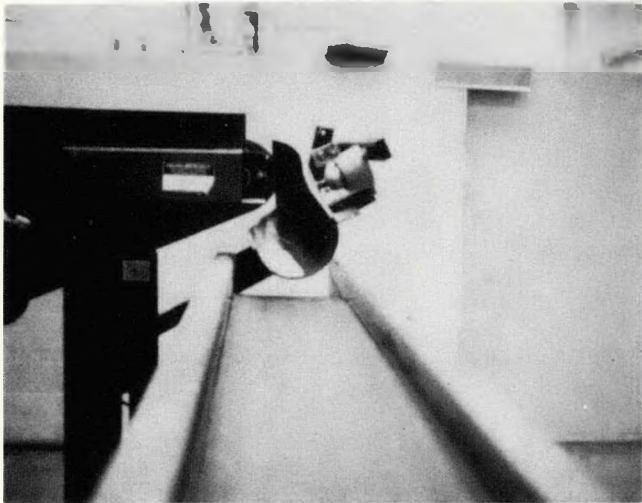


Figure 8-15C. Torus III Installation

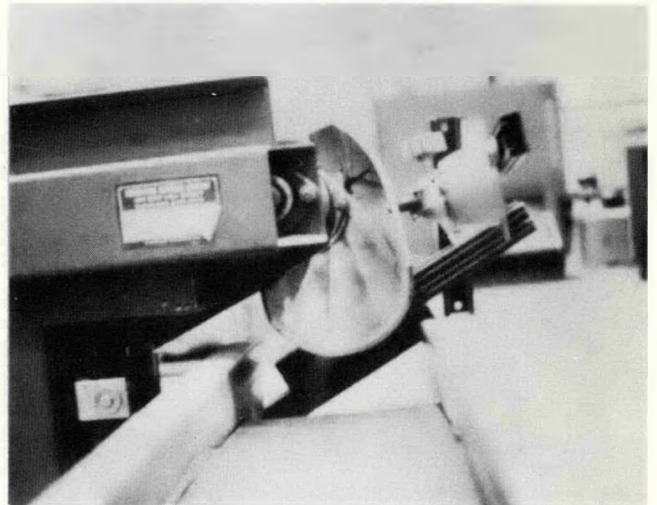


Figure 8-16. Torus I Installation for 350 FPM Feed

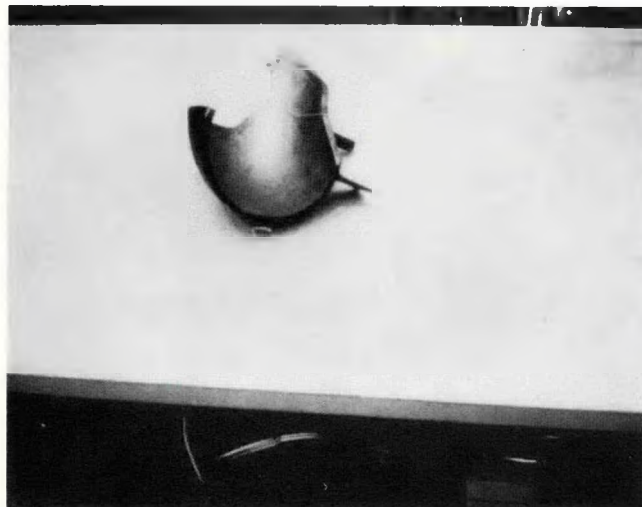


Figure 8-15B. Torus III Model

9.0 LABORATORY TESTING

9.1 FLOW MATERIALS UTILIZED

Flow materials utilized at different phases during scale model testing included primarily Ottawa sand, with occasional use of run-of-mine coal, including rock. Apart from the advantages of cleanliness and consistency of flow through the hopper test fixture, the Ottawa sand was the most useful material from the standpoint of tracing flow patterns --- particularly at the impact area.

Table 9-1 summarizes the data on the specific mixtures utilized in testing, in addition to the original Ottawa sand grade constituents of the mixes. The majority of testing was performed with the Code C mix. This contains four different Ottawa grades covering the range of about 15 available, wherein Flint Shot and F-140 are the coarsest and finest, respectively. This mix gives a well-proportioned profile of particle sizes.

Figure 9-1 shows some coal samples made available to FSEC during the

Table 9-1
Sand Mixtures Used in Scale Model Testing

Item	Description	Test Use Code	% Retained on (Sieve #)								Remarks
			30	40	50	70	140	200	270	Pan	
1	Flint Shot	A	30	65	5						Ottawa Std
2	Crystal	-	1	31	51	13	3	T			Ottawa Std
3	#17 Silica	-			45	29	13	4	1	T	Ottawa Std
4	F-140	-		T	2	8	36	31	12	11	Ottawa Std
5	Items 1 & 2	B	16	48	28	7	1	T			Equal Parts
6	Items 1, 2, 3, 4	C	8	26	26	12	13	9	4	2	Equal Parts

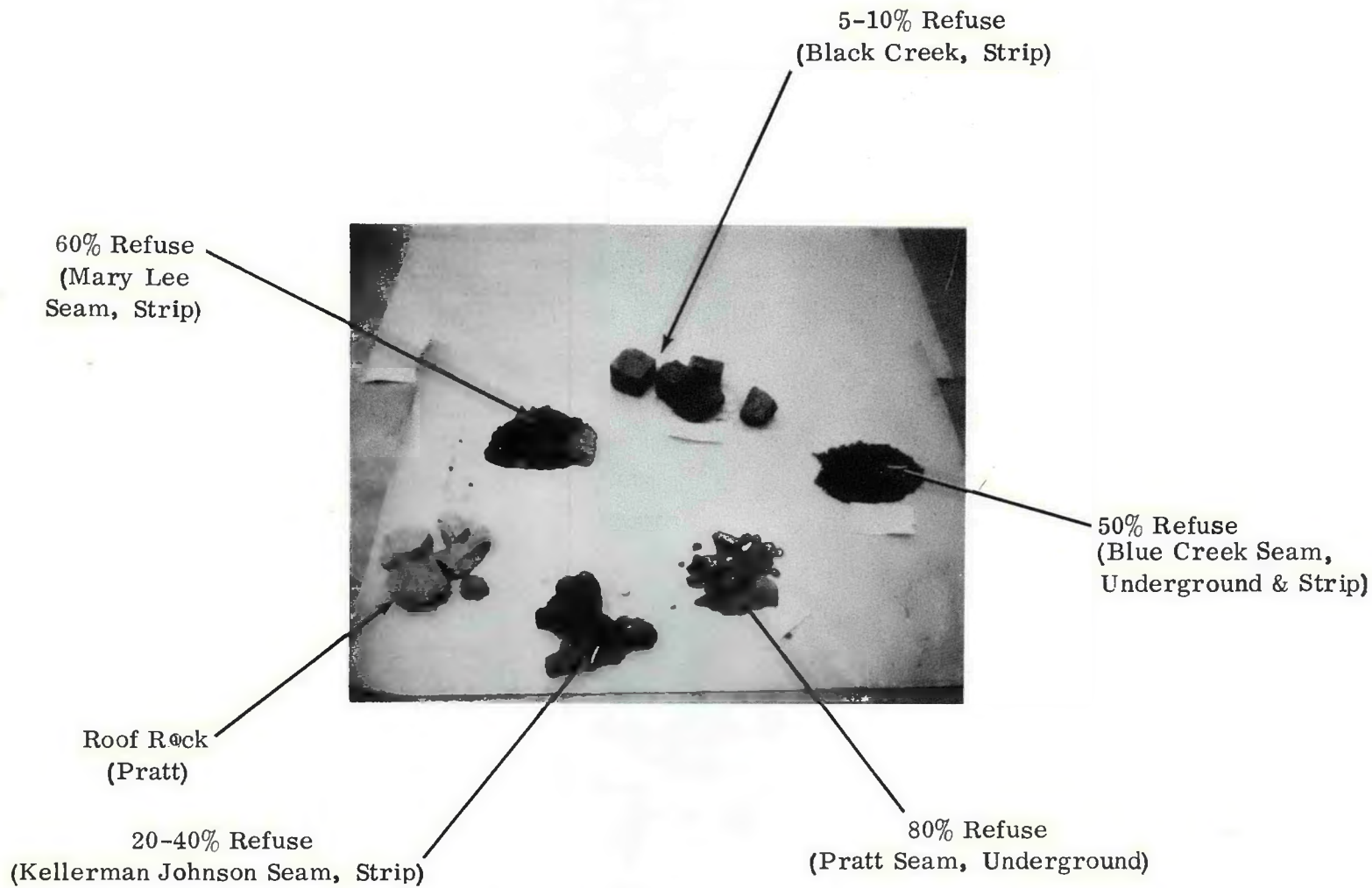


Figure 9-1. Run of Mine Coal Samples

study program. Informal lab testing was performed with a number of these; and the results, within the limitations of the method of feeding this coarse material, did not appear to deviate significantly from those for the sand flow pattern. Close hand observation of the coal frictional flow, because of the variation in particle size and the scale size used, was not an efficient method for parametric optimization of the chute performance; and on this account sand was the preferred test material for scale model testing.

Periodically during testing, roof rock (Figure 9-1) was introduced onto the feed belt (Figure 9-7), to verify chute clearance with the head pulley.

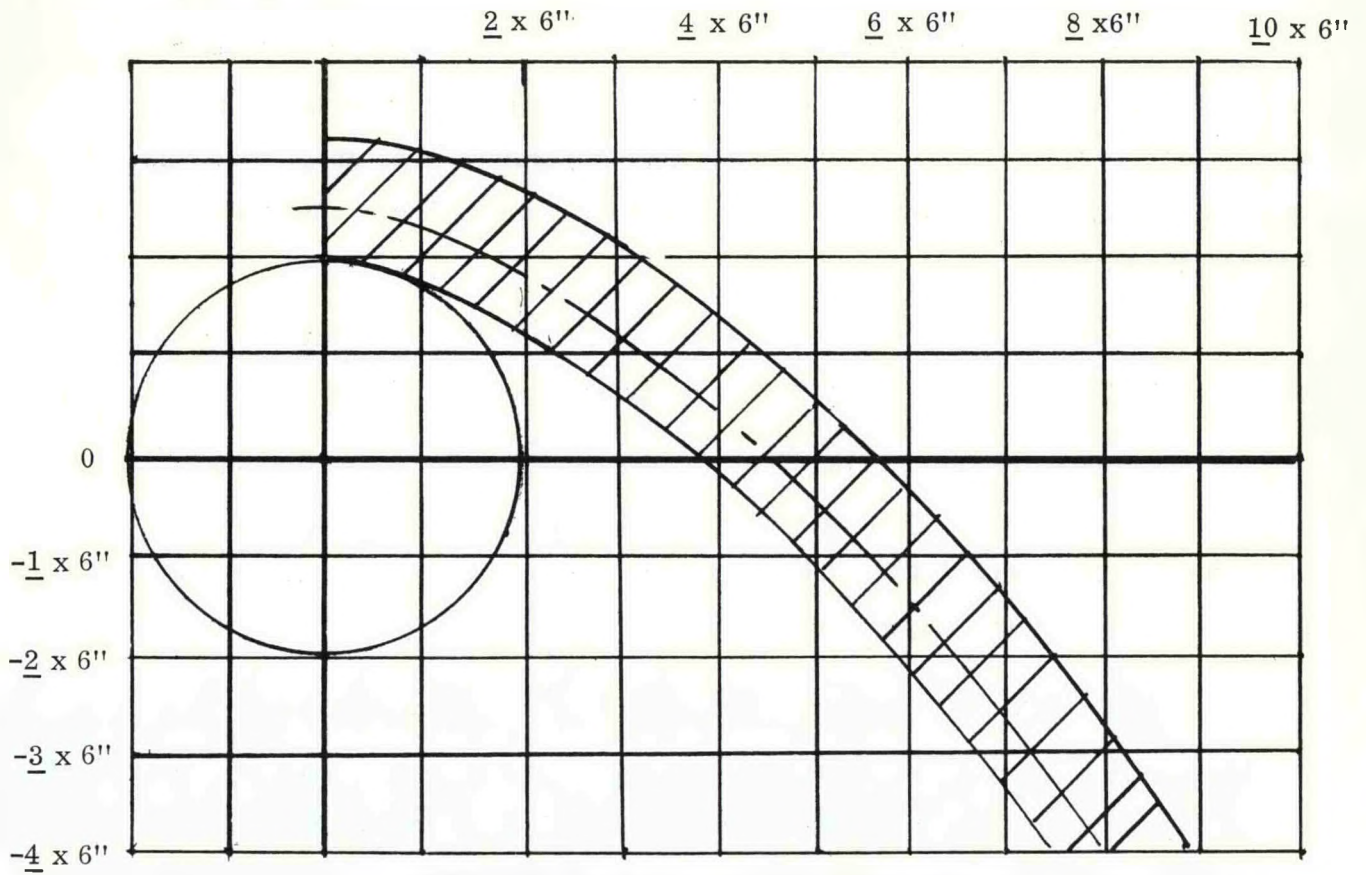
At the beginning of the laboratory testing program, a confirming comparison was made between the CEMA trajectory theory (5.1.2) and the velocity scale down theory (8.1.1). As shown in Figure 9-2, very good agreement was found between the two trajectory shapes.

9.2 INITIAL LAB TESTING OF DEVELOPMENT CONCEPTS

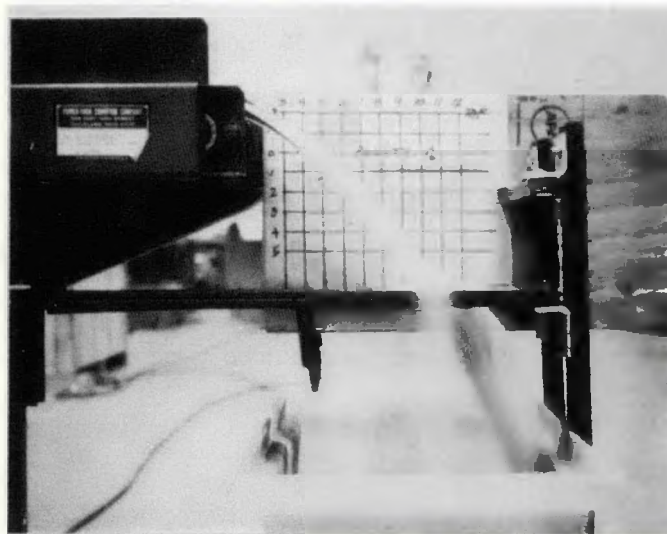
Laboratory scale model testing results constituted a major criterion in screening of initial chute configuration concepts, which is covered in Appendix G. This section covers the details of the test results. The test run data are provided in the form of tables and in photos referenced to the run numbers.

9.2.1 Cone Model Tests

The tests of the various cone configuration are summarized in Table 9-2, and in Figures 9-3 to 9-11. The overriding disadvantage with the opening angle cone configurations was inherent divergence of flow during descent (Runs 201-206). Although repositioning of the cone relative to the free fall trajectory made it possible to prevent the impact split, the divergence problem could not be resolved. (Next text page: 9-9).



600 FPM Trajectory (CEMA Theory)



246 FPM Test Trajectory (1/6 Scale)

Figure 9-2. Correlation Between Theoretical and Test Trajectory Shapes

TABLE 9-2

SCALE MODEL TEST RESULTS FOR CONE CHUTE CONFIGURATIONS

Run No.	Chute Config.		Flow Material	Locating Coord*			Y Min. In.	G _L Attitude			Deviation From 90° Turn	Remarks		
	Half Angle	Other Features		X In.	Y In.	Z In.		Roll o	Pitch o	Yaw o		Figure No.	Cohesion	Spillage
201	15°	Flat Impact Pl.	Sand - A**	4.8	1.6	0	-	0	25.5	0	20	9-3	Impact Split	Considerable Scatter
201A	15°	Flat Impact Pl.	ROM ***	4.8	1.6	0	-	0	25.5	0	20	9-4	Poor	Major Scatter
202	15°	No Impact Pl.	Sand - A	4	0.3	0	-	0	25	0	20	9-5	Impact Split	Slight Improvement
203	15°	No Impact Pl.	Sand - A	3.5	0.3	0	-	0	25	0	20	-	Divergence	No Change
204	15°	No Impact Pl.	Sand - A	3.5	0.3	0	-	0	25	11.5	0-5°	9-6	Improved	Some Scatter
205	15°	No Impact Pl.	Rock	3.5	0.3	0	-	0	25	11.5	0-5°	9-7, 8	-	None
206	15°	No Impact Pl.	Coal	3.5	0.3	0	-	0	25	11.5	-	9-9	Poor	Major Scatter
151	0	8" Dia. (Cyl.)	Sand - C	-1.9	6.2	2.4	-7.5	37.5	22.5	27	0	9-10	Good	-
152	0	6" Dia. (Cyl.)	Sand - C	-1.2	6.2	1.8	-7.0	44	30	23	0	9-11	Good	-

*G_L at top end, Runs 201-206

Aft outboard corner, Runs 211, 212

**See Mix Description, Table 9-1

*** Mary Lee, Figure 1

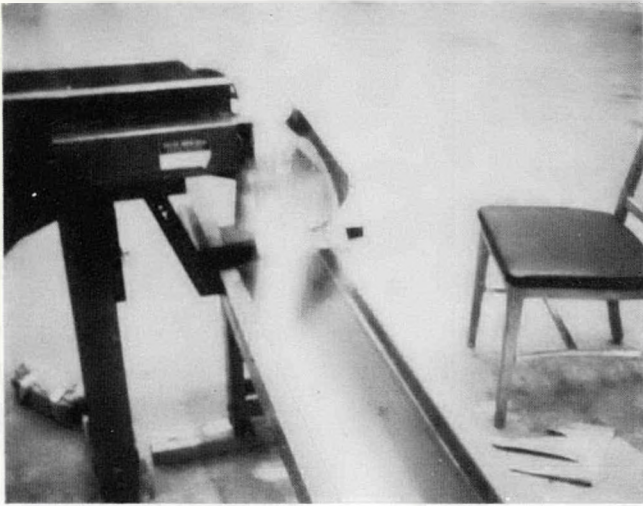


Figure 9-3. Run 201

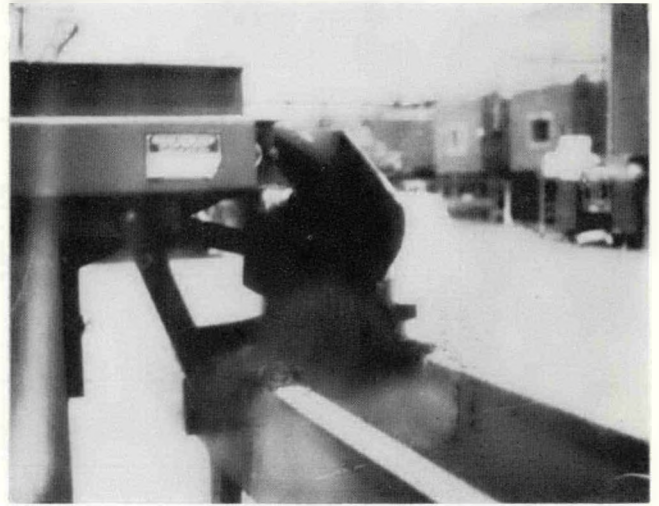


Figure 9-4. Run 201A

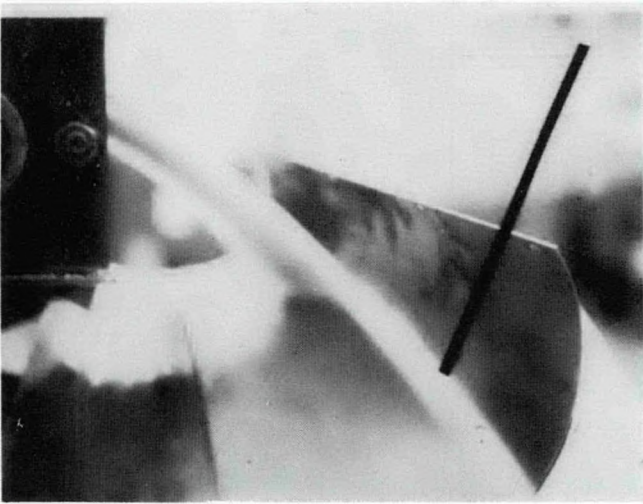


Figure 9-5. Run 202

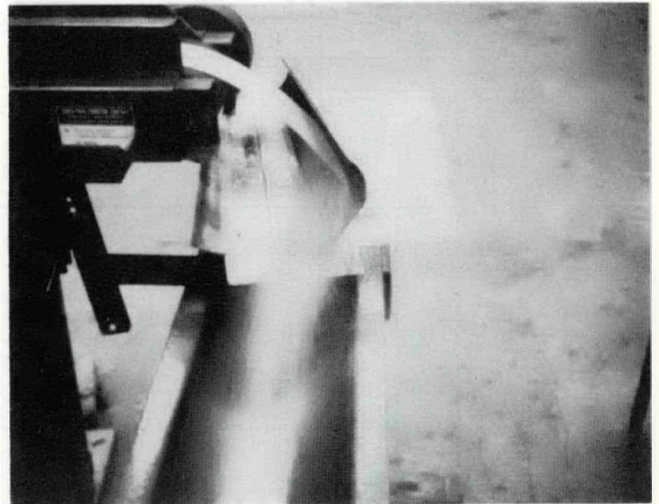


Figure 9-6. Run 204

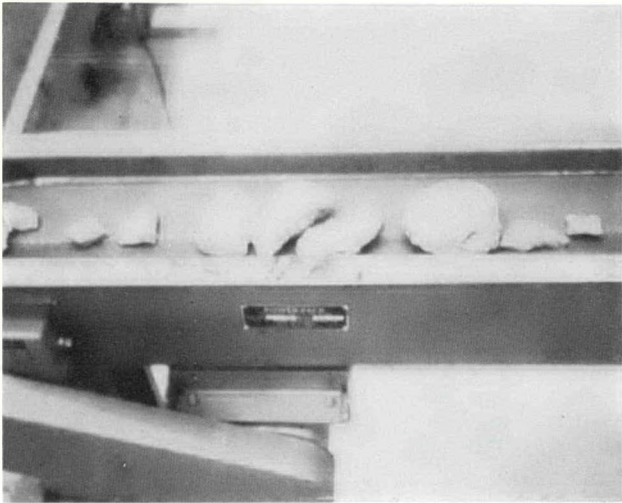


Figure 9-7. Run 205



Figure 9-8. Run 205



Figure 9-9. Run 206



Figure 9-10. Run 151

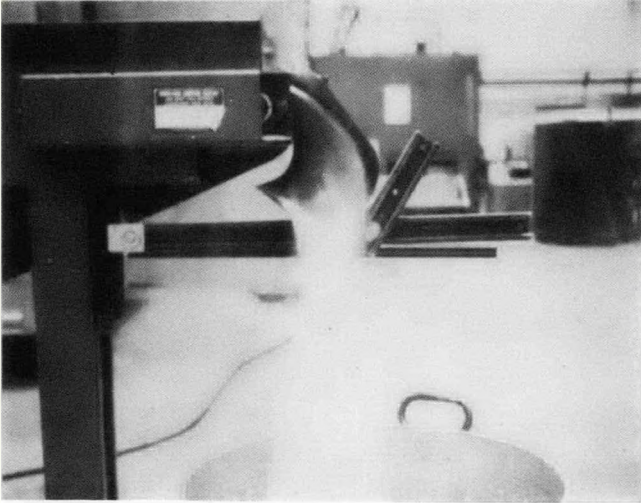


Figure 9-11. Run 152

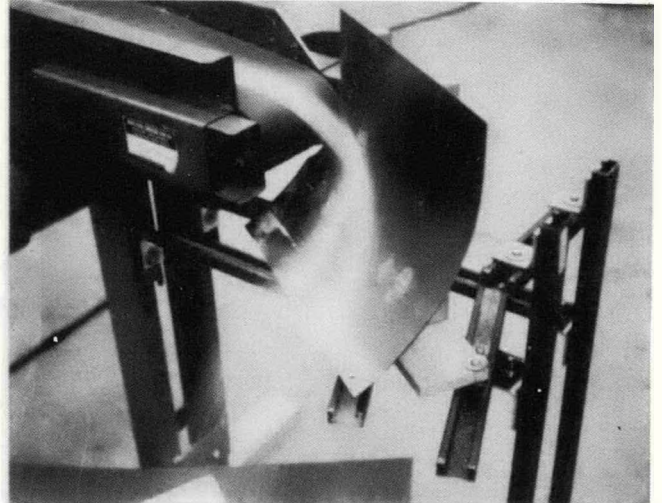


Figure 9-12. Run 1

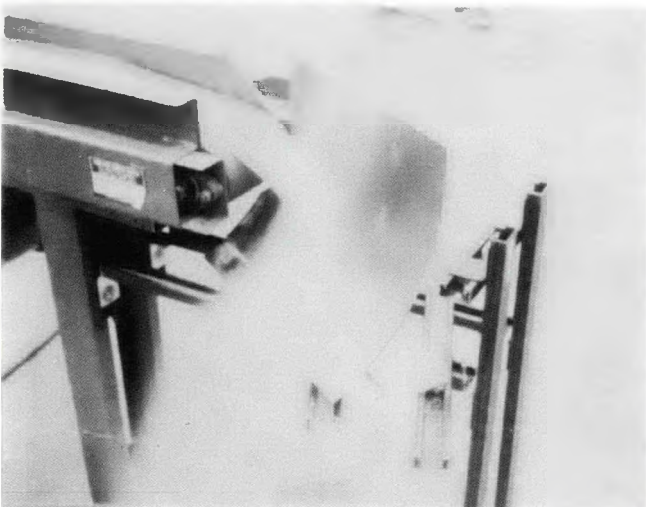


Figure 9-13. Run 3

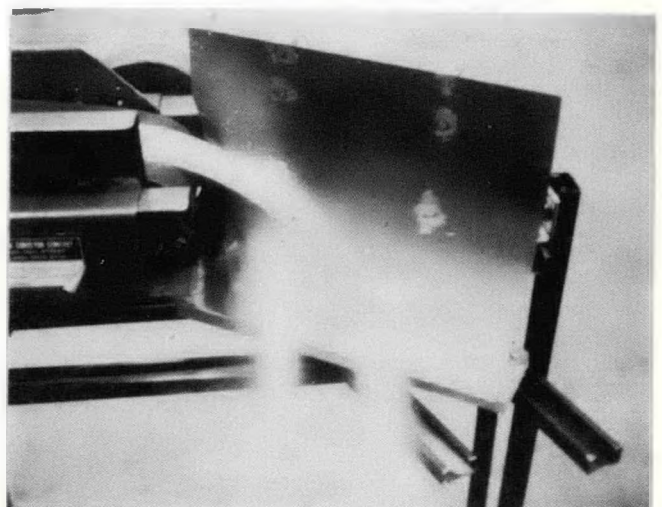


Figure 9-14. Run 4

This consideration led to the origin of the so-called "zero opening angle" cone, wherein the divergence was inherently eliminated. An unforeseen characteristic of this configuration, however, was the need for moving it too close to the head pulley, in order to provide a smooth (non-forking) impact condition (Runs 151, 152).

9.2.2 Cylinder Model Tests

Tables 9-3 and Figures 9-12 to 9-25 summarize the results of tests on the cylindrical configurations. The first tests, 1-8, were devoted to attainment of the optimum yaw angle of the cylinder axis with the input direction of flow, relative to achieving a 90° turn. This angle was found to be about 30 degrees.

The single surface cylinder (Test Runs 1 to 8) exhibited scatter, due partly to the absence of side constraints, but basically due to the constantly changing angle of impact of the free fall trajectory, at different points across the flow mass width. This resulted in a characteristic forking of the stream into two parts, or at least into a generalized fan pattern. Testing of the chute model at a variety of height positions relative to the feed conveyor yielded the same result. Control of the spillage feature of this forking phenomenon was attempted by the side walls provided in the compound cylinder configuration (Runs 9 to 13). While this attempt was successful, it was still apparent that the forking, which still persisted, corresponded to an undesirable, dust-producing turbulence in a full scale configuration.

In a final search for a non-forking impact flow, cylindrical radii tighter than the 10 inch one used in the above tests were tried. These included 6 and 8 inch radii (Runs 21 - 25).

9.2.3. Initial Torus Configuration Tests

The early torus chute tests are detailed in Table 9-4 and in Figures 9-27 to 9-50. (Next text page: 9-22).

TABLE 9-3

SCALE MODEL TEST RESULTS FOR CYLINDRICAL CHUTE CONFIGURATIONS

Run No.	Chute Config.			Flow Material	Height, Horiz. Cylindrical Axis Above Belt	Y Min.	ϕ Attitude			Deviation From 90° Turn	Remarks		
	Cylind. Descr.	Rad (In.)	Arc o				Roll o	Pitch o	Yaw o		Figure No.	Cohesion	Spillage
1	Plain	10"	64	Sand A	1.75	-7.2	0	0	38	15°	9-12	Sharp* Impact Fork	Scatter
2	Plain	10"	56	Sand A	1.75	-6.6	0	0	38	0-5	-	Sharp* Impact Fork	Scatter
3	Plain	10"	56	Sand A	1.75	-6.6	0	0	31	5°	9-13	Sharp* Impact Fork	Scatter
4	Plain	10"	64	Sand A	1.75	-7.2	0	0	31	5°	9-14	Sharp* Impact Fork	Scatter
5	Plain	10"	56	Sand A	0.12	-8.2	0	0	31	0°	9-15	Sharp* Impact Fork	Scatter
6	Plain	10"	56	Sand A	-1.31	-9.6	0	0	31	0°	9-16	Sharp* Impact Fork	Scatter
7	Plain	10"	56	Sand A	-4.31	-12.6	0	0	31	0°	9-17	Sharp* Impact Fork	Scatter
8	Plain	10"	56	ROM	-1.19	-9.5	0	0	30	0°	9-18	Less Pronounced Fork	Scatter
9	Compound	10"	64	Sand A	-1.0	-10.0	0	0	30	0°	9-19	Fork Recombined on Belt	Controlled
10	Compound	10"	64	ROM	-1.0	-10.0	0	0	30	0°	9-20	Not Visible	Dusting
11	Compound	10"	64	Sand A	1.0	-8.0	0	0	30	0°	9-21	Fork Maintained	None

* Trajectory Impacts
into Frictional Flow Path

TABLE 9-3 (Continued)

SCALE MODEL TEST RESULTS FOR CYLINDRICAL CHUTE CONFIGURATIONS

Run No.	Chute Config.			Flow Material	Height, Horiz. Cylindrical Axis Above Belt	Y Min.	☉ Attitude			Deviation From 90° Turn	Remarks		
	Cylind. Descr.	Rad (In.)	Arc °				Roll °	Pitch °	Yaw °		Figure No.	Cohesion	Spillage
12	Compound	10"	64	Rock	2.0	-7.0	0°	0°	30°	0°	9-22	-	None
13	Compound	10"	64	Sand A	2.0	-7.0	0°	0°	30°	0°	9-23	Fork	Controlled
21	Plain	6"	90	Sand A	2.25	-7.8	0°	0°	30°	0°	-	Fork	Scatter
22	Plain	6"	90	Sand A	4.0	-6	0°	0°	30°	0°	9-24	Fan-Out	Scatter
23	Plain	6"	90	Sand A	-1.0	-11	0°	0°	30°	0°	9-25	Fan-Out	Scatter
24	Plain	8"	90	Sand A	-1.0	-11	0°	0°	30°	0°	-	Fan-Out	Scatter
25	Plain	8"	90	Sand A	3.62	-6.8	0°	0°	30°	0°	9-26	Fork	Scatter

Table 9-4

Scale Model Test Results for Initial Torus Chute Configurations

Run #	Chute Config.	Flow Material	Locating Coord*			Y min in	Attitude			Dev. from 90° Turn °	Fig#	Remarks	
			X in	Y in	Z in		Roll °	Pitch °	Yaw °			Cohesion	Other
			101	Torus I/6	Sand-A		-	-	-			-	30
102	Torus I/6	"	-	-	-	-	42	0	0	30	9-28	"	"
103	Torus I/8	"	-	-	-	-	45	0	0	0 avg	9-29	Impact Fork	Diverge
104	"	"	-	-	-	-	45	0	0	10 avg	9-30	"	"
105	Torus I/6*	"	-	-	-	-	30	0	0	0 avg	9-31	"	"
106	Torus I/8*	Sand-A	-	-	-	-	30	0	0	10 avg	9-32	"	"
111	S/P I/8	Sand-B	3	-3.2	3.6	-	30	24.5	28	20	9-33	No Impact Split	Too tight
112	S/P II/8	"	5	-4	0	-	5	15	5	0	9-34, 35	Impact Fork	Clear OK
113	"	"	6	-5.4	5.1	-	10	23	9	0	-	"	Scatter
114	"	"	6.5	-4.2	4.2	-	0	30	20	30	9-36	Major Fork	Broad Scatter
115	"	"	4.8	-5.1	5	-	14	25	15	15	9-37	Smaller Fork	Some Scatter
116	"	"	4.8	-4.9	5.4	-	12.5	29	11	5°	9-38	Large Fork	Scatter
117	"	"	5.4	-4.5	5.4	-	5.5	30.5	10	25°	9-39	Minor Fork	Right Scatter

** Output side constraints added **

* To outboard edge of upper circle for Runs 111-126, See Fig. 9-34.

Table 9-4 continued

Scale Model Test Results for Initial Torus Chute Configurations

Run #	Chute Config.	Flow Material	Locating Coord*			Y min in	Attitude			Dev. From 90° Turn °	Fig. #	Remarks	
			X in	Y in	Z in		Roll °	Pitch °	Yaw °			Cohesion	Other
118	S/P II/8	Sand-C	5.4	-4.5	5.4	—	5.5	30.5	10°	25	—	Neg. 1 Fork	
119	↑	↑	5.4	-4.5	5.4	—	5.5	27	10	5	9-40	Same Fork	
120			5.4	-4.5	5.4	—	5.5	30	10	5	9-41	No Fork	1" extra added
121			5.4	-4.5	5.4	—	5.5	27	10	0	9-42, 43	Slight Fork	2" extra added
122			3.6	-6.7	4.4	—	5.5	25.5	12	0	9-44	Fork	
123			7	-6.7	4.1	—	0	26.5	22	0 avg.	9-45	Major Fork	Scatter
124			1	-7.8	4.2	—	25.5	22	23	0	9-46	Definite Fork	Good Reconverg.
125			↓	↓	-0.5	-7.9	5	-6.5	40.5	38	8	10	9-47
126	S/P II/8	↓	-0.5	-7.9	5	-7.0	40.5	38	8	0	9-48	No Fork	2" ext. added
131	S/P II/6	Sand-C	4.0*	-7.0*	4.5*	-6.5	20	20	10	0	9-49, 50	No Fork	2" ext. added

* To bottom of circle at lowest section prior to extension (Figure 9-50)

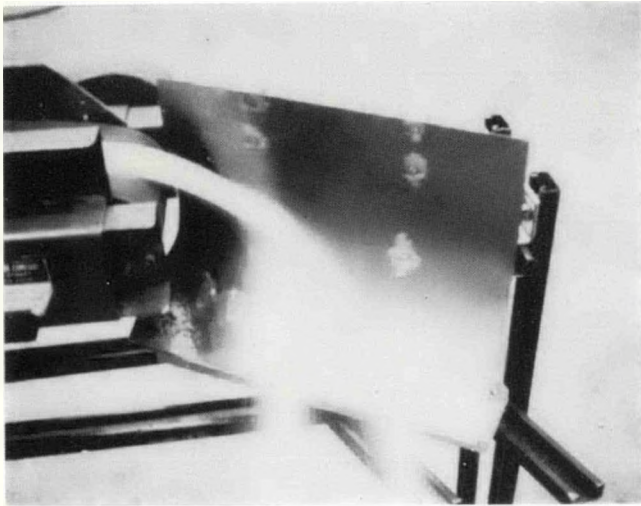


Figure 9-15. Run 5

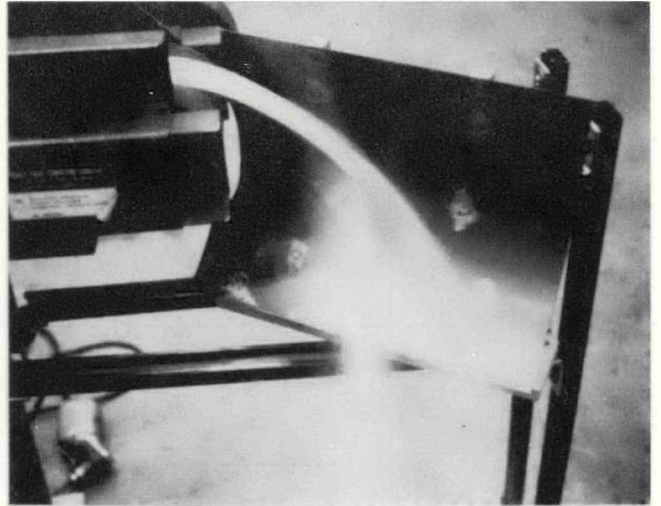


Figure 9-16. Run 6

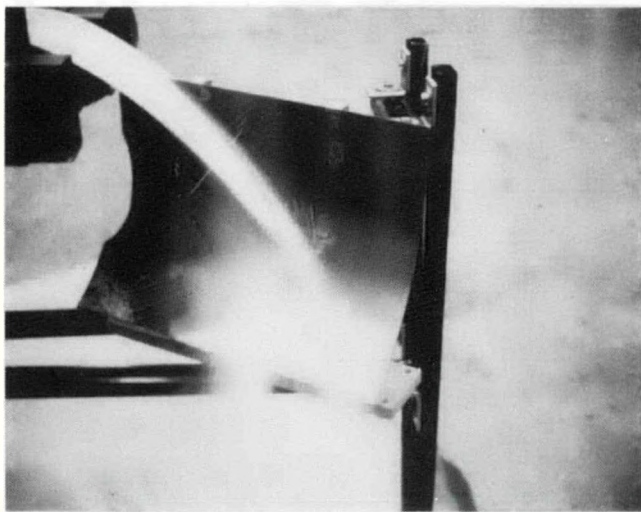


Figure 9-17. Run 7

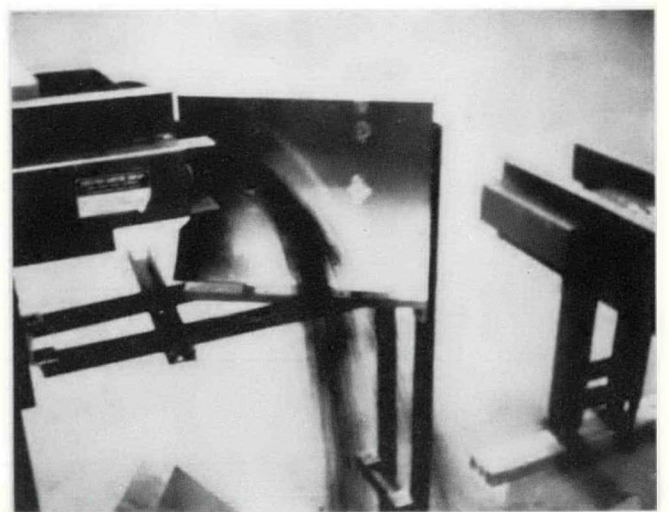


Figure 9-18. Run 8

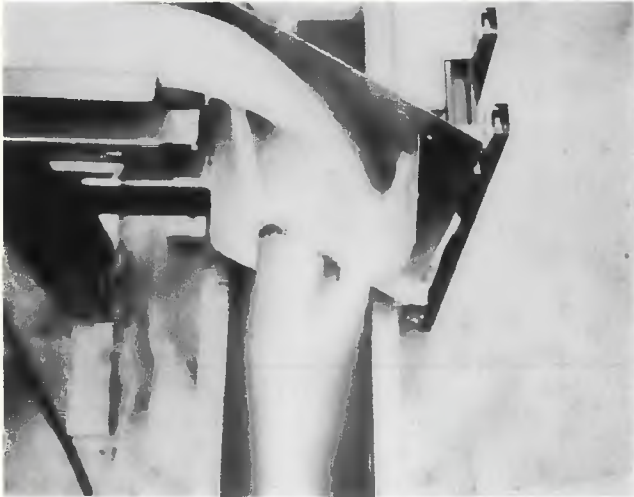


Figure 9-19. Run 9



Figure 9-20. Run 10

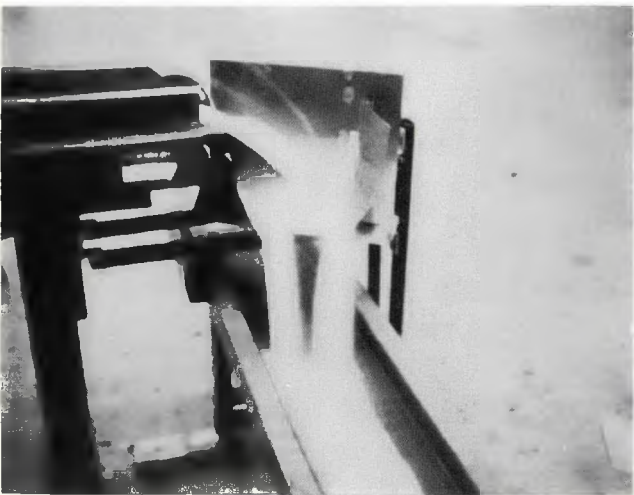


Figure 9-21. Run 11

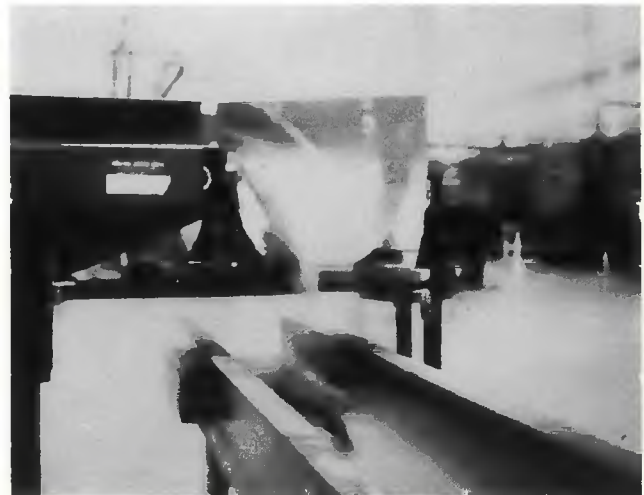


Figure 9-22. Run 12

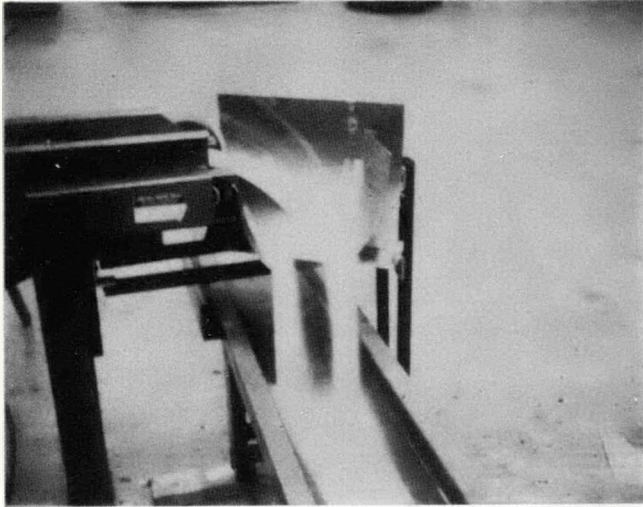


Figure 9-23. Run 13

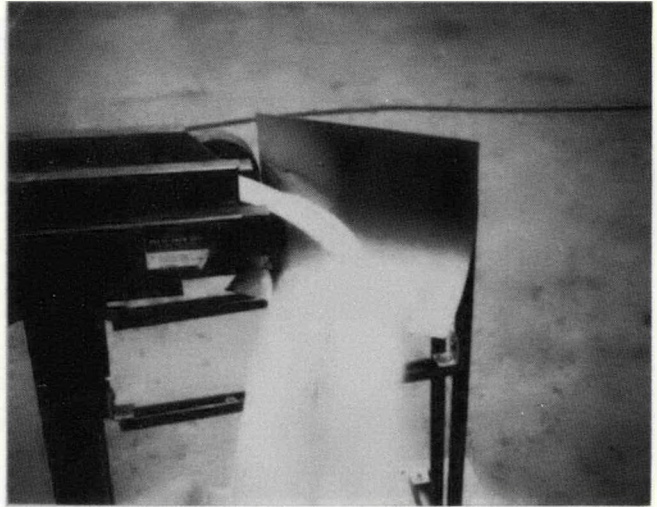


Figure 9-24. Run 22

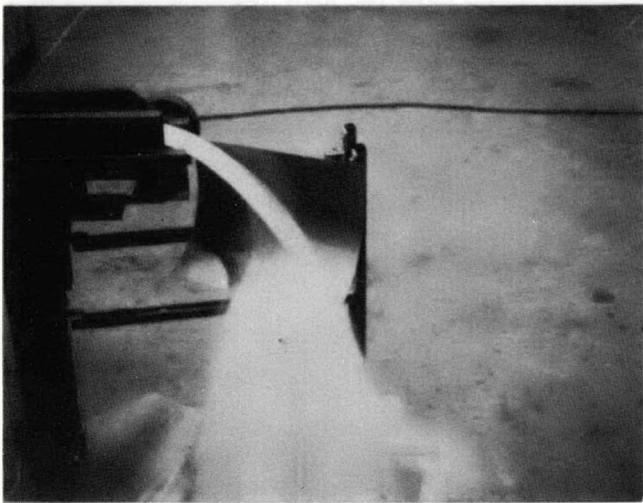


Figure 9-25. Run 23

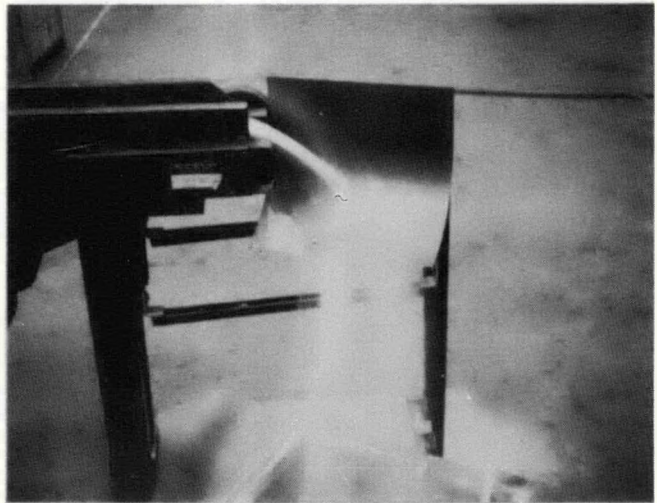


Figure 9-26. Run 25

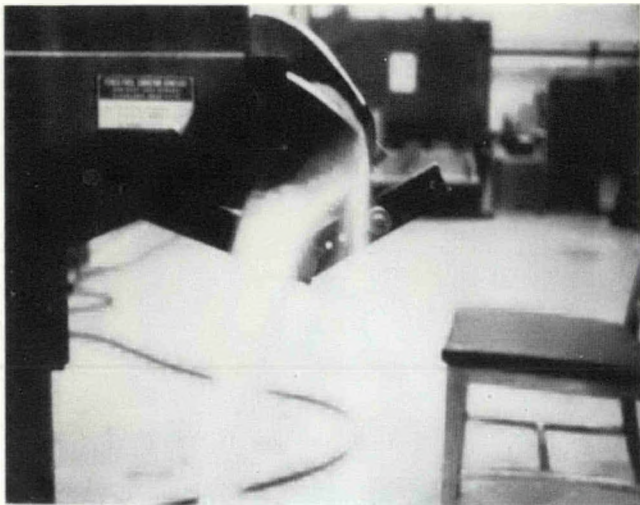


Figure 9-27. Run 101

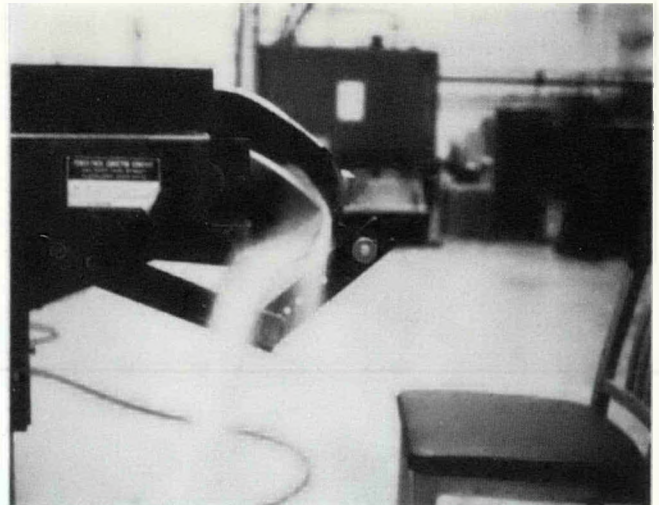


Figure 9-28. Run 102



Figure 9-29. Run 103

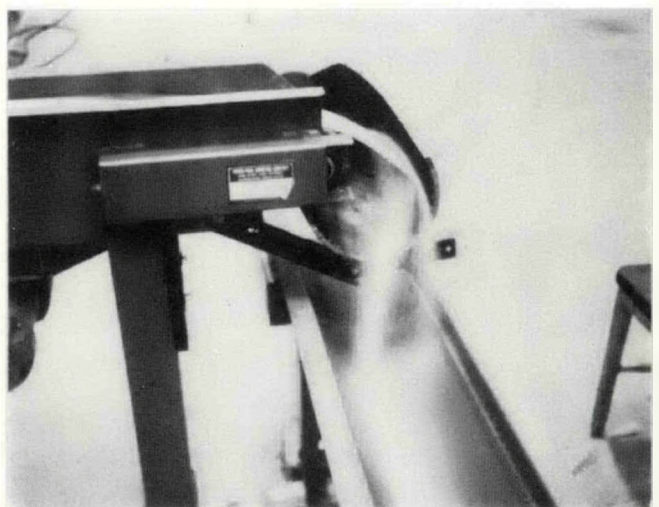


Figure 9-30. Run 104

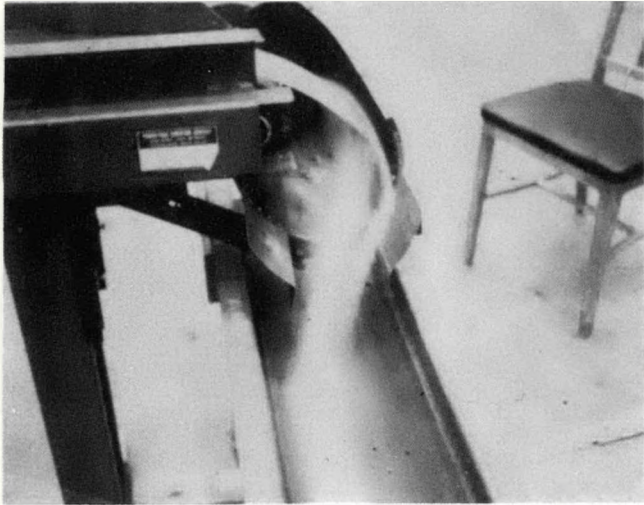


Figure 9-31. Run 105

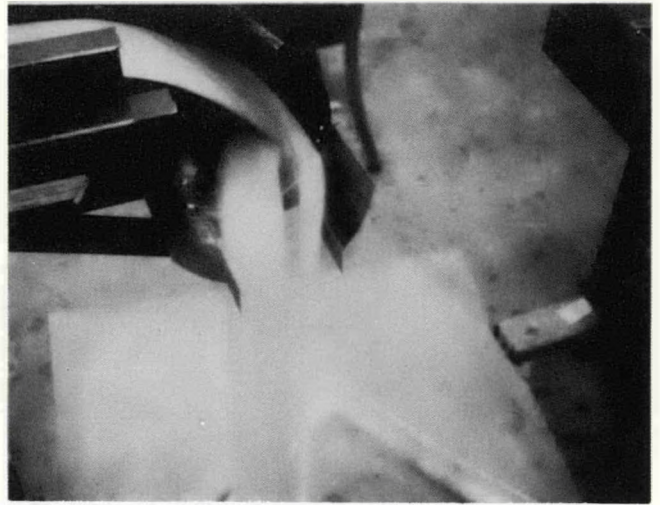


Figure 9-32. Run 106

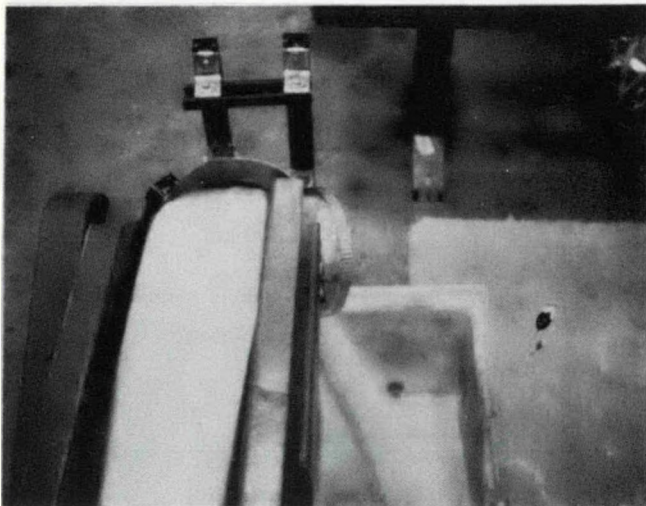


Figure 9-33. Run 107



Figure 9-34. Run 111

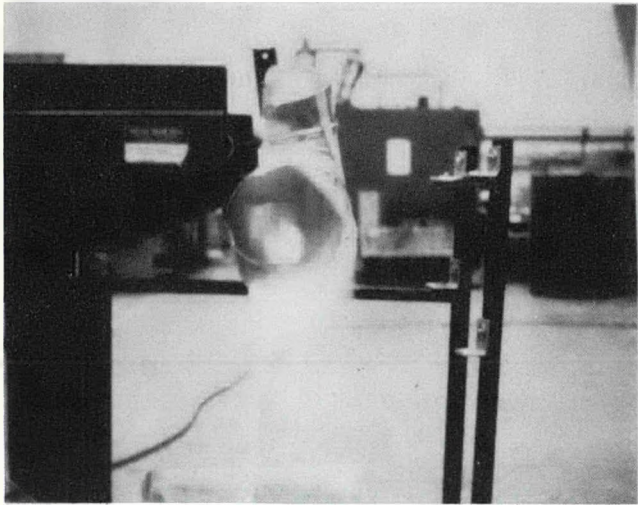


Figure 9-35. Run 112

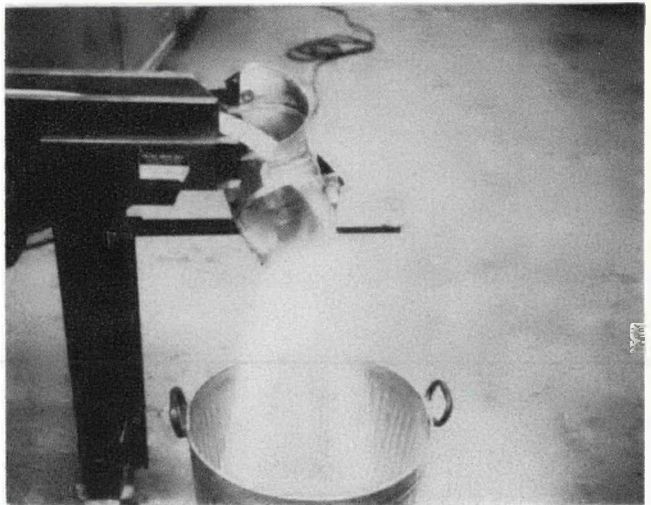


Figure 9-36. Run 114

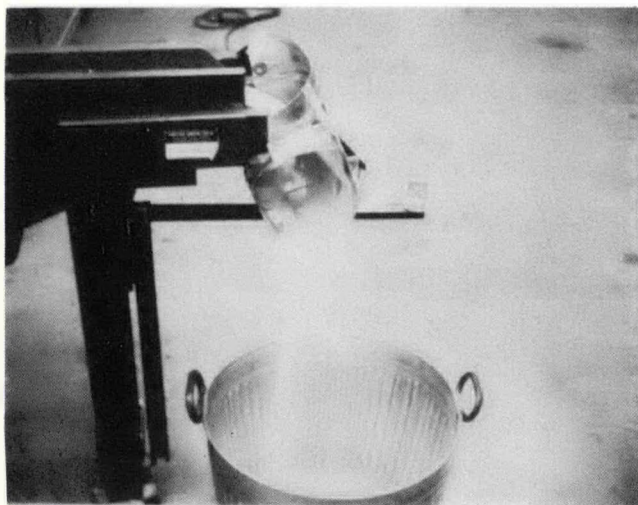


Figure 9-37. Run 115

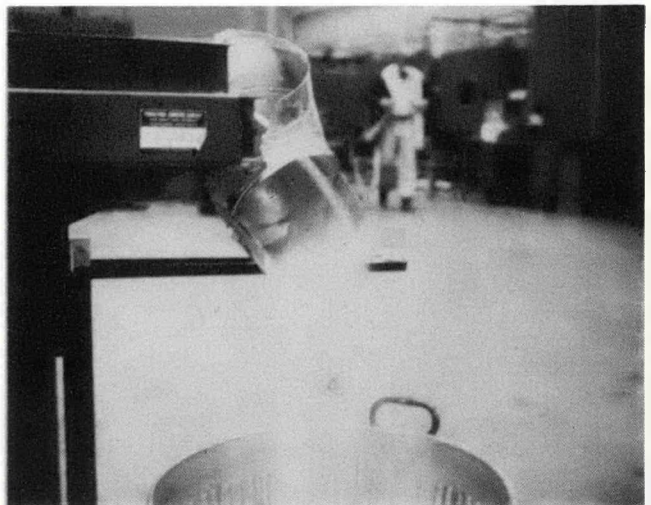


Figure 9-38. Run 116

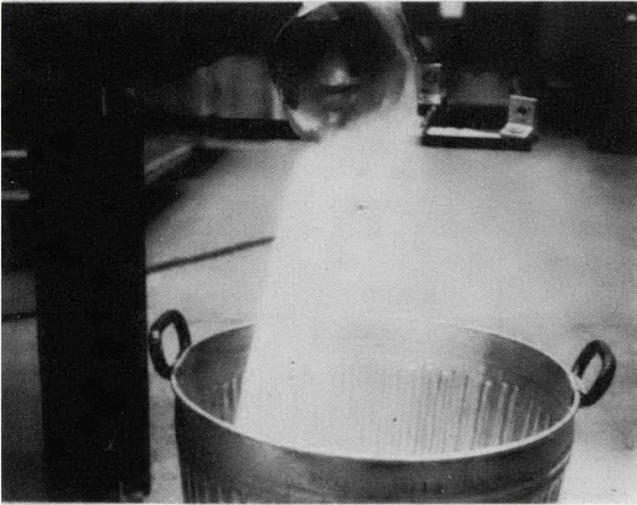


Figure 9-39. Run 117

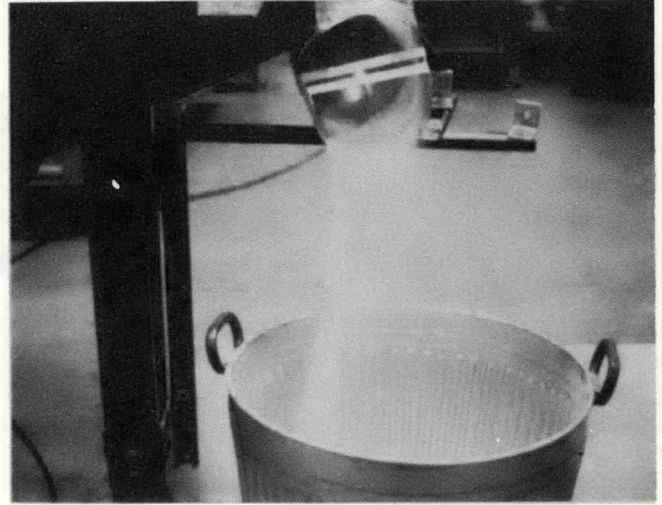


Figure 9-40. Run 119

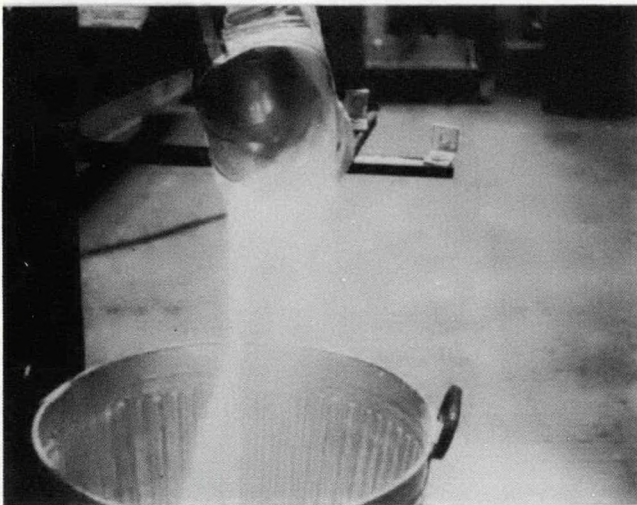


Figure 9-41. Run 120

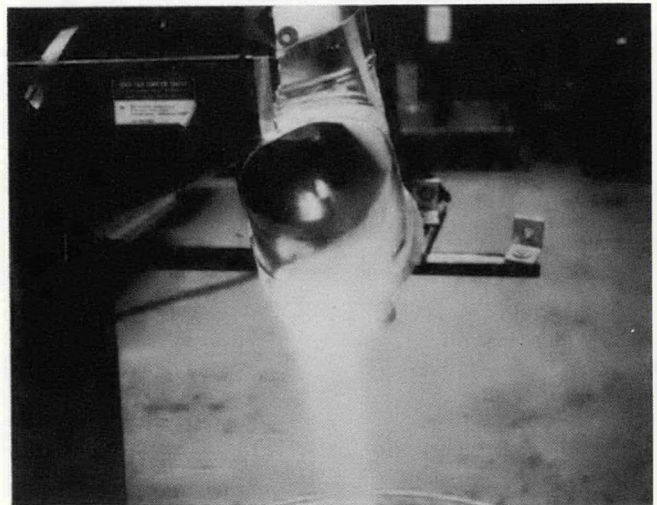


Figure 9-42. Run 121

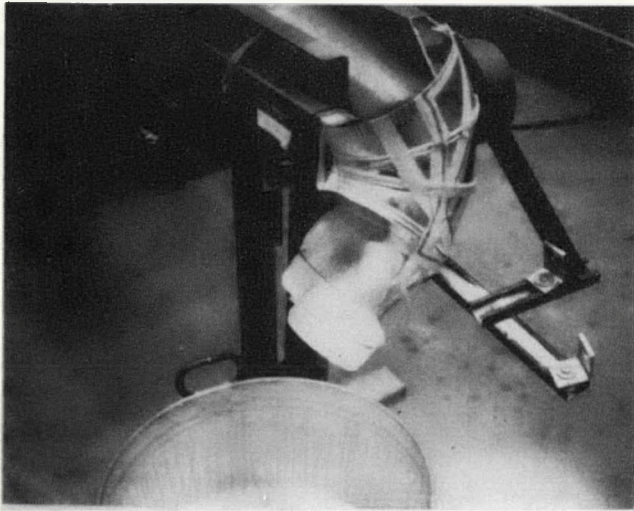


Figure 9-43. Run 121

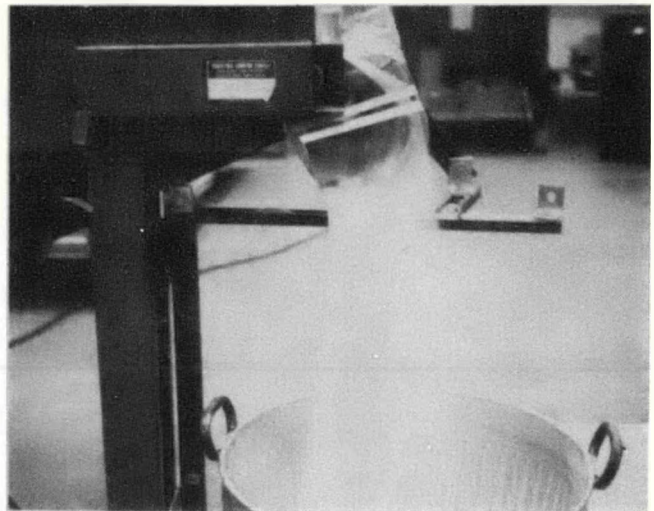


Figure 9-44. Run 122

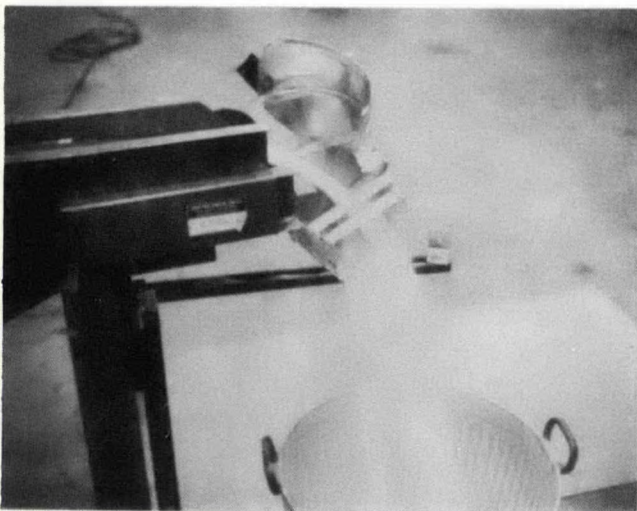


Figure 9-45. Run 123

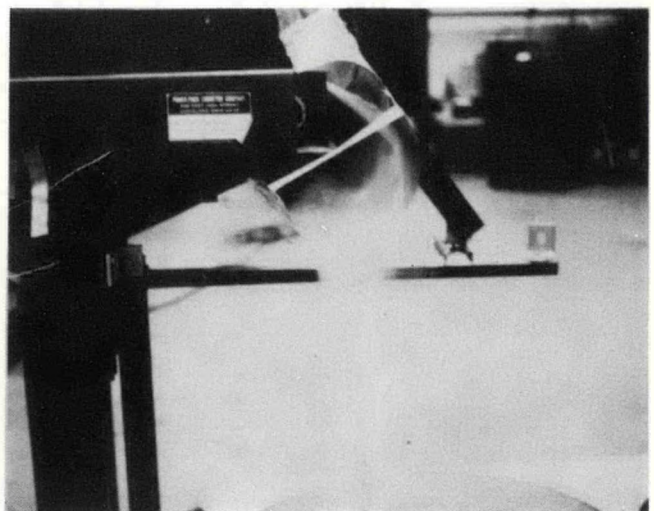


Figure 9-46. Run 124

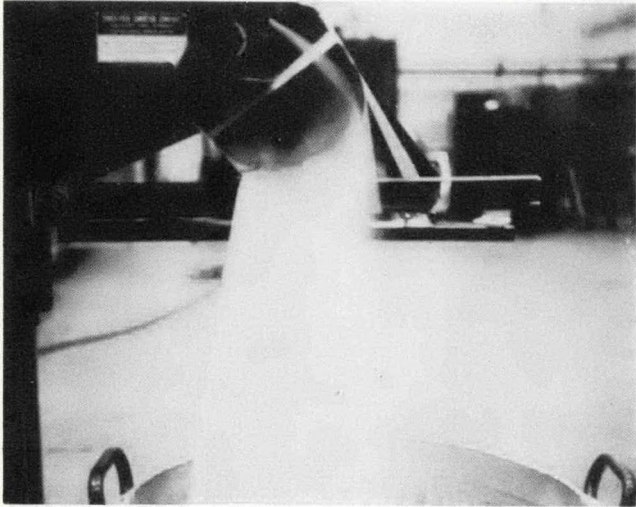


Figure 9-47. Run 125

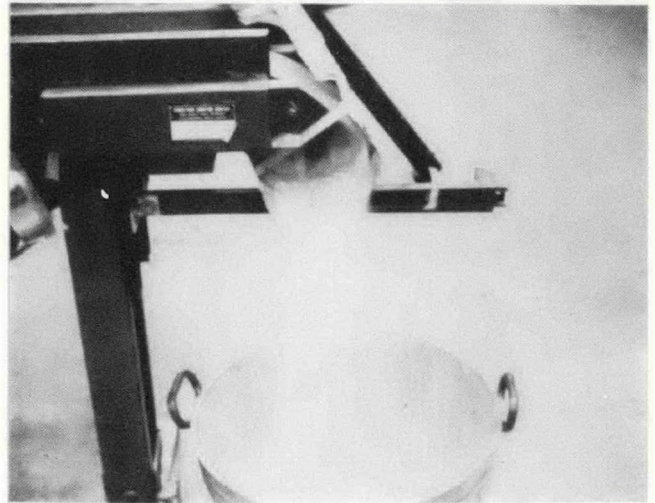


Figure 9-48. Run 126

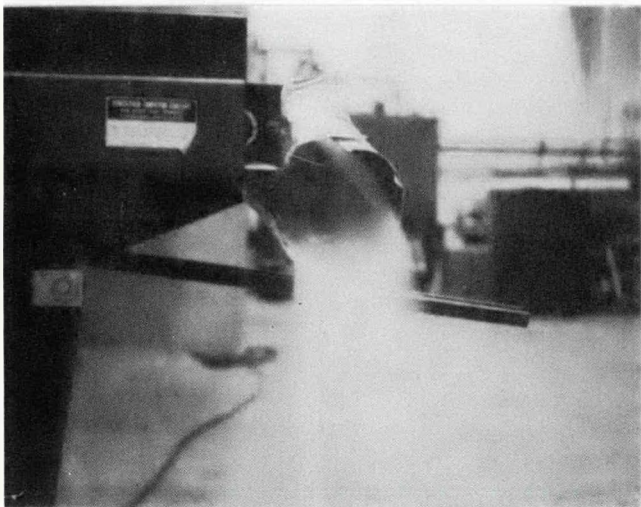


Figure 9-49. Run 131

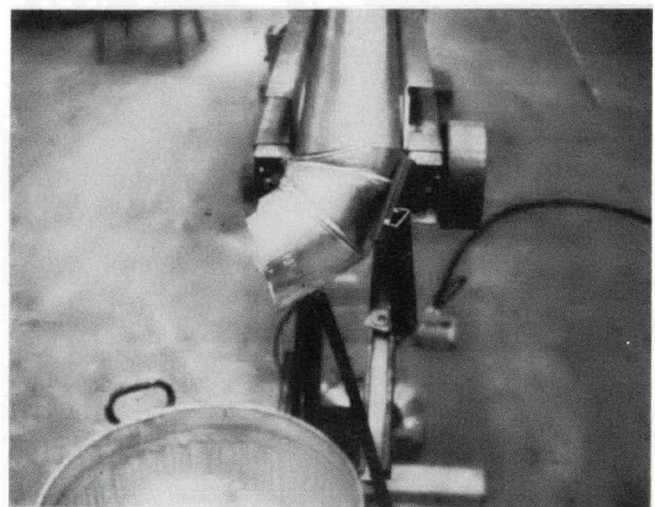


Figure 9-50. Run 131

The first torus configurations (Torus I, 6 and 8 inch sizes) were found to have the outboard side wall cut excessively low, requiring roll angles that caused the impacting stream to interfere with the subsequent frictional flow (Runs 101 to 106).

Simultaneously with the "true", or smooth surface torus models, ones with segmented sections were also tested. As noted in Section 8.0, the most convenient raw material for these scale model chutes were sheet metal, smoke pipes. Dimensional consistency and appearance of the numerous configurations tested here were not of the same quality as for the machined smooth torus chutes; but the primary objectives of these particular tests were satisfied: namely, 1) to confirm general agreement with the corresponding smooth torus configurations, and in particular 2) to verify that the joint intersections between successive cylindrical portions did not result in adverse flow patterns.

The other principal objectives in the many test runs involved with the smoke pipe torus involved achieving a non-splitting impact flow and a 90 degree turn. Of the various positions investigated, that for Run 126 appeared to achieve the best impact conditions and required turn, in the 8 inch minor diameter torus. This involved the addition of a chute extender, which caused the flow to return from an "over"-turn, i. e. , one past 90° , back to the center of the chute output area.

In order to enhance the headroom requirements, reflected in the "Y MIN" column of the table, a 6 inch minor diameter chute was also built and tested. Its optimum configuration was achieved in Run 131. (Y MIN is the distance of the lowest point on the chute from the pulley center axis and corresponds to the identical term used in the analytical chapter.)

Owing to the unsuitable dynamic characteristics encountered with the first smooth torus configurations (I/8" and I/6"), a number II chute was introduced for testing. Only a 6 inch minor diameter case was now investigated, it by now having been verified that this smaller diameter shape was of adequate size to "catch" and turn the

entire flow cross section width for a 6 inch wide (36 inch full size) belt. The results of this second torus cut from a 90 degree pipe elbow are presented in Table 9-5, and in associated Figures 9-51 to 9-64. At this point, the torus chute was the evident stand-out among chute concepts, and the range of possible input belt velocities was investigated, i. e., at 350, 450, and 600 FPM. While the Torus II chute was found, at respectively different attitudes and locations, to be suitable for the higher velocities, the shallowness of the 350 fpm velocity dictated a different solution. It was determined that the Torus I/6" chute, oriented differently from the position attempted in Runs 101, 102, and 105, was optimum for handling this low trajectory (Figures 9-60, 61).

It was found in general that the Torus II chute for the upper velocities was only marginally long enough, measuring length as the arc angle around the major diameter. In the earlier Runs, 61 to 65, the slot area provided in the basic design was covered up by various strip widths to resolve the original internal surface. Subsequent runs (66, 67) achieved reasonably good flow performance with the original slot restored, but optimal flow output, it was judged, would be gained by an additional slide surface extension.

The outboard wall of the Torus II configuration had been raised significantly, to correct the features in the Torus I tests, resulted in the Torus II wall now being too high, and some interference with the upper edge with the free fall stream was now noted. Notching of the wall was performed incrementally (See Figure 9-57) to eliminate the interference.

9.3 REVISED TORUS MODEL TESTS

The need to evolve a third torus configuration arose from five considerations, including some previously identified:

- The outboard side wall shape required optimization
- The chute needed to be longer to optimize the flow output shape
- A more accurate reference surface was needed to measure angular and positional offsets.
- There was need also to raise the chute inboard wall to control and turn flow at the higher roll angles tested (Next text page: 9-29)

Table 9-5

Scale Model Test Results for Second Group of Torus
Chute Configurations

Run#	Belt Velocity	Chute Config	Flow Matl	Locating Coord*			Y Min in	Attitude			Dev. from 90° Turn	Fig#	Remarks	
				X in	Y in	Z in		Roll °	Pitch °	Yaw °			Cohes.	Other
61	246	Torus II/6	Sand-C	2.5	-3.5	3.5	-7.2	37.5	16.9	7	10	9-51,52	Good	Slot Covrd
62	↑ (600 FPM, Full Scale) ↓	↑ ↓	↑ ↓	2.0	-3.5	3.2	-7.0	40.3	16	2	0-5	9-53,54	Good	2 1/8" Strip
63				2.2	-4.4	3.2	-6.6	32.2	12.	0	0-5	9-55	Good	"
64				2.0	-4	3.2	-7.0	36.0	16	0	0-5	-	Slight Fork	"
65				2.2	-3.6	2.6	-6.4	35.4	4	0	0-5	9-56,57	"	Filler removed
66				2.1	-3.5	3.1	-6.8	39.3	9.8	0	15°	9-58	No Fork	-
67	246	Torus II/6		3.0	-2.9	2.9	-7.0	28.5	10	13	0-5	9-59	No Fork	-
71	143**	Torus I/6		1.0	-2.8	-0.1	-6.2	11	6	0	10-15	9-60	Fork	-
72	143	"		-0.2	-2	-0.5	-6.4	24.4	0	0	0	9-61	Slight	-
73	143	"		-0.2	-2	-0.5	-6.4	24.4	0	0	0	-	"	Extension Added
81	184***	Torus I/6		1.0	-2.8	-0.1	-6.2	"	6	0	15	9-62	"	-
82	184	Torus II/6		3.4	-2.8	2.8	-7.4	25	4.5	0	5-10	9-63	No Fork	-
83	184	Torus II/6	Sand-C	2.0	-3.5	3.0	-6.4	35	6.0	0-5	0-5	9-64	"	-

** 350 FPM, Full Scale
*** 450 FPM, Full Scale

* To Outboard edge of upper circle for runs 61-67, 82, 83
To Aft edge of upper circle for runs 71-73, 81.

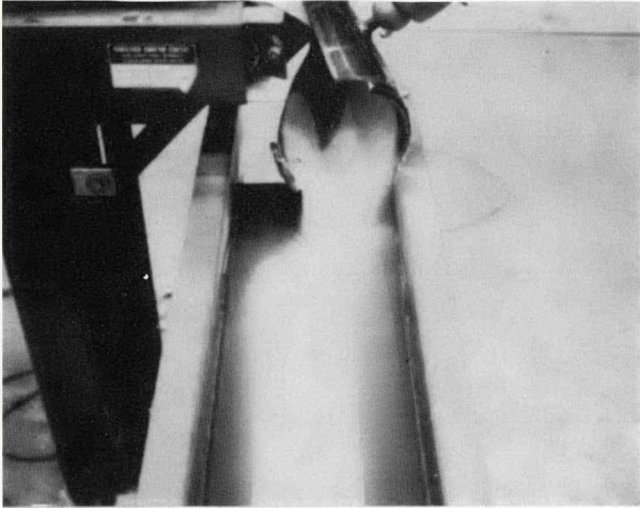


Figure 9-51. Run 61

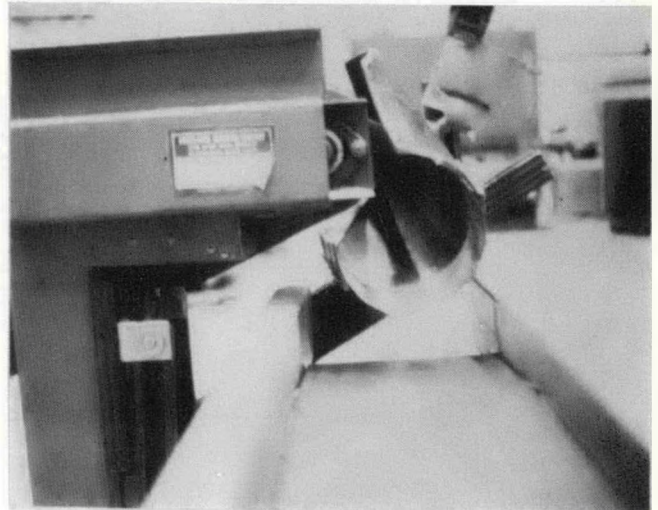


Figure 9-52. Run 61

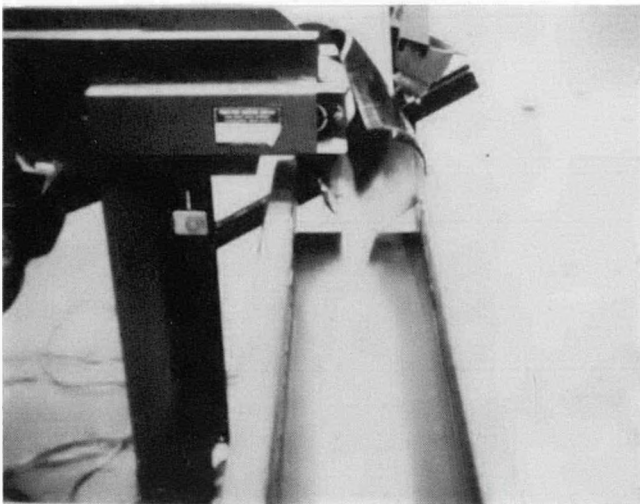


Figure 9-53. Run 62

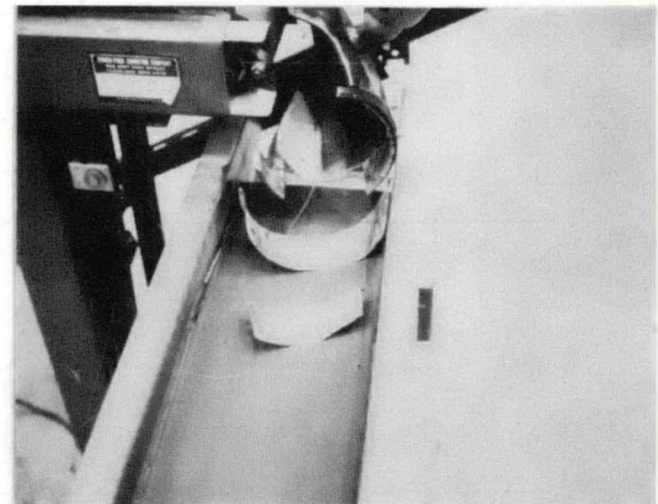


Figure 9-54. Run 62



Figure 9-55. Run 63



Figure 9-56. Run 65

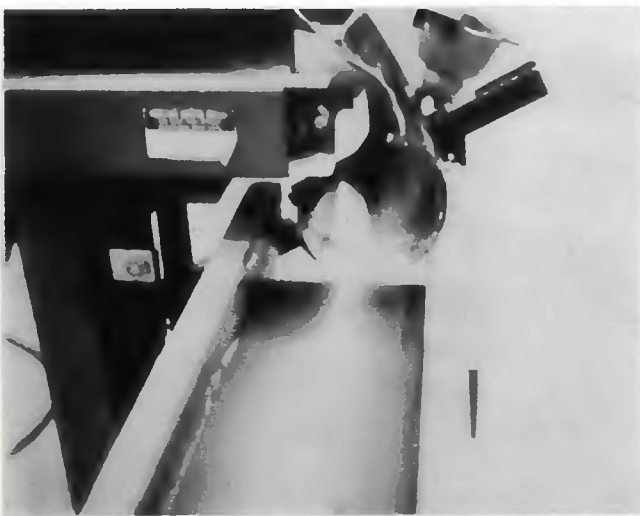


Figure 9-57. Run 65

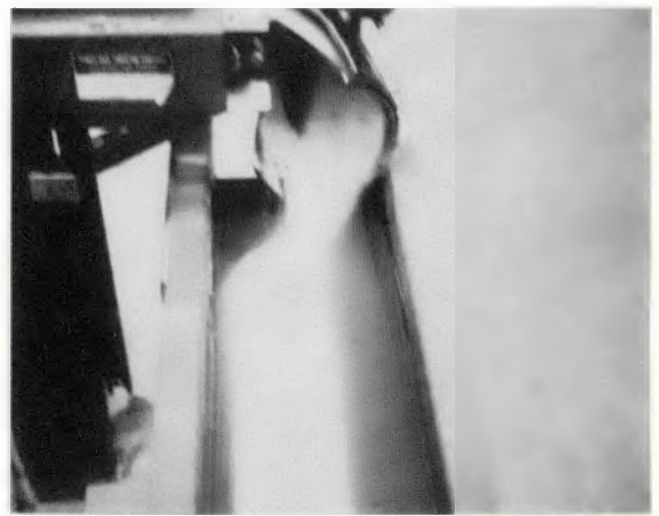


Figure 9-58. Run 66

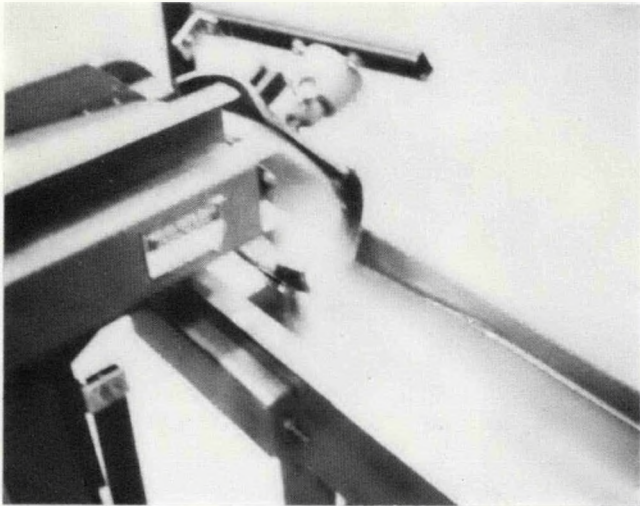


Figure 9-59. Run 67

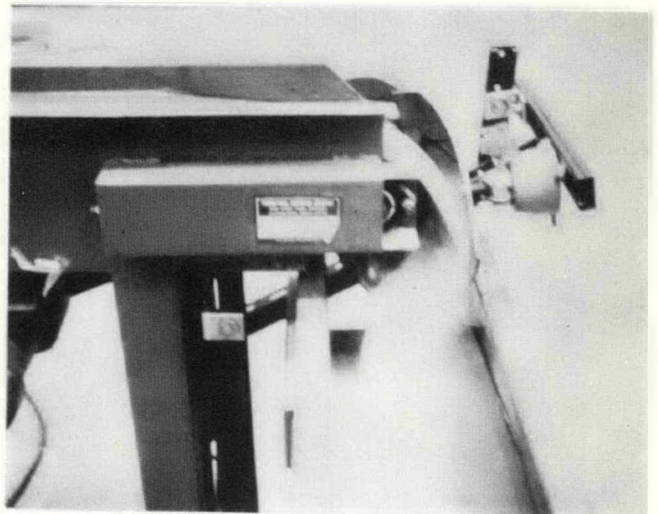


Figure 9-60. Run 71

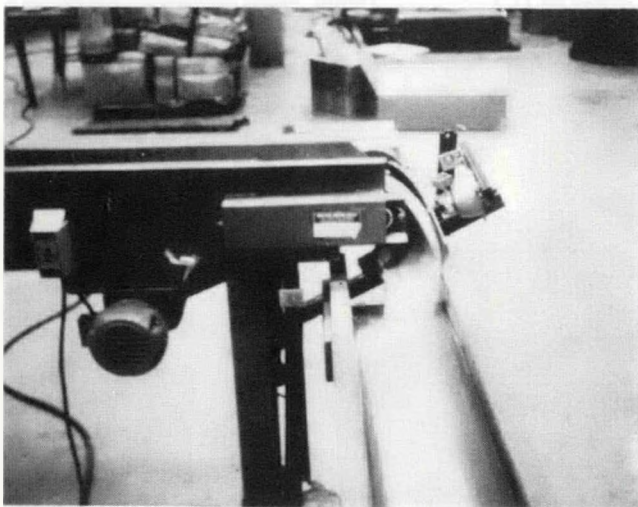


Figure 9-61. Run 72

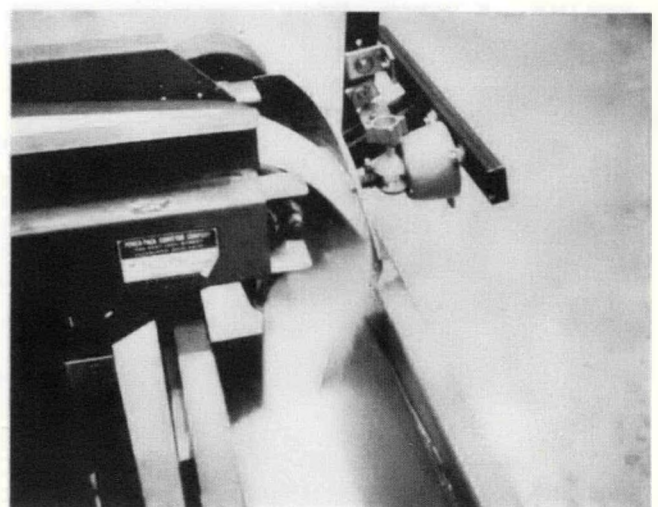


Figure 9-62. Run 81

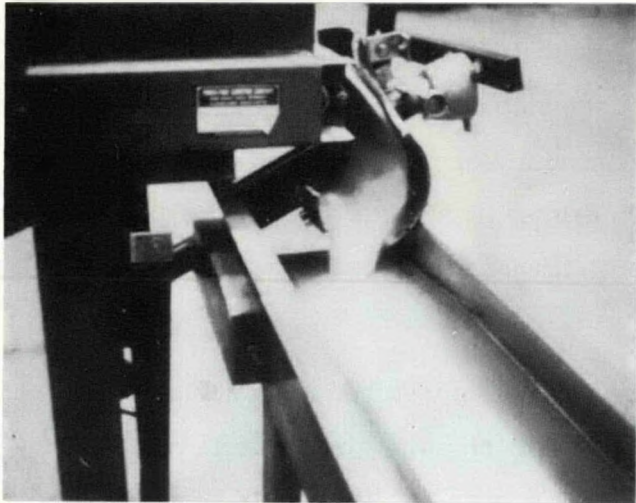


Figure 9-63. Run 82

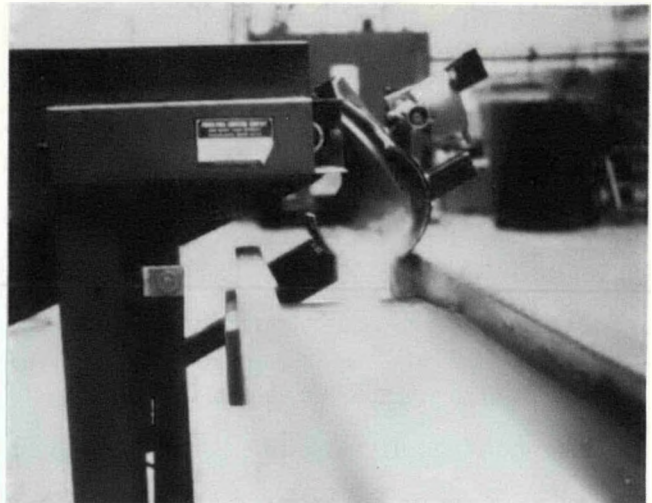


Figure 9-64. Run 83

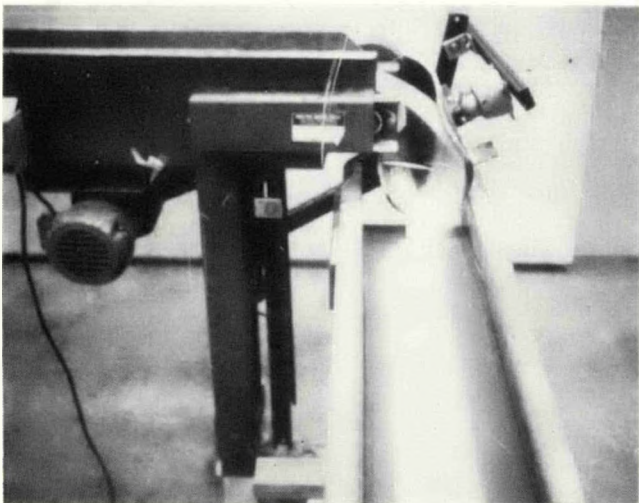


Figure 9-65. Run 461

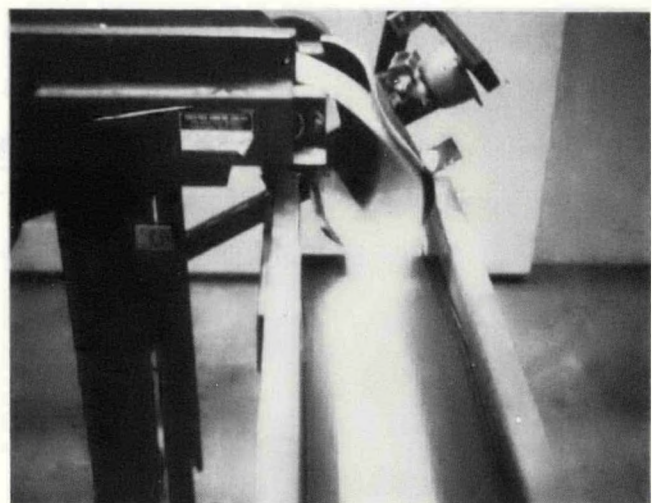


Figure 9-66. Run 462

- To establish baseline configurations for comparison with the analytical results, at the higher speeds of interest.

The Torus III chute was evolved accordingly. Test results involving this configuration are covered in Table 9-6 and Figures 9-65 to 9-69.

One of the test phenomena increasingly recognized through the iterations investigated was the development of a significant flow down the inboard side of the chute, the origin of which was the very fine material falling from the belt after the main flow trajectory had departed. This secondary flow had the effect of turning the main flow to the outboard direction, particularly if this main flow still had a significant velocity vector to the inboard side by the time it arrived at the bottom of the chute. This had a generally beneficial effect from the standpoint of minimizing the length of the chute required to center the flow and achieve a 90 degree turn. However, some disturbance in the flow at the convergence areas is an inherent penalty, although of an apparently second-order magnitude.

Of greater question is whether this phenomenon is matched in an actual transfer point configuration. It was observed during field trips that the effluent from the belt cleaner is sometimes quite significant in volume, although its role in current chute flow situations is not a factor, with the chute being normally clear of the effluent drop area. It is judged that the more conservative approach is to ignore the role of this secondary flow, from the standpoint of making worst case assumptions relating to the length of chute necessary to turn the flow. Thus, chute lengths in some configurations may have to be slightly longer, proportionately, than in these tests, although this is also a function of wall friction. In these tests, the angle of wall friction was measured at about 32° for both the steel pipe elbows and the galvanized steel smoke pipe elbows. For higher frictions, the flows will turn more quickly, and so the length can be shorter, and conversely for lower frictions. Ultimately, the chute design should be sufficiently flexible for varying local situations that the location of the lower chute termination can be varied to suit.

Table 9-6

Scale Model Test Results for Torus III Chute Configuration

Run #	Velocity (FPM)	Flow Material	Locating Coord. *			Y Min in	Attitude			Dev. from 90° Turn °	Fig. # **	Remarks	
			X in	Y in	Z in		Roll °	Pitch °	Yaw °			Cohesion	Other
461	246(600)	Sand-C	7.6	-2.8	6.8	-7.2	19	16	11.5	10	9-65	Good	Slight Scatter
462	246(600)	"	7.5	-2.5	6.8	-7.2	32	20	11	5-10	9-66	Good	Fines Buildup
461	184(450)	"	6.8	-2.8	7.2	-7.4	28.5	19.5	7	5-10	9-67	"	"
482	184(450)	"	6.2	-2.8	7.2	-7	29	17	3	0-5	-	"	"
483	184(450)	"	6.4	-2.5	7.5	-7	22	15	6	0	9-68	"	"
484	184(450)	Sand-C	6.5	-2.5	7.5	-7	27	14	6.5	0-5	9-69	"	"

* To outboard edge of lower circle

** Original black coating on pipe elbow removed after Run 482.

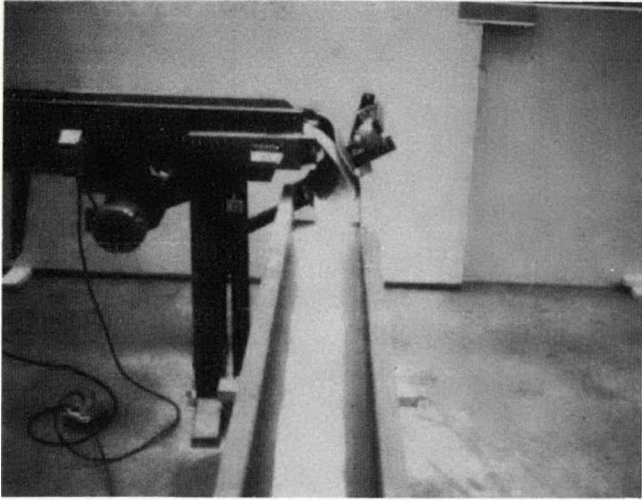


Figure 9-67. Run 481

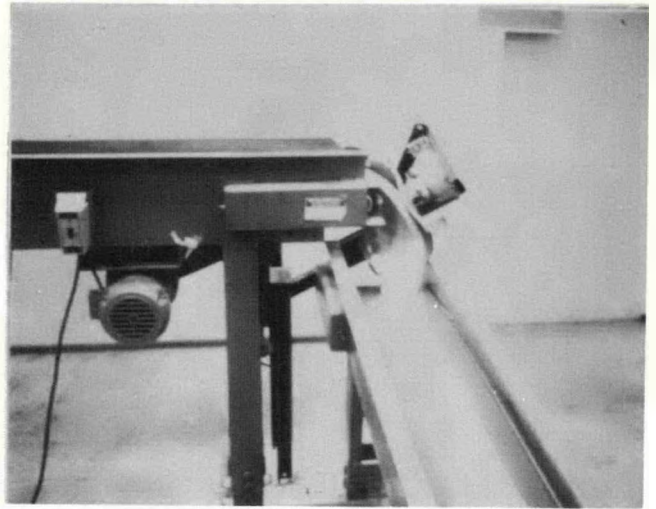


Figure 9-68. Run 483

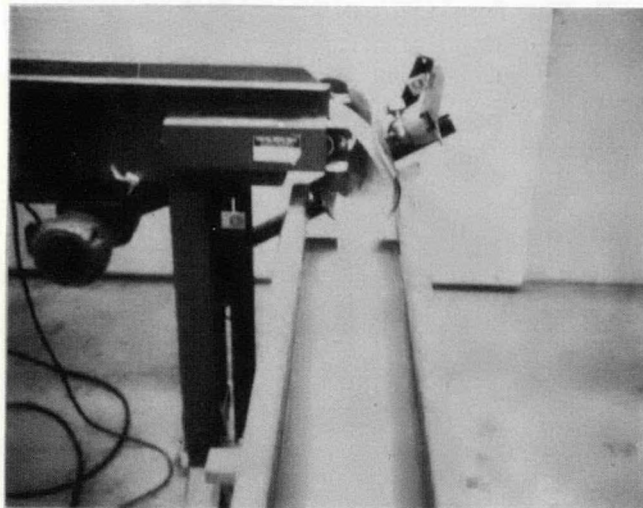


Figure 9-69. Run 484

APPENDIX A

BIBLIOGRAPHY ACCESSED IN TECHNOLOGY SURVEY

FOR LOW HEADROOM TRANSFER CHUTE PROGRAM

A. Chute Design, General

1. Flow of Coal, F. D. Cooper & J. R. Garvey, Mechanical Engineering, May 1958
2. Factors in Good Chute Design, W. H. VanBuren, Modern Materials Handling, Sept. 1953
3. Belt Conveyor Transfer Points, H. Colijn, P. J. Conners, Soc. Mining Engr. AIME, Vol. 252, Page 204 - 210, June 1972
4. Chutes - A Preview of Development of Chutes Underground, Colliery Guardian, September 20, 1962
5. A Chute Designed to Spread Uniformly a Stream of Bulk Solids, J. C. Richards
6. Design and Performance of Spiral Chute Installations in India and Abroad, R. N. Gupta Scientist and B. Singh, Assistant Director, Central Mining Research Station, Journal of Mines, Metals & Fuels, July 1970
7. Tips on Designing Chutes & Spouts, Colley, Material Handling Engineering, January 1966

*

8. Typical Coal Chutes and Coal Liners - Sketches

B. Chute Materials

1. Stainless Steel Coal Ducts Stop Trouble in Maintenance and Operation, J. L. Raymond, Mechanical Engineering, May 1955.
2. Plastic Liner for Chutes, Bins Shows Promising Results, Coal Age, August 1973
3. Plastic Sheeting - Fluid BedDryer, Coal Age, January 1976
4. Steels for coal Handling and Preparation, Wayne E. Tuomi, Coal Age, Sept. 1968
5. New Coal Chute Lining Saves Wear and Maintenance Costs, Power Engineering, May 1971
6. New Materials for Slidability Plus Longer Wear, Jack B. Blankenship, Mining Congress Journal, October 1975
7. Linings Made of Hostalen Gur (UHMW-PE) for Bins Containing Bulk Materials, American Hoechst Corp.

C. Coal Mining at Face

1. Technological Innovations Abound in Coal Mountains of Appalachia, Coal Age, Mid-May 1975.
2. SME Mining Engineering Handbook, Arthur B. Cummins, U. S. Bureau of Mines, 1973
3. Underground Mining, J. A. Reeves, Society of Mining Engineers, Feb. 1975

* Proprietary

4. Underground Coal Mining - 1971, George L. Judy, Mining Congress Journal, 1972
5. Underground Mining - 1972, William F. Distler, Douglas E. Julin, Mining Congress Journal, February 1973
6. Underground Mining of Coal, Robert L. Raines, Mining Congress Journal, 1975.
7. Principal Mining Enner, Energy Sources Division, Kaiser Engineers, C. B. Tillson, Jr., Mining Congress Journal, February 1975.
8. Mechanical Mining of Coal, William F. Diamond, Mining Congress Journal, February 1968
9. Research and Development, Robert L. Frantz, Society of Mining Engineers, March 1976
10. Continuous Mining in Thin Seams, C. Lynch Christian, Jr., Mining Congress Journal, July 1964

D. Underground Haulage

1. Belt Conveyors, Belting and Auxiliaries, Coal Age, Operating Guide, Jan. 1968
2. A System with the Right Angle, Mechanical Engineering, August 1972
3. Speedier Coal Haulage, Coal Age, February 1976
4. World's Longest Belt Conveyor, Coal Age, February 1970
5. Continuous Underground Slurry Transport of Coal, H. Douglas Dahl, D. L. McCain, Mining Congress Journal, May 1974
6. History, Present Use and Near-Term Potential of Continuous Haulage, A. W. Calder, Mining Congress Journal, August 1972
7. Evaluation of Underground Coal Haulage Systems, Arthur E. Belton, Mining Congress Journal, 1975.
8. Bulk Materials Handling, Hawk, Vol. 3: - with the following specific papers:
 - a. Editor's Remarks
 - b. General Design and Selection of Conveyor Systems, H. Colijn
 - c. The Effects of Physical Properties on the Design of Conveyor Syst, R. W. Christensen, R. W. Heins and K. K. Wu
 - d. Mathematical Modeling of Conveyor Systems, C. B. Manula
 - e. Conveyor Belting in the '70s, E. T. Gregory
 - f. Belt Conveyor Transfer Points, H. Colijn, P. J. Conners (Also item 3 under Chute Design, General

E. Dust

1. Environmental Control Applied to Belt Conveyor Transfer Points, Joseph N. Morrison, Jr., Dravo Corporation
2. Coal Dust: Hazards, Control, Coal Age, March, 1970
3. Dust Control on Underground Coal Conveyors, N. Levo, Jr. Mining Congress Journal, December 1965
4. What's New in Dust Control?, Robert D. Saltsman, Mining Congress Journal, August 1965
5. Dust Abatement Activities in Coal Operations, Robert R. Godard, Mining Congress Journal, April 1968
6. Coal Industry's Progress in Dust Control, Kenneth M. Morse, Mining Congress Journal, July 1969
7. Dust Control Methods, Coal Age, August 1967
8. Field Notes - A Coal Dust Suppression System, Power Engineering, June 1974

F. Specific Coal Mines

1. Peabody Coal Company - Tops in Reserves and Productive Zeal, Coal Age, October 1971

G. Safety - Fire

1. Standard Method of Test for Surface Burning Characteristics of Building Materials, ASTM E84-70
2. Standard Method of Test for Surface Flammability of Materials Using a Radiant Heat Energy Source, ASTM E 162-67

H. Bulk Flow General

1. Bulk Materials Handling - University of Pittsburg, Vol. 1:
 - a. State-of-the-Art of Bulk Materials Systems, E. R. Palowitch, R. S. Fowkes, and C. A. Goode
 - b. Gravity Flow of Bulk Materials: Hoppers and Bins, Chutes and Feeders, H. Colijn, and P. J. Carroll
 - c. Physical Properties of Bulk Materials, D. E. Frisque and L. C. Marraccini
2. Causes of "Hanging" in Ore Chutes Pipes and Its Solution, Vedat Aytaman, Canadian Mining Journal, November 1960
3. Energy System Problems - How Can We Stop Coal Sticking to Bunker Walls?, Francis P. Sullivan, Power, March 1966
4. Discharge Trajectories, CEMA Bulk Materials Conveyor Handbook.

I. Bulk Flow Theory

1. Stress and Velocity Fields in Gravity Flow of Bulk Solids, Jerry Ray Johanson and Andrew W. Jenike, Bulletin No. 116 of the Utah Engineering Experiment Station, May 1962 (Early edition of Item I-13) Extract
2. Storage and Flow of Solids, Andrew W. Jenike, Bulletin No. 123 of the Utah Engineering Experiment Station, November 1964 (Revised - See Item 10) Extract
3. Gravity Flow of Bulk Solids, Andrew W. Jenike, Bulletin No. 108 Utah Engineering Experiment Station, October 1961 Extract
4. Gravity Flow of Bulk Solids and Transportation of Solids in Suspension, Alexey J. Stepanoff, 1969
5. On the Theory of Bin Loads, A. W. Jenike, J. R. Johanson
6. Principles of Flow of Solids in Bins, Andrew W. Jenike, J. R. Johanson, Society of Mining Engineers of AIME, February 1968
7. Storage and Flow of Solids, A. W. Jenike, Society of Mining Engineers, Sept 1966
8. Bin Hopper Engineering and Bulk Materials Flow: A State-of-the-art Report on Empirical and Theoretical Analyses, U. S. Dept. of Interior, Bureau of Mines Information Circular, 1972, Pariseau and Fowkes
9. An Investigation of the Gravity Flow of Noncohesive Granular Materials Through Discharge Chutes, A. W. Roberts, Transactions of the ASME.
10. Storage and Flow of Solids, A. W. Jenike, Bulletin No. 123, Utah Engineering Experiment Station, March 1970 (Revision of Item 3)
11. A Flow-No Flow Criterion in the Gravity Flow of Powders in Converging Channels, A. W. Jenike and T. Leser.
12. Gravity Flow of Frictional-Cohesive Solids-Convergence to Radial Stress Fields, A. W. Jenike, Journal of Applied Mechanics, March 1965
13. Stress and Velocity Fields in the Gravity Flow of Bulk Solids, J. R. Johanson, ASME, 1964
14. Feeding, J. R. Johanson, Chemical Engineering, October, 1969
15. Steady Gravity Flow of Frictional-Cohesive Solids in Converging Channels, A. W. Jenike, Journal of Applied Mechanics, ASME, Paper No. 63-WA-177
16. New Design Concepts for Coal Bins and Hoppers, J. R. Johanson, Coal Age, Jan. 1966

17. Why Bins Don't Flow, A. W. Jenike, Mechanical Engineering, May 1964
18. New Design Criteria for Hoppers and Bins, J. R. Johanson and H. Colijn, Iron and Steel Engineer, Oct. 1964
19. Effect of Initial Pressures on Flowability of Bins, Journal of Engineering for Industry, ASME, Paper No. 68-MH-9, Nov. 25, 1976
20. In-Bin Blending, J. R. Johanson, Chemical Engineering Progress, June 1970
21. Handling Bulk Materials from Bins, A. W. Jenike, Mining Engineering, May 1968
22. Settlement of Powders in Vertical Channels Caused by Gas Escape, J. R. Johanson & A. W. Jenike, Journal of Applied Mechanics, ASME, Dec. 1972
23. Bin Loads, Journal of Engineering for Industry, Paper No. 72-MH-1, through MH-3 1972
24. A Measure of Flowability for Powders and Other Bulk Solids, A. W. Jenike, Powder Technology, 1975
25. Feeding Solids with Mass-Flow Bins, A. W. Jenike and J. W. Carson, Chemical Engineering Progress, February 1975
26. Method of Calculating Rate of Discharge from Hoppers and Bins., J. R. Johanson, Transactions of Society of Mining Engineers, March, 1965
27. Quantitative Designs of Mass Flow Bins, A. W. Jenike, Powder Technology, 1967, Vol. 1.
28. Flow characteristics of Shelled Corn Through Chutes, McCurdy and Buelow, Michigan Quarterly Bulletin, Vol. 46, No. 2
29. Profile of Flow of Granules Through Apertures, R. L. Brown and J. C. Richards, Transactions of Institution of Chemical Engineers, Vol. 38, 1960
30. The mixing of Powder Layers on a Chute: The Effect of Particle Size and Shape, K. Ridgeway and R. Rupp, Powder Technology, Vol. 4, 1970-71
31. Flow in a Hopper Discharge Chute System, A. W. Roberts and G. J. Montagner, Chemical Engineering Progress, Feb. 1975
32. Optimum Chute Profiles in Gravity Flow of Granular Materials: A Discrete Segment Solution Method, C. Chiarella, W. Charlton, and A. W. Roberts, Journal of Engineering for Industry, ASME, Feb. 1975
33. Application of Pseudo-Random Test Signals and Cross Correlation to the Identification and Cross Correlation to the Identification of Bulk Handling Plant Dynamic Characteristics, A. W. Roberts and W. H. Charlton, Journal of Engineering for Industry, ASME, February 1973

34. Gravity Flow of Granular Materials, Analysis of Particle Transit Time, W. H. Charlton and A. W. Roberts, W. H. Charlton and A. W. Roberts, ASME Paper 72-MH-73, 1972
35. The Dynamics of Granular Material Flow Through Curved Chutes, A. W. Roberts, Mechanical and Chemical Engineering Transactions, November 1967

* 36. Transfer Chute Study

J. Coal Properties

1. Classifying Flow Properties of Solids, Ralph L. Carr, Jr., Chemical Engineering, February 1965
2. Evaluating Flow Properties of Solids, Ralph Carr, Jr., Chemical Engineering, January 1965
3. Flow Properties of Bulk Solids, Jenike, Elsey and Woolley, Proceedings of ASTM, 1960
4. Too Coarse Too Fine, Clay Colley, Mechanical Engineering, May 1963
5. Physical Properties of Bulk Materials, D. E. Frisque, L. C. Marraccini
6. Experimental Study of the Flow of Coal in Chutes at Riverside Generating Station, E. F. Wolf, H. L. vonHohenleiten
7. Friction Between Coal and Metal Surfaces, Structure, Fracture, and Workability of Coal
8. Coal Selection and Handling, Power, February 1974
- * 9. Measured Wall Friction, Correspondence to T. L. Holliday, 7/28/76
10. Coal Preparation, Leonard/Mitchell, AIMMPE, 1968, Extract

K. Sampling

1. Introduction to Sampling and Blending Systems, H. Colijn, Bulk Materials Handling, Vol. 2
2. Statistical Sampling Techniques, A. A. Orning, Bulk Materials Handling, Vol. 2
3. Sampling System Guidelines, James A. Redding, Bulk Materials Handling, Vol. 2
4. Sampling Practices, Robert J. King, Bulk Materials Handling, Vol. 2
5. Continuous Sampling Equipment, Fred Huntington, Bulk Materials Handling, Vol. 2

* Proprietary

6. Practical Considerations in Sampling Standards and Procedures,
R. L. Zickefoose, Bulk Materials Handling, Vol. 2
7. Bulk Solids in Transit - Several articles on weighing, analyzing, etc.

L. Scale Modeling

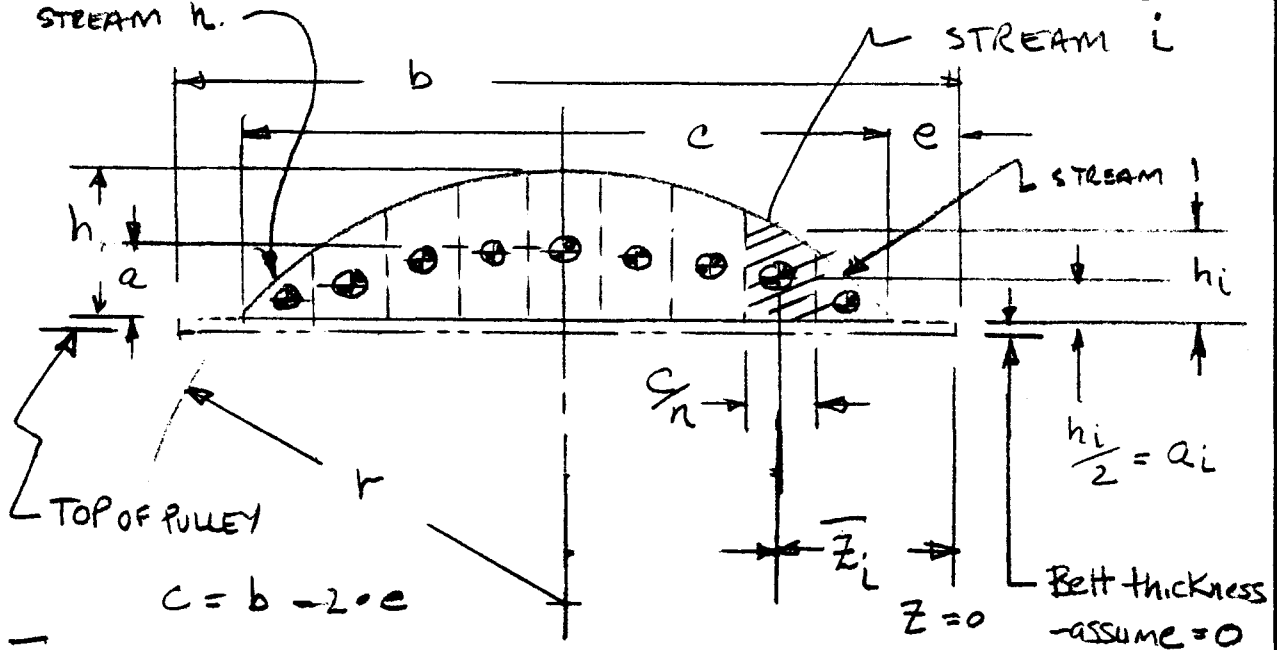
1. Modeling Flow of Bulk Solids, J. R. Johanson, Power Technology,
May 14, 1971

APPENDIX B

**MATH MODEL FOR PHASE I DYNAMICS
FREE FALL AND IMPACT DYNAMICS PHASE**



1. DIVIDE FLOW CROSS SECTION INTO n (ODD) STREAMS



z_i

$$z_i = e + i \times \left(\frac{c}{n}\right) + \frac{c}{2n} = e + \frac{c}{n} \left(i + \frac{1}{2}\right)$$

r

$$r - \sqrt{r^2 - \left(\frac{c}{2}\right)^2} = h$$

$$r^2 - 2rh + h^2 = r^2 - \frac{c^2}{4}$$

$$r = \frac{h}{2} + \frac{c^2}{8h} *$$

USING ABOVE VALUES FOR z_i and r ,
THE HEIGHT OF THE STREAM C.G. ABOVE PULLEY IS

$$\frac{h_i}{2} = \frac{\sqrt{r^2 - \left(\frac{b}{2} - z_i\right)^2} - \sqrt{r^2 - \frac{c^2}{4}}}{2}$$

* see next page for "h"

PREPARED BY

CHECKED BY

DATE

REV.



1 CONTINUED

DERIVATION OF h

REFER TO TABLE A-1 EXTRACT FROM CEMA BULK FLOW TRAJECTORIES, WHERE h IS GIVEN AS FUNCTION OF IDLER TYPE, BELT WIDTH, AND SURCHARGE ANGLE. DATA IS EXTRACTED FROM 20° , 35° , AND 45° IDLER & PLOTTED ON FIGURES A-1 & A-2 TO DETERMINE OTHER MINE IDLER TYPE, 27° , FOR 30 INCH AND 36 INCH BELT WIDTHS. FROM THESE GRAPHS ARE DERIVED THE FOLLOWING DATA TO BE TABULARLY ENTERED INTO THE COMPUTER MODEL.

IDLER ANGLE	SURCHARGE ANGLE	h^* - INCHES	
		$b = 30''$	$b = 36''$
27°	20°	5.07	6.24
	25°	5.57	6.86
	30°	5.99	7.50
35°	20°	5.71	6.95
	25°	6.04	7.52
	30°	6.38	8.09

* ADJUSTED FOR 2-INCH EDGE DISTANCE (e) CASE

PREPARED BY	CHECKED BY	DATE	REV.
-------------	------------	------	------



Type of idlers	Surcharge angle	"h" and "a," values, inches, for Standard Edge Distance of 0.055b + 0.9 inch													
		Belt width, inches													
		14	16	18	20	24	30	36	42	48	54	60	66	72	
20° Three-equal-length-roll troughing idlers	0°	h	0.9	1.0	1.1	1.4	1.7	2.1	2.7	3.1	3.7	4.1	4.7	5.3	5.7
		a ₁	0.4	0.4	0.4	0.6	0.7	0.8	1.1	1.3	1.5	1.7	1.9	2.1	2.3
	5°	h	1.0	1.2	1.4	1.6	2.0	2.6	3.2	3.9	4.5	5.1	5.6	6.3	6.8
		a ₁	0.4	0.5	0.6	0.6	0.8	1.0	1.3	1.6	1.8	2.1	2.3	2.5	2.7
	10°	h	1.2	1.4	1.6	1.9	2.4	3.1	3.7	4.5	5.2	6.0	6.7	7.4	8.1
		a ₁	0.5	0.6	0.6	0.8	1.0	1.3	1.5	1.8	2.1	2.4	2.7	3.0	3.3
20°	h	1.6	1.9	2.2	2.5	3.1	3.8	4.8	5.7	6.8	7.5	8.5	9.5	10.4	
	a ₁	0.6	0.8	0.9	1.0	1.3	1.6	1.9	2.3	2.7	3.0	3.4	3.8	4.2	
25°	h	1.8	2.1	2.5	2.8	3.5	4.5	5.4	6.4	7.5	8.5	9.6	10.5	11.6	
	a ₁	0.7	0.8	1.0	1.1	1.4	1.8	2.2	2.6	3.0	3.4	3.8	4.2	4.6	
30°	h	2.0	2.3	2.7	3.1	3.8	5.0	6.0	7.1	8.2	9.4	10.6	11.5	12.7	
	a ₁	0.8	0.9	1.1	1.3	1.5	2.0	2.4	2.9	3.3	3.8	4.3	4.6	5.1	
35° Three-equal-length-roll troughing idlers	0°	h	1.3	1.6	1.9	2.2	2.7	3.5	4.3	5.0	6.0	6.7	7.4	8.4	9.0
		a ₁	0.5	0.6	0.8	0.9	1.1	1.4	1.7	2.0	2.4	2.7	3.0	3.4	3.6
	5°	h	1.5	1.8	2.1	2.4	3.0	3.8	4.8	5.5	6.4	7.4	8.1	9.2	10.0
		a ₁	0.6	0.7	0.8	1.0	1.2	1.5	1.9	2.2	2.6	3.0	3.3	3.7	4.0
	10°	h	1.7	2.0	2.3	2.6	3.2	4.2	5.2	6.1	7.2	8.2	9.0	10.0	11.0
		a ₁	0.7	0.8	0.9	1.0	1.3	1.7	2.1	2.5	2.9	3.3	3.6	4.0	4.4
20°	h	1.9	2.3	2.7	3.1	3.9	5.1	6.1	7.3	8.4	9.5	10.7	11.7	13.0	
	a ₁	0.8	0.9	1.1	1.3	1.6	2.1	2.5	2.9	3.4	3.8	4.3	4.7	5.2	
25°	h	2.1	2.5	3.0	3.4	4.2	5.4	6.6	7.8	9.1	10.3	11.6	12.7	13.9	
	a ₁	0.8	1.0	1.2	1.4	1.7	2.2	2.7	3.1	3.7	4.1	4.6	5.1	5.6	
30°	h	2.3	2.7	3.2	3.6	4.5	5.7	7.1	8.4	9.8	11.1	12.4	13.7	14.9	
	a ₁	0.9	1.1	1.3	1.5	1.8	2.3	2.9	3.4	4.0	4.5	5.0	5.5	6.0	
45° Three-equal-length-roll troughing idlers	0°	h	1.6	1.9	2.2	2.5	3.1	4.0	5.0	6.0	6.8	7.7	8.6	9.5	10.5
		a ₁	0.6	0.8	0.9	1.0	1.3	1.6	2.0	2.4	2.7	3.1	3.5	3.8	4.2
	5°	h	1.7	2.1	2.4	2.8	3.4	4.4	5.4	6.4	7.4	8.4	9.5	10.4	11.4
		a ₁	0.7	0.8	1.0	1.1	1.4	1.8	2.2	2.6	3.0	3.4	3.8	4.2	4.6
	10°	h	1.9	2.2	2.6	3.0	3.7	4.7	5.8	7.0	7.9	9.0	10.2	11.3	12.2
		a ₁	0.8	0.9	1.0	1.2	1.5	1.9	2.3	2.8	3.2	3.6	4.1	4.6	4.9
20°	h	2.1	2.6	2.9	3.4	4.1	5.4	6.6	7.8	9.1	10.3	11.5	12.8	14.0	
	a ₁	0.8	1.0	1.2	1.4	1.7	2.2	2.7	3.1	3.7	4.2	4.6	5.2	5.6	
25°	h	2.3	2.7	3.1	3.6	4.4	5.7	7.0	8.3	9.7	10.9	12.3	13.6	14.8	
	a ₁	0.9	1.1	1.2	1.4	1.8	2.3	2.8	3.3	3.9	4.4	4.9	5.5	5.9	
30°	h	2.4	2.9	3.3	3.8	4.7	6.0	7.4	8.8	10.2	11.5	13.0	14.3	15.6	
	a ₁	1.0	1.2	1.3	1.5	1.9	2.4	3.0	3.5	4.1	4.6	5.2	5.8	6.3	

TABLE EXTRACTED FROM CEMA
BULK MATERIALS HANDBOOK, DISCHARGE
TRAJECTORIES

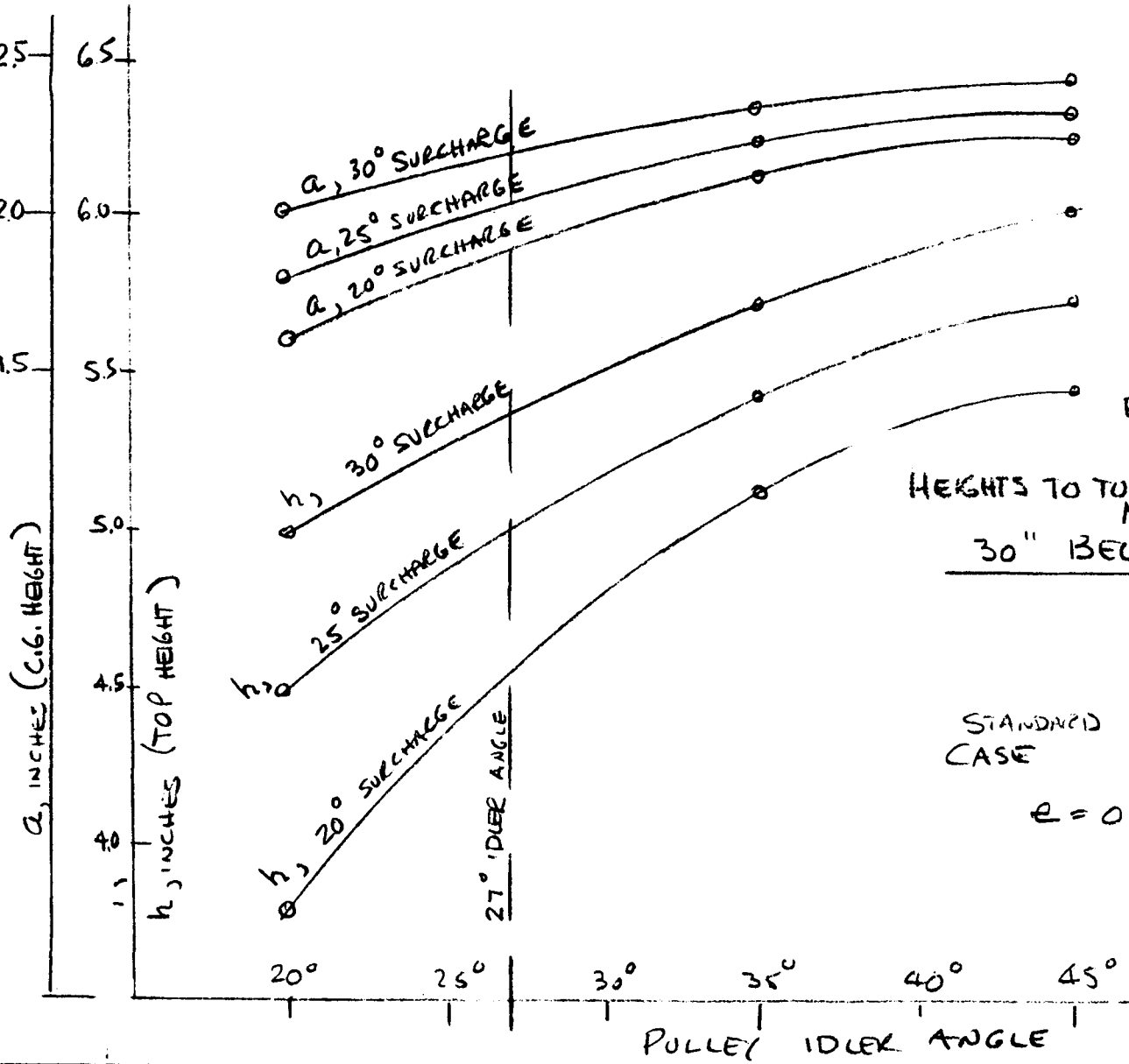
PREPARED BY	CHECKED BY	DATE	REV.
-------------	------------	------	------



1. CONTINUED

FIGURE A-1
HEIGHTS TO TOP AND G.G. OF FLOW
MASS
30" BELT CASE

STANDARD EDGE DISTANCE
CASE
 $e = 0.55b + 0.9$



PREPARED BY _____

CHECKED BY _____

DATE _____

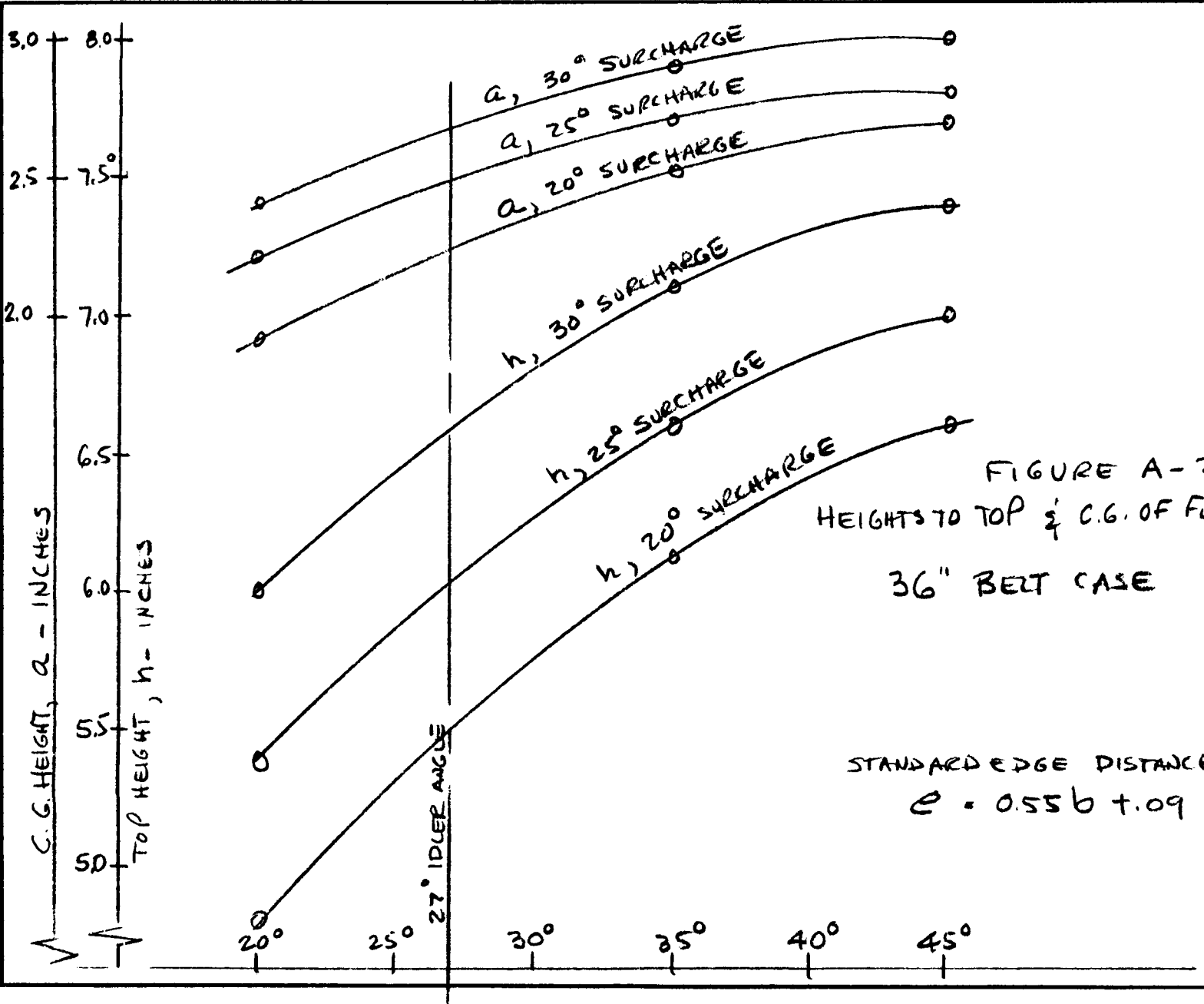
REV. _____



10 - CONTINUED

FIGURE A-2
HEIGHTS TO TOP $\frac{1}{2}$ C.G. OF FLOW MASS
36" BELT CASE

STANDARD EDGE DISTANCE
 $e = 0.55b \pm 0.09$



PREPARED BY	CHECKED BY	DATE	REV.

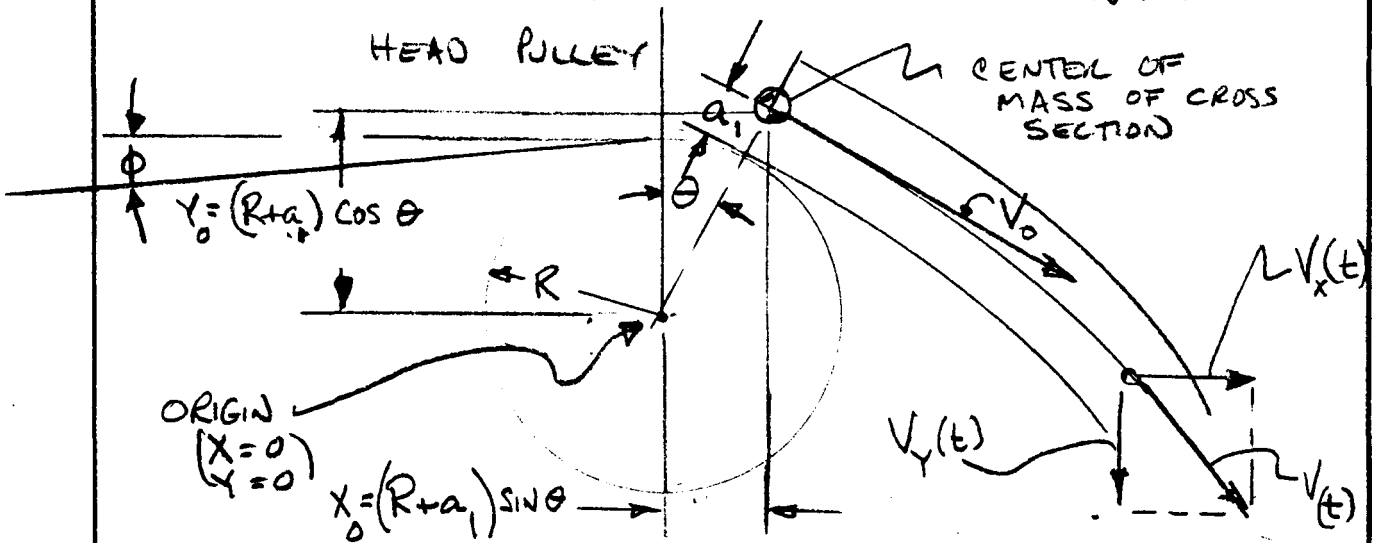
FORM 0006 REV. A 5-71

B-6



1.

2. DETERMINE POSITION AND DIRECTION OF TRAJECTORY CROSS SECTION LEAVING HEAD PULLEY



V = BELT SPEED

ϕ = BELT INCLINATION (+ = CLIMBING)

θ = ANGLE AT WHICH STREAM LEAVES PULLEY

$$\theta = f(R, \phi, V, a_1, g)$$

CASE 1: $\phi = 0$

IA. $\frac{V^2}{g(R+a_1)} \geq 1 \quad \therefore \theta = 0$

IB. $\frac{V^2}{g(R+a_1)} \leq 1 \quad \therefore \theta = \cos^{-1} \left(\frac{V^2}{g(R+a_1)} \right)$

PREPARED BY

CHECKED BY

DATE

REV.



CASE 2 $\phi > 0$

2A : $\frac{V^2}{g(R+a_1)} > 1 \quad \therefore \theta = -\phi$

2B : $\frac{V^2}{g(R+a_1)} = 1 \quad \therefore \theta = 0$

2C : $\frac{V^2}{g(R+a_1)} < 1 \quad \therefore \theta = \cos^{-1}\left(\frac{V^2}{g(R+a_1)}\right)$

CASE 3 $\phi < 0$ - NOT ADDRESSED AS APPLICABLE

OF THE ABOVE INDEPENDENT PARAMETERS INFLUENCING θ , ALL ARE INDEPENDENTLY SPECIFIED EXCEPT THE HEIGHT TO THE CENTER OF MASS OF THE FLOW CROSS SECTION, a_1 . THIS PARAMETER IS ITSELF A FUNCTION OF BELT WIDTH, EDGE DISTANCE, SURCHARGE ANGLE, AND IDLER ANGLE -- AS IN THE CASE FOR h . PLOTS FOR a_1 ARE INCLUDED IN FIGURES A1 AND A2, WHEREIN IS DERIVED VALUES FOR A 27° IDLER ANGLE FOR 30 INCH AND 36 INCH BELT WIDTHS THE DATA FOR THE 20° , 35° , AND 45° IDLER ANGLE CASES IS EXTRACTED FROM TABLE A-1

PREPARED BY	CHECKED BY	DATE	REV.
-------------	------------	------	------



2., CON'T.

THE FOLLOWING DATA ARE TABULATED HERE FOR ENTRY INTO THE COMPUTER MODEL.

IDLER ANGLE	SURCHARGE ANGLE	a_1 (INCHES)	
		$b = 30''$	$b = 36''$
27°	20°	2.48	2.23
	25°	2.75	2.29
	30°	2.97	2.45
35°	20°	2.35	2.85
	25°	2.46	3.08
	30°	2.58	3.31

THUS, θ IS NOW COMPLETELY SPECIFIED.

USING THE ABOVE DATA, AND ASSUMING THE ORIGIN AT THE CENTER OF THE PULLEY, THE FOLLOWING LOCATIONS ARE THEN APPLICABLE FOR THE TOP, CENTER OF GRAVITY, AND BOTTOM OF A STREAM L , USING THE COORDINATE SYSTEM DEFINED IN FIGURE A-3, WHEN IT LEAVES THE HEAD PULLEY.

PREPARED BY	CHECKED BY	DATE	REV.
-------------	------------	------	------



REPORT NO. APPENDIX B

FAIRCHILD
SPACE & ELECTRONICS DIVISION

MODEL _____

FIGURE A-3

PAGE 9

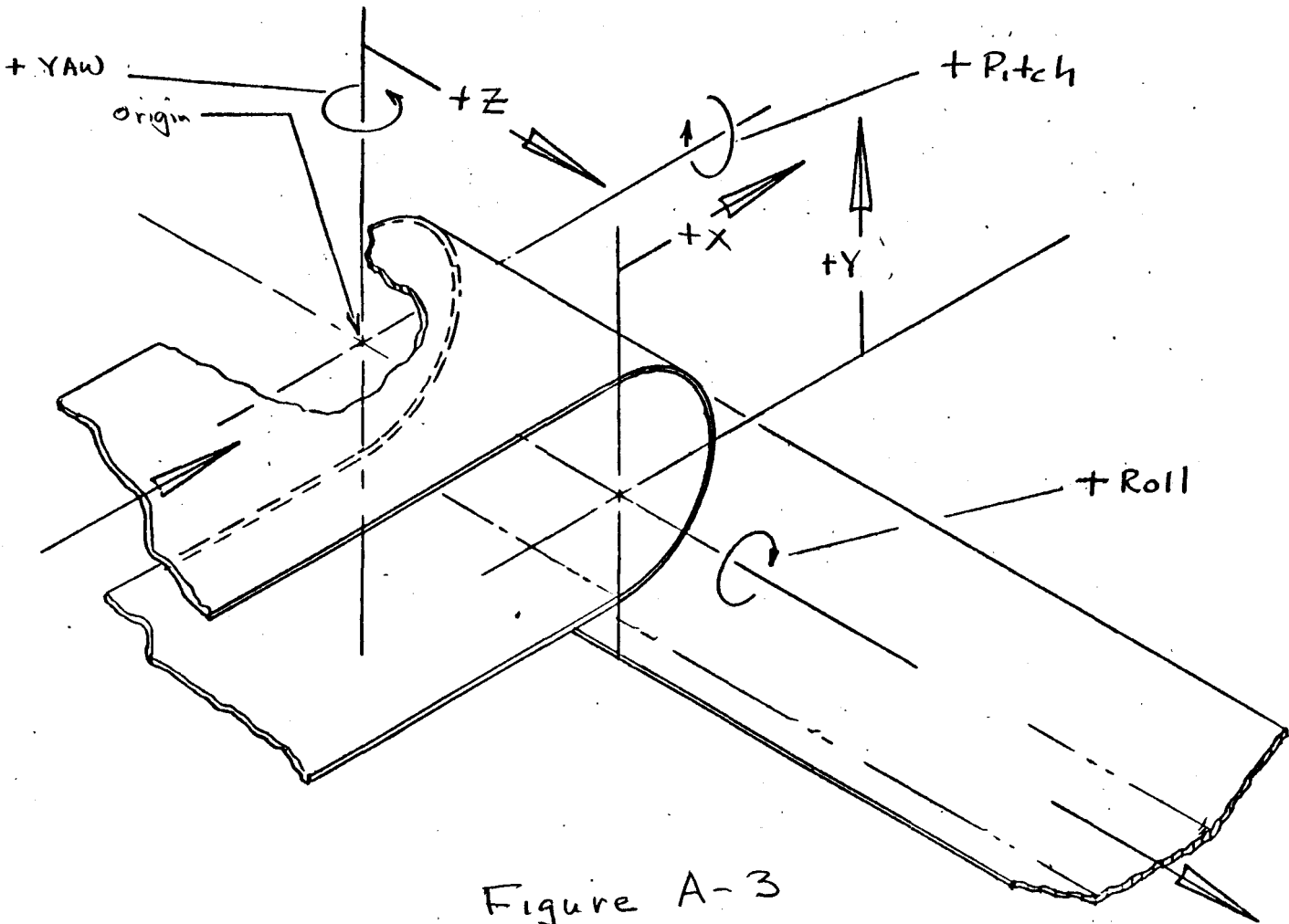


Figure A-3

PREPARED BY _____

CHECKED BY _____

DATE _____

REV. _____

FSGD 0085 REV. A 5-71

B-10



2. CONT

STREAM i LOCATION AT TIME
LEAVING PULLEY ($t=0$)

COORDINATE	TOP	C.G.	BOTTOM
x_0	$(R + \frac{h_i}{2}) \sin \theta$	$(R+a) \sin \theta$	$R \sin \theta$
y_0	$(R + \frac{h_i}{2}) \cos \theta$	$(R+a) \cos \theta$	$R \cos \theta$
z_0	$e + \frac{g}{n}(t + \frac{1}{2})$	$e + \frac{g}{n}(t + \frac{1}{2})$	$e + \frac{g}{n}(t + \frac{1}{2})$

3. DEFINE THE FREE FALL TRAJECTORY PATH

THE FOLLOWING DYNAMIC PARAMETERS APPLY
AT TIME t :

COORDINATE	LOCATION	VELOCITY
x_t	$x_0 + (V \cdot \cos \theta)t$	$V \cos \theta$
y_t	$y_0 - V \sin \theta t + \frac{1}{2}gt^2$	$V \sin \theta + gt$
z_t	$e + \frac{g}{n}(t + \frac{1}{2})$	0

PREPARED BY

CHECKED BY

DATE

REV.



4. LOCATION OF IMPACT POINT OF STREAM
L WITH CHUTE

THE IMPACT POINT OF STREAM L (TOP, C.G., AND BOTTOM, RESPECTIVELY) WITH THE CHUTE IS THE INTERCEPT BETWEEN THE FREE FALL TRAJECTORY, A PARABOLIC EQUATION, WITH THE $Z = e + \frac{y}{h}(l + \frac{y}{2})$ LINE EQUATION IN THE PARTICULAR PLATE INTERCEPTED. ASSUME THE RECTANGULAR PLATES TO BE DIVIDED INTO TWO TRIANGLES EACH FOR THIS SOLUTION, WHICH ADDRESSES THE C.G. TRAJECTORY, BUT IS READILY CONVERTED FOR THE INTERCEPTS OF THE TOP AND BOTTOM TRAJECTORY EQUATIONS

$$X_t = V_0 \cos \theta + X_0 \quad (1)$$

$$Y_t = Y_0 - V_0 \sin \theta t - \frac{1}{2} g t^2 \quad (2)$$

WHERE

$$t = \frac{X - X_0}{V \cos \theta} \quad (3)$$

PREPARED BY	CHECKED BY	DATE	REV.
-------------	------------	------	------



4. CONT

SUBSTITUTING VALUE FOR t INTO 1ST EQUATION FOR Y ,

$$Y = \left[\frac{-\frac{1}{2}g}{(V \cos \theta)^2} \right] X^2 + \left[\frac{g X_0}{(V \cos \theta)^2} - \text{TAN} \theta \right] X + \left[Y_0 + X_0 \text{TAN} \theta - \frac{0.5g X_0^2}{(V \cos \theta)^2} \right] \quad (4)$$

LET $\alpha = X^2$, OR 1ST TERM FACTOR (4a)

$\beta = X$, OR SECOND TERM FACTOR (4b)

$\gamma = \text{CONSTANT}$, OR THIRD TERM (4c)

4.2 EQUATIONS OF PLANE TRIANGLE \hat{j}
(GIVEN X, Y, Z COORDINATES FOR THREE CORNERS 1, 2, AND 3)

EVALUATE PLANE EQUATION CONSTANTS FOR GENERAL EQUATION FOR PLANE TRIANGLE :

$$ax + by + cz = 1 \quad (5)$$

PREPARED BY	CHECKED BY	DATE	REV.
-------------	------------	------	------



4 CONT

$$a = \frac{\begin{vmatrix} 1 & Y_1 & Z_1 \\ 1 & Y_2 & Z_2 \\ 1 & Y_3 & Z_3 \end{vmatrix}}{\begin{vmatrix} X_1 & Y_1 & Z_1 \\ X_2 & Y_2 & Z_2 \\ X_3 & Y_3 & Z_3 \end{vmatrix}} \quad (6)$$

$$b = \frac{\begin{vmatrix} X_1 & 1 & Z_1 \\ X_2 & 1 & Z_2 \\ X_3 & 1 & Z_3 \end{vmatrix}}{\begin{vmatrix} X_1 & Y_1 & Z_1 \\ X_2 & Y_2 & Z_2 \\ X_3 & Y_3 & Z_3 \end{vmatrix}} \quad (7)$$

$$c = \frac{\begin{vmatrix} X_1 & Y_1 & 1 \\ X_2 & Y_2 & 1 \\ X_3 & Y_3 & 1 \end{vmatrix}}{\begin{vmatrix} X_1 & Y_1 & Z_1 \\ X_2 & Y_2 & Z_2 \\ X_3 & Y_3 & Z_3 \end{vmatrix}} \quad (8)$$

PREPARED BY	CHECKED BY	DATE	REV.
-------------	------------	------	------



4. CONT

SOLVING EQUATION 5 FOR x , (9)

$$x = \frac{1 - cz - by}{a}$$

SINCE THE z INTERCEPT COORDINATE IS FIXED FOR ANY ONE STREAM, I.E.,

$$z_i = e + \frac{y}{n} \left(l + \frac{1}{2} \right)$$

THEN LET

$$k = (1 - cz) \quad (10)$$

HENCE

$$x = \frac{k - by}{a} \quad (11)$$

IS THE EQUATION OF THE LINE INTERSECTION BETWEEN THE $z = z_i$ PLANE AND THE PLANE OF THE PLATE.

THE POSSIBLE INTERCEPT POINTS ARE THEN OBTAINED BY SOLVING EQUATIONS (11) AND (4) SIMULTANEOUSLY.

PREPARED BY	CHECKED BY	DATE	REV.
-------------	------------	------	------



4.0 CONT

SUBSTITUTING X IN EQUATION 11 INTO EQUATION 4

$$y = \alpha \left(\frac{k-by}{a} \right)^2 + \beta \left(\frac{k-by}{a} \right) + \gamma \quad (12)$$

SIMPLIFYING TERMS & SETTING UP IN QUADRATIC FORM

$$0 = \left(\frac{\alpha}{a^2} \cdot b^2 \right) y^2 - \left[2kb \left(\frac{\alpha}{a^2} \right) + \frac{b\beta}{a} - 1 \right] y + \left[\frac{\alpha k^2}{a^2} + \frac{\beta}{a} k + \gamma \right]$$

LETTING

Q = CONSTANT FACTOR IN FIRST TERM

R = CONSTANT FACTOR IN 2ND TERM

S = THIRD TERM

$$y = \frac{-R \pm \sqrt{R^2 - 4QS}}{2Q}$$

THEN SOLVE FOR X

PROPER VALUE FOR Y & X IS DETERMINED BY FOLLOW CRITERIA :

PREPARED BY	CHECKED BY	DATE	REV.
-------------	------------	------	------



4. CAN'T

CRITERIA

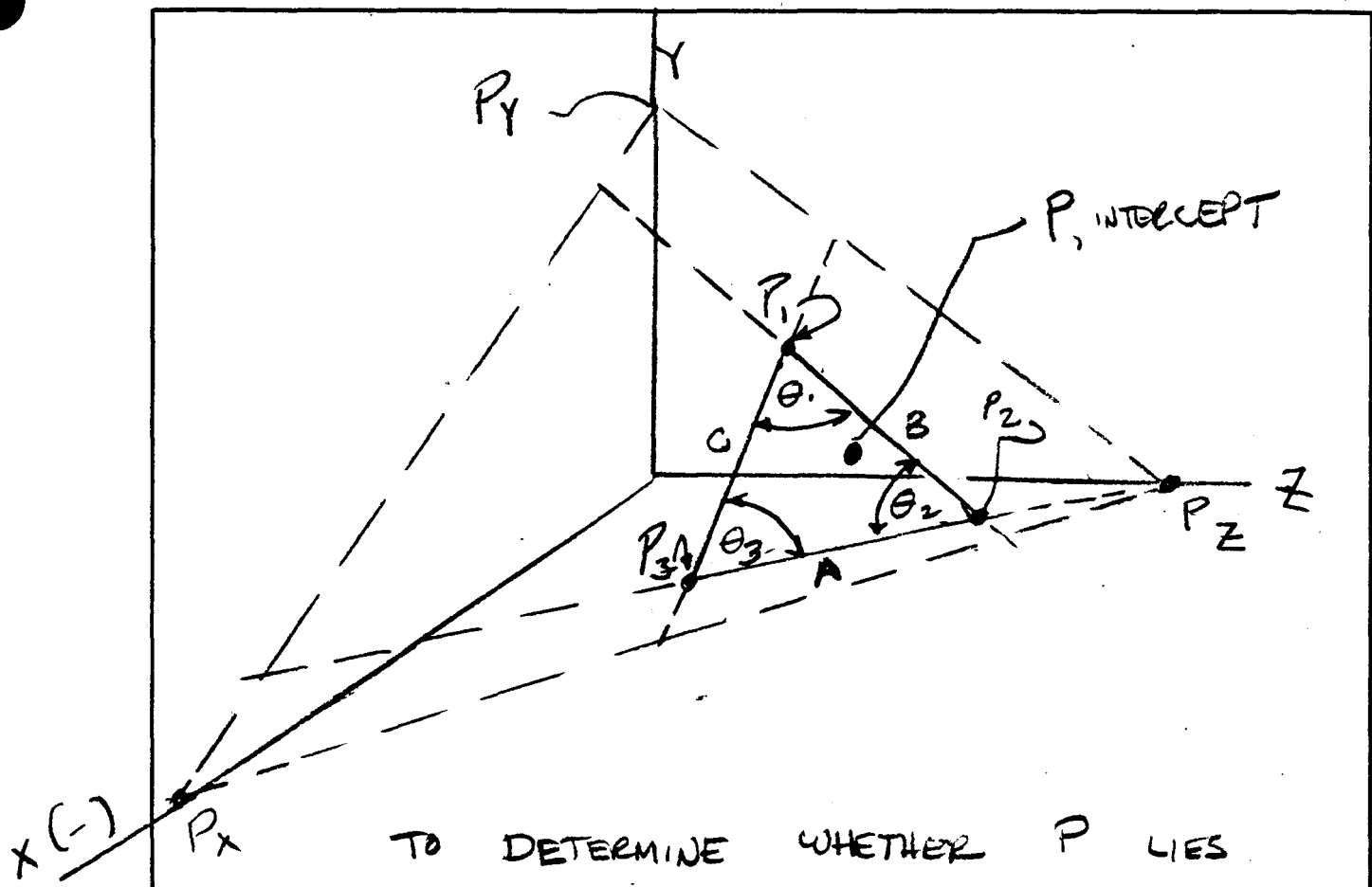
① IF $R^2 - 4QS < 0$, THEN NO INTERCEPT OCCURS

② IF $R = 4QS$, THEN
$$Y = \frac{-R}{2Q}$$

③ IF $R - 4QS > 0$, THEN OF TWO ROOTS Y_{MAX} & Y_{MIN} ,
1) CHOOSE Y_{MAX} IF $X_{FOR Y_{MAX}} > 0$
2) CHOOSE Y_{MIN} IF $X_{FOR Y_{MAX}} < 0$

SINCE ONLY A PORTION OF THE INFINITE PLANE $ax + by + cz = 1$ IS PART OF THE CHUTE, IT IS NECESSARY TO DETERMINE WHETHER THE INTERCEPT POINT P LIES IN THE TRIANGLE WITH CORNERS P_1, P_2, P_3 , OR OUTSIDE IT WHILE STILL WITHIN SOME LARGER EXTENSION OF THE PLANE, DEFINED BY P_x, P_y, P_z , ON THE NEXT PAGE

PREPARED BY	CHECKED BY	DATE	REV.
-------------	------------	------	------



TO DETERMINE WHETHER P LIES
 WITHIN P_1, P_2, P_3 , THE FOLLOWING MUST BE
 TRUE, INVOLVING ANGLES (\angle)

- $\angle P P_1 P_2 \leq \theta_1$
- $\angle P P_1 P_3 \leq \theta_1$
- $\angle P P_2 P_1 \leq \theta_2$
- $\angle P P_2 P_3 \leq \theta_2$
- $\angle P P_3 P_1 \leq \theta_3$
- $\angle P P_3 P_2 \leq \theta_3$

PREPARED BY	CHECKED BY	DATE	REV.
-------------	------------	------	------



4. CONT

WHERE

$$\Theta_1 = \cos^{-1} \left(\frac{A^2 - B^2 - C^2}{-2BC} \right)$$

$$\Theta_2 = \cos^{-1} \left(\frac{B^2 - C^2 - A^2}{-2CA} \right)$$

$$\Theta_3 = \cos^{-1} \left(\frac{C^2 - A^2 - B^2}{-2AB} \right)$$

AND A, B, & C ARE THE LENGTHS
OF THE SIDES OF THE TRIANGLES WITH
VERTEX POINTS P₁, P₂ & P₃, GIVEN
BY,

$$A^2 = (X_2 - X_3)^2 + (Y_2 - Y_3)^2 + (Z_2 - Z_3)^2$$

$$B^2 = (X_3 - X_1)^2 + (Y_3 - Y_1)^2 + (Z_3 - Z_1)^2$$

$$C^2 = (X_1 - X_2)^2 + (Y_1 - Y_2)^2 + (Z_1 - Z_2)^2$$

PREPARED BY

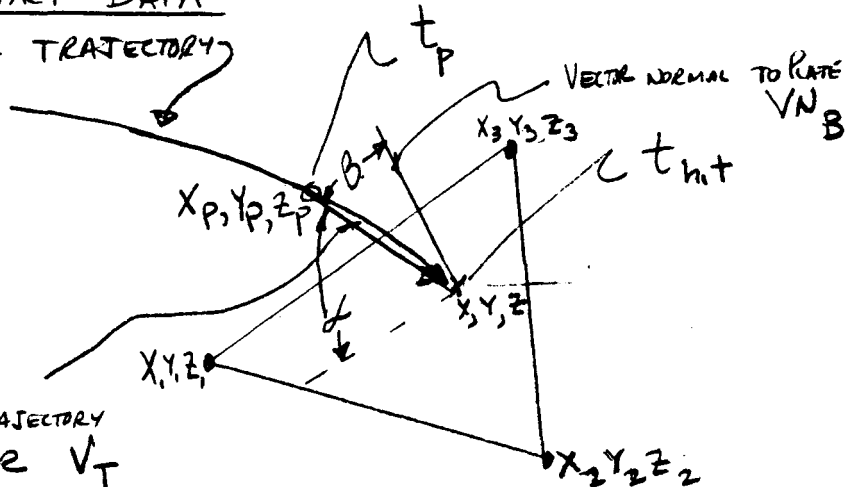
CHECKED BY

DATE

REV.

5. OTHER IMPACT DATA

FREE FALL TRAJECTORY

ASSUMED TRAJECTORY
HIT VECTOR V_T 5.1 IMPACT VECTOR DEFINITION

TO DEFINE VELOCITY VECTOR DIRECTION, ASSUME SAME AS FOR SEGMENT FROM IMPACT POINT UP TO POINT P ON TRAJECTORY 0.02 SECONDS EARLIER

$$t_p = t_{hit} - 0.02$$

$$X_p = V \cos \theta \cdot t_p + X_0$$

$$Y_p = Y_0 - V \sin \theta \cdot t_p - 0.5 g (t_p)^2$$

5.2 VECTOR NORMAL COMPONENTS : DOT CROSS PRODUCTS INVOLVING TRIANGULAR PLATE VERTEX COORDINATES

$$\overline{VN}_x = (Y_3 - Y_1) \cdot (Z_2 - Z_1) - (Y_2 - Y_1) \cdot (Z_3 - Z_1)$$

$$\overline{VN}_y = (Z_3 - Z_1) \cdot (X_2 - X_1) - (Z_2 - Z_1) \cdot (X_3 - X_1)$$

$$\overline{VN}_z = (X_3 - X_1) \cdot (Y_2 - Y_1) - (X_2 - X_1) \cdot (Y_3 - Y_1)$$

PREPARED BY

CHECKED BY

DATE

REV.



5. CONT

$$\overline{VN}_B = \sqrt{\overline{VN}_x^2 + \overline{VN}_y^2 + \overline{VN}_z^2}$$

5.3 ANGLE BETWEEN IMPACT VECTOR & PLANE NORMAL

$$\overline{VT}_x = X_p - x$$

$$\overline{VT}_y = Y_p - y$$

$$\overline{VT}_z = 0$$

$$\therefore \overline{VT}_B = \sqrt{\overline{VT}_x^2 + \overline{VT}_y^2}$$

$$\cos \beta = \frac{-(\overline{VT}_x \cdot \overline{VN}_x + \overline{VT}_y \cdot \overline{VN}_y)}{\overline{VN}_B \cdot \overline{VT}_B}$$

$$\alpha = 90 - \beta$$

5.4 VELOCITY VECTOR AFTER IMPACT

IMPACT VECTOR MAGNITUDES —

$$\overline{VV}_x = \overline{V} \cos \theta$$

$$\overline{VV}_y = \overline{V} \sin \theta - g(t_{hit})$$

$$\overline{VV}_z = 0$$

PREPARED BY

CHECKED BY

DATE

REV.



S.O CONT

$$\overline{V}_{VB} = \sqrt{\overline{V}_{Vx}^2 + \overline{V}_{Vy}^2}$$

$$\cos(P) = \frac{\overline{V}_{Vx} \cdot \check{n}_x + \overline{V}_{Vy} \cdot \check{n}_y}{\overline{V}_{VB}}$$

WHERE \check{n}_x & \check{n}_y are x & y components of UNIT NORMAL TO PLANE
 $\cos(Q) = -\cos(P)$

$$\sin(P) = \sqrt{1 - \cos^2(P)}$$

$$\tan(P) = \frac{\sin(P)}{\cos(P)}$$

FOR $P > \phi$, THE COMPONENTS OF THE VELOCITY VECTOR AFTER IMPACT ARE *

$$V_{Ex} = \left(1 - \frac{\tan \phi}{\tan(P)}\right) \cdot \left(\overline{V}_{Vx} + \check{n}_x \cdot \cos(P) \cdot \overline{V}_{VB}\right)$$

$$V_{Ey} = \left(1 - \frac{\tan \phi}{\tan(P)}\right) \cdot \left(\overline{V}_{Vy} + \check{n}_y \cdot \cos(P) \cdot \overline{V}_{VB}\right)$$

$$V_{Ez} = \left(1 - \frac{\tan \phi}{\tan(P)}\right) \cdot \left(\check{n}_z \cdot \cos(P) \cdot \overline{V}_{VB}\right)$$

* SEE APPENDIX C, SECTION 3

PREPARED BY

CHECKED BY

DATE

REV.

APPENDIX C

PHASE I DYNAMICS COMPUTER PROGRAM
FREE FALL AND IMPACT DYNAMICS PHASE


```

0009 C.....
      DIMENSION IPL(22,3)
0010 C
      NAMELIST /COLOUT/ LAMDA , XF , YF , ZF , Q , CHLN , NP, APT
      *
      , THETCN, H,A1,H2 , YMIN
0011 C
      NAMELIST /COALIN/ V,RADIUS,PHI,SECT,IDLANG,SURANG,BELTWD
      *
      , ND1 , ND2, FLAT , GAMMA,RADUP,DISP
      *
      ,MODET,EPS,RUNNO
      *
      , PHIP, GAMD, EL1, KC, DELTF, NP, NT, BMAR, YAW,ZIH
C.....
0012 C
      CALL DATCHR ( DATE)
0013 C
      V = 120
C
0014      EL1=1.
0015      EL=EL1
0016      JTP=99
0017      PHIP=35.
0018      PHIPR=PHIP/57.29578
0019      MU=TAN(PHIPR)
0020      GAMD = 50
0021      EL1 = 1
0022      KC = 0.5
0023      DELTF = 50
0024      RADIUS = 12.
0025      PHI = 0.
0026      SECT = 21
0027      IDLANG = 35.
0028      SURANG = 25.
0029      BELTWD = 36.
0030      BMAR = 2
0031      ND1 = 6
0032      ND2 = 10.
0033      FLAT = 12.
0034      GAMMA = 0
0035      ZIH = 0
0036      YAW = 0
0037      RADUP=12.
0038      MODET = 1
0039      EPS = 10.
C
0040      DISP = 6
0041      RT1 = 36
0042      RT2 = 18
0043      XT = 12
0044      YT = 16

```

C-2

```

C
C**** GURSENS DEBUGING CONSTANTS
0045      ND1 = 2
0046      ND2 = 2
0047      NT1 = 7
0048      NT2 = 8

C
C
C.....
0049      READ ( 5,C,DALIN,END=600)

C
0050      WRITE ( 6,905)
0051      905 FORMAT( '1' )
0052      WRITE ( 6,901)
0053      901 FORMAT( // )
0054      WRITE ( 6,916)
0055      916 FORMAT ( /1X,132( ' * ' ) )
0056      WRITE ( 6,901)
0057      WRITE ( 6,918) RUNNO , DATE
0058      918 FORMAT ( 1X,10X, 'BEGIN INDEPENDENT RUN OF CUAL CHUTE DESIGNER',
*          30X, 'RUN NUMBFR',13,5X, 'DATE ',5A4)
0059      WRITE ( 6,919)
0060      919 FORMAT ( /1X,31X,10( ' . ' ),5X,
*          ' INDEPENDENT VARIABLES FOR THIS RUN ', 5X,10( ' . ' ) // )
0061      WRITE(6,4000)
0062      4000 FORMAT(5X, ' A. INPUT DATA' )
0063      WRITE(6,4001)
0064      4001 FORMAT(//20X, ' FEED CONVEYOR DATA',50X, ' TORUS CHUTE DATA' )
0065      WRITE(6,4002) V,RT1
0066      4002 FORMAT(//5X, ' BELT SPEED V , IPS.', F7.2 ,40X, ' MAJOR RADIUS RT1,
* IN',F7.2 )
0067      WRITE(6,4003) RADIUS,RT2
0068      4003 FORMAT(//5X, ' PULLEY RADIUS R, IN.', F7.2 ,40X, ' MINOR RADIUS RT2,
* IN',F7.2)
0069      WRITE(6,4004) BELTWD,GAMMA,YAW , ZIH
0070      4004 FORMAT(//5X, ' BELT WIDTH BELTWD IN.',F7.2,40X, ' ROTATIONS,DEG.',
* /70X,
* ' Z-AXIS-GAMMA',F7.2,/70X, ' Y AXIS-YAW ',F7.2,/70X, ' X-AXIS-ZIH'
* ,F7.2)
0071      WRITE (6,4010) BMAR
0072      4010 FORMAT(//5X, ' BELT EDGE DISTANCE BMAR IN.', F7.2)
0073      WRITE(6,4005) IDLANG,DISP
0074      4005 FORMAT (//5X, ' TROUGH ANGLE IDLANG DEG.',F7.2,40X, ' EXTRA LENGTH
* DISP IN.', F7.2)
0075      WRITE(6,4006) SURANG,XT,YT
0076      4006 FORMAT(//5X, ' SURCHARGE ANGLE SURANG DEG.',F7.2,40X, ' COORDINATES
* PRIOR TO ROTATION',/65X, ' XT IN.',F7.2,/65X, ' YT IN.', F7.2)
0077      WRITE (6,4007) PHI,NT1,NT2

```

```

0078      4007  FORMAT(/75X,' INCLINATION ANGLE PHI DEG.',F7.2,40X,' FLAT PLATE
          *DIVISION',/65X,
          * ' MAJOR RADIUS-NT1',/17,/65X,' MINOR RADIUS-NT2',/17)
0079      WRITE ( 6,901)
0080      WRITE (6,4111)
0081      4111  FORMAT(/20X,' RUN OF MINE COAL DATA',50X,' RUN CONVENTION
          * CONSTANTS')
0082      WRITE (6,4112) GAMD
0083      4112  FORMAT(/75X,' DENSITY, GAMD LBS./CU. FT. ', F7.2)
0084      WRITE (6,4113) DELTF , EL1
0085      4113  FORMAT(/75X,' EFFECTIVE ANGLE OF FRICTION DELTF DEG.',F7.2,
          *40X,' FRICTION STEP DISTANCE - NOM.,FL1, IN.', F7.2)
0086      WRITE (6,4114) PHIP , SECT
0087      4114  FORMAT(/75X,' DYNAMIC ANGLE OF WALL FRICTION PHIP DEG.',F7.2, 40X,
          * ' NO OF STREAM SUBDIVISIONS SECT ', /17)
0088      WRITE ( 6,901)
0089      WRITE ( 6,COALIN)
0090      WRITE ( 6,916)

```

```

C
C      WRITE A CARD FOR PLOT PROGRAM IDENTIFIG THE RUN NUMBER
C

```

```

0091      WRITE ( 11,930) RUNNO , DATE
0092      930  FORMAT ( 40X,'RUN NO',/13,5X,'DATE ',/5A4)

```

```

C
C.....
C      USE BELTWD , SURANG , IDLANG TO GET 'A1' , 'HH' , AND '2' ARRAY

```

```

0093      IX = 1
0094      IF ( IDLANG.EQ. 35.) IX = 2

```

```

0095      SX = 1
0096      IF ( SURANG.EQ. 25.) SX= 2
0097      IF ( SURANG.EQ.30.) SX=3

```

```

0098      BX = 1
0099      IF ( BELTWD.EQ.36.) BX=2
0100      IF ( BELTWD.EQ.42.) BX=3

```

```

0101      H = HHH( 1,BX,SX,IX)

```

```

0102      A1 = A11( 1,BX,SX,IX)

```

```

0103      C = BELTWD - 2.*BMAR
0104      R = H/2. + C**2/(B.*H)

```

```

0105      DLT = C/SECT
0106      MID = SECT/2 + 1

```

```

0107      DO 40 K=1,SECT

```

```

0108      B = SQRT(R**2 - C**2/4)
0109      N = ABS(MID-K)
0110      XI = N*ULT
0111      A = SQRT( R**2 - XI**2)
0112      H2(K) = (A-B)/2.
0113      40 CONTINUE
C        CALL TRAJECTORY TO GET 'THETCN'. ONLY. THIS IS REQUIRED BY
C        THE CHUTE DESIGN SUBROUTINE 'KLUDGE'
0114      RSE = RADIUS + A1
C        .. INPUT...../ ... OUTPUT.....
0115      CALL TRAJ (V , RSE , PHI , NC , XO,YG, THETCN )
0116      THETR=RADC(THETCN)
C.....
C        CALL APPROPRIATE SUB-ROUTINE WHICH GENERATES A COAL CHUTE.
C.....
C        REQUIRED INPUT WILL VARY.
C        OUTPUT-  PTDAT  ARRAY CONTAINING X,Y,Z COORDINATES
C                NP    NO OF 4 SIDED PLATES.
C                YMIN  MINIMUM 'Y' (VERTICAL) VALUE.
C        GO TO 50
C 51 CONTINUE
C        .. INPUT FOR CONE CHUTE ..
C        CALL CONE ( RADIUS , A1 ,THETCN, V , GAMMA, RADUP , BELTWD
C        *          , DISP , H ,MODET , FPS
C        *          , YAW, RUNNO
C        *          , FLAT , ND1 , ND2
C        *          ,... OUTPUT OF CONE .....
C        *          ,PTDAT , NP , YMIN
C        *          , LAMDA,CHIN
C        *          ,BETA ,RHO , L11,L12,L13,L14,L15,XF,YF,ZF,Q )
C        GOTO 55
0117      50 CONTINUE
0118      CALL TORUS ( RADIUS , GAMMA , BELTWD , DISP
C        *          ,RT1,RT2,NT1,NT2
C        *          , XT, YT, ZIH, YAW
C        *          ,... OUTPUT OF TORUS .....
C        *          ,PTDAT,NP,YMIN,Z1,DZ1,BETAT,XG,YG)
C.....
C        PUT CHUTE GEOMETRY AND A ROLLER INTO A NASTRAN PLOT FILE
C
0119      55 CONTINUE
0120      ID = 0
0121      NE = 0
C        CALL ROLRI NE,BELTWD,RADIUS,ID,PHI)
0122      NI = 1000
C

```

```

0123      DO 90 J=1,NP
0124      DO 80 L=1,4
0125      CALL GRIDCD ( ID , PTDAT(1,L,J))
0126      IPTS(L) = ID
0127      80 CONTINUE
0128      CALL CGDCD( NE, IPTS)
0129      90 CONTINUE

```

C

C

C

C

```

      CONVERT PLATES INTO TRIANGULAR ELEMENTS FOR INTERNAL USE.

```

C

C

```

      NP = NO. OF PLATE IN CHUTE   NT = NO. OF SUBDIVIDED TRIANGLES.

```

C

```

0130      NT = 0
0131      DO 130 J=1,NP

```

C

```

0132      NT = NT + 1
0133      DO 110 K=1,3
0134      DO 110 L=1,3
0135      110 PT(L,K,NT) = PTDAT(L,K,J)

```

C

```

0136      NT = NT + 1
0137      M=0
0138      DO 125 K=1,4
0139      IF (K.EQ.2) GO TO 125
0140      M=M + 1
0141      DO 120 L=1,3
0142      120 PT(L,M,NT) = PTDAT(L,K,J)
0143      125 CONTINUE
0144      130 CONTINUE

```

C

```

0145      WRITE (7,COALIN)
0146      WRITE(7,3001)
0147      3001  FORMAT(' COORDS OF PLATE')
0148      DO 135 J=1,NP
0149      DO 135 K=1,4
0150      WRITE(7,151) (PTDAT(L,K,J),L=1,3)
0151      CONTINUE
0152      WRITE(7,3002)
0153      3002  FORMAT(' COORDS OF TRIANGLES')
0154      DO 138 J=1,NT
0155      DO 138 K=1,3
0156      WRITE(7,151) (PT(L,K,J),L=1,3)
0157      138 CONTINUE

```

C

C

C

```

C   CONSTRUCT UNIT NORMALS TO EACH TRIANGLE AND STORE IN UN(3,80)
C.....
C
0158      WRITE(7,3003)
0159      3003   FORMAT(' UNIT NORMALS ARE')
0160      DO 140 J=1,NT
C
0161      X1= PT(1,1,J)
0162      Y1= PT(2,1,J)
0163      Z1= PT(3,1,J)
C
0164      X2=PT(1,2,J)
0165      Y2=PT(2,2,J)
0166      Z2=PT(3,2,J)
C
0167      X3=PT(1,3,J)
0168      Y3=PT(2,3,J)
0169      Z3=PT(3,3,J)
C
C
0170      VNX= (Y3-Y1)*(Z2-Z1)-(Y2-Y1)*(Z3-Z1)
0171      VNY= (Z3-Z1)*(X2-X1) -(Z2-Z1)*(X3-X1)
0172      VNZ= (X3-X1)*(Y2-Y1)-(X2-X1)*(Y3-Y1)
0173      VNB=SQRT(VNX**2+VNY**2+VNZ**2)
C
0174      UN(1,J)=VNX/VNB
C
0175      UN(2,J)=VNY/VNB
C
0176      UN(3,J)=VNZ/VNB
0177      WRITE(7,151) (UN(L,J),L=1,3)
0178      151   FORMAT (3F20.8)
C
0179      140   CONTINUE
C
C      GET A,B , C AND THETAS FOR AL PLATES.
C
0180      DO 150 J=1,NT
0181      CALL PLATE( PT(1,1,J) , PT(1,2,J) , PT(1,3,J) ,
*      ABC(1,J) , THET(1,J) )
0182      150   CONTINUE
0183      WRITE(7,3004)
0184      3004   FORMAT(' ABC FOR PLATES ARE')
0185      DO 153 J=1,NT
0186      153   WRITE(7,151) (ABC(L,J),L=1,3)
0187      WRITE(7,3006)
0188      3006   FORMAT(' THETAS FOR PLATES ARE')
0189      DO 154 J=1,NT

```

```

0190      WRITE(7,251) (THE(I,J),L=1,3)
0191      CONTINUE
C
C.....
C      PRINT OUT INPUT CONDITIONS , CALCULATED PARAMETERS AND FINAL
C      CHUTE XYZ GEOMETRY.
C
0192      WRITE ( 6,905)
0193      WRITE ( 6,901)
0194      WRITE ( 6,920)
0195      920 FORMAT ( 31X,10(' '),5X
*,'SUMMARY OF KEY CALCULATED PARAMETERS AND FINAL PLATE '
*      , 'COORDINATES',5X,10(' '),/)
0196      WRITE(6,5000)
0197      5000 FORMAT(5X,' B. OUTPUT DATA ')
0198      WRITE(6,5001) THEICN,H,BETAT,YMIN
0199      5001 FORMAT(/10X,' PULLEY CONTACT DEP. ANGLE,DEG., ',F7.2,
*/10X,' INITIAL LOAD HEIGHT,IN. ',F7.2,
*/10X,' TORUS CUTOFF ANGLE,DEG.,',F7.2,
*/10X,' MINIMUM Y COORDINATE',F7.2)
C      WRITE ( 6,COLOUT)
0200      DO 160 L=1,NP
0201      WRITE ( 6,901)
0202      WRITE ( 6,907) L
0203      907 FORMAT ( 36X,'PLATE',I3/)
0204      WRITE ( 6,921) ((PTDAT(J,K,L),K=1,4),J=1,3)
0205      921 FORMAT ( 1X,4(5X,F15.3))
0206      160 CONTINUE
C
C.....
C      END OF CHUTE DEFINITION PHASE.
C.....
C
C      A THIS POINT A 'COAL CHUTE' OF TRIANGULAR FLAT PLATES IS CREATED
C      IN THE 'PT' ARRAY. TEST IT BY 'SHOOTING' ATE IT FROM
C      VARIOUS POINTS AND HEIGHTS ON THE BELT.
C      RECORD THE LOCATIONS OF INITIAL IMPACT AND OTHER ANGLES ETC.
C
0207      165 CONTINUE
0208      NHC = 0
0209      NF = 2000
0210      DO 510 II=1,3
0211      NS=)
0212      JF = 0
C
0213      DO 500 LL=1,SECT
C

```

```

0214      ZO = BMAR + DLT/2. + ( LL-1)*DLT
C        GET TRAJECTORY FROM INITIAL CONDITIONS
0215      IF ( LL.EQ. 1) A=0.
0216      IF ( LL.EQ.2) A = H2(LL)
0217      IF (LL.EQ. 3) A=2.*H2(LL)
0218      RSE = RADIUS + A
0219      VZ = V
0220      XU=RSE*SIN(THETR)
0221      YU=RSE*COS(THETR)
C        GO THRU ALL PLATES . CHECK IF TRAJECTORY INTERSECTS PLAT.
C        GET TIME OF INTERSECT AND FIN MINUM TIME.
0222      THIT = 1.0F10
0223      JP = 0
C
0224      N11=0
0225      NIT = NT+1
0226      189 CONTINUE
0227      DO 200 J = 1,NTT
0228      IF(J.EQ.NTT) ZO = ZO + 0.05
0229      IF(N11.EQ.1) GO TO 200
0230      IF(J.EQ.NTT) N11 = 1
0231      IF(J.EQ.NTT) GO TO 189
0232      KP = (J-1)/2 + 1
0233      CALL INTERX ( J, XO,YO,ZO,VZ,THETCN, PZ , TS , TAL , TKAP,TOEL,VL
* ,PHIP)
0234      IF ( TS.LT.0) GOTO 200
0235      IF ( TS.GT.THIT) GOTO 200
C
C        THIS IS THE NEAREST HIT SO FAR. SAVE TIME ETC.
C
0236      DO 190 L=1,6
0237      190 PX(L) = PZ(L)
0238      THIT = TS
0239      ALPHA = TAL
0240      KAPPA = TKAP
0241      DELTA = TOEL
0242      JP = KP
0243      JT=J
0244      GO TO 222
0245      200 CONTINUE
0246      222 CONTINUE
C
0247      908 FORMAT (//1X,12,' VFL=',F6.1,' PHI=',F4.1,
* ,XO,YO,ZO=',3F7.2,' DELTRAD=',F5.2)
0248      IF ( JP .NE. 0) GOTO 255
0249      903 FORMAT ( 1X,4X,'MISSED')
0250      GO TO 500
L

```

```

C      A THIS POINT THE JP'ITH PLATE WAS INTERSECT BY THE TRAJ.
C      THE XY/ OF THE INTERSECTION IS IN THE PX ARRAY.
C
0251      255 CONTINUE
0252      NHC = NHC + 1
0253      NS=NS+1
0254      IT(NS)=JT
0255      DO 195 KK=1,3
0256      VV(KK,NS)=VL(KK)
0257      AI(KK,NS)=PX(KK)
0258      1001   FORMAT(/,1X,2F7.2,13)
0259      195 CONTINUE
0260      IF(NS.NE.SECT) GO TO 333
0261      IF(II.NE.2) GO TO 333
0262      WRITE (7,3010)
0263      3010   FORMAT(' THE VELOCITIES AFTER IMPACT ARE ')
0264      DO 196 I=1,NS
0265      196   WRITE (7,151) (VV(KK,I),KK=1,3)
0266      WRITE (7,3020)
0267      3020   FORMAT(' THE COORDS OF HIT POINTS ARE ')
0268      DO 197 I=1,NS
0269      197   WRITE (7,151) (AI(KK,I),KK=1,3)
0270      WRITE (7,3025)
0271      3025   FORMAT(' THE SURFACES ARE ')
0272      DO 199 I=1,NS
0273      WRITE (7,3026) IT(I)
0274      3026   FORMAT(I8)
0275      199 CONTINUE
0276      333 CONTINUE
C
0277      909 FORMAT ( 5X,'HIT PLATE',I3,' AT',3F8.3,5X,' TIME=',F6.3
*           /5X,' ALPHA=',F6.1,' KAPPA=',F6.1,' DELTA=',F6.1)
0278      TIME(LL,II)=THIT
0279      AL(LL,II)=ALPHA
0280      HPT(1,LL,II)=PX(1)
0281      HPT(2,LL,II)=PX(2)
0282      HPT(3,LL,II)=PX(3)
0283      IPL(LL,II)=JP
C
C      DRAW LINE CONNECTING HIT POINTS OD CHUTE
C
0284      IF ( JF.EQ. 0) GOTO 280
0285      CALL GRIDCD ( ID, PX)
0286      IPTS(1) = ID
0287      CALL GRIDCD ( ID, PS)
0288      IPTS(2) = ID
0289      CALL CHARCD ( NE, IPTS )
0290      280 CONTINUE

```

```

0291      JF = 1
0292      DO 290 J=1,3
0293      290 PS(J)=PX(J)
0294      500 CONTINUE
0295      999 CONTINUE
0296      510 CONTINUE
0297      WRITE(6,905)
0298      WRITE(6,901)
0299      WRITE(6,916)
0300      WRITE(6,901)
0301      WRITE(6,6000)
0302      6000  FORMAT(/75X,' B. OUTPUT DATA')
0303      WRITE(6,6001)
0304      6001  FORMAT(/75X,' 1. HIT DATA')
0305      WRITE(6,6002)
0306      6002  FORMAT(/75X,' STREAM          C.G.
          *          BOTTOM          TOP')
0307      WRITE(6,6003)
0308      6003  FORMAT('          TIME  ANGLE  CX  Y  Z
          *          ANGLE  X  Y  PLATE  ANGLE  X
          *          Y  PL')
0309      DO 8000 LL=1,SECT
0310      WRITE(6,6010) LL,TIME(LL,2),AL(LL,2),(HPT(K,LL,2),K=1,3),
          * IPL(LL,2),AL(LL,1),(HPT(K,LL,1),K=1,2),IPL(LL,1),
          * AL(LL,3),(HPT(K,LL,3),K=1,2),IPL(LL,3)
0311      6010  FORMAT(/71X,I6,F9.2,4F9.1,I6,5X,3F9.1,I6,5X,3F9.1,I5)
0312      8000  CONTINUE
0313      600  CONTINUE
0314      STOP
0315      910  FORMAT(1X,3F15.5)
0316      END
    
```

C-11

```

0001      SUBROUTINE TORUS (R, GAMA, BL, DDF, RT1, RT2, NFI, NF2
*          , XT1, YTT, ZIHH, YAWW
*          , P, NP, YMIN, ZIT, DZTT, BETATT, XGG, YCG)
0002      DIMENSION P(3,4,1)
0003      DIMENSION PA(3) , PB(3)
0004      DATA P1/3.14159/
0005      NAMELIST / TORS / XT, YT, ZT, ALP, BETAT, XG, YG, GAMMA
*          , ZIHH, YAW, DZT
*          , ZU, YU, ZYGR, APS, YUR, XUR, ZUR
*          , TYUR, TXUR, TZUR, XLR, YLR, ZLR, TXLR, TYLR, TZLR

```

C
C
C

DU CHUTE COORDINATES PRE-PROCESSING

```

0006      GAMMA = GAMA
0007      GMR = RADC(GAMMA)
0008      SNG = SIN(GMR)
0009      CSG = COS(GMR)
0010      TNG = TAN(GMR)
0011      XT = XT1
0012      YT = YTT
0013      ZIH = ZIHH
0014      ZHR = RADC(ZIH)
0015      SNZ = SIN(ZHR)
0016      CSZ = COS(ZHR)
0017      YAW = YAWW
0018      YWR = RADC(YAW)
0019      REAL LAMDA, LMDA
0020      LAMDA = YAW
0021      ZT = ZTT
0022      DZT = DZTT
C
0023      T = ( YT + XT*TNG) / ( RT1 + RT2 )
0024      ALPR = ARSIN(T)
0025      ALP = DEGC(ALPR)
0026      CSA = COS(ALPR)
C
0027      ZT = ( RT1 + RT2)*(1.-CSA)
0028      F = SNZ * CSG
0029      Q = ARSIN (F)
0030      T = ( RT1 + RT2 - ( BL + DDF)/(COS(YWR)))/ ( RT1 + RT2)
0031      BETR = ARCCOS (T) + Q
0032      BETAT = DEGC(BETR)
0033      BETAT = 105.335
0034      BETR = RADC(BETAT)
0035      BETATT=DEGC(BETR)
C
0036      ZT = -ZT + RT1 + RT2
C

```

C-12

```

C
C*****
C
C      CREAT A PHYSICAL 'TORUS' SHAPED CHUTE IN PT ARRAY
0037      NP = 0
C
0038      BETD = BETR/ NT1
0039      SCR = ( PI + PI/3)/ NT2
C
0040      DO 200 J=1,NT1
0041      A1 = PI + {J-1}*BETD
0042      A2 = PI + J*BETD
0043      SNB1 = SIN(A1)
0044      CSB1 = COS(A1)
C
0045      SNB2 = SIN(A2)
0046      CSB2 = COS(A2)
C
0047      NX = NT2 + 1
0048      DO 150 K=1,NX
0049      PSI = 1.5*PI - (K-1)*SCR+ PI/3
C
C
0050      CSY = COS(PSI)
0051      SNY = SIN(PSI)
0052      PA(1) = RT2*SNY
0053      PA(2) = (RT1 - RT2*CSY) * SNB1
0054      PA(3) = (RT1-RT2*CSY)*CSB1
C
0055      PB(1) = RT2*SNY
0056      PB(2) = (RT1-RT2*CSY)*SNB2
0057      PB(3) = (RT1-RT2*CSY)*CSB2
0058      IF ( K.EQ. 1 ) GOTO 140
C
0059      CALL LOADP ( P,2,NP,PA)
0060      CALL LOADP ( P,3,NP,PB)
C
0061      IF ( K.EQ. NX ) GOTO 150
0062      140 CONTINUE
0063      NP = NP + 1
0064      CALL LOADP ( P,1,NP , PA )
0065      CALL LOADP ( P,4,NP , PB )
0066      150 CONTINUE
0067      200 CONTINUE
C
0068      JO = NP
0069      J1 = NP-1

```

C-14

```

0070      J2 = NP-2
0071      J3 = NP-3
0072      J4 = NP-4
0073      J5 = NP-5
0074      J6 = NP-6
0075      IF (NT2.EQ.8) J6 = NP
0076      J7 = NP-7
0077      IF (NT2.EQ.7) J7 = NP
0078      IF (NT2.EQ.8) J7 = NP-1
0079      J8 = NP-8
0080      IF (NT2.EQ.7) J8 = NP- 1
0081      IF (NT2.EQ.8) J8 = NP-2
0082      J9 = NP-9
0083      IF (NT2.EQ.7) J9 = NP- 2
0084      IF (NT2.EQ.8) J9 = NP-3
0085      J10= NP-10
0086      IF (NT2.EQ.7) J10= NP- 3
0087      IF (NT2.EQ.8) J10= NP-4
0088      J11= NP-11
0089      IF (NT2.EQ.7) J11= NP- 4
0090      IF (NT2.EQ.8) J11= NP-5
0091      J12= NP-12
0092      IF (NT2.EQ.7) J12= NP- 5
0093      IF (NT2.EQ.8) J12= NP-6
0094      J13= NP-13
0095      IF (NT2.EQ.7) J13= NP- 6
0096      IF (NT2.EQ.8) J13= NP-7
0097      EXT = DOF
0098      UY = P(2,1,J13)
0099      UZ = P(3,1,J13)
0100      LY = P(2,4,J13)
0101      LZ = P(3,4,J13)
0102      SLOPE = (LY - UY)/(LZ - UZ)
0103      SLOPE = ATAN(SLOPE)
0104      SNSL = SIN(SLOPE)
0105      CSSL = COS(SLOPE)
0106      ESNS = EXT*SNSL
0107      ECSS = (EXT) * (CSSL)
0108      NP = NP + 1
0109      P(1,1,NP) = P(1,4,J13)
0110      P(2,1,NP) = P(2,4,J13)
0111      P(3,1,NP) = P(3,4,J13)
0112      P(1,2,NP) = P(1,3,J13)
0113      P(2,2,NP) = P(2,3,J13)
0114      P(3,2,NP) = P(3,3,J13)
0115      P(1,3,NP) = P(1,3,J13)
0116      P(2,3,NP) = P(2,3,J13) + ESNS
0117      P(3,3,NP) = P(3,3,J13) + ECSS
    
```

C-15

0115 P(2,3,NP) = P(2,3,J13) + ESNS
 0116 P(3,3,NP) = P(3,3,J13) + ECSS
 0117 P(1,4,NP) = P(1,4,J13)
 0118 P(2,4,NP) = P(2,4,J13) + ESNS
 0119 P(3,4,NP) = P(3,4,J13) + ECSS
 0120 NP = NP + 1
 0121 P(1,1,NP) = P(1,4,J12)
 0122 P(2,1,NP) = P(2,4,J12)
 0123 P(3,1,NP) = P(3,4,J12)
 0124 P(1,2,NP) = P(1,3,J12)
 0125 P(2,2,NP) = P(2,3,J12)
 0126 P(3,2,NP) = P(3,3,J12)
 0127 P(1,3,NP) = P(1,3,J12)
 0128 P(2,3,NP) = P(2,3,J12) + ESNS
 0129 P(3,3,NP) = P(3,3,J12) + ECSS
 0130 P(1,4,NP) = P(1,4,J12)
 0131 P(2,4,NP) = P(2,4,J12) + ESNS
 0132 P(3,4,NP) = P(3,4,J12) + ECSS
 0133 NP = NP + 1
 0134 P(1,1,NP) = P(1,4,J11)
 0135 P(2,1,NP) = P(2,4,J11)
 0136 P(3,1,NP) = P(3,4,J11)
 0137 P(1,2,NP) = P(1,3,J11)
 0138 P(2,2,NP) = P(2,3,J11)
 0139 P(3,2,NP) = P(3,3,J11)
 0140 P(1,3,NP) = P(1,3,J11)
 0141 P(2,3,NP) = P(2,3,J11) + ESNS
 0142 P(3,3,NP) = P(3,3,J11) + ECSS
 0143 P(1,4,NP) = P(1,4,J11)
 0144 P(2,4,NP) = P(2,4,J11) + ESNS
 0145 P(3,4,NP) = P(3,4,J11) + ECSS
 0146 NP = NP + 1
 0147 P(1,1,NP) = P(1,4,J10)
 0148 P(2,1,NP) = P(2,4,J10)
 0149 P(3,1,NP) = P(3,4,J10)
 0150 P(1,2,NP) = P(1,3,J10)
 0151 P(2,2,NP) = P(2,3,J10)
 0152 P(3,2,NP) = P(3,3,J10)
 0153 P(1,3,NP) = P(1,3,J10)
 0154 P(2,3,NP) = P(2,3,J10) + ESNS
 0155 P(3,3,NP) = P(3,3,J10) + ECSS
 0156 P(1,4,NP) = P(1,4,J10)
 0157 P(2,4,NP) = P(2,4,J10) + ESNS
 0158 P(3,4,NP) = P(3,4,J10) + ECSS
 0159 NP = NP + 1
 0160 P(1,1,NP) = P(1,4,J9)
 0161 P(2,1,NP) = P(2,4,J9)
 0162 P(3,1,NP) = P(3,4,J9)

0163 P(1,2, NP) = P(1,3, J9)
0164 P(2,2, NP) = P(2,3, J9)
0165 P(3,2, NP) = P(3,3, J9)
0166 P(1,3, NP) = P(1,3, J9)
0167 P(2,3, NP) = P(2,3, J9) + ESNS
0168 P(3,3, NP) = P(3,3, J9) + ECSS
0169 P(1,4, NP) = P(1,4, J9)
0170 P(2,4, NP) = P(2,4, J9) + FSNS
0171 P(3,4, NP) = P(3,4, J9) + ECSS
0172 NP = NP + 1
0173 P(1,1, NP) = P(1,4, J8)
0174 P(2,1, NP) = P(2,4, J8)
0175 P(3,1, NP) = P(3,4, J8)
0176 P(1,2, NP) = P(1,3, J8)
0177 P(2,2, NP) = P(2,3, J8)
0178 P(3,2, NP) = P(3,3, J8)
0179 P(1,3, NP) = P(1,3, J8)
0180 P(2,3, NP) = P(2,3, J8) + ESNS
0181 P(3,3, NP) = P(3,3, J8) + ECSS
0182 P(1,4, NP) = P(1,4, J8)
0183 P(2,4, NP) = P(2,4, J8) + ESNS
0184 P(3,4, NP) = P(3,4, J8) + ECSS
0185 NP = NP + 1
0186 P(1,1, NP) = P(1,4, J7)
0187 P(2,1, NP) = P(2,4, J7)
0188 P(3,1, NP) = P(3,4, J7)
0189 P(1,2, NP) = P(1,3, J7)
0190 P(2,2, NP) = P(2,3, J7)
0191 P(3,2, NP) = P(3,3, J7)
0192 P(1,3, NP) = P(1,3, J7)
0193 P(2,3, NP) = P(2,3, J7) + ESNS
0194 P(3,3, NP) = P(3,3, J7) + ECSS
0195 P(1,4, NP) = P(1,4, J7)
0196 P(2,4, NP) = P(2,4, J7) + ESNS
0197 P(3,4, NP) = P(3,4, J7) + ECSS
0198 IF (NT2.EQ.7) GO TO 220
0199 NP = NP + 1
0200 P(1,1, NP) = P(1,4, J6)
0201 P(2,1, NP) = P(2,4, J6)
0202 P(3,1, NP) = P(3,4, J6)
0203 P(1,2, NP) = P(1,3, J6)
0204 P(2,2, NP) = P(2,3, J6)
0205 P(3,2, NP) = P(3,3, J6)
0206 P(1,3, NP) = P(1,3, J6)
0207 P(2,3, NP) = P(2,3, J6) + ESNS
0208 P(3,3, NP) = P(3,3, J6) + ECSS
0209 P(1,4, NP) = P(1,4, J6)
0210 P(2,4, NP) = P(2,4, J6) + ESNS

0211 P(3,4, NP) = P(3,4, J6) + ECSS
0212 IF (INT2.EQ.8) GO TO 220
0213 NP = NP + 1
0214 P(1,1, NP) = P(1,4, J5)
0215 P(2,1, NP) = P(2,4, J5)
0216 P(3,1, NP) = P(3,4, J5)
0217 P(1,2, NP) = P(1,3, J5)
0218 P(2,2, NP) = P(2,3, J5)
0219 P(3,2, NP) = P(3,3, J5)
0220 P(1,3, NP) = P(1,3, J5)
0221 P(2,3, NP) = P(2,3, J5) + ESNS
0222 P(3,3, NP) = P(3,3, J5) + ECSS
0223 P(1,4, NP) = P(1,4, J5)
0224 P(2,4, NP) = P(2,4, J5) + ESNS
0225 P(3,4, NP) = P(3,4, J5) + ECSS
0226 NP = NP + 1
0227 P(1,1, NP) = P(1,4, J4)
0228 P(2,1, NP) = P(2,4, J4)
0229 P(3,1, NP) = P(3,4, J4)
0230 P(1,2, NP) = P(1,3, J4)
0231 P(2,2, NP) = P(2,3, J4)
0232 P(3,2, NP) = P(3,3, J4)
0233 P(1,3, NP) = P(1,3, J4)
0234 P(2,3, NP) = P(2,3, J4) + ESNS
0235 P(3,3, NP) = P(3,3, J4) + ECSS
0236 P(1,4, NP) = P(1,4, J4)
0237 P(2,4, NP) = P(2,4, J4) + ESNS
0238 P(3,4, NP) = P(3,4, J4) + ECSS
0239 NP = NP + 1
0240 P(1,1, NP) = P(1,4, J3)
0241 P(2,1, NP) = P(2,4, J3)
0242 P(3,1, NP) = P(3,4, J3)
0243 P(1,2, NP) = P(1,3, J3)
0244 P(2,2, NP) = P(2,3, J3)
0245 P(3,2, NP) = P(3,3, J3)
0246 P(1,3, NP) = P(1,3, J3)
0247 P(2,3, NP) = P(2,3, J3) + ESNS
0248 P(3,3, NP) = P(3,3, J3) + ECSS
0249 P(1,4, NP) = P(1,4, J3)
0250 P(2,4, NP) = P(2,4, J3) + ESNS
0251 P(3,4, NP) = P(3,4, J3) + ECSS
0252 NP = NP + 1
0253 P(1,1, NP) = P(1,4, J2)
0254 P(2,1, NP) = P(2,4, J2)
0255 P(3,1, NP) = P(3,4, J2)
0256 P(1,2, NP) = P(1,3, J2)
0257 P(2,2, NP) = P(2,3, J2)
0258 P(3,2, NP) = P(3,3, J2)

```

0259      P(1,3,NP) = P(1,3,J2 )
0260      P(2,3,NP) = P(2,3,J2 ) + ESNS
0261      P(3,3,NP) = P(3,3,J2 ) + ECSS
0262      P(1,4,NP) = P(1,4,J2 )
0263      P(2,4,NP) = P(2,4,J2 ) + ESNS
0264      P(3,4,NP) = P(3,4,J2 ) + ECSS
0265      NP = NP + 1
0266      P(1,1,NP) = P(1,4,J1 )
0267      P(2,1,NP) = P(2,4,J1 )
0268      P(3,1,NP) = P(3,4,J1 )
0269      P(1,2,NP) = P(1,3,J1 )
0270      P(2,2,NP) = P(2,3,J1 )
0271      P(3,2,NP) = P(3,3,J1 )
0272      P(1,3,NP) = P(1,3,J1 )
0273      P(2,3,NP) = P(2,3,J1 ) + ESNS
0274      P(3,3,NP) = P(3,3,J1 ) + ECSS
0275      P(1,4,NP) = P(1,4,J1 )
0276      P(2,4,NP) = P(2,4,J1 ) + ESNS
0277      P(3,4,NP) = P(3,4,J1 ) + ECSS
0278      NP = NP + 1
0279      P(1,1,NP) = P(1,4,J0 )
0280      P(2,1,NP) = P(2,4,J0 )
0281      P(3,1,NP) = P(3,4,J0 )
0282      P(1,2,NP) = P(1,3,J0 )
0283      P(2,2,NP) = P(2,3,J0 )
0284      P(3,2,NP) = P(3,3,J0 )
0285      P(1,3,NP) = P(1,3,J0 )
0286      P(2,3,NP) = P(2,3,J0 ) + ESNS
0287      P(3,3,NP) = P(3,3,J0 ) + ECSS
0288      P(1,4,NP) = P(1,4,J0 )
0289      P(2,4,NP) = P(2,4,J0 ) + ESNS
0290      P(3,4,NP) = P(3,4,J0 ) + ECSS
0291      220 CONTINUE
0292      DIMENSION NUPLT(50) , INX(50)
0293      DATA NUPLT/ 1,2,3,4,5,6,7,8,9,10,11,12,17,25,33,41,0/
C
0294      IF ( NUPLT(1) .EQ. 0) GOTO 290
C
0295      K=0
0296      J=1
0297      DO 250 M=1,NP
C
0298      IF ( NUPLT(J).NE. M) GOTO 240
0299      J=J + 1
0300      GOTO 250
C
0301      240 CONTINUE

```

```
0302      K=K + 1
0303      INX(K) = M
0304      250 CONTINUE
0305      NP = K
C
0306      DO 280 J=1,NP
0307      DO 280 K=1,4
0308      280 CALL LOADP ( P , K , J , P(1,K,INX(J)) )
0309      290 CONTINUE
C
C
C      ROTATE TORUS AN MOVE IT TO REQUIRED PPSITION
C
0310      CALL THREEED ( ZIH, LAMDA, GAMMA, XT, YT, ZT)
C
0311      YMIN = 1.0E50
0312      DO 300 J=1,NP
0313      DO 300 K=1,4
0314      CALL THRZYX ( X , Y , Z , P(1,K,J) , P(2,K,J) , P(3,K,J) )
0315      P(1,K,J) = X
0316      P(2,K,J) = Y
0317      P(3,K,J) = Z
0318      YMIN = AMIN1( P(2,K,J) , YMIN)
0319      300 CONTINUE
0320      RETURN
0321      END
```

```

0001      SUBROUTINE KLUGE ( RADIUS , A1 , THETCN , V , GAMMA , RADUP , BELTWD
*          , DISP , H , MODE1 , EPS
*          , YAW , RUNNU
*          , FLAT , ND1 , ND2
*          , PIDAT , LP , YMIN
*          , LAMDA , CHLN
*          , BETA , RHO , L11 , L12 , L13 , L14 , L15 , XF , YF , ZF , Q )

```

```

0002      INTEGER PARAM
0003      DIMENSION PIDAT ( 3 , 4 , 1 ) , APT( 3 , 2 )

```

```

C.....
C

```

```

C      FOR THIS TRAJECTORY GET CRITICAL PARAMETERS FOR CHUTE DESIGN.

```

```

0004      WRITE ( 6 , 905 )
0005      905  FORMAT ( '11' )

```

```

0006      C      ..... INPUT TO KLUGE .....
      CALL KLUGE ( RADIUS , A1 , THETCN , V , GAMMA , RADUP , BELTWD
*          , DISP , H , MODE1 , EPS
*          , YAW , RUNNU

```

```

C      ..... OUTPUT FROM KLUGE .....
*          , LAMDA , XF , YF , ZF , Q , CHLN , APT
*          , BETA , RHO , L11 , L12 , L13 , L14 , L15 )

```

```

0007      YFM = -YF

```

```

C      HAS KLUGE BLOWN UP AGAIN .....

```

```

0008      IF ( ABS(XF) .GT. 1000. ) GOTO 55
0009      IF ( ABS(YF) .GT. 1000. ) GOTO 55
0010      IF ( MODE1 .EQ. 2 ) GOTO 60
0011      DO 50 J=1,3
0012      DO 50 K=1,2
0013      IF ( ABS( APT(J,K) ) .GT. 1000. ) GOTO 55
0014      50  CONTINUE
0015      GO TO 60
0016      55  CONTINUE
0017      WRITE ( 6 , 931 )
0018      931  FORMAT ( '///18,251(5)STOP ' ) // 25X

```

```

* * PROGRAM STOPPED BECAUSE OF IMPOSSIBLE NUMBERS CALCULATED BY*,
* * THE KLUGE ROUTINE '///18,251(5)STOP '*

```

```

0019      STOP

```

```

C      CREATE THE CHUTE IN THE PIDAT ARRAY IN XYZ COORDINATES.

```

```

0020      60  CONTINUE

```

C-20

0030 STUB = PI/2. - ZHR
0031 PSUB = DGLLSYHU

C

0032 XH=VS*CS1*TH+H*SN1
0033 X6 = XH-(H-A1)*SIN(ZHR)

0034 YA=YH(H-A1)*COS(ZHR)

C

PAGE 1A

C

0035 K1 = .5*(D**2)*TNI

C

0036 EQ . 40 TO 54
K19 = VS*SN1*TNE

0037 K20 = VS*CS1-K19

0038 K21 = H*A1*CS1 + YH

0039 K22 = VS*(SH+CS1*TNE)

0040 K23 = H*A1*SN1-XH

C

0041 K2 = 0*(VS*CS1-.5*K20) + K19

0042 K3 = VS*(CS1*K22 - SN1*K20) + L*(K23-K21*TNE)

0043 K4 = (K22*K23 + K20*K21)

C

SELECT PROPER CALCULATION FOR TI DEPENDING ON MODEL T PARAMETER

C

0044 IF (MODEL .NE. 1) GOTO 50

0045 K11 = K3**2-4*K2*K4

0046 X = (-K3+SQRT(K11)) / (2*K2)

0047 Y = (-K3-SQRT(K11)) / (2*K2)

0048 C = AMIN(X,Y)

0049 IF (C.LT.TH) C=AMAX(X,Y)

0050 T1 = C

0051 GOTO 200

C

50 CONTINUE

0052 IF (MODEL .NE. 2) GOTO 60

0053 T1 = TH

0054 K11=KH

0055 GO TO 200

C

C*****

C CLIC SOLUTION FOR TI = F(K1,K2,K3,K4)

C

PAGE 2A

C

0057 60 CONTINUE

C-23

0050 K6 = K7/11
 0051 K7 = K2/11
 0060 K8 = K4/11
 0061 K9 = 3*10/3.14*2-K7
 0062 K10 = 2*310/3.14*3.14/6/3. - K8
 0063 K11 = K9/3
 0064 K12 = K10/2
 0065 K13 = K12**2 - K11**3

C
 C PAGE 2B
 C

0066 W3 = 1./3.
 0067 IF (K13.LE. 0.) GO TO 100
 0068 RK13 = SQRT(K13)
 0069 T1A = ROOT(K12+RK13,W3) + ROOT(K12-RK13,W3) -K6/3.
 0070 GO TO 150

C
 100 CONTINUE
 0071 IF (K13.LE. 0.) GO TO 110
 0072 T1A = 2.*ROOT(K12,W3) -K6/3.
 0073 T1B = -ROOT(K12,W3) -K6/3.
 0074 GO TO 150

0076 110 CONTINUE
 0077 X = 2+SQRT(K11)
 0078 Y = ARCSIN(K12/(K11*SQRT(K11)))
 0079 Z = PI/3.
 0080 T1A = X*COS(Y/3.) -K6/3.
 0081 T1B = X*COS(Y/3. + 2.*Z) - K6/3.
 0082 T1C = X*COS(Y/3. + 4.*Z) - K6/3.

C-24

C
 150 CONTINUE

0084 X = T1A
 0085 IF (X.LT. TH) X=T1B
 0086 IF (X.LT.TH) X = T1C
 0087 T1 = X
 0088 GO TO 200

C
 C
 C PAGE 2C
 C

0089 200 CONTINUE
 C
 0090 IF (T1.LT. TH) STOP
 0091 IF (T1.LT. 0.) STOP

C

0092 X1 = VS*(S11) + BAI*SI1
 0093 Y1 = VS*(S11**2 + VS*SI1**2) + BAI*CS1
 0094 Z1R = WTAN((VS*SI1 + G*11)/ (VS*CS1))
 0095 Z1I = DLOC(Z1R)

0096 S1Y = P1/Z1 - Z1R - BPR
 0097 H1I = TAN(S1Y)
 0098 P5I = DLOC(S1Y)

0099 BEI = WTAN (H1I*SNG)
 0100 BETA = DLOC(BEI)
 0101 H (RUNDG.GF.30) BET = G
 0102 H (RUNDG.GF.30) L = 18

0103 M = 1 + BL*TAN(BET)/(2.*CSG)
 0104 Q1 = SIN(BET)*TAN(GAMA+BET)+COS(BET)
 0105 Q2 = SIN(BET)*(BL+DNE)/COS(GAMA+BET) + L*TAN(LGAMA)*Q1+L

0106 U = M*(CSG + SNG*TAN(GAMA+BET))
 0107 W = M*(CSG+SNG*TAN(GAMA-BET))

PAGE 3

0108 A = (U+W)/2.
 0109 B = SQRT((U+ (U-W)*SNG*TAN(BET)/2.)**2 -
 * ((U-W)/2.)**2)*CSG**2)

C25

0110 K5 = SQRT(A**2*TN1**2+B**2)
 0111 DY1=A**2+TAN(S1Y)/K5
 0112 DX1 = K5-TN1*DY1
 0113 X2 = X1-DX1
 0114 Y2 = Y1 + DY1 - (U-W)/2.
 0115 Y3 = Y2-BL*INC/2.
 0116 H (MULT.(G,2) Y3=Y3-1.
 0117 X3 = X2
 0118 BTR = EABC(BETA)
 0119 CBR = COS (BTR)
 0120 SBR = SIN (BTR)
 0121 X4 = X3 + CBR + (BL/2) * SBR
 0122 X5 = X4 - X3
 0123 H (RUNDG.GF.20) X3 = X3 - X5
 0124 Z3 = 0.

PAGE 4

0125 MZ = B- (DY1-(U-W)/2.)*SNG*TAN(BET)
 0126 L = (DY1-(U-W)/2.)*SG

```

0127     LAMBDA = ARSIN(1/PA)
0128     LAMBDA = DEGC(LAMBDA)
0129     CHLN = (C - 1) / TAN(BET)
0130     KROCK = ATAN(INI*CSG)
0131     KBL = DLE(LRIBK)
C
C
C
C   CALCULATE COORDINATES OF 'A' PLATE. PUT IN APT ARRAY FOR USE IN CHUTE ROUTINE
C
0132     K31 = DY1 - (U-K1/2. + (Y1 - YH)
0133     K32 = BL*ING/2.
0134     K33 = K31 - K32
0135     K34 = K33/ING
C
C
0136     DV1 = (L - BL + K34)*SNG + 1.
0137     DV2 = K33*CSG + 1.
0138     APT(2,1) = DV2
0139     APT(2,2) = DV1
C
C
0140     DW1 = K23*SNG
0141     DW2 = (BL + K34)*CSG - DW1 - K34*CSG
C
0142     APT(3,1) = -DW2
0143     APT(3,2) = DW1
C
C
C-26 0144     R2 = L - DW2*TAN(BET)
0145     R1 = L + DW1*TAN(BET)
0146     CSL = COS(LAMBDA)
0147     SNL = SIN(LAMBDA)
0148     DU1 = R1*CSL - TAN(RIBK)*(DV1 - R1*SNL)
0149     DU2 = R2*CSL - TAN(RHBL) * (DV2 - R2*SNL)
C
0150     APT(1,2) = DU1
0151     APT(1,1) = DU2
C
0152     L11 = SQRT((APT(1,2) - APT(1,1))**2 + (APT(2,2) - APT(2,1))**2 +
11APT(3,2) - APT(3,1))**2)
0153     L12 = SQRT((U*CSL - APT(1,2))**2 + (U*SNL - APT(2,2))**2 + (CHLN - APT(3,2))
1**2)
0154     L13 = SQRT((L*CSL - U*CSL)**2 + (L*SNL - U*SNL)**2 + CHLN**2)
0155     L14 = SQRT((APT(1,1) - L*CSL)**2 + (APT(2,1) - L*SNL)**2 + APT(3,1)**2)
0156     L15 = SQRT((U*CSL - APT(1,1))**2 + (U*SNL - APT(2,1))**2 + (CHLN - APT(3,1))
1**2)
0157     RETURN

```

0158

900 FORMAT (1X,4(2),10)

```

C.....
C
C      DEBUG IN LOGIC
C.....

```

0159

DEBUG IN IIC, AI, VS, GMA, I, BL, DDF, H

```

C.....
*      IIA, IIB, IIC, IY, YB, XA, YA, YA
*      ,K1,K2,K3,K4,K5,K6,K7,K8,K9,K11,K12,K13,KK13,K10
*      ,K19,K20,K21,K22,K23,K23,K31,K32,K33,K34,DV1,DV2
*      ,IJA,IJB,IJC,IJ,IJ,I,OHZ,IBW1,K2,KL,DO1,DO2
*      ,X1,Y1,C,C,B,W
*      ,A,B, DY1,DX1,X2,Y2,Y3,X3,Z3
*      ,IHA,LAMDA,BHC,BETA,Z11,Z10,EPS,PSI,PSIH
*      ,L11,L12,L13,L14,L15
*      ,M2,I,CHLN,APT )

```

0160

AI 1

0161

END

C-27

```

0001      SUBROUTINE INTERX( N,X0,Y0,Z0,V,ANG,PX,THIT,ALPHA,KAPPA,DELT,VE
          ,PHIP)
0002      REAL K,KAPPA,MU
          C
0003      COMMON THET ( 3,200 ) , ABC (3,200) , PT ( 3,3,200 ) , UN ( 3,200 )
          C
0004      DIMENSION PX(6) , DUM(3) , ANT(3)
0005      DIMENSION VE(3)
          C
0006      DATA G/386.4/
          C
0007      PHIPR=PHIP/57.29578
0008      MU=TAN(PHIPR)
0009      A = ABC(1,N)
0010      B = ABC(2,N)
0011      C=ABC(3,N)
          C
0012      IF ( A.EQ. 0. ) A=1.0E-10
          C
0013      THIT = -1.
0014      THR = RADG(ANG)
0015      VC = V*COS(THR)
0016      VCQ = VC**2
          C
          C
          C      GET ALPHA BETA GAMMA
          C
0017      AL = -.5*G/VCQ
0018      BET = G*X0/VCQ-TAN(THR)
0019      GAM = Y0 + X0*TAN(THR)-.5*G*X0**2/VCQ
          C
0020      K=1.-C*Z0
          C
0021      Q = ( AL*B**2)/A**2
0022      R = (-AL**2.*K*B)/A**2 - BET*B/A -1.
0023      S = (AL*K**2)/A**2 + BET*K/A + GAM
          C
0024      Y = -S/R
0025      IF ( Q.EQ. 0. ) GOTO 110
          C
0026      RCL = R**2-4*Q*S
0027      IF ( RCL.GE.0. ) GOTO 100
0028      900 FORMAT(///10X,'NEG ROOT INTERX')
0029      RETURN
          C
          C
0030      100 CONTINUE
0031      RCL = SQRT(RCL)
0032      Y1 = (-R+RCL)/(2*Q)

```

C-28

```

0033      Y2 = (-R-RC1)/(2*Q)
0034      Y = AMAX1(Y1,Y2)
C
0035      110 CONTINUE
0036      X = (K-B*Y) / A
0037      IF(X.LE.0.) Y=AMIN1(Y1,Y2)
0038      X = (K - B*Y)/A
C
0039      PX(1) = X
0040      PX(2) = Y
0041      PX(3) = Z0
C
C      IS THIS INTERSECT POINT ON THE PHYSICAL PLATE
C
0042      TH1 = DEGC(THET(1,N))
0043      TH2 = DEGC(THET(2,N))
0044      TH3 = DEGC(THET(3,N))
C
0045      CALL PLATE ( PX, PT(1,1,N) , PT(1,2,N) , DUM,ANT )
C
C      ANT(2)=P P1 P2      ANT(3) =P P2 P1
C
0046      D2 = DEGC(ANT(2))
0047      D3 = DEGC(ANT(3))
0048      NN = 0
0049      IF (D2.GT.TH1) NN = 1
0050      IF (D3.GT.TH2) NN= 1
0051      IF (N.NE.47.AND.N.NE.48.AND.N.NE.61.AND.N.NE.62.AND. NN.EQ.1)RETURN
0052      IF (N.EQ.47.OR.N.EQ.48.OR.N.EQ.61.OR.N.EQ.62)
C-29 *WRITE(6,111) D2,TH1,D3,TH2,N,NN
0053      111 FORMAT (4(F8.4,1X),2(13,1X))
C
0054      CALL PLATE( PX,PT(1,2,N) , PT(1,3,N) , DUM , ANT )
C
C      ANT(2) = P P2 P3      ANT(3) = P P3 P2
C
0055      D2 = DEGC(ANT(2))
0056      D3 = DEGC(ANT(3))
0057      IF (D2.GT.TH2) NN = 1
0058      IF (D3.GT.TH3) NN = 1
0059      IF (N.NE.47.AND.N.NE.48.AND.N.NE.61.AND.N.NE.62.AND. NN.EQ.1)RETURN
0060      IF (N.EQ.47.OR.N.EQ.48.OR.N.EQ.61.OR.N.EQ.62)
C *WRITE(6,111) D2,TH2,D3,TH3,N,NN
C
0061      CALL PLATE( PX, PT(1,3,N) , PT(1,1,N) , DUM,ANT)
C
C      ANT(2)= P P3 P1      ANT(3) = P P1 P3
C

```

```

0062      D2 = DEGC(ANT(2))
0063      D3 = DLGC(ANT(3))
0064      IF (D2.GT.TH3) NN = 1
0065      IF (D3.GT.TH1) NN = 1
0066      IF (N.NE.47.AND.N.NE.48.AND.N.NE.61.AND.N.NE.62.AND. NN.EQ.1)RETURN
0067      IF (N.EQ.47.OR.N.EQ.48.OR.N.EQ.61.OR.N.EQ.62)
*WRITE(6,111) D2,TH3,D3,TH1,N,NN
0068      IF (NN.EQ.1) RETURN

```

```

C
C      THIS POINT IS ON THE N TH PLATE IN THE LIST
C      GET TIME OF INTERSECTION
C

```

```

0069      THIT = (X-X0)/VC

```

```

C
C      THIS SECTION CALCULATE ALPHA THE ANGLE OF INTERSECT OF THE YRAJECTORY
C      WITH THE PLATE.
C

```

```

C      GET LOCATION OF POINT NEAR POINT OF INTERSECTION
C

```

```

0070      TP = THIT - .02
0071      XP = VC*TP + X0
0072      YP = Y0 - V*SIN(THR)*TP - .5*G*TP**2

```

```

C
C      PX(4) = XP
0073      PX(5) = YP
0074      PX(6) = Z0
0075

```

```

C
0076      X1 = PT(1,1,N)
0077      Y1 = PT(2,1,N)
0078      Z1 = PT(3,1,N)

```

```

C
0079      X2 = PT(1,2,N)
0080      Y2 = PT(2,2,N)
0081      Z2 = PT(3,2,N)

```

```

C
0082      X3 = PT(1,3,N)
0083      Y3 = PT(2,3,N)
0084      Z3 = PT(3,3,N)

```

```

C
C      ***** GET ALPHA *****
C

```

```

0085      VNX = (Y3-Y1)*(Z2-Z1) - (Y2-Y1)*(Z3-Z1)
0086      VNY = (Z3-Z1)*(X2-X1) - (Z2-Z1)*(X3-X1)
0087      VNZ = (X3-X1)*(Y2-Y1) - (X2-X1)*(Y3-Y1)
C
0088      VNB = SQRT ( VNX**2 + VNY**2 + VNZ**2)
C

```

```

0089      VTX = XP - X
0090      VTY = YP - Y
      C
0091      VTB = SQRT( VTX**2 + VTY**2)
      C
0092      CSB = -(VTX*VNX + VTY*VNY) / ( VNB*VTB)
      C
0093      I      CONTINUE
0094      VVX=VC
0095      VVY=V*SIN(THR)-G*THIT
0096      VVB=SQRT(VVX**2+VVY**2)
0097      CSP=-(VVX*UN(1,N)+VVY*UN(2,N))/VVB
0098      CSQ=-CSP
0099      IF(CSQ.GT.1) CSP=1
0100      XXX = 1.-CSP**2
0101      SNP = SQRT(XXX)
0102      TNP=SNP/CSP
      C  CALC. VELOCITIES OF STREAM AFTER IMPACT
      C
      C
      C
0103      IF (INP.GT.MU) GO TO 50
      C
0104      VE(1)=0.
      C
0105      VE(2)=0.
      C
0106      VE(3)=0.
0107      GO TO 60
0108      CONTINUE
      C
0109      VE(1)=(1.-MU/TNP)*(VVX+UN(1,N)*CSP+VVB)
      C
0110      VE(2)=(1.-MU/TNP)*(VVY+UN(2,N)*CSP+VVB)
      C
0111      VE(3)=(1.-MU/TNP)*(UN(3,N)*CSP+VVB)
      C
0112      60  CONTINUE
      C
0113      BETA = ARCUS(CSB)
0114      BETA = DEGC(BETA)
0115      ALPHA = 90. - BETA
      C
      C      ***** GET KAPPA *****
      C
0116      K = VNX*VTY - VNY*VTX

```

```
C
0117 VTSX = VNY*K - VNZ*VNZ*VTX
0118 VTSY = - VNZ*VNZ*VTY + VNX*K
0119 VTSZ = VNX*VNZ*VTX + VNY*VNZ*VTY
C
0120 VTSB = SQRT( VTSX**2 + VTSY**2 + VTSZ**2 )
0121 VBDR = SQRT ( (X3-X1)**2 + (Y3-Y1)**2 + (Z3-Z1)**2 )
C
0122 K = ( (X3-X1)*VTSX+ (Y3-Y1)*VTSY + (Z3-Z1)*VTSZ )/(VTSB*VBDR)
0123 KAPPA = DEGC( ARCCOS(K) )
C
C
C
C ***** GET DELTA *****
C
0124 VGX = -VNX*VNZ
0125 VGY = -VNZ*VNZ
0126 VGZ = VNZ*VNY + VNX*VNX
C
0127 VGGB = SQRT ( VGX**2 + VGY**2 + VGZ**2 )
0128 K = ( (X3-X1)*VGX + (Y3-Y1)*VGY + (Z3-Z1)*VGZ ) / (VBDR*VGGB)
C
0129 DFLT = DEGC(ARCCOS(K))
C
0130 RETURN
0131 END
```

```
0001      SUBROUTINE DIST ( P,NT2)
0002      DIMENSION P(3,4,1)
0003      DIMENSION
0004      *ADIS(40), BDIS(40),CDIS(40),DDIS(40), EDIS(40), FDIS(40), GDIS(40)
0005      DO 100 J = 1, NT2
0006      R=(P(1,1,J) - P(1,2,J))**2
0007      S=(P(2,1,J)-P(2,2,J))**2
0008      T=(P(3,1,J)- P(3,2,J))**2
0009      ADIS(J) = SQRT( R+S+T)
0010      R=(P(1,2,J)-P(1,3,J))**2
0011      S=(P(2,2,J)-P(2,3,J))**2
0012      T=(P(3,2,J)-P(3,3,J))**2
0013      BDIS(J) = SQRT( R+T+S)
0014      R=(P(1,3,J)-P(1,4,J))**2
0015      S=(P(2,3,J)-P(2,4,J))**2
0016      T=(P(3,3,J)-P(3,4,J))**2
0017      CDIS(J) = SQRT( R+S+T)
0018      R=(P(1,4,J)-P(1,1,J))**2
0019      S=(P(2,4,J)-P(2,1,J))**2
0020      T=(P(3,4,J)-P(3,1,J))**2
0021      DDIS(J) = SQRT(R+S+T)
0022      R=(P(1,1,J)-P(1,3,J))**2
0023      S=(P(2,1,J)-P(2,3,J))**2
0024      T=(P(3,1,J)-P(3,3,J))**2
0025      EDIS(J) = SQRT( R+T+S)
0026      FDIS(J) = (BDIS(J))/2
0027      GDIS(J) = (DDIS(J))/2
0028      100 CONTINUE
0029      WRITE (6,900) ADIS,BDIS,CDIS,DDIS,EDIS,FDIS,GDIS
0030      900 FORMAT(1X,10F13.4)
0031      RETURN
0032      END
```

APPENDIX D

MATH MODEL FOR PHASE II DYNAMICS
FRICTIONAL FLOW PHASE

MATHEMATICAL MODEL OF
COAL TRANSFER CHUTE
Fairchild Space and Electronics Corp.

76 - 37

Jenike & Johanson, Inc.
Storage and Flow of Solids
No. Billerica, Massachusetts

October 1976

MATHEMATICAL MODEL OF
COAL TRANSFER CHUTE

Fairchild Space and Electronics Corp.

Scope of the work

A mathematical model of the sliding of coal on a belt-to-belt transfer chute is presented along with a calculation procedure to solve the various equations describing the flow of the coal.

1. Introduction

1.1 Design concepts

The typical approach to transferring material from one belt to another, particularly at a right angle, is simply to drop the material off the end of the initial belt into an enclosure. The material is thereby confined to the belt area during the period that it must be accelerated to the speed of the receiving belt. The depth of material may vary from side-to-side on the belt and bouncing of particles is likely to occur. This type of approach has been used with some degree of success for several years. With low speed belt transfer conditions, the results are reasonable; however, with high speed belt transfer, problems of wear, spillage, and non-uniformity of loading on the belt become significant.

The ideal belt-to-belt transfer chute would transfer the material cross-section from the initial belt essentially intact to the receiving belt - in the same direction and at the same speed as the belt. Such a transfer would eliminate belt wear, dusting and any off-center loading on the receiving belt. In addition, this should be accomplished with a minimum amount of head room for underground coal mining applications. These constraints, combined with the flow properties of coal, constitute a well-posed problem.

The chute must be able to handle reasonable variations in coal properties and incoming belt speed, and also cope with transient starting and stopping conditions. The chute must be fairly easy to fabricate and be equipped with replaceable wear liners. The allowable degree of deviation from an ideal transfer of the coal must be determined by empirical data and field experience.

1.2 Mathematical approach

The mathematical analysis of the behavior of material on transfer chutes consists of a dynamic force analysis with restraints. Forces acting on a stream of material sliding on a chute can be summarized as follows: gravity, normal and frictional forces from the chute surface, lateral forces between streams of material, and the stream-to-stream frictional drag. These forces are created by or restrained by the physical shape of the chute and are limited by the friction coefficient on the chute, the plastic deformation of the coal and the coal slip-line condition between streams. In addition, continuity of the solid provides the means for determining the thickness of the stream as a function of velocity of the material.

1.3 Assumptions for mathematical model

- a) The coal sliding on the chute behaves as a Coulomb frictional solid in a steady flow state. This means that the coal is yielding at all times in accordance with the effective yield concepts.* This yield condition is described entirely by the effective angle of internal friction ϕ .
- b) The frictional drag τ on the chute is proportional to the pressure σ_N perpendicular to the chute surface

$$\tau = \mu \sigma_N$$

where $\mu = \tan \phi'$

In general ϕ' (the kinematic angle of surface friction) is not constant but a function of σ_N to be determined empirically.

- c) The sliding sheet of coal can be approximated by a series of interacting streams of rectangular cross-section, constantly in lateral contact with each other.
- d) Compressive yielding, or shortening of the width between streams, occurs at a stress level on the interactive surface of adjoining streams equal to the yield stress for converging plastic flow across the stream.

* A. W. Jenike, Bulletin No. 108, "Gravity Flow of Bulk Solids," and Bulletin 123, "Storage and Flow of Solids," University of Utah, Engineering Experiment Station, Salt Lake, Utah

J. R. Johanson, "Stress and Velocity Fields in the Gravity Flow of Bulk Solids," ASME Journal of Applied Mechanics, Vol 31, Ser E, No. 3 Sept. 1964.

- e) Expansive yielding, or increasing of the width between streams, occurs at a stress level on the interactive surface of adjoining streams equal to the yield stress for diverging plastic flow across the stream. Note that the diverging stress level is much lower than the converging stress.
- f) Forces on the various stream faces are in balance with the various components of acceleration and gravitational force components (Newton's law applies).
- g) The streams are, in general, of different thicknesses and, because of the force balance, the thinner stream has a larger interactive stress level than the thicker adjoining stream. Consequently, if two adjoining streams converge, only the thinner stream yields in compression and becomes thicker. If two adjoining streams diverge, only the thicker stream yields in expansion and becomes thinner.
- h) The streams are initially defined by slicing the coal on the incoming conveyer belt into vertical strips of a given area and uniform velocity and hence a given mass flow rate that is maintained constant throughout the calculation for that stream.
- i) The chute catches the incoming stream of coal sufficiently close to the direction of the trajectory from the conveyor belt as to negate any effects of bouncing of lumps of coal.
- j) The chute consists of a single continuously smooth surface in space. If this is not satisfied (e.g. if the surface is specified as a series of flat plates joined at the edges), the non-smooth surface must be approximated by a smooth surface by means of a suitable interpolation scheme.
- k) The stress acting in the direction of flow is always in a state of yielding and hence is constant on a given element.

1.4 Use of the report

The report is divided into subsections each describing a particular part of the theory with the last section providing the method of calculation relating all of the parts. The theory is not exact nor

does it cover all possible chute configurations. For example, chute edges are not treated by the theory but would have to be taken into account in some approximate manner at a later date. Before any extensive calculation of a variety of surfaces or any parametric study of chute geometry is undertaken, the theory should be verified with small-scale experiments. These experiments should be related to the full scale conditions by the scaling laws discussed in the following section.

2. Velocity and Length Scaling for Subscale Experiments

Two experiments involving belts and chutes will be called "dynamically similar" if

- 1) The experiments involve the same belt and chute materials, and the same coal.
- 2) The setups are geometrically similar, with characteristic lengths l_1 and l_2 respectively.
- 3) The corresponding belt velocities are proportional with characteristic velocities V_1 and V_2 respectively

$$4) \frac{l_1 g}{V_1^2} = \frac{l_2 g}{V_2^2}, \text{ whence } \frac{l_1}{V_1^2} = \frac{l_2}{V_2^2} \quad (2.1)$$

If two experiments are dynamically similar, the coal trajectories in the chutes should be geometrically similar; one experiment can be used to predict the results of the other.*

For example, suppose we wish to model a chute for a 36" wide, 600 fpm belt, with a 1/6 scale chute and a 6" wide belt. The required subscale belt velocity V_2 is given by

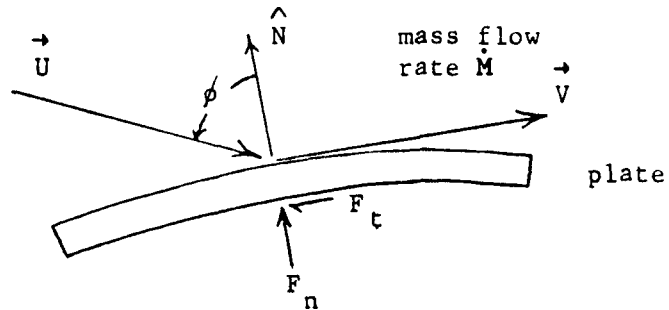
$$\frac{V_2}{V_1} = \sqrt{\frac{l_2}{l_1}} = \sqrt{\frac{1}{6}} = 0.408, \text{ whence}$$

$$V_2 = (0.408) (600 \text{ fpm}) = 245 \text{ fpm}$$

$\frac{lg}{V^2}$ is the only dimensionless quantity which can be formed from the gravitational acceleration g , the characteristic length l , and the characteristic velocity V . When the equations governing the motion of the coal are written in dimensionless form, the parameter $\frac{lg}{V^2}$ appears naturally.

* Some reservations: the largest lumps in the coal should be small compared to the characteristic length scales of both experiments. Effects due to air trapped in the coal should be negligible

3. Coal stream - plate impact model



The impacting coal is regarded as being composed of a number of individual streams. Consider one such stream. Let \vec{U} and \vec{V} be the coal velocity vectors just before and just after impact, respectively. Let \hat{N} be the unit vector normal to the curved plate at the impact point. The outgoing stream is assumed to be tangent to the plate at the impact point, and coplanar with \vec{U} and \hat{N} .

Let F_n , F_t be the total normal and tangential impact forces exerted on the stream by the plate. A momentum balance in the $+N$ direction gives $F_n = \dot{M} U \cos \phi$, with $U = |\vec{U}|$ the speed of the incoming stream, \dot{M} (Slugs/sec.) the mass flow rate associated with this stream, and ϕ the angle between the incoming velocity vector \vec{U} and the normal vector \hat{N} . (see diagram)

We have $F_t = \mu F_n$, where μ is the coefficient of sliding friction for this particular plate material and type of coal. Another momentum balance, in the \vec{V} direction, now leads to

$$V = U (\sin \phi - \mu \cos \phi) \quad (3.1)$$

$$[\tan \phi > \mu] \quad (3.2)$$

$$V = 0 \quad (3.3)$$

$$[\tan \phi \leq \mu] \quad (3.4)$$

with $V = |\vec{V}|$ the speed of the stream after impact.

In vector form, the impact model may be summarized as

$$\left. \begin{aligned} \vec{V} &= \left(1 - \frac{\mu}{\tan \phi}\right) (\vec{U} + \hat{N} U \cos \phi) \\ \text{with } U \cos \phi &= -U \cdot \hat{N} \\ [\tan \phi > \mu] \end{aligned} \right\} \quad (3.5)$$

After impacting on the plate, the coal stream is assigned a width as described in section 5 below.

Equation (3.3) predicts that the outgoing velocity will be zero whenever $\tan \phi \leq \mu$. If this should occur, any subsequent calculation of either sliding or free fall should start with zero initial velocity at the point of impact. In practice, this condition should be avoided because of the excessive coal build-up or chute wear that will occur at the impact point.

4. Equations of motion for steady sliding of a layer of coal on a curved plate

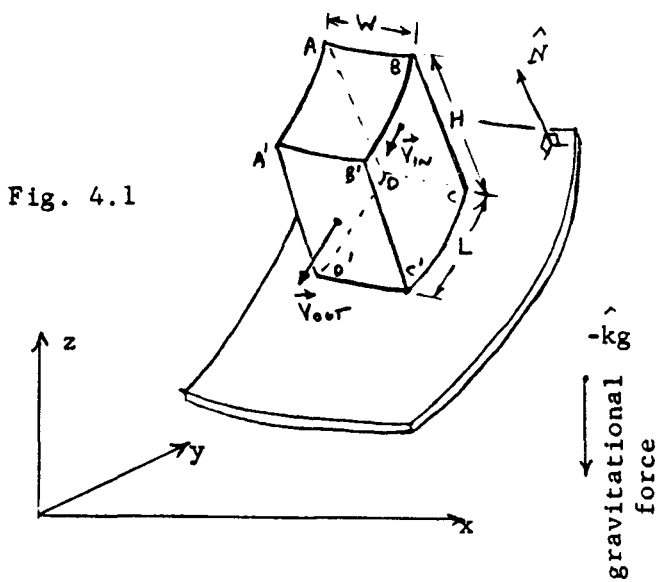


Fig. 4.1

Adopt a rectangular Cartesian coordinate system (x, y, z) in which the $+z$ axis points vertically upward. Let $\hat{i}, \hat{j}, \hat{k}$ be unit vectors parallel to the x -, y -, and z -axes respectively. Let \hat{N} be the unit vector normal to the plate, directed towards the side of the plate on which the coal is sliding. For force calculations, it is assumed that the coal velocity \vec{V} is independent of distance along the local normal to the curved plate, and that $\vec{V} \cdot \hat{N} = 0$; thus

the coal always moves "locally parallel" to the curved plate.

Consider the small volume element of Fig. 4.1, which represents a short section of one stream of coal. Mass enters and leaves the element only through the faces ABCD and A'B'C'D'; the other four faces are stream surfaces. All the lateral faces are composed of lines normal to the plate.

\vec{V}_{in} is normal to ABCD; \vec{V}_{out} is normal to A'B'C'D'

Mass conservation requires

$$\dot{M} = W H \rho |\vec{V}| = \text{const.} \quad (4.1)$$

for any given stream of coal. ($\rho = \text{coal density, slugs/ft}^3 = \gamma/g$, where γ is the bulk density of the coal in lbs/ft^3). Since this model assumes that the coal density ρ is constant, (4.1) gives the stream depth H in terms of the width W and $|\vec{V}|$.

A momentum balance for this volume element gives

$$\dot{M}(\vec{V}_{out} - \vec{V}_{in}) = \dot{M} \Delta \vec{V} = -M g \hat{k} + WL \cdot P \cdot \hat{N} - WL \cdot P \mu \frac{\vec{V}}{|\vec{V}|} + \vec{F}_I \quad (4.2)$$

where $M = LWH\rho$ is the mass of coal in the volume element.

The force terms on the righthand side of (4.2) are:

1. Body force due to gravity
2. Normal force exerted on the coal by the curved plate. [P (lbs/ft²) is the associated pressure at the plate surface]
3. Friction force acting opposite the direction of motion. (μ = coefficient of sliding friction).
4. The \vec{F}_I are interaction forces arising from adjacent coal streams. They are assumed to act at right angles to \hat{N} , and are discussed in detail below.

The plate pressure P is found as follows:

$$\hat{N} \cdot \vec{V} = 0 \text{ implies that } \Delta(\hat{N} \cdot \vec{V}) \approx \Delta \hat{N} \cdot \vec{V} + \hat{N} \cdot \Delta \vec{V} = 0 \quad (4.3)$$

Take the dot product of (4.2) with \hat{N} and use (4.1), (4.3) to get

$$P = \rho H (\hat{g} \hat{N} \cdot \hat{k} - |\vec{V}| \hat{V} \cdot \frac{\Delta \hat{N}}{L}) \quad (4.4)$$

The coal will fall off the plate unless $P > 0$.

$$(4.5)$$

The quantity $\hat{V} \cdot \frac{\Delta \hat{N}}{L}$ in (4.4) is just $\frac{|\vec{V}|}{R}$, with "R" the plate radius of curvature along the local coal trajectory, reckoned positive if the plate bends away from \hat{N} when following the coal. The assumptions made here concerning the velocity and stress fields in the sliding coal layer become dubious if the layer is too thick relative to the local plate radius of curvature. It is recommended that the flow field calculations cease if the condition

$$H < \frac{1}{2} |R| \quad (4.6)$$

is violated.

$\hat{N} \cdot \hat{k}$ in (4.4) is the cosine of the plate tilt angle with respect to the horizontal; this angle is zero for a level plate with coal sliding on the top side.

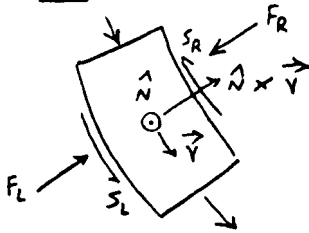


Fig. 4.2 top view of coal stream element

The interaction forces arising from adjacent streams are shown in Fig. 4.2. For the present model, it seems sufficient to write these stream interaction forces as

$$\vec{F}_I = (S_L - S_R) \frac{\vec{V}}{|\vec{V}|} + (F_L - F_R) \hat{N} \times \frac{\vec{V}}{|\vec{V}|} \quad (4.7)$$

The shear S and normal force F acting across the interface between two coal streams are related by

$$S = \pm F \sin \delta \quad (F > 0) \quad (4.8)$$

where δ is the effective angle of internal friction of the coal, and the sign in (4.8) is chosen to accelerate the slower-moving of the two streams.

For the normal force F , let the heights of the adjacent streams be H_A , H_B . Then if the center lines of the streams are inclined towards each other, the stream with the lower height yields plastically and

$$F = k_c \cdot PL \frac{H_A + H_B}{2} \quad (4.9A)$$

On the other hand, if the center lines of the streams are inclined away from each other, the higher stream yields plastically and

$$F = k_e \cdot PL \frac{H_A + H_B}{2} \quad (4.9B)$$

The values of k_c and k_e in general depend on the details of the stress distribution in a given element of material. As a first approximation

$$k_c = 0.5 \text{ and } k_e = 0.5 \left(\frac{1 - \sin \delta}{1 + \sin \delta} \right) \quad (4.10)$$

where δ is the effective angle of internal friction.

5. Method of solution of the equations of motion

5A. Extension of a streamline - following net across the curved plate

The streaming coal is divided into a network of small cells of the type considered in section 4. (see Fig. 5.1).

The sidewalls of this network are composed of local normals to the plate surface ξ . These normals spring from the arcs $\widehat{A_1 A_2}$, $\widehat{A_1 A_1'}$ etc. drawn on ξ . The arcs $\widehat{A_1 A_2}$, $\widehat{A_1 A_1'}$ etc are found as the intersections of ξ with certain planes, defined below.

The net is extended across the curved plate by constructing one new cross-stream row of cells at a time. The construction begins with the row of points $A_1, A_2, A_3 \dots$ on the plate surface ξ and the corresponding unit normals $\hat{N}_1, \hat{N}_2, \hat{N}_3, \dots$. Let (A,B) denote the distance between the points "A" and "B" in three dimensional space; then the initial stream widths are $W_1 = (A_1, A_2)$, $W_2 = (A_2, A_3)$ etc. The velocities $\vec{V}_1, \vec{V}_2, \vec{V}_3 \dots$ associated with the streams on the initial arc $A_1 A_2 A_3 \dots$ have the following properties:

$$\begin{aligned} \vec{V}_1 & \text{ is perpendicular to the line } \overline{A_1 A_2} \text{ in space,} \\ & \text{and also perpendicular to } \frac{\hat{N}_1 + \hat{N}_2}{2} \end{aligned} \tag{5.1}$$

$$\begin{aligned} \vec{V}_2 & \text{ is perpendicular to the line } \overline{A_2 A_3} \text{ in space,} \\ & \text{and also perpendicular to } \frac{\hat{N}_2 + \hat{N}_3}{2} \end{aligned}$$

The arc $\widehat{A_1 A_2}$ is defined as the intersection of ξ with the plane, perpendicular to \vec{V}_1 , passing through points A_1 and A_2 ; similarly $\widehat{A_2 A_3}$ is the intersection of ξ with the plane, perpendicular to \vec{V}_2 , passing through points A_2 and A_3 ; and so forth. The mass flow rates $\dot{M}_1, \dot{M}_2, \dot{M}_3, \dots$ are known for each stream, so equation (4.1) gives the initial stream heights as

$$H_1 = \frac{\dot{M}_1}{W_1 \rho |\vec{V}_1|}, \quad H_2 = \frac{\dot{M}_2}{W_2 \rho |\vec{V}_2|}, \quad \dots \tag{5.2}$$

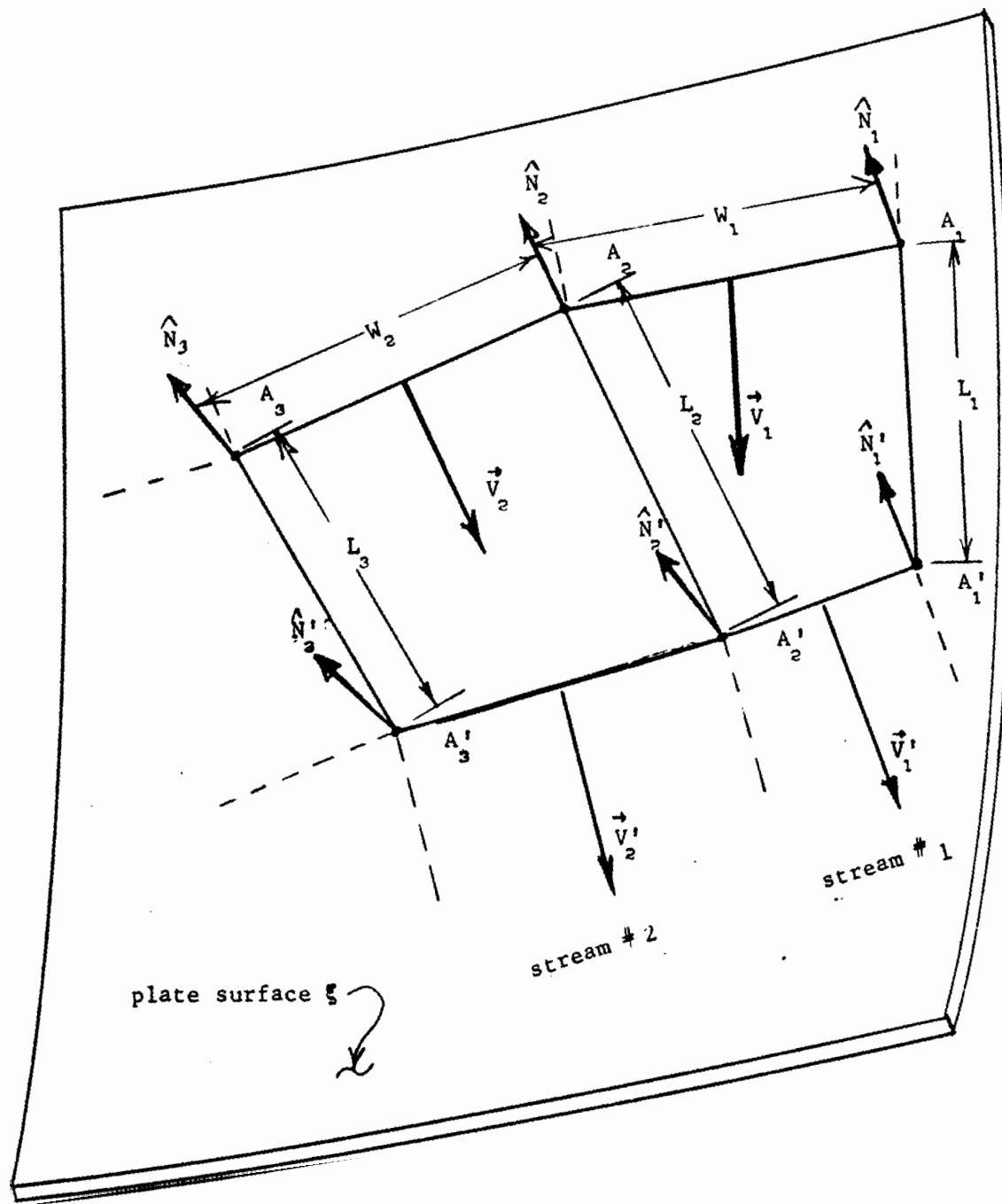


Fig. 5.1

Gridwork of Coal on Chute

To find the initial plate pressures P_i ($i = 1, 2, 3, 4, \dots$) we proceed as follows:

In equation (4.4) of section 4, take the limit as $L \rightarrow 0+$. $\frac{\hat{\Delta N}}{L}$ becomes $\frac{d\hat{N}}{dS}$, where dS is the arc length measured parallel to \vec{V} , and the formula for the local plate pressure is

$$P = \rho H \left[g \hat{N} \cdot \hat{k} - \left| \vec{V} \right| \vec{V} \cdot \frac{d\hat{N}}{dS} \right] \quad (5.3)$$

The calculation of the centrifugal force term $\left| \vec{V} \right| \vec{V} \cdot \frac{d\hat{N}}{dS}$ is discussed in detail in section 5c. Let $\left| \vec{V} \right| \vec{V} \cdot \left(\frac{d\hat{N}}{dS} \right)_i$ denote the centrifugal force term associated with the velocity \vec{V} and the point A_i on ξ . Then it is reasonable to approximate the initial plate pressures P_i as

$$P_i = \rho H_i \cdot \left\{ g \left(\frac{\hat{N}_i + \hat{N}_{i+1}}{2} \right) \cdot \hat{k} - \frac{1}{2} \left[\left| \vec{V}_i \right| \vec{V}_i \cdot \left(\frac{d\hat{N}}{dS} \right)_i + \left| \vec{V}_i \right| \vec{V}_i \cdot \left(\frac{d\hat{N}}{dS} \right)_{i+1} \right] \right\} \quad (5.4)$$

(see note at the end of this section)

Now let f_i, s_i denote the normal and shearing interaction forces per unit length, exerted on the i th stream by the $(i-1)$ th stream. [The sign conventions used are those of Fig. 4.2] The equations of section 4 give

$$\left. \begin{aligned} \frac{M_i (\vec{V}_i' - \vec{V}_i)}{L_i} &= -W_i H_i \rho g \hat{k} + W_i P_i \left(\frac{\hat{N}_i + \hat{N}_{i+1}}{2} - \mu \frac{\vec{V}_i}{\left| \vec{V}_i \right|} \right) \\ &+ (f_{i+1} - f_i) \left(\frac{\hat{N}_i + \hat{N}_{i+1}}{2} \right) \times \frac{\vec{V}_i}{\left| \vec{V}_i \right|} + (s_{i+1} - s_i) \frac{\vec{V}_i}{\left| \vec{V}_i \right|} \end{aligned} \right\} \quad (5.5)$$

($i = 1, 2, 3, 4, \dots$)

The stream surface separating the i th and $(i-1)$ th streams consists of local normals to ξ , springing from the arc $\widehat{A_i A_i'}$ on ξ . $\widehat{A_i A_i'}$ is the intersection of ξ with a "dividing plane" \mathbb{P}_i which has the following properties:

1. \mathbb{P}_i passes through the point A_i
2. \mathbb{P}_i is parallel to \hat{N}_i
3. \mathbb{P}_i is parallel to either \vec{V}_i or \vec{V}_{i-1} ,

depending on which of these two adjoining streams is yielding near the dividing plane \mathbb{P}_i . (e.g. If the i stream is non-yielding \mathbb{P}_i is parallel to \vec{V}_i . If the $i+1$ stream is non-yielding \mathbb{P}_i is parallel to \vec{V}_{i+1})

Now consider the i th and $(i-1)$ th streams.

$$\text{Let } C_i = (\vec{V}_{i-1} \times \vec{V}_i) \cdot \hat{N}_i \quad (5.6)$$

If $C_i > 0$, the streams are converging:

$$\left\{ \begin{array}{l} \text{If } H_i > H_{i-1}, \text{ the } (i-1)\text{th stream yields plastically near the} \\ \text{dividing plane } \mathbb{P}_i, \text{ and } \mathbb{P}_i \text{ is parallel to } \vec{V}_i. \\ \text{If } H_i < H_{i-1}, \text{ the } i\text{th stream yields near } \mathbb{P}_i, \text{ and } \mathbb{P}_i \text{ is parallel} \\ \text{to } \vec{V}_{i-1} \end{array} \right\} \quad (5.7)$$

$$f_i = k_c \left(\frac{P_i + P_{i-1}}{2} \right) \left(\frac{H_i + H_{i-1}}{2} \right) \quad (5.8)$$

$$s_i = \left\{ \begin{array}{l} f_i \sin \delta \left(\left| \vec{V}_i \right| > \left| \vec{V}_{i-1} \right| \right) \\ -f_i \sin \delta \left(\left| \vec{V}_i \right| < \left| \vec{V}_{i-1} \right| \right) \end{array} \right\} \quad (5.9)$$

If $C_i < 0$, the streams are diverging:

$$\left\{ \begin{array}{l} \text{If } H_i > H_{i-1}, \text{ the } i\text{th stream yields near } \mathbb{P}_i, \text{ and } \mathbb{P}_i \text{ is} \\ \text{parallel to } \vec{V}_{i-1}. \\ \text{If } H_i < H_{i-1}, \text{ the } (i-1)\text{th stream yields near } \mathbb{P}_i, \text{ and } \mathbb{P}_i \text{ is} \\ \text{parallel to } \vec{V}_i. \end{array} \right\} \quad (5.10)$$

$$f_i = k_e \left(\frac{P_i + P_{i-1}}{2} \right) \left(\frac{H_i + H_{i-1}}{2} \right) \quad (5.11)$$

$$s_i = \left\{ \begin{array}{l} f_i \sin \delta \left(\left| \vec{V}_i \right| > \left| \vec{V}_{i-1} \right| \right) \\ -f_i \sin \delta \left(\left| \vec{V}_i \right| < \left| \vec{V}_{i-1} \right| \right) \end{array} \right\} \quad (5.12)$$

Suppose that the net currently contains j separate streams of coal. Then (5.5) applies with $i = 1, 2, 3, \dots, j$ and the interaction forces

$$(f_1, s_1), (f_2, s_2), \dots, (f_j, s_j), (f_{j+1}, s_{j+1})$$

are called for. Since the edges of the coal sheet are regarded as traction-free and non-yielding in this model, we want to ensure that

$$\left. \begin{array}{l} f_1 = s_1 = f_{j+1} = s_{j+1} = 0 \\ \mathbb{P}_1 \text{ (the right-hand edge plane) is parallel to } \vec{V}_1 \\ \mathbb{P}_{j+1} \text{ (the left-hand edge plane) is parallel to } \vec{V}_j \end{array} \right\} \quad (5.13)$$

(5.13) can be satisfied if we apply the equations (5.6) - (5.12) for $i = 1, 2, 3, \dots, j+1$

$$\text{and choose } \left\{ \begin{array}{l} \vec{V}_0 = \vec{V}_1, H_0 = -H_1, P_0 = -P_1 \\ \vec{V}_{j+1} = \vec{V}_j, H_{j+1} = -H_j, P_{j+1} = -P_j \end{array} \right\} \quad (5.14)$$

We have now found all the dividing planes \mathbb{P}_i ($i = 1, 2, \dots, j+1$). Moreover, if the lengths L_i ($i = 1, 2, \dots, j$) were known, we could find the final velocity vectors \vec{V}_i from (5.5). To complete the construction of the new row of cells, one further piece of information is required; namely, the point A_1' on the right hand edge of the coal sheet. A_1' can be chosen to make the length L_1 a pre-determined fixed value (it is not important to get L_1 exactly right); or A_1' can be determined by a coal stream impact point to the right of the net. (see section 5B below)

Given A_1' , the final row of points A_2', A_3', \dots, A_j' is found sequentially, working from right to left as follows:

Find $L_1 = (A_1, A_1')$.

Get \vec{V}_1' from (5.5).

Pass a plane ϵ_1 through A_1' , perpendicular to \vec{V}_1' .

ϵ_1 and \mathbb{P}_2 intersect in a straight line ℓ_2 , and ℓ_2 intersects ξ at A_2' .

Find $L_2 = (A_2, A_2')$

Get \vec{V}_2' from (5.5).

Pass a plane ϵ_2 through A_2' , perpendicular to \vec{V}_2' .

ϵ_2 and \mathbb{P}_3 intersect in a straight line ℓ_3 , and ℓ_3 intersects ξ at A_3' .

etc.

(5.15)

Note that the cell lengths L_i are not equal, in general.

We are almost back to the situation we started in, with a row of points A_i' and corresponding velocity vectors \vec{V}_i' . But the \vec{V}_i' do not satisfy the criteria (5.1), because \vec{V}_i' is not exactly perpendicular to $\frac{\hat{N}_i' + \hat{N}_{i+1}'}{2}$, in general.

[The use of the plate pressure (5.4) ensures that the velocity vectors \vec{V}_i' are almost parallel to the surface at the end of the cell row construction process; but small errors will arise owing to the finite cell lengths L_i .]

To avoid the possibility of a progressive buildup of errors in the velocities, we produce corrected velocity vectors \vec{V}_i'' at the end of each cell row construction, according to

$$\vec{V}_i'' = \left| \vec{V}_i' \right| \frac{\vec{v}_i' \times \vec{a}_i'}{\left| \vec{v}_i' \times \vec{a}_i' \right|} \quad (5.16)$$

where $\vec{v}_i' = \frac{\hat{N}_i' + \hat{N}_{i+1}'}{2}$ and \vec{a}_i' is a vector pointing from A_i' to A_{i+1}' .

$$\left. \begin{aligned}
 \text{We then have } \vec{V}_i'' \cdot \vec{a}_i' &= \vec{V}_i' \cdot \vec{a}_i' = 0 \\
 \left| \vec{V}_i'' \right| &= \left| \vec{V}_i' \right| \\
 \text{and also } \vec{V}_i'' \cdot \vec{V}_i' &= 0
 \end{aligned} \right\} \quad (5.17)$$

The cell row construction process is now complete; the final points are the A_i' , and the final associated velocity vectors are the \vec{V}_i'' .

If we wish to find A_1' , given an approximate value of L_1 , it suffices to calculate the intersection of ξ with a line in the plane \mathbb{P}_1 , parallel to \hat{N}_1 and a distance L_1 from A_1 .

Note: the details of the arcs $\widehat{A_1 A_2}$, $\widehat{A_1 A_1'}$, etc. are not important; only the corner points A_i , A_i' require calculation.

The net extension process described in this section requires computer subroutines to perform the following computations about the chosen curved plate surface ξ :

- Intersection of ξ with a given straight line in three-dimensional space.
- Calculation of unit normal \hat{N} at a given point on ξ .
- Calculation of centrifugal force term $\left| \vec{V} \right| \vec{V} \cdot \frac{d\hat{N}}{dS}$ for a given point on ξ and a given tangential velocity vector \vec{V} .

Note to follow equation (5.4):

At this point, the two inequality checks mentioned in section 4 should be made for each cell. The computation halts unless $P_i > 0$ and also $H_i < \frac{1}{2} |R_i|$, where

$$R_i = \frac{\left| \vec{V}_i \right|^2}{\frac{1}{2} \left[\left| \vec{V}_i \right| \vec{V}_i \cdot \left(\frac{d\hat{N}}{dS} \right)_i + \left| \vec{V}_i \right| \vec{V}_i \cdot \left(\frac{d\hat{N}}{dS} \right)_{i+1} \right]}$$

is the local plate radius of curvature in the direction \vec{V}_i

5B. Method of starting the net, given a set of coal stream impact points.

5B.1 General procedure for widening a net to incorporate an additional stream on the right hand edge

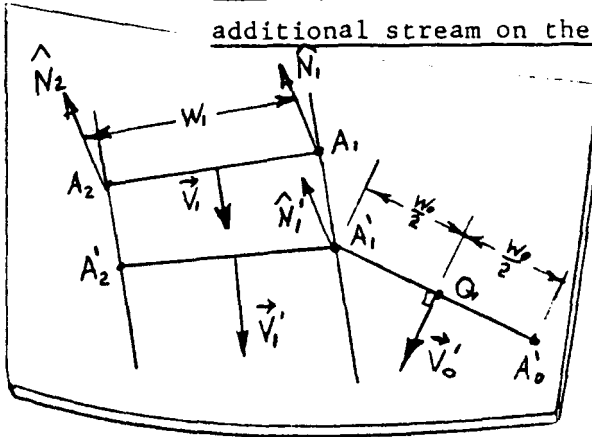


Fig. 5.2

Let the points A_1, A_2, \dots and velocities $\vec{V}_1, \vec{V}_2, \dots$ belong to an existing net, and let Q be a new coal stream impact point to the right of the net. (If Q lies inside the net, the coal is falling on itself and the computation should be terminated.) The right hand edge plane EP_1 of the original net passes through A_1 and is parallel to \hat{N}_1 and \vec{V}_1 .

The coal stream plate impact model of section 3 will provide the velocity (\vec{V}'_0 , say) of the impacting stream just after impact. Pass the plane ϵ_0 through Q , perpendicular to \vec{V}'_0 . ϵ_0 intersects EP_1 in a straight line l , and l intersects the plate surface ξ at A'_1 . Use A'_1 to construct the arc $A'_1 A'_2 A'_3 \dots$ terminating this row of cells, as described in section 5A.

Let $(A'_1, Q) = \frac{W_0}{2}$, the half-width

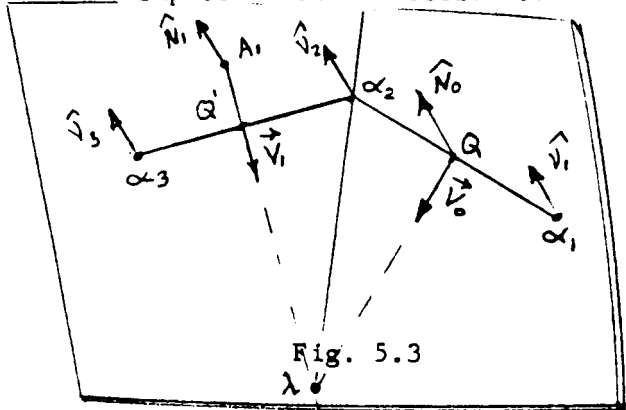
of a new right hand cell through which the impacting stream is sliding. Let l_0 be the line in the plane ϵ_0 , parallel to the normal N'_1 to ξ at A'_1 , and a distance W_0 from A'_1 . Find point A_0' , the intersection of the plate surface ξ with l_0 . A_0', A'_1, A'_2, \dots and the associated velocity vectors $\vec{V}_0', \vec{V}'_1, \vec{V}'_2, \dots$ constitute the beginning of a wider net, which incorporates the impacting stream; the computation now proceeds as described in section 5A. (The net points A_i and velocities \vec{V}_i can be renumbered if desired.)

5B.2 Special cases: one and two streams

The net-widening procedure just described is applicable if the existing net, prior to incorporation of the new stream, already contains at least two streams. An isolated stream, sliding on a plate, need not be assigned a width or height; in the absence of stream interaction forces, the equation of motion reduces to

$$\vec{V}_1 \frac{\vec{V}'_1 - \vec{V}_1}{L_1} = -g \mathbf{k} + \left\{ g N_1 \cdot \mathbf{k} - \vec{V}_1 \vec{V}_1 \cdot \left(\frac{dN}{dS} \right)_1 \right\} (N_1 - \mu \frac{\vec{V}_1}{V_1}), \quad (5.18)$$

where the normals \hat{N}_1 are taken on the stream center line. (5.18) describes the initial motion of the stream of coal originating at the top-most impact point on the chute. The initial value of \vec{V}_1 is found from the impact model of section 3.



At the Point A_1 of closest approach of the isolated stream, given by (5.18), to the second highest impact point Q on the chute, both streams are assigned widths and heights, and construction of the streamline - following net of section 5A is started.

Let \hat{N}_0, \hat{N}_1 be the unit normals to ξ at Q and A_1 , respectively; and let \vec{V}_0, \vec{V}_1 be the corresponding velocity vectors. (\vec{V}_0 is found from the impact model of section 3.) Let the plane FP_0 pass through Q and be parallel to \hat{N}_0 and \vec{V}_0 . Let the plane FP_1 pass through A_1 and be parallel to \hat{N}_1 and \vec{V}_1 . Let FP_0 and FP_1 intersect in a line l which cuts the plate surface ξ at the point λ . Let $FP_{\frac{1}{2}}$ denote the plane containing l which bisects the angle between FP_0 and FP_1 , and passes between Q and A_1 .

Now pass the plane ϵ_0 through Q perpendicular to \vec{V}_0 , and let ϵ_0 intersect $FP_{\frac{1}{2}}$ in a line l' which cuts ξ at α_2 . Let \hat{v}_2 be the unit normal to ξ at α_2 . $(Q, \alpha_2) = \frac{1}{2} W_0$, the half-width of the right hand stream.

Now find point α_1 as the intersection of ξ with a line in ϵ_0 , parallel to \hat{v}_2 , a distance W_0 from α_2 in the direction of Q .

Next pass the plane ϵ_1 through α_2 perpendicular to \vec{V}_1 ; let ϵ_1 intersect FP_1 in a line l'' which cuts ξ at Q' . Let $(\alpha_2, Q') = \frac{1}{2} W_1$, the half-width of the left hand stream. Find point α_3 as the intersection of ξ with a line in ϵ_1 , parallel to \hat{v}_2 , a distance W_1 from α_2 in the direction of Q' .

The points $\alpha_1, \alpha_2, \alpha_3$ and the velocity vectors \vec{V}_0, \vec{V}_1 are now used to start a two-stream net. The first step in this procedure is to adjust \vec{V}_0, \vec{V}_1 slightly to ensure that $\vec{V}_0 \cdot \left(\frac{\hat{v}_1 + \hat{v}_2}{2} \right) = \vec{V}_1 \cdot \left(\frac{\hat{v}_2 + \hat{v}_3}{2} \right) = 0$, as explained toward the end of section 5A.

5c. Calculation of the centrifugal forces produced by the curved plate

The quantity of interest here is the centrifugal force term

$|\vec{v}| \vec{v} \cdot \frac{d\hat{N}}{dS}$ ($S =$ distance parallel to \vec{v} where $\vec{v} \cdot \hat{N} = 0$) which appears in the equations of section 5A.

Let the plate surface ξ be defined by $F(x, y, z) = 0$ for some function F . Let F_x denote $\frac{\partial F}{\partial x}$, F_{xx} denote $\frac{\partial^2 F}{\partial x^2}$, F_{xy} denote $\frac{\partial^2 F}{\partial x \partial y}$ etc.

The vector field $\vec{N}(x, y, z) = F_x(x, y, z) \hat{i} + F_y(x, y, z) \hat{j} + F_z(x, y, z) \hat{k}$ is normal, at any point (x_p, y_p, z_p) , to the surface $F(x, y, z) = F(x_p, y_p, z_p)$. Consequently \vec{N} is normal to ξ on ξ .

Now $\hat{N} = \pm \frac{\vec{N}}{|\vec{N}|}$, with the sign chosen to make \hat{N} point towards the side of the plate on which the coal is sliding.

So

$$\begin{aligned} \vec{v} \cdot \frac{d\hat{N}}{dS} &= \pm \vec{v} \cdot \frac{d}{dS} \left(\frac{\vec{N}}{|\vec{N}|} \right) = \pm \vec{v} \cdot \left(\frac{1}{|\vec{N}|} \frac{d\vec{N}}{dS} - \frac{\vec{N}}{|\vec{N}|^2} \frac{d}{dS} |\vec{N}| \right) = \\ &= \pm \frac{\vec{v}}{|\vec{N}|} \cdot \frac{d\vec{N}}{dS} \quad \text{since } \vec{v} \cdot \vec{N} = 0 \end{aligned}$$

But
$$\frac{d\vec{N}}{dS} = \frac{\partial \vec{N}}{\partial x} \frac{dx}{dS} + \frac{\partial \vec{N}}{\partial y} \frac{dy}{dS} + \frac{\partial \vec{N}}{\partial z} \frac{dz}{dS}$$

and
$$\frac{dx}{dS} \hat{i} + \frac{dy}{dS} \hat{j} + \frac{dz}{dS} \hat{k} = \frac{\vec{v}}{|\vec{v}|}$$

Thus
$$\begin{aligned} \frac{d\vec{N}}{dS} &= (\text{grad } F_x) \cdot \frac{\vec{v}}{|\vec{v}|} \hat{i} + (\text{grad } F_y) \cdot \frac{\vec{v}}{|\vec{v}|} \hat{j} \\ &+ (\text{grad } F_z) \cdot \frac{\vec{v}}{|\vec{v}|} \hat{k} \end{aligned}$$

and finally, after some algebra,

$$|\vec{v}| \vec{v} \cdot \frac{d\hat{N}}{dS} = \pm \frac{F_{xx} v_x^2 + F_{yy} v_y^2 + F_{zz} v_z^2 + 2F_{xy} v_x v_y + 2F_{yz} v_y v_z + 2F_{xz} v_x v_z}{\sqrt{F_x^2 + F_y^2 + F_z^2}}$$

The local plate radius of curvature along the coal trajectory is

$$R = \frac{|\vec{v}|^2}{|\vec{v}| \vec{v} \cdot \frac{d\hat{N}}{ds}} \quad ; \text{ with our sign}$$

convention for \hat{N} , R is positive if the plate bends away from \hat{N} when following the coal.

Example:

$F(x,y,z) = x^2 + y^2 + z^2 - r^2 = 0$ defines a sphere ξ of radius r , centered at the origin. We have $F_x = 2x$; $F_y = 2y$; $F_z = 2z$

$$F_{xx} = F_{yy} = F_{zz} = 2; F_{xy} = F_{yz} = F_{xz} = 0$$

and so

$$|\vec{v}| \vec{v} \cdot \frac{d\hat{N}}{ds} = \frac{v_x^2 + v_y^2 + v_z^2}{\sqrt{x^2 + y^2 + z^2}} = \frac{|\vec{v}|^2}{r} \quad [\text{ for any point on } \xi].$$

The local radius of curvature is $R = \frac{|\vec{v}|^2}{|\vec{v}| \vec{v} \cdot \frac{d\hat{N}}{ds}} = r.$

APPENDIX E

PHASE II DYNAMICS COMPUTER PROGRAM
FRICTIONAL FLOW DYNAMICS PHASE

```

0001      REAL MU
0002      REAL KC,KE
0003      DIMENSION IPL (22,50)
0004      DIMENSION VELOC(22,50),WIDTH(22,50),HGT(22,50),RAD(22,50),
* FORC(22,50),SHEA(22,50),CORD(3,22,50)

0005      DIMENSION MT(22)
0006      DIMENSION IPTS(22),PXSAV(3)
0007      DIMENSION AX(3)
0008      DIMENSION VQ(3)
0009      DIMENSION PI(4)

0010      DIMENSION PY(3), PXX(3), P5(3)
0011      DIMENSION P3(3), AIIQ(3), ANL(3)
0012      DIMENSION K(22)
0013      DIMENSION KK(50),BAI(3,50),BVI(3,50),BAMDOT(50),ITT(50)
0014      DIMENSION AI(3,22),AN(3,22),VI(3,22),VN(3,22),PP(4,22),TEM(22),
* IV(2),IVP(2),P4(3),
* VB(22),F(22),S(22),HE(22),PTDAT(3,4,100),
* IT(22),C(22),PX(3),VP(3),P12(4),E(4),
* W(22),PRI(22),AMDOT(22)

0015      DIMENSION H2(22), HHH(1,3,3,2),AIII(1,3,3,2)
0016      INTEGER X
0017      INTEGER X1
0018      LOGICAL TOOBIG
0019      LOGICAL FULL
0020      FULL =.FALSE.

0021      TOOBIG = .FALSE.
0022      DATA HHH/ 5.07,6.24,7.62, 5.57,6.86,8.14, 5.99,7.50,8.76
* ,5.71,6.95,8.47, 6.04,7.52,9.05, 6.38,8.09,9.74/
0023      DATA AIII/2.48,2.23,3.03, 2.75,2.29,2.91
* ,2.97,2.45,3.19, 2.35,2.85,3.36
* ,2.46,3.08,3.60, 2.58,3.31,3.94/

0024      DATA H2/15*0./
0025      NAMELIST /COLDUT/ LAMDA , XF , YF , ZF , Q , CHLN , NP, APT
* ,THETCN, H,A1,H2 , YMIN
0026      NAMELIST /CUALIN/ V,RADIUS,PHI,SECT,IDLANG,SURANG,BELTWD
* ,ND1 , ND2, FLAT , GAMMA,RADUP,DISP
* ,MODET,EPSS,RUNNO,PHIP,GAMD,EL1,KC,DELTE,NP,NI,BMAR
* ,YAW,ZIH

0027      REAL IDLANG , LAMDA,KAPPA
0028      INTEGER IX,SX,IX,SECT,RUNNO
0029      DATA G/386.4/

0030      COMMON THET(3,200),ABC(3,200),PT(3,3,200),UN(3,200)
0031      COMMON /DENS/GAMD

0032      DD=1.0E-10
0033      NF=3000

0034      ID=3000
0035      DO 5555 I=1,3

0036      DO 5555 J=1,3

```

```

0037      DO 5555 L=1,20
0038      ABC(I,L)=0.
0039      PT(I,J,L)=0.
0040      UN(I,L)=0.
0041      R(L)=100.
0042      5555 CONTINUE
0043      READ(5,CGALIN,FND=9999)
0044      DELTA = DELTF
0045      NS = SECT
0046      PHIPR=PHIP/57.29578
0047      MU=TAN(PHIPR)
0048      WRITE ( 6,905)
0049      905 FORMAT(*1*)
0050      WRITE ( 6,901)
0051      901 FORMAT(//)
0052      WRITE ( 6,916)
0053      916 FORMAT ( /1X,132(**))
0054      WRITE ( 6,901)
0055      WRITE ( 6,918) RUNNO ,DATE
0056      918 FORMAT ( 1X,10X,'BEGIN INDEPENDENT RUN OF COAL CHUTE DESIGNER',
*          30X,'RUN NUMBER',13,5X,'DATE ',5A4)
0057      919 FORMAT ( /1X,31X,10(*. '),5X,
*          'INDEPENDENT VARIABLES FOR THIS RUN ', 5X,10(*. ')/)
0058      WRITE ( 6,901)
0059      WRITE ( 6,916)
0060      930 FORMAT ( 40X,'RUN NO',13,5X,'DATE ',5A4)
0061      IX = 1
0062      IF ( IDLANG.EQ. 35.) IX = 2
0063      SX = 1
0064      IF ( SURANG.EQ. 25.) SX= 2
0065      IF ( SURANG.EQ.30.) SX=3
0066      BX = 1
0067      IF ( BELTWD.EQ.36.) BX=2
0068      IF ( BELTWD.EQ.42.) BX=3
0069      H = HHH( 1,BX,SX,IX)
0070      A1 = A111( 1,BX,SX,IX)
0071      CC=BELTWD-2.*BMAR
0072      RR=H/2.+CC**2/(8.*H)
0073      DLT=CC/SECT
0074      MID = SECT/2 + 1
0075      DO 10 K=1,SECT
0076      B=SQRT(RR**2-CC**2/4)
0077      N = IABS(MID-K)
0078      X1 = N*DLT
0079      A=SQRT(RR**2-X1**2)
0080      H2(K) = (A-B)/2.
0081      RHO=GAMD/(32.2*12**3)
0082      AM/DT(K)=DLT*H2(K)*RHO*V

```

```
0083      10      CONTINUE
0084          R12=100.
0085          DELTA =DELTA/57.29
0086          KF=KC*(1.-SIN(DELTA))/(1.+SIN(DELTA))
0087          READ(5,15)
0088      15      FORMAT(20A4)
0089      18      CONTINUE
0090          DO 20 J=1,NP
0091          DO 20 K=1,4
0092          READ(5,25) (PTDAT(L,K,J),L=1,3)
0093      25      FORMAT(3F20.8)
0094      20      CONTINUE
0095          READ(5,15)
0096          DO 30 J=1,NT
0097          DO 30 K=1,3
0098          READ(5,25) (PT(L,K,J),L=1,3)
0099      30      CONTINUE
0100          READ(5,15)
0101          DO 40 J=1,NT
0102          READ(5,25) (UN(L,J),L=1,3)
0103      40      CONTINUE
0104          READ(5,15)
0105          DO 50 J=1,NT
0106          READ(5,25) (ABC(L,J),L=1,3)
0107      50      CONTINUE
0108          READ(5,15)
0109          DO 60 J=1,NT
0110          READ(5,25) (THET(L,J),L=1,3)
0111      60      CONTINUE
0112          READ(5,15)
0113      1      CONTINUE
0114          DO 70 J=1,NS
0115          READ(5,25) (VI(L,J),L=1,3)
0116      70      CONTINUE
0117          READ(5,15)
0118          DO 80 J=1,NS
0119          READ(5,25) (AI(L,J),L=1,3)
0120      80      CONTINUE
0121          READ(5,15)
0122          DO 90 J=1,NS
0123          READ(5,35) IT(J)
0124      35      FORMAT(I8)
0125      90      CONTINUE
0126      2      CONTINUE
0127          WRITE(6,92)
0128      92      FORMAT(1X,'LISTING OF INPUTS BEFORE ARRANGEMENT!')
0129          WRITE (6,127)
0130          DO 91 J=1,NS
```

```

0131      WRITE(6,126)J,II(J),AI(1,J),AI(2,J),AI(3,J),VI(1,J),VI(2,J)
          + ,VI(3,J) ,AMDOT(J)
0132      91  CONTINUE
          C
          C  ARRANGE STREAMS IN ORDER OF ACCUMULATION TO MAIN FLOW
          C
          C  FIND HIGHEST HITTING STREAM
          C
0133      A=AI(2,1)
0134      KK(1)=1
0135      DO 21 J=1,NS
0136      IF(A.GT.AI(2,J))GO TO 21
0137      A=AI(2,J)
0138      KK(1)=J
0139      21  CONTINUE
          C
          C  FIND WHICH OF TWO STREAMS ADJACENT TO ALREADY ACCUMULATED STREAMS
          C  HITS HIGHER
          C
0140      JP=KK(1)+1
0141      JM=KK(1)-1
0142      IF(JP.GT.NS)GO TO 27
0143      IF(JM.EQ.0) GO TO 24
0144      DO 23 L=2,NS
0145      KK(L)= JP
0146      IF(AI(2,JP).GT.AI(2,JM)) GO TO 22
0147      KK(L)=JM
0148      JM=JM-1
0149      IF ( JM.EQ.0)GO TO 24
0150      GO TO 23
0151      22  JP=JP+1
0152      IF(JP.GT.NS) GO TO 27
0153      23  CONTINUE
0154      GO TO 29
          C
          C  NUMBER ALL REMAINING STREAMS
          C
0155      24  DO 26 J=JP,NS
0156      KK(J)=J
0157      26  CONTINUE
          C
0158      GO TO 29
0159      27  JMM=NS+1-JM
0160      DO 28 J=JMM,NS
0161      KK(J)=NS-J+1
0162      28  CONTINUE
0163      29  CONTINUE
          C
          C  TRANSFER DATA REQUIRED BY RENUMBERING OF STREAMS DUE TO REARRANGEMENT
    
```

E-4

```

0164      C      DO 31 J=1,NS
0165      DD 31 L=1,3
0166      BAI(L,J)= AI(L,KK(J))
0167      BVI(L,J)= VI(L,KK(J))
0168      BAMDOT(J)= AMDOT(KK(J))
0169      ITT(J) = IT(KK(J))
0170      31 CONTINUE
0171      DO 32 J=1,NS
0172      DD 32 L=1,3
0173      AI(L,J)=BAI(L,J)
0174      VI(L,J)=BVI(L,J)
0175      AMDOT(J)=BAMDOT(J)
0176      IT(J)=ITT(J)
0177      MT(J)=IT(J)
0178      32 CONTINUE
0179      1003  FORMAT(//1X,3I8)
0180      1002  FORMAT(//3X,8F7.2)
0181      121  CONTINUE
0182      C
0183      129  WRITE(6,129)
0184      FORMAT(1X,'LISTING OF INPUTS AFTER ARRANGEMENT')
0185      WRITE (6,127)
0186      DD 128 J=1,NS
0187      WRITE(6,126)J,IT(J),AI(1,J),AI(2,J),AI(3,J),VI(1,J),VI(2,J)
0188      * ,VI(3,J) ,AMDOT(J)
0189      128 CONTINUE
0190      126  FORMAT(1X,2(13,3X),6(F8.2,3X),F8.4)
0191      127  FURHAT (1X,'STREAM,TRIANGLES, HIT POINTS ,VELOCITIES ,FLOW RATES')
0192      C
0193      ISTEP=1
0194      JT=IT(1)
0195      EX=(AI(2,1)-AI(2,2))/5,
0196      125 CONTINUE
0197      C
0198      R12=9999
0199      C
0200      C FORMATION OF TWO STREAM NET
0201      C DETERMINE PATH OF STREAM 1 IN INCREMENTS EX AND POINT OF CLOSEST
0202      C APPROACH TO STREAM 2
0203      C
0204      PX(1)=AI(1,1)
0205      PX(2)=AI(2,1)
0206      PX(3)=AI(3,1)
0207      PY(1) =PX(1)
0208      PY(2) =PX(2)
0209      PY(3) =PX(3)
0210      VP(1)=VI(1,1)

```

```

0202      VP(2)=VI(2,1)
0203      VP(3)=VI(3,1)
0204      CALL PLANE(JT,PX,VP,E)
0205      PP(1,1)=E(1)
0206      PP(2,1)=E(2)
0207      PP(3,1)=E(3)
0208      PP(4,1)=E(4)

C
C   DRAW A LINE IN P1 WHICH INTER. JT IN A1*
0209      P4(1)=A1(1,1)
0210      P4(2)=A1(2,1)
0211      P4(3)=A1(3,1)
0212      P5(1)= P4(1)-VI (1,1)
0213      P5(2)= P4(2)-VI (2,1)
0214      P5(3)= P4(3)-VI (3,1)
0215      CALL LOCAT3 (JT,EX,E,P4,P5,PXX )
0216      CALL FIND (JT,NT,PY,PXX,E,PX,JTP )
0217      JT = JTP
0218      PY(1) = PX(1)
0219      PY(2) = PX(2)
0220      PY(3) = PX(3)
0221      PE=G*UN(2,JT)
0222      DO 130 I=1,NS
0223      VB(I)=SQRT(VI(1,I)**2+VI(2,I)**2+VI(3,I)**2)
0224      130 CONTINUE

C
C   CALCULATE VELOCITY OF STREAM 1
C
0225      VE=VB(1)
0226      VP(1)=VI(1,1)+(EX/VE)*PE*(UN(1,JT)-MU*VI(1,1)/VE)
C
0227      VP(2) = VI(2,1) + (EX/VE)* (-G + PE*(UN(2,JT)-MU*VI(2,1)/VE))
C
0228      VP(3) =VI(3,1) +(EX/VE) * PE* (UN(3,JT)-MU*VI(3,1)/VE)
0229      D=0.

C
0230      DO 140 L=1,3
0231      D=D+(PX(L)-A1(L,2))**2
0232      140 CONTINUE
0233      D=SQRT(D)
0234      IF(ISTEP.EQ.1) GO TO 160
0235      IF(D.GT.DOLD) GO TO 200
0236      160 CONTINUE
0237      DO 170 L=1,3
0238      A1(L,1)=PX(L)
0239      VI(L,1)=VP(L)
0240      170 CONTINUE
0241      DOLD=D

```

0242
0243

ISTEP=ISTEP+1
GO TO 125

C
C

0244
0245
0246

200 CONTINUE
WRITE(6,3001) DOLD
3001 FORMAT(' THE CLOSEST DIST. OF APPR. OF ISOLATED STREAM TO
1 SECOND HIGHEST IMPACT POINT IS =',F8.2)

C

0247
0248
0249
0250
0251
0252
0253
0254
0255
0256

JT1 = J1(2)
JT=IT(2)
DO 203 L= 1,4
F(L) = PP(L,1)
203 CONTINUE
DO 205 L= 1,3
P3(L) = AI(L,1)
P4(L) = AI(L,2)
P5(L) = AI(L,2)
205 CONTINUE

C
C
C
C

FIND LOCATION OF NET POINT 2 HALFWAY BETWEEN HIT POINT 2
AND STREAM 1'S PATH

0257
0258
0259
0260
0261
0262
0263

E(4)=0.
DO 210 L=1,3
E(L)=VI(L,2)
E(4)=E(4)+VI(L,2)*AI(L,2)
PXX(L)= 2.*P4(L)-P3(L)
210 CONTINUE
E(4)=-E(4)

C

0264
0265

CALL LOCATE(JT,E,F,PY)
DOLD= SQRT((PY(1)-AI(1,2))**2
* (PY(2)-AI(2,2))**2
* (PY(3)-AI(3,2))**2)

0266
0267

DOLD=DOLD/2.
CALL LOCAT3(IT(2),DOLD,E,P4,PXX,PX)

C

0268
0269
0270
0271
0272
0273
0274

JTP=100
CALL FIND (JT,NT,P4,PX,E,PY,JTP)
IF (JTP.EQ.100) WRITE(6,5000)
AN(1,2) = PY(1)
AN(2,2) = PY(2)
AN(3,2) = PY(3)
5000 FORMAT(' POINT NOT LOCATABLE')
C

0275
0276

IT(2)=JTP
HW=0.

7-E

```

0277      DO 230 L=1,3
0278      WW=WW+(AN(L,2)-A(L,2))*#2
0279      230  CONTINUE
0280      WW=2.0*SQRT(WW)

C
C      FIND OTHER NET POINT FOR 2ND HIGHEST HITTING STREAM *****
C
C      IGROUP = 1 MEANS Z COORDINATE LESS THAN Z COORDINATE OF PRECEEDING STREAMS
C      IGROUP OTHERWISE
C
0281      IGROUP=1
0282      IF ( A(3,2) .LT. AN(3,2) ) IGROUP = 2
0283      IF (IGROUP.EQ.1) W(1)=WW
0284      IF (IGROUP.EQ.2) W(2)=WW
0285      DO 220 L=1,3
0286      PXX(L)=A(L,2) + (A(L,2) -AN(L,2))
0287      220  CONTINUE
0288      JTP = 100
0289      CALL FIND ( JTT,NT,P5,PXX,E,PX,JTP)
0290      IF (JTP.EQ.100) WRITE( 6,5000 )
0291      DO 240 L=1,3
0292      IF (IGROUP.EQ.2) AN(L,3)=PX(L)
0293      IF (IGROUP.EQ.1) AN(L,1)=PX(L)
0294      240  CONTINUE
C
0295      IF (IGROUP.EQ.1) IT(1)=JTP
0296      IF (IGROUP.EQ.2) IT(3)=JTP

C
C      FIND LOCATION OF CENTER OF 1 ST HITTING STREAM *****
C
0297      F(4)=0.
0298      DO 250 L=1,3
0299      PXX(L) = PY(L)
0300      E(L)=VI(L,1)
0301      E(4)=E(4)+VI(L,1)*AN(L,2)
0302      250  CONTINUE
0303      E(4)=-E(4)

C
0304      F(1)=PP(1,1)
0305      F(2)=PP(2,1)
0306      F(3)=PP(3,1)
0307      F(4)=PP(4,1)
0308      KT=IT(2)
0309      CALL LUCATE(KT,E,F,PX)
0310      CALL FIND ( KT,NT,PXX,PX,E,PY,JTTP )

C
0311      WW=0.
0312      DO 260 L=1,3

```

E-8

```

0313      WW=WW + (AN(L,2)-PY(1)) **2
0314      260  CONTINUE
0315      WW=2.0*SQRT(WW)
0316      IF (IGROUP.EQ.1) W(2)=WW
0317      IF (IGROUP.EQ.2) W(1)=WW
    
```

C
C
C
C

FIND LOCATION OF OTHER NET POINT OF FIRST HITTING STREAM *****

```

0318      P4(1)=AN(1,2)
0319      P4(2)=AN(2,2)
0320      P4(3)=AN(3,2)
0321      DO 265 L=1,3
0322      PXX(L) = PY(L) + (PY(L) - AN(L,2))
0323      265  CONTINUE
0324      JTP = 100
0325      CALL FIND(JTTP,NT,PY,PXX,E,PX,JTP )
0326      IF ( JTP.EQ.100) WRITE (6,500) )
0327      DO 270 L=1,3
0328      IF (IGROUP.EQ.2) AN(L,1)=PX(L)
0329      IF (IGROUP.EQ.1) AN(L,3)=PX(L)
0330      270  CONTINUE
0331      IF (IGROUP.EQ.2) IT(1)=JTP
0332      IF (IGROUP.EQ.1) IT(3)=JTP
    
```

C
C
C

TRANSFER STREAM 1 AND STREAM 2 DATA IF IGROUP = 1

```

0333      IF (IGROUP.EQ.2) GO TO 275
0334      DO 273 L= 1,3
0335      VN(L,2) = VI(L,1)
0336      VN(L,1) = VI(L,2)
0337      VN(L,3) = VN(L,2)
0338      273  CONTINUE
0339      D=AMDOT(2)
0340      AMDOT(2)=AMDOT(1)
0341      AMDOT(1)=D
0342      GO TO 285
0343      275  CONTINUE
0344      DO 280 I=1,2
0345      DO 280 L=1,3
0346      VN(L,1)=VI(L,1)
0347      VN(L,3)=VN(L,2)
0348      280  CONTINUE
0349      285  CONTINUE
    
```

C
C
C

INITIAL VELOCITIES AND HEIGHTS FOR 2 STREAM NET *****

```

0350      DO 290 I=1,2
    
```

E-9

```

0351      VB(1)=SQRT(VN(1,1)**2+VN(2,1)**2+VN(3,1)**2)
0352      CONTINUE
0353      DO 300 I=1,2
0354      HE(I)=AMD(HT(I)/(W(I)*RHO+VB(I))
0355      JT=IT(I)
0356      K=I+1
0357      KT=JTK
0358      UNN=(UN(2,JT)+UN(2,KT))/2.
0359      PR(1)=RHO*HE(I)*UNN*G
0360      CONTINUE
0361      HE(3)=-HE(2)
0362      PR(3)=-PR(2)
0363      IF(IGROUP.EQ.2) PR(3)=PR(2)
0364      IF(IGROUP.EQ.2) PR(2)=PR(1)
0365      IF(IGROUP.EQ.2) PR(1)=-PR(2)
    
```

C
C FIND DIVIDING PLAND FOR TWO STREAM NET BASED ON STREAM HEIGHT(HE)
C AND DIVERGENCE OR CONVERGENCE
C

```

0366      JT=IT(1)
0367      DO 325 L= 1,3
0368      VP(L)= VN(L,2)
0369      VQ(L) = VN(L,1)
0370      PX(L) = AN(L,1)
0371      325 CONTINUE
0372      CALL PLANE(JT,PX,VQ,E)
0373      PP(1,1)=E(1)
0374      PP(2,1)=E(2)
0375      PP(3,1)=E(3)
0376      PP(4,1)=E(4)
0377      JT=IT(2)
0378      CALL DETR(VQ,VP,UN(1,JT),C(2))
    
```

C
C C(2) LESS THAN ZERO MEANS DIVERGENCE
C

```

0379      IF(C(2).LT.0.) GO TO 350
0380      PX(1)=AN(1,2)
0381      PX(2)=AN(2,2)
0382      PX(3)=AN(3,2)
0383      IF(HE(2).GT.HE(1)) CALL PLANE(JT,PX,VP,E)
0384      IF(HE(2).LT.HE(1)) CALL PLANE(JT,PX,VQ,E)
0385      GO TO 360
0386      350 CONTINUE
0387      IF(HE(2).GT.HE(1)) CALL PLANE(JT,PX,VQ,E)
0388      IF(HE(2).LT.HE(1)) CALL PLANE(JT,PX,VP,E)
0389      360 CONTINUE
0390      PP(1,2)=E(1)
0391      PP(2,2)=E(2)
    
```

E-10

```

0392      PP(3,2)=E(3)
0393      PP(4,2)=E(4)

C
0394      JT=IT(3)
0395      PX(1)=AN(1,3)
0396      PX(2)=AN(2,3)
0397      PX(3)=AN(3,3)
0398      CALL PLANE(JT,PX,VP,E)
0399      PP(1,3)=E(1)
0400      PP(2,3)=E(2)
0401      PP(3,3)=E(3)
0402      PP(4,3)=E(4)

C
0403      DO 365 J=1,3
0404          VB(J)=SQRT(VN(1,J)**2+VN(2,J)**2+VN(3,J)**2)
0405      365 CONTINUE
0406          ISTEP=0
0407          IQ=3

C *****
C REPETITIVE LOOP ADDING STREAMS *****
C *****
0408      370 CONTINUE
C
0409          IGROUP=9999
0410          IF(AI(3,IQ).GT.AN(3,1)) IGROUP=1
0411          IF(AI(3,IQ).LT.AN(3,1Q)) IGROUP=2
0412          IF(IGROUP.EQ.9999) GO TO 375
0413          GO TO 380
0414      375 WRITE(6,3003) IQ
0415      3003 FORMAT(' HIT POINT',I4,' LIES WITHIN NET')
0416          GO TO 1400
0417      380 CONTINUE
0418          WRITE(6,379) IGROUP
0419      379 FORMAT(' IGROUP=',I2)

C
C CHECK IF NEW STREAM ADDS NORMALLY ( I.E. WAVE FRONT THRU HIT POINT
C INTERSECTS EXISTING TOTAL FLOW BELOW LAST CALCULATED WAVE FRONT)
C
0420          K= IQ
0421          IF ( IGROUP .EQ.1) K=1
0422          BELOW =0.
0423          DO 381 L=1,3
0424              BELOW = BELOW +VI(L,IQ)*(AN(L,K)-AI(L,IQ))
0425      381 CONTINUE
0426          EX = 3FLOW/SQRT(VI(1,IQ)**2+VI(2,IQ)**2+VI(3,IQ)**2)
0427          EXLIM = 1.
0428          IF (BELOW.LT.0..AND. ABS(EX).GT.EXLIM) GO TO 388
0429          IF ( BELOW .LT.0.) GO TO 390

```

E-12

```

C
C ESTABLISH NON-NORMAL NET POINT *****
C
C FLOW ALONG HIT VELOCITY VECTOR IS ASSUMED UNTIL NLW WAVE FRONT
C JOINS EXISTING WAVE FRONT
C
0430      WRITE(6,385)IG
0431      385      FORMAT(' NON-NORMAL NET POINT',I3)
0432          DO 382 L=1,3
0433          A1(Q(L))= A1(L,IQ)
0434          VP(L)= V1(L,IQ)
0435          P4(L) = A1(Q(L))-V1(L,IQ)
0436          PY(L) = AN(L,K)
0437      382      CONTINUE
0438          CALL PLANE ( MT(IQ),A1IQ,VP,E)
0439          CALL LOCAT3(MT(IQ),EX,E,A1IQ,P4,PX)
0440          VP(1)= PX(1)-PY(1)
0441          VP(2)= PX(2)-PY(2)
0442          VP(3)= PX(3)-PY(3)
0443          VQ(1)=PY(1)-VP(1)
0444          VQ(2)=PY(2)-VP(2)
0445          VQ(3)=PY(3)-VP(3)
0446          CALL PLANE (IT(K),PY,VP,E)
0447          WW= 2.*SQRT(VP(1)**2+VP(2)**2+VP(3)**2)
0448          CALL LOCAT3 ( IT(K) , WW, E, PY,VQ,PX)
0449          CALL FIND ( IT(K),NT,PY,PX,E,PXX,JTTP)
0450          IF( IGROUP .EQ.1) GO TO 600
0451          DO 383 L=1,3
0452          AN(L,IQ+1) = PXX(L)
0453      383      CONTINUE
0454          GO TO 795
0455      388      CONTINUE
C
C IF WAVE FRONT DISPLACEMENT TO JOINING BY NEXT STREAM GREATER THAN
C EXLIM (I.E. TOOBIG = TRUE) THEN STREAM 1 MOVED EXLIM AND TOTAL
C WAVE FRONT ADVANCES
C
0456          TOOBIG=.TRUE.
0457          IGROUP = 1
0458          WRITE(6,387)
0459      387      FORMAT(1X,'STEP SIZE TOO BIG, FIXED STEP TAKEN,NO STREAM ADDED')
0460          DO 399 L=1,3
0461          P3(L)= AN(L,1)-VN(L,1)
0462      399      CONTINUE
0463          CALL LOCAT3(IT(1),EXLIM,PP(1,1),AN(1,1),P3,PY)
0464          CALL FIND (IT(1),NT,AN(1,1),PY,PP(1,1),PX,JTP)
0465          DO 391 L=1,3
0466          AN(L,1)=PX(L)

```

```

0467      391  CONTINUE
0468      EL=FXLTM
0469      IT(1)= JTP
0470      GO TO 444
0471      390  CONTINUE
C
C FIND JUNCTION TO NET OF ADDING STREAM *****
C
0472      E(4)=0.
0473      DO 400 L=1,3
0474      E(L)=VI(L,IQ)
0475      E(4)=E(4)+VI(L,IQ)*AI(L,IQ)
0476      400  CONTINUE
0477      E(4)=-E(4)
0478      AIQ(1) = AI(1,IQ)
0479      AIQ(2) = AI(2,IQ)
0480      AIQ(3) = AI(3,IQ)
C
0481      JT=IT(1)
0482      JP=(JT-1)/2+1
0483      F(1)=PP(1,1)
0484      F(2)=PP(2,1)
0485      F(3)=PP(3,1)
0486      F(4)=PP(4,1)
0487      DO 405 L=1,4
0488      405  IF(IIGROUP.EQ.2) F(L)=PP(L,IQ)
0489      CALL LOCATE ( MT(IQ) ,E,F,PY)
0490      CALL FIND ( MT(IQ),NT,AIQ,PY,E,PX,JTP)
C FIND RADIUS AT START OF STEP FOR OLD BOUNDARY
0491      IF(IIGROUP.EQ.1) CALL LOCAT3(IT(1),1.,F,AN(1,1),PY,P3)
0492      IF(IIGROUP.EQ.2) CALL LOCAT3(IT(IQ),1.,F,AN(1,IQ),PY,P3)
0493      IF(IIGROUP.EQ.1) CALL RA(IT(1),NT,AN(1,1),P3,F,R12)
0494      IF(IIGROUP.EQ.2) CALL RA (IT(IQ),NT,AN(1,IQ),P3,F,R12)
0495      IF(R12.LT.18.) R12=18.
C FIND NEW STREAM BOUNDARY POINT *****
0496      PY(1)= AI(1,IQ)+(AI(1,IQ)-PY(1))
0497      PY(2)= AI(2,IQ)+(AI(2,IQ)-PY(2))
0498      PY(3)= AI(3,IQ)+(AI(3,IQ)-PY(3))
0499      CALL FIND (MT(IQ),NT,AIQ,PY,F,PXX,JTTP)
0500      EL=0.
0501      DO 410 L=1,3
0502      IF(IIGROUP.EQ.2) EL=EL+(PX(L)-AN(L,IQ))*2
0503      IF(IIGROUP.EQ.1) EL=EL+(PX(L)-AN(L,1))*2
0504      IF(IIGROUP.EQ.2) AN(L,IQ)=PX(L)
0505      IF(IIGROUP.EQ.1) AN(L,1)=PX(L)
0506      410  CONTINUE
0507      EL=SQRT(EL)
0508      JPP=(JTP-1)/2+1

```

E-13

```

0539      450  CONTINUE
0510      444  CONTINUE
0511      1001  FORMAT(/,IX,F7.2)
          C
          C
0512      F(I)=0.
0513      S(I)=0.
0514      F(IQ)=0.
0515      S(IQ)=0.
          C
          C  FIND INNER DIVIDING PLANES BASED ON STREAM HEIGHT (HE) AND
          C  CONVERGENCE OR DIVERGENCE
          C
0516      IQ1=IQ-1
0517      DO 490 I=2,IQ1
0518      JT=IT(L)
0519      K=L-1
0520      PX(1)=AN(1,L)
0521      PX(2)=AN(2,L)
0522      PX(3)=AN(3,L)
0523      VP(1)=VN(1,L)
0524      VP(2)=VN(2,L)
0525      VP(3)=VN(3,L)
0526      VQ(1)=VN(1,K)
0527      VQ(2)=VN(2,K)
0528      VQ(3)=VN(3,K)
          C
          C  C(L) LESS THAN ZERO MEANS STREAMS DIVERGING
          C
0529      IF (C(L).LT.0.) GO TO 470
0530      F(L)=KC*(PR(L)+PR(K))*(HE(L)+HE(K))/4.
0531      S(L)=F(L)*SIN(DELTA)
0532      IF (VB(L).LT.VB(K)) S(L)=-S(L)
0533      IF (HE(L).GT.HE(K)) CALL PLANE(JT,PX,VP,E)
0534      IF (HE(L).LE.HE(K)) CALL PLANE(JT,PX,VQ,E)
0535      GO TO 480
0536      470  CONTINUE
0537      F(L)=KE*(PR(L)+PR(K))*(HE(L)+HE(K))/4.
0538      S(L)=F(L)*SIN(DELTA)
0539      IF (VB(L).LT.VB(K)) S(L)=-S(L)
0540      IF (HE(L).GT.HE(K)) CALL PLANE(JT,PX,VQ,E)
0541      IF (HE(L).LE.HE(K)) CALL PLANE(JT,PX,VP,E)
0542      480  CONTINUE
0543      PP(1,L)=E(1)
0544      PP(2,L)=E(2)
0545      PP(3,L)=E(3)
0546      PP(4,L)=E(4)
0547      490  CONTINUE

```

```

0548      C          IF (IGROUP.EQ.2) GO TO 699
      C
      C      NEW VELOCITY FOR STREAM 1 *****
      C
0549      JT=IT(1)
0550      IT(1)=JTP
0551      LT=IT(2)
0552      WW=W(1)
0553      VQ(1)=VN(1,1)
0554      VQ(2)=VN(2,1)
0555      VQ(3)=VN(3,1)
0556      R(1) = R12
0557      PR(1) =      RHO*HE(1)*(VB(1)**2/R(1)+G*UN(2,JT))
0558      CALL VEL(EL,AMDOT(1),JT,LT,HE(1),WW,F(1),F(2),S(1),S(2),PR(1),
      * VQ,VP,
      * MU)
0559      DO 500 L=1,3
0560      VN(L,1)=VP(L)
0561      500 CONTINUE
      C
      C      MAIN IGROUP.EQ.1 ROUTINE *****
      C
0562      DO 600 I=2,10
0563      K=I-1
0564      VB(K)=SQRT(VN(1,K)**2+VN(2,K)**2+VN(3,K)**2)
      C
      C      LOCATE NEW NET POINT I AT INTERSECTION OF DIVIDING PLANE THRU OLD NET POINT.
      C      CHUTE SURFACE AT OLD NET POINT AND PLANE NORMAL TO VELOCITY VECTOR THRU
      C      NEW NET POINT WITH INDEX I-1
      C
0565      JT=IT(I)
0566      JP=(JT-1)/2+1
0567      F(4)=0.
0568      DO 510 L=1,3
0569      E(L)=VN(L,K)
0570      510 E(4)=E(4)+VN(L,K)*AN(L,K)
0571      E(4)=-E(4)
0572      JT=IT(I)
0573      JP=(JT-1)/2+1
0574      PI(1)=PP(1,1)
0575      PI(2)=PP(2,1)
0576      PI(3)=PP(3,1)
0577      PI(4)=PP(4,1)
      C
0578      CALL LOCATE (JT,E,PI,PY)
0579      ANL(1)= AN(1,1)
0580      ANL(2)= AN(2,1)

```

```

0581      ANL(3)= AN(3,I)
0582      CALL FIND (JT,NT,ANL,PY,PI,PX,JTP )
0583      EL=0.
0584      DO 520 L=1,3
0585 520      EL=EL+(AN(L,I)-PX(L))**2
0586      EL=SQRT(EL)
0587      W(K) = 0.
0588      DO 560 L=1,3
0589      W(K) = W(K)+(PX(L)-AN(L,K))**2
0590 560      CONTINUE
0591      W(K) = SQRT(W(K))
0592      HE(K) = AMDOT(K)/(W(K)*RHO * VB(K) )
0593      CALL RA(IT(I),NT,AN(1,I),PX,PI,R12)
0594      IF(R12.LT.16.) R12=18.
0595      R(I)=R12
0596      PR(I) =      RHO*HE(I)*(VB(I)**2/R(I)+G*UN(2,IT(I)))
C
0597      IT(I)=JTP
0598      JPP=(JTP-1)/2+1
0599 550      CONTINUE
0600 544      CONTINUE
C
0601 2002      FORMAT(/2X,I8,10F7.2)
0602      IF(I.FQ.IQ) GO TO 565
C
0603      LT=IT(I)
0604      JT=IT(K)
0605      VQ(1)=VN(1,I)
0606      VQ(2)=VN(2,I)
0607      VQ(3)=VN(3,I)
0608      CALL VEL(EL,AMDOT(I),JT,LT,HE(I),W(I),F(I),E(I+1),
+ S(I),S(I+1),PR(I),VQ,VP ,
* MU)
0609      VB(I) = SQRT(VP(1)**2+VP(2)**2+VP(3)**2)
0610 565      CONTINUE
0611      DO 570 L=1,3
0612      VN(L,I)=VP(L)
0613      AN(L,I)=PX(L)
0614 570      CONTINUE
0615 600      CONTINUE
0616      IF ( TONBIG) GO TO 799
C
C TRANSFER ALL WAVE FRONT PARAMETERS TO ACCORD WITH RENUMBERING. REQUIRED.
C BY ADDFD STREAM
C
0617      DO 601 J=1,IQ
0618      I=IQ-J+1
0619      K=I+1

```

```

0620      DO 601 L=1,3
0621      AN(L,K)=AN(L,I)
0622      IT(K)=IT(I)
0623      VN(L,K)=VN(L,I)
0624      VB(K)=VB(I)
0625      W(K) = W(I)
0626      HE(K) = HE(I)
0627      AMDOT(K) = AMDOT(I)
0628 601  CONTINUE
0629      IT(1)=JTTP
0630      WW=0.
0631      DO 698 L=1,3
0632      VN(L,1)=V(L,IQ)
0633      AN(L,1)=PXX(L)
0634      WW=WW+(AN(L,1)-AN(L,2))**2
0635 698  CONTINUE
0636      W(1)= SQRT (WW)
0637      VB(1)=SQRT(VN(1,1)**2+VN(2,1)**2+VN(3,1)**2)
0638      AMDOT(1) =BAMDOT (IQ)
0639      HE(1)=AMDOT(1)/(W(1)*RHO*VB(1))
0640      GO TO 799
C *****
0641 699  CONTINUE
C
C NEW VELOCITY FOR STREAM IQ-1 *****
C
0642      JT=IT(IQ)
0643      IT(IQ)= JTP
0644      LT=IT(IQ-1)
0645      WW=W(IQ-1)
0646      VQ(1)=VN(1,IQ-1)
0647      VQ(2)=VN(2,IQ-1)
0648      VQ(3)=VN(3,IQ-1)
0649      R(IQ-1)=R12
0650      PR(IQ-1)= RHO*HE(IQ-1)*(VB(IQ-1)**2/R(IQ-1)+G*UN(2,LT))
0651      CALL VEL(EL,AMDOT(IQ),JT,LT,HE(IQ-1),WW,F(IQ-1),F(IQ),S(IQ-1),S(I
*Q),PR(IQ-1),VQ,VP,
* MU)
0652      DO 501 L=1,3
0653      VN(L,IQ-1)=VP(L)
0654 501  CONTINUE
0655 700  CONTINUE
C
C MAIN IGROUP.EQ.2 ROUTINE *****
C
0656 701  CONTINUE
0657      DO 795 I=2,IQ
0658      J=IQ-1+1

```

E-17

```

0659      K=J+1
0660      VB(J)=SQRT(VN(1,J)**2+VN(2,J)**2+VN(3,J)**2)
0661      E(4)=0.
0662      DO 710 L=1,3
0663      E(L)=VN(L,K)
0664 710    E(4)=E(4)+VN(L,J)*AN(L,K)
0665      E(4)=-E(4)
0666      JT=IT(J)
0667      JP=(JT-1)/2+1
0668      PI(1)=PP(1,J)
0669      PI(2)=PP(2,J)
0670      PI(3)=PP(3,J)
0671      PI(4)=PP(4,J)
C
C LOCATE NEW NET POINT J BASED ON INTERSECTION OF DIVIDING
C PLANE THRU OLD NET POINT, CHUTE SURFACE AT OLD NET POINT AND PLANE
C NORMAL TO VELOCITY VECTOR THRU NEW NET POINT WITH INDEX J+1
C
0672      CALL LOCATE (JT,E,PI,PY)
0673      ANL(1)= AN(1,J)
0674      ANL(2)= AN(2,J)
0675      ANL(3)=AN(3,J)
0676      CALL FIND (IT(J),NT,ANL,PY,PI,PX,JTP)
0677      IF (JTP.EQ.100) WRITE ( 6,1402) J
0678      IF (JTP.EQ.100) GO TO 1401
0679      EL=0.
0680      DO 720 L=1,3
0681 720    EL=EL+(ANL(L,J)-PX(L))**2
0682      EL=SQRT(EL)
0683      W(J)=0.
0684      DO 760 L=1,3
0685      W(J)=W(J)+(PX(L)-ANL(L,K))**2
0686 760    CONTINUE
0687      W(J)=SQRT(W(J))
0688      CALL RA (IT(J),NT,AN(1,J),PX,PI,R12)
0689      IF (R12.LT.18.) R12=18.
0690      R(J)=R12
0691      PR(J) =      RHO*HE(J)*(VB(J)**2/R(J)+G*UN(2,IT(J)))
0692      IT(J)=JTP
0693      JPP=(JTP-1)/2+1
0694      IF (J.EQ.1) GO TO 765
0695      LT=IT(J)
0696      N=J-1
0697      JT=IT(N)
0698      VQ(1)=VN(1,N)
0699      VQ(2)=VN(2,N)
0700      VQ(3)=VN(3,N)
0701      CALL VEL (EL,AMDOT(N),JT,LT,HE(N),W(N),F(N),F(J),S(N),S(J),PR(J),

```

```

      1  VQ,VP,
      *  MU)
0702  765  CONTINUE
      C PARAMETERS FOR NEW WAVE FRONT *****
0703      DO 770 L=1,3
0704      VN(L,N)=VP(L)
0705      AN(L,J)=PX(L)
0706      AN(L,IQ+1)=PXX(L)
0707  770  CONTINUE
0708      VB(J) = SQRT(VN(1,J)**2+VN(2,J)**2+VN(3,J)**2)
0709      HE(J)=AMDOT(J)/(W(J)*RHO*VB(J) )
0710  795  CONTINUE
0711      WW=0.
0712      DO 798 L=1,3
0713      VN(L,IQ)= VI(L,IQ)
0714      VN(L,IQ+1)= VI(L,IQ)
0715      WW=WW+(AN(L,IQ)-AN(L,IQ+1))**2
0716  798  CONTINUE
0717      W(IQ)= SQRT(WW)
0718      VB(IQ)= SQRT(VN(1,IQ)**2+VN(2,IQ)**2+VN(3,IQ)**2 )
0719      HE(IQ)=AMDOT(IQ)/(W(IQ)*RHO*VB(IQ) )
0720      IT(IQ+1)=J*ITP
0721  799  CONTINUE
      C
0722      IF ( TLOBIG) IQ=IQ-1
0723      TLOBIG = .FALSE.
      C
0724      DO 815 I=1,IQ
0725      JT=IT(I)
0726      K=I+1
0727      LT=IT(K)
0728      UNN=(UN(2,LT)+UN(2,JT))/2.
0729      PR(I) = RHO*HE(I)*(VB(I)**2/R(I)+G+UNN)
0730  815  CONTINUE
0731      IQ1= IQ+1
0732      HE(IQ1)=-HE(IQ)
0733      PR(IQ1)=-PR(IQ)
      C
      C FORCE VFLOCITY VECTOR TO BE NORMAL TO WAVE FRONT
      C
0734      DO 822 K=2,IQ1
0735      DO 820 L=1,3
0736      P3(L)= (AN(L,K)-AN(L,K-1))
0737      P4(L)= UN(L,IT(K))+UN(L,IT(K-1))
0738  820  CONTINUE
0739      P5(1)= P4(2)*P3(3)-P4(3)*P3(2)
0740      P5(2)=P4(3)*P3(1)-P4(1)*P3(3)
0741      P5(3)=P4(1)*P3(2)-P4(2)*P3(1)

```

```

0742      WW=0.
0743      DO 821 L=1,3
0744      WW=WW+P5(L)**2
0745      821  CONTINUE
0746      WW= SQRT(WW)
0747      VN(1,K-1)= P5(1)*VB(K-1)/WW
0748      VN(2,K-1)= P5(2)*VB(K-1)/WW
0749      VN(3,K-1)= P5(3)*VB(K-1)/WW
0750      822  CONTINUE
      C

0751      C(1)= 1.E10
0752      DO 830 L=2,IQ1
0753      K=L-1
0754      JT=IT(L)
0755      CALLDETR(VN(1,K),VN(1,L),UN(1,JT),C(L))
0756      830  CONTINUE
      C  STREAM BOUNDARY DIVIDING PLANES *****
0757      PX(1)=AN(1,1)
0758      PX(2)=AN(2,1)
0759      PX(3)=AN(3,1)
0760      VP(1)=VN(1,1)
0761      VP(2)=VN(2,1)
0762      VP(3)=VN(3,1)
0763      JT=IT(1)
0764      CALL PLANE(JT,PX,VP,E)
0765      PP(1,1)=E(1)
0766      PP(2,1)=E(2)
0767      PP(3,1)=E(3)
0768      PP(4,1)=E(4)
0769      PX(1)=AN(1,IQ1)
0770      PX(2)=AN(2,IQ1)
0771      PX(3)=AN(3,IQ1)
0772      VP(1)=VN(1,IQ)
0773      VP(2)=VN(2,IQ)
0774      VP(3)=VN(3,IQ)
0775      JT= IT(IQ+1)
0776      CALL PLANE(JT,PX,VP,E)
0777      PP(1,IQ1)=E(1)
0778      PP(2,IQ1)=E(2)
0779      PP(3,IQ1)=E(3)
0780      PP(4,IQ1)=E(4)
0781      891  FORMAT( ' COORD. OF AN',13,3X,3(F6.2,1X),3X,'TRI',14
* ,3X,'STEP',13,3X,'RAD',1X,F5.1,3X,'VEL',F6.1
* ,3X,'HGT',F7.3,3X,'WIDTH',F5.2,3X,'C',1X,F13.3)
      DO 892 I=1,IQ1
0782      WRITE(6,891) I,AN(1,I),AN(2,I),AN(3,I),IT(I),ISTEP,R(I),VB(I)
0783      * ,HE(I),W(I),C(I)
0784      892  CONTINUE

```

```

0785      IQ=IQ+1
0786      IF ( IQ.GT. NS) GO TO 900
0787      ISTEP=ISTEP-1
0788      GO TO 370
C *****
0789      900 CONTINUE
0790      IQ=IQ-1
0791      IQ1=IQ+1
0792      1401 CONTINUE
C
C WAVE FRONT PROGRESSION AS BEFORE BUT NO NEW STREAMS ADDED
C FIXED STEP ELI TAKEN BY STREAM 1 ( OR LOWEST NUMBERED STREAM STILL ON
C CHUTE). IF A STREAM LEAVES CHUTE ALL HIGHER NUMBERED STREAMS ARE
C ASSUMED OFF CHUTE ALSO. X= LOWEST NUMBERED STREAM ON CHUTE, NS1= HIGHEST
C NUMBERED STREAM STILL ON CHUTE.
C
0793      6999 CONTINUE
0794      NS=IQ1
0795      ISTEP=1
0796      X = 1
0797      NSS = NS
0798      NSM = NS - 1
0799      1000 CONTINUE
0800      DO 1010 I=X,NSS
0801      1010 VB(I)=SQRT(VN(1,I)**2+VN(2,I)**2+VN(3,I)**2)
0802      CONTINUE
0803      NS1 = NSS - 1
0804      FORC(X,ISTEP) = 0.
0805      SHEA(X,ISTEP) = 0.
0806      FORC(NSS,ISTEP) = 0.
0807      SHEA(NSS,ISTEP) = 0.
0808      F(X) = 0.
0809      S(X) = 0.
0810      F(NSS) = 0.
0811      S(NSS) = 0.
0812      JT = IT(X)
0813      DO 6001 L=1,3
0814      PX(L) = AN(L,X)
0815      6001 VP(L) = VN(L,X)
0816      CALL PLANE(JT,PX,VP,E)
0817      DO 6002 L=1,4
0818      6002 PP(L,X) = E(L)
0819      DO 6003 L=1,3
0820      PX(L) = AN(L,NSS)
0821      6003 VP(L)=VN(L,NS1)
0822      JT = IT(NSS)
0823      CALL PLANE(JT,PX,VP,E)
0824      DO 6004 L=1,4

```

```

0825 . 6004 PP(L,NSS) = E(L)
0826 PR(X) = RHO*HE(X)*(G*UN(2,IT(X))+VB(X)**2/R(X))
0827 X1=X+1
0828 DO 1200 L=X1,NS1
0829 JT=IT(L)
0830 PR(L)=RHO*HE(L)*(G*UN(2,JT)+VB(L)**2/R(L))
0831 K=L-1
0832 CALL DETR(VN(1,K),VN(1,L),UN(1,JT),C(L))

```

C

C C(L) LESS THAN ZERO MEANS STREAMS DIVERGING

C

```

0833 IF(C(L).LT.0.) GO TO 1020
0834 F(L)=KC*(PR(L)+PR(K))*(HE(L)+HE(K))/4.
0835 S(L)=F(L)*SIN(DELTA)
0836 IF(VB(L).LT.VB(K)) S(L)=-S(L)
0837 P5(1)=VN(1,L)/VB(L)+HE(K)/(HE(K)+HE(L))*
* (VN(1,K)/VB(K)-VN(1,L)/VB(L))
0838 P5(2)=VN(2,L)/VB(L)+HE(K)/(HE(K)+HE(L))*
* (VN(2,K)/VB(K)-VN(2,L)/VB(L))
0839 P5(3)=VN(3,L)/VB(L)+HE(K)/(HE(K)+HE(L))*
* (VN(3,K)/VB(K)-VN(3,L)/VB(L))
0840 CALL PLANE(JT,AN(1,L),P5,PP(1,L))
0841 GO TO 1030
0842 1020 CONTINUE
0843 F(L)=KE*(PR(L)+PR(K))*(HE(L)+HE(K))/4.
0844 S(L)=F(L)*SIN(DELTA)
0845 IF(VB(L).LT.VB(K)) S(L)=-S(L)
0846 P5(1)=VN(1,L)/VB(L)+HE(L)/(HE(K)+HE(L))*
* (VN(1,K)/VB(K)-VN(1,L)/VB(L))
0847 P5(2)=VN(2,L)/VB(L)+HE(L)/(HE(K)+HE(L))*
* (VN(2,K)/VB(K)-VN(2,L)/VB(L))
0848 P5(3)=VN(3,L)/VB(L)+HE(L)/(HE(K)+HE(L))*
* (VN(3,K)/VB(K)-VN(3,L)/VB(L))
0849 CALL PLANE(JT,AN(1,L),P5,PP(1,L))
0850 1030 CONTINUE
0851 FORC(L,ISTEP)=F(L)
0852 SHEA(L,ISTEP)=S(L)
0853 1200 CONTINUE
0854 PR(NSS)=-PR(NS1)
0855 NSKIP=0
0856 EL1 = 1.2
0857 NSS1 = NS1-1
0858 DO 1202 I = X,NSS1
0859 IF (ABS(VB(I) - VB(I+1)).LT.12.) GO TO 1202
0860 EL1 = EL1/2.
0861 GO TO 1203
0862 1202 CONTINUE
0863 1203 CONTINUE

```

```

0864 DO 2000 I = X,NSS
0865     JTP=100
0866     JT=IT(1)
0867     LT=JT
0868     IF (I.NE.X) GO TO 1230
0869     EL=FL1
0870     1201 CONTINUE
C
C LOCATE NEW SMALLEST NUMBERED NETPOINT
C
0871     P5(1)= AN(1,I)-VN(1,X)
0872     P5(2)= AN(2,I)-VN(2,X)
0873     P5(3)= AN(3,I)-VN(3,X)
0874     CALL LOCAT3(LT,EL,PP(1,I),AN(1,I),P5,PX )
0875     CALL FIND(JT,NT,AN(1,I),PX,PP(1,I),AX,JTP)
0876     IF (JTP.EQ.100) GO TO 1228
0877     CALL RA (JT,NT,AN(1,I),PX,PP(1,I),R12)
0878     IF (R12.LE.18.) R12=18.
0879     DO 1122 L=1,3
0880     1122     PX(L)=AX(L)
0881     1205 CONTINUE
0882     LLP=(JTP-1)/2+1
0883     IPL(I,ISTEP)=LLP
0884     GO TO 1240
0885     1228 CONTINUE
0886     WRITE (6,1121) I,ISTEP
0887     1121     FORMAT(1X,'STREAM',1X,13,3X,'OFF CHUTE DURING STEP',13)
0888     X=X+1
0889     IF (X.EQ.NSS-1) GO TO 2500
0890     GO TO 1000
0891     1229 CONTINUE
0892     WRITE (6,1121) I,ISTEP
0893     NSS=I-1
0894     IF (X.GE.NSS-1) GO TO 2500
0895     GO TO 1998
0896     1230 CONTINUE
C
C LOCATE REMAINDER OF NET POINTS STILL ON CHUTE
C
0897     K=I-1
0898     E(4)=0.
0899     DO 1235 L=1,3
0900     E(L)=VN(L,K)
0901     1235     E(4)=E(4)+VN(L,K)*AN(L,K)
0902     E(4)=-E(4)
0903     CALL LOCATE(LT,E,PP(1,I),PX)
0904     CALL FIND(JT,NT,AN(1,I),PX,PP(1,I),AX,JTP)
0905     IF (JTP.EQ.100) GO TO 1229

```

```

0906 CALL RA (JT,NT,AN(1,1),PX,PP(1,1),R12)
0907 IF (R12.LT.18.) R12=18.
0908 DO 1247 L=1,3
0909 1247 PX(L)=AX(L)
0910 CONTINUE
0911 1249 LLP=(JTP-1)/2+1
0912 IPL(I,ISTEP)=LLP
0913 LL=J.
0914 DO 1245 L=1,3
0915 FL=EL+(AN(L,1)-PX(L))**2
0916 1245 CONTINUE
0917 EL=SQRT(EL)
0918 W(K)=0.
0919 DO 1250 L=1,3
0920 W(K)=W(K)+(PX(L)-AN(L,K))**2
0921 1250 CONTINUE
0922 W(K)=SQRT(W(K))
0923 WIDTH(K,ISTEP)=W(K)
0924 HE(K)=AMDOT(K)/(W(K)*RHO*VB(K))
0925 HGT(K,ISTEP)=HE(K)
0926 1240 CONTINUE
0927 1241 CONTINUE
0928 CORD(1,I,ISTEP)=PX(1)
0929 CORD(2,I,ISTEP)=PX(2)
0930 CORD(3,I,ISTEP)=PX(3)
0931 IF (I.EQ.X) GO TO 9245
0932 XISTEP = ISTEP
0933 IF (ABS(XISTEP/7.-AINT(XISTEP/7.)).GT.Q.11) GO TO 9245
0934 CALL GRIDCD(ID,PXSAV)
0935 IPTS(1)=ID
0936 CALL GRIDCD(ID,PX)
0937 IPTS(2)=ID
0938 CALL CBARCD(INE,IPTS)
0939 9245 CONTINUE
0940 DO 9246 J=1,3
0941 9246 PXSAV(J)=PX(J)
0942 JP=(JT-1)/2+1
0943 JPP=(JTP-1)/2+1
0944 NCH=1
0945 IF (JPP.EQ.JP) NCH=0
0946 IF (JPP.EQ.JP) JPP=JP+1
0947 IF (JPP.LE.NP) GO TO 5001
0948 GO TO 5005
0949 1310 CONTINUE
0950 5001 CONTINUE
0951 P4(1)=PTDAT(1,4,JPP)
0952 P4(2)=PTDAT(2,4,JPP)
0953 P4(3)=PTDAT(3,4,JPP)

```

```

0954      AX(1)=PTDAT(1,3,JPP)
0955      AX(2)=PTDAT(2,3,JPP)
0956      AX(3)=PTDAT(3,3,JPP)
0957      VP(1)=PTDAT(1,2,JPP)
0958      VP(2)=PTDAT(2,2,JPP)
0959      VP(3)=PTDAT(3,2,JPP)
0960      VQ(1)=PTDAT(1,1,JPP)
0961      VQ(2)=PTDAT(2,1,JPP)
0962      VQ(3)=PTDAT(3,1,JPP)
0963      IF (I.EQ.X) FL = EL1
0964      5005 CONTINUE
0965      R(I) = R12
0966      RAD(I,ISTEP)=R(I)
0967      IF(I.EQ.NSS) GO TO 1275
0968      LT=IT(I)
0969      M=I+1
0970      KT=IT(M)
0971      UNN=(UN(2,LT)+UN(2,KT))/2.
0972      PR(I)=RHO*HE(I)*(G*UNN+VB(I))*2/R12)
0973      IF (I.EQ.X) EL = EL1
0974      VQ(1)=VN(1,I)
0975      VQ(2)=VN(2,I)
0976      VQ(3)=VN(3,I)
0977      CALL VFL(EL,AMDOT(I),JT,LT,HE(I),W(I),F(I),F(M),S(I),S(M),PR(I),
*      VQ,VP,
*      MU)
0978      IF (ISTEP.EQ.14.OR.ISTEP.EQ.15.OR.ISTEP.EQ.16)
*      WRITE(6,1274) HE(I),W(I),F(I),F(M),S(I),S(M),PR(I),VQ(1),
*      VQ(2),VQ(3),VP(1),VP(2),VP(3),MU
1274      FORMAT(14(F8.2,1X))
1275      CONTINUE
0981      VB(I)=SQRT(VP(1)**2+VP(2)**2+VP(3)**2)
0982      VELOC(I,ISTEP)=VB(I)
0983      DO 1280 L=1,3
0984      VN(L,I)=VP(L)
0985      AN(L,I)=PX(L)
0986      1280 CONTINUE
0987      IT(I)=JTP
0988      CONTINUE
0989      3333  FORMAT(' THE POINT',14,' DIST=',F7.2,' AFTER STEP',14)
0990      1999 CONTINUE
0991      2000 CONTINUE
0992      1998 CONTINUE
0993      DO 2004 I=1,NS
0994      IF(I.GE.X.AND. I.LE.NSS) GO TO 2004
0995      RAD(I,ISTEP)=0.
0996      FORC(I,ISTEP)=0.
0997      SHEA(I,ISTEP)=0.

```

```

0998      IPL(I,ISTEP)=0
0999      WIDTH(I,ISTEP)=0.
1000      HGT(I,ISTEP)=0.
1001      VFLOC(I,ISTEP)=0.
1002      CORD(1,I,ISTEP)=CORD(1,I,ISTEP-1)
1003      CORD(2,I,ISTEP)=CORD(2,I,ISTEP-1)
1004      CORD(3,I,ISTEP)=CORD(3,I,ISTEP-1)
1005 2004 CONTINUE
C FORCE VELOCITY VECTOR TO BE NORMAL TO WAVE FRONT
1006      X1=X+1
1007      DO 802 K=X1,NSS
1008      DO 800 L=1,3
1009      P3(L)=(AN(L,K)-AN(L,K-1))
1010      P4(L)=UN(L,IT(K))+UN(L,IT(K-1))
1011 800 CONTINUE
1012      P5(1)=P4(2)*P3(3)-P4(3)*P3(2)
1013      P5(2)=P4(3)*P3(1)-P4(1)*P3(3)
1014      P5(3)=P4(1)*P3(2)-P4(2)*P3(1)
1015      WW=0.
1016      DO 801 L=1,3
1017      WW=WW+P5(L)**2
1018 801 CONTINUE
1019      WW=SQRT(WW)
1020      VN(1,K-1)=P5(1)*VB(K-1)/WW
1021      VN(2,K-1)=P5(2)*VB(K-1)/WW
1022      VN(3,K-1)=P5(3)*VB(K-1)/WW
1023 802 CONTINUE
1024      DO 2005 I = X,NSS
1025      WRITE(6,891) I,AN(1,I),AN(2,I),AN(3,I),IT(I),ISTEP,R(I),VB(I)
* ,HE(I),W(I),C(I)
1026 2005 CONTINUE
1027      WRITE(6,901)
1028      ISTEP=ISTEP+1
1029      IF (ISTEP.GT.50) GO TO 3446
1030      GO TO 1000
1031 2500 CONTINUE
1032      WRITE(6,916)
1033      WRITE(6,901)
1034      WRITE(6,2501)
1035 2501 FORMAT(1X,' PARAMETERS WHEN EACH STREAM LEAVES CHUTE')
1036      WRITE(6,901)
1037      WRITE(6,916)
1038      DO 2345 I=1,NSM
1039      WRITE(6,2346) I,VN(1,I),VN(2,I),VN(3,I)
1040 2346 FORMAT('0',' THE VELOC. COMP. OF STREAM',I4,' ARE',3F10.2)
1041 2345 CONTINUE
1042      DO 2347 I=1,NS
1043      ZPLAN=ATAN(VN(2,I)/VN(1,I))

```

```

1044      ZPLAN = 57.2 * ZPLAN
1045      YPLAN=ATAN(VN(1,1)/VN(3,1))
1046      YPLAN = 57.2 * YPLAN
1047      XPLAN=ATAN(VN(2,1)/VN(3,1))
1048      XPLAN = 57.2 * XPLAN
1049      WRITE(6,5678) I,ZPLAN,YPLAN,XPLAN
5678      FORMAT('0', ' THE DIRECT. ANGLES FOR STR.',14, ' ARE',3E10,21)
1051      2347  CONTINUE
1052      WRITE(6,3000) ISTEP
1053      3446  IF (JTP.NE.100.OR.ISTEP.NE.51) WRITE(6,7890)
1054      7890  FORMAT(' SHORT RUN')
1055      NSTEP=ISTEP-1
1056      DO 4000 I=1,NSM
1057      WRITE(6,905)
1058      WRITE(6,916)
1059      WRITE(6,901)
1060      WRITE(6,3004)
1061      WRITE(6,3005)
1062      DO 3500 J=1,NSTEP
1063      IF (HGT(I,J).EQ.0.) RAT = 0.
1064      IF (HGT(I,J).EQ.0.) GO TO 3498
1065      RAT=RAD(I,J)/HGT(I,J)
1066      3498  CONTINUE
1067      WRITE(6,3010) I,J,VELOC(I,J),WIDTH(I,J),HGT(I,J),RAD(I,J),RAT,
*      FORC(I,J),SHEA(I,J),(CORD(L,I,J),L=1,3),IBL(I,J)
1068      3530  CONTINUE
1069      3010  FORMAT(3X,14,3X,14,5X,10(F6.1,3X),2X,12)
1070      3004  FORMAT(' STREAM STEP VELOCITY WIDTH HEIGHT RADIUS
1 RAD/HGT NORMAL SHEAR LOCATION')
1071      3005  FORMAT('
1 FORCE FORCE RIGHT EDGE')
1072      4000  CONTINUE
1073      1402  FORMAT(' NET POINT',13, 'OFF CHUTE')
1074      3000  FORMAT(' THE STREAMS HAVE LEFT THE CHUTE AFTER STEP',15)
1075      1400  CONTINUE
1076      9999  CONTINUE
1077      1500  STOP
1078      END

```

E-27

```

0001      SUBROUTINE RA ( JJT,NT,01,PZ,PP,KK)
0002      DIMENSION R(2), U(2,3), PPNN(3,3),UNIT(3) ,T(4)
0003      DIMENSION O1(3),PZ(3)
0004      DIMENSION O(3),P(3),PP(4),PX(3),MTR(2),OP(3),OY(3),PP1(3),PP2(3),
*      PP3(3),P1(3),P2(3),P3(3),PPN(3),PQ(3)

0005      DIMENSION PP4(3)
0006      C(IMMOV THET(3,200),ABC(3,200),PT(3,3,200),UN(3,200)
0007      REAL NP,NQ
0008      K1=1
0009      K2=0
0010      K3=0
0011      K4=0
0012      K5=0
0013      R(1)=100.
0014      R(2)=100.
0015      1000  CONTINUE
0016      K5=K2
0017      LET1=J
0018      LET2=0
0019      JT=JJT
0020      DO 1 L=1,3
0021      O(L)=O1(L)
0022      P(L)=PZ(L)
0023      1  CONTINUE
0024      5  CONTINUE

C FIND UNIT VECTOR OP
0025      DO 10 L=1,3
0026      O(L) = O(L)
0027      OP(L)=P(L)-O(L)
0028      10  CONTINUE
0029      OPB=SQRT(OP(1)**2+OP(2)**2+OP(3)**2)
0030      DO 20 L=1,3
0031      OP(L)=OP(L)/OPB
0032      OY(1) = UN(2,JT)* OP(3) -UN(3,JT)*OP(2)
0033      OY(2) = UN(3,JT)* OP(1) -UN(1,JT)*OP(3)
0034      OY(3) = UN(1,JT)* OP(2) -UN(2,JT)*OP(1)
0035      DO 30 L=1,3
0036      PP1(L) = PT(L,1,JT)
0037      PP2(L) = PT(L,2,JT)
0038      PP3(L) = PT(L,3,JT)
0039      30  CONTINUE
C FIND COORDS OF P1,P2,P3 WRT NEW ORIGIN AT O
0040      DO 35 L=1,2
0041      P1(L)=0.
0042      P2(L)=0.
0043      35  P3(L)=0.
0044      DO 40 L=1,3
0045      P1(L) = P1(L) +(PP1(L)-O(L))* OP(L)

```

```

0046      P2(1) = P2(1) + (PP2(L)-O(L))* OP(L)
0047      P3(1) = P3(1) + (PP3(L)-O(L))* OP(L)
0048      P1(2) = P1(2) + (PP1(L)-O(L))* OY(L)
0049      P2(2) = P2(2) + (PP2(L)-O(L))* OY(L)
0050      P3(2) = P3(2) + (PP3(L)-O(L))* OY(L)
0051      40      KK=1
0052      IF (K5.EQ.1) GO TO 48
0053      IF (LET1.EQ.1.AND.LET2.EQ.2) GO TO 48
0054      IF (LET2.EQ.1.AND.LET1.EQ.2) GO TO 48
0055      ON = ((P2(1)-P1(1)) / (P2(2)-P1(2))) * (-P1(2)) + P1(1)
0056      45      IF (ON.LE.P1(1).AND.ON.GE.P2(1).OR.ON.LE.P2(1).AND.ON.GE.P1(1)) GO
* TO 100
0057      48      CONTINUE
0058      IF (LET1.EQ.2.AND.LET2.EQ.3) GO TO 58
0059      IF (LET2.EQ.2.AND.LET1.EQ.3) GO TO 58
0060      KK=2
0061      IF (K5.EQ.2) GO TO 58
0062      ON = ((P3(1)-P2(1)) / (P3(2)-P2(2))) * (-P2(2)) + P2(1)
0063      55      IF (ON.LE.P2(1).AND.ON.GE.P3(1).OR.ON.LE.P3(1).AND.ON.GE.P2(1)) GO
* TO 110
0064      58      CONTINUE
0065      KK=3
0066      IF (K5.EQ.3) GO TO 97
0067      ON = ((P1(1)-P3(1)) / (P1(2)-P3(2))) * (-P3(2)) + P3(1)
0068      65      IF (ON.LE.P3(1).AND.ON.GE.P1(1).OR.ON.LE.P1(1).AND.ON.GE.P3(1)) GO
* TO 120
0069      97      WRITE(6,98)
0070      98      FORMAT (1X, ' ERROR IN RADIUS ROUTINE')
0071      RR = 54.
0072      RETURN
0073      100     CONTINUE
0074      DO 70 L=1,3
0075      PP1(L)=PT(L,1,JT)
0076      PP2(L)=PT(L,2,JT)
0077      GO TO 200
0078      110     DO 80 L=1,3
0079      PP1(L) = PT(L,2,JT)
0080      PP2(L)=PT(L,3,JT)
0081      GO TO 200
0082      120     DO 90 L=1,3
0083      PP1(L)= PT(L,3,JT)
0084      PP2(L)= PT(L,1,JT)
0085      90      CONTINUE
0086      200     CONTINUE
0087      K5=0
0088      IF (K2.EQ.0) K2=KK
0089      IF (K4.EQ.1) K2=10

```

C FIND TRIANGLE HAVING SIDE DEFINED BY PP1,PP2

```

0090      DO 300 M=1,NT
0091      IF(M.EQ.JT) GO TO 300
0092      LET1=0
0093      LET2=0
0094      NV=0
0095      DO 310 J=1,3
0096      DO 320 K=1,3
0097      IF (PP1(K).NE.PT(K,J,M)) GO TO 324
0098      320 CONTINUE
0099      LET1=J
0100      NV=NV+1
0101      324 CONTINUE
0102      DO 325 K=1,3
0103      IF (PP2(K).NE.PT(K,J,M)) GO TO 308
0104      325 CONTINUE
0105      LET2=J
0106      NV=NV+1
0107      308 IF (NV.EQ.2) GO TO 350
0108      310 CONTINUE
0109      300 CONTINUE
0110      350 CONTINUE
0111      JTP=M
0112      IF (NV.NE.2) GO TO 204
0113      JT=JTP
0114      204 CONTINUE
0115      DO 205 L=1,3
0116      205 PP4(L) = PP1(L) + 100.*UN(L,JT)
0117      T(1) = PP1(2)*(PP2(3)-PP4(3))
0118      * -PP1(3)*(PP2(2)-PP4(2))
0119      * + (PP2(2)*PP4(3)-PP4(2)*PP2(3))
0120      T(2) = - (PP1(1)*(PP2(3)-PP4(3))
0121      * -PP1(3)*(PP2(1)-PP4(1))
0122      * + (PP2(1)*PP4(3)-PP2(3)*PP4(1)))
0123      T(3) = PP1(1)*(PP2(2)-PP4(2))
0124      * - PP1(2)*(PP2(1)-PP4(1))
0125      * + (PP2(1)*PP4(2)-PP4(1)*PP2(2))
0126      T(4) = - (PP1(1)*(PP2(2)*PP4(3)-PP4(2)*PP2(3))
0127      * -PP1(2)*(PP2(1)*PP4(3)+PP4(1)*PP2(3))
0128      * + PP1(3)*(PP2(1)*PP4(2)-PP4(1)*PP2(2)))
0129      CALL LOCATE(JT,T,PP,PPN)
0130      IF (NV.NE.2) GO TO 390
0131      N=0
0132      V=0
0133      DO 360 L=1,3
0134      IF (UN(L,JTP).LE.UN(L,JJT)+1.E-5.AND.UN(L,JTP).GT.UN(L,JJT)-1.E-5)
0135      * N=N+1
0136      U(K1,L)=(UN(L,JTP)+UN(L,JJT))
0137      PPNN(K1,L)=PPN(L)

```

```

0129      V=V+U(K1,L)**2
0130      360 CONTINUE
0131      DO 361 L=1,3
0132      U(K1,L) = U(K1,L)/SQRT(V)
0133      361 CONTINUE
0134      IF(N.EQ.3) GO TO 368
0135      K1=K1+1
0136      K3=K3+1
0137      IF(K1.EQ.4) GO TO 400
0138      IF(K3.EQ.2) GO TO 362
0139      GO TO 368
0140      362 CONTINUE
0141      IF (K1.EQ.4) GO TO 400
0142      K3=0
0143      K4=1
0144      GO TO 1000
0145      390 DO 395 L=1,3
0146      PPNN(K1,L) = PPN (L)
0147      395 CONTINUE
0148      R(K1) = 1.E10
0149      K1=K1+1
0150      IF(R(1).EQ.1.E10 .AND.R(2).EQ.1.E10) WRITE (6,367)
0151      367 FORMAT(1X,' COMPUTATION FOR RADIUS INVALID')
0152      IF(R(1).EQ.1.E10 .AND.R(2).EQ.1.E10) RR=54
0153      IF(R(1).EQ.1.E10 .AND.R(2).EQ.1.E10) RETURN
0154      GO TO 362
0155      368 NP=100.
0156      369 CONTINUE
0157      CALL LOCAT3 (JTP,NP,PP,PPN,OI,PX)
0158      370 CONTINUE
0159      DO 380 L=1,3
0160      P(L)=PX(L)
0161      380 U(L)=PPN(L)
0162      GO TO 5
0163      400 CONTINUE
0164      DO 450 L=1,3
0165      OP(L)=PZ(L)-OI(L)
0166      450 CONTINUE
0167      OPB=SQRT(OP(1)**2+OP(2)**2+OP(3)**2)
0168      DO 460 L=1,3
0169      UP(L)=OP(L)/OPB
0170      460 CONTINUE
0171      X1= (PPNN( 1,1)-OI(1))*OP(1)+(PPNN( 1,2)-OI(2))*OP(2)
*      +(PPNN( 1,3)-OI(3))*OP(3)
0172      X2= (PPNN( 2,1)-OI(1))*OP(1)+(PPNN( 2,2)-OI(2))*OP(2)
*      +(PPNN( 2,3)-OI(3))*OP(3)
0173      X3= (PPNN( 3,1)-OI(1))*OP(1)+(PPNN( 3,2)-OI(2))*OP(2)
*      +(PPNN( 3,3)-OI(3))*OP(3)

```

```
0174      Y1= (PPNN( 1,1)-O1(1))*UN(1,JJT)+(PPNN(1,2)-O1(2)) *UN(2,JJT)
*      +(PPNN( 1,3)-O1(3))*UN(3,JJT)
0175      Y2= (PPNN( 2,1)-O1(1))*UN(1,JJT)+(PPNN(2,2)-O1(2)) *UN(2,JJT)
*      +(PPNN( 2,3)-O1(3))*UN(3,JJT)
0176      Y3= (PPNN( 3,1)-O1(1))*UN(1,JJT)+(PPNN(3,2)-O1(2)) *UN(2,JJT)
*      +(PPNN( 3,3)-O1(3))*UN(3,JJT)
0177      Z1=- (X1**2+Y1**2)
0178      Z2=- (X2**2+Y2**2)
0179      Z3=- (X3**2+Y3**2)
0180      DENOM=X1*Y2+X2*Y3+X3*Y1-X3*Y2-X2*Y1-X1*Y3
0181      ANUM=Z1*Y2+Z2*Y3+Z3*Y1-Z3*Y2-Z2*Y3-Z1*Y3
0182      BNUM=X1*Z1+X2*Z3+X3*Z1-X3*Z2-X2*Z1-X1*Z3
0183      CNUM=X1*Y2*Z3+X2*Y3*Z1+X3*Y1*Z2-X3*Y2*Z1-X2*Y1*Z3-X1*Y3*Z2
0184      A=ANUM/DENOM
0185      B=BNUM/DENOM
0186      C=CNUM/DENOM
0187      RR=      -C+(-A/2.)**2+(-B/2.)**2
0188      IF (RR.LT.0) WRITE(6,98)
0189      IF (RR.LT.0) RR = 324.
0190      RR = SQRT(RR)
0191      IF (RR.GT.54.) RR=54.
0192      RETURN
0193      END
```

```
0001      SUBROUTINE GRIDCD ( ID,XYZ)
      C
0002      910 FORMAT ( 'GRID',4X,18,8X,3F8.3)
0003      911 FORMAT ( 'CBAR',4X,18,8X,218)
0004      915 FORMAT ( 'CQMEM',2X,18,8X,418)
      C
      C
0005      DIMENSION XYZ(1)
0006      ID = ID + 1
0007      WRITE ( 10,910) ID,XYZ(3) , XYZ(1) , XYZ(2)
0008      RETURN
      C
      C
0009      ENTRY CQDCD ( NE, PTS)
      C
0010      INTEGER PTS(4)
      C
0011      NE = NE + 1
0012      WRITE ( 10,915) NE , PTS
0013      RETURN
      C
      C
0014      ENTRY CHARCD ( NE, PTS)
      C
0015      NE = NE + 1
0016      WRITE ( 10,911) NE,PTS(1) , PTS(2)
0017      RETURN
0018      END
```

```
0001      SUBROUTINE DETR(A,B,C,DT)
      C
0002      DIMENSION A(1) , B(1) , C(1)
      C
0003      D=A(1)*B(2)*C(3)
0004      D = D + A(2)*B(3)*C(1)
0005      D=D+ A(3)*B(1)*C(2)
      C
0006      D = D -A(3)*B(2)*C(1)
0007      D=D-A(2)*B(1)*C(3)
0008      DT= D-A(1)*B(3)*C(2)
      C
0009      RETURN
0010      END
```

THIS PAGE INTENTIONALLY BLANK

```

0001 SUBROUTINE FIND( JJT,NT,01,PZ,PP,PX,JIP)
0002 DIMENSION O1(3),PZ(3)
0003 DIMENSION O(3),P1(3),PP(4),PX(3),MTR(2),OP(3),OY(3),PP1(3),PP2(3),
* PP3(3),P1(3),P2(3),P3(3),PPN(3),PQ(3)
0004 DIMENSION R(4)
0005 DIMENSION PP4(3)
0006 COMMON THET(3,200),ABC(3,200),PT(3,3,200),UN(3,200)
0007 REAL NP,NQ
0008 JT=JJT
0009 LET1=0
0010 LET2=0
0011 DO 1 L=1,3
0012 O(L)=O1(L)
0013 P(L)=PZ(L)
0014 1 CONTINUE
0015 5 CONTINUE
C FIND UNIT VECTOR OP
0016 DO 10 L=1,3
0017 O(L) = O(L)
0018 OP(L)=P(L)-O(L)
0019 10 CONTINUE
0020 OPB=SQRT(OP(1)**2+OP(2)**2+OP(3)**2)
0021 DO 20 L=1,3
0022 20 OP(L)=OP(L)/OPB
0023 OY(1) = UN(2,JT)* OP(3) -UN(3,JT)*OP(2)
0024 OY(2) = UN(3,JT)* OP(1) -UN(1,JT)*OP(3)
0025 OY(3) = UN(1,JT)* OP(2) -UN(2,JT)*OP(1)
0026 DO 30 L=1,3
0027 PP1(L) = PT(L,1,JT)
0028 PP2(L) = PT(L,2,JT)
0029 PP3(L) = PT(L,3,JT)
0030 30 CONTINUE
C FIND COORDS OF P1,P2,P3 WRT NEW ORIGIN AT O
0031 DO 35 L=1,2
0032 P1(L)=0.
0033 P2(L)=0.
0034 35 P3(L)=0.
0035 DO 40 L=1,3
0036 P1(1) = P1(1) +(PP1(L)-O(L))* OP(L)
0037 P2(1) = P2(1) +(PP2(L)-O(L))* OP(L)
0038 P3(1) = P3(1) +(PP3(L)-O(L))* OP(L)
0039 P1(2) = P1(2) +(PP1(L)-O(L))* OY(L)
0040 P2(2) = P2(2) +(PP2(L)-O(L))* OY(L)
0041 40 P3(2) = P3(2) +(PP3(L)-O(L))* OY(L)
0042 K=1
0043 IF(LET1.EQ.1.AND.LET2.EQ.2) GO TO 48
0044 IF(LET2.EQ.1.AND.LET1.EQ.2) GO TO 48
0045 ON = ((P2(1)-P1(1)) / (P2(2)-P1(2))) * (-P1(2)) + P1(1)

```

```

0046      IF ( ON .GT.1.E-4 .AND.ON .LT.OPB ) GO TO 45
0047      GO TO 48
0048      45  IF (ON.LE.P1(1).AND.ON.GE.P2(1).OR.ON.LE.P2(1).AND.ON.GE.P1(1)) GO
          * TO 60
0049      48  CONTINUE
0050          K=2
0051          IF(LET1.EQ.2.AND.LET2.EQ.3) GO TO 58
0052          IF(LET2.FQ.2.AND.LET1.EQ.3) GO TO 58
0053          ON =(P3(1)-P2(1)) / (P3(2)-P2(2)) * (-P2(2)) + P2(1)
0054          IF ( ON .GT.1.E-4 .AND.ON .LT.OPB ) GO TO 55
0055          GO TO 58
0056      55  IF (ON.LE.P2(1).AND.ON.GE.P3(1).OR.ON.LE.P3(1).AND.ON.GE.P2(1)) GO
          * TO 60
0057      58  CONTINUE
0058          K=3
0059          ON =(P1(1)-P3(1)) / (P1(2)-P3(2)) * (-P3(2)) + P3(1)
0060          IF ( ON .GT.1.E-4 .AND.ON .LT.OPB ) GO TO 65
0061          GO TO 68
0062      65  IF (ON.LE.P3(1).AND.ON.GE.P1(1).OR.ON.LE.P1(1).AND.ON.GE.P3(1)) GO
          * TO 60
0063      68  CONTINUE
0064          JTP=JT
0065          PX(1)=P(1)
0066          PX(2)=P(2)
0067          PX(3)=P(3)
0068          RETURN
0069      60  CONTINUE
0070          GO TO (100,110,120),K
0071      100  DO 70 L=1,3
0072          PP1(L)=PT(L,1,JT)
0073      70  PP2(L)=PT(L,2,JT)
0074          GO TO 200
0075      110  DO 80 L=1,3
0076          PP1(L) = PT(L,2,J1)
0077      80  PP2(L)=PT(L,3,JT)
0078          GO TO 200
0079      120  DO 90 L=1,3
0080          PP1(L)= PT(L,3,JT)
0081          PP2(L)= PT(L,1,JT)
0082      90  CONTINUE
0083      200  CONTINUE
          C FIND TRIANGLE HAVING SIDE DEFINED BY PP1,PP2
0084          DO 300 M=1,NT
0085          IF(M.EQ.JT) GO TO 300
0086          LET1=3
0087          LET2=0
0088          NV=0
0089          DO 310 J=1,3

```

```

0090      DO 320 K=1,3
0091      IF (PP1(K).NE.PT(K,J,M)) GO TO 324
0092 320    CONTINUE
0093      LET1=J
0094      NV=NV+1
0095 324    CONTINUE
0096      DO 325 K=1,3
0097      IF (PP2(K),NE.PT(K,J,M)) GO TO 308
0098 325    CONTINUE
0099      LET2=J
0100      NV=NV+1
0101 308    IF (NV.EQ.2) GO TO 350
0102 310    CONTINUE
0103 300    CONTINUE
0104 350    CONTINUE
0105      JTP=M
0106      IF (NV.NE.2) JTP=100
0107      IF (JTP.EQ.100) RETURN
0108      JT=JTP
0109      DO 205 L=1,3
0110 205    PP4(L) = PP1(L) + 100.*UN(L,JT)
0111      R(1) = PP1(2)*{PP2(3)-PP4(3)}
*         -PP1(3)*{PP2(2)-PP4(2)}
*         +{PP2(2)*PP4(3)-PP4(2)*PP2(3)}
0112      R(2)=-{PP1(1)*{PP2(3)-PP4(3)}
*         -PP1(3)*{PP2(1)-PP4(1)}
*         +{PP2(1)*PP4(3)-PP2(3)*PP4(1)}}
0113      R(3)=PP1(1)*{PP2(2)-PP4(2)}
*         - PP1(2)*{PP2(1)-PP4(1)}
*         +{PP2(1)*PP4(2)-PP4(1)*PP2(2)}
0114      R(4)=-{PP1(1)*{PP2(2)*PP4(3)-PP4(2)*PP2(3)}
*         -PP1(2)*{PP2(1)*PP4(3)-PP4(1)*PP2(3)}
*         + PP1(3)*{PP2(1)*PP4(2)-PP4(1)*PP2(2)}}
0115      CALL LOCATE(JT,R,PP,PPN)
C: FIND COORDS OF P*
0116      NP=OPB-ON
0117      CALL LOCAT3 (JTP,NP,PP,PPN,O1,PX)
0118 370    CONTINUE
0119      DO 380 L=1,3
0120      P(L)=PX(L)
0121 380    U(L)=PPN(L)
0122      GO TO 5
0123      END

```

```

0001      SUBROUTINE LOCAT3(IT,EL,P1,A1,AX,A2)
0002      DIMENSION P1(4),A1(3),A2(3),AX(3),X(3,3),PX(3)
0003      DIMENSION E(4),D(2)
0004      COMMON THET(3,200),ABC(3,200),PT(3,3,200),UN(3,200)
0005      1 CONTINUE
0006      P1MAG = ABS(P1(4)/SQRT(P1(1)**2 + P1(2)**2 +P1(3)**2))
C UNIT VECTOR NORMAL TO P1
0007      U1=-P1MAG*P1(1)/P1(4)
0008      U2=-P1MAG*P1(2)/P1(4)
0009      U3=-P1MAG*P1(3)/P1(4)
C E IS VECTOR NORMAL TO BOTH IT AND P1 PLANES NORMAL VECTORS
0010      E1= UN(2,IT)*U3-UN(3,IT)*U2
0011      E2= UN(3,IT)*U1-UN(1,IT)*U3
0012      E3= UN(1,IT)*U2-UN(2,IT)*U1
0013      ER= SQRT(E1**2 +E2**2 +E3**2 )
0014      E1=+E1/ER
0015      E2=+E2/ER
0016      E3 =+E3/ER
0017      E(4)=-1.
0018      PE=A1(1)*E1+A1(2)*E2+A1(3)*E3
0019      Y= 1.
0020      IF ( PE.LT.0. ) Y=-1.
0021      IF (PE .LT.0. ) PE =-PE
0022      D(1) = PE-EL
0023      D(2)=PE+EL
0024      DO 10 L=1,2
0025      E(L) =(E1/D(L))*Y
0026      E(L) =(E2/D(L))*Y
0027      E(L) =(E3/D(L))*Y
0028      CALL LOCATE ( IT,P1,E,PX)
0029      X(1,L) = PX(1)
0030      X(2,L) = PX(2)
0031      X(3,L) = PX(3)
0032      10 CONTINUE
0033      DIST1=0.
0034      DIST2=0.
0035      DO 30 L=1,3
0036      DIST1= DIST1+(AX(L)-X(L,1))**2
0037      DIST2= DIST2+(AX(L)-X(L,2))**2
0038      30 CONTINUE
0039      K=2
0040      IF ( DIST1.GT.DIST2) K=1
0041      A2(1)=X(1,K)
0042      A2(2)=X(2,K)
0043      A2(3)=X(3,K)
0044      RETURN
0045      END

```

E-39

```

0001      SUBROUTINE LOCATE(JT,P,Q,PX)
0002      COMMON THE(3,200),ABC(3,200),PT(3,3,200),UN(3,200)
0003      DIMENSION P(4),Q(4),R(4),PX(3)
0004      I
0005      CONTINUE
0006      R(1)=ABC(1,JT)
0007      R(2)=ABC(2,JT)
0008      R(3)=ABC(3,JT)
0009      R(4)=1
0010      P(4)=-P(4)
0011      Q(4)=-Q(4)
0012      A=P(4)*(Q(2)*R(3)-R(2)*Q(3))
0013      *   -P(2)*(Q(4)*R(3)-R(4)*Q(3))
0014      *   +P(3)*(Q(4)*R(2)-R(4)*Q(2))
0015      B=P(1)*(Q(4)*R(3)-R(4)*Q(3))
0016      *   -P(4)*(Q(1)*R(3)-R(1)*Q(3))
0017      *   +P(3)*(Q(1)*R(4)-R(1)*Q(4))
0018      C=P(1)*(Q(2)*R(4)-R(2)*Q(4))
0019      *   -P(2)*(Q(1)*R(4)-R(1)*Q(4))
0020      *   +P(4)*(Q(1)*R(2)-R(1)*Q(2))
0021      DR=P(1)*(Q(2)*R(3)-R(2)*Q(3))
0022      *   -P(2)*(Q(1)*R(3)-R(1)*Q(3))
0023      *   +P(3)*(Q(1)*R(2)-R(1)*Q(2))
0024      PX(1) = A/DR
0025      PX(2) = B/DR
0026      PX(3) = C/DR
0027      P(4) = - P(4)
0028      Q(4) = -Q(4)
0029      RETURN
0030      END

```

```
0001      SUBROUTINE VEL(FL,AMDOT,JT,LT,HE,W,F1,F2,S1,S2,PR,VI,VP,MU)
0002      COMMON THET(3,200),ABC(3,200),PT(3,3,200),UN(3,200)
0003      DIMENSION UNN(3),VI(3),ALPH(3),BET(3),GAM(3),LAM(3)
0004      DIMENSION VP(3)
0005      REAL LAM
0006      REAL MU
0007      COMMON /DENS/GAMD
0008      I      CONTINUE
0009      RHO=GAMD/(32.2*12**3)
0010      DO 495 L=1,3
0011      UNN(L)=(UN(L,JT)+UN(L,LT))/2.
0012      G=386
0013      495    CONTINUE
0014      ALPH(1)=0.
0015      ALPH(2)=-W*HE*RHO*G
0016      C      ALPH(3)=0.
0017      C      VB=SQRT(VI(1)**2+VI(2)**2+VI(3)**2)
0018      DO 10 L=1,3
0019      BET(L)=W*PR*(UNN(L)-MU*VI(L)/VB)
0020      C      LAM(L)=(S2-S1)*VI(L)/VB
0021      10    CONTINUE
0022      C      GAM(1)=(F2-F1)*(VI(3)*UNN(2)-VI(2)*UNN(3))/VB
0023      GAM(2)=(F2-F1)*(VI(1)*UNN(3)-VI(3)*UNN(1))/VB
0024      GAM(3)=(F2-F1)*(VI(2)*UNN(1)-VI(1)*UNN(2))/VB
0025      DO 20 L=1,3
0026      VI(L)=VI(L)+EL*(ALPH(L)+BET(L)+GAM(L)+LAM(L))/AMDOT
0027      VP(L)=VI(L)
0028      20    CONTINUE
0029      RETURN
0030      END
```

```

0001 SUBROUTINE PLANE ( JT , A , V , P )
0002 COMMON THET(5,200),ABC(3,200),PT(3,3,200),UN(3,200)
      C THIS SUB CAL FUN OF A PLANE DRAWN THROUGH A AND PAR TO V AND
      C PAR. TO NORMAL AT A
      C
0003 DIMENSION A(3), V(3) , P(4)
      C
0004 DD=1.0E-10
0005 CONTINUE
0006 A1=UN(1,JT)
0007 B1=UN(2,JT)
0008 C1=UN(3,JT)
0009 V1=V(1)
0010 V2=V(2)
0011 V3=V(3)
0012 DR= V(1)*UN(2,JT)-V(2)*UN(1,JT)-
0013 IF(DR.EQ.0.) DR=DD
0014 P(1)=(V(2)*UN(3,JT)-UN(2,JT)*V(3))/DR
0015 P(2)=(V(3)*UN(1,JT)-V(1)*UN(3,JT))/DR
0016 P(3)=1.
      C
      C
0017 P(4) = - (P(1) * A(1) + P(2) * A(2) + P(3) * A(3))
      C
0018 RETURN
0019 END
    
```

APPENDIX F

TRADEOFF STUDY OF CANDIDATE TRANSFER CHUTE CONCEPTS

TABLE OF CONTENTS

<u>Section</u>	<u>Title</u>	<u>Page, F-</u>
1.0	Introduction	3
2.0	Conclusions	3
3.0	Candidate Configurations	4
3.1	Geometrical Surfaces Considered	4
3.2	Specific Configurations	5
3.2.1	Conical Shapes	5
3.2.2	Quarter Cylinder Shapes	14
3.3.3	Toroidal Shapes	14
4.0	Evaluation	19
4.1	Methodology	19
4.1.1	Evaluation Criteria	19
4.1.2	Weighting of Evaluation Criteria	33
4.1.3	Rating Provision	37
4.2	Trade Off Evaluation	37
4.2.1	Summary Analysis	37
4.2.2	Analysis Details	39

LIST OF TABLES

<u>Table No.</u>	<u>Title</u>	
1	Evaluation Criteria Weighting	33
2	Trade Off Evaluation Analysis	38

LIST OF FIGURES

<u>No.</u>	<u>Title</u>	<u>Page(s) F-</u>
1	Concept 1, Opening Half Angle Cone	
	A. 1/6 Scale Test Configuration (1) & (2)	6, 7
	B. Typical Computer Plot Approximation	8
2	Concept 2, Flat Impact Plate Cone	
	A. 1/6 Scale Test Configuration	9
	B. Typical Computer Plot Approximation	10
3	Concept 3, Zero Half Angle Cone	
	A. 1/6 Scale Test Configuration (1) & (2)	11, 12
	B. Typical Computer Plot Approximation	13
4	Concept 4, Single Quarter Cylinder, 1/6 Scale Test Configuration (1) & (2)	15, 16
5	Concept 5, Compound Quarter Cylinder 1/6 Scale Test Configuration (1) & (2)	17, 18
6	Concept 6, True (Smooth) Torus	
	A. 1/6 Scale Test Configuration I (1) & (2)	20, 21
	B. 1/6 Scale Test Configuration II (1) & (2)	22, 23
	C. 1/6 Scale Test Configuration III (1) & (2)	24, 25
7	Concept 7, Smoke Pipe Torus	
	A. 1/6 Scale Test Configurations (1), (2), & (3)	26, 27, 28
	B. Typical Computer Plot Approximations	29
8	Flow Divergence, Cone Concepts (1, 2)	40
9	Stream Cohesion Cases	41
10	Stream Diffusion/Splitting Characteristics, Quarter Cylinder Concepts (4, 5)	42
11	Buildup and Dynamic Effects of Fines for Some Torus Configurations	44
12	Typical Cases of Interference Between Impacting and Frictional Flow Portions of Stream	47

1.0 INTRODUCTION

During the initial portion of the Low Headroom Transfer Point Chute Program numerous geometries have been conceived as possible chute configuration candidates. These have been given various degrees of evaluation, usually starting with layout drawings and cardboard models. The more promising ones were also defined mathematically for possible subsequent computer analysis and were constructed as a scale model for testing in a 1/6 scale belt conveyor transfer point set up.

The scope of this interim study is to provide a screening of the more serious candidates evolved, for which various evaluation data, including primarily scale model testing, have been compiled. Essentially seven different configurations are addressed, comprising one- and two-degree curvature surfaces: cones and cylinders in the former case and toroidal shapes in the latter. These different configurations have been evaluated and compared against ten criteria, which themselves have been weighted in relative order of importance.

2.0 CONCLUSIONS

It is the conclusion from the tradeoff analysis herein that a two degree of curvature shape --- the torus---offers the best means of achieving the optimum stream dynamics relative to dust suppression, spillage and belt wear, while 1) simultaneously obtaining the minimum possible headroom and 2) fulfilling operational and economic constraints related to underground coal mining. Potential risk areas, which will require close attention during remaining scale model testing and preliminary design, involve the following areas:

- Clearance with the head pulley: 15 inches is currently provided and must be increased
- Producibility of a two degree of curvature surface

Various means for increasing chute clearance will be investigated during more detailed scale model testing, now that the interim phase of scale modelling of a variety of chute candidates is complete. An additional degree of chute rotation, about a vertical axis, will be evaluated as a means of increasing chute clearance without comprising stream dynamics.

It is the plan to approximate a true toroidal surface by a series of intersecting cylinders, as in the case of a HVAC jointed duct elbow. Thus the problem of producibility will be essentially eliminated.

3.0 CANDIDATE CONFIGURATIONS

3.1 GEOMETRICAL SURFACES CONSIDERED

Geometrical surfaces investigated during conceptual chute design were selected with an eye to three initial dynamic considerations:

- Low angle of incidence at impact between the free fall trajectory and the chute, to avoid ricochet and scatter.
- Cohesiveness and low turbulence of mass flow during the frictional phase
- Convergency of chute flow output, sufficient to achieve clean transfer to the receiving belt.

These guidelines lead to the study of three different geometries:

1. Cone
2. Cylinder
3. Torus

Layout studies and preliminary analysis of these geometries, resulted in turn in the evolution of seven distinct configurations, which are described briefly in the following section.

3.2 SPECIFIC CONFIGURATIONS

3.2.1 CONICAL SHAPES

3.2.1.1 Opening Half Angle Concept

Early computer math modeling work in the study program resulted in evolution of a conical model whose shape and orientation were defined in part by the free fall trajectory of the coal leaving the head pulley. Given independent parameters of 1) conical axis inclination with the horizontal; 2) the minimum cone radius at the upstream end of the cone; and 3) the minimum clearance with the pulley, the computer program determined the cone half angle and its location relative to the pulley (Figure 1A (1)). Another independent parameter that controlled the cone configuration and location was an allowable angle of incidence at impact with the chute defined at the centroid of the flow mass. The test configuration is shown in Figure 1A (2) and a computer plot approximation in 1B.

3.2.1.2 Flat Impact Plate Cone Concept

Owing to a desire to control the impact incidence angle to be as nearly uniform as possible throughout the thickness of the flow mass, an alternative configuration was developed whereby the free fall trajectory would impact a flat surface located above, and tangent to, the conical surface described earlier (Figures 2A & 2B). In this way impact of the flow mass with a constantly curving surface, resulting in a variable incidence angle across the flow thickness, would be avoided. This method of optimizing smoothness of flow at impact has, however, the associated potential penalty of additional headroom requirement.

3.2.1.3 Zero Degree Half Angle Cone Concept

Subsequent testing of the two conical configurations defined above revealed a tendency toward divergency of flow at the output, with attendant failure to achieve a clean deposition of material on the second belt. This problem led to definition of a third version whereby the opening half angle defined by the math model was suppressed to be zero degrees (Figures 3A and 3B). This yields, in fact, a cylindrical configuration. Its

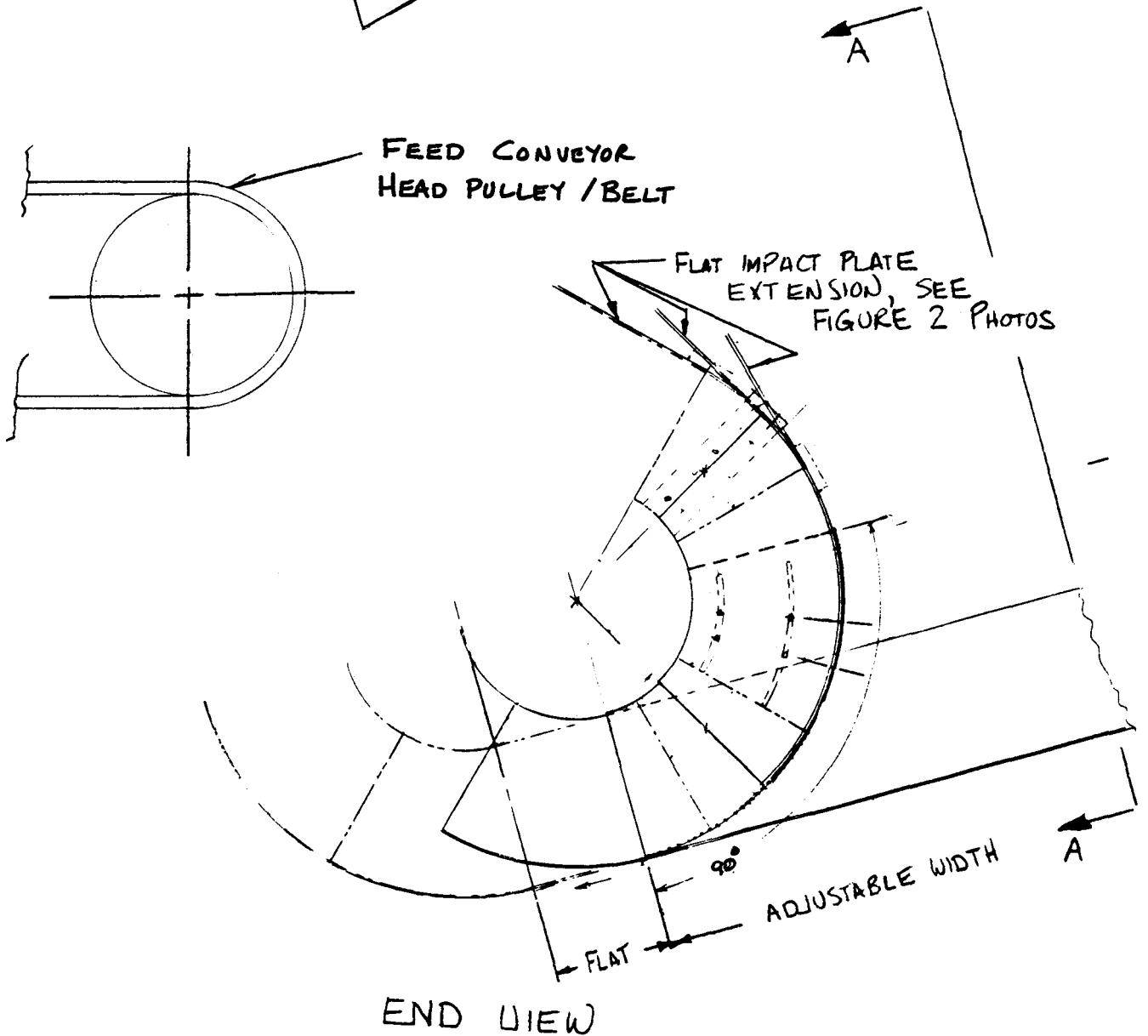
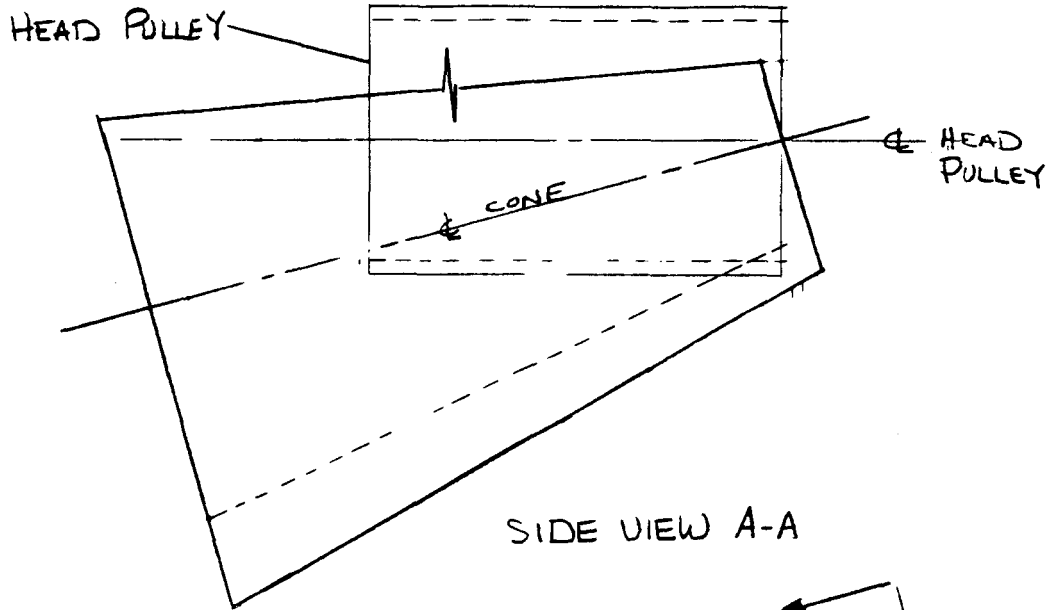
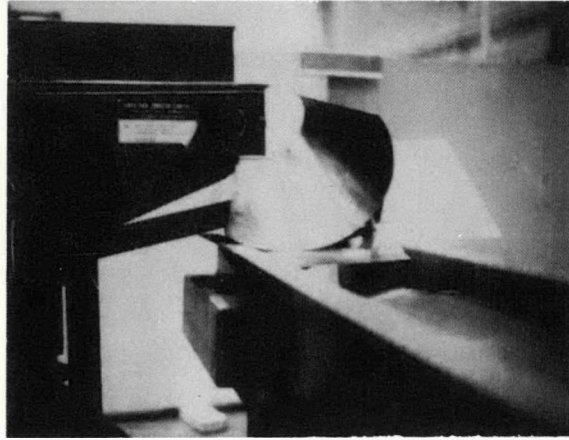
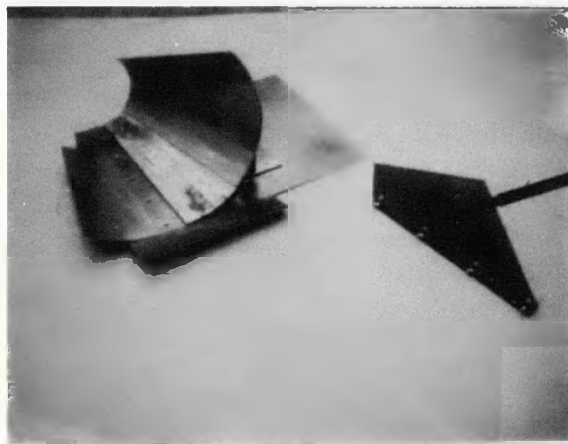


Figure 1A(1) Concept 1: Detail Layout



Installation



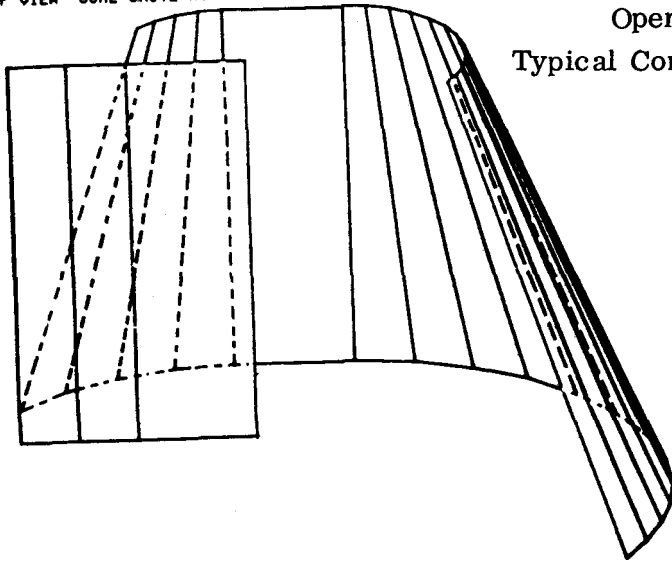
Flat Impact Plate -
Not Used in Concept
2 (Figure 2)

Details

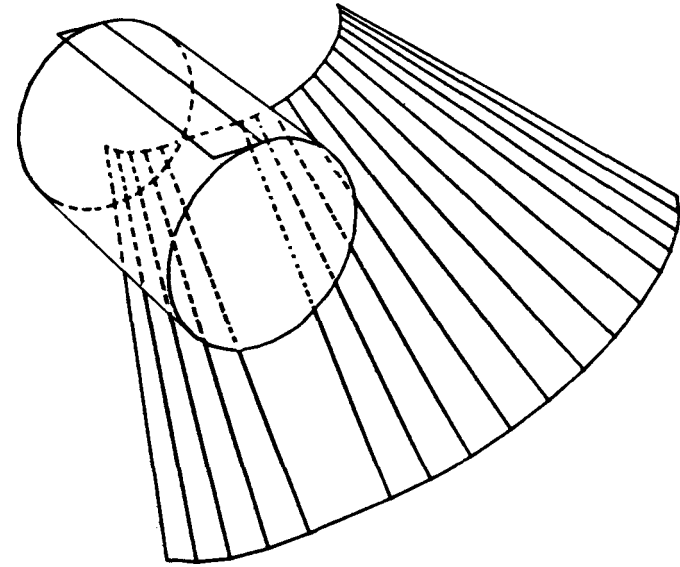
Figure 1A(2) Opening Half Angle Cone
1/6 Scale Test Configuration
Installation Set Up

Concept 1
Opening Angle Cone
Typical Computer Plot Approximation
Figure 1B

TOP VIEW COAL CHUTE RUN23

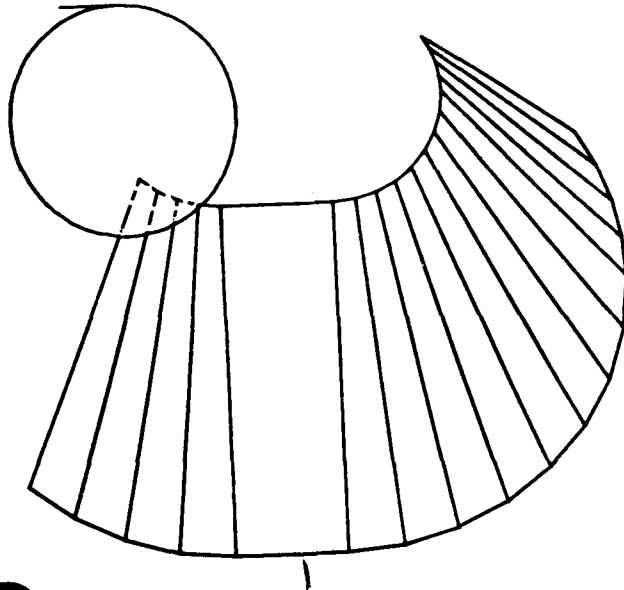


3-D VIEW COAL CHUTE RUN23

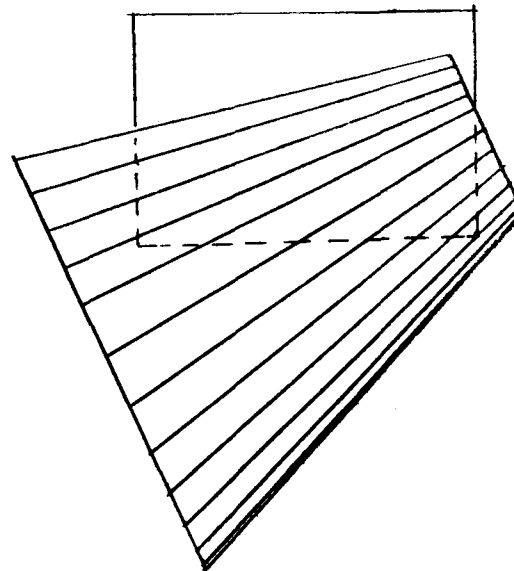


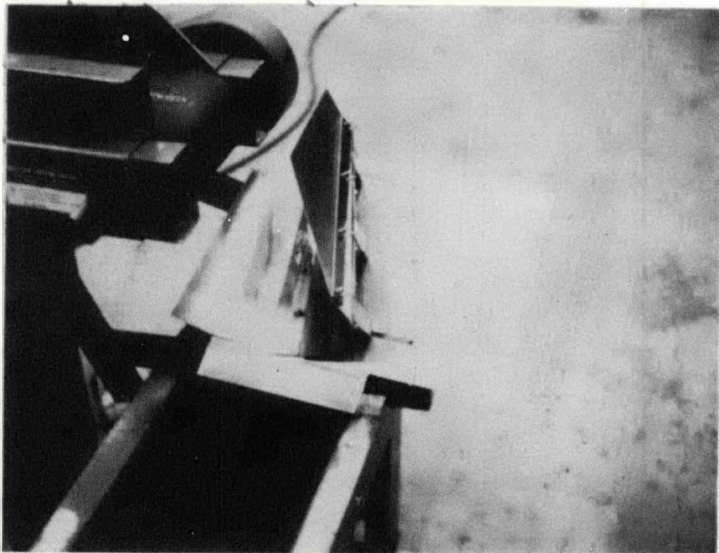
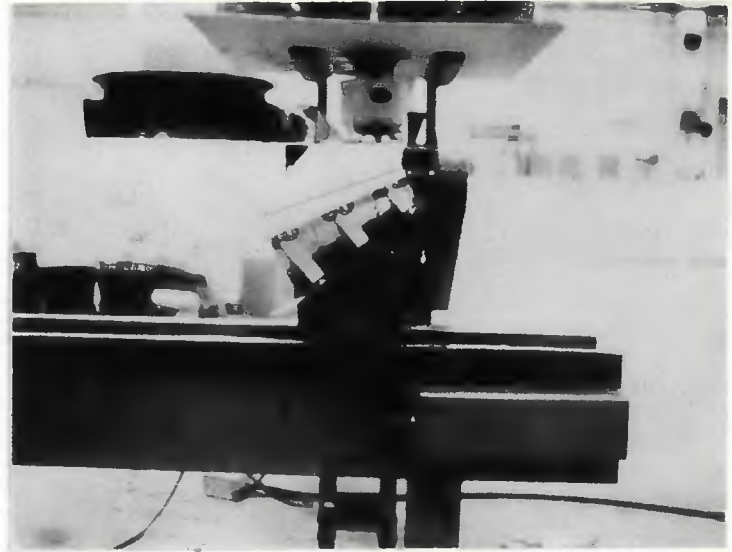
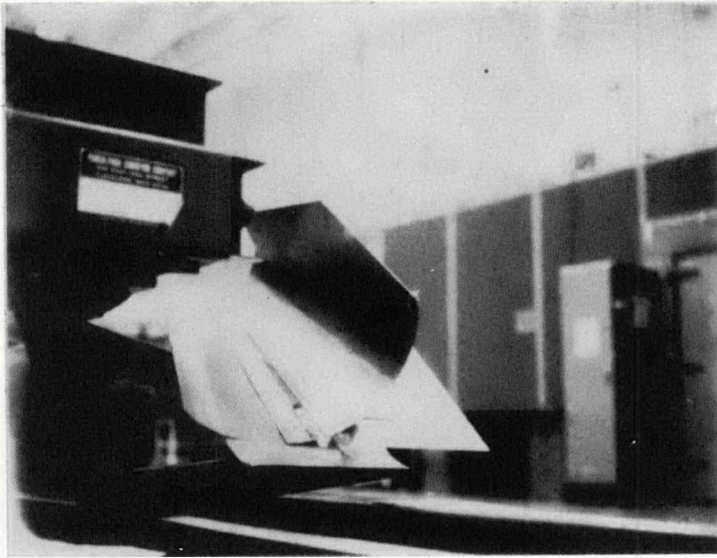
F-8

FRONT VIEW COAL CHUTE RUN23



SIDE VIEW COAL CHUTE RUN23





Flat Impact Plate Cone Concept
1/6 Scale Test Configuration

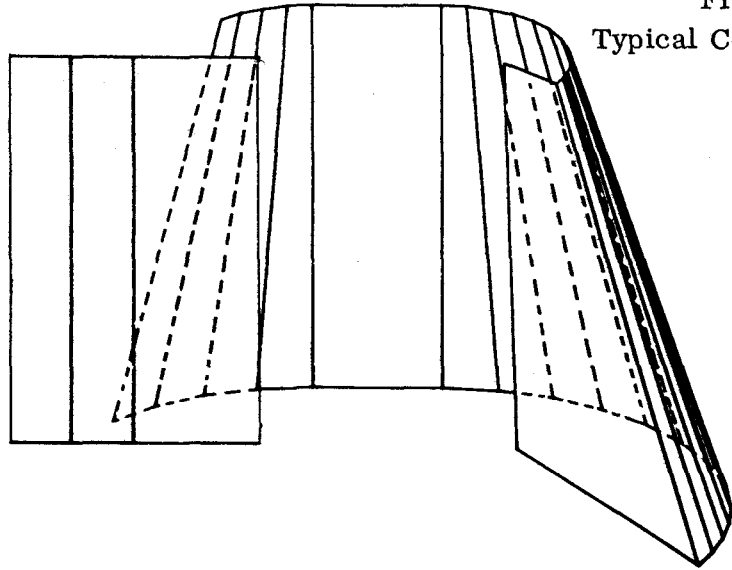
Figure 2A

Concept 2

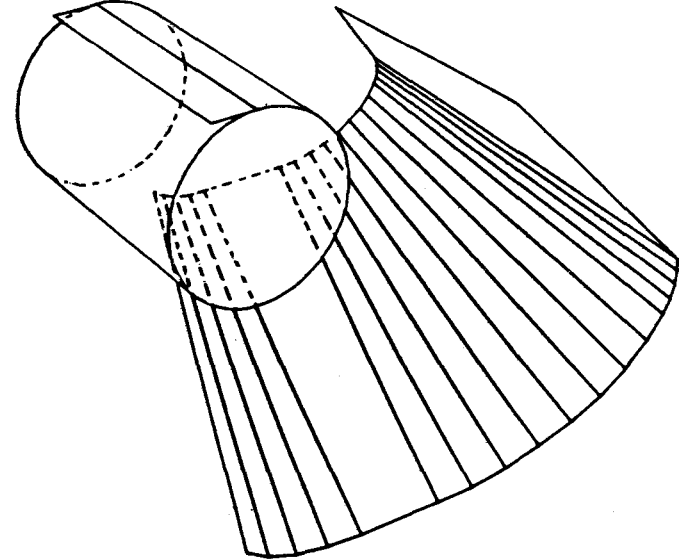
Flat Impact Plate Cone
Typical Computer Plot Approximation

Figure 2B

TOP VIEW COAL CHUTE

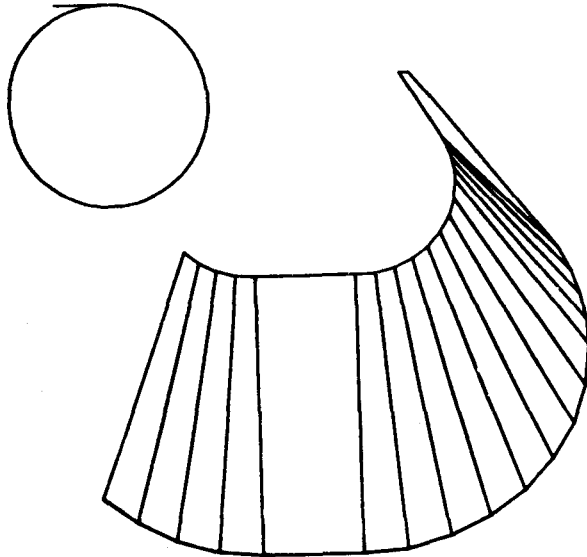


3-D VIEW COAL CHUTE

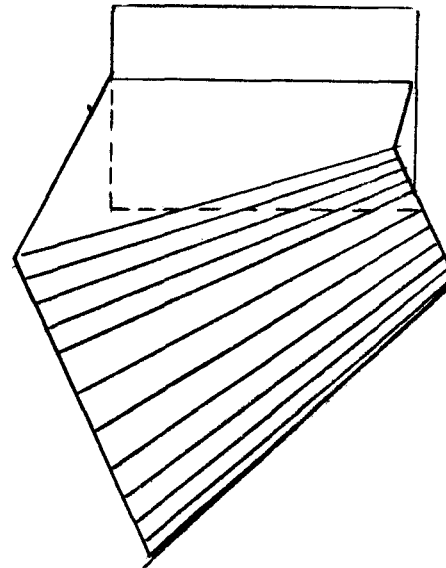


F-10

FRONT VIEW COAL CHUTE



SIDE VIEW COAL CHUTE



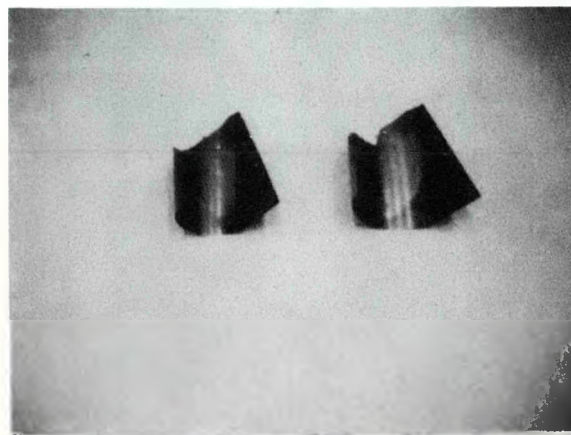
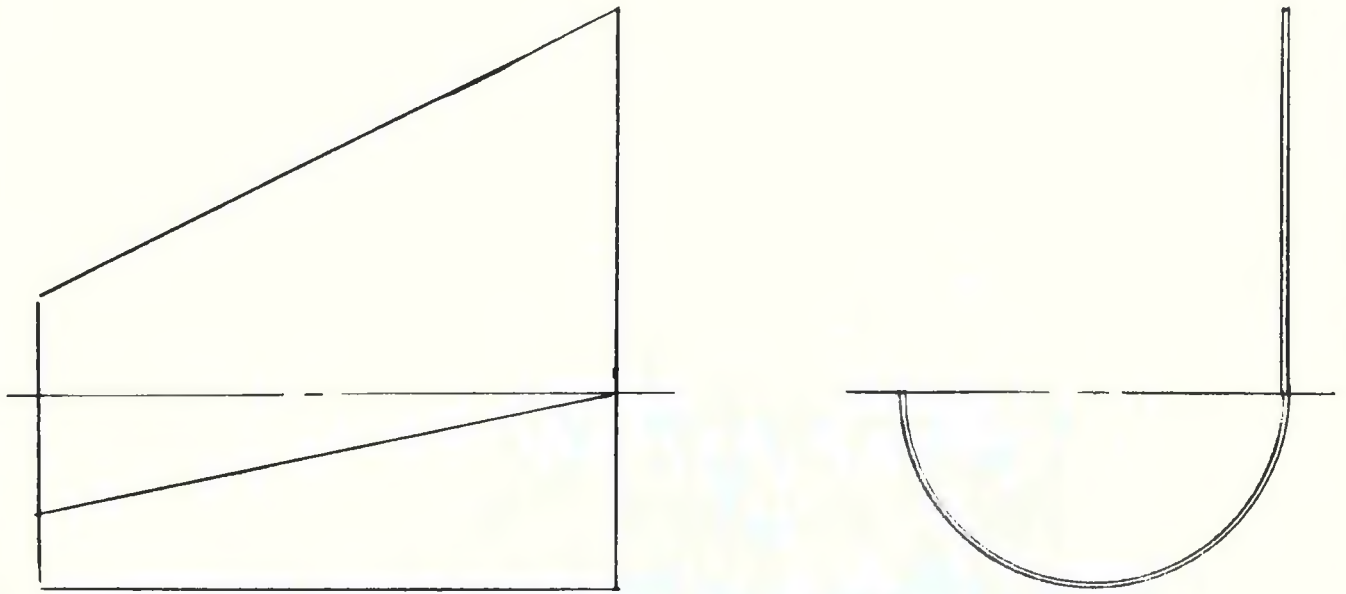


Figure 3A(1) Concept 3: Zero Half Angle Cone
1/6 Scale Test Configuration Details

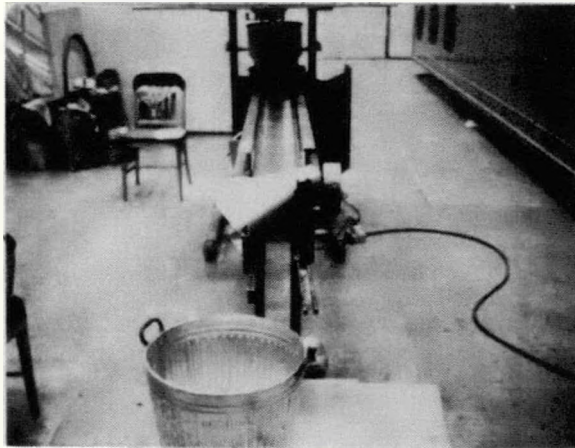
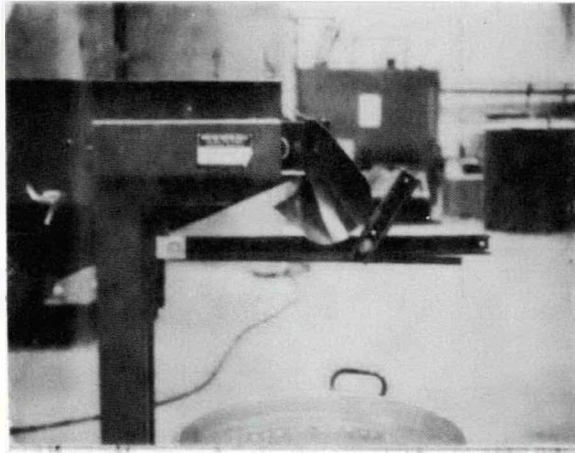
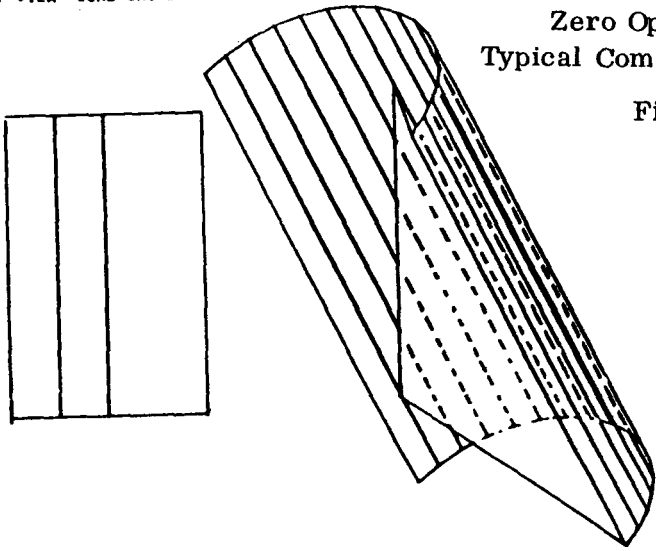


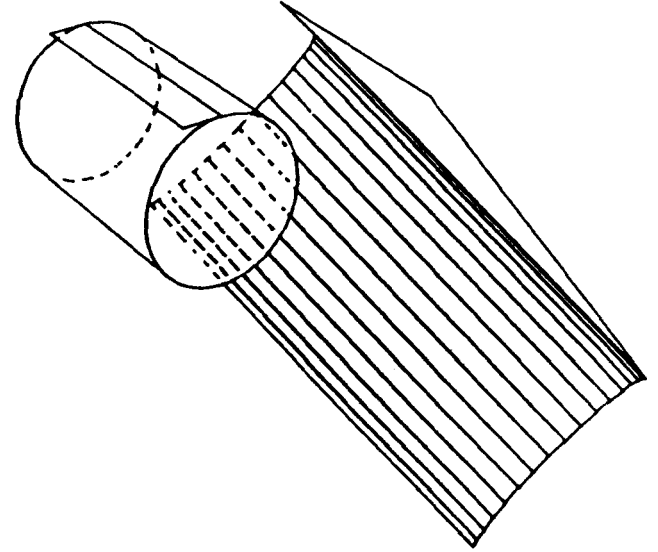
Figure 3A (2) Concept 3: Zero Half Angle Cor
1/6 Scale Test Configuration
Installation Set Up

TOP VIEW COAL CHUTE RUN NO 30



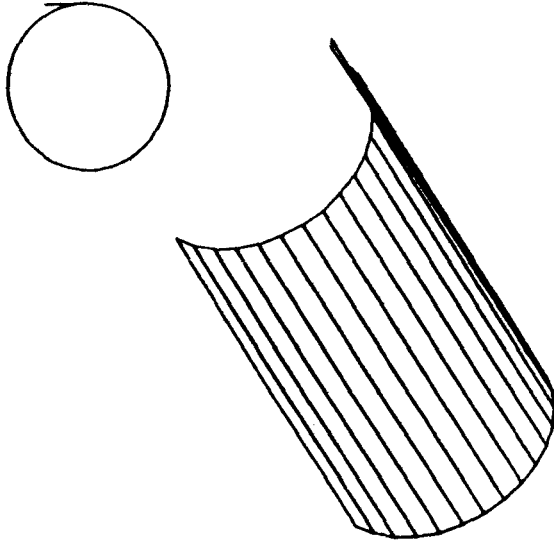
Concept 3
Zero Opening Angle Cone
Typical Computer Plot Approximation
Figure 3B

3-D VIEW COAL CHUTE RUN NO 30

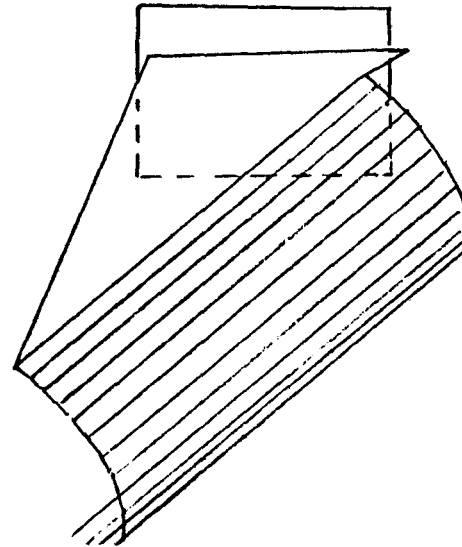


F-13

FRONT VIEW COAL CHUTE RUN NO 30



SIDE VIEW COAL CHUTE RUN NO 30



shape and orientation are quite different from the cylindrical concepts in the following paragraphs, however, in its philosophy of handling flow convergence.

3.2.2 QUARTER CYLINDER SHAPES

3.2.2.1 Single Cylindrical Surface Concept

Figures 4A and 4B show a chute configuration consisting of approximately a one-quarter cylinder shape, whose top edge is tangent to a vertical wall surface that intersects the direction of flow of the feed conveyor at about a 30 degree angle. Depending upon the height of the tangency line, material at different locations crosswise to the flow mass will impact either against the flat vertical surface or else against the cylindrical portion. The portions of initial flow progressively to the right, i. e., toward the final direction of flow, will impact at points progressively greater in horizontal and vertical distance from the feed pulley.

3.2.2.2 Compound Cylindrical Surface Concept

Although early evidence suggested that the above cylindrical configuration could be oriented and sized to turn all portions of the mass cross section through a common 90-degree angle, this did not guarantee adequate convergency of flow to ensure its proper deposition on the receiving belt. Concepts were, therefore, evolved to define side constraints to the flow once it had been turned. Simple flat side plates, arranged in a troughing fashion (Figure 5B), were considered for this purpose, but their intersection with the cylindrical surface formed Vee channels whose inclination with the horizontal was too shallow to insure flow. It was found that the use of cylindrical surfaces to provide the side wall constraints resulted in Vee channels adequately steep to insure flow at these intersections (Figure 5A).

3.3.3 TOROIDAL SHAPES

3.3.3.1 True Toroidal (Smooth) Concept

The toroidal configuration was evolved with the intent to evaluate the effectiveness of a double curvature surface. The minor radius of curvature would converge the flow cross section, as does the zero degree half angle conical configurations (3.2.1.3), with the other, major radius of curvature providing a vertical curve type chute profile, as afforded by the cylindrical configuration (3.2.2). In the case of a

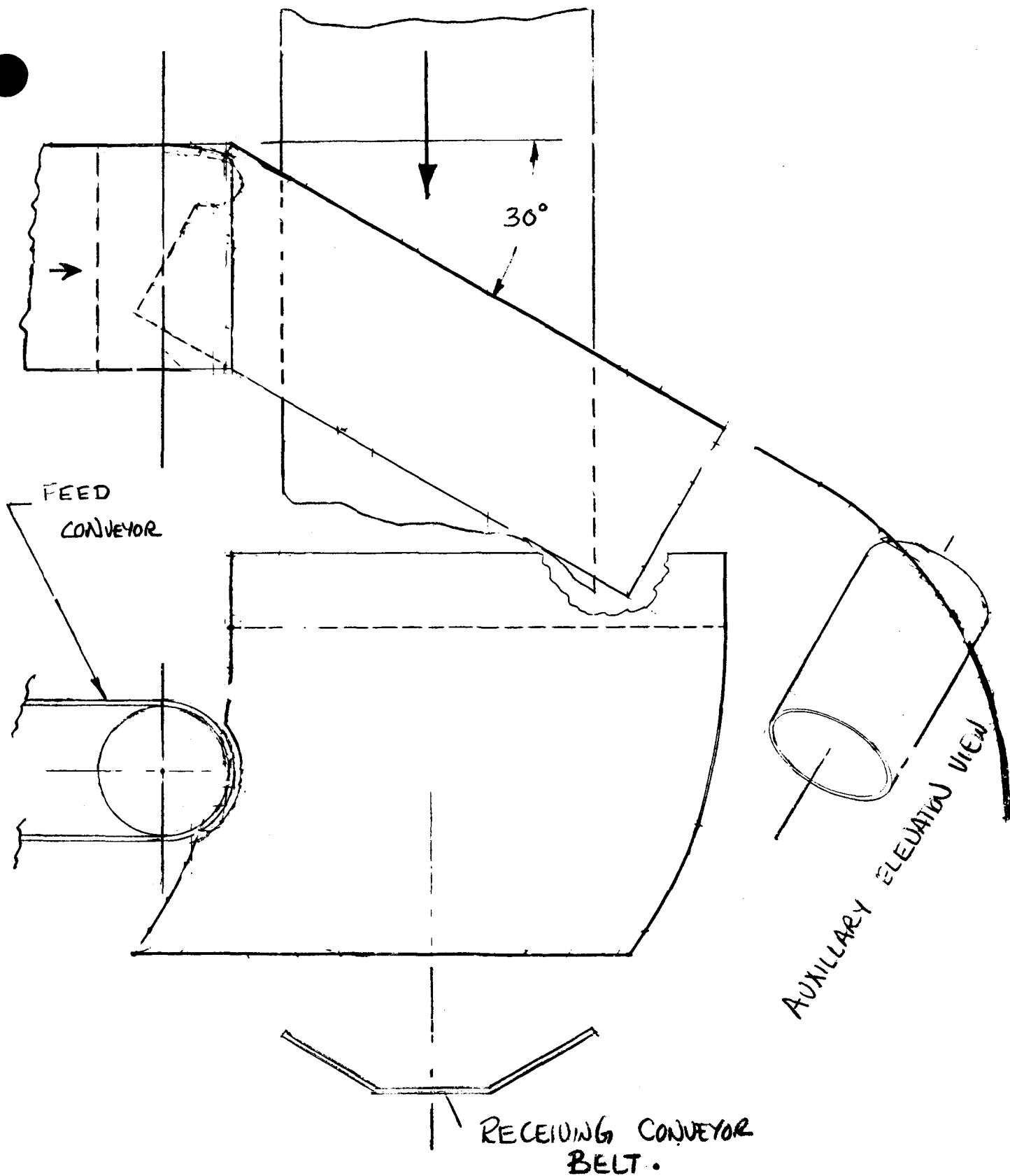
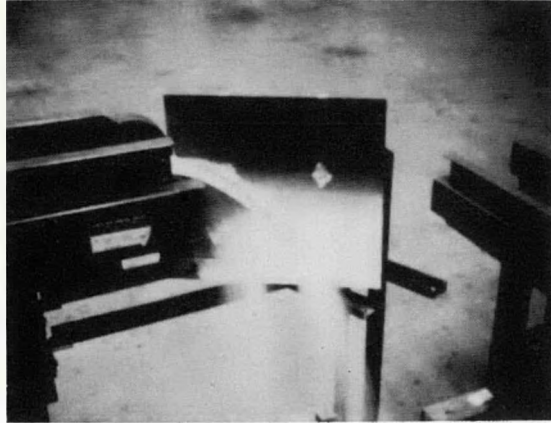


Figure 4A Concept 4 Single Quarter Cylinder
 1/6 Scale Configuration Detail Layout



Concept 4

Single Quarter Cylinder
1/6 Scale Test Configuration

Figure 4B

F-16

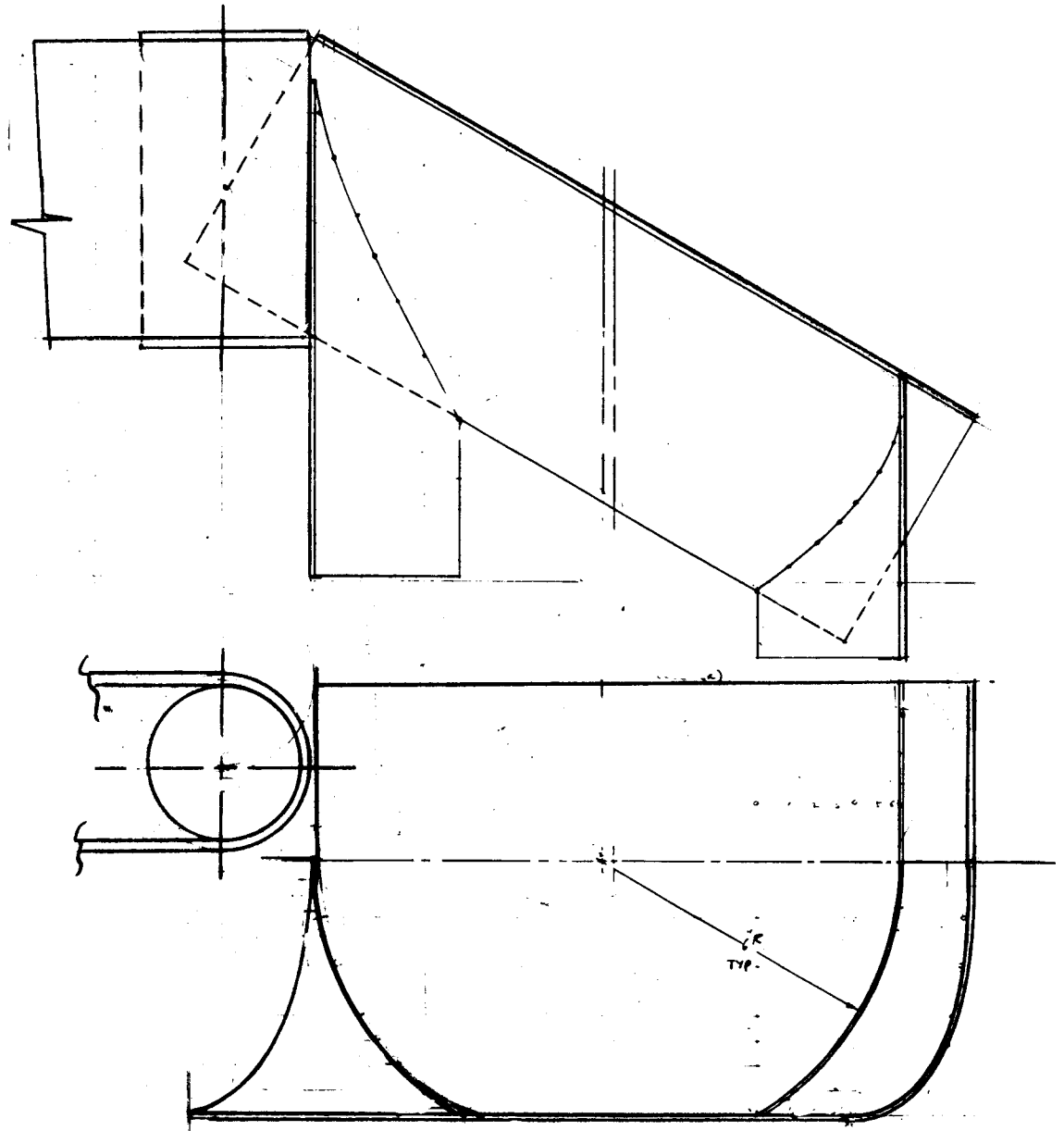
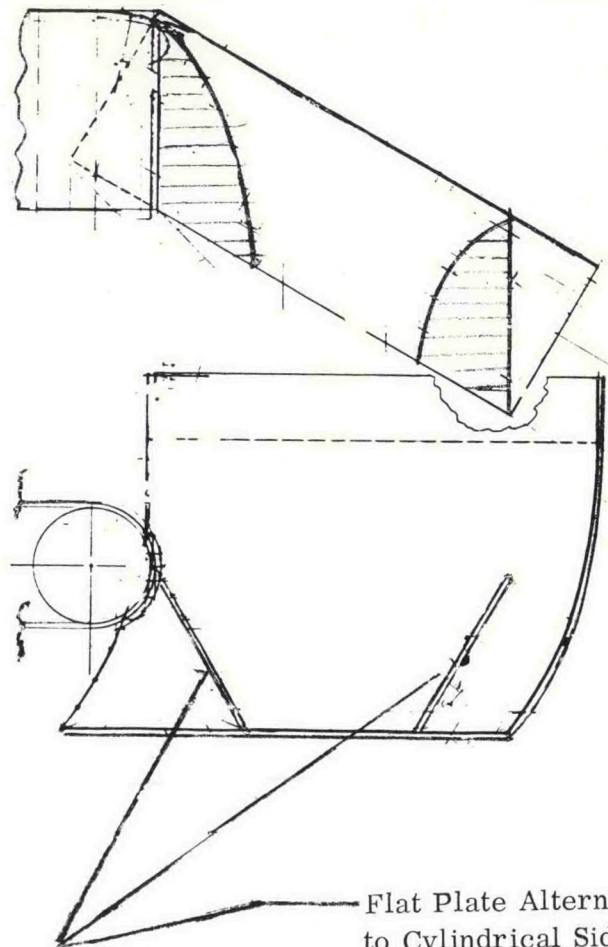
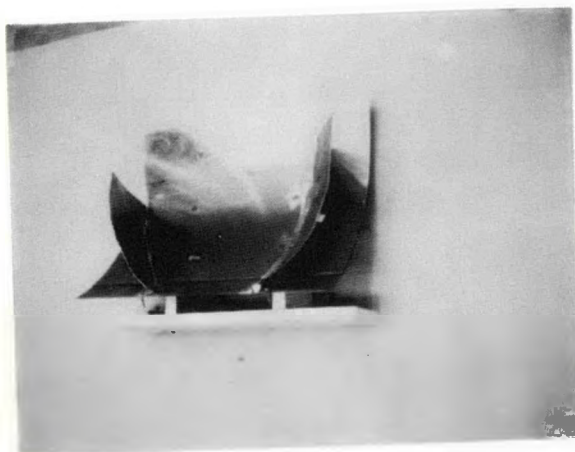
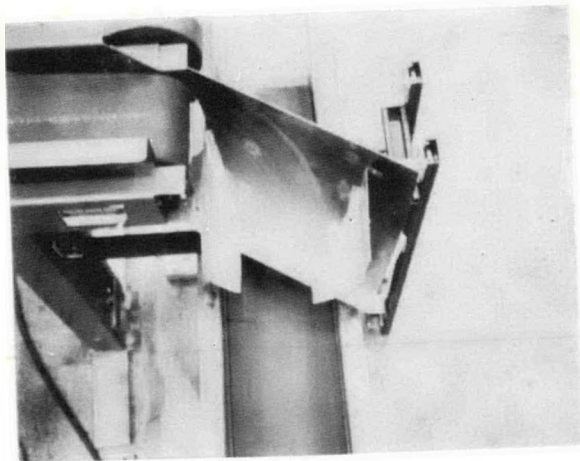


Figure 5A Concept 5: Compound Quarter Cylinder
1/6 Scale Test Configuration
Detail Layout



Flat Plate Alternative
to Cylindrical Side
Constraints

Figure 5 b. Concept 5: Compound Quarter Cylinder
1/6 Scale Test Configuration

single degree of curvature surface such as the cone, the coefficient of wall friction dictates a minimum slope angle upon the attitude of the central axis. This defines directly a minimum headroom clearance between belt surfaces, depending upon the width of the feeder belt. The objective with the vertical curve is to determine whether headroom reduction can be achieved by causing the material to the left* of the flow cross section, which lands upon the steep portion of the vertical profile slope and experiences great vertical acceleration, to drive out that portion on the right* of the flow mass, which falls on the shallow profile slope, where it experiences much lower vertical acceleration.

Figures 6A and 6B chute surfaces which correspond to a true, smoothly defined, toroidal shape, with cutouts as required to clear the feed belt pulley.

3.3.3.2 "Smoke-Pipe" Toroidal Concept

Owing to the inevitable question of producibility of a large double curvature surface, a second investigation was initiated of a modified torus, developed from a series of intersecting cylindrical shapes and corresponding to a portion of a "smoke pipe", or sheet metal, 90 degree elbow, as used in HVAC ductwork. This configuration is depicted in various sizes in Figures 7A (1), 7A (2), and 7A (3).

4.0 EVALUATION

4.1 METHODOLOGY

4.1.1 EVALUATION CRITERIA

The concepts identified in the previous section (3.0) have been evaluated against ten criteria, relating to 1) performance, 2) compatibility with mining operations and 3) economics. The essential considerations involved in defining these criteria are discussed here. The following section describes the weighting system for establishing comparative importance of these criteria.

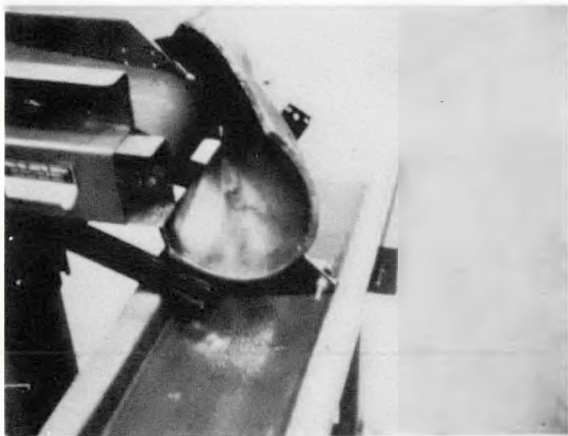
* Viewed by a person travelling with the flow toward a right hand turn transfer point.



Installation, 6" Minor Dia. Case



6" and 8" Minor Dia Cases



Installation, 8" Minor Dia Case

Figure 6A(2) Concept 6: True (Smooth) Torus
1/6 Scale Test Configuration 2
Installation Set Up Detail

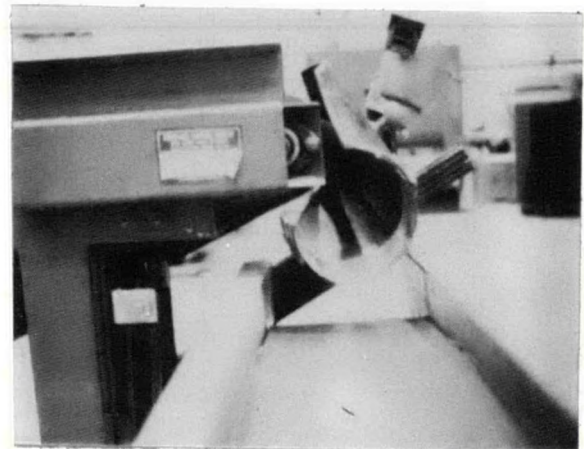
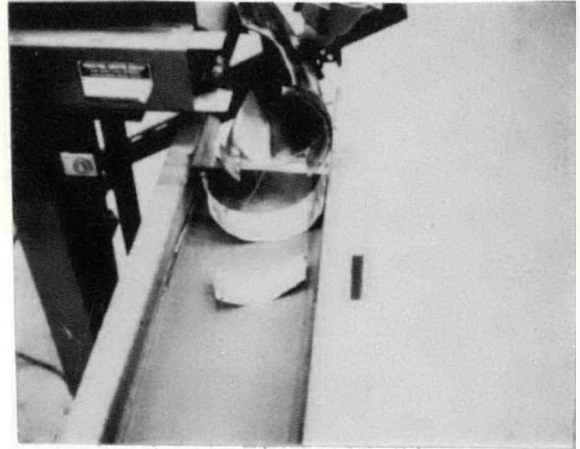
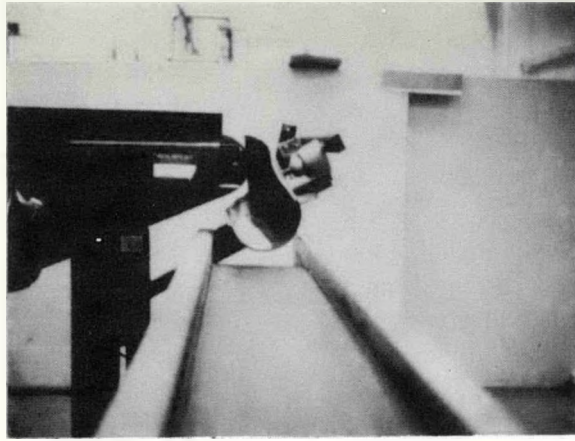
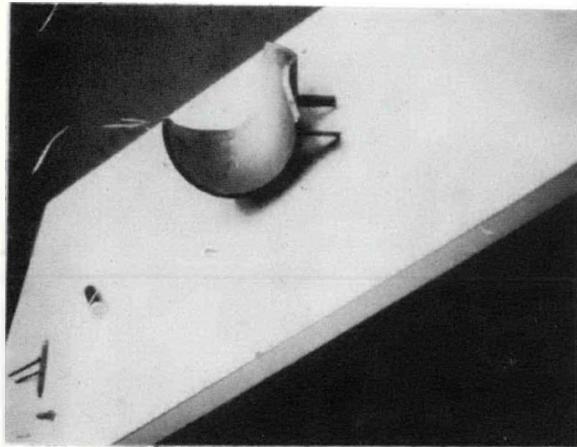


Figure 6B(2) Concept 6 True (Smooth) Torus
1/6 Scale Test Configuration II



Installation, 6" Minor Dia.



6" Minor Diameter Case

Figure 6C(2) Concept 6: True (Smooth) Torus
1/6 Scale Test Configuration
Installation Detail/Set Up

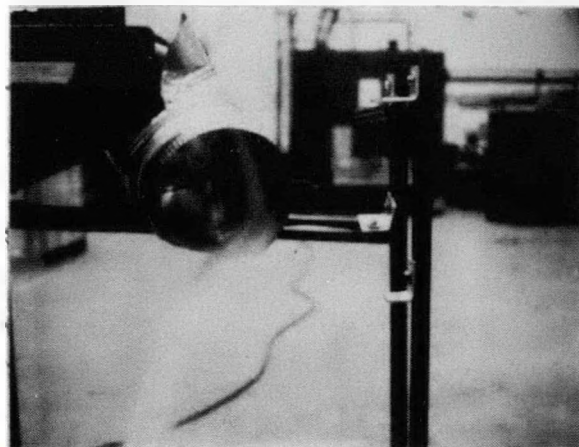


Figure 7A(1) Concept 7: Smoke Pipe Torus
1/6 Scale Model Test Configuration
8" Diameter Case Low Installation

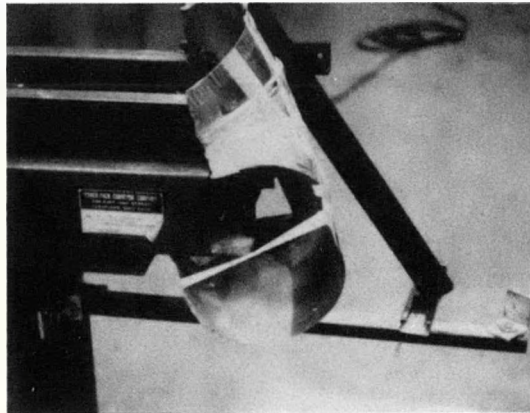
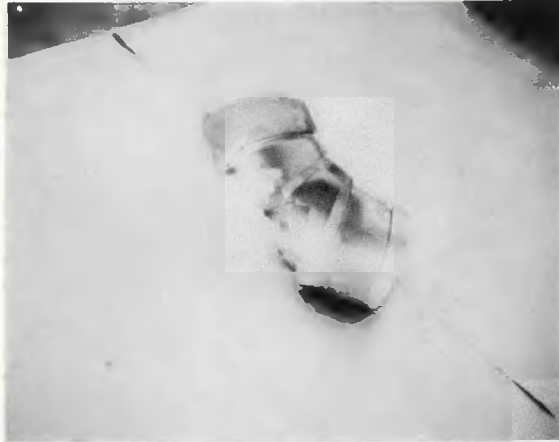


Figure 7A(2) Concept 7: Smoke Pipe Torus
1/6 Scale Test Configuration
8" Diameter Case, High Installation

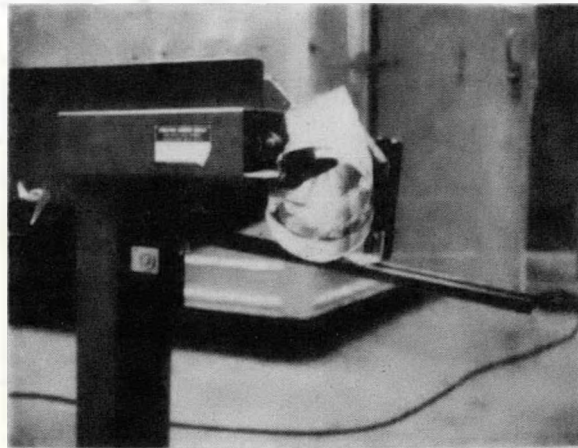
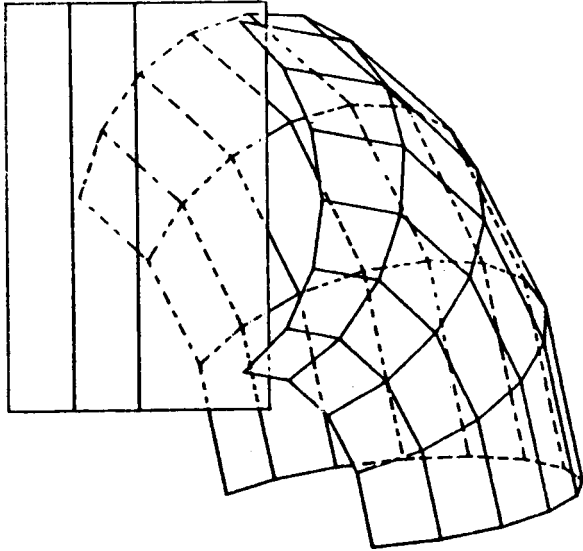
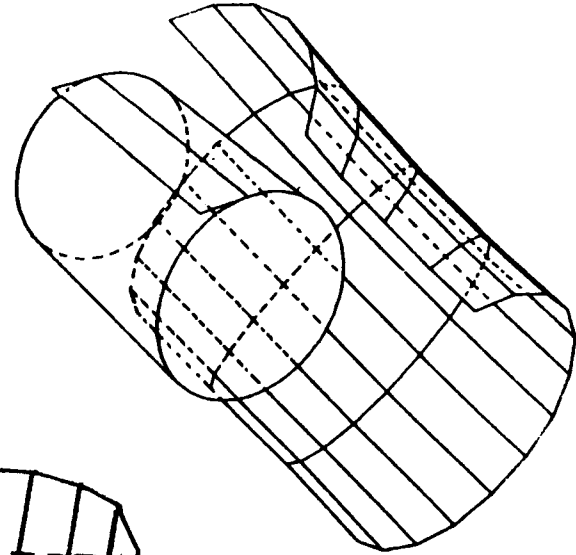


Figure 7A(3) Concept 7 Smoke Pipe Torus
1/6 Scale Test Configuration
6" Diameter Case, Installation

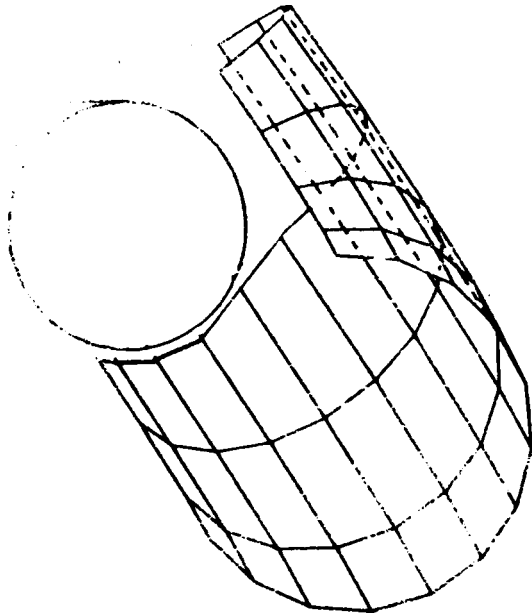
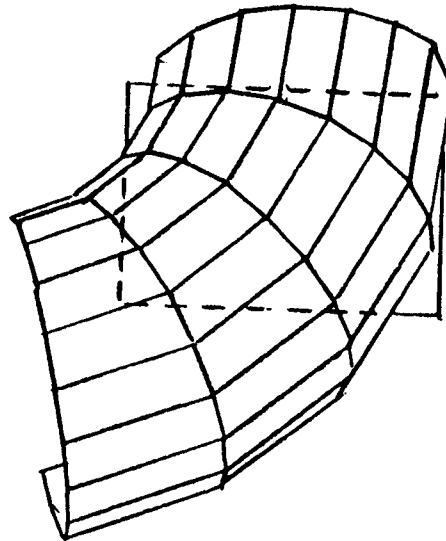
TOP VIEW COAL CHUTE



3-D VIEW COAL CHUTE



SIDE VIEW COAL CHUTE



F-29

Concept 7
Smoke Pipe Torus
Typical Computer Plot Approximation
Figure 7B

4.1.1.1 Performance Criteria

4.1.1.1.1 Stream Cohesion

The essential characteristic involved here is freedom from flow disintegration and turbulence, both within the coal mass and at the chute wall surface. This characteristic is one of two major measures of low dust evolution. Specific conditions whereby stream cohesion is considered to be degraded are 1) particle bounce upon impact; 2) interference between the impacting stream and flow moving on the surface; 3) material scatter during frictional flow down the chute. (One other source of dust evolution is addressed in the following paragraph.)

4.1.1.1.2 Belt Impact Vector

A design goal from the dynamic standpoint is to match the terminal flow vector leaving the chute with that of the receiving belt velocity. In particular, low belt wear as well as minimum dust evolution will be related to 1) minimizing the vertical component of this terminal vector, as well as 2) matching its horizontal magnitude with the belt speed. By total elimination of the vertical component of chute discharge velocity, it is seen the impact velocity will be confined only to that due to the height of the bottom of the chute above the belt.

4.1.1.1.3 Free-Flow

Freedom of flow along the frictional surface is a function of surface shape as well as material friction and is characterized by absence of a tendency to clog, due to heavy flow, sticky flow material, and related conditions. The primary objective here is prevention of spillage and associated lost personnel time.

4.1.1.1.4 Convergence

A second dynamic criterion essential to avoid spillage is that the flow be converged sufficiently by the chute to confine the impact area in the receiving belt to its central, primarily flat area. Exact definition of the width of this impact zone is somewhat arbitrary, but it is judged that a 12 to 18 inch figure should be a goal*. A secondary factor associated with this requirement is that the net flow vector leaving the chute be parallel to the receiving conveyor, in order to avoid disturbing belt tracking on this conveyor.

*for a 36 inch wide belt

4.1.1.2 Mine Operation - Related Criteria

4.1.1.2.1 Jam Clearance

In view of the fact that run of mine coal contains not only large pieces of rock, but also such unplanned items as roof bolts, it is necessary that there be adequate distance between the feed conveyor head pulley and the chute. A sampling of observations by mine personnel during FSEC's site survey indicates that the probable upper dimensional limit of such pieces will be adequately provided for by an 18 to 20 inch clearance.

4.1.1.2.2 Minimum Headroom

Defined narrowly here as the elevation distance between transfer point belt surfaces, a minimum headroom chute is, by original definition, an objective of this program. Associated with this is reduction in the amount of required roof cover removal at transfer points.

The background in this area is that, from observations of eight underground mines around the country, FSEC has seen only one where chutes were used at transfer points with less than a five foot elevation difference between belt surfaces. In three of the mines, where a 2 1/2 to 3 foot headroom clearance was involved, only simple deflector backboard provisions existed, resulting in no right angle acceleration of the flow prior to belt impact.

4.1.1.2.3 Installation

Ease of installation is measured not only by how little time is required for final field assembly and mounting of the chute at the transfer point but also by the simplicity of final alignment procedures. This latter includes absence of the following: 1) tight alignment tolerances; 2) marked sensitivity of the flow dynamics to small variations in chute attitude and location; and 3) requirements for special tools, etc.

4.1.1.3 Economic Criteria

4.1.1.3.1 Maintainability

At the mine sites visited, provision for repairing worn portions of a chute surface generally involved replacement on site of a localized plate section of the chute wall. Generally, torch cutting and welding procedures were utilized, although in one more ambitious maintenance program observed, the slide surface consisted of elements individually attached by flat head cap screws. This approach appears very desirable, as compared with replacement of an entire chute. The ease of maintenance then involves either 1) capability of local fabrication of an individual piece from a drawing or else 2) maintaining an inventory of such pieces, which have been produced in quantity using a more elaborate fabrication process by a regional or national manufacturer.

4.1.1.3.1 Producibility

Herein the essential characteristic is whether the chute dictates manufacturing processes that are normally not available in a local area or, more serious, not feasible in other than high quantity production. This does not necessarily invalidate use of special tooling, providing 1) its design is well documented and it is readily and cheaply reproducible, or else 2) it is perhaps available on loan through a regional or national association of mine owners. Another factor in this connection is the applicability of the same tooling to all possible dimensional configurations of a given basic design, which may vary, for example, for different belt speeds.

An intangible consideration in connection with producibility is saleability, or ease of acceptance among industry users. It is evident that exotic designs or complex geometrical surfaces, completely apart from questions of fabrication, are not going to be indulged by mine owners if they appear to involve production risks in terms of lead time or an inherent limitation on the number of sources where the chute can be obtained.

4.1.1.3.3 Initial Cost

The other consideration involved in industry wide acceptance is, of course, cost. Here a number of interrelated factors apply. However, depending upon an individual mine owner's sensitivity to such problems as dust evolution, belt wear, and spillage, a given chute design may warrant a considerably higher cost than ones in typical use now.

4.1.2 WEIGHTING OF EVALUATION CRITERIA

Table 1 shows the relative weighting importance considered to apply among the criteria previously described. The criteria are ranked on a scale of from 1 to 5.

Table 1
Evaluation Criteria Weighting

<u>Evaluation Area</u>	<u>Criterion</u>	<u>Weight Value</u>
Performance	1. Stream Cohesion	4
	2. Belt Impact Vector	4
	3. Free Flow (Non Clogging)	5
	4. Convergence	5
Mine Operation	5. Jam Clearance	5
	6. Minimum Headroom	2
	7. Installation Complexity	2
Economics	8. Maintainability	3
	9. Producibility	3
	10. Initial Cost	3

Assignment of the above weighing inevitably involves subjective rationale. It will be seen that three of the four criteria given the highest weight -- namely items 3, 4, and 5 --- relate to the most basic consideration: it has to handle the flow without 1) clogging (free flow); 2) missing or falling off the receiving belt (convergence); and 3) getting a large piece caught between the pulley and the chute (jam clearance). Of the three original considerations identified at the outset of this program --- spillage, dust, and belt wear --- the first is most directly related to the essential questions: Does the chute work? and, Are there any operational risks?

The next highest weight, 4, is given to the dust-related criteria of stream cohesion and belt impact vector. This reflects the outlook that dust suppression is, as of today, nearly as fundamental as the mechanics of the rightangle transfer itself.

While belt wear is, coincidentally, a factor in the belt impact vector criterion, it is not judged to be as overriding a concern as is dust suppression; and had it been possible to separate them in this area, belt wear would have been weighted 3 rather than 4. There appears to be some question among experts as to the sensitivity of belt life to the impact wear induced at transfer points, it being argued by at least one FSEC consultant that there is little correlation between the two and that catastrophic failures and edge wear are by far the pacing factors in belt life. Whether or not this viewpoint is common within the underground coal industry, or whether the subject is too subtle for the average mine maintenance operator, it is clear that current transfer point design practices observed by FSEC reflect little detailed concern over the wear impact mechanism. Apart from spillage, the provision of a chute to turn the flow appeared to arise primarily from the need to ensure against jams occurring in high volume situations or where more than one transfer point lies along a conveyor.

Three criteria have been weighted with a factor of three. Primarily economic in nature, maintainability, producibility, and initial cost are in reality overriding considerations in the probability of acceptance by the industry of a chute design, irrespective of its functional merits. The medium weighting assigned here reflects not so much a downgrading of these essential aspects as much as a recognition that even difficult design solutions in these areas cannot be ruled out at this R/D stage, and that performance - and operational-related criteria must dictate the cutting edge of this screening of conceptual candidates.

Two remaining criteria --- low headroom and installation --- are weighted at a factor of two. While this treatment of headroom may appear contradictory in view of its place in the title of this program, it appears consistent with the guidance provided for design of the full size chute; namely: "It shall be designed to minimize coal spillage, dust generation, and conveyor belt wear," and "The chute ----- shall have as low a profile as possible."

Of greater issue here, however, is the implicit relative weighting given these four characteristics in mine operations witnessed by FSEC. Concern over spillage and dust generation was clearly evident where these problems existed; and various types of corrective measures were uniformly in evidence. On the other hand, even though cost and roof stability considerations associated with removing significant amounts of rock cover --- up to nine-feet or more --- were found to be well-understood and acknowledged by mine personnel when specifically questioned on this subject, there simply appeared to be little sensitivity on this matter. The mood appeared to be that removing this additional material was a one-time problem, was not a overriding cost factor, and was, moreover, frequently dictated by considerations other than the headroom buildup required by the chute installation.

Apparent evidence of the desirability of low headroom was the stark absence of chutes at some 36 inch to 42 inch belt transfer points, where the elevation distance between belts was held to 30 to 36 inches. The conclusion here is, however, that this practice derived less from an intent to minimize headroom and more from a motivation to dispense with the inconvenience of installing a chute, where a low flow volume made it possible. The headroom utilized at these locations appeared to derive directly from the requirements of the deflector plate geometry, rather than from a conscious effort to minimize ceiling height.

The lower-than-average weighting given to chute installation is explained against the background of relocation and alignment tasks for other types of equipment in underground mines, involving far greater complexity than the relocation and/or installation of a chute. While complex alignment and mounting procedures for the chute are plainly undesirable, it is not anticipated that any serious chute candidate design will dictate unusual requirements in this area.

4. 1. 3 RATING PROVISION

Using the ten design criteria, each candidate configuration has been rated on a scale of from zero to ten, approximately as noted here:

10	Ideal
7.5	Good
5.0	Fair
2.5	Marginal
0	Totally Unsuitable

It will be seen that with this rating system and the criteria weighting previously established, the maximum possible score is 360.

4. 2 TRADEOFF EVALUATION

4. 2. 1 SUMMARY ANALYSIS

Table 2 summarizes a comparative evaluation of the seven candidate configurations described in 3. 0. The following discussion summarizes the principal conclusions from this tradeoff analysis while section 4. 2. 2 reviews details of the analysis.

It will be seen that for the concepts evaluated, scores compared to the maximum possible ranged from about 60 to 70 percent, with the compound quarter cylinder and the smoke pipe torus leading, with about 70 percent. Because of lack of consistently good performance against all ten evaluation criteria, the scores tended to average out, and no one concept is a runaway. However, the two above mentioned concepts rank markedly above the rest.

It will be seen that the major flaw in the compound cylinder configuration is the serious absence of stream cohesion. This is characterized by a two-pronged split in the flow at impact and was found to persist for various cylindrical radii configurations as well as for various chute location and orientations tried. No solution to this problem has thus far been developed.

In general, the torus concepts ranked the best from the standpoint of performance criteria, but were less impressive when judged against operational and

Table 2. Tradeoff Evaluation Analysis

Evaluation Criterion				Cone						Quarter Cylinder				Torus			
				Opening 1/2Angle		Flat Plate		Zero 1/2Angl		Single		Comp		True, Smooth		Smoke Pipe	
Area		Description	Weight W	R	RW	R	RW	R	RW	R	RW	R	RW	R	RW	R	RW
Performance	1	Stream Cohesion	4	5.0	20	5.0	20	7.5	30	0	0	0	0	9	36	9	36
	2	Belt Impact Vector	4	4	16	4	16	4	16	9	36	9	36	9	36	9	36
	3	Free Flow	5	10	50	10	50	9	45	10	50	9	45	8	40	8	40
	4	Convergence	5	2	10	2	10	7.5	37.5	0	0	9	45	9	45	9	45
Mine Operation	5	Jam Clearance	5	7.5	37.5	7.5	37.5	0	0	10	50	10	50	6	30	6	30
	6	Minimum Headroom	2	6	10	6	10	5	10	9	18	9	18	5	10	5	10
	7	Installation Complexity	2	5	10	7.5	15	5	10	10	20	7.5	15	4	8	5	10
Econo- mics	8	Maintainability	3	7.5	22.5	7.5	22.5	7.5	22.5	8	24	5	15	1	3	5	15
	9	Producibility	3	7.5	22.5	7.5	22.5	7.5	22.5	7.5	22.5	5	15	1	5	5	25
	10	Initial Cost	3	6	18	6	18	7.5	22.5	7.5	22.5	4	12	0	0	3	9
		TOTAL RW	36		226		234.		216		243		251		213		256
		RATING AGAINST MAX POSSIBLE SCORE PERCENT			62.9		64.3		60		67.5		69.7		59.2		71.1
		Code: W - Numerical weight assigned to criterion, 1 to 5 R - Numerical rating given to configuration for indicated criterion, 1 to 10 (See Table 1) RW - R x W															

economic criteria. In the areas of producibility and cost, the smoke pipe torus appears to be a prohibitive choice over the true torus, although in an absolute sense it is still not optimum. A principal area of sensitivity exists in jam clearance, where the chute impact area is estimated to be about 15 inches from the feeder pulley, at the centerline of the belt. This is a design risk area which must be evaluated further by testing and analysis during the balance of the study program.

In general, several of the ratings of the two leading candidates against specific criteria involved very imprecise and preliminary judgement factors, especially in the economic areas. There is not much doubt that the compound quarter cylinder configuration can be produced cheaply, but somewhat more design study is required to gain definition relative to the smoke pipe torus.

In order to select which candidate chute concept, or concepts, should be investigated during final analysis and testing, an initial decision involves the compound cylinder concept, in a tradeoff between the good headroom and the very poor stream cohesion characteristics. The judgment is that the cohesion problem appears irredeemable and that acceptance of this penalty to gain a headroom advantage would not contribute usefully to the state of the art. Too many other chute configurations, as well as deflection boards, now in use already achieve this tradeoff. On this basis, the tradeoffs summarized in Table 2 indicate the torus to be the sole candidate design concept to be further considered.

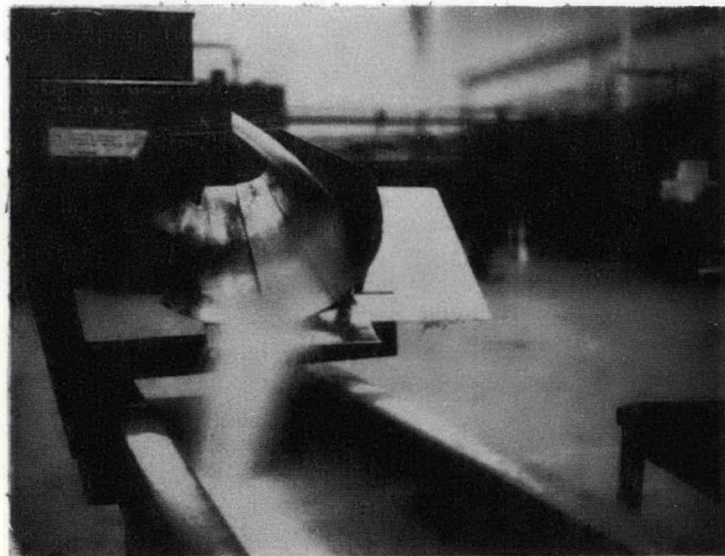
4.2.2 ANALYSIS DETAILS

This section reviews some of the details and rationale behind the trade-off analysis presented in Table 2, covered on a criterion-by-criterion basis.

4.2.2.1 Stream Cohesion

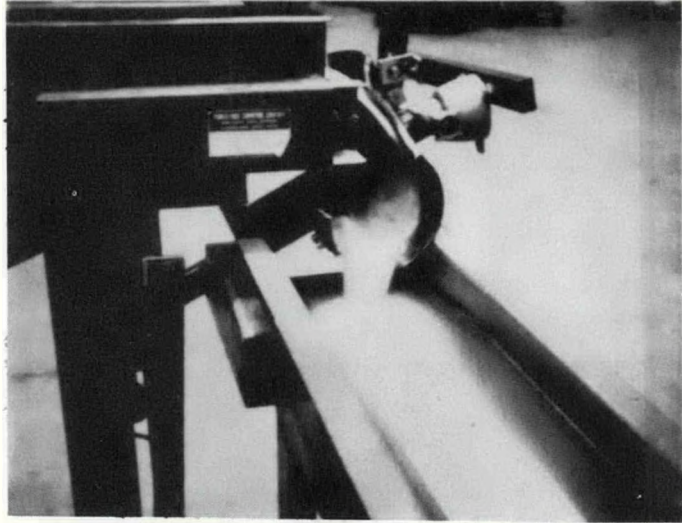
When properly aligned and located relative to the free fall trajectory from the head pulley, both the torus and the cone configurations possess good stream cohesion immediately after impact. The opening half angle cone concepts (1 and 2) tend to lose cohesiveness shortly after impact, however, due to the divergence of this opening angle (Figure 8). The torus and zero half angle cone maintain cohesion for specific positions and orientations (Figure 9).

In the case of the quarter cylinder configurations, impact of the free fall trajectory results in a stream pattern ranging from a diffuse fan to two broadly divergent forks (Figure 10). Movement of the chute in a vertical direction tended to vary the

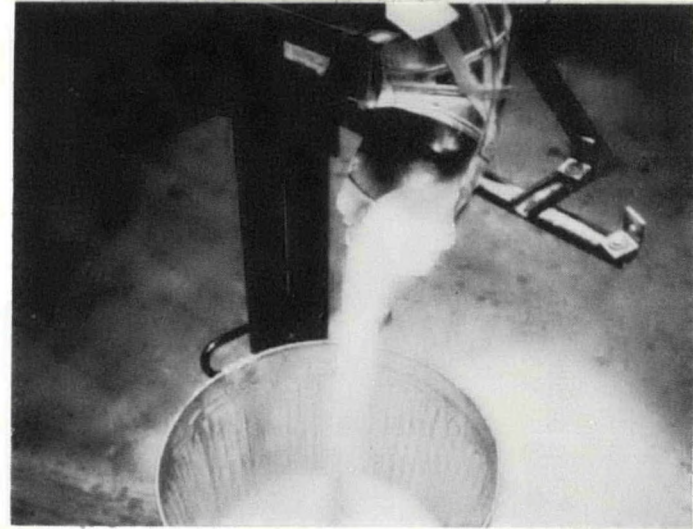


Flow Divergence
Cone Concepts (1, 2)

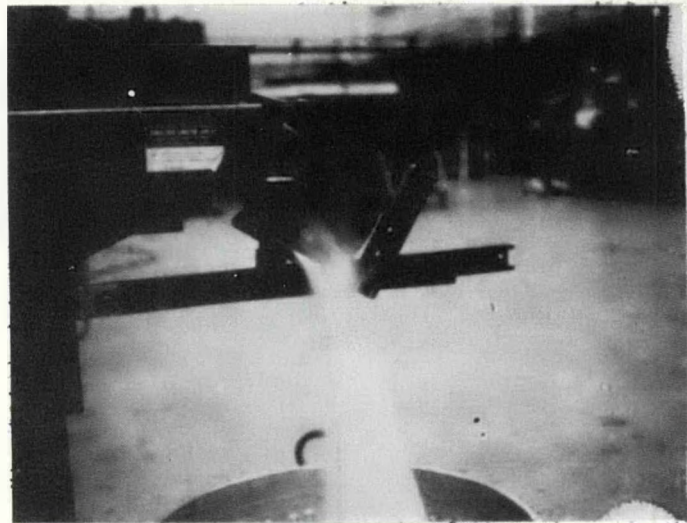
Figure 8



True (Smooth) Torus



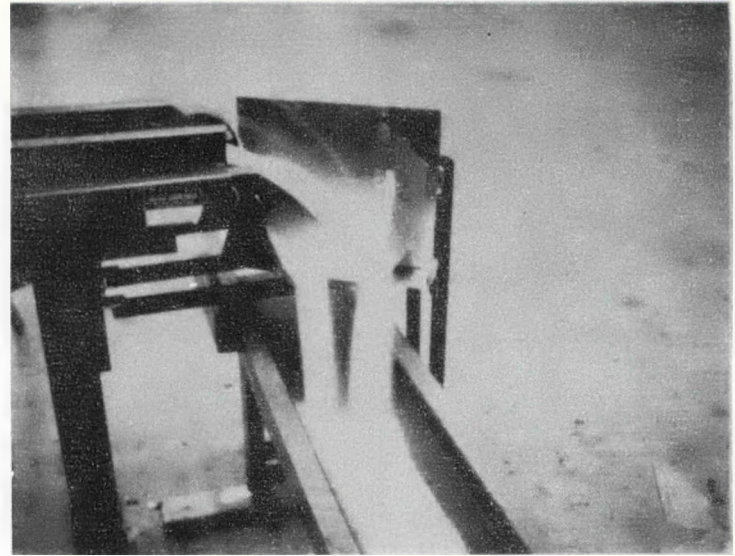
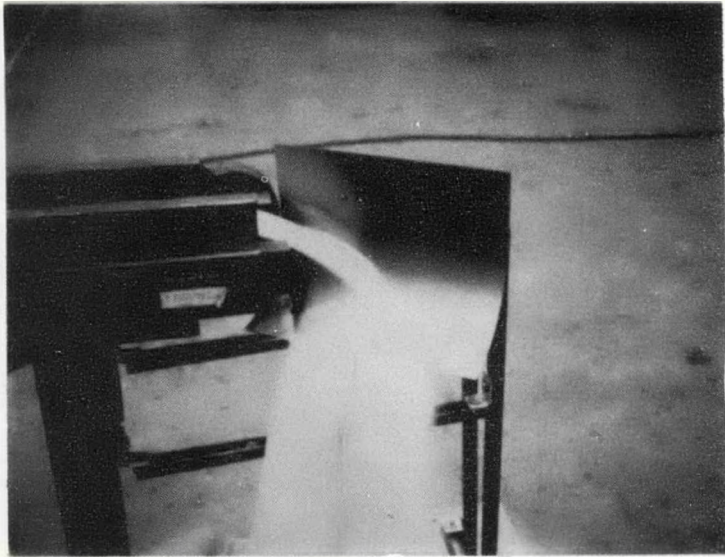
Smokepipe Torus



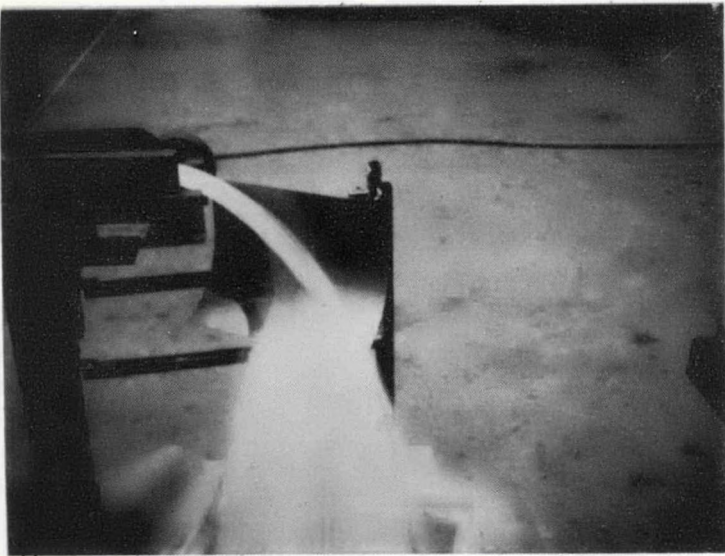
Zero Half Angle Cone

Stream Cohesion Cases

Figure 9



F-42



Stream Diffusion/Splitting Characteristics
Quarter Cylinder Concepts (4, 5)

Figure 10

pattern somewhat, with the least divergent corresponding to an extremely large headroom figure in excess of 78 inches (full scale) from the top of the feeder belt to the lower edge of the chute.

4. 2. 2. 2 Belt Impact Vector

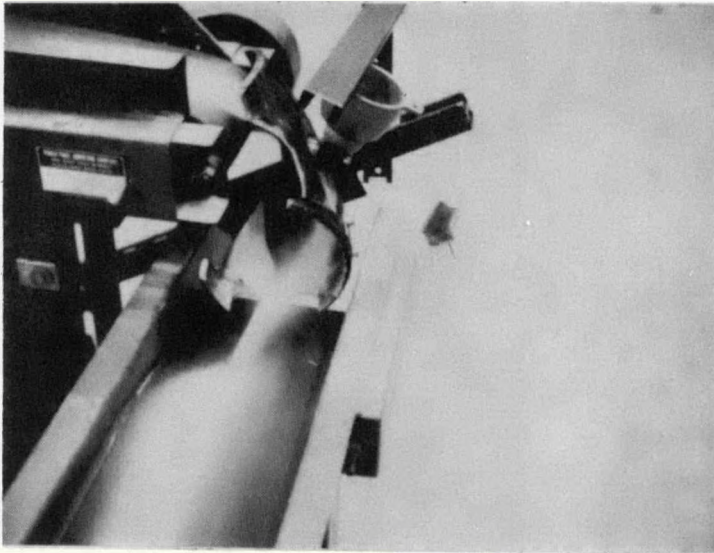
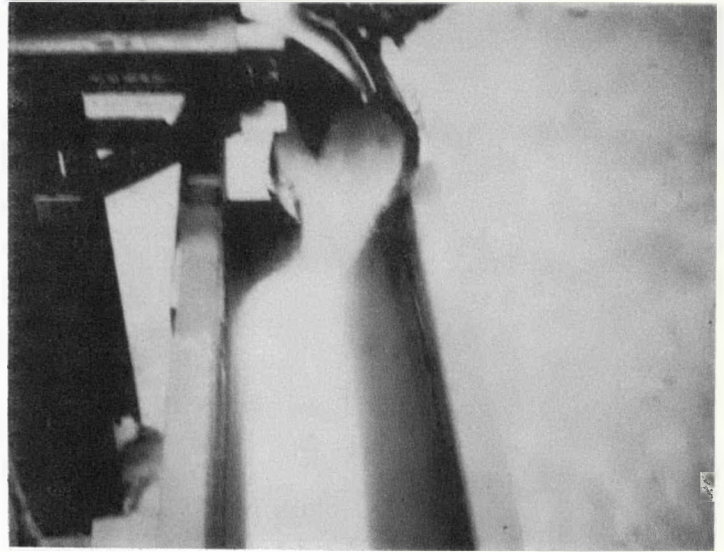
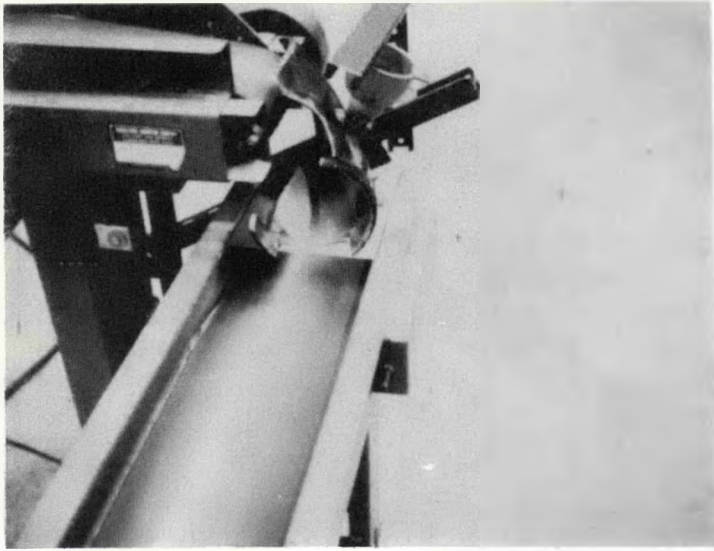
The quarter cylinder and toroidal configurations rank well in this area because of the common characteristic of a vertical curve in the direction of forced flow. Thus, the flow can be caused to leave the chute at a direction not more than 10 to 15 degrees down from the horizontal.

Lacking this vertical curve, the cone configurations will necessarily have a 35 to 45 degree output inclination angle. In an attempt to reduce the downward velocity component, a short curved lip was provided at the lower edge of the cone tested (Figure 2A), but it appeared that this substantial change of direction over a short distance tended to scatter the flow.

Tests revealed no significant clogging sensitivity among any of the candidate configurations, although the vertical curve shape identified previously, did sometimes demonstrate a slight tendency to build up flow depth in the case of the torus. In another area it was found that fine particles tended to travel a considerable distance around the pulley radius before falling and sometimes then tended to build up in the chute immediately below the pulley, for some chute altitudes (Figure 11). This build-up was frequently instrumental in turning the main flow coming down and across the chute from the opposite, or outboard, side relative to the head pulley.

4. 2. 2. 4 Convergence

Convergency of the different candidate shapes in retrospect, should have been relatively predictable. The opening angle cones were divergent, as was the single quarter cylinder configuration. It was found that the addition of the side walls in the case of the compound cylinder configuration achieved an artificial convergency, howbeit a rather turbulent one.



Buildup and Dynamic Effects of Fines
for Some Torus Configurations

Figure 11

4. 2. 2. 5 Jam Clearance

Jam clearance is defined here as the distance between the feed pulley surface and the free fall impact point on the chute at the center of flow. It is an arbitrary measure of the likelihood of large pieces of rock to clear between the pulley and the chute and to execute the turn to the lower without jamming. The reason it is a factor at all in chute configurations evaluated here relates to the stream cohesion requirement, whereby impacting flow must meet the chute surface at a relatively low angle of incidence. To achieve this, the tangent to the local wall surface in this impact area needs to be at an altitude ranging between vertical to one leaning slightly toward the pulley. Moreover, the location of this impact point must be as close as possible to the pulley surface to minimize headroom. Based on these criteria, the resulting jam clearances achieved during scale model testing of the different configurations are summarized below, as adjusted to full scale:

<u>Configuration</u>	<u>Jam Clearance (inches)</u>
1. Cone, Opening Angle	24
2. Cone , Flat Impact Plate	24
3. Cone, Zero Half Angle	9
4. Quarter cylinder, Angle	N/A
5. Quarter cylinder, Compound	N/A
6. Torus, True	17
7. Torus, Smoke Pipe	15

It can be concluded that the clearance for all but the zero half angle core are generally viable, although, as noted earlier, the clearances for the torus configurations as presently defined are slightly too small for good design and must be increased.

4. 2. 2. 6 Minimum Headroom

Allowing an additional 8 inches clearance between the bottom of the chute and the receiving belt, the preliminary headroom requirements for the various candidate configurations are summarized below, these figures reflecting test data:

<u>Configuration</u>	<u>Elevation Difference Belt-to-Belt, Inches</u>
Cone, Opening Angle	58

(Cont)	<u>Configuration</u>	<u>Elevation Difference</u>
2.	Cone, Flat Impact Plate	58
3.	Cone, Zero Half Angle	62
4.	Quarter cylinder, Single	40
5.	Quarter cylinder, Compound	40
6.	Torus, True	62
7.	Torus, Smoke Pipe	62

With the exception of configurations 4 and 5, these figures correspond to the minimum headroom positions for which stream cohesion is maintained. The effect of further decreasing the elevation difference in each case resulted in a part of the frictional stream being diverted above, rather than below the top of the impact zone. (Fig 12)

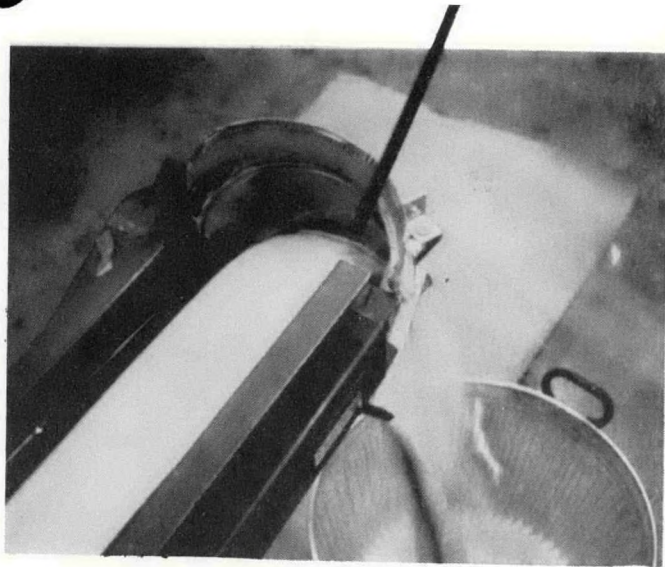
4.2.2.7 Installation Complexity

This area of evaluation, as well as the remaining three criteria, reflect very preliminary judgements. The ratings given to ease of installation are deliberately conservative and indicative of the need for more care in chute alignment to optimize stream cohesion, than is presently observed. Current alignment procedures, which emphasize centering the chute output flow on the receiving conveyor, will have to be broadened to obtain a smooth chute stream flow as well. However, it is not expected that this will introduce any special hardship or significant expenditure of time.

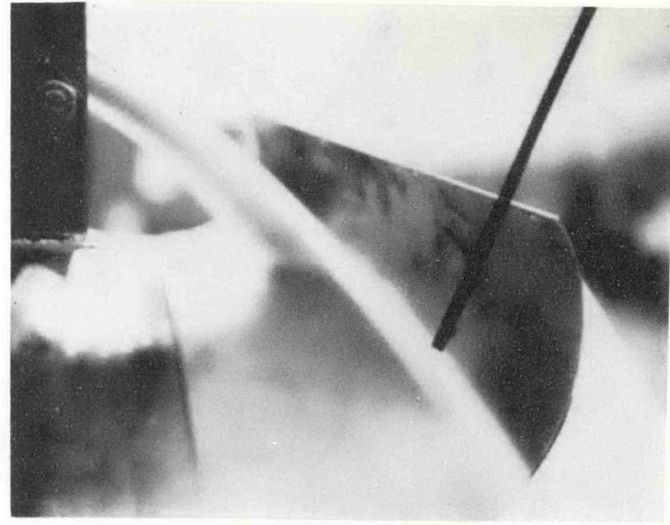
The relatively high scores given to the cylindrical configurations in ease of installation are somewhat misleading, in the sense that alignment efforts will not significantly improve stream cohesion.

4.2.2.8 Maintainability

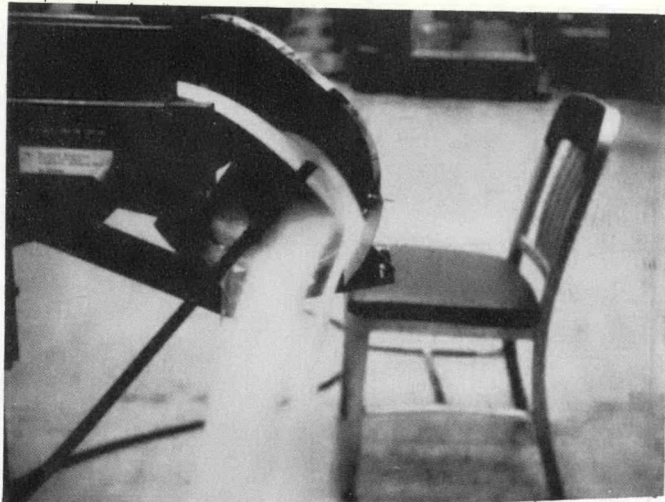
It is envisioned that, with the exception of the "true" torus, the slide surfaces of any of the candidate chute configurations would consist of piece-wise replaceable liner elements. These elements would be flat or single-degree-of-curvature plates and would be bolted to a support structure with flat head screws. The true torus slide surface, it is envisioned, would be made in a similar piece-wise



Smoke Pipe Torus



Cone



True (Smooth) Torus

F-47

Figure 12.
Typical Cases of Interference
between impacting and frictional flow
portions of stream

fashion of die-formed, two-degree-of-curvature elements. In this context, replacement time for worn portions of any of the candidate configurations should be essentially the same, although matching pieces with curvature is apt to require more care to achieve surface continuity. In general, maintainability here is a measure of the difficulty of procuring and maintaining an inventory of replacement elements. Flat patterns plainly can be fabricated locally, ensuring no inventory problem for linear configurations constructed of flat plates elements. This includes all cone and cylinder concepts. A single degree of curvature element, as might be required for the smoke pipe torus, should generally entail very little more fabrication capability. On the other hand, a die-formed piece, required for a true torus surface, most likely will involve some lead time,

4. 2. 2. 9 Producibility

This subject has already been largely covered in the previous section. Only the true torus involves a potential problem from the standpoint of construction. The support structure design for the liner wall mosaic will necessarily involve moderate tolerances to ensure surface smoothness, and this may dictate some jiggling, especially where single or double curvature is involved.

4. 2. 2. 10 Initial Cost

Here the highest ratings are arbitrarily given on the basis of surface shape simplicity, with the simplest shapes being the zero half angle cone---in reality a 180 degree cylinder --- and the single quarter cylinder. The other cone configurations involve a little more structural jiggling cost, and the compound cylinder still more due to the cylindrical intersections involved. The torodial configuration ratings on cost are quite conservative, and probably more nearly reflect prototype development rather than production.

APPENDIX G

TORUS CHUTE MATH MODEL



1. BASIC OFFSETS PRIOR TO ROTATION

a. LINEAR OFFSETS, FROM ORIGIN

- INDEPENDENT {
- X_T - X OFFSET TO ϕ OF BASIC TORUS PRIOR TO ROTATIONS
 - Y_T - Y OFFSET TO TOP OF BASIC TORUS PRIOR TO ROTATIONS
 - Z_T - Z OFFSET OF ϕ OF BASIC TORUS AT TOP PRIOR TO ROTATIONS

b. ROTATIONS ABOUT ORIGIN

- INDEPENDENT {
- GAMMA (γ) = ROLL, ABOUT Z AXIS
 - ZIH (θ) = PITCH, ABOUT X AXIS
 - LAMDA (λ) = YAW, ABOUT Y AXIS (NOT SHOWN BELOW)

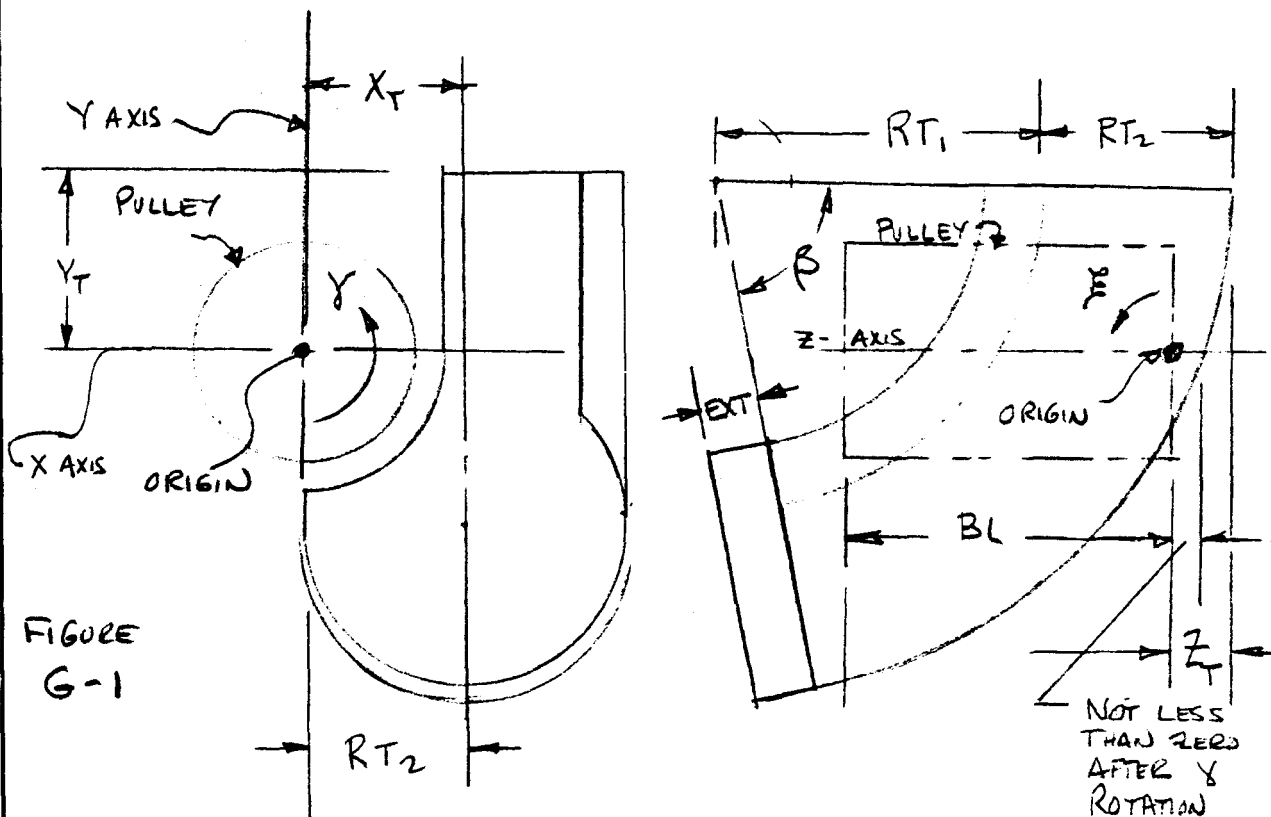


FIGURE
G-1

CHUTE PRIOR TO ROTATIONS

PREPARED BY	CHECKED BY	DATE	REV.
-------------	------------	------	------



2. DERIVATION OF CASE PARAMETERS

a. ZT OFF SET, REQ'D PRIOR TO ROTATION

SET BACK SURFACE OF CHUTE AT
PULLEY & LEVEL EVEN WITH RIGHT
HAND END OF PULLEY (Z=0)
AFTER ROLL ROTATION (γ)

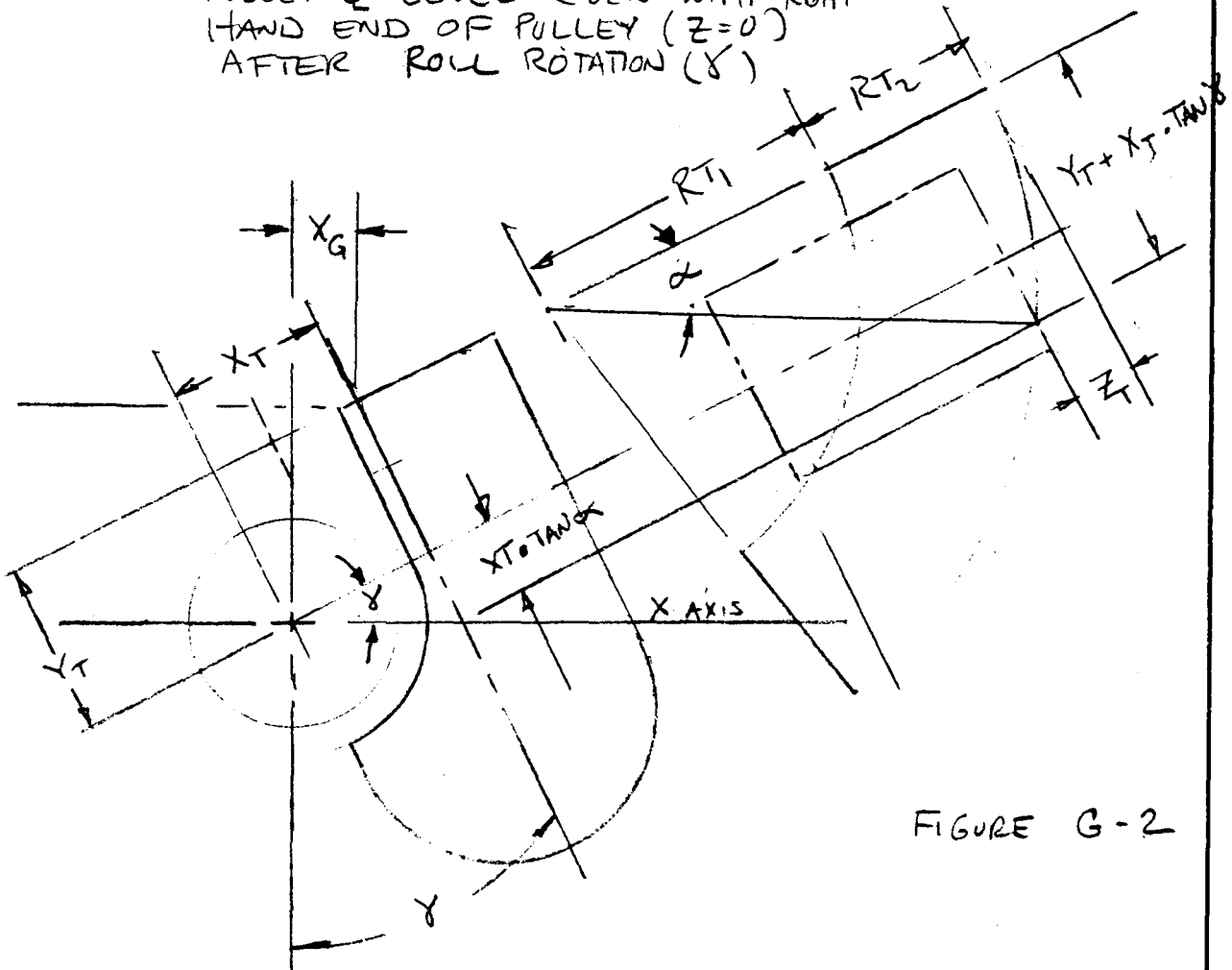


FIGURE G-2

$$\alpha = \sin T$$

$$\text{WHERE } T = \frac{Y_T + X_T \cdot \tan(\gamma)}{R_{T1} + R_{T2}}$$

PREPARED BY

CHECKED BY

DATE

REV.



20 CONT.

$$Z_T = (R_{T1} + R_{T2}) (1 - \cos \alpha)$$

$$X_G = (Y_T + X_T \cdot \tan \gamma) \cos \delta$$

$$Y_G = X_T \cos \delta - Y_T \sin \delta$$

b. AFTER ROTATION - β

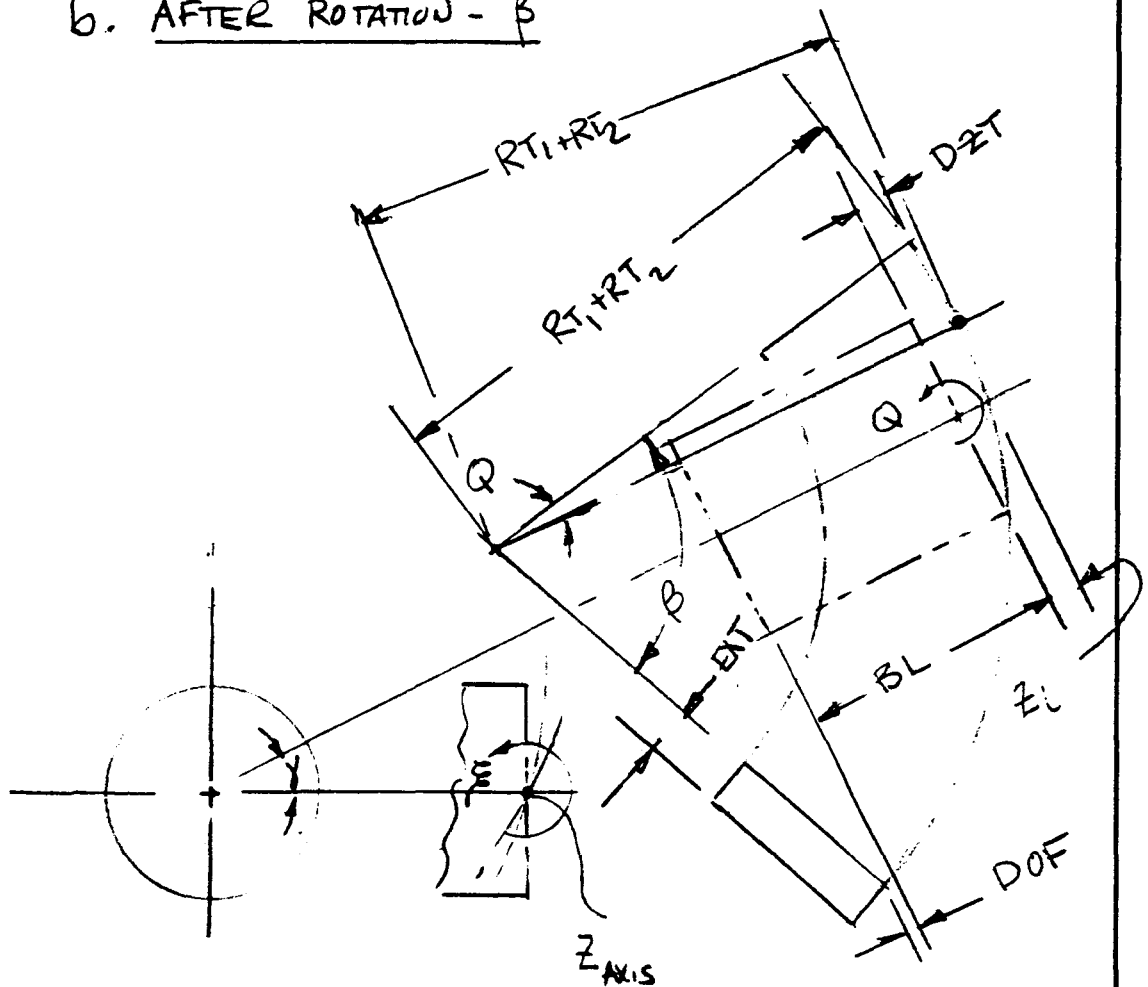


FIGURE G-3

PREPARED BY	CHECKED BY	DATE	REV.
-------------	------------	------	------



2 CONT

$$Q = \sin^{-1} \left[\frac{2 RT_2 \cdot \sin \xi \cdot \cos \gamma}{2 RT_2} \right]$$

$$= \sin^{-1} (\sin \xi \cdot \cos \gamma)$$

$$\cos(\beta - Q) = \frac{RT_1 + RT_2 - (BL + DOF + Z_L)}{RT_1 + RT_2}$$

$$\beta = \cos^{-1} \left[\frac{(RT_1 + RT_2) - (DOF + BL + Z_L)}{RT_1 + RT_2} \right] - Q$$

CORRECTING FORESHORTENING DUE TO
YAW AND NEGLECTING Z_L ,

$$\beta_{\text{APPROX}} = \cos^{-1} \left[\frac{(RT_1 + RT_2) - (DOF + BL)}{\cos(\text{YAW})(RT_1 + RT_2)} \right] - Q$$

3. SUBDIVISION INTO RECTANGULAR PLATES

A FLAT PATTERN OF A TOROIDAL SECTION WITH $NT_1 \times NT_2$ SUBDIVIDED PLATES IS SHOWN IN FIGURE G-4, WITH A TYPICAL PLATE NP HAVING CORNERS 1, 2, 3 & 4. DEFINITION OF WRAP-AROUND ANGLES A AND ψ IN RT_1 AND RT_2 PLANES IS SHOWN IN FIGURES G-5 & G-6, RESPECTIVELY.

PREPARED BY	CHECKED BY	DATE	REV.
-------------	------------	------	------

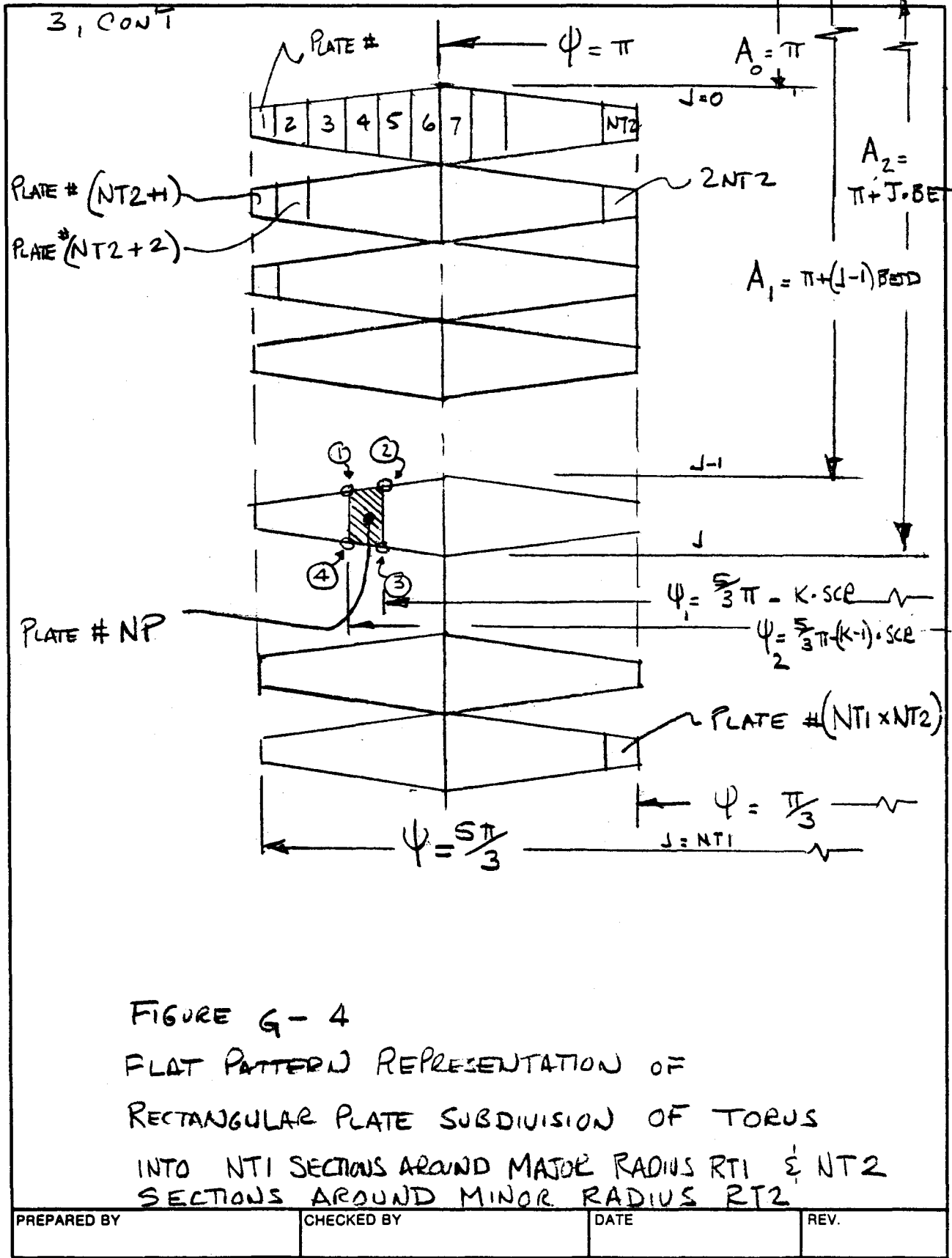


FIGURE G-4
 FLAT PATTERN REPRESENTATION OF
 RECTANGULAR PLATE SUBDIVISION OF TORUS
 INTO NT1 SECTIONS AROUND MAJOR RADIUS RT1 & NT2
 SECTIONS AROUND MINOR RADIUS RT2

PREPARED BY	CHECKED BY	DATE	REV.
-------------	------------	------	------



3. CONT

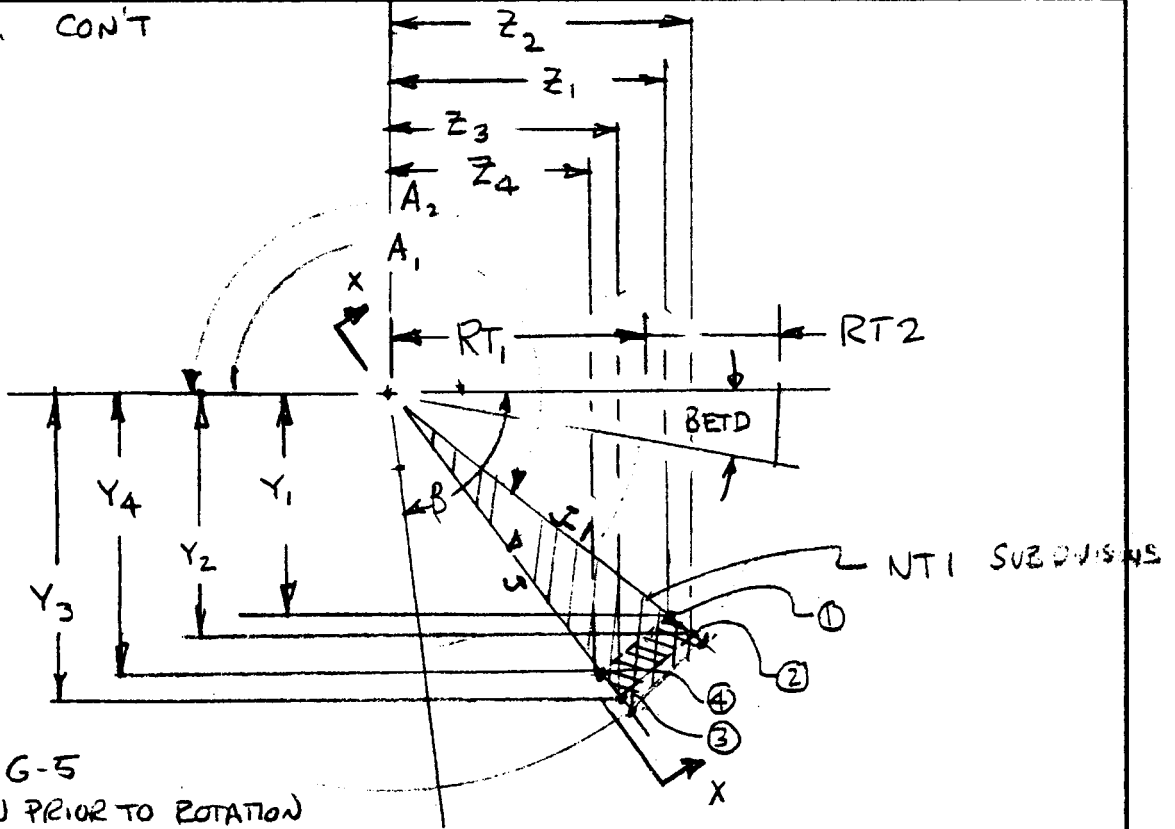


FIGURE G-5
VIEW PRIOR TO ROTATION

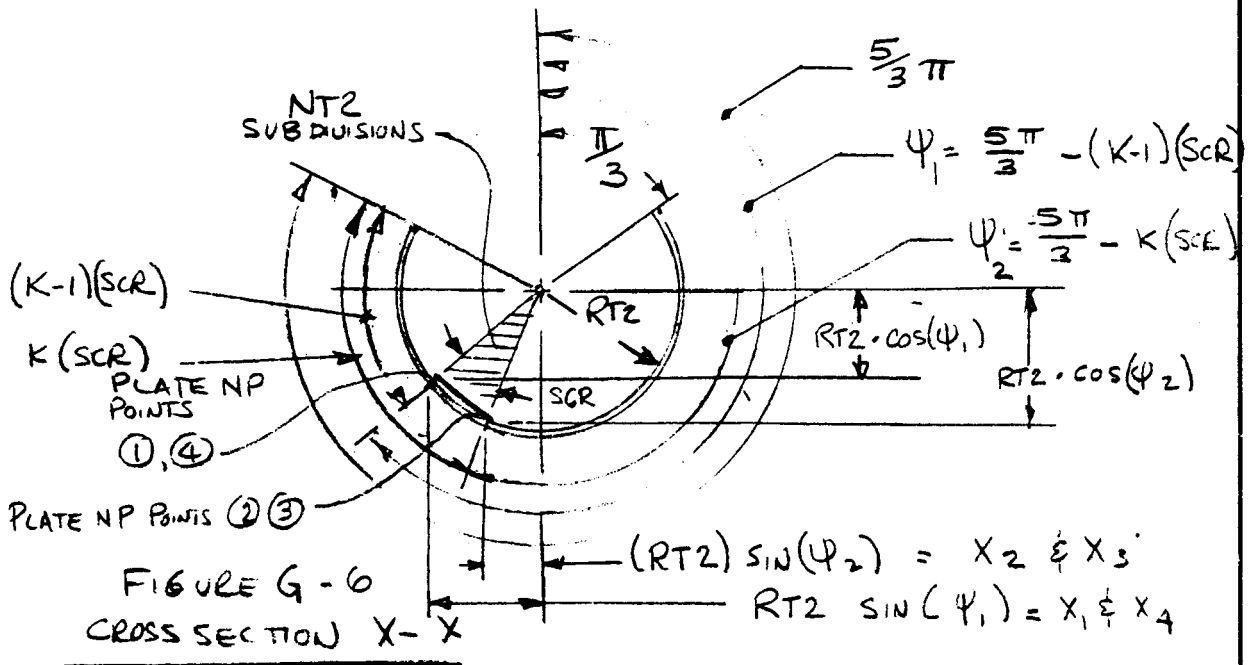


FIGURE G-6
CROSS SECTION X-X

PREPARED BY	CHECKED BY	DATE	REV.
-------------	------------	------	------



3. CONT

THE COORDINATES FOR THE 4 CORNERS OF TYPICAL PLATE NP ARE THE FOLLOWING, REFERRING TO FIGURES G-5 & G-6

CORNER #	CORNER		
	X	Y	Z
1	$RT_2 \cdot \sin \psi_1$	$(RT_1 - RT_2 \cdot \cos \psi_2) \sin A_1$	$(RT_1 - RT_2 \cdot \cos \psi_2) \cos A_1$
2	$RT_2 \cdot \sin \psi_2$	$(RT_1 - RT_2 \cdot \cos \psi_1) \sin A_1$	$(RT_1 - RT_2 \cdot \cos \psi_1) \cos A_1$
3	$RT_2 \cdot \sin \psi_2$	$(RT_1 - RT_2 \cdot \cos \psi_1) \cdot \sin A_2$	$(RT_1 - RT_2 \cdot \cos \psi_1) \cos A_2$
4	$RT_2 \cdot \sin \psi_1$	$(RT_1 - RT_2 \cdot \cos \psi_2) \cdot \sin A_2$	$(RT_1 - RT_2 \cdot \cos \psi_2) \cos A_2$

PREPARED BY

CHECKED BY

DATE

REV.

APPENDIX H

COMPUTER ANALYTICAL RESULTS

Appendix H Contents

<u>Section</u>	<u>Description</u>	<u>Page</u>
H-1	Free Fall/Impact Analysis Results	H-1
	350 FPM Trajectory Case (Runs 626, 627)	H-2
	450 FPM Trajectory Case (Runs 746, 706)	H-2
	600 FPM Trajectory Case (Runs 846, 806)	H-44
H-2	Frictional Flow Analysis Results	H-65

SECTION H-1

FREE FALL/IMPACT ANALYSIS RESULTS

350 FPM TRAJECTORY IMPACT CASE

RUNS 626, 627

BEGIN INDEPENDENT RUN OF COAL CHUTE DESIGNER

RUN NUMBER626

DATE 27 APR 77 20 16 27

..... INDEPENDENT VARIABLES FOR THIS RUN

A. INPUT DATA

FEED CONVEYOR DATA

TORUS CHUTE DATA

BELT SPEED V , IPS. 70.00

MAJOR RADIUS RT1, IN 36.00

PULLEY RADIUS R, IN. 12.00

MINOR RADIUS RT2, IN. 18.00

BELT WIDTH BELTWD IN. 36.00

ROTATIONS,DEG.
Z-AXIS-GAMMA 25.00
Y AXIS-YAW 0.0
X-AXIS-ZIH 0.0

H-3

BELT EDGE DISTANCE BMAR IN. 2.00

TROUGH ANGLE IDLANG DEG. 35.00

EXTRA LENGTH DISP IN. 0.0

SURCHARGE ANGLE SURANG DEG. 25.00

COORDINATES PRIOR TO ROTATION
XT IN. 5.00
YT IN. 10.00

INCLINATION ANGLE PHI DEG. 0.0

FLAT PLATE DIVISION
MAJOR RADIUS-NT1 7
MINOR RADIUS-NT2 7

RUN OF MINE COAL DATA

RUN CONVENTION CONSTANTS

DENSITY, GAMD LBS./CU. FT. 50.00

EFFECTIVE ANGLE OF FRICTION DELTF DEG. 50.00

FRICTION STEP DISTANCE - NOM.,EL1, IN. 1.00

DYNAMIC ANGLE OF WALL FRICTION PHIP DEG. 30.00

NO OF STREAM SUBDIVISIONS SECT 21

===== SUMMARY OF KEY CALCULATED PARAMETERS AND FINAL PLATE COORDINATES =====

U. OUTPUT DATA

PULLEY CONTACT DEP. ANGLE, DEG., 32.76
INITIAL LOAD HEIGHT, IN. 7.52
TORUS CUTOFF ANGLE, DEG. 105.33
MINIMUM Y COORDINATE -39.38

PLATE 1

0.305	8.462	14.122	6.230
11.176	14.980	2.841	-1.530
-1.427	0.985	2.754	0.425

PLATE 2

8.462	14.433	19.371	14.122
14.980	17.764	7.176	2.841
0.985	7.573	9.116	2.754

PLATE 3

14.433	16.619	20.569	19.371
17.764	18.783	10.313	7.176
7.573	16.573	17.808	9.116

PLATE 4

16.619	14.433	17.396	20.569
18.783	17.764	11.411	10.313
16.573	25.573	26.499	17.808

PLATE 5

6.230	14.122	19.395	11.749
-1.530	2.841	-8.465	-13.365
0.425	2.754	7.939	5.853

PLATE 6

14.122	19.371	23.970	19.395
2.841	7.176	-2.687	-8.465
2.754	9.116	13.640	7.939

H-4

19.371	20.569	24.248	23.970
7.176	10.313	2.423	-2.687
9.116	17.808	21.426	13.640

PLATE 8

20.569	17.396	20.155	24.248
10.313	11.411	5.494	2.423
17.808	26.499	29.213	21.426

PLATE 9

-8.379	-4.286	-0.341	-5.223
-12.792	-15.863	-24.322	-19.559
21.426	13.639	20.833	27.181

PLATE 10

-4.286	3.081	7.604	-0.341
-15.863	-16.072	-25.771	-24.322
13.639	7.939	16.186	20.833

PLATE 11

3.081	11.749	16.483	7.604
-16.072	-13.365	-23.516	-25.771
7.939	5.853	14.485	16.186

PLATE 12

11.749	19.395	23.917	16.483
-13.365	-8.465	-18.164	-23.516
5.853	7.939	16.186	14.485

PLATE 13

19.395	23.970	27.914	23.917
-8.465	-2.687	-11.146	-18.164
7.939	13.640	20.833	16.186

PLATE 14

23.970	24.248	27.404	27.914
-2.687	2.423	-4.345	-11.146
13.640	21.426	27.181	20.833

PLATE 15

24.248	20.155	22.522	21.404
2.423	5.494	0.418	-4.345
21.426	29.213	33.529	27.181

PLATE 16

-5.223	-0.341	2.679	-2.807
-19.559	-24.322	-30.800	-24.741
27.181	20.833	30.203	34.677

PLATE 17

-0.341	7.604	11.066	2.679
-24.322	-25.771	-33.196	-30.800
20.833	16.186	26.928	30.203

PLATE 18

7.604	16.483	20.107	11.066
-25.771	-23.516	-31.289	-33.196
16.186	14.485	25.729	26.928

PLATE 19

16.483	23.917	27.380	20.107
-23.516	-18.164	-25.589	-31.289
14.485	16.186	26.928	25.729

PLATE 20

23.917	27.914	30.935	27.380
-18.164	-11.146	-17.624	-25.589
16.186	20.833	30.203	26.928

PLATE 21

27.914	27.404	29.820	30.935
-11.146	-4.345	-9.527	-17.624
20.833	27.181	34.677	30.203

PLATE 22

27.404	22.522	24.544	29.820
-4.345	0.418	-3.468	-9.527
27.181	33.529	39.151	34.677

PLATE 23

-2.807	2.679	4.568	-1.296
--------	-------	-------	--------

34.677

30.203

41.103

43.401

PLATE 24

2.679
-30.800
30.203

11.066
-33.196
26.928

13.231
-37.839
39.429

4.568
-34.850
41.108

PLATE 25

11.066
-33.196
26.928

20.107
-31.289
25.729

22.374
-36.149
38.815

13.231
-37.839
39.429

PLATE 26

20.107
-31.289
25.729

27.380
-25.589
26.928

29.545
-30.232
39.429

22.374
-36.149
38.815

PLATE 27

27.380
-25.589
26.928

30.935
-17.624
30.203

32.823
-21.674
41.108

29.545
-30.232
39.429

PLATE 28

30.935
-17.624
30.203

29.820
-9.527
34.677

31.331
-12.767
43.401

32.823
-21.674
41.108

PLATE 29

29.820
-9.527
34.677

24.334
-3.468
39.151

25.467
-5.899
45.694

31.331
-12.767
43.401

PLATE 30

-1.296
-27.981
43.401

4.568
-34.850
41.108

5.195
-36.195
52.798

-0.794
-29.058
52.753

PLATE 31

4.568
-34.850
41.108

13.231
-37.839
39.429

13.951
-39.382
52.831

5.195
-36.195
52.798

PLATE 32

13.231
-37.839
39.429

22.374
-36.149
38.815

23.126
-37.764
52.843

13.951
-39.382
52.831

PLATE 33

22.374
-36.149
38.815

29.545
-30.232
39.429

30.264
-31.775
52.831

23.126
-37.764
52.843

"R"

PLATE 34

29.545
-30.232
39.429

32.823
-21.674
41.108

33.451
-23.019
52.798

30.264
-31.775
52.831

PLATE 35

32.823
-21.674
41.108

31.331
-12.767
43.401

31.833
-13.843
52.753

33.451
-23.019
52.798

PLATE 36

31.331
-12.767
43.401

25.467
-5.899
45.694

25.844
-6.706
52.708

31.833
-13.843
52.753

B. OUTPUT DATA

1. HIT DATA

6-H

STREAM	TIME	ANGLE	X	C.G.		Z	ANGLE	BOTTOM		PLATE	TOP			
				Y	Z			X	Y		ANGLE	X	Y	PL
1	0.12	-24.3	14.1	2.7	2.8	5	-24.3	13.8	2.3	5	-13.5	13.8	3.8	2
2	0.14	-21.9	15.5	1.7	4.3	6	-23.5	15.7	-0.5	5	-12.4	15.4	4.0	2
3	0.16	-20.5	16.9	0.5	5.8	6	-19.1	17.2	-3.2	6	-22.1	16.7	3.9	6
4	0.18	-19.1	18.4	-1.2	7.3	6	-17.5	18.7	-6.1	6	-21.0	18.1	3.5	6
5	0.20	-17.8	19.8	-3.2	8.9	6	-26.2	20.0	-8.8	13	-19.8	19.5	2.6	6
6	0.22	-16.6	21.3	-5.5	10.4	6	-25.4	20.8	-10.6	13	-18.6	20.9	1.2	6
7	0.24	-25.7	22.3	-7.1	11.9	13	-24.7	21.6	-12.5	13	-17.4	22.3	-0.6	6
8	0.25	-25.1	23.1	-8.6	13.4	13	-24.1	22.5	-14.4	13	-16.3	23.8	-2.9	6
9	0.26	-24.4	24.0	-10.3	15.0	13	-23.5	23.3	-16.4	13	-25.5	24.7	-4.3	13
10	0.28	-23.8	24.8	-12.1	16.5	13	-31.4	24.0	-18.3	20	-8.3	25.4	-5.4	14
11	0.29	-23.3	25.6	-14.1	18.0	13	-48.6	24.5	-19.5	19	-7.5	26.2	-7.4	14
12	0.30	-31.3	26.2	-15.6	19.5	20	-48.4	24.9	-20.6	19	-23.6	27.2	-9.8	13
13	0.31	-31.0	26.6	-16.9	21.0	20	-48.2	25.3	-21.7	19	-31.5	27.8	-11.9	20
14	0.32	-30.6	27.0	-18.3	22.6	20	-48.1	25.7	-22.8	19	-31.1	28.2	-13.4	20

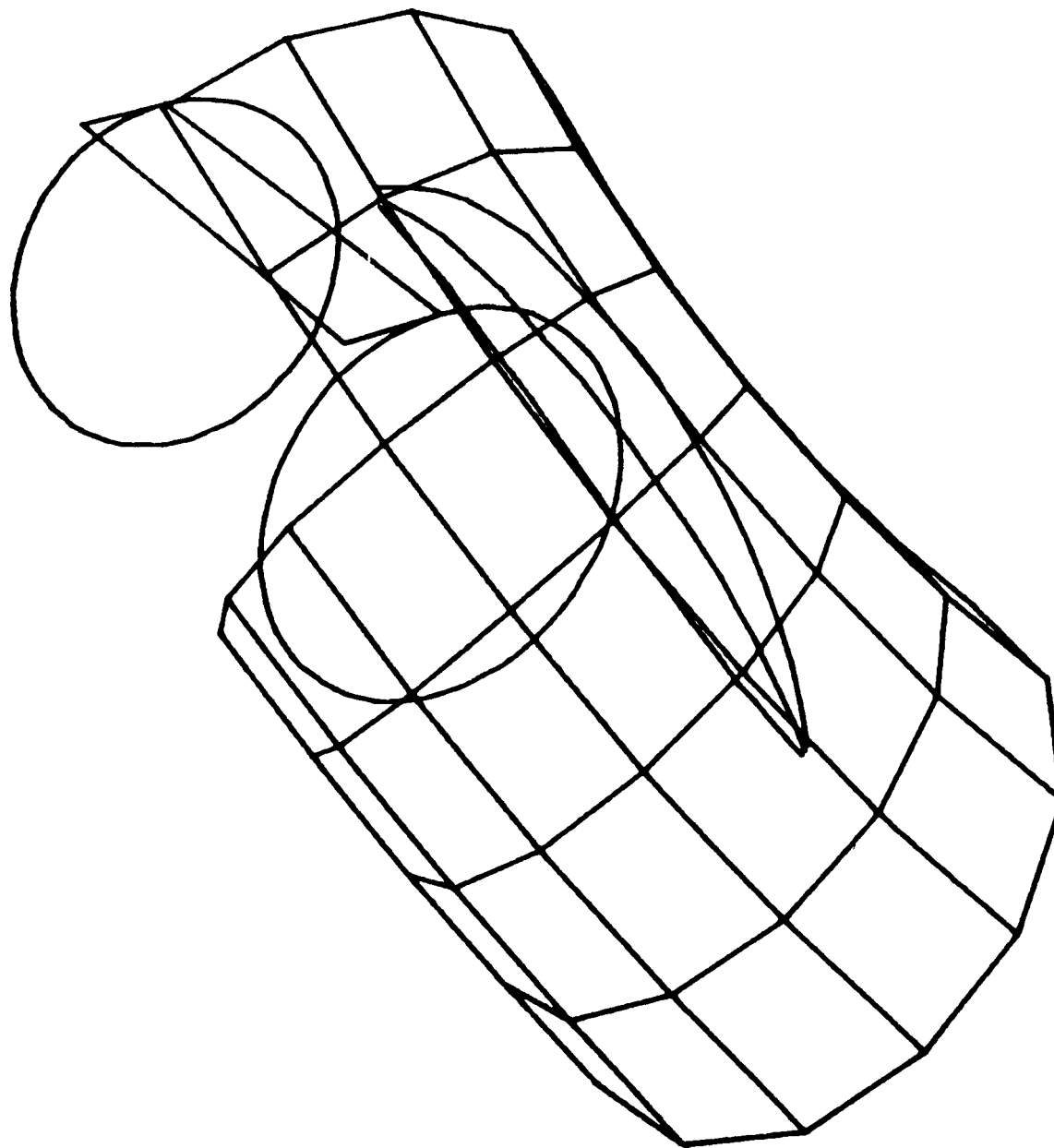
15	0.32	-30.3	27.4	-19.8	24.1	20	-47.9	26.1	-24.0	19	-30.7	28.0	-19.2	20
16	0.33	-30.0	27.8	-21.4	25.6	20	-47.8	26.5	-25.1	19	-30.4	28.8	-17.2	20
17	0.34	-29.7	28.1	-23.2	27.1	20	-59.8	26.9	-26.2	26	-30.0	29.0	-19.4	20
18	0.35	-35.7	28.2	-24.6	28.7	27	-59.7	27.1	-26.8	26	-35.9	29.1	-21.7	27
19	0.35	-35.5	28.2	-25.9	30.2	27	-59.6	27.3	-27.4	26	-35.7	29.0	-23.7	27
20	0.36	-35.3	28.2	-27.3	31.7	27	-59.5	27.5	-28.0	26	-35.4	28.7	-25.8	27
21	0.36	-59.4	28.0	-28.4	33.2	26	-59.4	-7.7	-28.6	26	-59.4	28.2	-28.1	26

3-D VIEW

RUN 626

ELEMENTS

1,99999



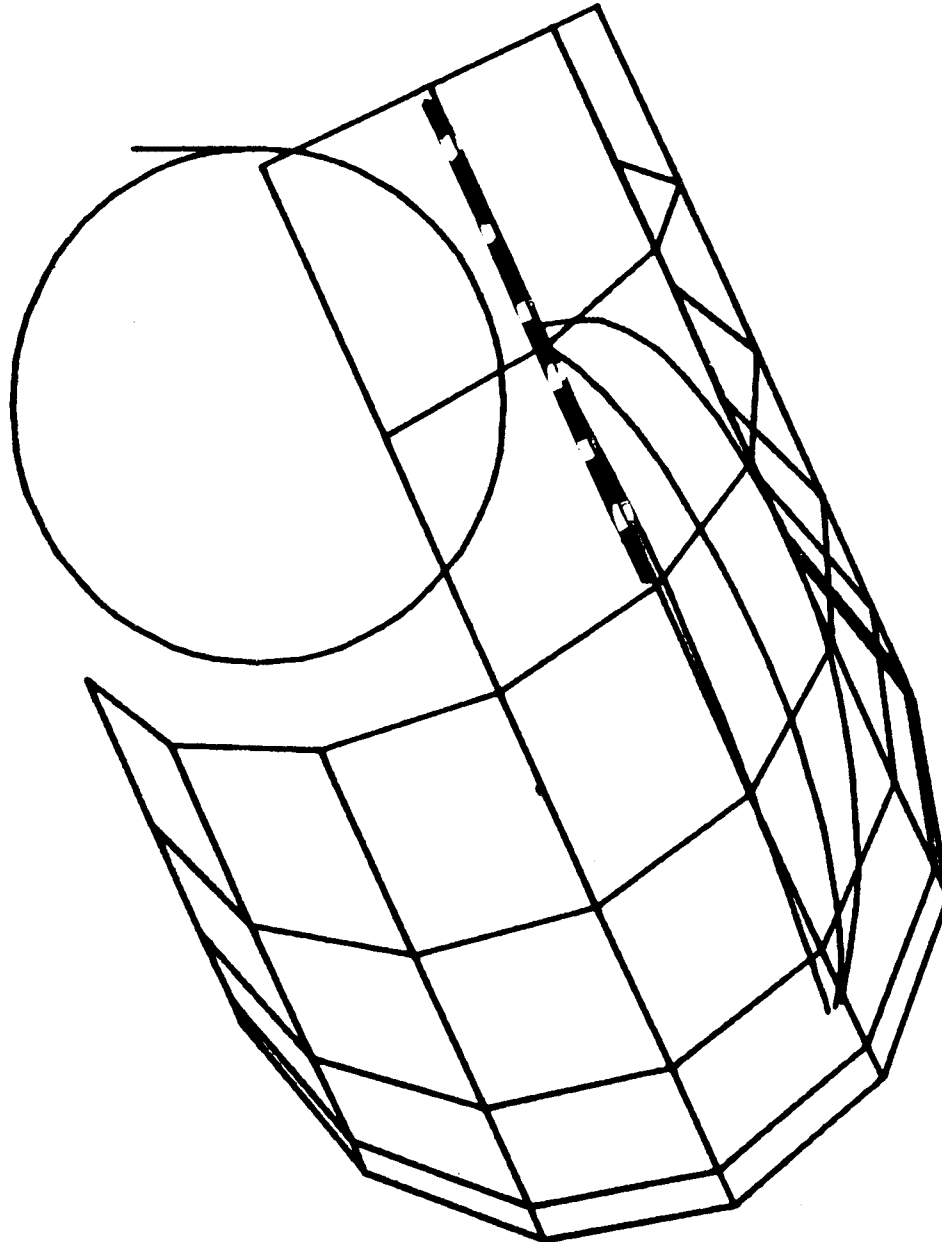
H-11

FRONT VIEW

RUN 626

ELEMENTS

1,99999



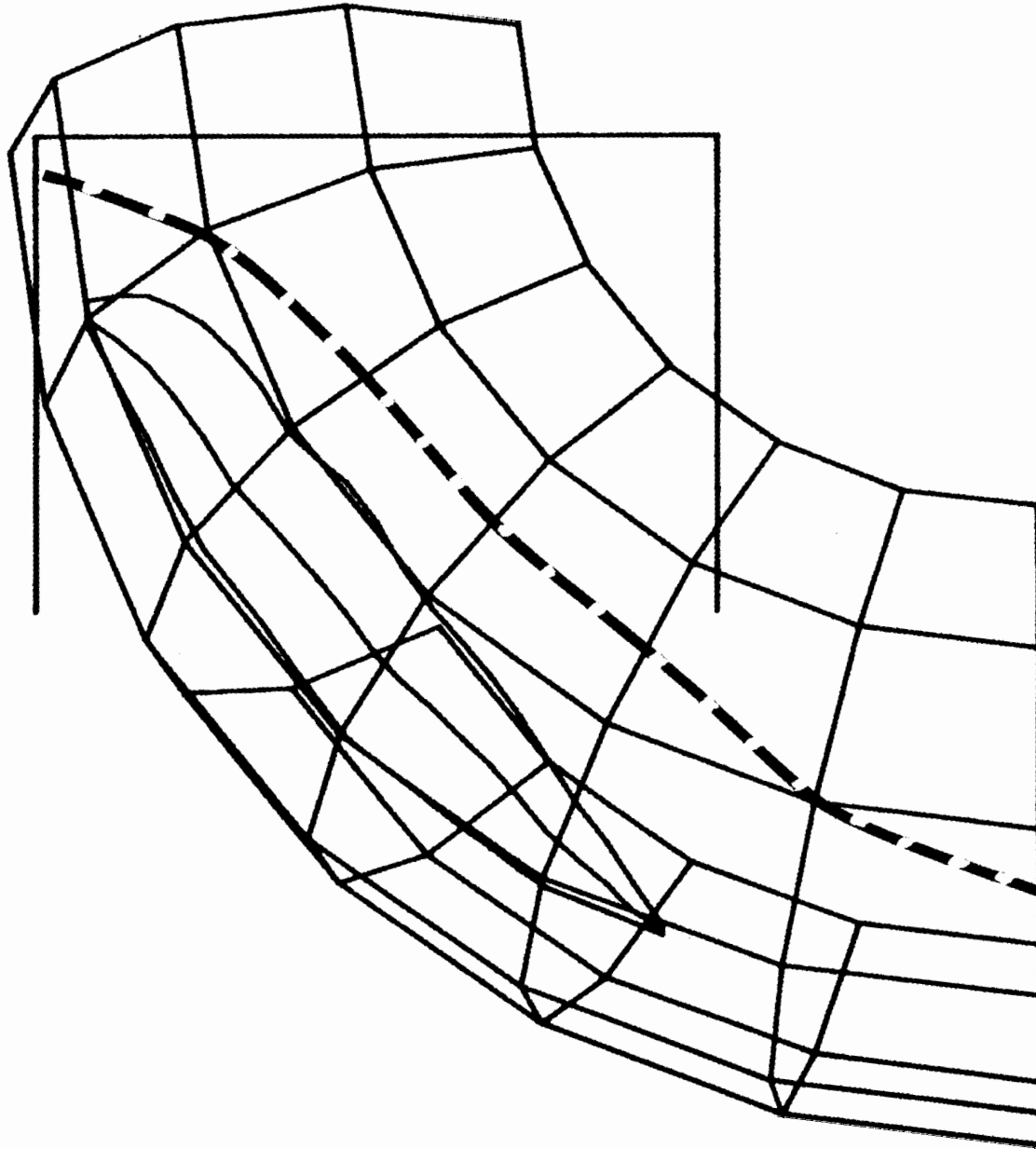
H-12

SIDE VIEW

RUN 626

ELEMENTS

1,99999



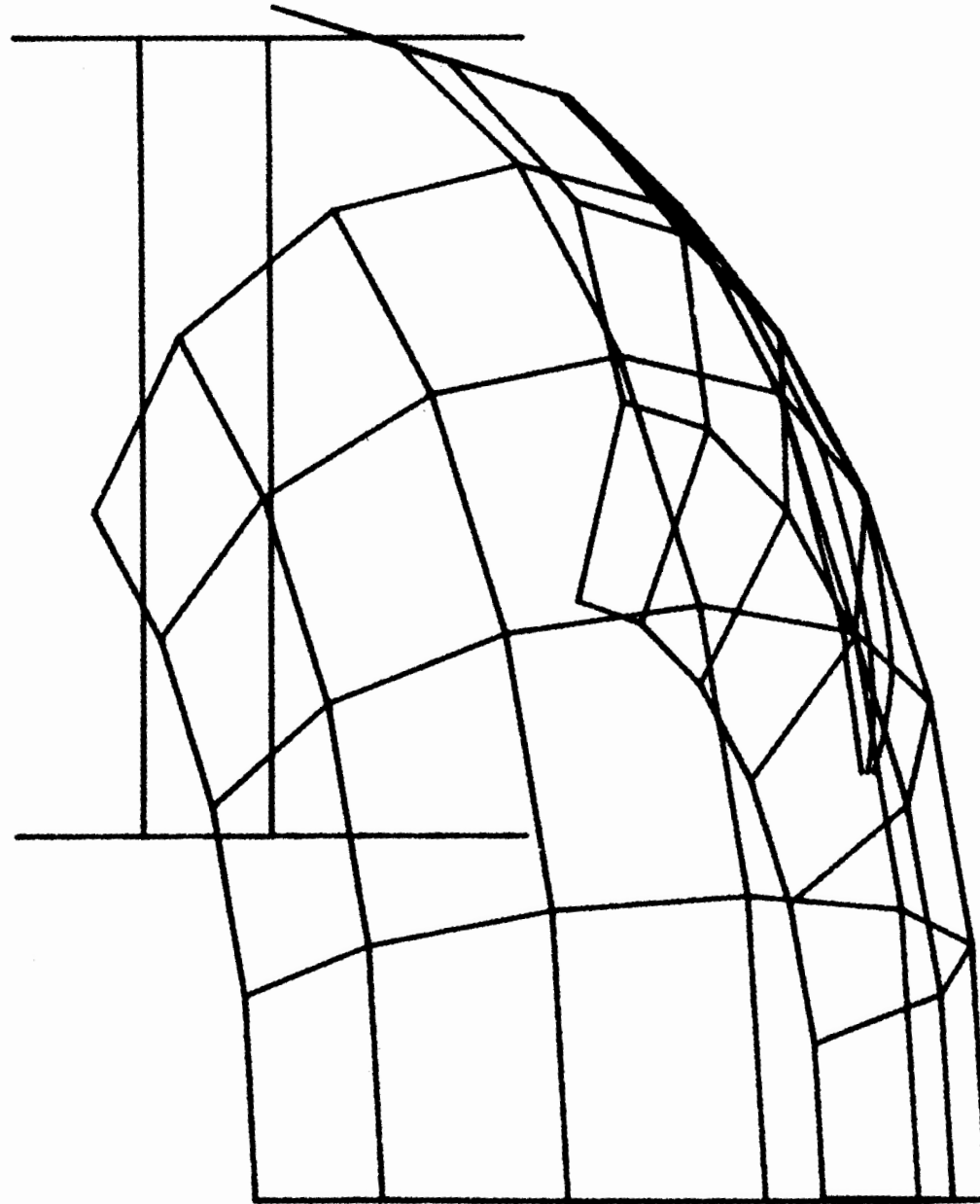
H-13

TOP VIEW

RUN 626

ELEMENTS

1,99999



H-14

BEGIN INDEPENDENT RUN OF COAL CHUTE DESIGNER

RUN NUMBER 627

DATE 27 APR 77 20 18 30

..... INDEPENDENT VARIABLES FOR THIS RUN

A. INPUT DATA

FEED CONVEYOR DATA

TORUS CHUTE DATA

BELT SPEED V , IPS. 70.00

MAJOR RADIUS RT1, IN 36.00

PULLEY RADIUS R, IN. 12.00

MINOR RADIUS RT2, IN. 18.00

BELT WIDTH BELTWD IN. 36.00

ROTATIONS, DEG.
Z-AXIS-GAMMA 25.00
Y AXIS-YAW 0.0
X-AXIS-ZIH 0.0

BELT EDGE DISTANCE BMAR IN. 2.00

TROUGH ANGLE IDLANG DEG. 35.00

EXTRA LENGTH DISP IN, 0.0

SURCHARGE ANGLE SURANG DEG. 25.00

COORDINATES PRIOR TO ROTATION
XT IN. 4.00
YT IN. 10.00

INCLINATION ANGLE PHI DEG. 0.0

FLAT PLATE DIVISION
MAJOR RADIUS-NT1 7
MINOR RADIUS-NT2 7

RUN OF MINE COAL DATA

RUN CONVENTION

CONSTANTS

DENSITY, GAMD LBS./CU. FT. 50.00

EFFECTIVE ANGLE OF FRICTION DELTF DEG. 50.00

FRICTION STEP DISTANCE - NOM., EL1, IN. 1.00

DYNAMIC ANGLE OF WALL FRICTION PHIP DEG. 30.00

NO OF STREAM SUBDIVISIONS SECT 21

ST-H

B. OUTPUT DATA

1. HIT DATA

H-16

STREAM	TIME	ANGLE	X	C.G.			Z	ANGLE	BOTTOM		PLATE	TOP		
				Y					X	Y		ANGLE	X	Y
1	0.09	-15.8	12.2	5.2	2.8	2	-14.8	12.6	4.1	2	-16.9	11.9	6.3	2
2	0.12	-13.0	14.3	3.5	4.3	2	-22.4	14.5	1.3	6	-15.7	13.3	6.8	2
3	0.14	-22.0	15.8	2.4	5.8	6	-20.4	16.0	-1.1	6	-13.9	15.0	6.4	2
4	0.16	-20.5	17.2	0.9	7.3	6	-18.7	17.5	-3.8	6	-22.5	16.9	5.3	6
5	0.18	-19.0	18.7	-0.9	8.9	6	-17.1	19.1	-6.8	6	-21.3	18.3	4.5	6
6	0.20	-17.7	20.1	-3.1	10.4	6	-26.1	20.1	-8.9	13	-19.9	19.7	3.3	6
7	0.23	-26.4	21.5	-5.4	11.9	13	-25.4	20.9	-10.8	13	-10.4	20.5	2.8	7
8	0.24	-25.7	22.4	-6.9	13.4	13	-24.7	21.7	-12.7	13	-10.2	20.9	2.8	7
9	0.25	-25.0	23.3	-8.6	15.0	13	-24.0	22.6	-14.6	13	-9.5	21.5	2.2	7
10	0.26	-24.4	24.1	-10.3	16.5	13	-23.4	23.4	-16.6	13	-8.4	22.4	0.9	7
11	0.28	-23.8	24.9	-12.3	18.0	13	-31.5	24.0	-18.1	20	-10.5	23.4	-1.1	14
12	0.29	-31.7	25.7	-14.2	19.5	20	-31.1	24.4	-19.3	20	-9.4	24.3	-3.2	14
13	0.30	-31.3	26.1	-15.5	21.0	20	-30.8	24.9	-20.6	20	-8.1	25.5	-6.1	14
14	0.31	-31.0	26.5	-16.9	22.6	20	-30.5	25.3	-21.8	20	-9.3	27.0	-10.3	21

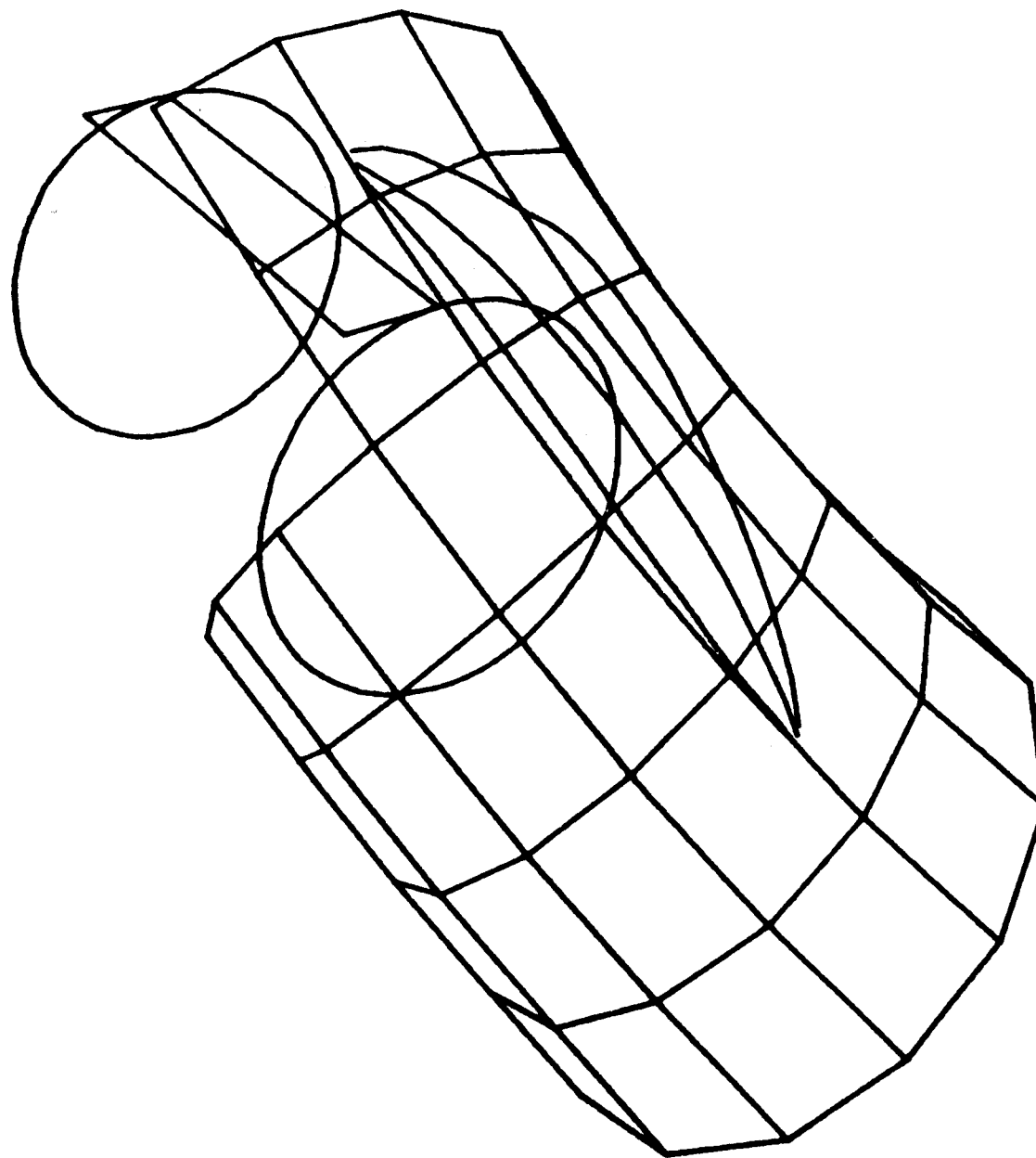
16	0.32	-30.3	27.2	-20.0	25.6	20	-29.9	26.2	-24.3	20	-30.7	28.3	-15.8	20
17	0.33	-30.0	27.6	-21.7	27.1	20	-29.6	26.6	-25.5	20	-30.3	28.5	-17.9	20
18	0.34	-36.0	27.8	-23.4	28.7	27	-35.7	26.9	-26.2	27	-29.9	28.7	-20.3	20
19	0.35	-35.8	27.8	-24.7	30.2	27	-35.6	27.1	-26.9	27	-35.9	28.6	-22.5	27
20	0.35	-35.6	27.8	-26.1	31.7	27	-35.5	27.3	-27.6	27	-35.7	28.3	-24.6	27
21	0.36	-35.3	27.7	-27.7	33.2	27	-35.3	27.6	-28.2	27	-35.4	27.9	-27.2	27

3-D VIEW

RUN 627

ELEMENTS

1,99999



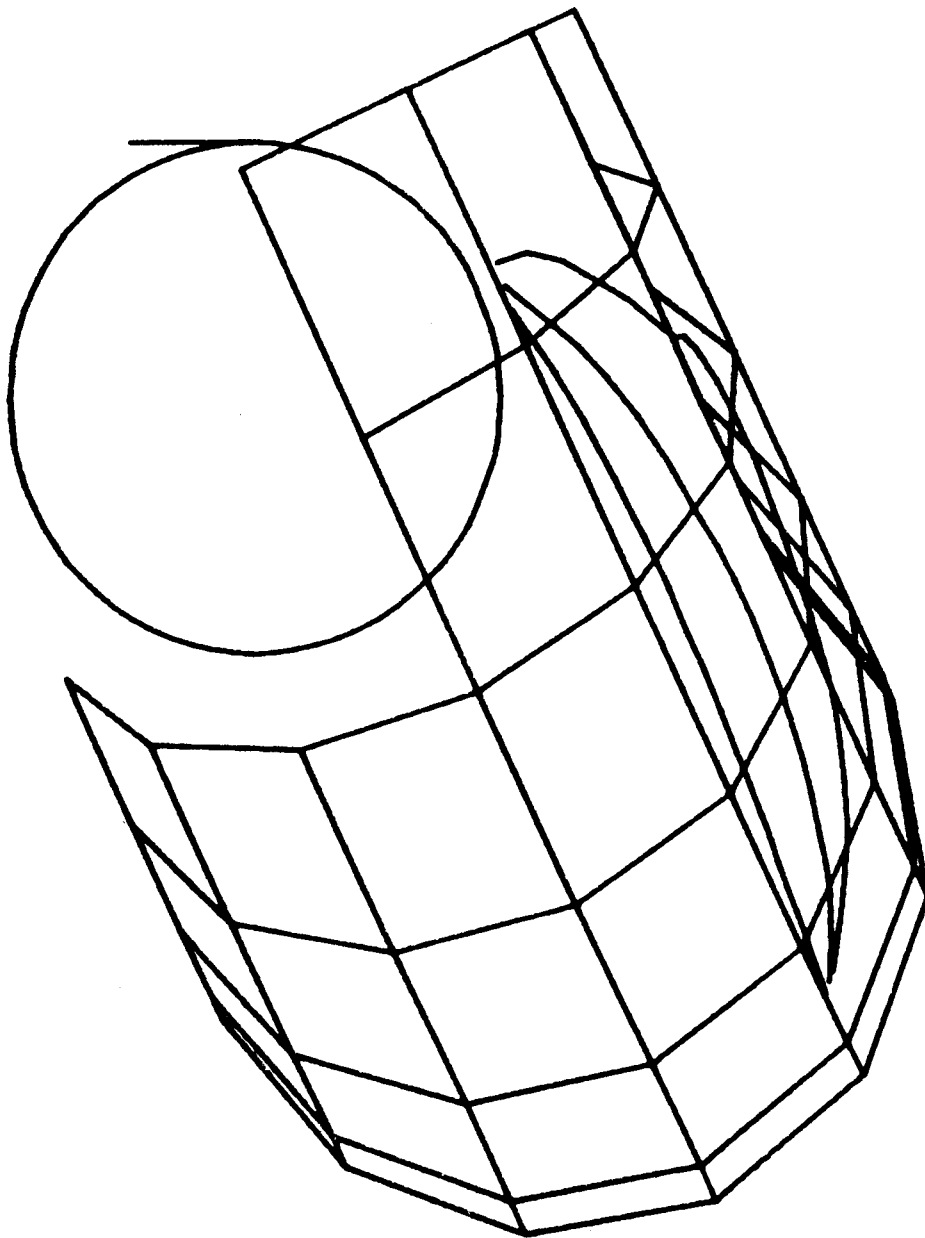
H-18

FRONT VIEW

RUN 627

ELEMENTS

1,99999



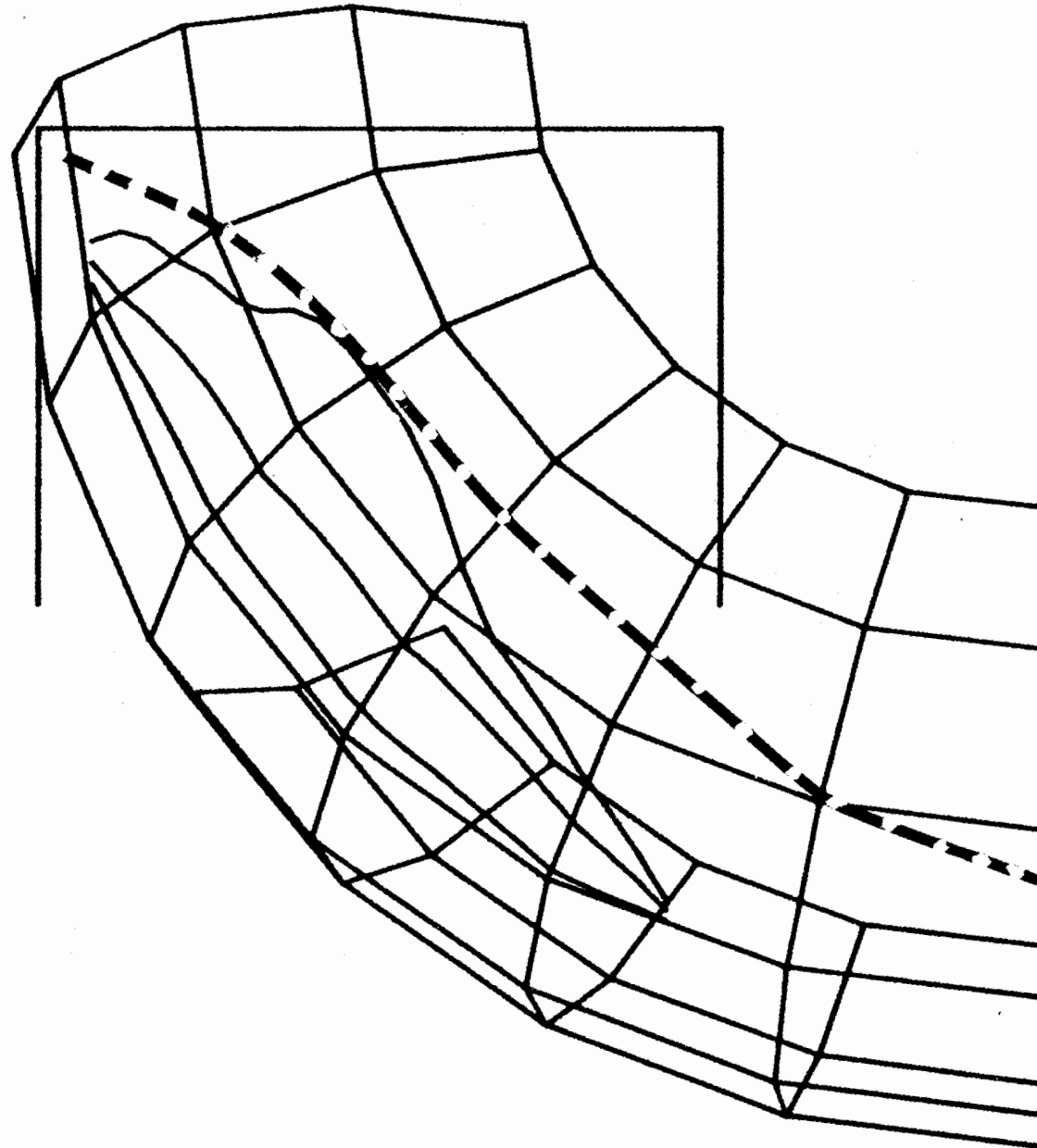
H-19

SIDE VIEW

RUN 627

ELEMENTS

1,99999



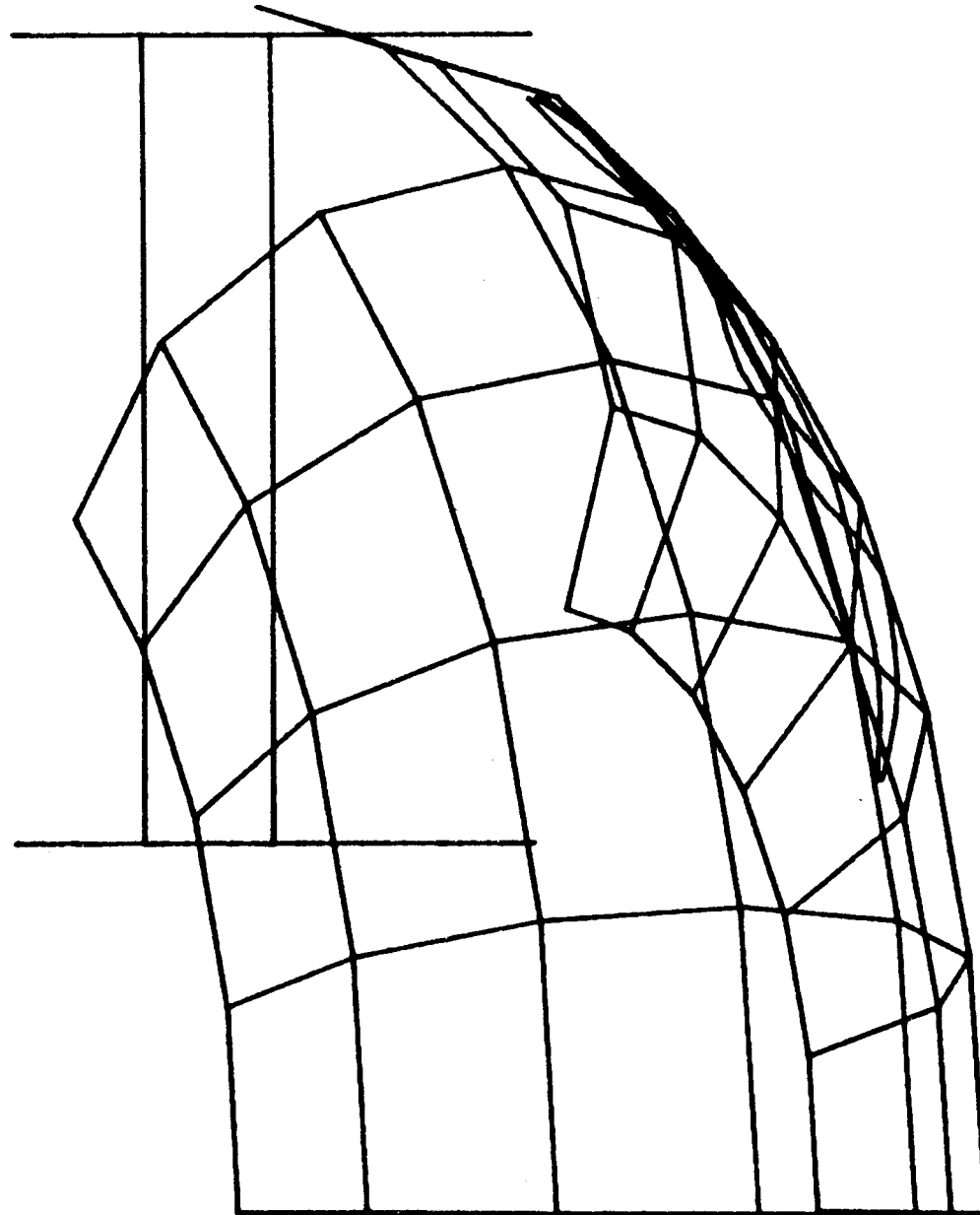
H-20

TOP VIEW

RUN 627

ELEMENTS

1,99999



H-21

450 FPM TRAJECTORY CASE

RUNS 746, 706

BEGIN INDEPENDENT RUN OF COAL CHUTE DESIGNER

RUN NUMBER746

DATE 27 APR 77 18 55 12

..... INDEPENDENT VARIABLES FOR THIS RUN

A. INPUT DATA

FEEED CONVEYOR DATA

TORUS CHUTE DATA

BELT SPEED V , IPS. 90.00

MAJOR RADIUS RT1, IN 36.00

PULLEY RADIUS R, IN. 12.00

MINOR RADIUS RT2, IN. 18.00

BELT WIDTH BELTWD IN. 36.00

ROTATIONS,DEG.
Z-AXIS-GAMMA 30.00
Y AXIS-YAW 5.00
X-AXIS-ZIH 15.00

BELT EDGE DISTANCE BMAR IN. 2.00

TROUGH ANGLE IDLANG DEG. 35.00

EXTRA LENGTH DISP IN. 6.00

SURCHARGE ANGLE SURANG DEG. 25.00

COORDINATES PRIOR TO ROTATION
XT IN. 12.00
YT IN. 16.00

INCLINATION ANGLE PHI DEG. 0.0

FLAT PLATE DIVISION
MAJOR RADIUS-NT1 7
MINOR RADIUS-NT2 7

RUN OF MINE COAL DATA

RUN CONVENTION

CONSTANTS

DENSITY, GAMD LBS./CU. FT. 50.00

EFFECTIVE ANGLE OF FRICTION DELTF DEG. 50.00

FRICTION STEP DISTANCE - NOM.,EL1, IN. 1.00

DYNAMIC ANGLE OF WALL FRICTION PHIP DEG. 30.00

NO OF STREAM SUBDIVISIONS SECT 21

H-23

===== SUMMARY OF KEY CALCULATED PARAMETERS AND FINAL PLATE COORDINATES =====

B. OUTPUT DATA

PULLEY CONTACT DEP. ANGLE, DEG., 0.0
 INITIAL LOAD HEIGHT, IN. 7.52
 TORUS CUTOFF ANGLE, DEG. 105.33
 MINIMUM Y COORDINATE -42.88

PLATE 1

9.082	16.738	23.404	16.060
8.504	12.943	1.311	-3.671
-1.929	0.987	2.655	-0.183

PLATE 2

16.738	22.125	27.939	23.404
12.943	16.025	5.878	1.311
0.987	7.937	9.392	2.655

PLATE 3

22.125	23.799	28.450	27.939
16.025	16.924	8.807	5.878
7.937	17.058	18.223	9.392

PLATE 4

23.799	21.312	24.801	28.450
16.924	15.399	9.311	8.807
17.058	25.907	26.781	18.223

PLATE 5

-2.608	1.042	6.318	1.613
-9.283	-9.788	-19.346	-16.930
16.189	7.631	12.067	19.738

PLATE 6

1.042	7.875	13.924	6.318
-9.788	-7.734	-18.691	-19.346
7.631	1.638	6.725	12.067

H-24

PLATE 7

7.875	16.060	22.391	13.924
-7.734	-3.671	-15.141	-18.691
1.638	-0.183	5.141	6.725

PLATE 8

16.060	23.404	29.453	22.391
-3.671	1.311	-9.646	-15.141
-0.183	2.655	7.742	5.141

PLATE 9

23.404	27.939	33.215	29.453
1.311	5.878	-3.680	-9.646
2.655	9.392	13.829	7.742

PLATE 10

27.939	28.450	32.671	33.215
5.878	8.807	1.160	-3.680
9.392	18.223	21.772	13.829

PLATE 11

28.450	24.801	27.966	32.671
8.807	9.311	3.577	1.160
18.223	26.781	29.443	21.772

PLATE 12

1.613	6.318	10.695	5.114
-16.930	-19.346	-27.660	-23.581
19.738	12.067	19.181	25.429

PLATE 13

6.318	13.924	18.941	10.695
-19.346	-18.691	-28.222	-27.660
12.067	6.725	14.880	19.181

PLATE 14

13.924	22.391	27.643	18.941
-18.691	-15.141	-25.117	-28.222
6.725	5.141	13.678	14.880

22.391	29.453	34.470	27.643
-15.141	-9.646	-19.177	-25.117
5.141	7.742	15.897	13.678

PLATE 16

29.453	33.215	37.592	34.470
-9.646	-3.680	-11.993	-19.177
7.742	13.829	20.943	15.897

PLATE 17

33.215	32.671	36.173	37.592
-3.680	1.160	-5.491	-11.993
13.829	21.772	27.463	20.943

PLATE 18

32.671	27.966	30.592	36.173
1.160	3.577	-1.411	-5.491
21.772	29.443	33.711	27.463

PLATE 19

5.114	10.695	13.871	7.655
-23.581	-27.660	-34.159	-28.780
25.429	19.181	28.484	32.871

PLATE 20

10.695	18.941	22.582	13.871
-27.660	-28.222	-35.673	-34.159
19.181	14.880	25.545	28.484

PLATE 21

18.941	27.643	31.455	22.582
-28.222	-25.117	-32.917	-35.673
14.880	13.678	24.841	25.545

PLATE 22

27.643	34.470	38.111	31.455
-25.117	-19.177	-26.628	-32.917
13.678	15.897	26.562	24.841

PLATE 23

-19.177
15.897

-11.993
20.943

-18.493
30.246

-26.628
26.562

PLATE 24

37.592
-11.993
20.943

36.173
-5.491
27.463

38.714
-10.690
34.906

40.768
-18.493
30.246

PLATE 25

36.173
-5.491
27.463

30.592
-1.411
33.711

32.498
-5.311
39.293

38.714
-10.690
34.906

PLATE 26

7.655
-28.780
32.871

13.871
-34.159
28.484

15.629
-38.398
39.338

9.062
-32.172
41.555

PLATE 27

13.871
-34.159
28.484

22.582
-35.673
25.545

24.598
-40.533
37.988

15.629
-38.398
39.338

PLATE 28

22.582
-35.673
25.545

31.455
-32.917
24.841

33.565
-38.004
37.866

24.598
-40.533
37.988

PLATE 29

31.455
-32.917
24.841

38.111
-26.628
26.562

40.127
-31.488
39.005

33.565
-38.004
37.866

"R"

PLATE 30

38.111
-26.628
26.562

40.768
-18.493
30.246

42.527
-22.732
41.100

40.127
-31.488
39.005

PLATE 31

40.768
-18.493

38.714
-10.690

40.120
-14.082

42.527
-22.732

PLATE 32

38.714	32.498	33.553	40.120
-10.690	-5.311	-7.855	-14.082
34.906	39.293	45.805	43.589

PLATE 33

9.062	15.629	15.849	9.238
-32.172	-38.398	-40.087	-33.522
41.555	39.338	50.999	50.884

PLATE 34

15.629	24.598	24.850	15.849
-38.398	-40.533	-42.469	-40.087
39.338	37.988	51.357	50.999

PLATE 35

24.598	33.565	33.829	24.850
-40.533	-38.004	-40.030	-42.469
37.988	37.866	51.860	51.357

PLATE 36

33.565	40.127	40.379	33.829
-38.004	-31.488	-33.424	-40.030
37.866	39.005	52.374	51.860

PLATE 37

40.127	42.527	42.746	40.379
-31.488	-22.732	-24.421	-33.424
39.005	41.100	52.761	52.374

PLATE 38

42.527	40.120	40.296	42.746
-22.732	-14.082	-15.432	-24.421
41.100	43.589	52.918	52.761

PLATE 39

40.120	33.553	33.685	40.296
-14.082	-7.855	-8.868	-15.432
43.589	45.805	52.802	52.918

PLATE 40

9.238	15.849	15.698	9.087
-33.522	-40.087	-40.501	-33.936
50.884	50.999	56.983	56.867

PLATE 41

15.849	24.850	24.699	15.698
-40.087	-42.469	-42.883	-40.501
50.999	51.357	57.340	56.983

PLATE 42

24.850	33.829	33.678	24.699
-42.469	-40.030	-40.444	-42.883
51.357	51.860	57.843	57.340

PLATE 43

33.829	40.379	40.228	33.678
-40.030	-33.424	-33.838	-40.444
51.860	52.374	58.357	57.843

PLATE 44

40.379	42.746	42.596	40.228
-33.424	-24.421	-24.834	-33.838
52.374	52.761	58.745	58.357

PLATE 45

42.746	40.296	40.145	42.596
-24.421	-15.432	-15.846	-24.834
52.761	52.918	58.901	58.745

PLATE 46

40.296	33.685	33.534	40.145
-15.432	-8.868	-9.282	-15.846
52.918	52.802	58.786	58.901

B. OUTPUT DATA

1. HIT DATA

H-30

STREAM	TIME	ANGLE	X	C.G.			PLATE	BOTTOM			TOP				
				Y	Z			ANGLE	X	Y	ANGLE	X	Y	PL	
1	0.26	-25.1	23.1	-0.2	2.8	8	-25.2	22.9	-0.6	8	-25.1	23.2	0.1	8	
2	0.28	-23.4	25.3	-2.1	4.3	9	-24.5	25.1	-3.0	8	-23.6	25.1	-0.6	9	
3	0.30	-22.2	26.8	-3.3	5.8	9	-23.9	27.1	-5.6	8	-22.6	26.3	-1.0	9	
4	0.31	-21.1	28.2	-4.7	7.3	9	-20.6	28.8	-7.8	9	-21.5	27.7	-1.7	9	
5	0.33	-19.9	29.8	-6.4	8.9	9	-22.1	30.1	-10.8	16	-20.4	29.1	-2.8	9	
6	0.35	-15.7	31.1	-10.8	10.4	16	-31.0	31.1	-10.8	16	-19.4	30.6	-4.2	9	
7	0.36	-19.1	32.0	-10.8	11.9	16	0.0*****				-11.3	32.0	-10.8	16	
8	0.37	-24.9	33.0	-10.8	13.4	16	-0.0*****		0.0*****		-12.9	33.0	-10.8	16	
9	0.00*****			0.0*****			*****	1.1	0.0*****		-15.5	33.9	-10.7	16	
10	-0.00*****						*****		0.0	1		-19.8	34.8	-10.7	16
11	*****			-0.0*****			4.0*****	-35.0	35.5	-18.1	23	-28.1	35.8	-10.7	16
12	0.41	-34.4	36.5	-16.0	19.5	23	-34.7	36.1	-19.0	23	*****	0.0	0.0*****		
13	0.41	-34.1	37.0	-17.0	21.0	23	-34.3	36.6	-19.9	23	-33.9	37.4	-14.0	23	
14	0.42	-33.8	37.5	-18.0	22.6	23	-34.0	37.1	-20.9	23	-33.6	37.9	-15.2	23	

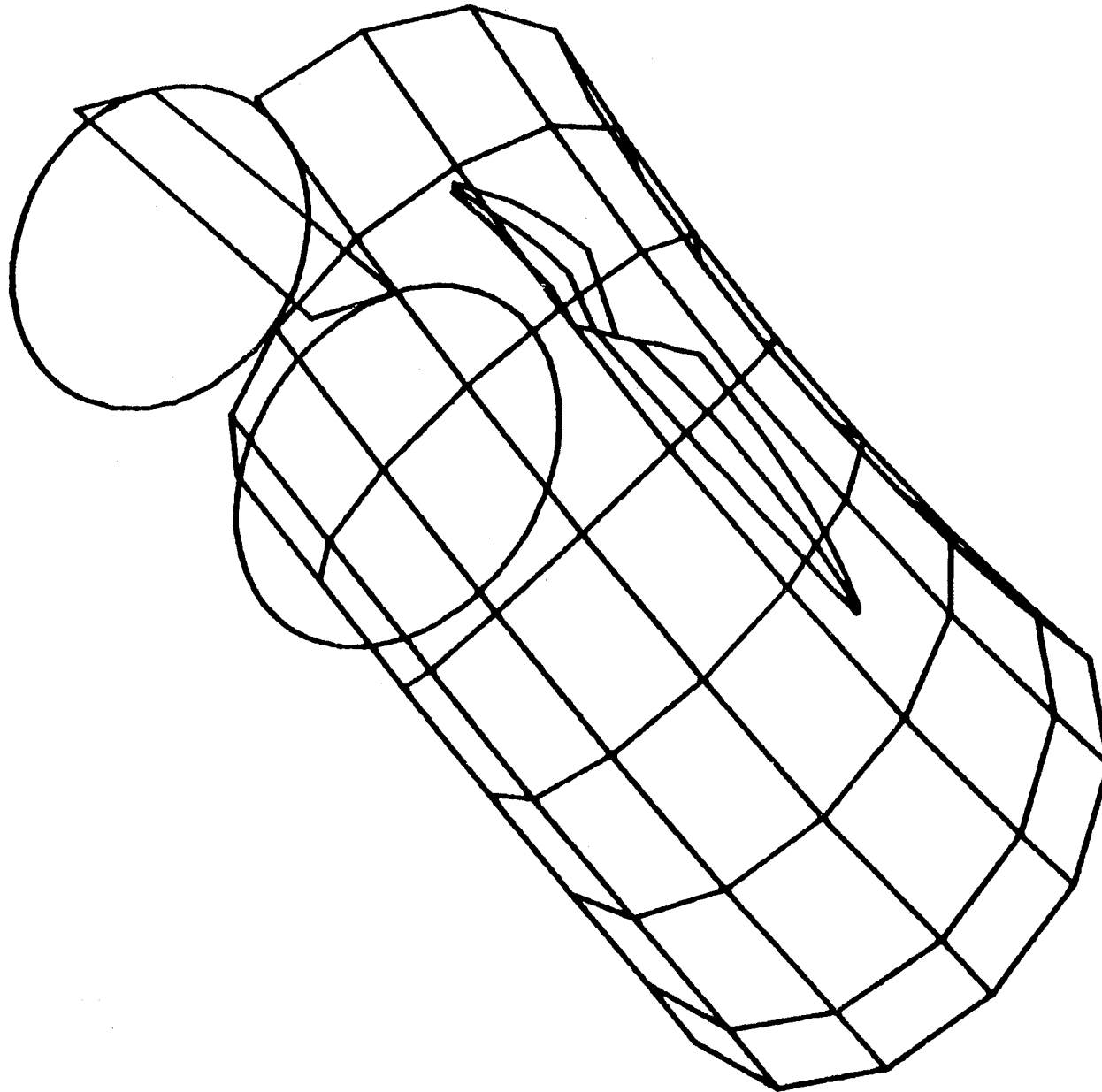
15	0.42	-33.5	38.0	-19.2	24.1	23	-33.7	37.7	-21.8	23	-33.3	38.4	-16.5	23
16	0.43	-33.2	38.5	-20.4	25.6	23	-33.4	38.2	-22.8	23	-33.0	38.8	-17.9	23
17	0.43	-32.9	39.0	-21.6	27.1	23	-33.1	38.7	-23.8	23	-32.8	39.3	-19.4	23
18	0.44	-39.3	39.4	-22.8	28.7	30	-39.5	39.1	-24.5	30	-32.5	39.7	-21.1	23
19	0.44	-39.2	39.6	-23.7	30.2	30	-39.4	39.4	-25.0	30	-39.1	39.9	-22.4	30
20	0.44	-39.1	39.8	-24.6	31.7	30	-39.2	39.6	-25.5	30	-39.0	40.0	-23.8	30
21	0.44	-39.0	40.0	-25.7	33.2	30	-39.1	39.9	-26.0	30	-39.0	40.0	-25.4	30

3-D VIEW

RUN 746

ELEMENTS

1,99999



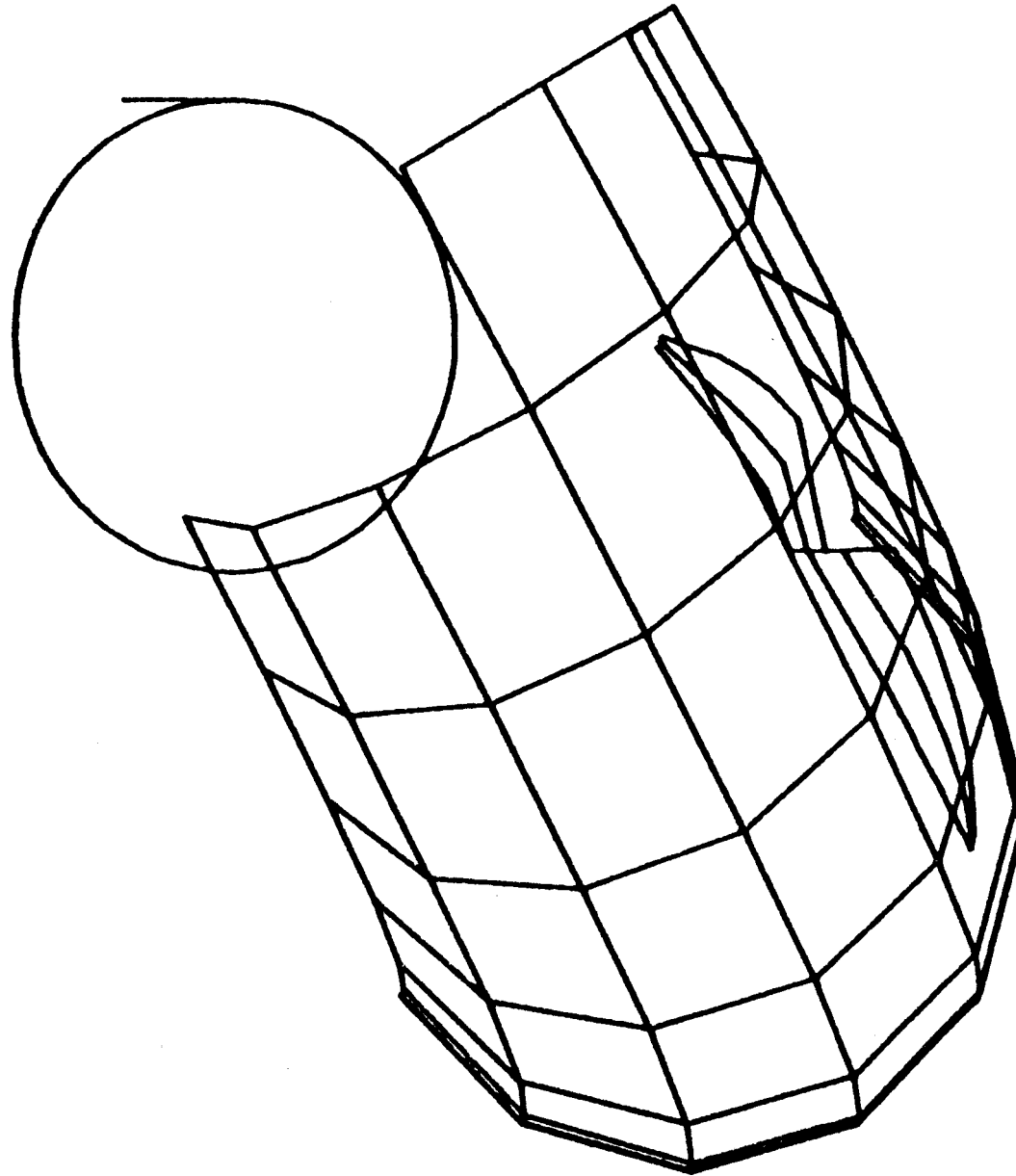
H-32

FRONT VIEW

RUH 746

ELEMENTS

1,99999



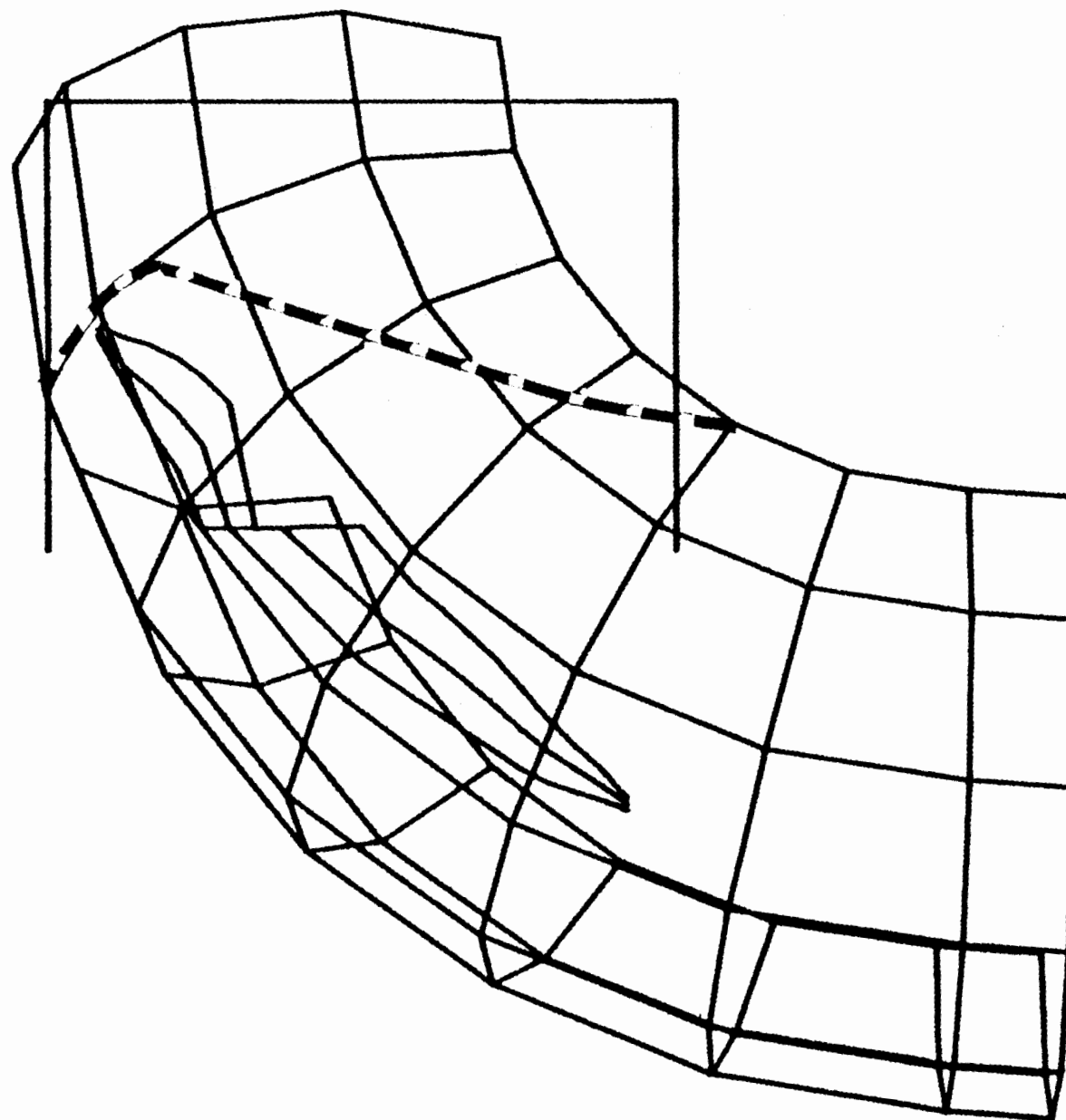
H-33

SIDE VIEW

RUN 746

ELEMENTS

1,99999



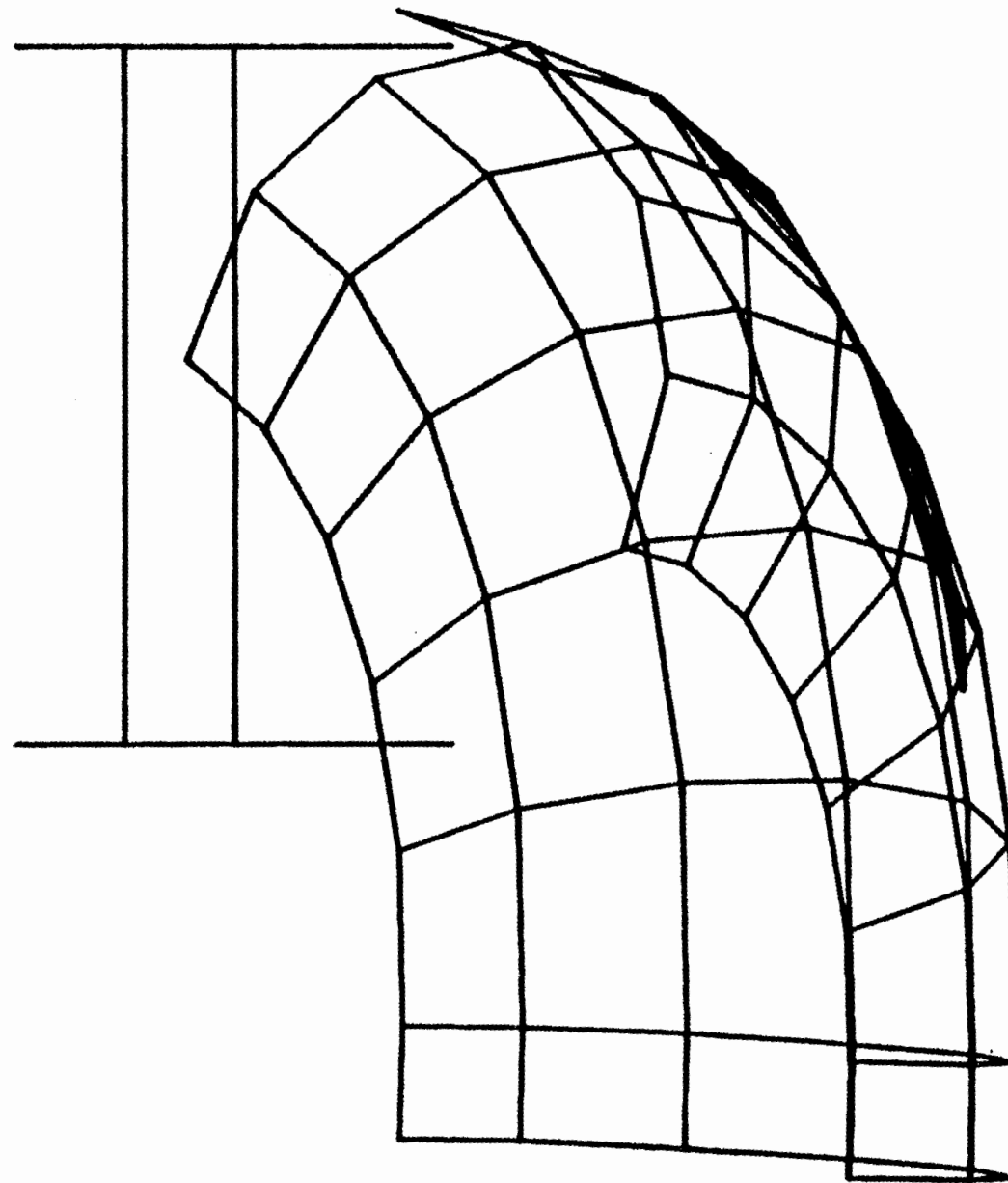
H-34

TOP VIEW

RUN 746

ELEMENTS

1,99999



H-35

BEGIN INDEPENDENT RUN OF COAL CHUTE DESIGNER

RUN NUMBER706

DATE 27 APR 77 18 56 18

..... INDEPENDENT VARIABLES FOR THIS RUN

A. INPUT DATA

FEED CONVEYOR DATA

TORUS CHUTE DATA

BELT SPEED V , IPS. 90.00

MAJOR RADIUS RT1, IN 36.00

PULLEY RADIUS R, IN. 12.00

MINOR RADIUS RT2, IN. 18.00

BELT WIDTH BELTWD IN. 36.00

ROTATIONS,DEG.
Z-AXIS-GAMMA 20.00
Y AXIS-YAW 5.00
X-AXIS-ZIH 20.00

BELT EDGE DISTANCE BMAR IN. 2.00

EXTRA LENGTH DISP IN. 6.00

TROUGH ANGLE IOLANG DEG. 35.00

SURCHARGE ANGLE SURANG DEG. 25.00

COORDINATESPRIOR TO ROTATION

XT IN. 12.00
YT IN. 16.00

INCLINATION ANGLE PHI DEG. 0.0

FLAT PLATE DIVISION
MAJOR RADIUS-NT1 7
MINOR RADIUS-NT2 7

RUN OF MINE COAL DATA

RUN CONVENTION

CONSTANTS

DENSITY, GAMD LBS./CU. FT. 50.00

EFFECTIVE ANGLE OF FRICTION DELTF DEG. 50.00

FRICTION STEP DISTANCE - NOM.,EL1, IN. 1.00

DYNAMIC ANGLE OF WALL FRICTION PHIP DEG. 30.00

NO OF STREAM SUBDIVISIONS SECT 21

H-36

B. OUTPUT DATA

1. HIT DATA

STREAM	TIME	ANGLE	X	C.G.			ANGLE	BOTTOM		PLATE	TOP			PL
				Y	Z		X	Y			ANGLE	X	Y	
1	0.25	-18.3	22.8	0.1	2.8	2	-18.1	23.0	-0.6	2	-18.5	22.5	0.8	2
2	0.28	-16.5	24.8	-1.4	4.3	2	-26.8	25.1	-3.0	9	-17.1	24.1	0.5	2
3	0.29	-25.8	26.4	-2.8	5.8	9	-25.7	26.5	-4.8	9	-15.6	25.9	-0.5	2
4	0.31	-24.8	27.8	-4.1	7.3	9	-24.6	28.0	-6.7	9	-24.9	27.6	-1.6	9
5	0.32	-23.8	29.2	-5.6	8.9	9	-23.6	29.4	-8.7	9	-23.9	29.0	-2.6	9
6	0.34	-22.8	30.6	-7.4	10.4	9	-22.7	30.9	-10.8	9	-23.0	30.4	-3.9	9
7	0.36	-21.9	32.1	-9.3	11.9	9	-32.5	32.1	-12.5	16	-18.6	30.8	-4.1	10
8	0.37	-20.5	33.0	-10.4	13.4	17	-31.9	33.0	-13.9	16	-18.3	31.2	-4.3	10
9	0.37	-20.2	33.4	-10.9	15.0	17	-31.4	33.9	-15.3	16	-17.9	31.7	-4.7	10
10	0.38	-19.8	33.8	-11.5	16.5	17	-30.9	34.7	-16.8	16	-17.4	32.2	-5.3	10
11	0.38	-19.5	34.2	-12.2	18.0	17	-18.5	35.5	-18.1	17	-17.0	32.8	-6.1	10
12	0.39	-19.1	34.7	-13.0	19.5	17	-18.2	36.0	-18.9	17	-20.1	33.4	-7.2	17
13	0.39	-18.8	35.2	-13.8	21.0	17	-21.1	36.3	-19.5	24	-19.7	33.9	-8.1	17
14	0.40	-18.4	35.7	-14.8	22.6	17	-20.9	36.6	-20.0	24	-19.3	34.5	-9.3	17

H-37

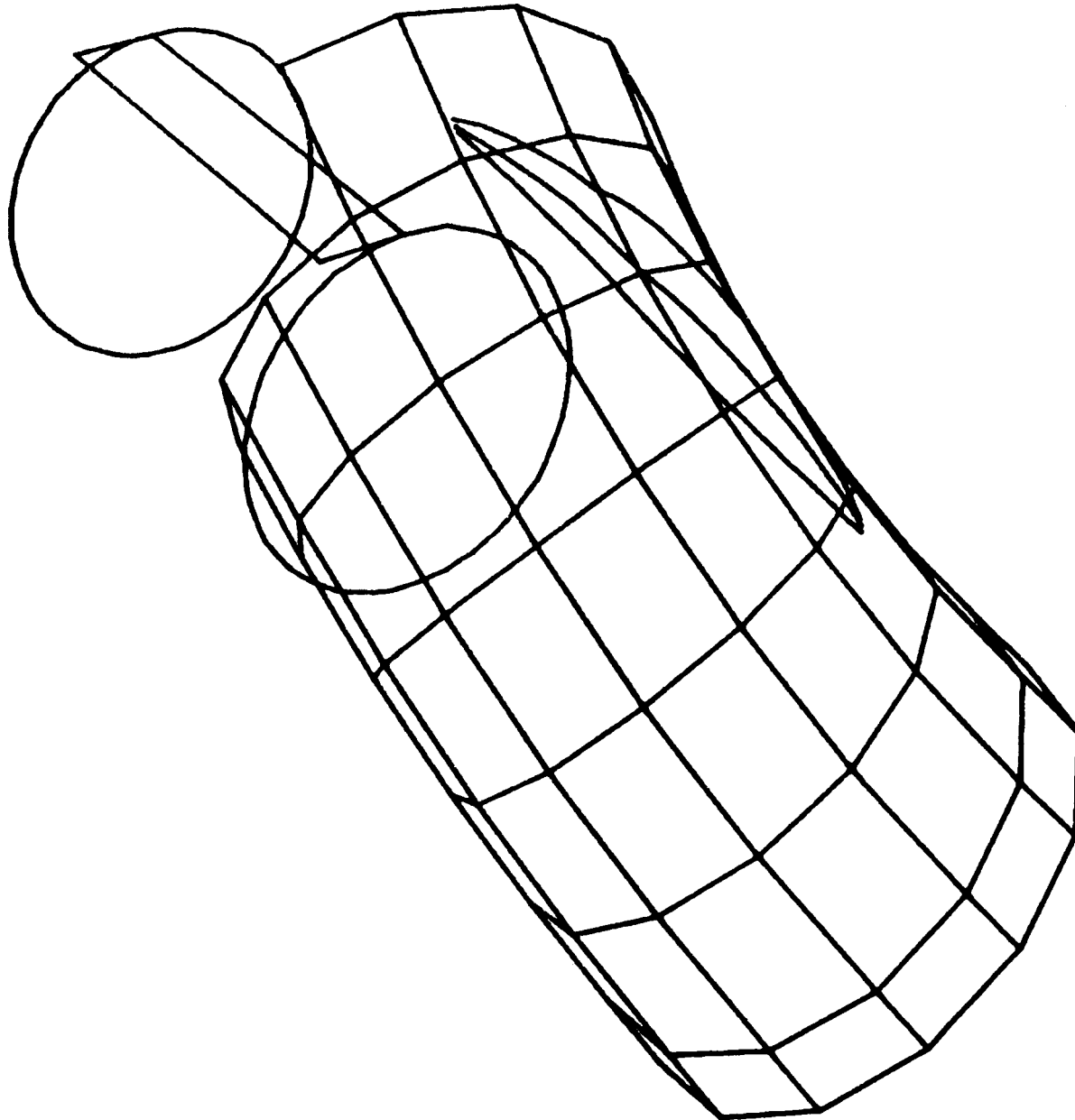
15	0.40	-21.2	36.2	-15.9	24.1	24	-20.7	36.9	-20.5	24	-3.4	34.1	-9.1	18
16	0.41	-20.9	36.5	-16.8	25.6	24	-20.5	37.2	-21.0	24	-4.5	32.7	-7.4	18
17	0.41	-20.7	36.9	-17.0	27.1	24	-20.3	37.5	-21.6	24	-5.0	32.1	-7.1	18
18	0.41	-20.4	37.3	-18.9	28.7	24	-20.1	37.8	-22.1	24	-5.1	32.0	-7.8	18
19	0.42	-20.1	37.7	-20.2	30.2	24	-19.9	38.1	-22.7	24	-4.6	32.5	-9.7	18
20	0.42	-22.2	38.2	-21.6	31.7	31	-22.1	38.4	-23.1	31	-20.0	37.9	-19.9	24
21	0.43	-22.0	38.5	-22.8	33.2	31	-22.0	38.5	-23.4	31	-22.1	38.4	-22.3	31

3-D VIEW

RUN 706

ELEMENTS

1,99999



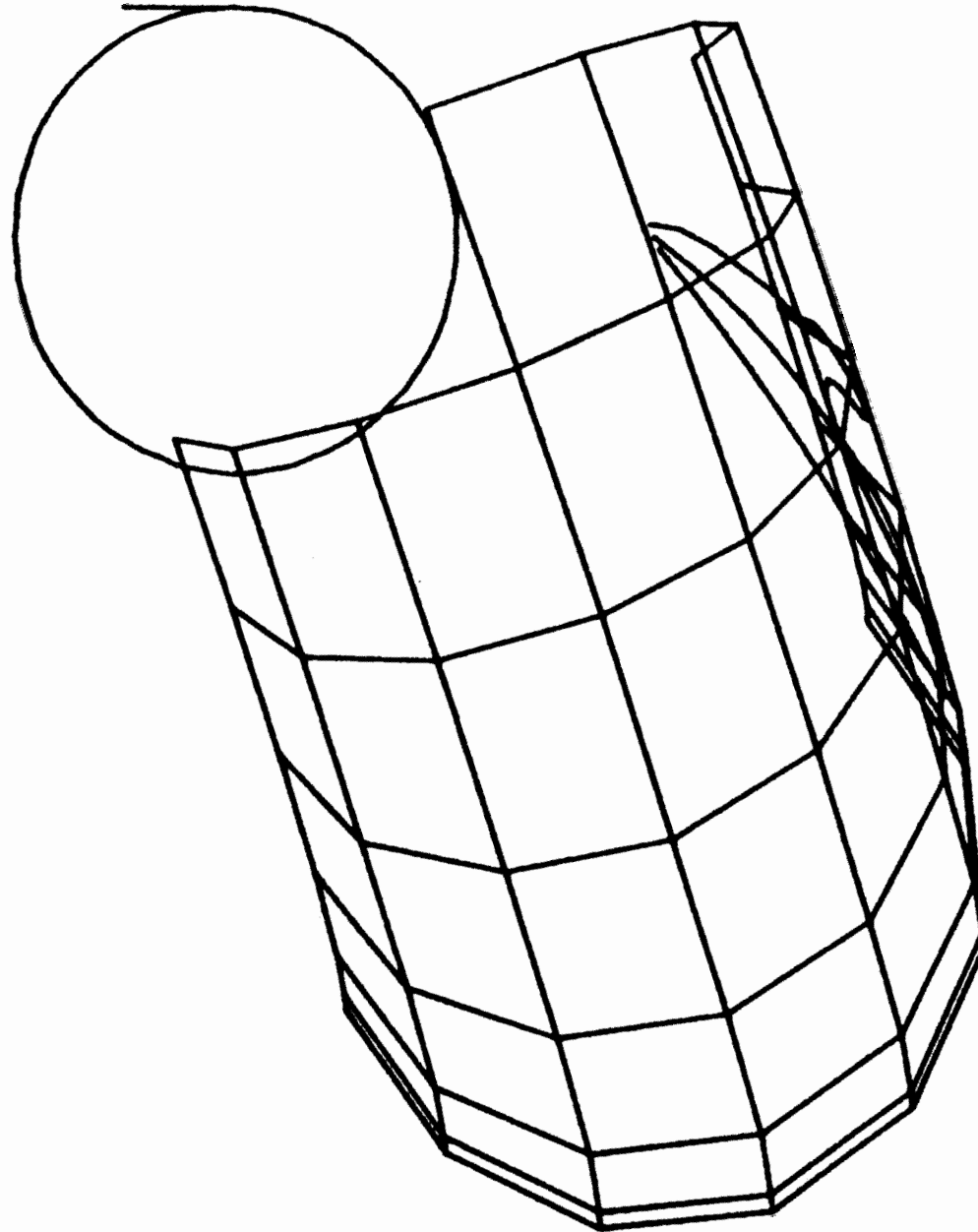
H-39

FRONT VIEW

RUN 706

ELEMENTS

1,99999



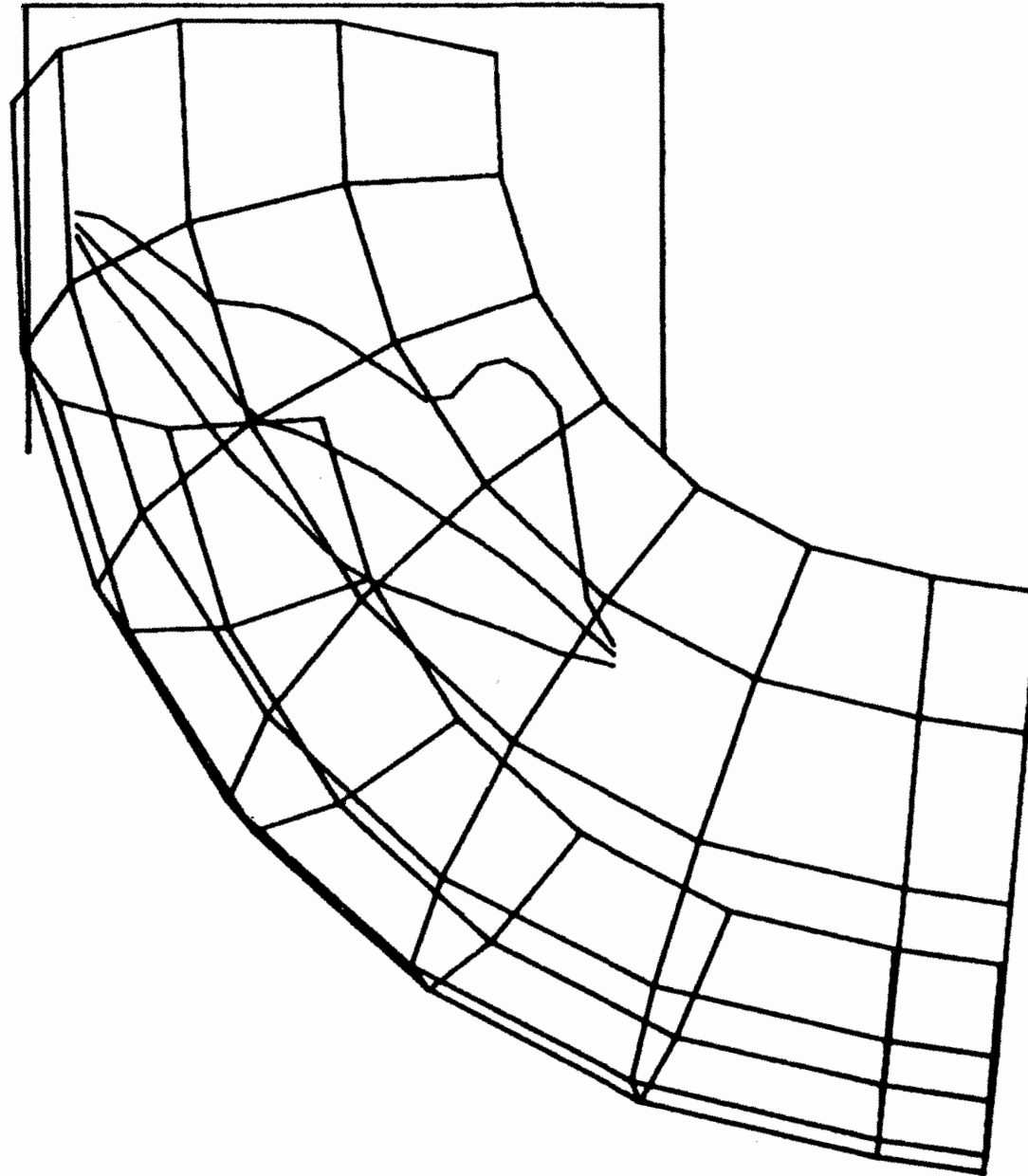
H-40

SIDE VIEW

RUN 706

ELEMENTS

1,99999



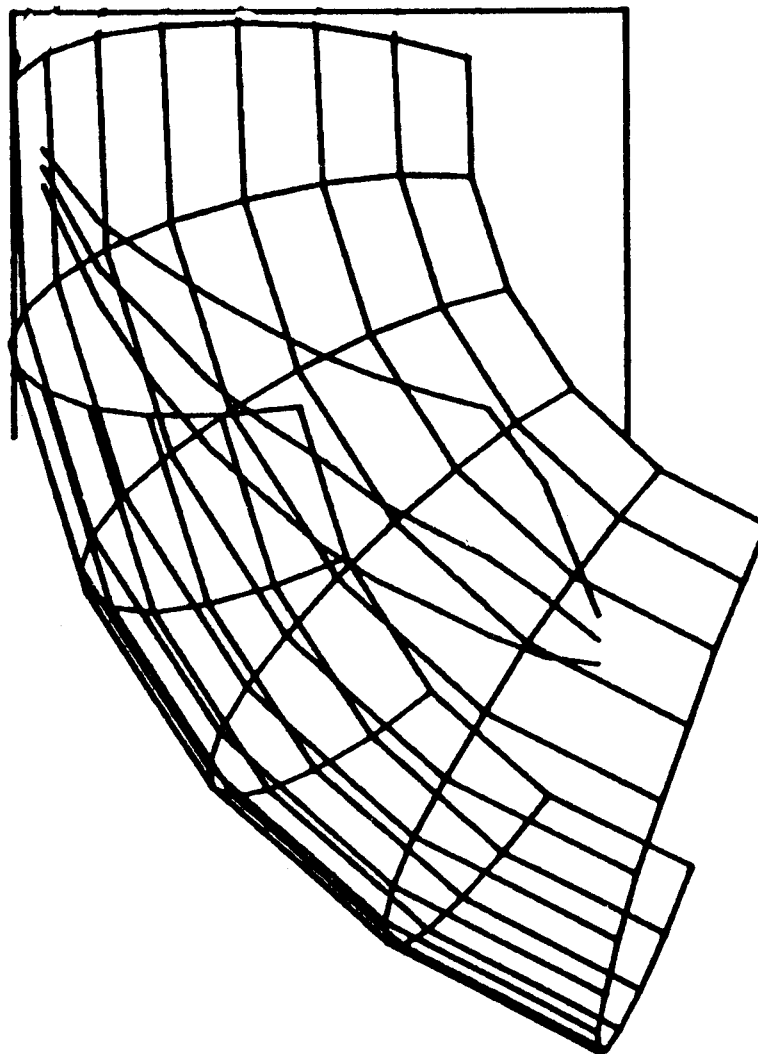
H-41

SIDE VIEW TEKPL0T NASDEK1

348,12,16

ELEMENTS

1,99999



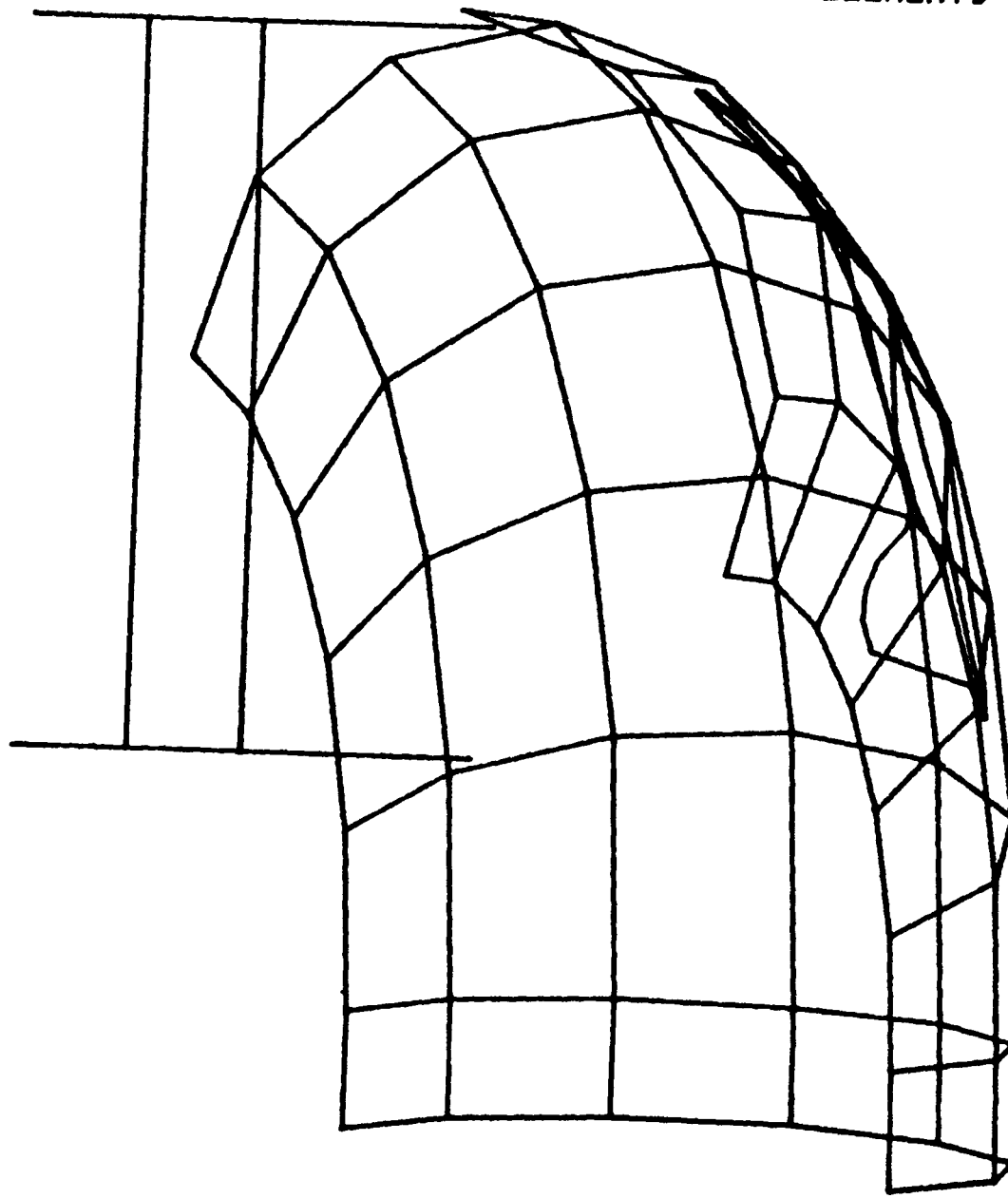
H-42

TOP VIEW

RUN 706

ELEMENTS

1,99999



H-43

600 FPM TRAJECTORY CASE

RUNS 846, 806

BEGIN INDEPENDENT RUN OF COAL CHUTE DESIGNER

RUN NUMBER846

DATE 27 APR 77 18 57 23

..... INDEPENDENT VARIABLES FOR THIS RUN

A. INPUT DATA

FEED CONVEYOR DATA

TORUS CHUTE DATA

BELT SPEED V , IPS. 120.00

MAJOR RADIUS RT1, IN 36.00

PULLEY RADIUS R, IN. 12.00

MINOR RADIUS RT2, IN. 18.00

BELT WIDTH BELTWD IN. 36.00

ROTATIONS,DEG.
Z-AXIS-GAMMA 30.00
Y-AXIS-YAW 10.00
X-AXIS-ZIH 20.00

BELT EDGE DISTANCE BMAR IN. 2.00

TROUGH ANGLE IDLANG DEG, 35.00

EXTRA LENGTH DISP IN. 6.00

SURCHARGE ANGLE SURANG DEG. 25.00

COORDINATESPRIOR TO ROTATION
XT IN. 15.00
YT IN. 17.00

INCLINATION ANGLE PHI DEG. 0.0

FLAT PLATE DIVISION
MAJOR RADIUS-NT1 7
MINOR RADIUS-NT2 7

RUN OF MINE COAL DATA

RUN CONVENTION

CONSTANTS

DENSITY, GAMD LBS./CU. FT. 50.00

EFFECTIVE ANGLE OF FRICTION DELTF DEG. 50.00

FRICTION STEP DISTANCE - NOM.,EL1, IN. 1.00

DYNAMIC ANGLE OF WALL FRICTION PHIP DEG. 30.00

NO OF STREAM SUBDIVISIONS SECT 21

H-45

===== SUMMARY OF KEY CALCULATED PARAMETERS AND FINAL PLATE COORDINATES =====

B. OUTPUT DATA

PULLEY CONTACT DEP. ANGLE, DEG., 0.0
INITIAL LOAD HEIGHT, IN. 7.52
TORUS CUTOFF ANGLE, DEG. 105.33
MINIMUM Y COORDINATE -44.08

PLATE 1

10.521 18.293 25.336 17.893
11.717 16.115 4.587 -0.350
-2.718 -0.059 0.027 -2.628

PLATE 2

18.293 24.174 30.318 25.336
16.115 18.748 8.692 4.587
-0.059 6.671 6.746 0.027

PLATE 3

24.174 26.590 31.505 30.318
18.748 18.910 10.865 8.692
6.671 15.669 15.729 6.746

PLATE 4

26.590 24.892 28.578 31.505
18.910 16.557 10.523 10.865
15.669 24.523 24.568 15.729

PLATE 5

0.801 3.728 9.574 5.478
-7.931 -7.560 -17.302 -15.695
14.660 5.820 8.951 17.164

PLATE 6

3.728 9.984 16.686 9.574
-7.560 -4.796 -15.965 -17.302
5.820 -0.507 3.082 8.951

H-46



PLATE 7

9.984	17.893	24.908	16.686
-4.796	-0.350	-12.041	-15.965
-0.507	-2.628	1.129	3.082

PLATE 8

17.893	25.336	32.037	24.908
-0.350	4.587	-6.582	-12.041
-2.628	0.027	3.616	1.129

PLATE 9

25.336	30.318	36.163	32.037
4.587	8.692	-1.050	-6.582
0.027	6.746	9.877	3.616

PLATE 10

30.318	31.505	36.181	36.163
8.692	10.865	3.071	-1.050
6.746	15.729	18.233	9.877

PLATE 11

31.505	28.578	32.085	36.181
10.865	10.523	4.678	3.071
15.729	24.568	26.446	18.233

PLATE 12

5.478	9.574	14.720	9.595
-15.695	-17.302	-26.062	-22.703
17.164	8.951	14.922	21.941

PLATE 13

9.574	16.686	22.585	14.720
-17.302	-15.965	-26.007	-26.062
8.951	3.082	9.927	14.922

PLATE 14

16.686	24.908	31.083	22.585
-15.965	-12.041	-22.552	-26.007
3.082	1.129	8.295	9.927

24.908	32.037	37.937	31.083
-12.041	-6.582	-16.624	-22.552
1.129	3.616	10.462	8.295

PLATE 16

32.037	36.163	41.310	37.937
-6.582	-1.050	-9.810	-16.624
3.616	9.877	15.848	10.462

PLATE 17

36.163	36.181	40.298	41.310
-1.050	3.071	-3.937	-9.810
9.877	18.233	23.010	15.848

PLATE 18

36.181	32.085	35.173	40.298
3.071	4.678	-0.578	-3.937
18.233	26.446	30.029	23.010

PLATE 19

9.595	14.720	18.814	12.870
-22.703	-26.062	-33.239	-28.445
21.941	14.922	23.325	28.663

PLATE 20

14.720	22.585	27.279	18.814
-26.062	-26.007	-34.235	-33.239
14.922	9.927	19.561	23.325

PLATE 21

22.585	31.083	35.996	27.279
-26.007	-22.552	-31.165	-34.235
9.927	8.295	18.378	19.561

PLATE 22

31.083	37.937	42.630	35.996
-22.552	-16.624	-24.852	-31.165
8.295	10.462	20.095	18.378

PLATE 23

41.310	49.505	42.190
--------	--------	--------

10.027
10.462

15.848

24.251

20.095

PLATE 24

41.310
-9.810
15.848

40.298
-3.937
23.010

43.573
-9.678
29.733

45.404
-16.987
24.251

PLATE 25

40.298
-3.937
23.010

35.173
-0.578
30.029

37.629
-4.884
35.071

43.573
-9.678
29.733

PLATE 26

12.870
-28.445
28.663

18.814
-33.239
23.325

21.575
-38.341
33.583

15.079
-32.526
36.870

PLATE 27

18.814
-33.239
23.325

27.279
-34.235
19.561

30.444
-40.083
31.320

21.575
-38.341
33.583

PLATE 28

27.279
-34.235
19.561

35.996
-31.165
18.378

39.309
-37.287
30.688

30.444
-40.083
31.320

PLATE 29

35.996
-31.165
18.378

42.630
-24.852
20.095

45.795
-30.700
31.855

39.309
-37.287
30.688

PLATE 30

42.630
-24.852
20.095

45.404
-16.987
24.251

48.165
-22.089
34.509

45.795
-30.700
31.855

PLATE 31

45.404
-16.987

43.573
-9.678

49.782
-13.760

48.165
-22.089

PLATE 32

43.573	37.629	39.286	45.782
-9.678	-4.884	-7.945	-13.760
29.733	35.071	41.226	37.939

PLATE 33

15.079	21.575	22.814	16.070
-32.526	-38.341	-41.018	-34.667
36.870	33.583	44.993	45.997

PLATE 34

21.575	30.444	31.864	22.814
-38.341	-40.083	-43.152	-41.018
33.583	31.320	44.400	44.993

PLATE 35

30.444	39.309	40.796	31.864
-40.083	-37.287	-40.499	-43.152
31.320	30.688	44.379	44.400

PLATE 36

39.309	45.795	47.216	40.796
-37.287	-30.700	-33.769	-40.499
30.688	31.855	44.935	44.379

PLATE 37

45.795	48.165	49.403	47.216
-30.700	-22.089	-24.766	-33.769
31.855	34.509	45.919	44.935

PLATE 38

48.165	45.782	46.773	49.403
-22.089	-13.760	-15.901	-24.766
34.509	37.939	47.067	45.919

PLATE 39

45.782	39.286	40.029	46.773
-13.760	-7.945	-9.551	-15.901
37.939	41.226	48.071	47.067

PLATE 40

16.070	22.814	23.177	16.433
-34.667	-41.018	-41.948	-35.598
45.997	44.993	50.909	51.914

PLATE 41

22.814	31.864	32.227	23.177
-41.018	-43.152	-44.083	-41.948
44.993	44.400	50.317	50.909

PLATE 42

31.864	40.796	41.159	32.227
-43.152	-40.499	-41.430	-44.083
44.400	44.379	50.295	50.317

PLATE 43

40.796	47.216	47.578	41.159
-40.499	-33.769	-34.700	-41.430
44.379	44.935	50.851	50.295

PLATE 44

47.216	49.403	49.766	47.578
-33.769	-24.766	-25.696	-34.700
44.935	45.919	51.835	50.851

PLATE 45

49.403	46.773	47.136	49.766
-24.766	-15.901	-16.832	-25.696
45.919	47.067	52.983	51.835

PLATE 46

46.773	40.029	40.392	47.136
-15.901	-9.551	-10.482	-16.832
47.067	48.071	53.988	52.983

B. OUTPUT DATA

1. HIT DATA

STREAM	TIME	ANGLE	X	C.G.			ANGLE	BOTTOM		PLATE	TOP			
				Y	Z			X	Y		ANGLE	X	Y	PL
1	0.24	-26.5	28.9	1.2	2.8	9	-26.4	29.1	0.7	9	-26.6	28.7	1.8	9
2	0.25	-25.5	30.4	0.7	4.3	9	-25.1	30.9	-0.8	9	-25.8	30.0	2.3	9
3	0.27	-24.4	32.1	-0.0	5.8	9	-24.0	32.8	-2.5	9	-24.9	31.4	2.4	9
4	0.28	-23.4	33.8	-1.0	7.3	9	-33.6	34.5	-4.0	16	-23.9	32.9	2.1	9
5	0.30	-33.0	35.5	-2.2	8.9	16	-32.8	35.8	-5.2	16	-23.0	34.5	1.5	9
6	0.31	-32.3	36.7	-3.0	10.4	16	-32.1	37.0	-6.4	16	-20.1	34.8	1.8	10
7	0.32	-21.3	37.9	-3.9	11.9	17	-31.4	38.2	-7.6	16	-19.9	35.0	2.1	10
8	0.32	-21.0	38.3	-4.2	13.4	17	-30.7	39.5	-8.9	16	-19.6	35.4	2.2	10
9	0.32	-20.6	38.8	-4.6	15.0	17	-30.1	40.7	-10.2	16	-19.2	35.9	2.0	10
10	0.33	-20.2	39.4	-5.1	16.5	17	-39.6	41.6	-11.2	23	-22.5	36.4	1.7	17
11	0.33	-19.8	40.0	-5.7	18.0	17	-39.1	42.3	-12.0	23	-22.0	36.9	1.2	17
12	0.34	-19.3	40.6	-6.4	19.5	17	-38.7	43.1	-12.9	23	-21.6	37.6	0.5	17
13	0.34	-22.2	41.1	-7.1	21.0	24	-20.5	43.5	-13.4	24	-6.7	36.9	1.0	18
14	0.35	-21.8	41.7	-7.8	22.6	24	-20.2	44.0	-14.0	24	-7.8	35.5	2.1	18

H-52

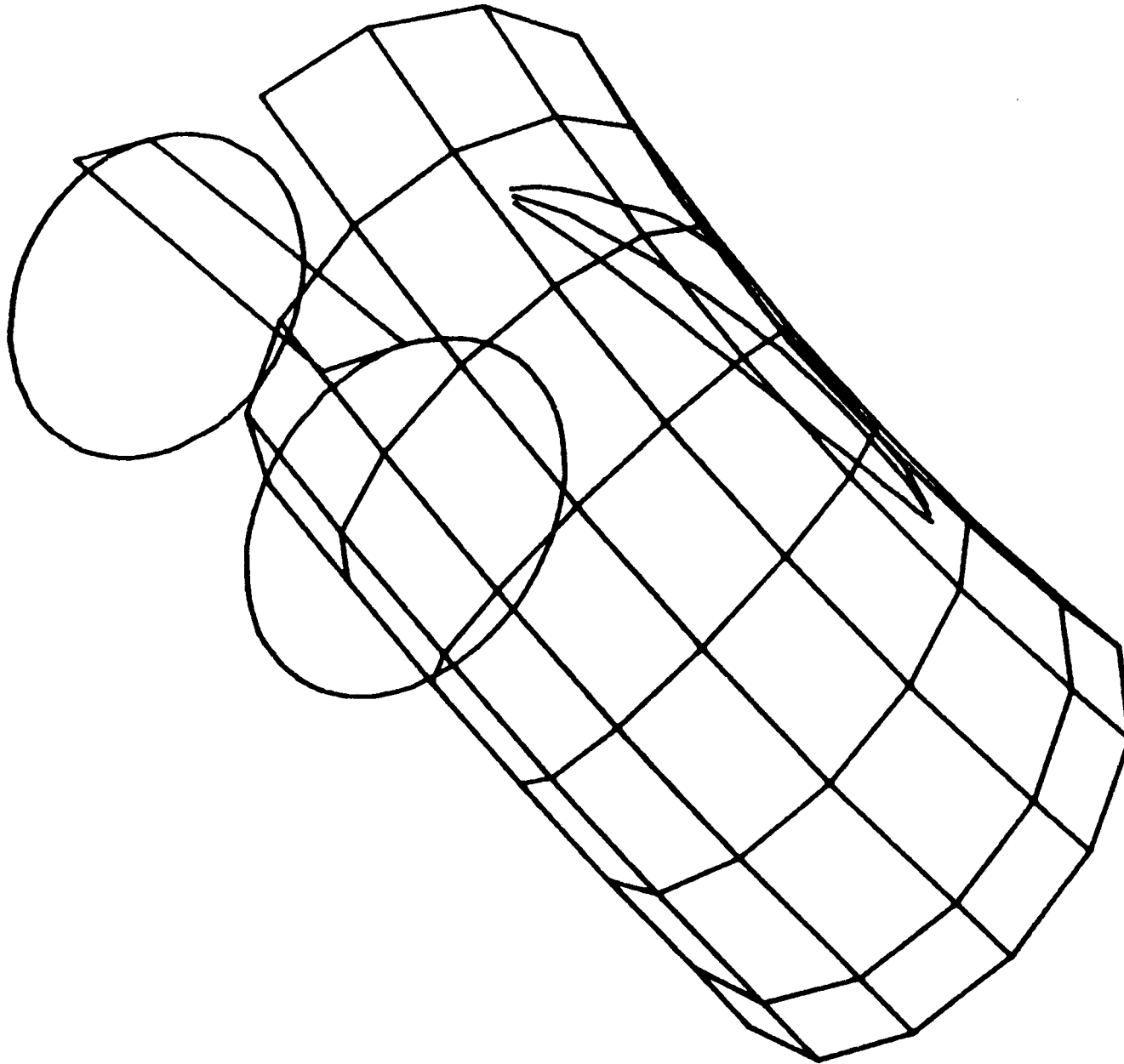
15	0.35	-21.4	42.2	-8.6	24.1	24	-19.9	44.4	-14.5	26	-8.5	34.7	2.4	18
16	0.36	-21.0	42.9	-9.6	25.6	24	-19.6	44.9	-15.1	24	-8.7	34.4	2.2	18
17	0.36	-20.5	43.5	-10.7	27.1	24	-21.9	45.2	-15.4	31	-8.6	34.5	1.4	18
18	0.37	-22.6	44.2	-11.9	28.7	31	-21.8	45.4	-15.7	31	-8.0	35.2	-0.1	18
19	0.37	-22.2	44.7	-13.1	30.2	31	-21.6	45.7	-16.0	31	-1.8	39.4	-5.3	25
20	0.38	-21.8	45.3	-14.4	31.7	31	-21.4	46.0	-16.4	31	-22.2	44.7	-12.4	31
21	0.38	-21.4	46.0	-16.0	33.2	31	-21.2	46.3	-16.7	31	-21.5	45.8	-15.2	31

3-D VIEW

RUN 846

ELEMENTS

1,99999



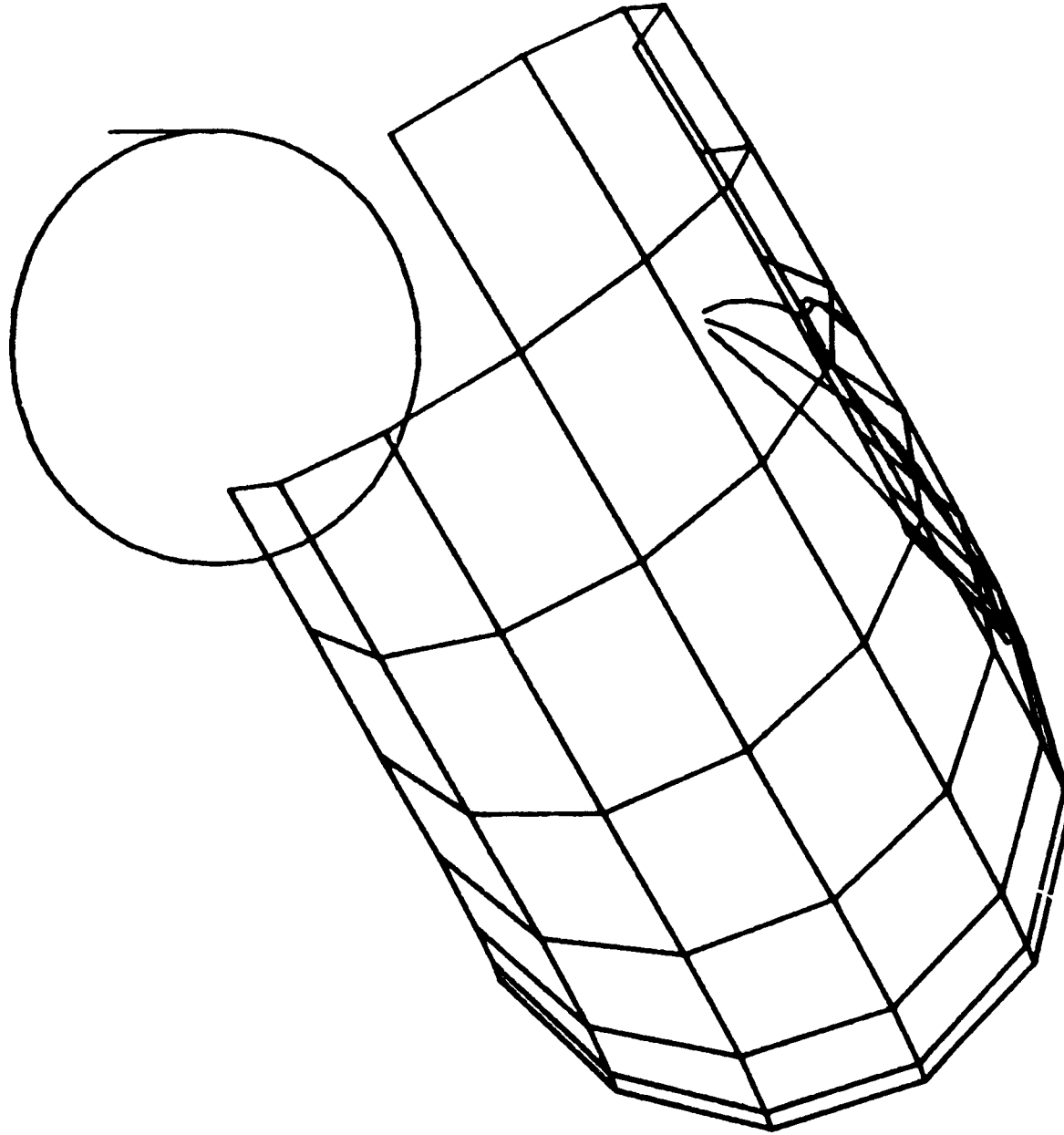
H-54

FRONT VIEW

RUN 846

ELEMENTS

1,99999



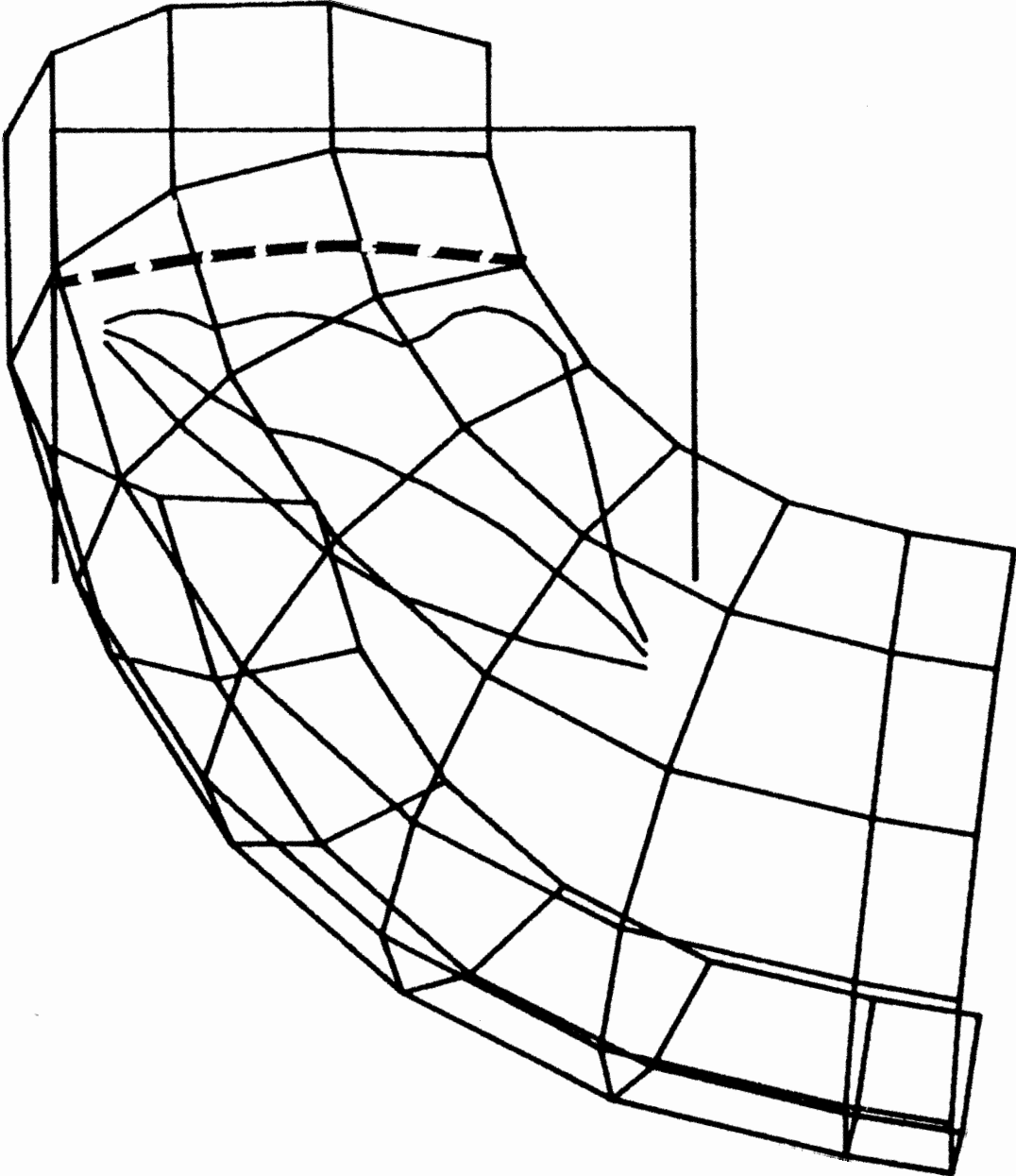
H-55

SIDE VIEW

RUN 846

ELEMENTS

1,99999



H-56

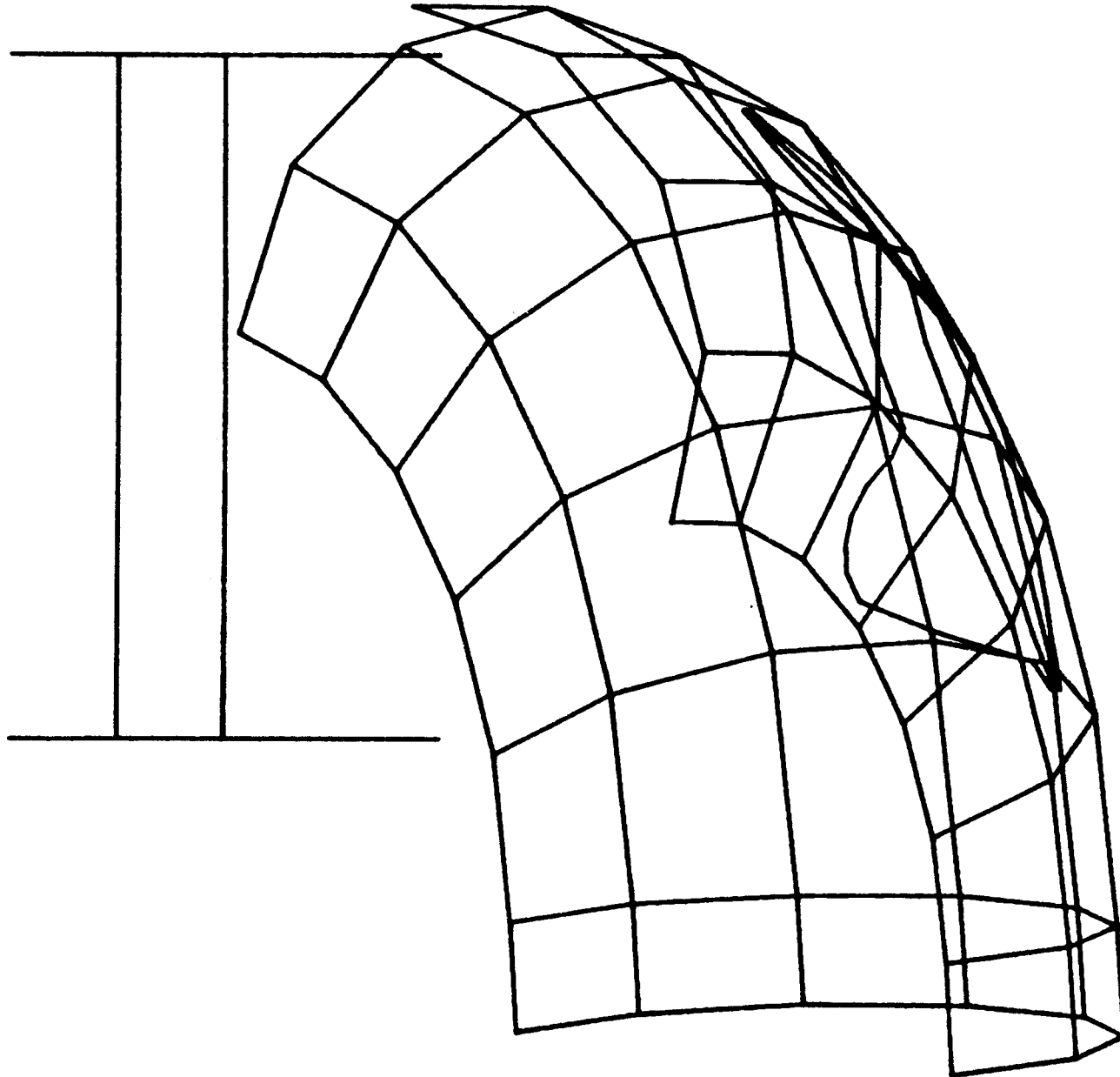


TOP VIEW

RUN 846

ELEMENTS

1,99999



H-57

BEGIN INDEPENDENT RUN OF COAL CHUTE DESIGNER

RUN NUMBER806

DATE 27 APR 77 18 58 38

..... INDEPENDENT VARIABLES FOR THIS RUN

A. INPUT DATA

FEED CONVEYOR DATA

TORUS CHUTE DATA

BELT SPEED V , IPS. 120.00

MAJOR RADIUS RT1, IN 36.00

PULLEY RADIUS R, IN. 12.00

MINOR RADIUS RT2, IN. 18.00

BELT WIDTH BELTWD IN. 36.00

ROTATIONS,DEG.
Z-AXIS-GAMMA 20.00
Y-AXIS-YAW 10.00
X-AXIS-ZIH 15.00

BELT EDGE DISTANCE BMAR IN. 2.00

TROUGH ANGLE IDLANG DEG. 35.00

EXTRA LENGTH DISP IN. 6.00

SURCHARGE ANGLE SURANG DEG. 25.00

COORDINATESPRIOR TO ROTATION
XT IN. 15.00
YT IN. 17.00

INCLINATION ANGLE PHI DEG. 0.0

FLAT PLATE DIVISION
MAJOR RADIUS-NT1 7
MINOR RADIUS-NT2 7

RUN OF MINE COAL DATA

RUN CONVENTION

CONSTANTS

DENSITY, GAMD LBS./CU. FT. 50.00

EFFECTIVE ANGLE OF FRICTION DELTF DEG. 50.00

FRICTION STEP DISTANCE - NOM.,EL1, IN. 1.00

DYNAMIC ANGLE OF WALL FRICTION PHIP DEG. 30.00

NO OF STREAM SUBDIVISIONS SECT 21

H-58

B. OUTPUT DATA

L. HIT DATA

STREAM	TIME	ANGLE	X	C.G.			PLATE	ANGLE	BOTTOM		PLATE	TOP		
				Y	Z	X			Y	ANGLE		X	Y	PL
1	0.24	-33.4	28.8	1.3	2.8	9	-33.4	28.8	0.8	9	-33.4	28.8	1.7	9
2	0.25	-32.6	30.4	0.8	4.3	9	-32.6	30.4	-0.4	9	-32.7	30.4	2.0	9
3	0.27	-31.8	32.0	0.1	5.8	9	-31.8	32.0	-1.8	9	-31.9	31.9	1.9	9
4	0.28	-31.1	33.5	-0.8	7.3	9	-31.0	33.6	-3.2	9	-31.2	33.0	2.0	10
5	0.29	-30.0	34.5	-1.2	8.9	10	-30.3	35.2	-4.6	9	-30.9	33.4	2.5	10
6	0.29	-29.5	35.0	-1.4	10.4	10	-28.5	36.3	-5.7	10	-30.5	33.8	2.7	10
7	0.30	-29.0	35.7	-1.8	11.9	10	-31.8	36.9	-6.3	17	-30.1	34.3	2.8	10
8	0.30	-28.5	36.3	-2.2	13.4	10	-31.3	37.5	-6.9	17	-29.7	34.9	2.7	10
9	0.31	-28.0	37.0	-2.7	15.0	10	-30.9	38.1	-7.5	17	-29.2	35.5	2.4	10
10	0.31	-31.3	37.6	-3.2	16.5	17	-30.5	38.7	-8.1	17	-19.4	36.0	2.0	11
11	0.32	-30.9	38.2	-3.8	18.0	17	-30.0	39.3	-8.7	17	-20.0	35.4	2.7	11
12	0.32	-30.4	38.8	-4.4	19.5	17	-29.6	39.9	-9.4	17	-20.4	34.8	3.2	11
13	0.32	-13.8	38.9	-4.7	21.0	18	-29.2	40.5	-10.0	17	-20.8	34.4	3.4	11
14	0.32	-14.2	38.5	-4.4	22.6	18	-32.1	41.0	-10.6	24	-21.1	34.1	3.4	11

H-59

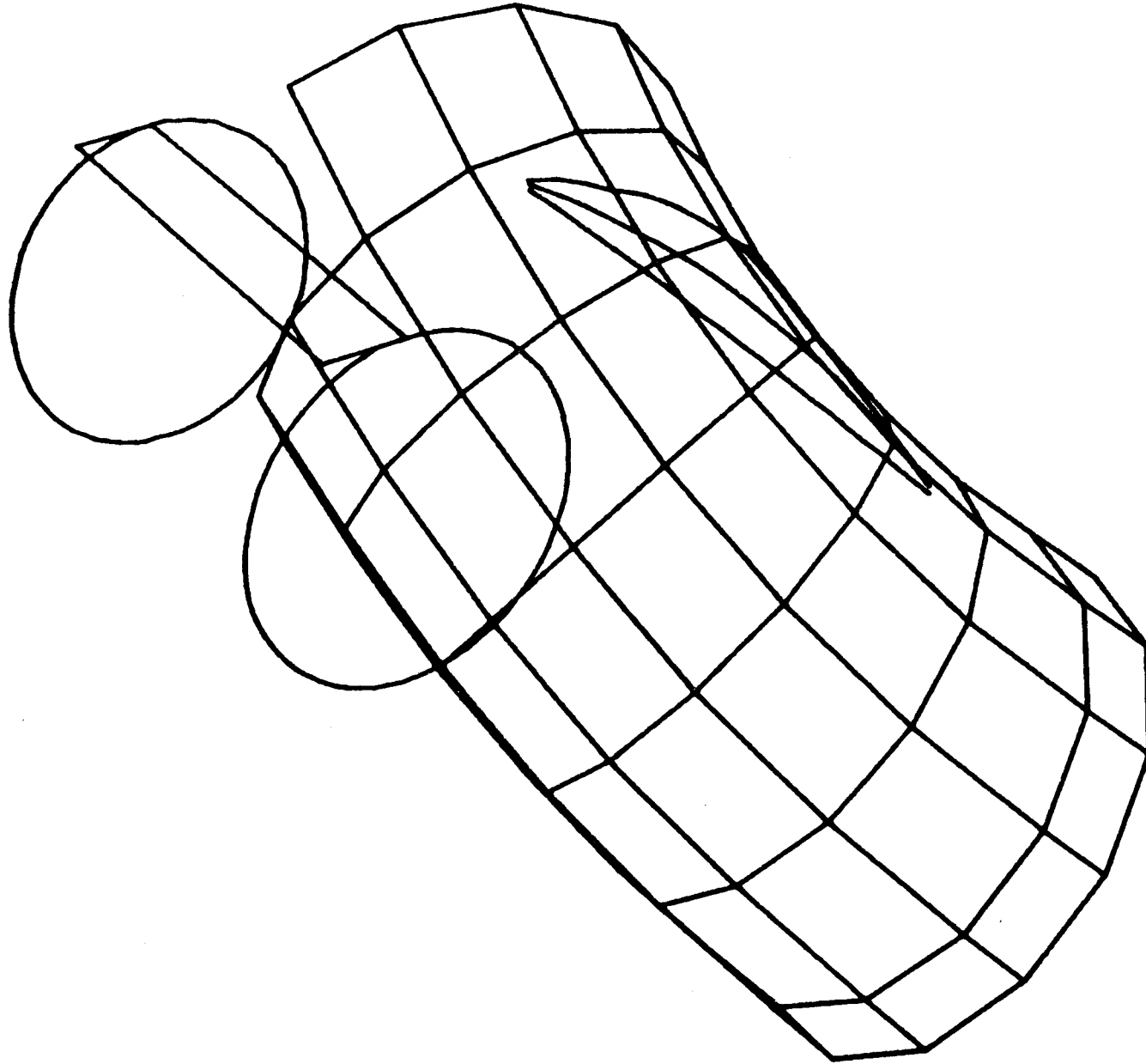
16	0.32	-14.7	37.8	-4.2	25.6	18	-31.4	41.9	-11.6	24	*****	0.0*****
17	0.31	-14.8	37.7	-4.4	27.1	18	-31.1	42.4	-12.1	24	*****	-0.0 0.0*****
18	0.31	-12.0	37.7	-4.8	28.7	25	-30.8	42.9	-12.6	24	*****	0.0 0.0*****
19	0.32	-11.6	38.2	-5.8	30.2	25	-8.6	42.4	-12.1	25	*****	0.0*****
20	0.32	-11.1	38.9	-7.1	31.7	25	-9.1	41.6	-11.3	25	*****	0.0*****
21	0.33	-10.3	39.9	-9.0	33.2	25	-7.4	41.0	-10.6	32		-11.0 39.0 -7.5 25

3-D VIEW

RUN 807

ELEMENTS

1,99999



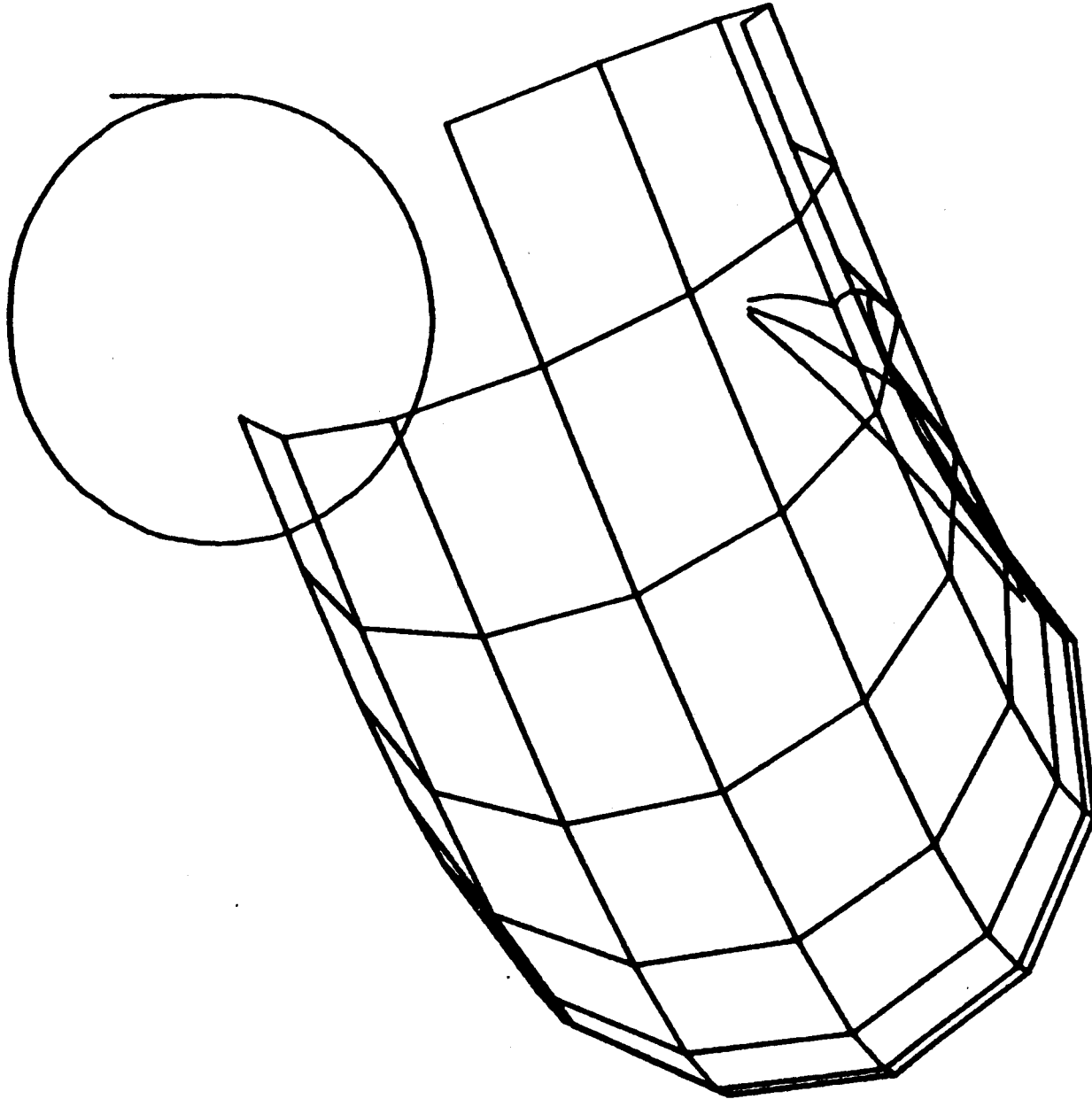
H-61

FRONT VIEW

RUN 807

ELEMENTS

1,99999



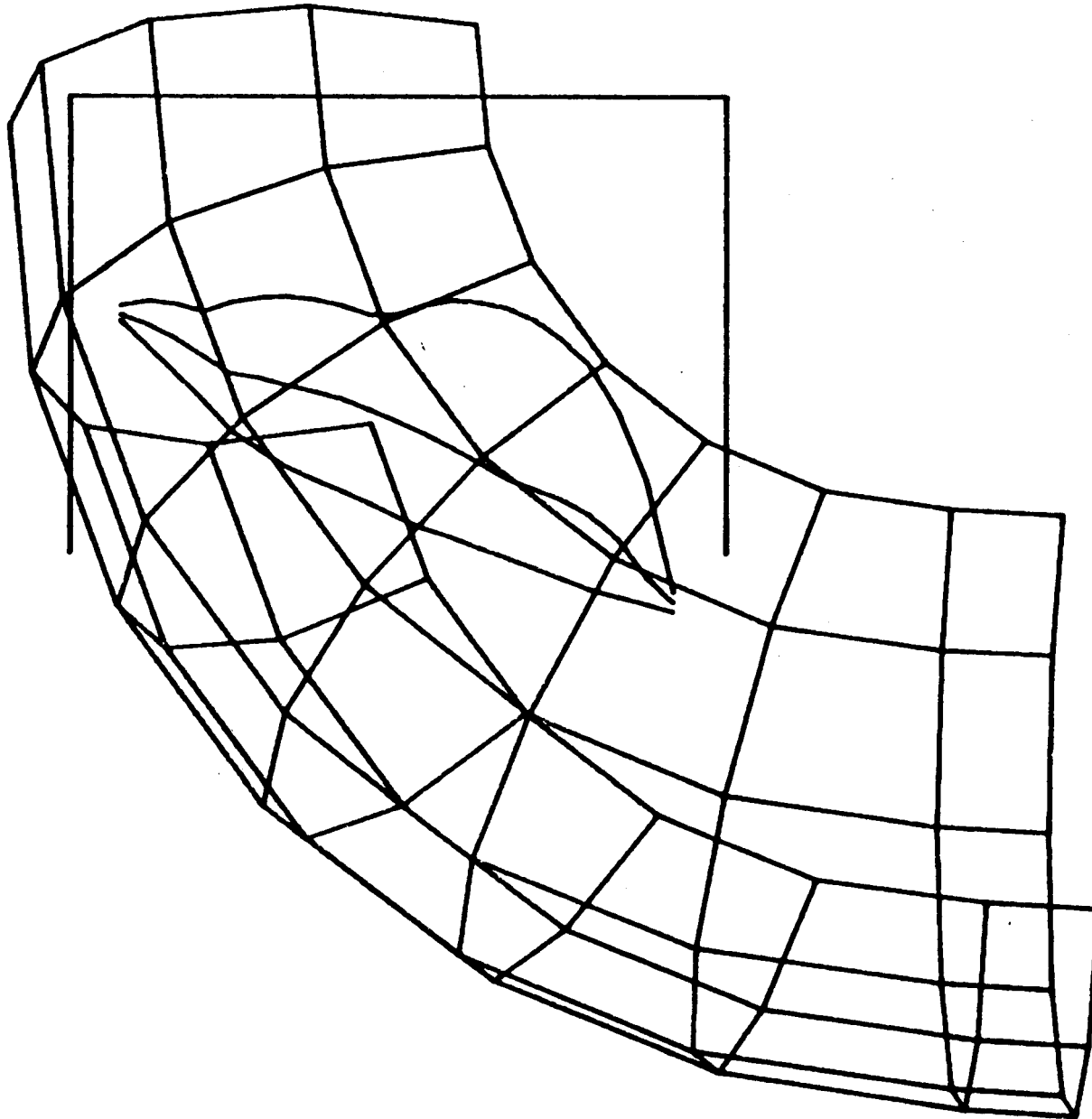
H-62

SIDE VIEW

RUN 807

ELEMENTS

1,99999



H-63

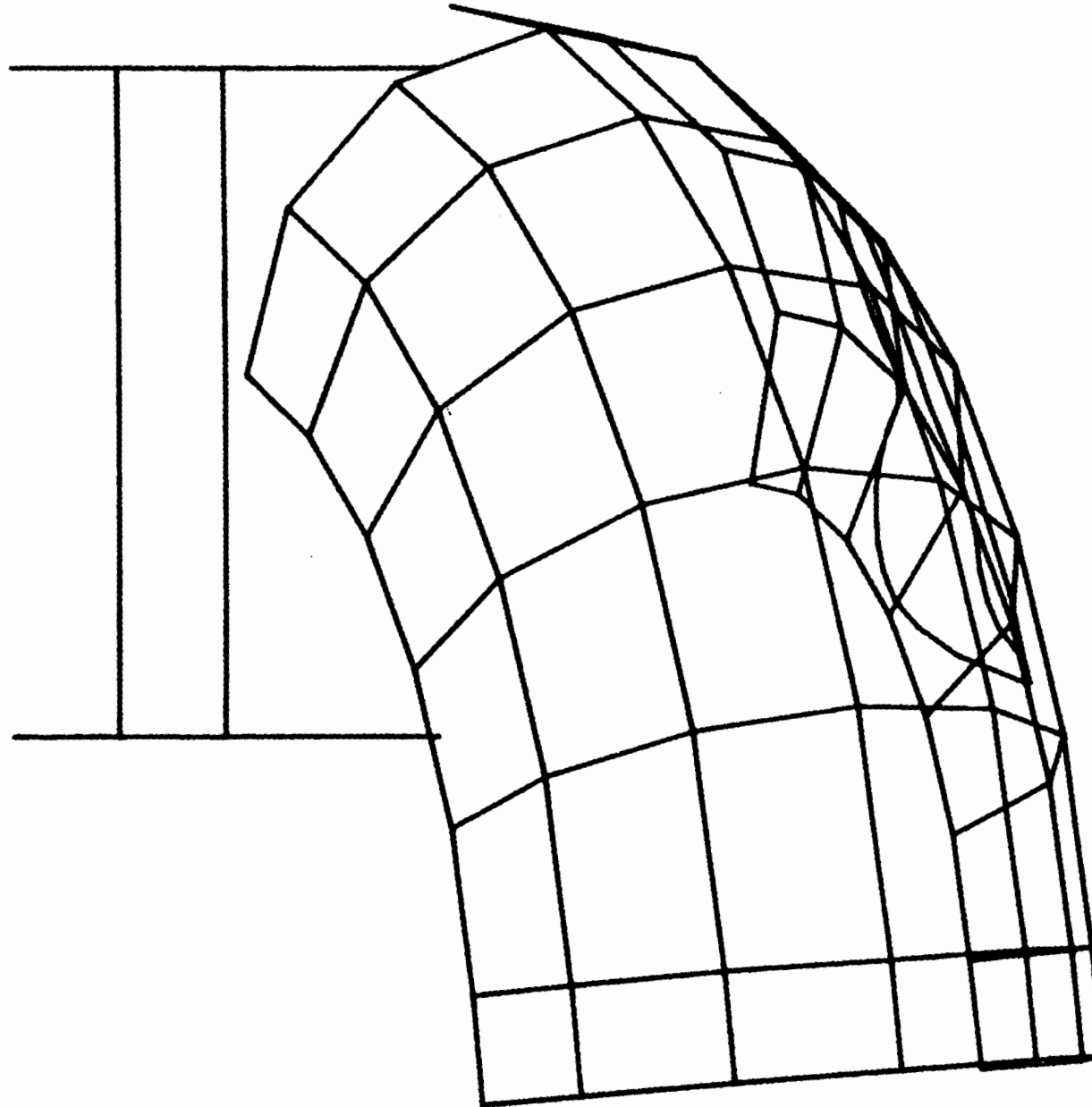
TOP VIEW

RUN 807

ELEMENTS

1,99999

F9-H



H-2

FRictional FLOW ANALYSIS RESULTS

H-65

TYPICAL STREAM DATA LOG

STREAM	STEP	VELOCITY (IN./SEC)	WIDTH (IN)	HEIGHT (IN)	RADIUS (IN)	RAD/HGT	NORMAL		SHEAR		LOCATION, RIGHT EDGE			PLATE LOCATION
							FORCE*	FORCE*	FORCE*	FORCE*	X	Y	Z	
3	1	153.3	1.4	1.5	31.1	21.2	0.4	0.3	46.1	-16.7	31.2	31		
3	2	155.2	1.4	1.5	33.7	23.2	0.1	-0.1	46.4	-17.9	31.3	31		
3	3	156.3	1.4	1.4	38.7	26.7	0.5	0.4	46.6	-18.5	31.3	31		
3	4	157.4	1.4	1.4	41.4	28.7	0.4	0.3	46.8	-19.1	31.4	31		
3	5	159.0	1.4	1.4	44.2	30.9	0.0	0.0	47.0	-19.6	31.4	31		
3	6	159.4	1.5	1.4	46.9	33.4	0.3	0.3	47.2	-20.2	31.5	31		
3	7	161.4	1.5	1.4	49.6	35.8	0.0	0.0	47.3	-20.8	31.5	30		
3	8	160.3	1.5	1.4	48.6	34.7	0.4	0.3	47.3	-21.4	31.6	30		
3	9	162.7	1.5	1.4	46.8	33.9	0.4	-0.3	47.2	-22.0	31.7	30		
3	10	161.3	1.4	1.4	44.9	32.2	0.4	0.3	47.2	-22.5	31.9	30		
3	11	163.8	1.4	1.4	43.0	31.2	0.4	-0.3	47.1	-23.1	32.0	30		
3	12	162.2	1.4	1.4	41.1	29.5	0.4	0.3	47.0	-23.7	32.1	30		
3	13	163.6	1.4	1.4	39.2	28.3	0.4	-0.3	47.0	-24.3	32.2	30		
3	14	165.3	1.4	1.4	37.5	27.4	0.1	0.0	46.9	-24.9	32.3	30		
3	15	163.3	1.4	1.4	35.6	25.6	0.5	0.4	46.9	-25.5	32.4	30		
3	16	166.0	1.4	1.4	33.7	24.5	0.5	-0.4	46.8	-26.1	32.6	30		
3	17	163.7	1.4	1.4	31.7	22.7	0.5	0.4	46.8	-26.7	32.7	30		
3	18	164.8	1.4	1.4	29.6	21.4	0.5	-0.4	46.7	-27.3	32.8	30		
3	19	163.1	1.4	1.4	28.0	20.0	0.1	-0.1	46.6	-27.9	33.0	37		
3	20	164.8	1.4	1.4	54.0	38.8	0.5	-0.4	46.5	-28.5	33.1	37		
3	21	163.6	1.4	1.4	54.0	38.5	0.0	-0.0	46.4	-29.1	33.3	37		
3	22	164.5	1.4	1.4	54.0	38.7	0.4	-0.3	46.3	-29.6	33.4	37		
3	23	163.6	1.4	1.4	54.0	38.2	0.4	-0.3	46.2	-30.2	33.6	37		
3	24	162.7	1.4	1.4	54.0	37.8	0.4	-0.3	46.1	-30.8	33.7	37		
3	25	165.6	1.4	1.4	54.0	37.9	0.4	-0.3	45.9	-31.3	33.9	36		
3	26	163.3	1.4	1.5	54.0	36.7	0.5	0.4	45.5	-31.8	34.1	36		
3	27	162.6	1.3	1.5	54.0	36.0	0.6	-0.4	45.2	-32.2	34.3	36		
3	28	165.2	1.3	1.5	54.0	36.0	0.5	-0.4	44.8	-32.7	34.5	36		
3	29	162.6	1.3	1.5	54.0	34.9	0.5	0.4	44.5	-33.1	34.8	36		
3	30	165.4	1.3	1.5	54.0	34.9	0.6	-0.4	44.1	-33.6	35.0	36		
3	31	162.6	1.3	1.6	54.0	33.8	0.6	0.4	43.8	-34.1	35.2	36		
3	32	165.6	1.2	1.6	54.0	34.1	0.6	-0.4	43.4	-34.5	35.5	36		
3	33	162.7	1.2	1.6	54.0	33.2	0.6	0.5	43.1	-35.0	35.7	36		
3	34	165.7	1.2	1.6	54.0	33.5	0.6	-0.5	42.8	-35.4	35.9	36		
3	35	162.7	1.2	1.7	54.0	32.7	0.6	0.5	42.4	-35.9	36.2	36		
3	36	163.5	1.2	1.6	54.0	32.8	0.6	-0.5	42.1	-36.3	36.4	36		
3	37	161.6	1.2	1.7	54.0	32.3	0.1	-0.1	41.7	-36.8	36.7	36		
3	38	163.0	1.2	1.7	54.0	32.5	0.6	-0.5	41.4	-37.2	36.9	36		
3	39	161.1	1.2	1.7	54.0	32.0	0.1	-0.1	41.1	-37.7	37.2	36		
3	40	162.5	1.2	1.7	54.0	32.2	0.6	-0.5	40.8	-38.1	37.4	36		
3	41	160.6	1.2	1.7	54.0	31.8	0.1	-0.1	40.4	-38.6	37.7	36		
3	42	162.3	1.2	1.7	54.0	32.4	0.6	-0.5	40.1	-39.0	38.0	35		
3	43	159.2	1.2	1.7	54.0	31.7	0.1	0.1	39.6	-39.2	38.3	35		
3	44	163.1	1.2	1.7	54.0	31.7	0.7	-0.5	39.2	-39.4	38.6	35		
3	45	158.2	1.2	1.7	54.0	31.1	0.7	-0.6	38.7	-39.7	38.9	35		
3	46	161.4	1.2	1.7	54.0	31.7	0.8	-0.6	38.2	-39.9	39.3	35		
3	47	158.9	1.2	1.8	54.0	30.8	0.8	0.6	37.8	-40.1	39.6	35		
3	48	157.5	1.2	1.7	54.0	31.0	0.8	-0.6	37.3	-40.4	40.0	35		
3	49	154.6	1.2	1.8	54.0	30.2	0.1	0.1	36.9	-40.6	40.3	35		
3	50	156.1	1.2	1.8	54.0	30.7	0.8	-0.6	36.4	-40.8	40.7	35		
3	51	155.8	1.2	1.8	54.0	30.3	0.8	0.6	35.9	-41.1	41.1	35		
3	52	152.4	1.2	1.8	54.0	29.6	0.1	0.1	35.5	-41.3	41.4	35		
3	53	153.5	1.2	1.8	54.0	29.9	0.8	-0.6	35.1	-41.5	41.8	35		
3	54	150.0	1.2	1.9	54.0	29.2	0.1	0.1	34.6	-41.7	42.2	35		
3	55	151.1	1.2	1.8	54.0	29.4	0.8	-0.6	34.2	-42.0	42.6	35		
3	56	157.7	1.2	1.9	54.0	29.8	0.1	0.1	33.7	-42.3	43.0	35		

*LBS/IN²

12-68

3	57	148.8	1.2	1.9	54.0	26.1	0.8	-0.6	33.3	-42.4	43.3	35
3	58	149.4	1.2	1.9	54.0	26.5	0.1	0.1	32.9	-42.7	43.7	35
3	59	146.5	1.2	1.9	54.0	26.8	0.8	-0.6	32.5	-42.9	44.1	35
3	60	146.5	1.2	1.9	50.0	26.2	0.1	0.1	31.6	-43.2	44.9	41
3	61	140.9	1.2	2.0	54.0	27.0	0.9	0.7	31.2	-43.1	45.3	41
3	62	141.4	1.2	2.0	54.0	27.0	0.9	-0.7	30.8	-43.1	45.8	41
3	63	144.0	1.1	2.0	54.0	27.3	0.9	-0.7	30.3	-43.0	46.2	41
3	64	138.2	1.1	2.1	54.0	26.2	0.9	0.7	29.5	-43.0	47.1	41
3	65	134.0	1.1	2.1	54.0	25.1	0.1	-0.1	29.1	-42.9	47.6	41
3	66	138.6	1.1	2.1	54.0	25.9	0.1	-0.1	28.2	-42.8	48.6	41
3	67	134.4	1.1	2.1	20.1	9.4	1.0	0.7	27.8	-42.8	49.0	41
3	68	129.0	1.2	2.2	18.0	8.2	0.0	0.0	27.1	-42.8	50.0	41
3	69	132.4	1.1	2.1	54.0	25.2	0.0	0.0	26.7	-42.8	50.5	41
3	70	0.0	0.0	0.0	0.0	0.0	0.0	0.0	26.7	-42.8	50.5	0
3	71	0.0	0.0	0.0	0.0	0.0	0.0	0.0	26.7	-42.8	50.5	0
3	72	0.0	0.0	0.0	0.0	0.0	0.0	0.0	26.7	-42.8	50.5	0
3	73	0.0	0.0	0.0	0.0	0.0	0.0	0.0	26.7	-42.8	50.5	0
3	74	0.0	0.0	0.0	0.0	0.0	0.0	0.0	26.7	-42.8	50.5	0
3	75	0.0	0.0	0.0	0.0	0.0	0.0	0.0	26.7	-42.8	50.5	0

TYPICAL STREAM DATA LOG

450 FPM TRAJECTORY CASE

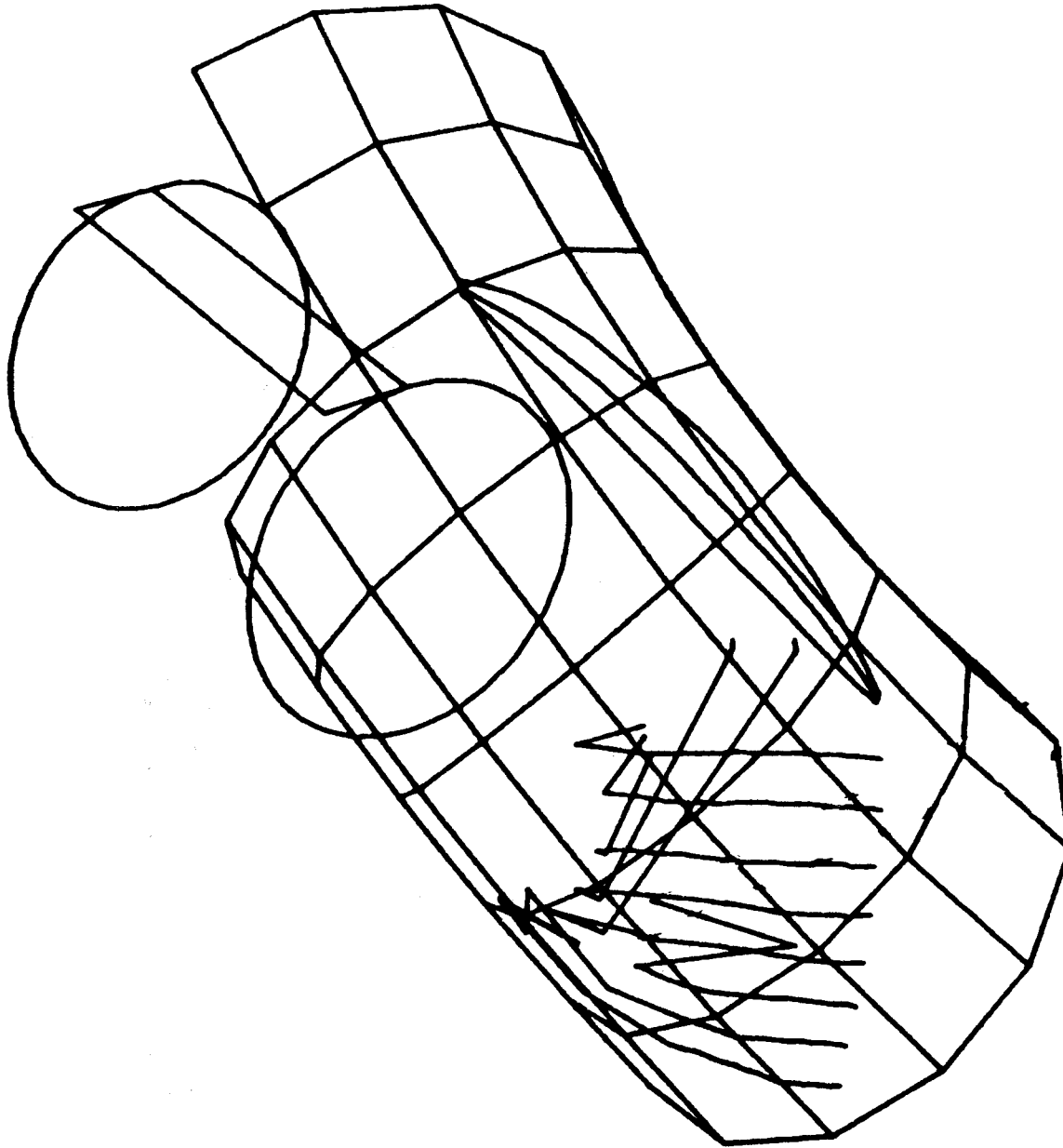
<u>RUN</u>	<u>ANGLE OF WALL FRICTION</u>
746	0°
747	20°

3-D VIEW

RUN 746 1

ELEMENTS

1,99999



H-69

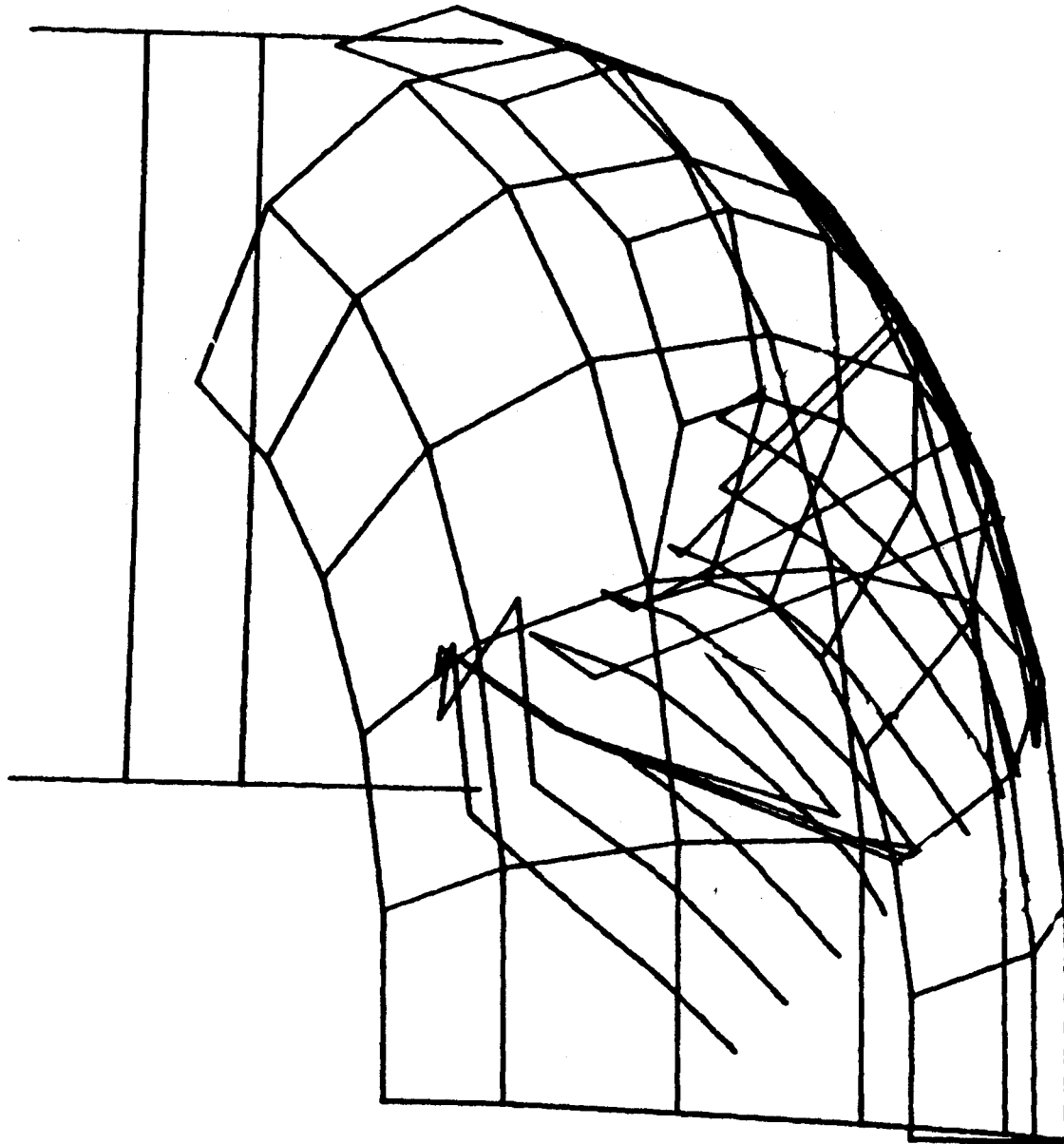
TOP VIEW

RUN 746 1

ELEMENTS

1,99999

H-70

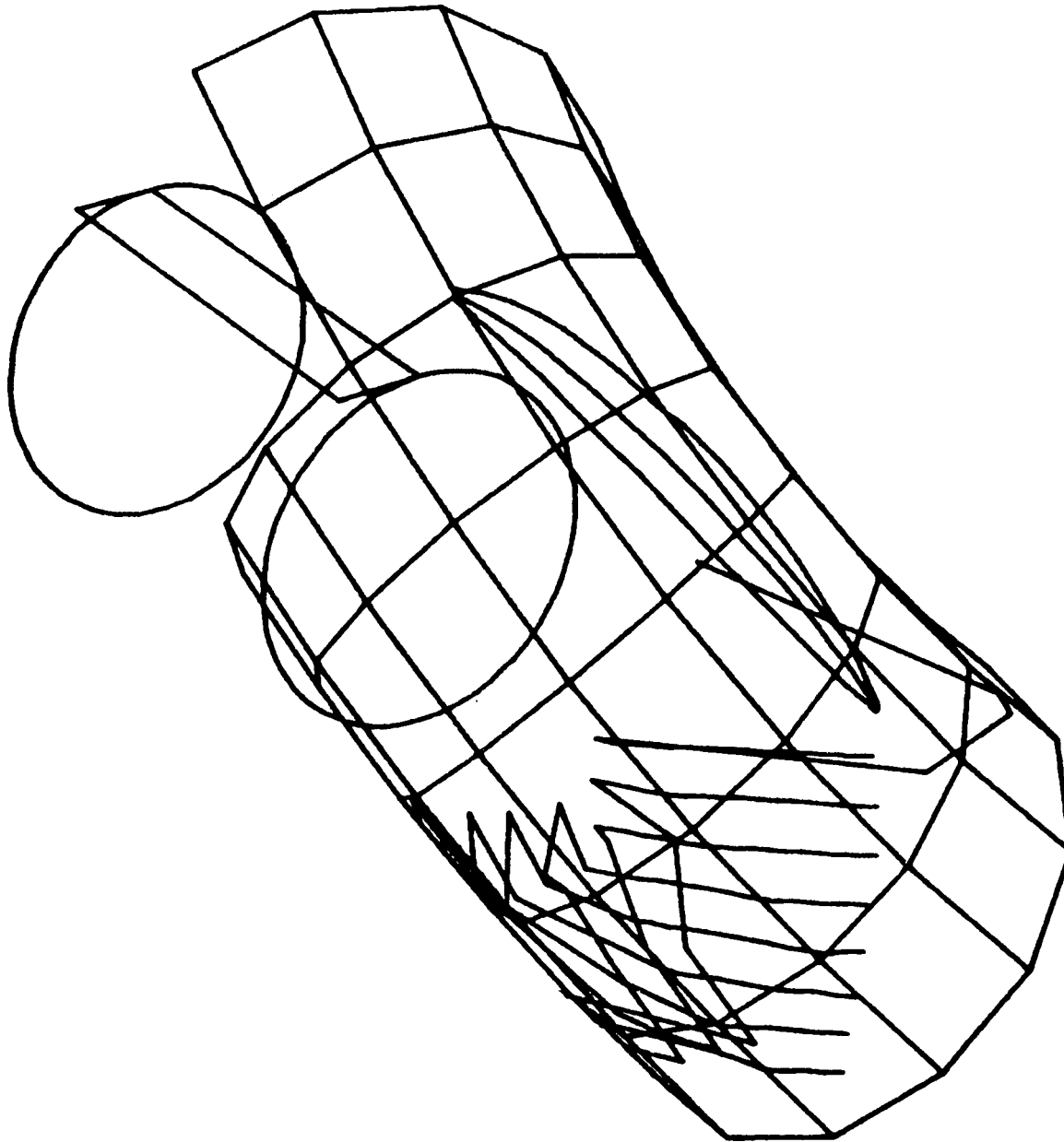


3-D VIEW

RUN 747 2

ELEMENTS

1,99999



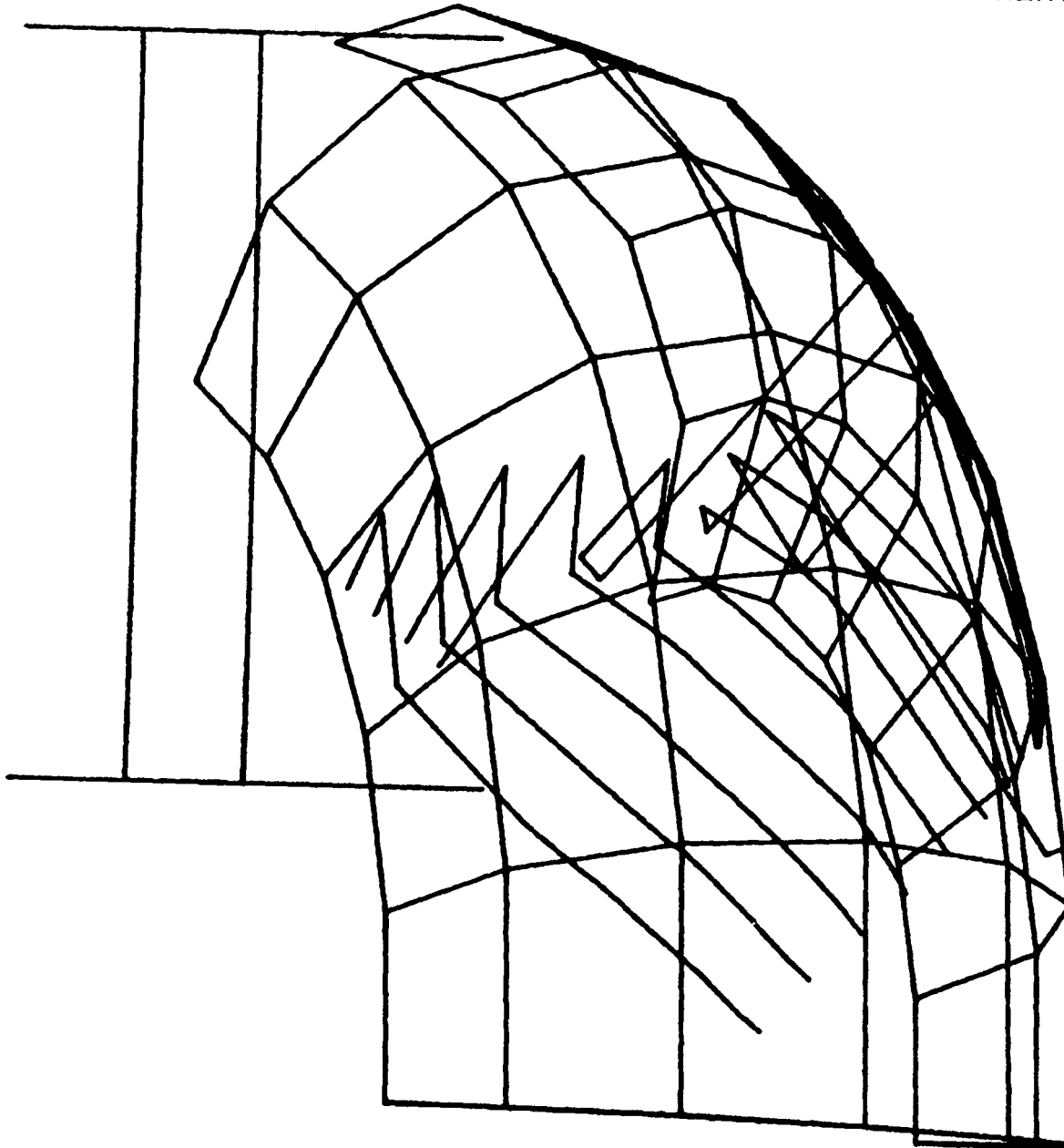
H-71

TOP VIEW

RUN 747 2

ELEMENTS

1,99999



H-72

600 FPM TRAJECTORY CASE

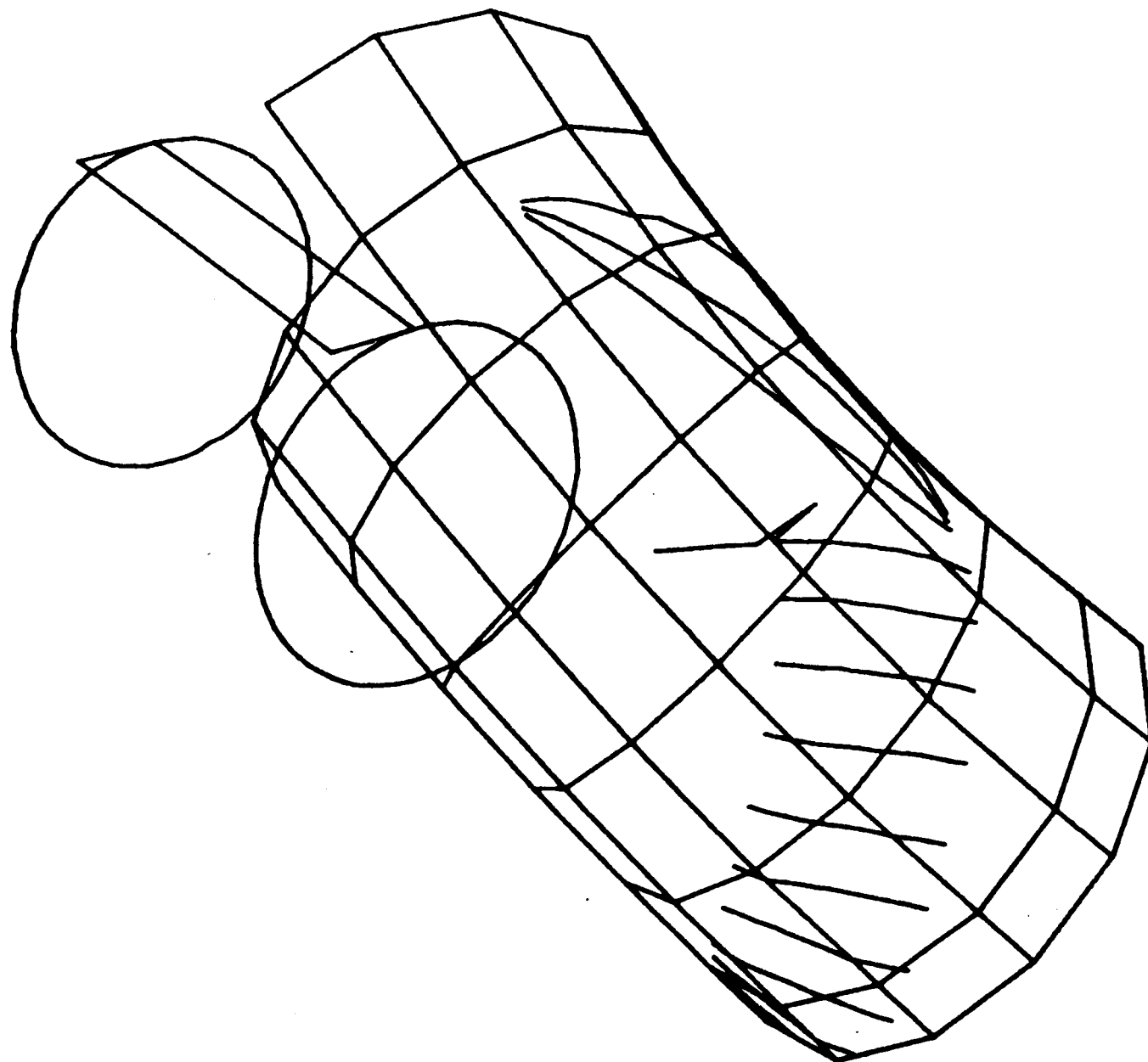
<u>RUN</u>	<u>ANGLE OF WALL FRICTION</u>
846	0
847	20

3-D VIEW

RUN 846 6

ELEMENTS

1,99999



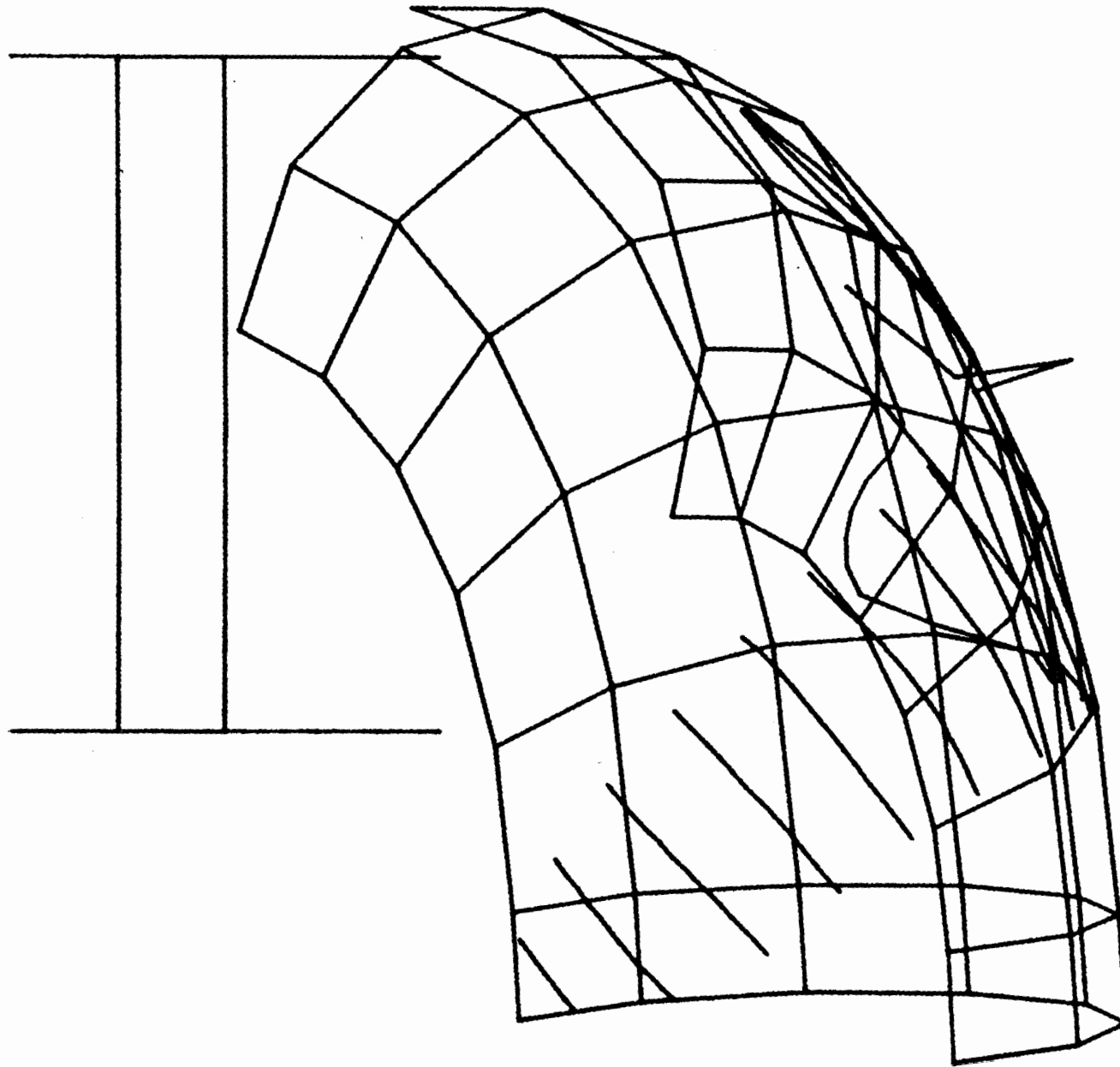
H-74

TOP VIEW

RUN 846 6

ELEMENTS

1,99999



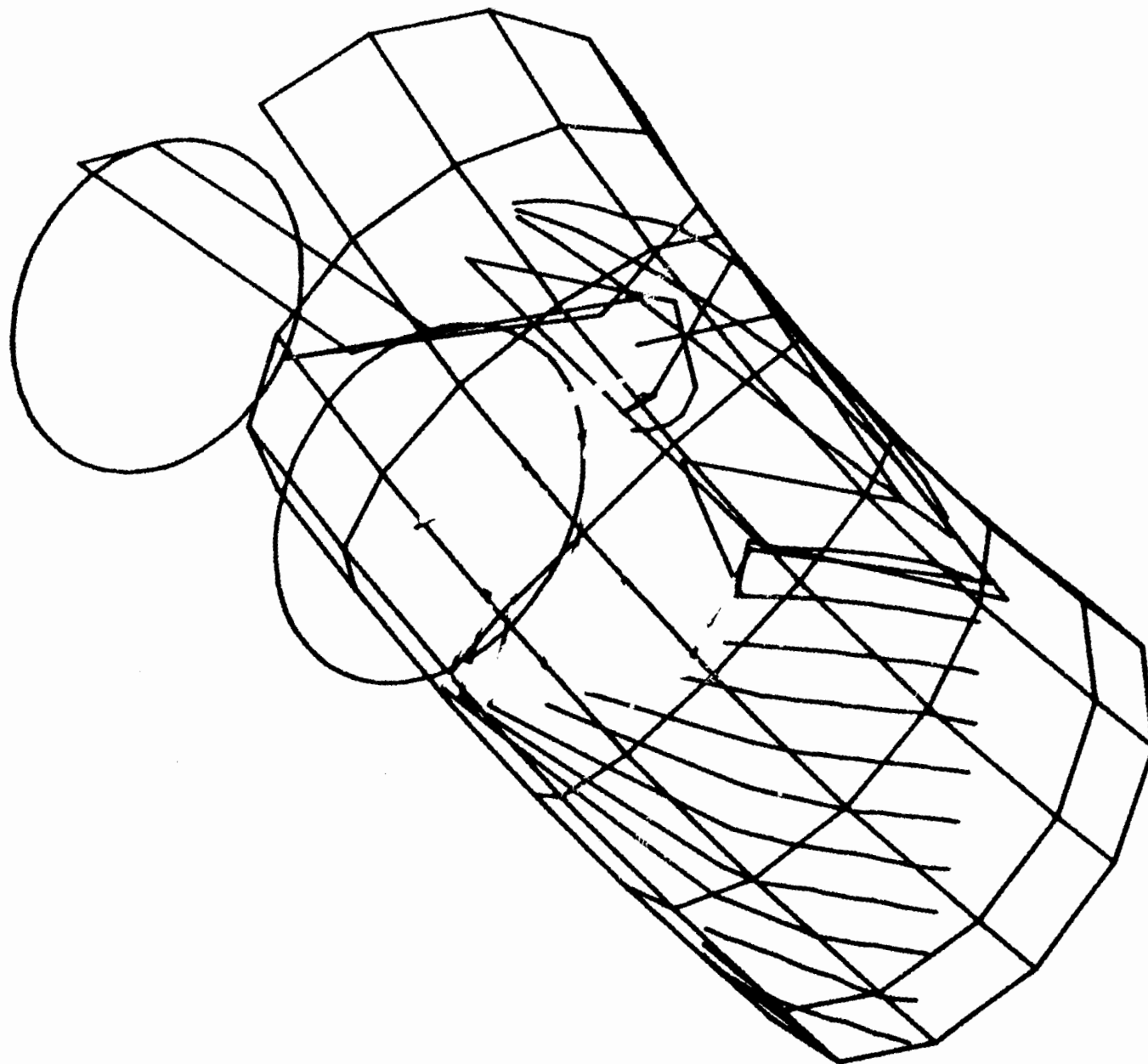
H-75

3-D VIEW

RUN 847 7

ELEMENTS

1,99999



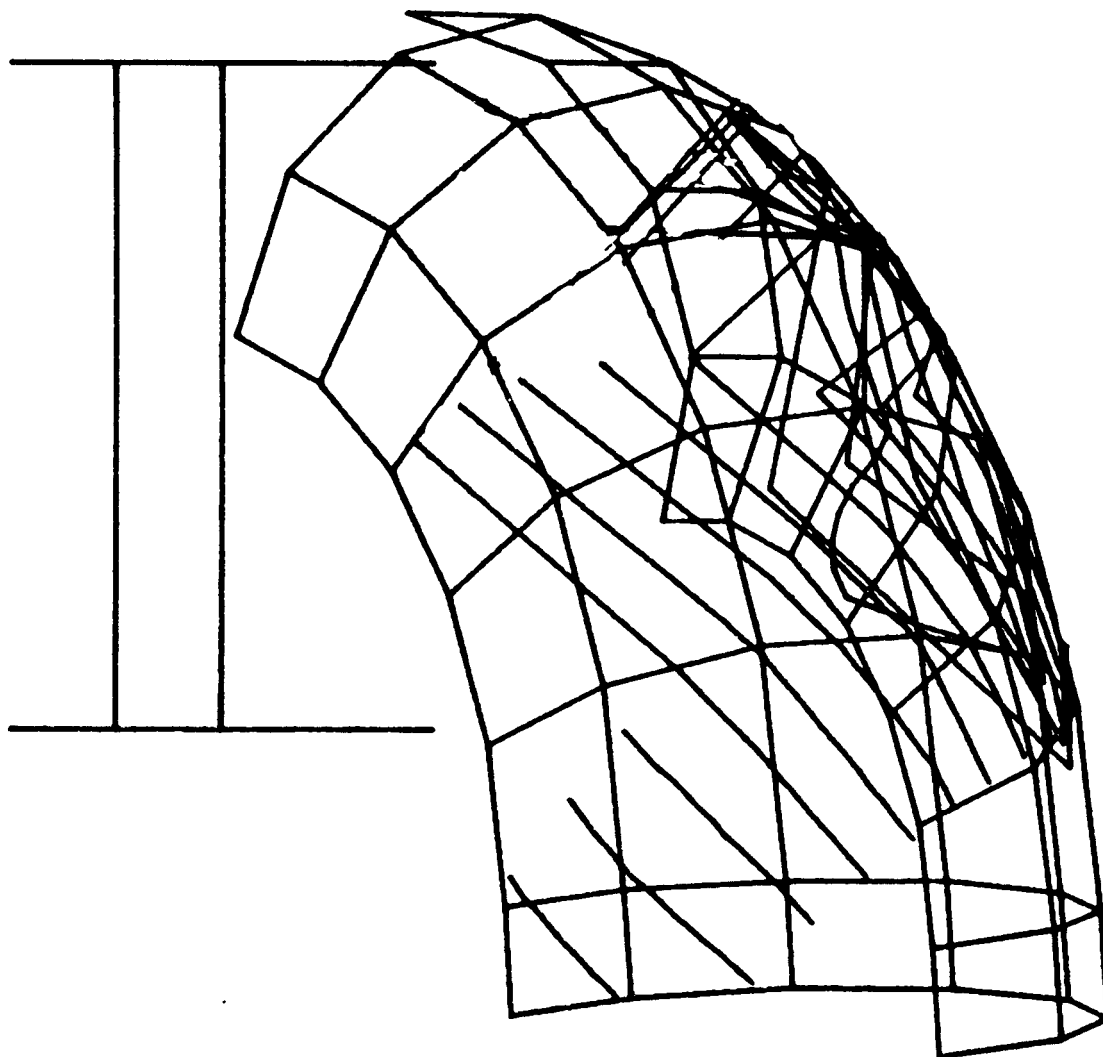
H-76

TOP VIEW

RUN 847 7

ELEMENTS

1,99999



H-77